FOODS and raw materials

Volume 14
Issue 1
2026

ISSN 2308-4057 (print)
ISSN 2310-9599 (online)

FRM

food production technology

food production processes and equipment

nutrition

veterinary

biotechnology

biological sciences

chemistry and ecology

standardization, certification, quality and safety

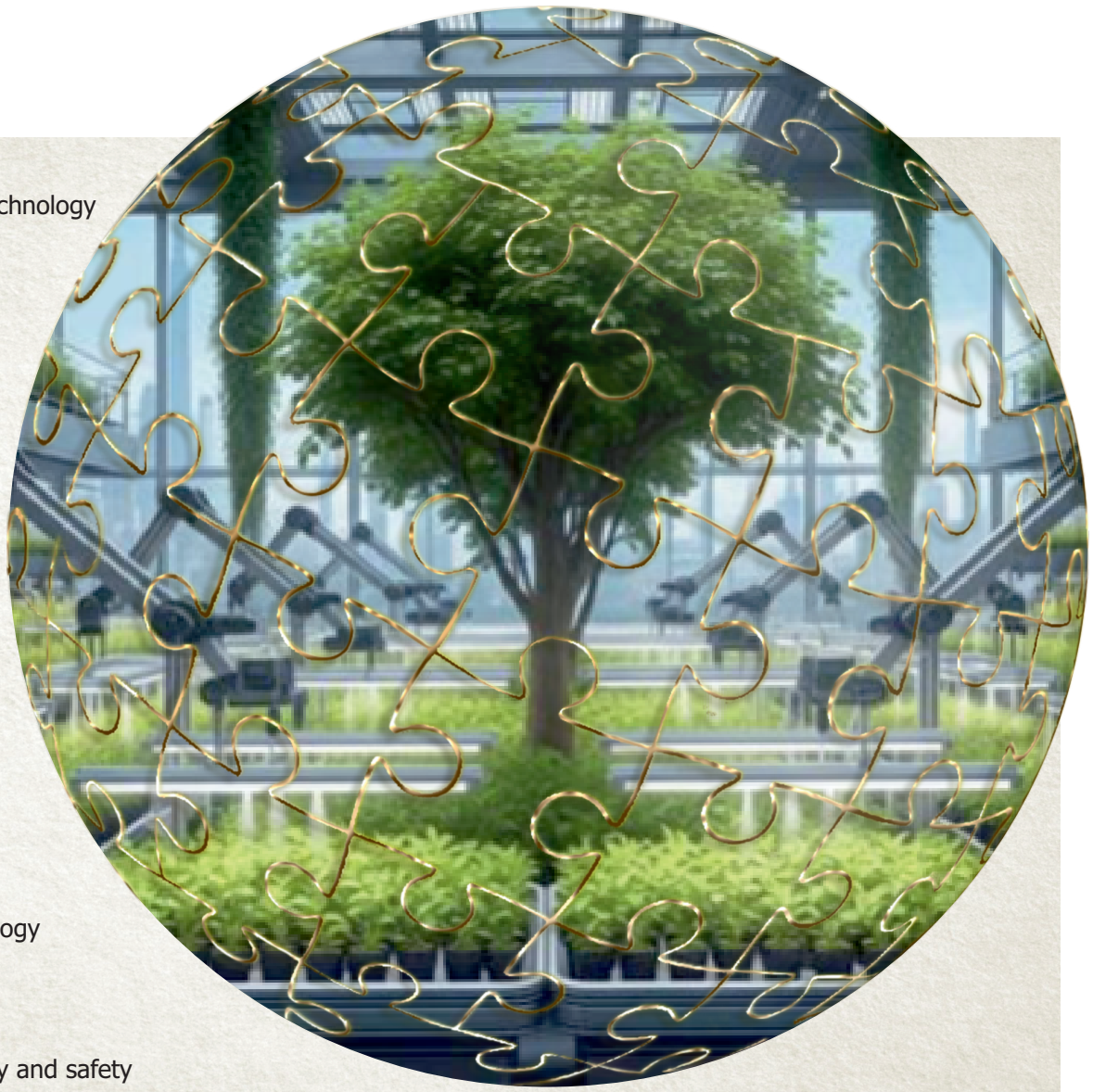

FOODS AND RAW MATERIALS

Kemerovo State University

Vol. 14, no. 1, 2026

ISSN 2308-4057 (Print) ISSN 2310-9599 (Online)

Foods and Raw Materials – рецензируемый высококвартильный научный журнал, освещающий широкий круг вопросов пищевой промышленности и смежных отраслей. Издается на английском языке с 2013 г.

В журнале публикуются результаты фундаментальных и прикладных исследований в виде научных оригинальных и обзорных статей, кратких научных сообщений по направлениям: технология пищевых производств; биотехнология; процессы, оборудование и аппараты пищевых производств; питание; стандартизация, сертификация, качество и безопасность; химия и экология; вопросы общей ветеринарии; сельскохозяйственные и биологические науки; экономика.

Foods and Raw Materials является научным изданием открытого доступа (open access). Опубликованные материалы распространяются на условиях лицензии CC BY 4.0. Политика открытого доступа соответствует Budapest Open Access Initiative, все статьи доступны онлайн сразу после публикации на *jfrm.ru* и *elibrary.ru*.

Foods and Raw Materials индексируется в следующих базах данных: Scopus (Q1/Q2), ESCI (Web of Science Core Collection), DOAJ, CAS, FSTA, ResearchBib, WJCI, Dimensions, LENS.ORG, Scilit, CNKI, ProQuest, CABI, Agricola, Google Scholar, Ulrich's, OCLC WorldCat и BASE.

Согласно рекомендациям ВАК № 3-пл/1 от 21 декабря 2023 г. *Foods and Raw Materials* приравнивается к журналам Перечня ВАК категории К1. ЕГПНИ (Белый список) – первый уровень.

Финансирование журнала осуществляется за счет средств учредителя – Кемеровский государственный университет. Для публикации статей необходимо вносить плату (APC).

Более подробно с журналом можно ознакомиться на сайте *jfrm.ru*

Главный редактор

Просеков Александр Юрьевич, академик РАН, д-р техн. наук, д-р биол. наук, профессор, Заслуженный работник высшей школы РФ, Лауреат премии Правительства РФ в области науки и техники, Почетный работник высшего профессионального образования РФ, Кемеровский государственный университет, Кемерово, Россия.

Заместитель главного редактора

Бабич Ольга Олеговна, д-р техн. наук, доцент, Балтийский федеральный университет имени Иммануила Канта, Калининград, Россия.

Редакционная коллегия

Бат Левент, Ph.D., профессор, Синопский университет, Синоп, Турция;

Гат Йогеш Шринивас, Ph.D., Институт химической технологии, Мумбаи, Индия;

Донник Ирина Михайловна, академик РАН, д-р биол. наук, профессор, Национальный исследовательский центр «Курчатовский институт», Москва, Россия;

Кумар Нишант, Ph.D., Национальный институт предпринимательства и менеджмента пищевых технологий, Сонепат, Индия;

Кючукбай Ф. Зехра, Ph.D., профессор, Университет Инону, Малатья, Турция;

Лисицын Андрей Борисович, академик РАН, д-р техн. наук, профессор, Лауреат Государственной премии РФ, Федеральный научный центр пищевых систем им. В. М. Горбатова РАН, Москва, Россия;

Ли Янг, д-р техн. наук, профессор, Колледж пищевых наук Северо-Восточного сельскохозяйственного университета, Харбин, Китай;

Мариод Абдалбасит Адам, Ph.D., профессор, Университет Джидды, Алкамил, Саудовская Аравия;

Мишу Филипп, Ph.D., профессор, Университет Клермон-Овернь, Политехнический институт Клермон-Ферран, Обье, Франция;

Моради Мехран, D.V.M-Ph.D., доцент, Университет Урмия, Урмия, Иран;

Пасторе Глосия Мария, Ph.D., профессор, Университет Кампинаса, Кампинас, Бразилия;

Сонаване Шириш Хари, Ph.D., профессор, Национальный институт технологии, Телангана, Индия;

Ходай Дьяко, Ph.D., Дублинский технологический университет, Дублин, Ирландия.

Научные редактора

Гуринович Галина Васильевна, д-р техн. наук, профессор, Кемеровский государственный университет, Кемерово, Россия;

Киселева Татьяна Федоровна, д-р техн. наук, профессор, Кемеровский государственный университет, Кемерово, Россия;

Осинцев Алексей Михайлович, д-р техн. наук, профессор, Кемеровский государственный университет, Кемерово, Россия.

Выпускающий редактор

Лосева Анна Ивановна, д-р техн. наук, Кемеровский государственный университет, Кемерово, Россия.

Учредитель, издатель, редакция: Кемеровский государственный университет, 650000, Россия, Кемеровская обл. – Кузбасс, г. Кемерово, Красная, 6 тел.: +7 (3842) 58-81-19; e-mail: fjournal@mail.ru

Адрес типографии: Кемеровский государственный университет, 650000, Россия, Кемеровская обл. – Кузбасс, г. Кемерово, пр. Советский, 73

Ответственные за выпуск: Дмитриева Е.В.
Литературный редактор: Николаева К.А.
Переводчики: Павлова О.Ю., Рабкина Н.В.
Дизайн и компьютерная верстка: Волкова Е.В.
Изображение на обложке: *https://ru.pinterest.com/pin/818388563579612336/*
Изображения, используемые в статьях, предоставлены авторами

Дата выхода в свет 24.02.2026

16+

Тираж 500 экз. Цена свободная. Выходит 2 раза в год
Подписной индекс по интернет-каталогу агентства «Урал-Пресс» – 40539

Регистрационный номер СМИ серия ПИ № ФС77-72606 выдан Роскомнадзор

© Составление, сопроводительный текст, редакционно-издательское оформление, Кемеровский государственный университет, 2026

FOODS AND RAW MATERIALS

Kemerovo State University

Vol. 14, no. 1, 2026

ISSN 2308-4057 (Print) ISSN 2310-9599 (Online)

Foods and Raw Materials reports pioneering research in the food industry and agricultural science. We publish the results of fundamental and applied research as scientific papers, peer reviews, brief scientific reports, etc. The Journal is a single platform for scientific communication.

Foods and Raw Materials has been published in the English language since 2013. Two volumes a year come out in print and online.

All submitted manuscripts are checked for plagiarisms via *antiplagiat.ru* and undergo a double-blind peer review. Authors are responsible for the content of their article.

Foods and Raw Materials is supported by the Kemerovo State University. Authors are charged an Article Publication Charge (APC).

Foods and Raw Materials is an open access journal (CC BY 4.0). Our open access policy follows the Budapest Open Access Initiative (BOAI), which means that all our articles are available online immediately upon publication. Full-text electronic versions of all published materials appear in open access on *jfrm.ru/en* and *elibrary.ru*

Foods and Raw Materials is included in the following international data-bases: Scopus, Emerging Sources Citation Index (Web of Science Core Collection), DOAJ, CAS, FSTA, ResearchBib, WJCI, Dimensions, LENS.ORG, Scilit, CNKI, ProQuest, CABI, Agricola, Ulrich's, Google Schoar, OCLC WorldCat, and "White list" (Russia) – 1 level.

For submission and subscription instructions, please visit us online at *jfrm.ru/en*

Editor-in-Chief

Alexander Yu. Prosekov, Dr. Sci. (Eng.), Dr. Sci. (Biol.), Professor, Academician of RAS, Kemerovo State University, Kemerovo, Russia.

Deputy Editor-in-Chief

Olga O. Babich, Dr. Sci. (Eng.), Associate Professor, Immanuel Kant Baltic Federal University, Kaliningrad, Russia.

Editorial Board

Levent Bat, Ph.D., Professor Dr., University of Sinop, Sinop, Turkey;

Yogesh Shrinivas Gat, Ph.D., Institute of Chemical Technology, Mumbai, India;

Irina M. Donnik, Dr. Sci. (Biol.), Professor, Academician of RAS, Kurchatov Institute, Moscow, Russia;

Nishant Kumar, Ph.D., National Institute of Food Technology Entrepreneurship and Management, Sonepat, India;

Fatumetuzzehra Küçükbay, Ph.D., Professor Dr., İnönü University, Malatya, Turkey;

Andrey B. Lisitsyn, Dr. Sci. (Eng.), Professor, Academician of RAS, V. M. Gorbatov Federal Research Center for Food Systems of Russian Academy of Sciences, Moscow, Russia;

Yang Li, Dr. Sci. (Eng.), Professor, College of Food Science, Northeast Agricultural University, Harbin, China;

Abdalbasit Adam Mariod, Ph.D., Professor, University of Jeddah, Alkamil, Saudi Arabia;

Philippe Michaud, Ph.D., Professor, Universite Clermont Auvergne, Polytech Clermont Ferrand, Aubiere, France;

Mehran Moradi, Doctor of Veterinary Medicine, Ph.D., Urmia University, Urmia, Iran;

Gláucia Maria Pastore, Ph.D., Professor, Campinas University, Campinas, Brazil;

Shirish Hari Sonawane, Ph.D., Professor, National Institute of Technology Warangal, Telangana, India;

Diako Khodaei, Ph.D., Technical University of Dublin, Dublin, Ireland.

Scientific Editor

Galina V. Gurinovich, Dr. Sci. (Eng.), Professor, Kemerovo State University, Kemerovo, Russia;

Tatyana F. Kiseleva, Dr. Sci. (Eng.), Professor, Kemerovo State University, Kemerovo, Russia;

Alexey M. Osintsev, Dr. Sci. (Eng.), Professor, Kemerovo State University, Kemerovo, Russia.

Executive Editor

Anna I. Loseva, Dr. Sci. (Eng.), Kemerovo State Universty, Kemerovo, Russia.

Founder and Publisher: Kemerovo State University, 6, Krasnaya St., Kemerovo, Kemerovo region – Kuzbass, 650000, Russia

Editorial Office: Kemerovo State University, 6, Krasnaya St., Kemerovo, Kemerovo Region – Kuzbass, 650000, Russia; phone: +7(3842)58-81-19; e-mail: fjournal@mail.ru

Printing Office: Kemerovo State University, 73, Sovetskiy Ave., Kemerovo, Kemerovo Region – Kuzbass, 650000, Russia

Translators: Oxana Yu. Pavlova, Nadezda V. Rabkina

Publishing editors: Ekaterina V. Dmitrieva

Literary editor: Ksenia A. Nikolaeva

Computer layout and design: Elena V. Volkova

Cover image: image from *https://ru.pinterest.com/pin/818388563579612336/*

Photos credits: contributors

Date of publishing

February 24, 2026

16+

Circulation 500 ex. Open price.

Subscription index in the Ural-Press online catalog – 40539.

The Federal Service for Supervision of Communications, Information Technology, and Mass Media (Roskomnadzor)

Media registration number PI series No. FS77-72606

© Layout, accompanying text, editorial and publishing design, Kemerovo State University, 2026

Foods and Raw Materials. 2025;13(2)
ISSN 2310-9599 (Print)
ISSN 2308-4057 (Online)

Editorial
Open Access

Available online at https://jfrm.ru/en

Editor's column

Russia's agro-industrial complex is a cornerstone of national food security and economic independence. Despite new challenges, it maintains an upward growth trajectory, constantly expanding its export potential.

2025 was a year of market challenges and climatic volatility. Yet, it saw the third-largest grain harvest in the national history: it totaled 142 million tons, including over 93 million tons of wheat. Farmers provided the country with ample supplies of grain, meat, fish, oil, and sugar while closing the gap on the targets set by the Russian Food Security Doctrine for milk, potatoes, and vegetables.

The rapid proliferation of advanced technologies, including digital solutions and process automation, have been a driver of efficiency across the entire agro-industrial chain, from primary production and food processing to each single food industry. Our agro-industrial complex is going through profound technological transformations. But despite the numerous threats and challenges, it is emerging as a global frontliner of agricultural innovations. While being in line with global trends, this progress is anchored in the national strategic objectives of food security, export expansion, and international competitiveness.

As they permeate all spheres of agriculture, advanced technologies bolster the efficiency and sustainability of agricultural production. More than 40% of agricultural businesses have integrated digital tools into their workflows. The tactical deployment of artificial intelligence has a potential to generate over $6 billion in annual operating profit.

State support, strategizing, digitalization, robotics, automation, and agrobiotechnologies catalyze the technological development in the Russian agro-industrial complex.

The government implements a wide range of support measures to stimulate technological innovations. This centralized support guarantees the stability of the agro-industrial complex while accelerating its technological development.

Agricultural digitalization encompasses such innovations as precision farming, advanced agricultural data analytics, the Internet of Things (IoT), etc. It introduces modern information and communication technologies into all facets of agricultural production. Robotics means that production processes are managed by automated systems based on autonomous machinery, Unmanned Aerial Vehicles (UAVs), and AI-powered management systems. The synergy of these tech-nologies bolsters the efficiency, operational precision, and stability of agricultural production, reducing its dependence on human labor in conditions of labor shortages and rising costs.

Agricultural biotechnology serves as a powerful catalyst of crop yields and provides agricultural sustainability. The spectrum of agricultural advancements involves genetically modified varieties, bio-based pesticides, environmentally friendly biofertilizers, cell selection and marker-assisted selection technologies, etc. Their development and scaling are fundamental to maintaining Russia's domestic and international competitiveness.

Digital information platforms transform the agro-industrial complex by optimizing all stages of agricultural production. An AI digital platform for the agro-industry and fisheries is slated for completion in Russia by the end of 2026 by order of the Chairman of the Government. By integrating federal information systems, the platform will provide a service-based management model for the entire agro-industrial complex. Its main objective is to disseminate the agricultural knowledge through academic programs, scientific achievements, and practical innovations.

This strategic initiative has earned universal acclaim within the Russian scientific community, notably from Professor Viktor A. Panfilov, Doctor of Engineering Sciences, Academician of the Russian Academy of Sciences, Honored Scientist of the Russian Federation. In his extensive research, Professor Panfilov promotes the idea of a radical technological breakthrough to secure the future of Russia's agro-industrial complex. According to Professor Panfilov, the dialectical development of innovative technologies will facilitate the historic transition to the Sixth Technological Paradigm.

Professor Panfilov has made distinguished contributions to crop processing, food technology, and food production engineering. His contributions to highly efficient processing systems are pivotal to the domestic food subcomplex and, hence, to national food security.

Professor Panfilov pioneered the scientific field of Systemology of Food and Processing Industries. He developed a comprehensive theory of process flow rooted in technological integrity, system analysis and synthesis, process flow models, quantitative assessment of technology, and production line diagnostics. He spearheaded the System of Scientific and Engineering Support for the Food and Processing Industries of the Russian Agro-Industrial Complex.

We congratulate Professor Viktor A. Panfilov on his 85th birthday, celebrated on February 7, 2026! We sincerely wish him robust health, abundant energy, and continued inspiration for new ideas and achievements in the company of his loved ones, colleagues, and the many students he has mentored.

Editor-in-Chief,
Academician of the Russian Academy of Sciences,
Honored Worker of Higher Education of the Russian Federation,
Laureate of the Russian Federation Government Prize in Science and Technology,
Professor A. Yu. Prosekov



Copyright © 2026, Prosekov. This is an open access article distributed under the terms of the Creative Commons Attribution 4.0 International License (https://creativecommons.org/licenses/by/4.0/), allowing third parties to copy and redistribute the material in any medium or format and to remix, transform, and build upon the material for any purpose, even commercially, provided the original work is properly cited and states its license.

Foods and Raw Materials. 2026;14(1)

ISSN 2308-4057 (Print)
ISSN 2310-9599 (Online)

Review Article
Open Access

Available online at http://jfrm.ru/en
https://doi.org/10.21603/2308-4057-2026-1-653
https://elibrary.ru/UMGKPZ

Biological value of berry polyphenols and prospects for supercritical extraction application for their isolation: A review

Elena V. Guseva*, Natalya Yu. Khromova, Boris A. Karetkin, Artem I. Artemiev, Kirill M. Demkin, Julia M. Puzankova, Irina V. Shakir, Victor I. Panfilov

Dmitry Mendeleev University of Chemical Technology of Russia, Moscow, Russia

* e-mail: guseva.e.v@muctr.ru

Received 10.07.2024; Revised 26.08.2024; Accepted 03.09.2024; Published online 25.12.2024

Abstract:
Plant polyphenols are known for their numerous health-promoting properties. This article reviews the current state of research in two related fields, namely beneficial effects of flavonoids for human health, e.g., gut microbiome, and supercritical fluid extraction applied to flavonoids of plant origin. The review covered research articles registered in eLIBRARY.RU, PubMed, and Science Direct in 2005–2025. Polyphenolic compounds obtained from various berries were reported to have a positive impact on gut microbiota, e.g., they stimulated the growth of lactobacilli, bifidobacteria, and other beneficial microorganisms, as well as improved the adhesion of probiotic and pathogenic microbes to intestinal epithelial cells.
The review revealed some promising application areas for berry extracts in the functional food industry. Polyphenols can be part of meat formulations due to their strong antioxidant activity. Their antimicrobial effect against a wide range of contaminants renders them good prospects in protecting food products from microbial spoilage. Supercritical extraction is a promising method that isolates biologically active substances from plant materials. The review summarizes its advantages and limitations, as well as the range of prospective co-solvents.
Ultrasonication, pulse electric field, and enzymic pretreatment make supercritical extraction more efficient. In general, this extraction method proved to be an excellent means of isolating flavonoids and related compounds from various plants and their parts.

Keyworlds: Plant materials, flavonoids, prebiotics, biological activity, intestinal microbiota, extraction, green technologies, supercritical fluid

Funding: The research was supported by the Russian Science Foundation, grant no. 24-19-00298, https://rscf.ru/project/24-19-00298/

Please cite this article in press as: Guseva EV, Khromova NYu, Karetkin BA, Artemiev AI, Demkin KM, Puzankova JM, *et al.* Biological value of berry polyphenols and prospects for supercritical extraction application for their isolation: A review. Foods and Raw Materials. 2026;14(1):1–13. https://doi.org/10.21603/2308-4057-2026-1-653

INTRODUCTION

Biologically active substances of plant origin, e.g., polyphenolic compounds and flavonoids, are known for a number of beneficial effects on human health. That is why the effect of flavonoids on gut microbiota has attracted much scientific attention in the last decade [1]. According to The International Scientific Association for Probiotics and Prebiotics (2017), prebiotics include not only carbohydrates, but also polyphenols, and all of them can be used as food components to improve gut microbiome [2]. Flavonoids are abundant in fruits. Russia boasts a wide diversity of wild and cultivated berries, which are part of many food products. Yet, their nutraceutical value seems to attract few domestic scientists [3, 4] although this area possesses an obvious research potential, especially in the sphere of public health.

The list of extractants that isolate biologically active compounds from plant materials includes alcohol, aqueous and alcoholic solutions, ethers, or carbon dioxide (CO_2). Each solvent has its advantages and disadvantages [5]. Currently, the food and pharmaceutical industries are trying to avoid organic and toxic solvents. The diffusion rate through the diffusive boundary layer

Copyright © 2024, Guseva *et al.* This is an open access article distributed under the terms of the Creative Commons Attribution 4.0 International License (https://creativecommons.org/licenses/by/4.0/), allowing third parties to copy and redistribute the material in any medium or format and to remix, transform, and build upon the material for any purpose, even commercially, provided the original work is properly cited and states its license.

between the plant material and the solvent is the most important extraction factor. The extraction yield depends on the efficiency of the extraction method. Inactive and inert solvents preserve the nutraceutical properties of the target plant components. They make it possible to skip some labor-intensive and energy-consuming production stages. Supercritical fluid extraction (SCFE) is a fast-developing method in Russia, China, and the USA. Supercritical fluids have been employed to isolate natural components since the late 1970s. Initially, their use was rare. Today, supercritical fluid technologies and equipment are a promising research direction [6].

This article reviews publications that describe the beneficial properties of flavonoids on gut microbiota and the method of supercritical fluid extraction applied to isolate flavonoids from plant materials.

STUDY OBJECTS AND METHODS

The review covered scientific publications registered in the Russian Research Citation Index (eLIBRARY.RU), PubMed, and Science Direct in 2005–2024. The articles under analysis featured flavonoids, their beneficial properties, and action mechanisms, as well as the method of supercritical extraction of polyphenols as biologically active compounds. The keyword list included *flavonoids*, *microbiota*, *supercritical fluid extraction*, and *plant materials*.

RESULTS AND DISCUSSION

Berry extracts in the food industry and medicine. Fruits and berries are a reliable source of bioactive extracts, and their biological properties are a popular research subject. Polyphenolic compounds of berry extracts are antioxidants with strong anti-inflammatory, anticancer, and neuroprotective effects. They are able to modulate gut microbiota, which has been confirmed both *in vitro* and *in vivo*. Berries owe their nutraceutical value to their phytochemical composition, represented by a wide variety of phenols, e.g., phenolic acids (derivatives of cinnamic and benzoic acids), flavonoids (anthocyanins, flavanols, and flavonols), tannins, stilbenes, etc. [7]. The growing scientific interest stimulates the market of functional foods and supplements, where berry extracts serve as biologically active ingredients [8]. This fact, in turn, encourages researchers to explore new applications of berry extracts that can improve the quality of human life. This section reviews relevant scientific data on the prospects of berry extracts in medicine and food.

Berry polyphenolic compounds in medicine. Polyphenolic compounds exert a positive effect on human health by interacting with gut microbiome. The colon microbiome is a complex ecosystem of diverse bacteria that controls the metabolism of chemical compounds that are consumed with food [9]. Unfortunately, most polyphenolic compounds, depending on their chemical composition and polymerization, demonstrate poor bioavailability in the digestive tract as a result of poor absorption and rapid excretion, which means they fail to reach the bloodstream in their natural form [10]. They need hydrolysis by either intestinal enzymes or intestinal microbiota to transform polyphenols into bioactive molecules that would be absorbed and transported to the target organ [11]. Many studies assess the prebiotic effect of polyphenolic compounds and how they affect probiotics.

Prebiotic effect of polyphenolic compounds in berry extracts on gut microbiota. Food polyphenols interact bidirectionally with the intestinal microbiota, stimulating beneficial bacteria or inhibiting potential pathogens. This phenomenon is called a selective prebiotic effect. Such representatives of beneficial microbiota as *Lactobacillus* spp. and *Bifidobacterium* spp. produce more short-chain fatty acids, e.g., butyric acid, when affected by polyphenols, especially catechins, anthocyanins, and proanthocyanidins [12].

Pan *et al.* [13] modeled healthy fecal culture fermentation *in vitro* to study the effect of flavonoids on structure and metabolism of the intestinal microbiota. They tested hesperidin, hesperetin 7-O-glucoside, naringin, prunin, rutin, isoquercitrin, and quercetin. Hesperetin 7-O-glucoside, prunin, and isoquercitrin had the greatest effect on the structure of the human intestinal microbiota at a concentration of 4 mg/mL, increasing the count of *Bifidobacterium*, *Lactobacillus*, and *Prevotella* after 24 h of simulated fermentation *in vitro.*

Perz *et al.* [14] studied the effect of flavonoids on the growth kinetics and count of pathogenic and probiotic microorganisms. Chalcones, flavans, and flavones substituted with -Br, -Cl, $-CH_3$, and $-NO_2$ inhibited or suppressed the growth of pathogenic bacteria without affecting health-beneficial probiotics. In the same research, 6-methyl-8-nitroflavone and 8-bromo-6-chloroflavone showed a positive modulation of gut microbiome in *in-vitro* digestion, raising the count of beneficial bacteria and reducing the count of potential pathogens.

Meng *et al.* [15] studied the metabolism of quercitrin in the colon and its effect on the colon microbiota in mice *in vivo.* Quercitrin changed the beta-diversity of gut microbiome, affecting such probiotics as *Akkermansia* and *Lactococcus*. In addition, it boosted the development of such short-chain fatty acids as propanoate, isovalerate, and hexanoate.

Multicomponent formulations of berry extracts had a positive effect on gut microbiome by increasing in the probiotic bacterial count. Attri *et al.* [16] studied *in vitro* the sustainability of sea-buckthorn polyphenols during digestion and their effect on colon microbiome. Fecal microbiota simulated digestion and fermentation by increasing the content of polyphenols and improving their antioxidant properties.

Sea-buckthorn juice increased the diversity of *Bacteroides*, *Prevotella*, *Lactobacteria*, and *Bifidobacteria*, which indicated a potential positive effect on colon microbiota. Molan *et al.* [17] reported prebiotic beneficial effects of aqueous bilberry extracts with pure and mixed human fecal cultures *in vitro.* Blueberry extracts stimulated the growth of pure *Lactobacillus rhamnosus* and

Bifidobacterium breve. A mixed fecal culture batch fermentation system demonstrated similar results. When administered daily to rats *per os*, bilberry extracts increased the population of lactobacilli and bifidobacteria.

Berry extracts proved effective as prebiotic supplements that restore the gut microbiota in various metabolic disorders. Lee *et al*. [18] studied the effect of blueberry extracts on microbiome, systemic inflammation, and insulin resistance in rats that received a high-fat diet. Blueberry increased the count of *Gammaproteobacteria*, decreased the villus length in the ileum, and improved the insulin sensitivity.

Li and Ming [19] described the effect of mulberry polyphenols on small and large intestinal microbiota during type 2 diabetes. Mulberry polyphenols improved the diversity of microbiota in both compartments. The small intestinal microbiota was found to affect the blood glucose balance. Mulberry polyphenols improved the pathophysiology of type 2 diabetes.

Polyphenolic compounds have a great potential as prebiotic supplements or synbiotic compositions that modulate or restore intestinal microbiota affected by chronic diseases or metabolic disorders.

Effect of polyphenolic compounds on probiotic activity: other mechanisms. Plant polyphenols promote probiotic adhesion. Yuan *et al*. [20] studied cell surface hydrophobicity and autoaggregation. Resveratrol enhanced the adhesion of *Lactobacillus acidophilus* NCFM to mucin (1.73 times), epicatechin (1.47 times), caffeic acid (1.30 times), and hesperidin (0.99 times). Quercetin demonstrated a certain degree of inhibition (0.84 times). According to a proteomic analysis, resveratrol altered proteins on the surface of *L. acidophilus* NCFM, as well as promoted the expression of mucin genes and glycosylation of mucins on the surface of HT-29 cells. Similar results were reported for resveratrol and ferulic acid [21].

Dietary flavan-3-ols altered the intestinal microecology by enhancing or inhibiting the adhesion of lactobacilli strains to intestinal cells. Flavan-3-ols inhibited the adhesion of *L. acidophilus* LA-5 and *Lactobacillus plantarum* IFPL379. Pigallocatechin gallate, on the contrary, enhanced the adhesion of *L. acidophilus* LA-5 to Caco-2. Procyanidins B1 and B2 improved the adhesion of *L. casei* LC115 to HT-29 cells, while epigallocatechin increased the adhesion of *L. casei* LC115 to Caco-2 [22].

Polyphenol-containing plant extracts and probiotics demonstrate a certain synergism. When combined with a probiotic, anthocyanin-rich blueberry extract reduced the count of adherent viable pathogenic cells on a mucin/BSA-treated surface more efficiently than in the sample where the probiotic was alone [23]. When combined with *Bifidobacterium animalis* Bo, blueberry extract was able to inhibit pathogen adhesion completely.

Polyphenolic compounds of berries in the food industry. ***Berry extracts as natural antioxidants in meat products.*** Berry extracts with polyphenolic compounds have good prospects as natural food preservatives because synthetic alternatives may be toxic. Berry extracts prevented the oxidation of lipids, proteins, and pigments in meat and meat products [24]. Grape seed and bearberry extracts reduced lipid oxidation during storage in pork chops while maintaining their sensory properties after cooking [25]. Blueberry extract increased the oxidative stability and antioxidant activity of a pork roll during storage at 8°C [26]. Blackcurrant extract (*Ribes nigrum* L.) in raw pork chops developed carbonyls and reduced the amount of substances that reacted with thiobarbituric acid during refrigerated storage. In addition, pork chops maintained the sulfhydryl level in a dose-dependent manner, indicating a significant inhibition of lipid and protein oxidation. [27]

Freeze-dried cranberries (*Vaccinium oxycoccus* L.) in nitrite-free fermented sausages with venison and pork fat reduced oxidative changes during storage [28]. Strawberry extracts (*Arbutus unedo* L.) proved more effective than rosehip (*Rosa canina* L.) in reducing lipid oxidation in sausages during refrigerated storage [29]. Chokeberry (*Aronia melanocarpa* L.) extract reduced oxidation processes in cooked ham or raw pork burgers [30].

Berry extracts demonstrated enough antioxidant activity for meat preservation as a prospective alternative to synthetic preservatives.

Berry extracts as antimicrobial agents against foodborne pathogens. Some berries have polyphenolic compounds that can disrupt the membrane of Gram-negative bacteria and reduce their viability [31]. Such berries are promising antimicrobial additives that protect foods from foodborne bacteria. Cranberry extracts demonstrated a dose-dependent antimicrobial activity against *Salmonella*, *Escherichia coli*, and *C. perfringens*, as well as *Staphylococcus*, *Listeria*, *Helicobacter*, *Bacillus*, and *Campylobacter* [31]. Cranberry extracts were more antimicrobial than those of blueberry, raspberry, and strawberry [32].

The antimicrobial profile of berry extracts may vary for one and the same species depending on where the berries grew. Georgescu *et al*. [33] studied antimicrobial activities of eight berry extracts (blueberry, blackcurrant, gooseberry, redcurrant, raspberry, sea buckthorn, strawberry, and cherry) collected simultaneously in Romania and Russia. The research featured seven pathogenic microorganisms, i.e., *Bacillus subtilis*, *Bacillus cereus*, *Staphylococcus aureus*, *E. coli*, *Salmonella typhi*, *Candida albicans*, and *Aspergillus niger*. Most of them showed resistance or intermediate activity against berry extracts from both countries. Raspberry and strawberry extracts had very low or no activity against Gram-positive pathogenic bacteria. Strawberry extract did not affect Gram-negative strains, while raspberry extract demonstrated zero or very low antifungal effect. *E. coli* proved to be the most berry-sensitive microorganism, especially to cherry extract, followed by sea buckthorn and blackcurrant. *S. typhi* proved to be the most berry-resistant microorganism. However, most Romanian berries showed higher antimicrobial efficacy against *B. subtilis*, *B. cereus*, *S. aureus*, *S. typhi*, and *C. albicans*, while Russian berries were more effective against *E. coli* and *A. niger*.

Polyphenolic compounds of berry origin as part of animal feed can affect the microbiological profile of products made from the meat of farm animals. For example, when pigs were fed an additive with cranberry pulp, lactic acid bacteria became the predominant microflora in meat stored under anaerobic conditions. It inhibited the growth of pathogenic bacteria [34]. A goji dietary supplement in the diet of rabbits improved the oxidative stability and increased the content of phenols in the meat [35]. Goji berries did not affect the hygienic profile of rabbit meat but boosted the growth of *Lactobacillus* spp., thus improving the sensory profile [36].

Berry extracts as antimicrobial additives are a good natural alternative to antibiotics. They satisfy the needs of consumers for high-quality and safe products, as well as allow producers to minimize the use of antibiotics in animal feed.

Berry extracts in functional foods. Fruit and berry juices are part of many fermented beverages, the most popular raw materials being pomegranate, mulberry, cherry, blueberry, blackberry, and goji. They act as a carrier matrix for probiotics [37]. Black goji juice (*Lycium ruthenicum* Murr.) developed more phenolic acids, gallic or chlorogenic, as well as flavonoids, amino acids, and dipeptides, when it was used to ferment *Lactobacillus rhamnosus* GG. Black goji juice also increased the production of lactic acid and the viability of probiotics during 24 h of fermentation [38].

When fermented with *L. plantarum*, sea-buckthorn (*Hippophae rhamnoides* L., subsp. *carpatica*) juice was used as a food matrix and caused a significant increase in phenols and flavonoids with a lactobacillus count of 8.5 log CFU/mL [39]. Markkinen *et al.* [40], who studied chokeberry, sea-buckthorn, and lingonberry juices fermented with *L. plantarum* and *Oenococcus oeni*, obtained different results. In their case, fermentation of chokeberry juice with DSM 10492 strain reduced the content of flavonols by 9–14% and hydroxycinnamic acids by 20–24%. The content of flavonol glycosides and sugar in sea buckthorn remained unchanged, as did the content of anthocyanins in chokeberry.

The phenolic profile of mulberry juice demonstrated an increase in the total concentration of anthocyanins, phenols, and flavonoids, when fermented with *L. plantarum*, *Lactobacillus acidophilus*, and *Lactobacillus paracasei*. The best result belonged to *L. plantarum* [41].

Therefore, fermentation with lactic acid bacteria in non-dairy functional drinks increases the bioavailability of polyphenolic compounds. The synergistic action of probiotics and prebiotics have a beneficial potential for consumers' health.

Polyphenolic compounds from plant extracts: other applications. Flavonoids with two aromatic rings linked by C-C bonds and a 3-C-oxygenated heterocycle are the most diverse group of berry polyphenols [42]. Flavonoids (pure, in plant extracts, or combined with probiotics) can be used in agriculture.

In aquaculture, the freshwater dark sleeper (*Odontobutis potamophila* Günther, 1861) improved its gut flora and increased the species range of probiotics *Bacillus* spp. and *Lactobacillus* spp. after exposure to 2.5 mg/L of quercetin. However, 5 and 10 mg/L of quercetin inhibited the growth of *Lactobacillus* spp. [43].

In cattle farming, natural plant extracts with flavonoids and probiotics proved to be a promising alternative to antibiotics. Weaned piglets that received flavonoids from Tartary buckwheat (*Fagopyrum tataricum* (L.) Gaertn.) supplements improved their average daily gain, immune capacity, and the antioxidant activity of *L. plantarum*. A combination of flavonoids from Tartary buckwheat and probiotics promoted nutrient digestibility [44].

In poultry farming, flavonoids from hawthorn-leaf in the diet of breeding hens affected the microbiota that the hens transmitted to chickens. The probiotic count in meconium increased, as did the average daily gain, while the feed conversion ratio of chickens went down [45].

Modern methods and trends in plant material extraction. ***Types of extraction.*** Plant materials are an important source of biologically active substances, e.g., polyphenolic compounds. When extracted, they are expected to maintain their initial integrity and biological activity. The content of valuable components in extracts varies greatly.

Polyphenolic compounds, such as flavonoids, are extracted with water vapor (lipid fraction), water, oil, glycerol, or organic solvents. Other methods include subcritical carbon dioxide extraction, supercritical extraction (desorption), and various combined techniques [46, 47].

Extraction is a popular method to obtain biologically active compounds. Table 1 summarizes the existing methods for extracting target components from plant materials with brief technological descriptions [48].

The extraction process should meet the following requirements: it is fast, simple, and cheap; the extract is rich in the target component; the target substance is yielded in a quantity sufficient enough to allow for final measurements to be conducted without additional concentration, and the waste is small and recyclable.

For many years, targeted extraction from oil have relied on hydrocarbon or chlorinated organic solvents in a Soxhlet extractor. Unfortunately, liquid extraction often fails to meet some important criteria. It takes several hours to obtain a satisfactory amount of the active component. Most organic solvents are expensive, and the resulting extracts are low in the target substance. As a result, the method needs additional concentration. However, some part of the target substance may decompose or get lost during this stage. Moreover, concentration often causes air-pollution [49].

Waters Corporation (USA) is a large manufacturer of supercritical extractors [50]. The Waters Prep Supercritical Fluid Extraction system (Fig. 1) makes it possible to substitute organic solvents with a supercritical CO_2 atmosphere. Waters Corporation systems extract and fractionate food fats and oils, allow obtaining biologically active substances from such plants as St. John's wort, ginger, garlic, or ginseng, as well as purify medicinal herbs and foods from pesticides and herbicides, etc.

Table 1 Extracting biologically active substances from plant materials: technical characteristics [48]

Extraction methods	Solvent	Temperature	Pressure	Time	Chances for organic solvent use	Polarity of target components
Maceration	Water and organic solvents	Room (295.2 K)	Atmospheric	Long	High	Depends on the extracting solvent
Soxhlet extractor	Organic solvents	Heating	Atmospheric	Long	Moderate	Depends on the extracting solvent
Hydrodistillation	Water	Heating	Atmospheric	Long	Moderate	Non-polar or moderately polar compounds
Pressurized liquid extraction	Aqueous and non-aqueous solvents	Heating	High	Short	Low	Depends on the extracting solvent
Subcritical water extraction	Water	Heating	High	Short	Low	Polar and moderately polar compounds
Supercritical fluid extraction	Supercritical fluid (CO_2), sometimes with organic co-solvents	Heating	High	Very short	No or low	Non-polar or moderately polar compounds
Ultrasonic extraction	Water and organic solvents	Room/heating	Atmospheric	Short or moderate	Low or moderate	Depends on the extracting solvent
Microwave extraction	Water and organic solvents	Room/heating	Atmospheric	Short	Low	Depends on the extracting solvent



Figure 1 Waters prep supercritical fluid extraction system (Waters Corporation, USA)



Figure 2 STS 316 supercritical fluid extraction system (Rexo Engineering, South Korea)

Rexo Engineering (South Korea) is a major supplier of supercritical extraction equipment [51]. Figure 2 shows its set for supercritical fluid extraction. The system consists of a cryostat circulator that cools CO_2, a pump that feeds it, an extractor with a tank for raw materials (0.5–20 L), a heated backpressure regulator, and a separator. The process is carried out at 40 MPa and 250°C, with an extractant flow rate of 100 mL/min. An STS 316 extractor is made of material that is inert to the solvent and the plant raw materials.

During supercritical fluid extraction, the solvent is in the supercritical state and is subjected to severe compression. The resulting supercritical fluid acquires the properties of both gas and liquid. It has the same diffusion rate, low viscosity, and compressibility as gas, and the same high density and dissolving capacity as liquid. The supercritical fluid can easily penetrate into small-diameter pores in the deep layers of the extracted material, where it dissolves and extracts the target components with the rapid mass transfer, which other solvents cannot provide. As the pressure increases, so does the supercritical fluid density, which makes the components more soluble. When the pressure is removed, the rapid expansion of supercritical solutions leads to the precipitation of finely dispersed solid particles. All flow reactors rely on this phenomenon. Unlike conventional solvents, supercritical fluids can dissolve gases, e.g., hydrogen and nitrogen, thus providing a rapid and pure hydrogenation.

A result, supercritical fluid extraction has become a popular method that targets specific components in various types of raw materials, including plants [52].

Supercritical solvents in obtaining biologically active components. To be used as an extractant for biologically active substances, a supercritical fluid is expected meet the following requirements [53]: the extract obtained has no unwanted smells or harmful

components; the extractant is highly selective and possesses a good dissolving capacity; the extractant is chemically inert to the target components and the equipment; the extractant is safe, non-flammable, and inexplosive; the extractant is cheap, harmless, and available, and the extractant is colorless and non-hydrophobic.

The list of efficient solvents includes CO_2, water, ethane, methane, etc. In the supercritical state, all liquids mix with each other; beyond the critical point, the mix becomes a single phase.

Table 2 presents the critical values of density, temperature, and pressure, at which solvents enter the supercritical state [54].

CO_2 is the most popular supercritical fluid due to its non-flammability and low critical parameters (304.15 K, 7.4 MPa). Unfortunately, its polarity in a supercritical state is quite low. However, polar modifiers assed as co-solvents can change the polarity of the supercritical fluid and increase its solvating ability with respect to target components [55].

High-pressure extractors: modernization and intensification. A supercritical extractor that relies on CO_2 must contain the following units: a cylinder to store CO_2, a condenser to cool CO_2, a high-pressure pump, a tank for preheating CO_2, a high-pressure reactor, and a separator to collect the extract (Fig. 3) [56].

From a cylinder (1), CO_2 goes to a condenser (2), where it cools down and converts to liquid. Then, the liquid CO_2 is pumped by a high-pressure pump (4) into a thermostat (5), where it is heated to a temperature that exceeds the temperature of transition to the supercritical state. Then, the supercritical CO_2 enters a high-pressure extractor (6) loaded with plant raw materials. Penetrating the raw materials, the supercritical CO_2 dissolves the extracted substances. The supercritical mix flows from the high-pressure extractor through a fine adjustment valve (7) into an extract collector (8), where the extracted substances are condensed while the CO_2 turns back to gas. It can be discharged into the atmosphere or liquified for another extraction.

Supercritical CO_2 extraction is one of the most attractive methods for extracting biologically active substances from plant materials. Its main advantage is that it can extract heat-labile substances that are important for pharmacy, including polyphenolic compounds [57, 58]. A lot of attempts have been made to modify the existing methods of supercritical CO_2 extraction in order to increase the yield of target components [58, 59].

Co-solvent. A polar co-solvent facilitates the process of CO_2 extraction of polyphenolic compounds from plant materials. A small amount of co-solvent improves the properties of non-polar supercritical CO_2, as well as increases the rate of mass transfer and the solubility of polar compounds [60]. Ethanol, methanol, water, or their mixes facilitate the extraction of highly polar phenolic phytocompounds [61]. The amount of quercetin was

Table 2 Critical parameters of solvents used as supercritical extractants [54]

Solvent	Chemical formula	Critical density, g/cm^3	Critical temperature, K	Critical pressure, MPa
Water	H_2O	0.32	647.30	22.10
CO_2	CO_2	0.47	304.15	7.39
Methane	CH_4	0.16	191.05	4.64
Ethane	C_2H_6	0.20	305.45	4.88
Propane	C_3H_8	0.22	369.95	4.26
Propylene	C_3H_6	0.23	364.90	4.60
Methanol	CH_3OH	0.27	512.60	8.09
Ethanol	C_2H_5OH	0.28	513.90	6.14

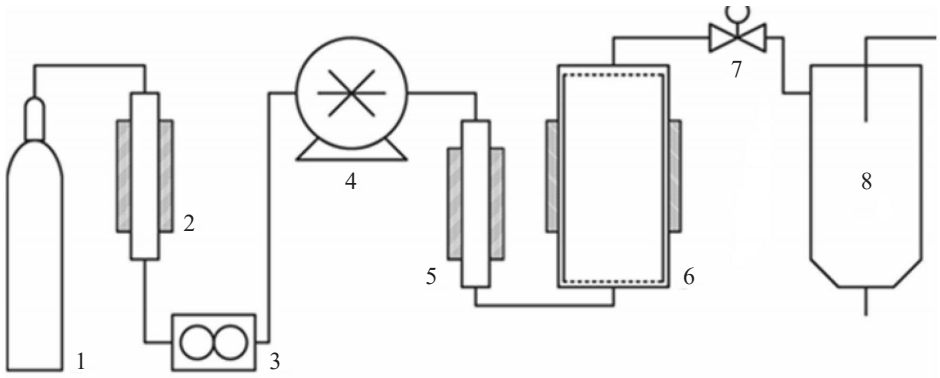

Figure 3 A supercritical extractor: CO_2 cylinder (1), refrigerator (2), flow meter (3), high-pressure pump (4), heater (5), extraction vessel in a heating jacket (6), automatic pressure regulator (7), polymer cyclone separator (8) [49]

reported to increase together with the ethanol content in supercritical CO_2 [62]. When extracted with pure CO_2, the quercetin content in the extract was 64 μg/100 g; when extracted with 7.36 mass.% ethanol, it was 2402 μg/100 g. However, this intensification method requires an additional step to remove the co-solvent from the extract, which should be taken into account when calibrating the amount of the co-solvent.

Temperature and pressure. Temperature and pressure affect such properties of supercritical fluids as density, viscosity, diffusion coefficient, and, eventually, their solvation capacity [63]. As the pressure increases, so does the density of the extractant and the solubility of the extracted substances. However, after a certain point, an increase in pressure can reduce the diffusion capacity of the supercritical extractant, thereby reducing the amount of the extract dissolved. For instance, when the pressure exceeded 200 atm, the extract yield went down, following a decrease in the diffusion coefficient [64].

The correlation between the extract yield and the temperature is more complex. On the one hand, a temperature increase raises the diffusion coefficient and improves the extraction yield. On the other hand, as the temperature falls down, the vapor pressure of the dissolved substances decreases while the extractant gains more density, which, in turn, increases the dissolving capacity. This chain leads to the phenomenon called crossover pressure. Below the crossover pressure, higher temperatures reduce the extract yield. Above the crossover pressure, higher temperatures increase the extract yield. For instance, the amount of eugenol extracted from *Ocimum sanctum* Linn. went down as the temperature increased at lower pressures. When the pressure exceeded 200 bar, an increase in temperature led to an increase in the eugenol yield [65].

Extractant flow rate. Solvent flow rate also exerts a significant effect on supercritical extraction. An increase in the CO_2 flow rate increased the extract yield as the extractant flow in the high-pressure reactor became turbulent. The driving force grew because dissolved substances were carried away faster than before. This phenomenon reduced the resistance to external mass transfer and increased the extract yield [66]. However, upon reaching a certain flow rate, further growth of the solvent flow does not affect the extract yield. On the contrary, the yield may decrease because the plant material grows more compact in the extractor [67, 68].

Ultrasound radiation. A particular mechanical action on plant raw materials may also increase the extract yield. Ultrasound intensifies the process of supercritical extraction. This phenomenon can be explained by mechanical, cavitation, and thermal effects: they destroy cell membranes, reduce the particle size, and increase the mass transfer through membranes. The collapse of cavitation bubbles generates microturbulence and high-speed interparticle collisions, which accelerates diffusion of the extracted substance [69]. The cavitation on the surface of the source material causes a collision of microflows, thus eroding or destroying the particles [70]. Ultrasound processing made it possible to increase the yield of flavonoids by 19% [71].

Pulse electric field. Electric field affects cell membranes through the phenomenon known as electroporation [72]. Electrodes produce high-voltage electric pulses for several seconds, and the charge of the cytoplasmic membrane increases. Upon reaching the threshold of transmembrane potential, small pores appear: it is through them that the target component exits the cell. This intensification method is efficient both during raw material processing and during extraction. The electric field method was reported to increase the yield of polyphenolic compounds from grape skins [72] and almond husks [73].

Enzymes. Enzymes also increase the yield of target components during supercritical CO_2 extraction. They destroy cell membranes in plant materials, thus improving the access of supercritical CO_2 to bioactive substances and increasing their extraction [74]. Enzymes break the bonds between non-extractable polyphenols and macromolecules of lignin or cellulose, converting them into more extractable forms. This approach is suitable for a bigger range of compounds and improves the quality of the extract. For example, tea waste treated with enzymes allowed for a five-fold higher extract yield [75].

Extracting biologically active substances from plant raw materials using supercritical extraction. Supercritical extraction is a popular method of extracting biologically active substances. Tomatoes extracted after a preliminary enzymatic treatment demonstrated a better solubility in supercritical CO_2 [76]. Cranberry (*Viburnum opulus* L.) contains such beneficial substances as chlorogenic and quinic acids. Kraujalis *et al*. [77] effectively extracted cranberries in a 50-mL Helix extractor between two layers of cotton wool. The obtained extract contained oleic and linoleic acids, as well as a wide range of tocopherols.

Tangerine peel proved to be a promising secondary raw material for obtaining flavonoids by supercritical extraction [78]. Kueh *et al*. [79] obtained essential oils, sesquiterpenes, and phenols from the leaves of *Melaleuca pentavesica*. A good yield of terpenoids and tocopherols was registered in *Thymus munbyanus* Boiss. & Reut. extracts [80].

Additional co-solvents may increase the yield of target components. Bayrak *et al*. [81] used methanol as a co-solvent to obtain extracts from *Colchicum* species. The yield of colchicine increased, and the process became more selective. Ethanol is another popular co-solvent. Ethyl alcohol added to the CO_2 flow affected the yield of triterpene saponins (ginsenosides) [82].

Mora *et al*. [83] considered the extraction of flavonoids and coumarins from industrial fruit peel waste. Atwi-Ghaddar *et al*. [84] extracted dihydrorobinetin and robinetin from *Robinia pseudoacacia* L. for their antimicrobial and antioxidant properties. Quercetin, kaempferol, and catechin were extracted from the flowers of medicinal *Dendrobium* plants [85]. The extracts demonstrated antitumor, hypoglycemic, anti-inflammatory, and

Table 3 Obtaining plant extracts using various extraction methods [76–89]

Plant raw material	Bioactive substances	Extractant	Temperature, K (Pressure, MPa)	Reference
Tomatoes	Lycopene	CO_2	359.2 (50)	[76]
Cranberries	Oleic acid, linoleic acid, tocopherols	CO_2	323.2 (57)	[77]
Tangerine peels	Flavonoids	CO_2	303.2 (3)	[78]
Melaleuca pentavecchia	Sesquiterpenes and phenols	CO_2	316.2 (25)	[79]
Thymus munbyanus	Phenolic compounds	CO_2	343.2 (450)	[80]
Colchicum	Colchicine	CO_2 + 3% methanol	308.2 (24.7)	[81]
Ginseng	Triterpene saponins	CO_2 + 6% ethanol	343.2 (20)	[82]
Citrus peels	Flavonoids, coumarins	80% CO_2, 20% ethanol	333 (30)	[83]
Robinia pseudoacacia	Flavonoids, phenolic compounds	80% CO_2, 20% ethanol	353 (10)	[84]
Dendrobium	Flavonoids	40% CO_2, 60% ethanol	323 (20)	[85]
Pueraria lobata	Flavonoids	CO_2, ethanol	323.54 (20.04)	[86]
Odentema	Flavonoids	85% CO_2, 15% ethanol	238.2 (20)	[87]
Ziziphus jujuba	Flavonoids	85% CO_2, 15% ethanol	324.7 (27.12)	[88]
Costus spicatus	Linoleic acid, flavonoids, phenols	90% CO_2, 10% ethanol	323.2 (14)	[89]

antibacterial potentials. The total yield of flavonoids was three times as high as in the extract obtained by ultrasonic circulating extraction.

Pueraria lobata Willd. is a source of five flavonoids, i.e., puerarin, daidzin, genistin, daidzein, and genistein. Its extracts are known for their anticancer, antigiardiasic, and antidiabetic properties. The supercritical extraction involved a Spe-ed SFE Basic laboratory extractor (250 mL, USA) [86].

Odentema leaves were reported to contain a complex of flavonoids, alkaloids, carbohydrates, glycosides, saponins, phytosterols, and tannins. The main target component was quercetin: its extracts help against hypertension and possess excellent antioxidant properties. The supercritical extraction involved an SFE 2 X 100 F extractor (USA) [87].

Ziziphus jujuba L. leaves were extracted in a high-pressure ASI Spe-ed SFE-2 extractor (USA). The extracts contained glycosides of kaempferol and quercetin, which are popular in the food industry due to their antioxidant, anti-inflammatory, antigenotoxic, and antiprotozoal activities [88].

Costus spicatus L. extracts were reported to possess analgesic, antioxidant, antimicrobial, antifungal, and nephroprotective properties. Its leaves and stems contained triterpenes, sterols, flavonoids, saponins, alkaloids, and tannins. A supercritical extraction with ultrasound pretreatment made it possible to rationalize the optimal technological variables with the maximal flavonoid extraction [89].

Table 3 provides data on supercritical extraction from various plant raw materials, including the most efficient extractants and the main technological variables, i.e., temperature and pressure.

Carefully selected parameters make it possible to control the flavonoid extraction from various types of plant raw materials. The method of supercritical extraction provides their complete extraction at low temperatures and requires small amounts of expensive co-solvents, such as ethanol. As a result, the method of supercritical extraction remains energetically and environmentally efficient.

CONCLUSION

Berries are rich in polyphenolic compounds and flavonoids. They boost the growth and metabolism of beneficial intestinal microorganisms while suppressing potential pathogens, which classifies them as prebiotics. In addition, they can stimulate the adhesion of probiotic microorganisms to intestinal epithelial cells. Polyphenols give berry extracts their strong antioxidant properties, which makes it possible to use them as natural ingredients in meat products. The ability to inhibit microbial contaminants in food makes them efficient biopreservatives.

New technologies yield more valuable bioactive substances than traditional extraction methods. Supercritical fluids are a promising alternative to such expensive solvents as hexane or dichloromethane. Carbon dioxide used as an extractant in supercritical extraction requires no additional stages and is environmentally neutral. In addition, the method of supercritical fluid extraction was approved by the Soil Association for organic foods.

Supercritical extraction is popular in Russia, China, the USA, and Brazil. Many research articles feature novel laboratory installations or extraction models with subsequent scaling to industrial volumes.

Process control makes it possible to vary the dissolving capacity of the extractant. The extraction efficiency depends on the selectivity: a highly-selective extractant makes it possible to obtain pure substances while maintaining their structural integrity. Flavonoids are diverse in structure. As a result, the extraction of target components from plant materials requires different conditions. The optimal parameters provide the maximal yield.

By varying the pressure, temperature, and quantity of the co-solvent in the extractant flow, producers optimize the extraction process, which is impossible in traditional methods.

CONTRIBUTION

N.Yu. Khromova, J.M. Puzankova, and I.V. Shakir wrote the first section about berry extracts in the food industry and medicine; E.V. Guseva, A.I. Artemiev, and K.M. Demkin wrote the second section about the method of supercritical extraction; B.A. Karetkin, and V.I. Panfilov reviewed and edited the original draft. All the authors proofread the final version.

CONFLICT OF INTEREST

The authors declare no conflict of interest.

REFERENCES

1. Fraga CG, Croft KD. Kennedy DO, Tomás-Barberán FA. The effects of polyphenols and other bioactives on human health. Food and Function. 2019;10:514–528. https://doi.org/10.1039/C8FO01997E
2. Gibson GR, Hutkins R, Sanders ME, Prescott SL, Reimer RA, Salminen SJ, *et al.* Expert consensus document: The International Scientific Association for Probiotics and Prebiotics (ISAPP) consensus statement on the definition and scope of prebiotics. Nature Reviews Gastroenterology and Hepatology. 2017;14:491–502. https://doi.org/10.1038/nrgastro.2017.75
3. Averyanova EV, Shkolnikova MN, Rozhnov ED, Batashov ES. Bioconversion of sea buckthorn meal into physiologically active ingredients. Khimija Rastitelnogo Syrja. 2023;(1):297–305. (In Russ.). https://doi.org/10.14258/jcprm.20230111884; https://elibrary.ru/YKDNFH
4. Razgonova MP, Senotrusova TA, Li NG, Timoschenko EE, Murzina OG, Rusakova EA, *et al.* Aspects of complex processing of far eastern berry crops. Siberian Herald of Agricultural Science. 2023;53(8):15–26. (In Russ.). https://doi.org/10.26898/0370-8799-2023-8-2; https://elibrary.ru/AYWAUO
5. Frolova AS, Fokina AD, Milentyeva IS, Asyakina LK, Proskuryakova LA, Prosekov AYu. The biological active Substances of *Taraxacum officinale* and *Arctium lappa* from the Siberian Federal District. International Journal of Molecular Sciences. 2024;25(6):3263. https://doi.org/10.3390/ijms25063263.
6. Zilfikarov IN, Chelombitko VA, Aliev AM. Medicinal plant materials processed with liquefied gases and supercritical fluids. Pyatigorsk. 2007. 244 p. (In Russ.).
7. Dumitrașcu L, Banu I, Patrașcu L, Vasilean I, Aprodu I. The Influence of Processing on the Bioactive Compounds of Small Berries. Applied Sciences. 2024;14(19):8713. https://doi.org/10.3390/app14198713
8. Nile SH, Park SW. Edible berries: bioactive components and their effect on human health. Nutrition. 2014;30(2):134–144. https://doi.org/10.1016/j.nut.2013.04.007
9. Duda-Chodak A, Tarko T, Satora P, Sroka P. Interaction of dietary compounds, especially polyphenols, with the intestinal microbiota: a review. European Journal of Nutrition. 2015;54:325–341. https://doi.org/10.1007/s00394-015-0852-y
10. Zhu B, Wang X, Li L. Human gut microbiome: the second genome of human body. Protein and Cell. 2010;1(8):718–725. https://doi.org/10.1007/s13238-010-0093-z
11. Lavefve L, Howard LR, Carbonero F. Berry polyphenols metabolism and impact on human gut microbiota and health. Food and Function. 2020;11:45–65. https://doi.org/10.1039/C9FO01634A
12. Plamada D, Vodnar DC. Polyphenols–Gut microbiota interrelationship: A transition to a new generation of prebiotics. Nutrients. 2021;14(1):137. https://doi.org/10.3390/nu14010137
13. Pan L, Ye H, Pi X, Liu W, Wang Z, Zhang Y, *et al.* Effects of several flavonoids on human gut microbiota and its metabolism by *in vitro* simulated fermentation. Frontiers in Microbiology. 2023;14:1092729. https://doi.org/10.3389/fmicb.2023.1092729
14. Perz M, Szymanowska D, Kostrzewa-Susłow E. The Influence of Flavonoids with -Br, -Cl Atoms and -NO_2, -CH_3 Groups on the Growth Kinetics and the Number of Pathogenic and Probiotic Microorganisms. International Journal of Molecular Sciences. 2024;25(17):9269. https://doi.org/10.3390/ijms25179269
15. Meng X, Xia C, Wu H, Gu Q, Li P. Metabolism of quercitrin in the colon and its beneficial regulatory effects on gut microbiota. Journal of the Science of Food and Agriculture. 2024;104(15):9255–9264. https://doi.org/10.1002/jsfa.13747
16. Attri S, Sharma K, Raigond P, Goel G. Colonic fermentation of polyphenolics from Sea buckthorn (*Hippophae rhamnoides*) berries: Assessment of effects on microbial diversity by Principal Component Analysis. Food Research International. 2018;105:324–332. https://doi.org/10.1016/j.foodres.2017.11.032
17. Molan AL, Lila MA, Mawson J, De S. In vitro and in vivo evaluation of the prebiotic activity of water-soluble blueberry extracts. World Journal of Microbiology and Biotechnology. 2009;25:1243–1249. https://doi.org/10.1007/s11274-009-0011-9

18. Lee S, Keirsey KI, Kirkland R, Grunewald ZI, Fischer JG, de La Serre C. B. Blueberry supplementation influences the gut microbiota, inflammation, and insulin resistance in high-fat-diet–fed rats. The Journal of Nutrition. 2018;148(2): 209–219. https://doi.org/10.1093/jn/nxx027

19. Li F, Ming J. Mulberry polyphenols restored both small and large intestinal microflora in *db/db* mice, potentially alleviating type 2 diabetes. Food and Function. 2024;15:8521–8543. https://doi.org/10.1039/D4FO01291G

20. Yuan Y, Zhang X, Pan S, Xu X, Wu T. Effects and Mechanisms of Resveratrol on the Adhesion of *Lactobacillus acidophilus* NCFM. Probiotics and Antimicrobial Proteins. 2023;15:1529–1538. https://doi.org/10.1007/s12602-022-10007-9

21. Celebioglu HU, Delsoglio M, Brix S, Pessione E, Svensson B. Plant Polyphenols Stimulate Adhesion to Intestinal Mucosa and Induce Proteome Changes in the Probiotic *Lactobacillus acidophilus* NCFM. Molecular Nutrition Food Research. 2018;62(4):1700638. https://doi.org/10.1002/mnfr.201700638

22. Bustos I, García-Cayuela T, Hernández-Ledesma B, Peláez C, Requena T, Martínez-Cuesta MC. Effect of flavan-3-ols on the adhesion of potential probiotic lactobacilli to intestinal cells. Journal of Agricultural and Food Chimistry. 2012;60(36):9082–9088. https://doi.org/10.1021/jf301133g

23. Silva S, Costa EM, Oliveira H, Freitas V, Morais RM, Calhau C, *et al*. Impact of a Purified Blueberry Extract on In Vitro Probiotic Mucin-Adhesion and Its Effect on Probiotic/Intestinal Pathogen Systems. Molecules. 2022;27(20):6991. https://doi.org/10.3390/molecules27206991

24. Lorenzo JM, Pateiro M, Domínguez R, Barba FJ, Putnik P, Kovačević DB, *et al.* Berries extracts as natural antioxidants in meat products: A review. Food Research International. 2018;106:1095–1104. https://doi.org/10.1016/j.foodres.2017.12.005

25. Carpenter R, O'Grady MN, O'Callaghan YC, O'Brien NM, Kerry JP. Evaluation of the antioxidant potential of grape seed and bearberry extracts in raw and cooked pork. Meat Science. 2007;76(4):604–610. https://doi.org/10.1016/j.meatsci.2007.01.021

26. Muzolf-Panek M, Waśkiewicz A, Kowalski R, Konieczny P. The effect of blueberries on the oxidative stability of pork meatloaf during chilled storage. Journal of Food Processing and Preservation. 2016;40(5):899–909. https://doi.org/10.1111/jfpp.12668

27. Jia N, Kong B, Liu Q, Diao X, Xia X. Antioxidant activity of black currant (*Ribes nigrum* L.) extract and its inhibitory effect on lipid and protein oxidation of pork patties during chilled storage. Meat Science. 2012;91(4):533–539. https://doi.org/10.1016/j.meatsci.2012.03.010

28. Karwowska M, Dolatowski ZJ. Effect of acid whey and freeze-dried cranberries on lipid oxidation and fatty acid composition of nitrite-/nitrate-free fermented sausage made from deer meat. Asian-Australasian Journal of Animal Sciences. 2017;30(1):85–93. https://doi.org/10.5713/ajas.16.0023

29. Armenteros M, Morcuende D, Ventanas S, Estévez M. Application of natural antioxidants from strawberry tree (*Arbutus unedo* L.) and dog rose (*Rosa canina* L.) to frankfurters subjected to refrigerated storage. Journal of integrative agriculture. 2013;12(11):1972–1981. https://doi.org/10.1016/S2095-3119(13)60635-8

30. Tamkutė L, Vaicekauskaitė R, Melero B, Jaime I, Rovira J, Venskutonis PR. Effects of chokeberry extract isolated with pressurized ethanol from defatted pomace on oxidative stability, quality and sensory characteristics of pork meat products. LWT. 2021;150:111943. https://doi.org/10.1016/j.lwt.2021.111943

31. Das Q, Islam R, Marcone MF, Warriner K, Diarra MS. Potential of berry extracts to control foodborne pathogens. Food Control. 2017;73:650–662. https://doi.org/10.1016/j.foodcont.2016.09.019

32. Khalifa HO, Kamimoto M, Shimamoto T, Shimamoto T. Antimicrobial effects of blueberry, raspberry, and strawberry aqueous extracts and their effects on virulence gene expression in *Vibrio cholerae.* Phytotherapy Research. 2015;29(11):1791–1797. https://doi.org/10.1002/ptr.5436

33. Georgescu C, Frum A, Virchea L-I, Sumacheva A, Shamtsyan M, Cligor F-G, *et al.* Geographic variability of berry phytochemicals with antioxidant and antimicrobial properties. Molecules. 2022;27(15):4986. https://doi.org/10.3390/molecules27154986

34. Fortier MP, Saucier L, Guay F. Effects on microbial quality of fresh pork loin during storage from oregano oil and cranberry pulp diet supplementation in pigs. Canadian Journal of Animal Science. 2012;92(4):465–471. https://doi.org/10.4141/cjas2012-078

35. Menchetti L, Brecchia G, Branciari R, Barbato O, Fioretti B, Codini M, *et al.* The effect of Goji berries (*Lycium barbarum*) dietary supplementation on rabbit meat quality. Meat Science. 2020;161:108018. https://doi.org/10.1016/j.meatsci.2019.108018

36. Castrica M, Menchetti L, Balzaretti CM, Branciari R, Ranucci D, Cotozzolo E, *et al.* Impact of dietary supplementation with goji berries (*Lycium barbarum*) on microbiological quality, physico-chemical, and sensory characteristics of rabbit meat. Foods. 2020;9(10):1480. https://doi.org/10.3390/foods9101480

37. Doriya K, Kumar DS, Thorat BN. A systematic review on fruit-based fermented foods as an approach to improve dietary diversity. Journal of Food Processing and Preservation. 2022;46(11):e16994. https://doi.org/10.1111/jfpp.16994

38. Kamonsuwan K, Balmori V, Marnpae M, Chusak C, Thilavech T, Charoensiddhi S, *et al.* Black Goji Berry (*Lycium ruthenicum*) Juice Fermented with *Lactobacillus rhamnosus* GG Enhances Inhibitory Activity against Dipeptidyl Peptidase-IV and Key Steps of Lipid Digestion and Absorption. Antioxidants. 2024;13(6):740. https://doi.org/10.3390/antiox13060740

39. El-Sohaimy SA, Shehata MG, Mathur A, Darwish AG, Abd El-Aziz NM, Gauba P, *et al.* Nutritional Evaluation of Sea Buckthorn "*Hippophae rhamnoides*" Berries and the Pharmaceutical Potential of the Fermented Juice. Fermentation. 2022;8(8):391. https://doi.org/10.3390/fermentation8080391

40. Markkinen N, Laaksonen O, Nahku R, Kuldjärv R, Yang B. Impact of lactic acid fermentation on acids, sugars, and phenolic compounds in black chokeberry and sea buckthorn juices. Food Chemistry. 2019;286:204–215. https://doi.org/10.1016/j.foodchem.2019.01.189

41. Kwaw E, Ma Y, Tchabo W, Apaliya MT, Wu M, Sackey AS, *et al.* Effect of lactobacillus strains on phenolic profile, color attributes and antioxidant activities of lactic-acid-fermented mulberry juice. Food Chemistry. 2018;250:148–154. https://doi.org/10.1016/j.foodchem.2018.01.009

42. Manganaris GA, Goulas V, Vicente AR, Terry LA. Berry antioxidants: Small fruits providing large benefits. Journal of the Science of Food and Agriculture. 2014;94(5):825–833. https://doi.org/10.1002/jsfa.6432

43. Zhu C, Liu G, Gu X, Zhang T, Xia A, Zheng Y, *et al.* Effects of Quercetin on the Intestinal Microflora of Freshwater Dark Sleeper *Odontobutis potamophila.* Antioxidants. 2022;11(10):2015. https://doi.org/10.3390/antiox11102015

44. Cui K, Wang Q, Wang S, Diao Q, Zhang N. The Facilitating Effect of Tartary Buckwheat Flavonoids and *Lactobacillus plantarum* on the Growth Performance, Nutrient Digestibility, Antioxidant Capacity, and Fecal Microbiota of Weaned Piglets. Animals. 2019;9(11):986. https://doi.org/10.3390/ani9110986

45. Dai H, Huang Z, Shi F, Li S, Zhang Y, Wu H, *et al.* Effects of maternal hawthorn-leaf flavonoid supplementation on the intestinal development of offspring chicks. Poultry Science. 2024;103(9):103969. https://doi.org/10.1016/j.psj.2024.103969

46. Kafarov VV, Dorokhov IN. Systems analysis of chemical engineering processes: Fundamental strategy. Moscow: Yurayt. 2018. 499 p. (In Russ.). https://elibrary.ru/ZCYHSC

47. Gumerov FM, Yarullin LY, Hung TN, Gabitov FR, Kayumova VA. Sub- and supercritical fluid media in food, perfume, and pharmacy. Herald of Technological University. 2017;20(8):30–35. (In Russ.). https://elibrary.ru/YLFXJH

48. Mazzutti S, Pedrosa RC, Ferreira SRS. Green processes in foodomics. Supercritical fluid extraction of bioactives. In: Cifuentes A, editor. Comprehensive Foodomics. Elsevier; 2021. pp. 725–743. https://doi.org/10.1016/B978-0-08-100596-5.22816-3

49. Gallego R, Bueno M, Herrero M. Sub-and supercritical fluid extraction of bioactive compounds from plants, food-by-products, seaweeds and microalgae – An update. TrAC Trends in Analytical Chemistry. 2019;116:198–213. https://doi.org/10.1016/j.trac.2019.04.030

50. Waters: official website [Internet]. [cited 2024 Jul 14]. Available from: https://waters.com/

51. Rexo Engineering: official website [Internet]. [cited 2024 Jul 14]. Available from: https://rexo.co.kr/en/product

52. Sapkale GN, Patil SM, Surwase US, Bhatbhage PK. Supercritical fluid extraction. International Journal of Chemical Sciences. 2010;8(2):729–743.

53. Arumugham T, Rambabu K, Hasan SW, Show PL, Rinklebe J, Banat F. Supercritical carbon dioxide extraction of plant phytochemicals for biological and environmental applications – A review. Chemosphere. 2021;271:129525. https://doi.org/10.1016/j.chemosphere.2020.129525

54. Zaharil HA. An investigation on the usage of different supercritical fluids in parabolic trough solar collector. Renewable Energy. 2021;168:676–691. https://doi.org/10.1016/j.renene.2020.12.090

55. Menshutina NV, Kazeev IV, Artemiev AI, Bocharova OA, Khudeev II. Application of supercritical extraction for isolation of chemical compounds. ChemChemTech. 2021;64(6):4–19. (In Russ.). https://doi.org/10.6060/ivkkt.20216406.6405

56. Griffiths MW, Walkling-Ribeiro M. Pulsed electric field processing of liquid foods and beverages. In: Sun D-W, editor. Emerging technologies for food processing. Academic Press; 2014. pp. 115–145. https://doi.org/10.1016/B978-0-12-411479-1.00007-3

57. Rombaut N, Savoire R, Thomasset B, Bélliard T, Castello J, Van Hecke É, *et al*. Grape seed oil extraction: Interest of supercritical fluid extraction and gas-assisted mechanical extraction for enhancing polyphenol co-extraction in oil. Comptes Rendus Chimie. 2014;17(3):284–292. https://doi.org/10.1016/j.crci.2013.11.014

58. Avilés-Betanzos KA, Scampicchio M, Ferrentino G, Ramírez-Sucre MO, Rodríguez-Buenfil IM. *Capsicum chinense* Polyphenols Extraction by Supercritical Fluids Using Response Surface Methodology (RSM). Processes. 2023;11(7):2055. https://doi.org/10.3390/pr11072055

59. Vinitha UG, Sathasivam R, Muthuraman MS, Park SU. Intensification of supercritical fluid in the extraction of flavonoids: A comprehensive review. Physiological and Molecular Plant Pathology. 2022;118:101815. https://doi.org/10.1016/j.pmpp.2022.101815

60. Panja P. Green extraction methods of food polyphenols from vegetable materials. Current Opinion in Food Science. 2918;*23*:173–182. https://doi.org/10.1016/j.cofs.2017.11.012

61. Lee YH, Charles AL, Kung HF, Ho CT, Huang TC. Extraction of nobiletin and tangeretin from *Citrus depressa* Hayata by supercritical carbon dioxide with ethanol as modifier. Industrial Crops and Products. 2010;31(1):59–64. https://doi.org/10.1016/j.indcrop.2009.09.003

62. Mohamed M, Mahmood, Daud WRW, Markom M. Cosolvent selection for supercritical fluid extraction (SFE) of bioactive compounds from *Orthosiphon stamineus*. Sains Malaysiana. 2018;47(8):1741–1747. https://doi.org/10.17576/jsm-2018-4708-13

63. Ekinci MS. Supercritical fluid extraction of quercetin from sumac (*Rhus coriaria* L.): effects of supercritical extraction parameters. Separation Science and Technology. 2022;57(2):256–262. https://doi.org/10.1080/01496395.2021.1893333

64. Bimakr M, Rahman RA, Ganjloo A, Taip FS, Salleh LM, Sarker MZI. Optimization of supercritical carbon dioxide extraction of bioactive flavonoid compounds from spearmint (*Mentha spicata* L.) leaves by using response surface methodology. Food and Bioprocess Technology. 2012;*5*:912–920. https://doi.org/10.1007/s11947-010-0504-4

65. Ghosh S, Chatterjee D, Das S, Bhattacharjee P. Supercritical carbon dioxide extraction of eugenol-rich fraction from *Ocimum sanctum* Linn and a comparative evaluation with other extraction techniques: process optimization and phytochemical characterization. Industrial Crops and Products. 2013;47:78–85. https://doi.org/10.1016/j.indcrop.2013.02.030

66. Da Porto C, Natolino A. Supercritical fluid extraction of polyphenols from grape seed (*Vitis vinifera*): Study on process variables and kinetics. The Journal of Supercritical Fluids. 2017;130:239–245. https://doi.org/10.1016/j.supflu.2017.02.013

67. Fachri BA, Sari P, Yuwanti S, Subroto E. Experimental study and modeling on supercritical CO_2 extraction of Indonesian raw propolis using response surface method: Influence of pressure, temperature and CO_2 mass flowrate on extraction yield. Chemical Engineering Research and Design. 2020;153:452–462. https://doi.org/10.1016/j.cherd.2019.11.014

68. Moges A, Barik CR, Sahoo L, Goud VV. Optimization of polyphenol extraction from *Hippophae salicifolia* D. Don leaf using supercritical CO_2 by response surface methodology. 3 Biotech. 2020;12:292. https://doi.org/10.1007/s13205-022-03358-1

69. Shirsath SR, Sonawane SH, Gogate PR. Intensification of extraction of natural products using ultrasonic irradiations–A review of current status. Chemical Engineering and Processing: Process Intensification. 2012;53:10–23. https://doi.org/10.1016/j.cep.2012.01.003

70. Balachandran S, Kentish SE, Mawson R, Ashokkumar M. Ultrasonic enhancement of the supercritical extraction from ginger. Ultrasonics Sonochemistry. 2006;13(6):471–479. https://doi.org/10.1016/j.ultsonch.2005.11.006

71. Yang Y-C, Wang C-S, Wei M-C. Kinetics and mass transfer considerations for an ultrasound-assisted supercritical CO_2 procedure to produce extracts enriched in flavonoids from *Scutellaria barbata*. Journal of CO_2 Utilization. 2019;32:219–231. https://doi.org/10.1016/j.jcou.2019.04.008

72. Ćurko N, Lukić K, Tušek AJ, Balbino S, Pavičić TV, Tomašević M, *et al.* Effect of cold pressing and supercritical CO_2 extraction assisted with pulsed electric fields pretreatment on grape seed oil yield, composition and antioxidant characteristics. LWT. 2023;184:114974. https://doi.org/10.1016/j.lwt.2023.114974

73. Salgado-Ramos M, Martí-Quijal FJ, Huertas-Alonso AJ, Sánchez-Verdú MP, Cravotto G, Moreno A, *et al.* Sequential extraction of almond hull biomass with pulsed electric fields (PEF) and supercritical CO_2 for the recovery of lipids, carbohydrates and antioxidants. Food and Bioproducts Processing. 2023;139:216–226. https://doi.org/10.1016/j.fbp.2023.04.003

74. Bogolitsin KG, Druzhinina AS, Ovchinnikov DV, Parshina AE, Shulgina EV, Turova PN. Polyphenols of brown algae. Khimija Rastitelnogo Syrja. 2018;(3):5–21. (In Russ.). https://doi.org/10.14258/jcprm.2018031898; https://elibrary.ru/YABURN

75. Mushtaq M, Sultana B, Akram S, Anwar F, Adnan A, Rizvi SS. Enzyme-assisted supercritical fluid extraction: An alternative and green technology for non-extractable polyphenols. Analytical and Bioanalytical Chemistry. 2017;409:3645–3655. https://doi.org/10.1007/s00216-017-0309-7

76. Lenucci MS, De Caroli M, Marrese PP, Iurlaro A, Rescio L, Böhm V, *et al*. Enzyme-aided extraction of lycopene from high-pigment tomato cultivars by supercritical carbon dioxide. Food Chemistry. 2015;170:193–202. https://doi.org/10.1016/j.foodchem.2014.08.081
77. Kraujalis P, Kraujalienė V, Kazernavičiūtė R, Venskutonis PR. Supercritical carbon dioxide and pressurized liquid extraction of valuable ingredients from *Viburnum opulus* pomace and berries and evaluation of product characteristics. The Journal of Supercritical Fluids. 2017;122:99–108. https://doi.org/10.1016/j.supflu.2016.12.008
78. Ko M-J, Kwon H-L, Chung M-S. Pilot-scale subcritical water extraction of flavonoids from satsuma mandarin (*Citrus unshiu* Markovich) peel. Innovative Food Science and Emerging Technologies. 2016;38:175–181. https://doi.org/10.1016/j.ifset.2016.10.008
79. Kueh BWB, Yusup S, Osman N. Supercritical carbon dioxide extraction of *Melaleuca cajuputi* leaves for herbicides allelopathy: Optimization and kinetics modelling. Journal of CO2 Utilization. 2018;24:220–227. https://doi.org/10.1016/j.jcou.2018.01.005
80. Bendif H, Adouni K, Miara MD, Baranauskienė R, Kraujalis P, Venskutonis PR, *et al.* Essential oils (EOs), pressurized liquid extracts (PLE) and carbon dioxide supercritical fluid extracts (SFE-CO_2) from Algerian *Thymus munbyanus* as valuable sources of antioxidants to be used on an industrial level. Food Chemistry. 2018;260:289–298. https://doi.org/10.1016/j.foodchem.2018.03.108
81. Bayrak S, Sökmen M, Aytac E, Sökmen A. Conventional and supercritical fluid extraction (SFE) of colchicine from *Colchicum speciosum.* Industrial Crops and Products. 2019;128:80–84. https://doi.org/10.1016/j.indcrop.2018.10.060
82. Wang H-C, Chen C-R, Chang CJ. Carbon dioxide extraction of ginseng root hair oil and ginsenosides. Food Chemistry. 2001;72(4):505–509. https://doi.org/10.1016/S0308-8146(00)00259-4
83. Mora JJ, Tavares HM, Curbelo R, Dellacassa E, Cassel E, Apel MA, *et al.* Supercritical fluid extraction of coumarins and flavonoids from citrus peel. The Journal of Supercritical Fluids. 2025;215:106396. https://doi.org/10.1016/j.supflu.2024.106396
84. Atwi-Ghaddar S, Destandau E, Lesellier E. Optimization of supercritical fluid extraction of polar flavonoids from *Robinia pseudoacacia* L. heartwood. Journal of CO2 Utilization. 2023;70:102440. https://doi.org/10.1016/j.jcou.2023.102440
85. Hu Y, Yang L, Liang Z, Chen J, Zhao M, Tang Q. Comparative analysis of flavonoids extracted from *Dendrobium chrysotoxum* flowers by supercritical fluid extraction and ultrasonic cold extraction. Sustainable Chemistry and Pharmacy. 2023;36:101267. https://doi.org/10.1016/j.scp.2023.101267
86. Wang L, Yang B, Du X, Yi C. Optimisation of supercritical fluid extraction of flavonoids from *Pueraria lobata*. Food chemistry. 2008;108(2):737–741. https://doi.org/10.1016/j.foodchem.2007.11.031
87. Ouédraogo JCW, Dicko C, Kini FB, Bonzi-Coulibaly YL, Dey ES. Enhanced extraction of flavonoids from *Odontonema strictum* leaves with antioxidant activity using supercritical carbon dioxide fluid combined with ethanol. The Journal of Supercritical Fluids. 2018;131:66–71. https://doi.org/10.1016/j.supflu.2017.08.017
88. Song L, Liu P, Yan Y, Huang Y, Bai B, Hou X, *et al.* Supercritical CO_2 fluid extraction of flavonoid compounds from Xinjiang jujube (*Ziziphus jujuba Mill*.) leaves and associated biological activities and flavonoid compositions. Industrial Crops and Products. 2019;139:111508. https://doi.org/10.1016/j.indcrop.2019.111508
89. Laurintino TKS, Laurintino TNS, Tramontin DP, Cruz AB, Paiva DW, Bolzan A, *et al.* Ultrasound pretreatment combined with supercritical CO_2 extraction of *Costus spicatus* leaf extract. The Journal of Supercritical Fluids. 2024;213:106372. https://doi.org/10.1016/j.supflu.2024.106372

ORCID IDs
Elena V. Guseva https://orcid.org/0000-0002-6835-4513
Natalya Yu. Khromova https://orcid.org/0000-0001-9852-9401
Boris A. Karetkin https://orcid.org/0000-0002-0976-9700
Artem I. Artemiev https://orcid.org/0000-0001-8388-4806
Kirill M. Demkin https://orcid.org/0000-0002-3299-6397
Julia M. Puzankova https://orcid.org/0000-0002-7776-2922
Irina V. Shakir https://orcid.org/0000-0002-1787-5773
Victor I. Panfilov https://orcid.org/0000-0002-8158-7012

Foods and Raw Materials. 2026;14(1)

ISSN 2308-4057 (Print)
ISSN 2310-9599 (Online)

Research Article
Open Access

Available online at http://jfrm.ru/en
https://doi.org/10.21603/2308-4057-2026-1-658
https://elibrary.ru/AZEHNG

Dietary consumption of pre-carcinogenic amines and mutagenicity in humans: An evidence-based study

Ishrat Perveen[1,*], Nazia Koser[2], Rozina Shahadat Khan[3], Maryam Maqsood[2], Nida Saleem[4], Farhat Naseem Alvi[5], Syed Muhammad Aun[6], Maria Fareed Siddiqui[2], Tallat Anwar Faridi[2], Hafiz Muhammad Abrar Awan[7], Yasar Saleem[1,], Naaz Abbas[1], Sania Mazhar[1], Shaista Nawaz[1], Quratulain Syed[1], Syed Hussain Imam Abidi[8]**

[1] Food and Biotechnology Research Centre, Lahore, Pakistan
[2] University of Lahore, Lahore, Pakistan
[3] Ameer-ud-din Medical College, Lahore General Hospital, Lahore, Pakistan
[4] University of Education, Lahore, Pakistan
[5] University of Sargodha, Sargodha, Pakistan
[6] Superior University, Lahore, Pakistan
[7] University of the Punjab, Lahore, Pakistan
[8] Pakistan Council of Scientific and Industrial Research, Islamabad, Pakistan

e-mail: *drishratperveen51214@outlook.com; **ysaleem73@hotmail.com

Received 08.01.2024; Revised 23.03.2024; Accepted 02.04.2024; Published online 27.12.2024

Abstract:
Dietary consumption of heterocyclic aromatic amines (HAA) is considered to be a high-risk factor that substantially contributes to the development of mutagenicity and carcinogenicity in humans. This study provides ample evidence for the plausible association between mutagenicity or carcinogenicity development and dietary intake of heterocyclic amines in humans. The current study intends to assess the degree of heterocyclic amine contaminants in high-temperature cooked meats, their subsequent food intake, and potential health risk estimations.

The meat samples were homogenized, filtered, extracted, and eluted. The list of heterocyclic amines to be identified and quantified included PhIP (2-amino-1-methyl-6-phenylimidazo[4,5-b] pyridine), IQ (2-amino-3-methyl-imidazo[4,5-f] quinolone), and MeIQx (2-amino-3,8-dimethylimidazo[4,5-f] quinoxaline). They were simultaneously isolated and studied using the method of high-pressure liquid chromatography (HPLC). The highest heterocyclic amine concentration was found in chicken (2705.99 ± 6.12 ng/g), beef (574.09 ± 1.52 ng/g), and mutton (342.41 ± 3.69 ng/g). PhIP (73%) was the main heterocyclic amine in chicken. The estimated daily dietary intake or exposure in chicken, mutton, and beef was 0.690, 0.050, and 0.144 ng/kg body weight, respectively. The values for margin of exposure were within the range identified by the European Food Safety Authority for mutton (102.06) and chicken (13.250), but not for beef (3.784).

This significantly high prevalence of heterocyclic amines and the associated health risks are sufficient to warn the public about the high dietary intake of meat and its carcinogenic health hazards. The mutational patterns induced by heterocyclic amines resemble those in human tumors, requiring the use of specific biomarkers like HAA-DNA and HAA-protein adducts. Future prospects are high for integrating these biomarkers into epidemiological studies, which could provide a comprehensive assessment of health risks associated with dietary heterocyclic aromatic amines in human cancer.

Keywords: Cytotoxicity, meat, heterocyclic amines, high pressure liquid chromatography, biomarkers, carcinogenicity, health risk

Please cite this article in press as: Perveen I, Koser N, Khan RS, Maqsood M, Saleem N, Alvi FN, *et al.* Dietary consumption of pre-carcinogenic amines and mutagenicity in humans: An evidence-based study. Foods and Raw Materials. 2026;14(1):14–25. https://doi.org/10.21603/2308-4057-2026-1-658

INTRODUCTION

Dietary exposure of humans to heterocyclic amines significantly contributes to the development of mutagenicity and carcinogenicity [1]. The amount and structure of various types of heterocyclic amines depend on the temperature and cooking methods. Heterocyclic amines in varying concentrations were discovered in the deep-fried, roasted, charcoal-grilled (high heat, 20 min), and

Copyright © 2024, Perveen *et al.* This is an open access article distributed under the terms of the Creative Commons Attribution 4.0 International License (https://creativecommons.org/licenses/by/4.0/), allowing third parties to copy and redistribute the material in any medium or format and to remix, transform, and build upon the material for any purpose, even commercially, provided the original work is properly cited and states its license.

barbecued (177–260 and 339–365°C) chicken flesh samples [2]. High-temperature cooking procedures, antioxidant presence, lipid oxidation, meat precursor types, creatine levels, and free amino acids also increase the presence of heterocyclic amines in meat products [3].

PhIP(2-amino-1-methyl-6-phenylimidazo[4,5-b] pyridine), one of the 25 detectable heterocyclic amines, was identified as a carcinogenic heterocyclic amine, abundantly prevalent in high-flame-cooked proteinaceous foods, such as beef, pork, and fish [4].

Heterocyclic compounds are organic compounds with a minimum of one hetero atom [5]. A carbocyclic compound is an organic cyclic molecule with rings, with the most common heterocycles consisting of oxygen, nitrogen, or sulfur atoms [3]. Diverse natural products, physiologically active molecules, functional materials, ligands, and catalysts all comprise heterocyclic compounds with nitrogen, oxygen, and sulfur atoms. These compounds serve as versatile components in synthesizing organic compounds [6]. Heterocyclic moieties are particularly common in commercially available medications and agrochemicals [7]. Significant work has been put into developing synthetic techniques to create heterocyclic molecules [7]. Pyridine, pyrrole, thiophene, and furan are well-known heterocyclic compounds with six-atom rings [8]. Five-membered rings in furan, thiophene, and pyrrole molecules consist of four carbon atoms and one atom of oxygen, sulfur and nitrogen, respectively [9–11].

According to several epidemiological studies and cohort experiments, consumption of processed red meats quadruples the health risk concern of developing colorectal cancer [9]. Additionally, consumption of cooked or processed meat was linked to the development of malignancies in the esophagus, stomach, endometrial lining, pancreas, prostate, and lungs [10]. Busquets *et al*. [11], who conducted a survey based on a food frequency questionnaire, reported that an average daily intake of 13 meat dishes raised heterocyclic amines up to 285.6 ng/g. In addition, the average daily intake of heterocyclic amines could grow by 475.6 ng in the presence of co-mutagens. Kobets *et al*. wrote that a daily dietary intake of heterocyclic amines might bring their level up to 103 and 160 ng, which may trigger the development of various carcinogenic effects [12].

DNA adduct identification and measurement are crucial to understand exposure to genotoxic chemicals and their role in cancer development. Tissues embedded in paraffin and fixed with formalin offer unexplored biosamples for studying cancerogens by adducting DNA biomarkers [13].

Hazardous carcinogenic compounds in the diet and environment can facilitate the formation of genomic DNA adducts, leading to development of cancer and mutations. DNA adduct identification and measurement involve methods like liquid chromatography-mass spectrometry (LC/MS), mass spectrometry, immunoassays, and 32P-postlabeling. New developments in formalin-fixed paraffin-embedded tissues offer untapped biosamples for tumor-causing DNA adduct biomarker research through mass spectrometry-based human biomonitoring (Fig. 1) [14].

Annual poultry consumption in Pakistan is 16 kg per person [15]. In 2020, the consumption of sheep, beef, and veal in Pakistan amounted to 6.62, 2.02, and 6.42 kg/per person, respectively [16]. Sohaib and Jamil reported the per capita meat consumption as 11.7, 13.8, and 14.7 kg in 2000, 2006, and 2009, respectively; the authors expected it to surge and reach 47 kg/per capita by 2020 [17]. The mean values for annual per capita consumption of beef were 2.7 (total), 2.4 (rural), and 3.0 (urban) kg, as reported in 2018 by the Household Integrated Economic Survey. However, a field survey

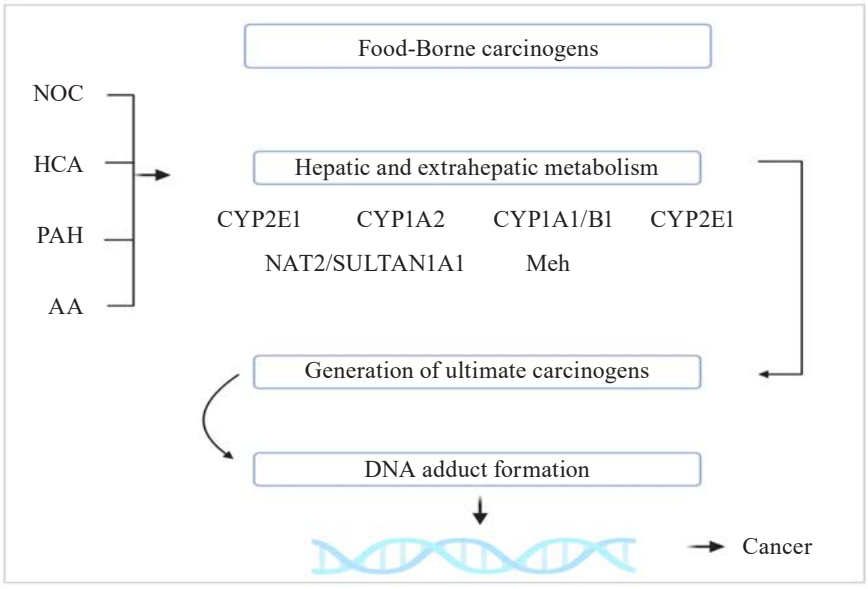

Figure 1 Mutations and cancer as a result of carcinogenic substances in food and environment

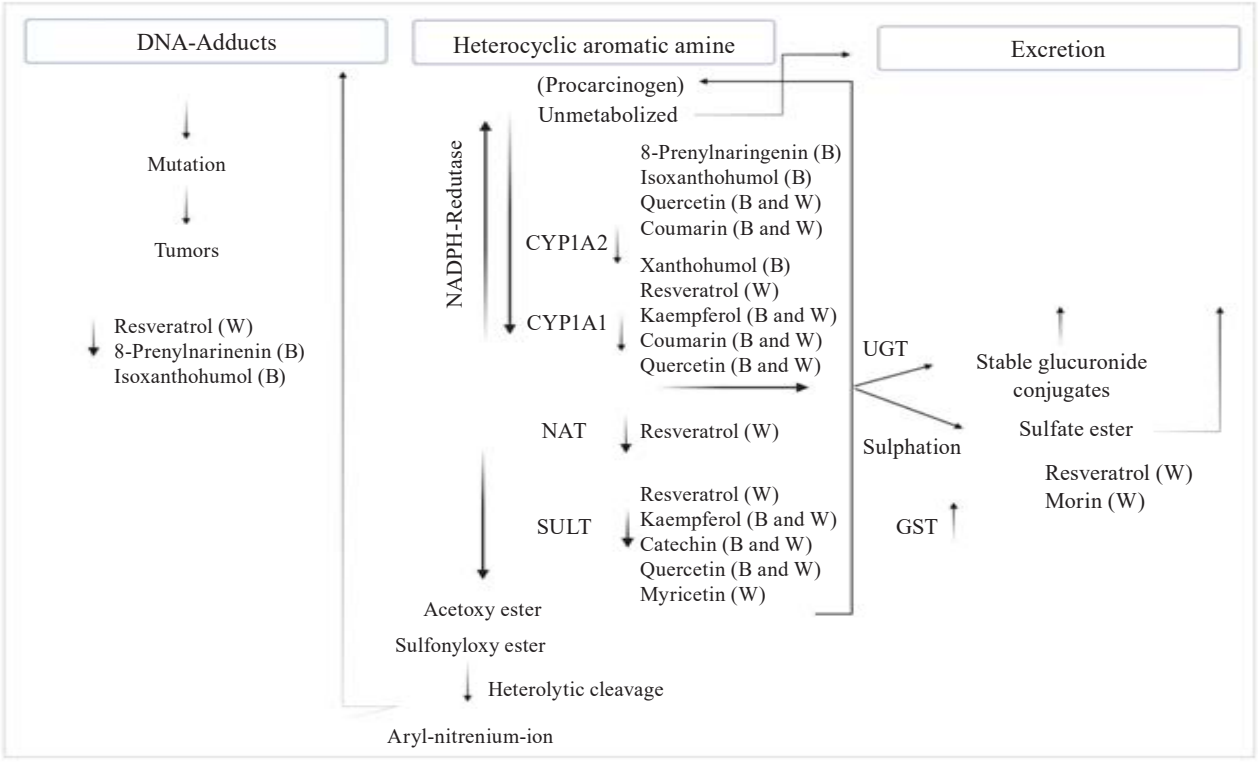

Figure 2 Biomarkers and metabolism of heterocyclic amines in human beings [19, 20]

performed that yielded different mean values, i.e., 3.8 (total), 4.2 (rural), and 3.4 (urban) kg [18].

N-oxidation of exocyclic amine groups results in the production of HONH-HAAs, i.e., genotoxic metabolites of heterocyclic aromatic amines. In rodents, the liver exhibits the highest metabolic activity, especially following enzyme induction with polychlorinated biphenyl or 3-methylcholanthrene. HONH-HAAs form mutation-prone DNA adducts by covalently attaching to DNA. Hepatic cytochrome CYP1A2, extrahepatic CYP1A1, and CYP1B1 are the main cytochromes that catalyze N-oxidation of heterocyclic aromatic amines in humans. CYP1A2 is responsible for 70% of the total metabolism of PhIP and 91% metabolism of MeIQx. The interspecies variations in heterocyclic aromatic amine metabolism occur by cytochromes in nonhuman primates, humans, and rodents. The primary causes are attributed to the cytochrome expression levels, catalytic activity variations, and cytochrome regioselectivities towards heterocyclic aromatic amines. MeIQx is mainly produced in human hepatocytes as the detoxicated metabolite IQx-8-COOH, which is primarily formed in the urine of meat consumers. This metabolite is catalyzed by human CYP1A2. Compared to rat CYP1A2, recombinant human CYP1A2 exhibits catalytic effectiveness of PhIP and MeIQx N-oxidation that are 10–19 times higher. These interspecies differences must be considered when determining the risk of heterocyclic aromatic amines to human health using experimental animal toxicity data because they have an impact on the biological effects of heterocyclic aromatic amines [20].

Food contains such toxic substances as polycyclic aromatic hydrocarbons and mycotoxins, which can pose serious problems for the modern world. Mycotoxin exposure to agricultural products is spreading around the world, and eating processed red meat raises risks of developing cancer, especially colorectal cancer. The International Agency for Research on Cancer has categorized processed meat as a human carcinogen (Group 1) and red meat as a potential human carcinogen (Group 2A). Meat is often subjected to high asparagine levels, baking, frying, drying, combustion products from fossil fuels, heating fats or oils to high temperatures, fermenting, salting, pickling, and rotting. These processing techniques can result in the formation of carcinogenic compounds. Many genotoxic substances found in food undergo biotransformation within the body, which turns them from initial mutagens or carcinogens into ultimate ones. Food procarcinogens are metabolized by Phase I functioning reactions (Phase I) and conjugation reactions (Phase II), which are catalyzed by xenobiotic, or drug-metabolizing enzymes, preferentially (XMEs/DMEs) [12].

As food-genotoxic substances undergo biotransformation, turning into carcinogens or mutagens, they are metabolized through phase I and II reactions, being catalyzed by xenobiotic enzymes. Metabolism (Phase I) of the abovementioned carcinogens in food is affected by cytochrome P450. DNA sites that are vulnerable to electrophilic compounds include: adenine N_3, N_1, and N_7 atoms, guanine O_6, N_7, and N_3 atoms, thymine N_3, O_4, and O_2 atoms, cytosine N_3 and O_2 atoms, phosphodiester

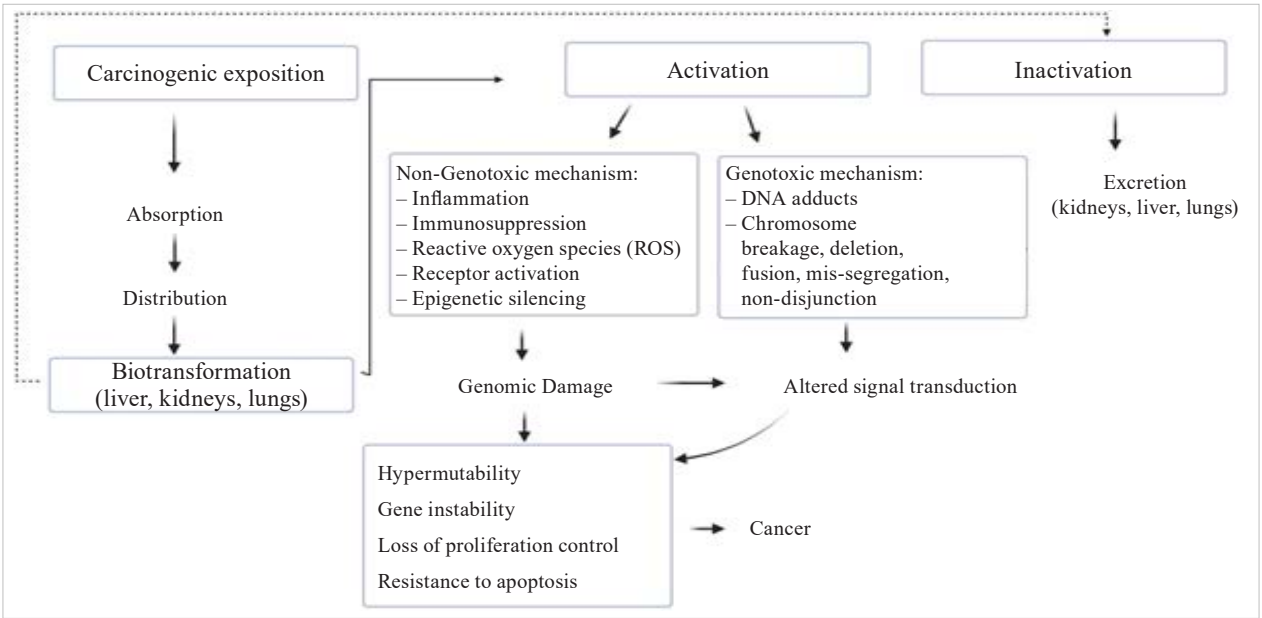

Figure 3 Food-borne carcinogens, metabolism, and development of mutagenicity in humans [21]

skeleton in the phosphate group, etc. When guanine or adenine is alkylated at the N_7 position, they trigger such reactions as spontaneous depurination with the formation of purine sites (AP) or conversion of alkylated bases into a stable formamidopyrimidone (FAPy) form [22].

The O6 positional modifications of pyrimidine and purine bases typically result in mismatched base pairing and mutations in daughter cells. Chemicals with electrophilic properties that bind to DNA covalently have the potential to cause carcinogenesis, which could lead to neoplastic transformation. These chemicals could change into electrophilic forms that bind to nucleophilic sites in DNA, making them mutagenic [14].

Food contains harmful compounds that can pose significant health risks, e.g., mycotoxins, processed red meat, and contaminated grains. The food industry must address these issues and develop effective strategies to prevent and treat these harmful substances in food production. At home and in restaurants, cooking techniques often include grilling, broiling, deep frying, and pan-frying. All these high-temperature treatments, cooking time, meat type, and some cooking utensils lead to high contents of carcinogenic heterocyclic amines in food. High-temperature cooking of meats was found associated with the development of powerfully carcinogenic heterocyclic amines in commercially available ready-to-eat and ready-to-cook meat products [23].

The current study investigated and verified the presence, formation, and quantification of carcinogenic heterocyclic amines and their subsequent health risks in high-temperature cooked chicken, mutton, and beef.

STUDY OBJECTS AND METHODS

Chemicals. Heterocyclic amines from high proteinaceous muscle foods, such as beef, poultry, and mutton, were isolated, identified, and quantified. The methods were in line with those described in [24, 25], with some changes connected with affordability, effective compatibility, and economic viability [23]. In this study, we used three heterocyclic amine standards imported from Toronto Chemical Company, Canada. They included PhIP (2-amino-1-methyl-6-phenylimidazo[4,5-b] pyridine), IQ (2-amino-3-methyl-imidazo[4,5-f] quinolone), and MeIQx (2-amino-3,8-dimethylimidazo[4,5-f] quinoxaline). Sodium hydroxide (NaOH), methanol (CH_3OH), ethyl acetate ($CH_3COOC_2H_5$), and ACN (acetonitrile) were purchased from Sigma-Aldrich, USA. All chemicals and solvents involved in the mobile phase preparation and extraction process were of HPLC-grade. The syringe filters (0.22 µm, 25 mm), diatomaceous earth, and filter papers (0.22 µm, 47 mm) were acquired from Integrated Biosciences, Pakistan. The purity values of MeIQx, IQ, and PhIP were 99.78, 98, and 99%, respectively. The internal standard of 4,7,8-TriMeIQx was added at a constant concentration to the purified samples and standards. Figure 4 illustrates the chemical structures of the four heterocyclic amine standards.

Stock standard solutions and their preparations. We prepared a stock solution (200 µg/mL) for three heterocyclic amine standards, i.e., IQ, MeIQx, and PhIP, in methanol to be used for spiking standards. The calibration curves with three heterocyclic amine standard mixes were obtained between 0.0000001 to 1 µg of heterocyclic amine per 1 mL to establish a linearity range. Figure 2 demonstrates the linearity range for the calibration curves of PhIP, IQ, and MeIQx standards. Prior to the injection of sample extracts and standards in high-performance liquid chromatography (HPLC), we filtered them by using syringe filters (0.22 µm, 25 mm).

Preparing meat samples. Meat samples were barbecued, homogenized, and stored in a refrigerator at –20°C until further use. Then we mixed 1 g of defrosted

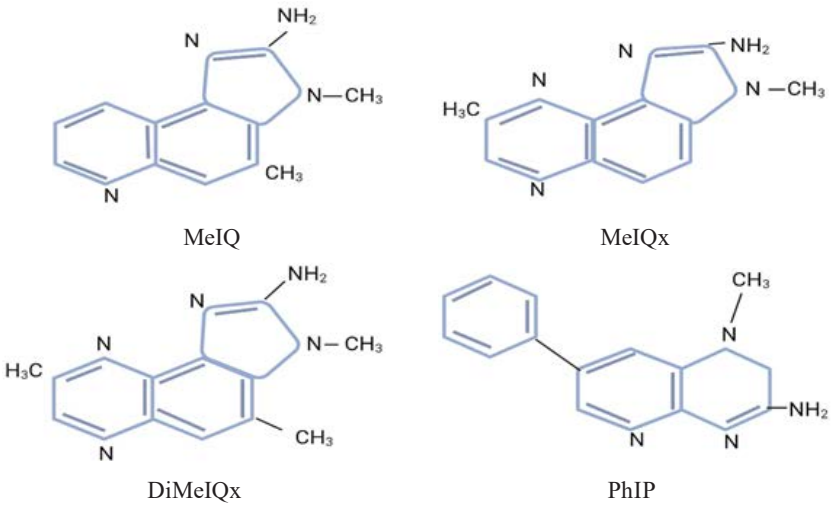

Figure 4 Structural depiction of heterocyclic amines [20]

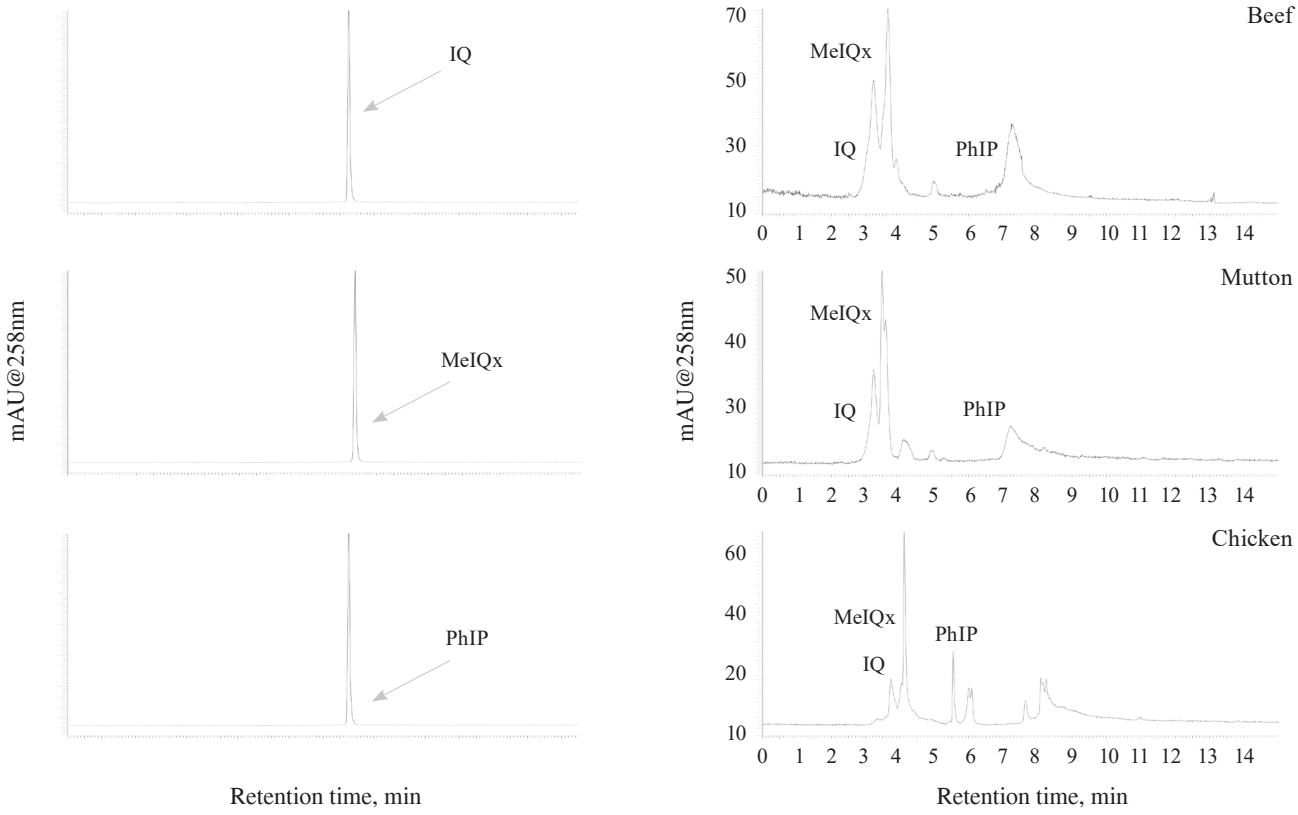

Figure 5 Chromatograms of heterocyclic amines, i.e., PhIP, IQ, and MeIQx standards (on the left) in beef, mutton, and chicken (on the right)

meat with 12 mL of 1N NaOH and turned it into a homogenous suspension by using magnetic stirring at 600–700 rpm for 1 h. After the mix passed through the EXtrelut columns packed with diatomaceous earth, we added ethyl acetate $CH_3COOC_2H_5$ (20 mL), 0.1 N HCl (2 mL), and MeOH (2 mL). The resultant analyte was eluted by using 2 mL of 25% NH_4OH (ammonium hydroxide) and MeOH (1:19, v/v).

Identification and subsequent quantification of heterocyclic amines. We identified and quantified heterocyclic amines by using a PerkinElmer HPLC system. The procedure involved an Ultra-Violet/Visible detector and C18-Column (4.6 mm, 250 L, 100Aº). The flow rates of mobile phase A (H_2O/MeOH/CH_3COOH/ACN 76/8/2/14 mL) and mobile phase B (ACN) were at 0.7 mL/min; the analyte injection volume was 10 µL. Figure 5 illustrates the chromatograms for PhIP, IQ, and MeIQx standards.

Method validation. We validated this analytical method by various experimental studies. The limits of quantitation and detection (LOQ and LOD) values along with the linearity range were established and calculated

for each of the three heterocyclic amines. Linearity was calculated by spiking the heterocyclic amine standards at six different concentration levels. Graphs were plotted between a peak area and the concentration of the heterocyclic amines to produce calibration curves. We also calculated the linear regression to define the correlation coefficient, intercept, and slope of each calibration line. Figure 6 shows the calibration curves of MeIQx, IQ, and PhIP standards (μg/mL) with the corresponding linear regression and R^2 value. The detection and quantitation limits for MeIQx, PhIP, and IQ were in the ranges of 10–1000, 0.1–100, and 0.1–10 ng/g.

Dietary exposure and health risks estimation. The daily dietary exposure data for heterocyclic amine contamination in meats came from various sources. As it was mentioned above, the annual poultry consumption in Pakistan is 16 kg per person [15]. In 2020, the annual consumption of poultry, sheep, and beef reached 6.62, 2.02, and 6.42 kg/per person, respectively [16]. The Food and Agriculture Organization offers different statistics, according to which the per capita annual meat consumption in Pakistan mainly consists of buffalo (1.7 kg), beef (6.3 kg), chicken (4.5 kg), goat (1.6 kg), and sheep (2.1 kg) [26]. In this research, we accepted 70 kg as the average body weight of an adult meat consumer. To calculate the estimated daily meat intake, we used the formula proposed by Bogdanović *et al*. [27]:

$$\text{EDI} = \frac{C_c \times C_i}{\text{BW}} \quad (1)$$

where C_c is the stands for the average daily meat consumption by person, g; C_i is the designates the content of the heterocyclic amine, ng/g; BW is the average body weight of consumers, kg; EDI is the means the estimated daily meat intake expressed as 1 ng/kg body weight/day.

Calculating margin of exposure. Margin of exposure (MOE) calculation made it possible to estimate the health risks. This experiment followed the recommendations of the European Food Safety Authority Panel [32] and the procedure for polycyclic aromatic hydrocarbons (PAH) [28]. The benchmark dose limit ($BMDL_{10}$) value for PhIP was reported as 2.71, 0.74, and 0.4 mg per 1 kg of body weight per day for their association with the

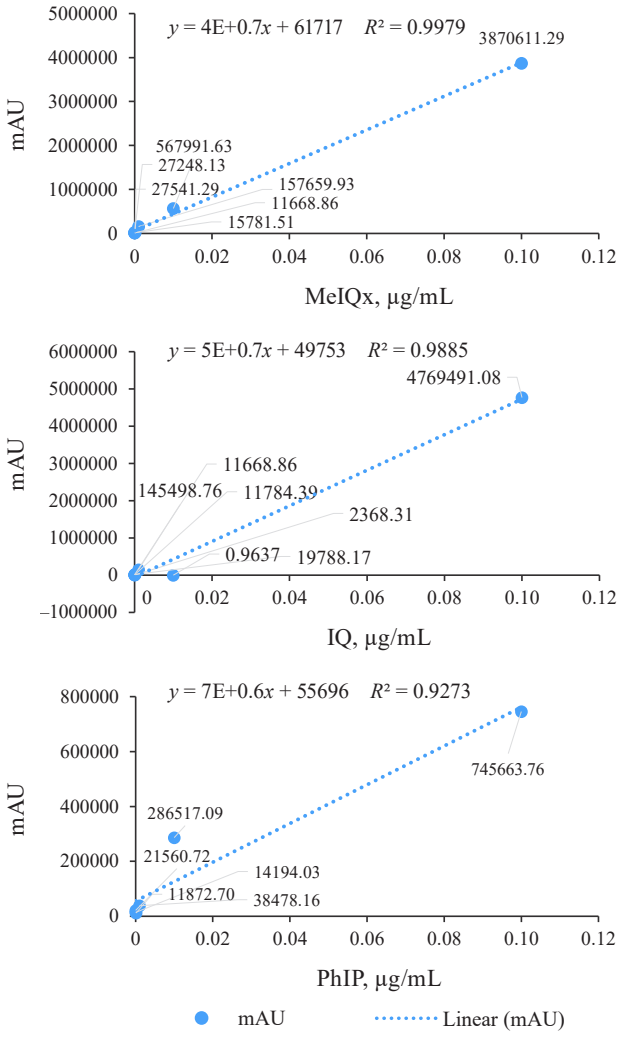

MeIQx				
Concentration, μg/mL	mAU	R^2 value	LOQ, ng/g	LOD, ng/g
0.1	3870611.29	0.9979	100	0.1
0.01	567991.63			
0.001	157659.93			
0.0001	27541.29			
0.0001	15781.51			
0.000001	27248.13			
0.0000001	11668.86			

IQ				
Concentration, μg/mL	mAU	R^2 value	LOQ, ng/g	LOD, ng/g
0.1	4769491.08	0.9637	10	0.1
0.01	1395448.11			
0.001	145498.76			
0.0001	19788.17			
0.00001	11784.39			
0.0000001	2368.31			
0.0000001	11668.86			

PhIP				
Concentration, μg/mL	mAU	R^2 value	LOQ, ng/g	LOD, ng/g
0.1	745663.76	0.9278	1000	10
0.01	286517.09			
0.001	38478.16			
0.0001	11872.70			
0.00001	14194.03			
0.000001	21560.72			

LOQ = Signal: Noise (1:9) ; LOD = Signal: Noise (1:3)

Figure 6 Calibration curves of MeIQx, IQ, and PhIP standards with corresponding linear regression, R^2 values, limits of quantitation (LOQ), and limits of detection (LOD)

colon, mammary, and prostate tumors, respectively [29]. The benchmark dose limit for MeIQx was 8.8 μM (0.001876 mg/kg) [30]. The benchmark dose limit for IQ came from a study conducted on GST-P positive foci, which indicated a significant increase in its numbers at $BMDL_{10}$ = 1.44 ppm (1.44 mg/kg) [31]. These values for $BMDL_{10}$ were used as references in the following formula:

$$MOE = \frac{BMDL_{10}}{EDI} \quad (2)$$

where EDI is the dietary intake of heterocyclic amines, mg/kg body weight/day; $BMDL_{10}$ is the stands for the benchmark lower dose limit for heterocyclic amine per 1 kg of body weight per day at 10% and measurable response.

Statistical analysis. We used a complete block experiment in a randomized pattern with repeated measurements. Each experimental unit was repeated four times. For statistical analysis, the average of two measurements was made on the same experimental unit. The data were processed using SAS 9.1 to examine all statistical significance. The analysis involved a multiple comparison test and a variance analysis (ANOVA). Means at $p \leq 0.05$ served to assess the significance of the findings [32].

RESULTS AND DISCUSSION

Contamination of barbecued meats with heterocyclic amines. The total heterocyclic amine concentrations in barbecued meat, i.e., mutton, beef, and chicken, ranged between 342.41 ± 3.69 and 2705.99 ± 6.12 ng/g. Table 1 gives the quantitative analysis data of PhIP (2-amino-1-methyl-6-phenylimidazo[4,5-b]pyridine), IQ (2-amino-3-methyl-imidazo[4,5-f]quinolone), and MeIQx (2-amino-3,8-dimethylimidazo[4,5-f]quinoxaline) in charcoal-barbecued mutton, beef, and chicken. The resulting heterocyclic amine contents in barbecued chicken (2705.99 ± 6.12 ng/g), mutton (342.41 ± 3.69 ng/g), and beef (574.09 ± 1.52 ng/g) appeared to be considerably higher.

As a rule, heterocyclic amine formation depends on the cooking temperature and time [33]. The PhIP contents for pan and deep-fried samples ranged from 18.33 to 70.00 ng/g and from 21.3 to 22.21 ng/g, respectively. In contrast, microwave treatment at different treatment times were reported to increase the heterocyclic amine level by 0.70–35.00 μg/g [23].

Barbecuing is universally regarded as one of the most prevalent cooking methods. Duck and chicken breasts cooked by grilling were found to contain 112 and 32 ng/g of total heterocyclic amines, respectively [34]. Our findings were consistent with the high PhIP (270 ng/g) and AαC (180.4 ng/g) in chicken breasts grilled at high temperatures [33]. The respective production of mutagens in commercially processed chicken products, i.e., chicken nuggets, olive oil sardines, and tomato sauce sardines, was 166.44, 61.10, and 47.33 ng/g [33].

Predominant concentrations of individual heterocyclic amines. In this study, the predominant PhIP content in beef, mutton, and chicken ranged between 212.10 ± 1.35 and 1987.18 ± 5.73 ng/g. Our results support those published by Perveen *et al*., who found high heterocyclic amine quantities in high-temperature processed pan-fried (1.11–8.60 g/g), deep-fried (1.6–22.3 g/g), microwaved (0.7–35.0 μg/g), and ready-to-eat chicken kababs [23]. Thus, cooking food at different temperatures may result in various concentrations of PhIP in chicken flesh.

The extremely high PhIP content (1987.18 ± 5.73 ng/g) in this study was in line with the high PhIP contents in barbecued (480 ng/g) or grilled (270 ng/g) chicken [35]. Also, previous studies also detected the highest PhIP concentrations of 420, 320, and 92 ng/g in beef, chicken, and turkey meat, respectively [12].

Kobets *et al*. grilled chicken breast samples at 177–260°C and obtained 480 ng/g PhIP while the chicken samples barbecued at 339–365°C produced a total PhIP level of 330 ng/g [12]. However, Olalekan Adeyeye and Ashaolu [4] reported high MeIQx concentrations of > 100 ng/g.

IQ contents in barbecued meats. The grilled beef samples revealed no IQ quantified for heterocyclic amines. However, the barbecued mutton and chicken samples demonstrated IQ concentrations as high as 116.39 ± 2.20 and 692.33 ± 0.58 ng/g, respectively (Table 1).

Some other studies also verified no IQ content in processed meat products [36]. These findings were, however, found in contrast to the lower IQ contents ranging between 0.44 and 13.98 ng/g [37]. These high IQ quantifications, as detected in the chicken samples, were also in correspondence with our previous findings of IQ, which ranged from 0.25 to 4.97 μg/g [38].

MeIQx and PhIP in beef steaks were reported to be up to a respective level of 2.3 and 16.8 ng/g. A significant correlation occurred between the heterocyclic amine content and the drippings gravy intake. A quarter cup of gravy contained up to 62 ng/g DiMeIQx,

Table 1 Contamination level of heterocyclic amines MeIQx, IQ, and PhIP in various types of barbecued and/or charcoal grilled beef, mutton, and chicken

Meat	MeIQx, ng/g	IQ, ng/g	PhIP, ng/g	Σ, ng/g	*F*-value
Beef	48.34 ± 1.00^{c}	0.00 ± 0.00^{d}	525.75 ± 0.54^{b}	574.09 ± 1.52^{a}	308999.19
Mutton	13.91 ± 0.38^{d}	116.39 ± 2.20^{c}	212.10 ± 1.35^{b}	342.41 ± 3.69^{a}	11516.19
Chicken	26.48 ± 0.56^{d}	692.33 ± 0.58^{c}	1987.18 ± 5.73^{b}	2705.99 ± 6.12^{a}	249743.96

Means that do not share the same superscript are significantly different ($p \leq 0.05$); *P*-value was 0.000 for all samples

230 ng/g PhIP, and 398 ng/g MeIQx [4]. According to Omofuma *et al*., pan-fried hamburgers contained twice as much MeIQx as barbecued or grilled steaks. Figure 7 illustrates the process involved in the heterocyclic amine formation [39].

Higher PhIP contents in grilled/barbecued samples. In this study, the grilled beef samples revealed no IQ. Significant concentrations of PhIP (73%) followed by MeIQx (1%), and IQ (26%) were, however, present in barbecued chicken. The charcoal-grilled chicken samples demonstrated higher PhIP percentages than the mutton samples: 73 vs. 61.86%. The barbecued beef samples contained more PhIP (91.43%) and MeIQx (8.57%) than IQ. However, the MeIQx concentration in the barbecued mutton sample was substantially greater (4.18%) than that in the chicken sample (1%).

Our findings agreed with those reported by Zeng *et al*., who detected more PhIP (38.2–48.54 ng/g) than MeIQx in mutton, chicken, and beef [40]. Barbecued meat (270°C, > 6 h) was reported to result in a tenfold rise in PhIP contents (0–73 ng/g) as compared to MeIQx [41]. However, deep frying produced higher PhIP (31.97 ng/g) concentrations than MeIQx (293.86 ng/g). Thus, pan-fried fish had high PhIP (69.20 ng/g) contents, followed by MeIQx (6.44 ng/g) [39].

The high PhIP content reported by the abovementioned studies was consistent with the results of our investigation. However, Olalekan Adeyeye and Ashaolu found significant MeIQx (22.02 ng/g) and PhIP (19.77 ng/g) contents in fried mutton [4]. In our samples of grilled mutton, the high PhIP (61.86%) levels were followed by IQ (33.95%). These findings were in

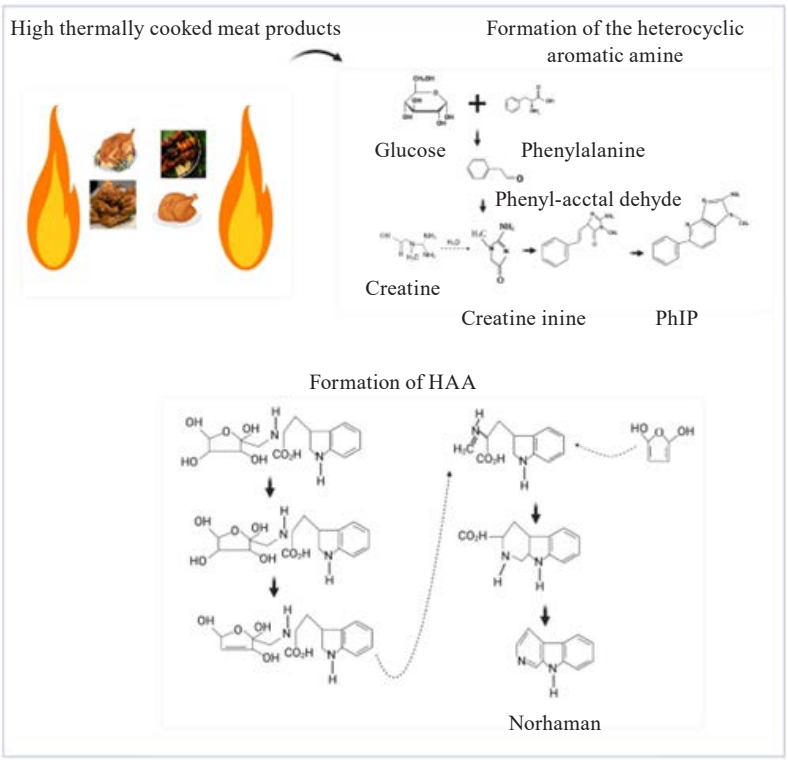

Figure 7 Mechanism involved in heterocyclic aromatic amine formation

Table 2 Estimated daily dietary intake, ng/kg body weight, and risk assessment (margin of exposure) in barbecued beef, mutton, and chicken

Meat	MeIQx		IQ		PhIP		Σ_3	
	Estimated daily dietary intake	Margin of exposure	Estimated daily dietary intake	Margin of exposure	Estimated daily dietary intake	Margin of exposure	Estimated daily dietary intake	Margin of exposure
Beef	0.0121	0.154	0	0	0.132	3.63	0.144	3.784
Mutton	0.0020	0.930	0.017	85.49	0.031	15.64	0.05	102.06
Chicken	0.0068	0.275	0.178	8.088	0.510	4.89	0.69	13.25

Estimated daily dietary intake = Average daily meat consumption by person, g × Heterocyclic amine, ng/g /body weight

Margin of exposure = Benchmark dose limit / Estimated daily dietary intake

Average daily meat consumption: beef = 6.42/365 = 0.0176, chicken = 6.62/365 = 0.018 [16], and mutton = 3.7/365 = 0.01013 [26]. Average body weight = 70 kg. Benchmark dose limit for PhIP = 0.48 mg/kg/body weight/day [29], MeIQx = 8.8 μM (0.001876 mg/kg) [29], IQ = 1.44 ppm (1.44 mg/kg) [31]

correspondence with Jahurul *et al*. [38], who reported total heterocyclic amines up to 38.7 ng/g, which was mainly comprised of PhIP followed by MeIQx and IQ.

Table 1 demonstrates the current heterocyclic amine quantifications. ng/g, in various types of barbecued and charcoal-grilled beef, mutton, and chicken detected by UV-Vis HPLC. Our results were in correspondence with those reported by other scientists. The resulting variation in concentrations as reported by different studies might be accredited to different varieties of meat, cooking time, and temperatures.

Estimating dietary exposure. Table 2 shows the daily dietary intake of IQ, PhIP, MeIQx, and Σ_3 heterocyclic amines in adult humans from barbecued or grilled beef, mutton, and chicken.

Dietary ingestion of respective heterocyclic amines in chicken, mutton, and beef was found as 0.69, 0.05, and 0.144 ng/kg body weight per day. A similar study [28] on polycyclic aromatic hydrocarbons (PAHs) reported 0.13–0.72 ng/kg body weight per day for meat doners and 0.03–0.24 ng/kg body weight per day for grilled fish.

The daily dietary intake of heterocyclic amines depends on the eating habits and/or patterns. Additionally, consumers' exposure to heterocyclic amines grows together with the consumption rates.

The estimated dietary exposure to heterocyclic amines in this research was in line the previous studies. According to a preliminary estimation, the mean daily dietary exposure to total heterocyclic amines was 4.43 ng/kg body weight, which fits better within the reported range [42]. Another Malaysian study stated the major contribution of grilled and fried chicken to the high average daily dietary ingestion of heterocyclic amines as up to 553.7 ng per person [38]. Similarly, Pouzou *et al.* [43] found an almost similar concentration of daily exposure to heterocyclic amines (PhIP and MeIQx) from meat and various kinds of bread in the United States as 565.3 ng per person. Sabally *et al*. [44] observed that the daily dietary exposure to MeIQx (0.93 ng/kg body weight) and PhIP (2.34 ng/kg body weight) was within the previously reported ranges for heterocyclic amines.

Dietary exposure to heterocyclic amines and risk assessment. The margin of exposure made it possible to estimate the health risk. If the margin of exposure is below 10.000 for any contamination level, human health may be at high risk [45]. Table 2 gives the estimated daily intake and the margin of exposure for heterocyclic amines in grilled or charcoal chicken, mutton, and beef. In this study, the margin of exposure indicated as lowest vs. highest values was found as 3.784 and 102.06, respectively, in beef and chicken samples. The lowest respective margins of exposure for PhIP as reported by Carthew and co-workers were 20 000, 40 000, and 150 000 for prostate, breast, and colon tumors [29].

Little information is available to estimate the margin of exposure for heterocyclic amines. Our findings of margin of exposure calculation were relatable to the prevalence and exposure to polycyclic aromatic hydrocarbons (PAH). Rozentale *et al*. [46] studied high-temperature produced carcinogenic polyaromatic compounds in foods and reported a respective margin of exposure for PAH4 and Benzo[a]pyrene (BaP) as 8.486 and 11.602, respectively, which suggests that middle-aged (39–50 y.o.) consumers may be at high risk. Duedahl-Olesen *et al*. [47] studied the daily consumption of extensively contaminated barbeque and home-cooked meat in Denmark and reported it to pose a health risk when the margin of exposure values exceeded 7.080 and 8.450, respectively. Sahin *et al*. [28], however, reported safe margin of exposure intervals for PAH4 in fish/shellfish (485.437), meat (25.634), and smoked food products (265.957).

CONCLUSION

Variable contents of heterocyclic amines in different meats can be attributed to varying cooking methods, surface heat transfer, cooking temperature, and cooking time. The current study considerably signifies high heterocyclic amine levels in barbecued or charcoal-grilled beef, mutton, and chicken as 574.09 ± 1.52, 342.41 ± 3.69, and 2705.99 ± 6.12 ng/g, respectively. High contents of PhIP (2-amino-1-methyl-6-phenylimidazo[4,5-b] pyridine) were quantified in beef, mutton, and chicken samples as 525.75 ± 0.54, 212.10 ± 1.35, and 1987.18 ± 5.73 ng/g, respectively. The estimated daily dietary consumption of heterocyclic amines, however, was 0.69, 0.05, and 0.144 ng per 1 kg of body weight in chicken, mutton, and beef, respectively. The margin of exposure values calculated for chicken, mutton, and beef proved to be 13.250, 102.060, and 3.784, respectively. The margin of exposure value for mutton and chicken exceeded the critical limit of 10.000 published by the European Food Safety Authority and hence remained within the reliable range. However, the margin of exposure for beef appeared to be far below the critical allowance limit and range, which is a matter of great health risk concern. High heterocyclic amine levels were found in barbecued and/or charcoal-grilled chicken, which necessitates immediate action by public health authorities. The food science needs to explore a variety of strategies to mitigate, reduce, prevent, and/or inhibit the heterocyclic amine formation at high temperatures in meats. The high consumption of proteinaceous foods containing such carcinogenic compounds has, thus, further quadrupled the health risk concerns for human beings.

High-temperature cooked meats and poultry produce harmful heterocyclic aromatic amines (HAA), which can induce cell mutations and contribute to cancers, especially in regions with high meat consumption. These mutational patterns resemble those found in human tumors, highlighting the need for specific biomarkers to understand their role in meat-related cancers. PhIP, a prominent heterocyclic aromatic amine in well-done meats, was identified as a carcinogen. However, biomarkers indicating the biologically effective dose, such as HAA-DNA and HAA-protein adducts, should be incorporated into epidemiological studies for a compre-

hensive assessment of health risks. Future studies integrating specific heterocyclic aromatic amine biomarkers and genetic factors could advance our understanding of the health risks associated with dietary heterocyclic aromatic amines in human cancer.

CONTRIBUTION

Conceptualization, Ishrat Perveen, and Yasar Saleem; methodology, Ishrat Perveen and Yasar Saleem; software, Shaista Nawaz, and Nida Saleem; validation, Yasar Saleem, and Ishrat Perveen; formal analysis, Ishrat Perveen, and Yasar Saleem; investigation, Ishrat Perveen, Tallat Anwar Faridi, and Rozina Shahadat Khan; resources, Maryam Maqsood; Ishrat Perveen; Rozina Shahadat Khan, data curation, Farhat Naseem Alvi, Syed Muhammad Aun, Maria Fareed Siddiqui, Hafiz Muhammad Abrar Awan and Ishrat Perveen; writing of original draft, Ishrat Perveen, Tallat Anwar Faridi, Maryam Maqsood, and Rozina Shahadat Khan; editing, and review Quratulain Syed, Syed Hussain Imam Abidi supervision and project administration Yasar Saleem, and Ishrat Perveen. The authors have reviewed and approved of the final version of manuscript.

CONFLICT OF INTEREST

The authors declared no conflict of interest regarding the publication of this article.

ACKNOWLEDGMENTS

The authors extend their thanks to the Director General PCSIR, LLC, Lahore, and Chairman PCSIR, Islamabad, for provoking the idea, stimulating thoughtful insights, and providing adequate research facilities along with ensuring a skillful and conducive environment.

REFERENCES

1. Shiri P, Roosta A, Ramezanpour S, Amani AM. Editorial: Six-membered heterocycles: their synthesis and bio applications. Frontiers in Chemistry. 2023;11:1229825. https://doi.org/10.3389/fchem.2023.1229825
2. Kabir E, Uzzaman M. A review on biological and medicinal impact of heterocyclic compounds. Results in Chemistry. 2022;4:100606. https://doi.org/10.1016/j.rechem.2022.100606
3. Chen J, Shi X, Zhao R, Tian Z, Zhang L, Yu Q, *et al.* Effect of pomegranate peel extract on the reduction of heterocyclic amines and quality characteristics of mutton meatballs. Food Quality and Safety. 2023;7:1–9. https://doi.org/10.1093/fqsafe/fyac073
4. Olalekan Adeyeye SA, Ashaolu TJ. Heterocyclic Amine Formation and Mitigation in Processed Meat and Meat Products: A Mini-Review. Journal of Food Protection. 2021;84:1868–1877. https://doi.org/10.4315/JFP-20-471
5. Teng H, Mi Y, Deng H, He Y, Wang S, Ai C, *et al.* Acylated anthocyanin inhibited the formation of heterocyclic amines in hybrid chemical model system and its underlying mechanism. Food Chemistry: X. 2023;17:100559. https://doi.org/10.1016/j.fochx.2023.100559
6. Hao T, Huang L, Wei Y, Shi M. Copper-Catalyzed Synthesis of Indolyl Benzo[*b*]carbazoles and Their Photoluminescence Property. Organic Letters. 2021;23(13):5133–5137. https://doi.org/10.1021/acs.orglett.1c01659
7. D'Souza A, D'Souza AS, Mendonca AP, Nayak P, Poddar RK, Sadananda V, *et al.* Review on green multicomponent synthesis of heterocyclic compounds. International Journal of Health Sciences. 2022;6(S8):4601–4623. https://doi.org/10.53730/ijhs.v6nS8.13250
8. Batool Z, Xia W, Chen J-H, Bi Y, Chen F, Wang M. Quantification of hetero-cyclic amines from different categories of braised beef by optimized UPLC-TQ-XS/ESI method. Food Chemistry. 2023;421:136191. https://doi.org/10.1016/j.foodchem.2023.136191
9. Farvid MS, Sidahmed E, Spence ND, Mante Angua K, Rosner BA, Barnett JB. Consumption of red meat and processed meat and cancer incidence: a systematic review and meta-analysis of prospective studies. European Journal of Epidemiology. 2021;36:937–951. https://doi.org/10.1007/s10654-021-00741-9
10. Niedermaier T, Gredner T, Hoffmeister M, Mons U, Brenner H. Impact of Reducing Intake of Red and Processed Meat on Colorectal Cancer Incidence in Germany 2020 to 2050 – A Simulation Study. Nutrients. 2023;15(4):1020. https://doi.org/10.3390/nu15041020
11. Busquets R, Mitjans D, Puignou L, Galceran MT. Quantification of heterocyclic amines from thermally processed meats selected from a small-scale population-based study. Molecular Nutrition Food Research. 2008;52(12):1408–1420. https://doi.org/10.1002/mnfr.200800048
12. Kobets T, Smith BPC, Williams GM. Food-Borne Chemical Carcinogens and the Evidence for Human Cancer Risk. Foods. 2022;11(18):2828. https://doi.org/10.3390/foods11182828
13. Fahrer J. Food-Borne Carcinogens. In: Schwab M. editor. Encyclopedia of Cancer. Berlin: Springer; 2016. pp. 1–5. https://doi.org/10.1007/978-3-642-27841-9_7235-1
14. Hwa Yun B, Guo J, Bellamri M, Turesky RJ. DNA adducts: Formation, biological effects, and new biospecimens for mass spectrometric measurements in humans. Mass Spectrometry Reviews. 2020;39(1–2):55–82. https://doi.org/10.1002/mas.21570

15. Ahmed T, Ameer HA, Javed S. Pakistan's backyard poultry farming initiative: impact analysis from a public health perspective. Tropical Animal Health Production. 2021;53:210. https://doi.org/10.1007/s11250-021-02659-6
16. Statista Research Department. Statista Research Department, https://www.statista.com/statistics/756924/pakistan-meat-consumption-per-capita-by-type / (2022, accessed 26 July 2023).
17. Sohaib M, Jamil F. An Insight of Meat Industry in Pakistan with Special Reference to Halal Meat: A Comprehensive Review. Korean Journal for Food Science of Animal Resources. 2017;37(3):329–341. https://doi.org/10.5851/kosfa.2017.37.3.329
18. Aujla KM, Sadiq N. Supply estimate and projection for poultry meat in Pakistan by the year 2030 AD. Pure and Applied Biology. 2018;7(2):460–465. https://doi.org/10.19045/bspab.2018.70057
19. Alsohaimi IH, Khan MR, Ali HM, Azam M. Emergence of mutagenic/carcinogenic heterocyclic amines in traditional Saudi chicken dishes prepared from local restaurants. Food and Chemical Toxicology. 2019;132:110677. https://doi.org/10.1016/j.fct.2019.110677
20. Bellamri M, Walmsley SJ, Turesky RJ. Metabolism and biomarkers of heterocyclic aromatic amines in humans. Genes and Environment. 2021;43:29. https://doi.org/10.1186/s41021-021-00200-7
21. National Cancer Institute. Nutritional Carcinogenesis. Qeios. 2020. https://doi.org/10.32388/DE0377
22. Bukowska B, Duchnowicz P, Tumer TB, Michałowicz J, Krokosz A. Precarcinogens in food – Mechanism of action, formation of DNA adducts and preventive measures. Food Control. 2023;152:109884. https://doi.org/10.1016/j.foodcont.2023.109884
23. Perveen I, Saleem Y, Qazi JI. Determination of Heterocyclic Amines in Ready to Eat Chicken Kabab Commercially Available from Pakistani Markets. Pakistan Journal Zoology. 2020;52(6):2027–2400. https://doi.org/10.17582/journal.pjz/20190509050501
24. Gross GA, Grüter A. Quantitation of mutagegnic/carcinogenic heterocyclic aromatic amines in food products. Journal of Chromatography A. 1992;592(1-2):271–278. https://doi.org/10.1016/0021-9673(92)85095-B
25. Messner C, Murkovic M. Evaluation of a new model system for studying the formation of heterocyclic amines. Journal of Chromatography B. 2004;802(1):19–26. https://doi.org/10.1016/j.jchromb.2003.11.015
26. OECD-FAO Agricultural Outlook 2022-2031. OECD; 2022. https://doi.org/10.1787/f1b0b29c-en
27. Bogdanović T, Pleadin J, Petričević S, Listeš E, Sokolić D, Marković K, *et al.* The occurrence of polycyclic aromatic hydrocarbons in fish and meat products of Croatia and dietary exposure. Journal of Food Composition and Analysis. 2019;75:49–60. https://doi.org/10.1016/j.jfca.2018.09.017
28. Sahin S, Ulusoy HI, Alemdar S, Erdogan S, Agaoglu S. The Presence of Polycyclic Aromatic Hydrocarbons (PAHs) in Grilled Beef, Chicken and Fish by Considering Dietary Exposure and Risk Assessment. Food Science of Animal Resources. 2020;40(5):675–688. https://doi.org/10.5851/kosfa.2020.e43
29. Carthew P, DiNovi M, Woodrow Setzer R. Application of the Margin of Exposure (MOE) approach to substances in food that are genotoxic and carcinogenic. Food and Chemical Toxicology. 2010;48:S98–S105. https://doi.org/10.1016/j.fct.2009.10.035
30. Zhang J, Empl MT, Schwab C, Fekry MI, Engels C, Schneider M, *et al.* Gut Microbial Transformation of the Dietary Imidazoquinoxaline Mutagen MeIQx Reduces Its Cytotoxic and Mutagenic Potency. Toxicological Sciences. 2017;159(1):266–276. https://doi.org/10.1093/toxsci/kfx132
31. Wei M, Wanibuchi H, Nakae D, Tsuda H, Takahashi S, Hirose M, *et al.* Low-dose carcinogenicity of 2-amino-3-methylimidazo [4,5-f] quinoline in rats: Evidence for the existence of no-effect levels and a mechanism involving $p21^{Cip/WAF1}$. Cancer Science. 2011;102(1):88–94. https://doi.org/10.1111/j.1349-7006.2010.01761.x
32. Benjamini Y, Braun H. John W. Tukey's contributions to multiple comparisons. The Annals of Statistics. 2002;30(6):1576–1594. https://doi.org/10.1214/aos/1043351247
33. Salmon CP, Knize MG, Felton JS, Zhao B, Seow A. Heterocyclic aromatic amines in domestically prepared chicken and fish from Singapore Chinese households. Food and Chemical Toxicology. 2006;44(4):484–492. https://doi.org/10.1016/j.fct.2005.08.022
34. Zaidi R, Rani Rawat P. Identification of Heterocyclic Amines in Indian Home Cooked and Commercially Available Meat Foods. Journal Nutrition and Food Sciences. 2011;1(3):1000107. https://doi.org/10.4172/2155-9600.1000107
35. Lu F, Kuhnle GK, Cheng Q. Vegetable oil as fat replacer inhibits formation of heterocyclic amines and polycyclic aromatic hydrocarbons in reduced fat pork patties. Food Control. 2017;81:113–125. https://doi.org/10.1016/j.foodcont.2017.05.043
36. Erdoğan B, Özdestan-Ocak Ö. Determination the effects of pumpkin and rosehip seed oils on heterocyclic aromatic amine formation in meatballs by high-performance liquid chromatography. Journal of Food Processing and Preservation. 2022;46(2):e16299. https://doi.org/10.1111/jfpp.16299

37. Jinap S, Mohd-Mokhtar MS, Farhadian A, Hasnol NDS, Jaafar SN, Hajeb P. Effects of varying degrees of doneness on the formation of Heterocyclic Aromatic Amines in chicken and beef satay. Meat Science. 2013;94(2):202–207. https://doi.org/10.1016/j.meatsci.2013.01.013
38. Jahurul MHA, Jinap S, Ang SJ, Abdul-Hamid A, Hajeb P, Lioe HN, et al. Dietary exposure to heterocyclic amines in high-temperature cooked meat and fish in Malaysia. Food Additives and Contaminants: Part A. 2010;27(8):1060–1071. https://doi.org/10.1080/19440041003801190
39. Omofuma OO, Steck SE, Olshan AF, Troester MA. The association between meat and fish intake by preparation methods and breast cancer in the Carolina Breast Cancer Study (CBCS). Breast Cancer Research and Treatment. 2022;193:187–201. https://doi.org/10.1007/s10549-022-06555-x
40. Zeng M, Wang J, Zhang M, Chen J, He Z, Qin F, *et al.* Inhibitory effects of Sichuan pepper (*Zanthoxylum bungeanum*) and sanshoamide extract on heterocyclic amine formation in grilled ground beef patties. Food Chemistry. 2018;239:111–118. https://doi.org/10.1016/j.foodchem.2017.06.097
41. Oz F, Kaya M. The inhibitory effect of black pepper on formation of heterocyclic aromatic amines in high-fat meatball. Food Control. 2011;22(3–4):596–600. https://doi.org/10.1016/j.foodcont.2010.10.010
42. Jain RB. Concentrations of selected heterocyclic aromatic amines among US population aged ≥6 years: data from NHANES 2013–2014. Environmental Science and Pollution Research. 2018;25:19859–19874. https://doi.org/10.1007/s11356-018-2210-0
43. Pouzou JG, Costard S, Zagmutt FJ. Probabilistic assessment of dietary exposure to heterocyclic amines and polycyclic aromatic hydrocarbons from consumption of meats and breads in the United States. Food and Chemical Toxicology. 2018;114:361–374. https://doi.org/10.1016/j.fct.2018.02.004
44. Sabally K, Sleno L, Jauffrit J-A, Iskandar MM, Kubow S. Inhibitory effects of apple peel polyphenol extract on the formation of heterocyclic amines in pan fried beef patties. Meat Science. 2016;117:57–62. https://doi.org/10.1016/j.meatsci.2016.02.040
45. Scientific Opinion of the Panel on Contaminants in the Food Chain on a request from the European Commission on Polycyclic Aromatic Hydrocarbons in Food. The EFSA Journal. 2008;724:1–114. https://doi.org/10.2903/j.efsa.2008.724
46. Rozentale I, Zacs D, Bartkiene E, Bartkevics V. Polycyclic aromatic hydrocarbons in traditionally smoked meat products from the Baltic states. Food Additives and Contaminants: Part B. 2018;11(2):138–145. https://doi.org/10.1080/19393210.2018.1440637
47. Duedahl-Olesen L, Aaslyng M, Meinert L, Christensen T, Jensen AH, Binderup M-L. Polycyclic aromatic hydrocarbons (PAH) in Danish barbecued meat. Food Control. 2015;57:169–176. https://doi.org/10.1016/j.foodcont.2015.04.012

ORCID IDs
Ishrat Perveen https://orcid.org/0009-0006-2243-1014
Nazia Koser https://orcid.org/0000-0003-2236-668X
Rozina Shahadat Khan https://orcid.org/0000-0001-7651-652X
Maryam Maqsood https://orcid.org/0000-0001-8515-5260
Syed Muhammad Aun https://orcid.org/0000-0001-8658-039X
Maria Fareed Siddiqui https://orcid.org/0000-0001-8515-5260
Yasar Saleem https://orcid.org/0000-0001-5799-5393
Naaz Abbas https://orcid.org/0000-0002-1284-2972
Shaista Nawaz https://orcid.org/0000-0001-8299-1423

Foods and Raw Materials. 2026;14(1)

ISSN 2308-4057 (Print)
ISSN 2310-9599 (Online)

Research Article
Open Access

Available online at http://jfrm.ru/en
https://doi.org/10.21603/2308-4057-2026-1-657
https://elibrary.ru/JOGQDD

Predictive analytics of cattle behavior using machine learning techniques: A case study

Khalid El Moutaouakil[1,*], Noureddine Falih[1], Karim Doumi[2]

[1] Sultan Moulay Slimane University, Beni Mellal, Morocco
[2] Mohammed V University, Rabat, Morocco

* e-mail: elmoutaouakil.kh@gmail.com

Received 08.12.2023; Revised 02.04.2024; Accepted 07.05.2024; Published online 30.12.2024

Abstract:
Livestock management is a critical aspect of agricultural sustainability and food security. Today, there is a pressing need for advanced tools in cattle behavior analysis to improve livestock welfare and productivity. We aimed to enhance cattle behavior classification by using accelerometers fitted in wearable collars. Deep learning techniques were employed to classify behavioral patterns in cattle such as feeding, moving, and lying. Ultimately, our study sought to improve livestock management practices, including the monitoring of health and overall well-being.

The study was conducted in a local barn, where cattle were outfitted with specially designed collars with accelerometer sensors. These sensors recorded intricate movements, facilitating the collection of comprehensive behavioral data. Deep learning algorithms were used to process and analyze the accelerometer data, enabling precise classification of various behaviors exhibited by the cattle.

Our results showed the effectiveness of AI-driven classification techniques in distinguishing cattle behaviors with a high degree of accuracy. Our findings underscore the potential of deep learning techniques in optimizing livestock management practices.

This research significantly advances livestock management by offering a simple continuous monitoring solution for cattle behavior. Deep learning techniques not only enhance our understanding of cattle behavior but also pave the way for intelligent systems that empower farmers to make informed decisions. By promoting healthier and more productive livestock, this research contributes to the broader goal of enhancing global food security and sustainability in the livestock industry.

Keywords: Precision agriculture, food security, livestock farming, cattle veterinary, accelerometer data, behavior classification, Convolutional Neural Networks

Please cite this article in press as: El Moutaouakil K, Falih N, Doumi K. Predictive analytics of cattle behavior using machine learning techniques: A case study. Foods and Raw Materials. 2026;14(1):26–36. https://doi.org/10.21603/2308-4057-2026-1-657

INTRODUCTION

Monitoring livestock behavior is a critical aspect of modern livestock management [1], offering a valuable means to detect health issues and ensure the overall well-being of the animals [2]. Cattle, like other domesticated livestock, exhibit distinct behavior patterns that can serve as early indicators of health problems [3]. Changes in behavior, such as reduced activity, changed feeding habits, or abnormal movements, can often signal underlying health issues [4], including illness, stress, or discomfort [5]. Recognizing these deviations in real-time is crucial, as it allows for timely intervention and veterinary care [6], potentially preventing the spread of diseases and reducing treatment costs [7]. By leveraging technology, such as accelerometer sensors, and employing artificial intelligence techniques, we can gain a deeper understanding of cattle behavior [8] and develop predictive models to promptly identify deviations from normal behavior [9].

Studies have successfully collected and analyzed data from cattle to identify and differentiate various behaviors such as standing, lying, walking, grazing, and ruminating [10]. This data provides valuable insights into animal activity patterns, time budgets, and potential health issues [11].

Machine learning algorithms have been employed to classify cattle behaviors [12] with high accuracy. These algorithms learn from labeled datasets, where video scene data is associated with specific behaviors based on visual observations or video recordings [13].

Copyright © 2024, El Moutaouakil *et al.* This is an open access article distributed under the terms of the Creative Commons Attribution 4.0 International License (https://creativecommons.org/licenses/by/4.0/), allowing third parties to copy and redistribute the material in any medium or format and to remix, transform, and build upon the material for any purpose, even commercially, provided the original work is properly cited and states its license.

Integrating accelerometer data or other sensors, such as GPS, gyroscopes, and magnetometers, can further enhance the accuracy and range of behavior classifications [14]. This allows for monitoring finer movements, tracking location, and identifying specific behaviors such as eating, drinking, and social interactions [15].

Accurate behavior monitoring helps optimize feeding, milking schedules, and environmental conditions, thus ultimately improving animal welfare, productivity, and profitability [16]. However, there are a number of challenges such as long-term sensor durability, data processing limitations, and ethical considerations [17].

Research on deep learning architectures and multimodal data fusion can improve accuracy and provide deeper insights [18]. The development of low-cost, lightweight, and long-lasting sensors will facilitate wider adoption [19]. Integrating behavior monitoring with precision livestock farming systems can further optimize resource allocation and improve overall farm management [20].

The emergence of deep learning has further revolutionized the field of cattle behavior recognition. Deep Neural Networks (DNNs) and Convolutional Neural Networks (CNNs) have demonstrated remarkable capabilities in extracting complex patterns from sensor data [21], leading to significant improvements in accuracy and performance. Notably, CNN models achieved 98% accuracy in classifying animal behaviors, highlighting the power of deep learning for analyzing more diverse activity patterns [22]. Additionally, using Long Short-Term Memory (LSTM) networks for analyzing time-series data proved highly accurate in identifying specific feeding behaviors [23], showcasing the potential of deep learning for exploring nuanced behavioral patterns.

Researchers have already explored the integration of video recordings, vocalizations, and physiological signals, to gain a comprehensive understanding of animal behavior and health [24]. This multimodal approach offers opportunities to analyze intricate aspects of well-being beyond simple activity levels. For instance, a study combined accelerometer and video data to identify lameness in dairy cows with 95% accuracy, which demonstrated the potential of this combined approach for detecting specific health issues [25]. Similarly, other researchers used acoustic signals and machine learning to detect respiratory diseases in cattle with 97% accuracy [26], highlighting the potential of analyzing vocalizations for early disease identification.

Several commercial solutions are now available that leverage the power of AI-driven behavior analysis to improve livestock management practices. These systems, such as Mootral, SmaXtec, and Calibrate, offer farmers real-time insights into animal activity, enabling them to optimize feeding schedules, monitor health, and improve overall well-being. This commercialization of AI technology signifies its growing impact on the livestock industry and its potential to revolutionize farming practices.

In this study, we used accelerometer sensors instead of video scenes for cattle behavior monitoring. Accelerometer sensors offer distinct advantages over video cameras. They provide non-intrusive, continuous monitoring of cattle behavior in real-time, capturing subtle changes and patterns without the need for extensive data storage. With lower power consumption, easy deployment, and reduced sensitivity to environmental conditions, accelerometer sensors are particularly suitable for outdoor settings. Focused data collection and the absence of visual images mitigate privacy concerns, making accelerometer sensors well-suited for agricultural and research applications. Additionally, they can be easily attached to cattle, allowing for efficient and cost-effective monitoring, especially in remote areas. Unlike monitoring through video scenes, accelerometer sensors do not require a lot of equipment and processing power. While accelerometer sensors excel in certain aspects, the choice between them and video cameras ultimately depends on the specific goals and requirements of the monitoring system.

Transforming raw data generated by accelerometer sensors into accurate predictions of actual behaviors in cattle involves several key steps. Initially, data is collected through wearable accelerometers which record motion and activity patterns. This raw sensor data is then preprocessed, which includes cleaning and filtering, to remove noise and ensure data quality [27]. The second step is extraction, where relevant characteristics of the data are identified and quantified, such as acceleration patterns during different activities [28]. Once the feature set is prepared, machine learning models, which often include supervised learning algorithms, are trained on labeled data by associating sensor readings with known cattle behaviors. The trained models are then applied to unlabeled data to predict behaviors in real-time. Regular model evaluation and refinement are crucial to enhance predictive accuracy and adapt to changing cattle behaviors or environmental conditions [29]. Finally, the predictions are translated into actionable insights for livestock managers, helping them make informed decisions for better cattle care and management practices [30].

We aimed to investigate the feasibility of using accelerometer data to automatically classify cattle behavior using the power of AI. Accelerometers are relatively inexpensive and non-invasive sensors that can be easily attached to cattle collars. This makes them a promising tool for continuous monitoring of cattle behavior [31]. By analyzing the acceleration patterns in cattle, we can identify distinct behavioral patterns associated with different activities, including feeding, ruminating, moving, and lying [32]. This information can be used to improve animal welfare, productivity, and health [33]. For example, by monitoring feeding patterns, we can identify cows that may be underfed or have feed of poor quality [34]. Additionally, by monitoring rumination time, we can identify cows that may be suffering from digestive problems [35]. Finally, by monitoring moving and lying patterns, we can identify cows that may be lame or stressed [36].

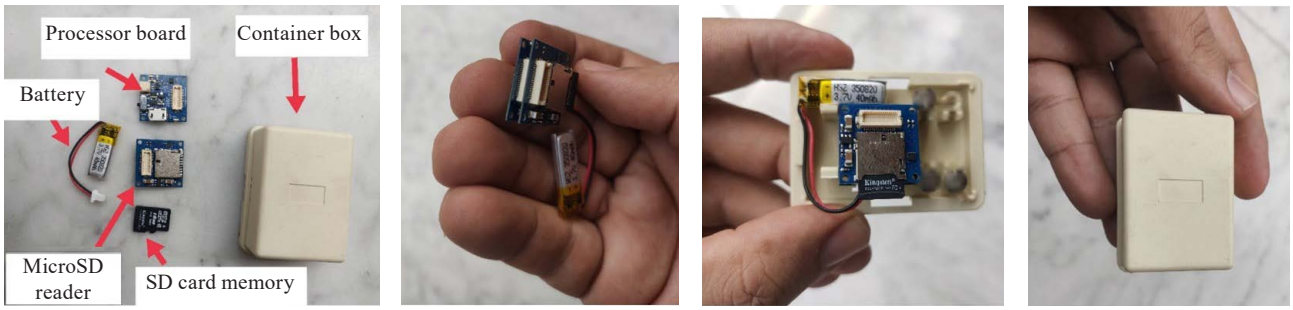

Figure 1 Data collection device components (a), the processor board and the MicroSD reader (b), the setup in the container box (c), and the closed container box (d)

Accelerometer-based monitoring systems have extensive potential applications [37]. They can significantly improve cattle welfare, productivity, and health [38], contributing to enhancing global food security [39].

STUDY OBJECTS AND METHODS

Data collection. We collected data in a local barn in the suburbs of Marrakesh city (Morocco) from 03 to 08 October 2023. There, six cows of multiple breeds were equipped with collars containing accelerometer sensors. These sensors recorded the acceleration and movement patterns of the cattle for five days. The cows moved freely while being filmed and the data was collected over this specific period to capture various behaviors such as moving, feeding, and other essential activities.

A small accelerometer and a data logger were employed for gathering cattle movement data. Specifically, we used a Tiny Zero processor board equipped with an Arduino-compatible microcontroller featuring a SAMD21 processor. The board included a Bosch BMA250 3-axis accelerometer. A Tiny Circuits MicroSD shield was used as a data logger. It stored data on a 16 GB MicroSD card, streamlining data collection. As a power source, we used a 290-mAh Tiny Circuits lithium polymer battery with compatible connectors.

The Tiny Zero processor board, which is central to the device's operation, offers a USB connectivity port, power management, and a battery charging capability in a compact 20×20-mm form. Also, the device features an accelerometer that integrates the low-power Bosch BMA250 3-axis accelerometer into the board without increasing its size. All 20 IO pins are readily available for use, making it a versatile platform for data collection.

This ultra-compact, lightweight, low-power, and cost-effective accelerometer is specifically tailored for our cattle behavior research. Its key features include a weight of less than 3 grams (excluding the battery and the box), a battery life ranging from 2 weeks to 1 month, and a total cost of under 60 United States dollars (USD). The device is constructed from easily attainable components and offers room for customization within the Arduino ecosystem. Figure 1 shows the components of this data collection device.



Figure 2 The data collection device attached to an adjustable neck-mounted collar (a) and its length (b)

Assembling the device is a straightforward process: the MicroSD shield is attached to the Tiny Zero processor board through the white connectors, the battery is connected to the designated battery connector on the processor board, and the MicroSD card is inserted into the SD slot on the MicroSD shield. When assembled, all the components are securely fixed inside the container plastic box.

The data collection devices with accelerometer sensors were attached to neck-mounted collars (Fig. 2).

Barn layout. The layout of the barn used for this study played a crucial role in the data collection process and in the interpretation of the observed cattle behaviors. The study took place in a rectangular barn with a total area of 600 square meters. The interior was divided into three sections: a freestall area housing 6 cows in individual stalls, a 200-square-meter runway for additional movement and interaction, and a dedicated feeding and watering area. Artificial lighting provided consistent brightness throughout the day. A ventilation system maintained the air quality and prevented overheating, which was particularly important during hot weather. Non-slip rubber matting covered the freestall area and runway for comfort and traction, while the feeding and watering area had a concrete floor for easy cleaning.

The layout encouraged linear movements between the stalls and the feeding area, facilitating data collection.

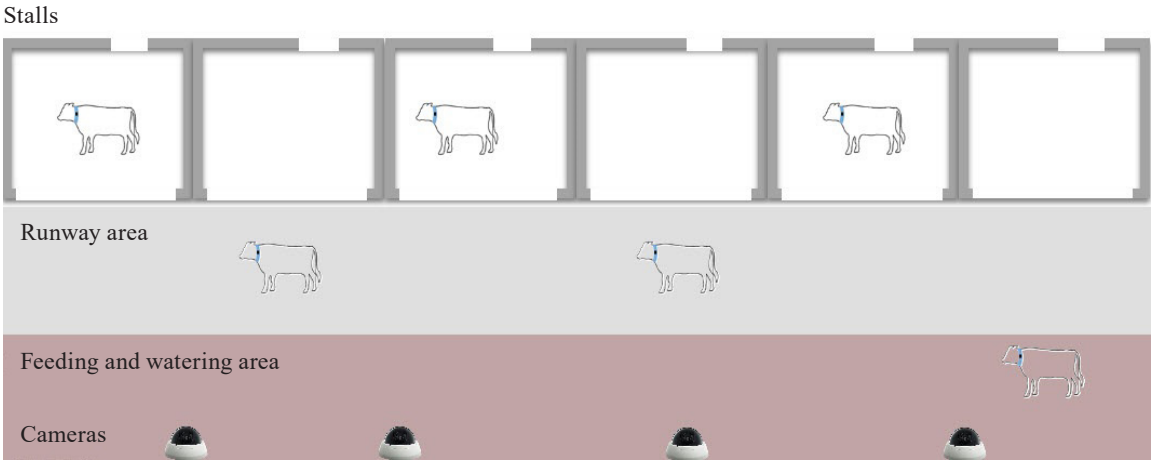

Figure 3 The overall layout of the barn

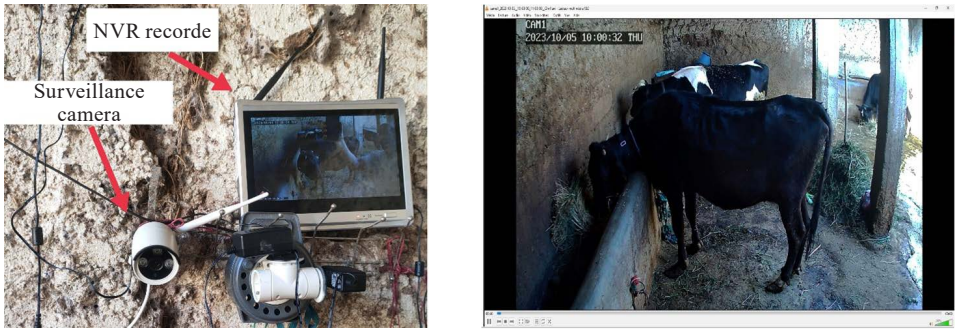

a b

Figure 4 Surveillance camera system components (a) and a screenshot from a recorded video file (b)



Figure 5 The three-axis neck-mounted accelerometer-based collar

The runway and the feeding area provided opportunities for social interactions important for mental health and natural behaviors. The comfortable stalls with mattresses encouraged lying down, providing ample data for identifying lying behavior patterns. The feeding area offered easy access to both hay and grain, allowing for efficient data collection on feeding duration and frequency.

While the barn size may have limited the range of observed movements and interactions, the controlled environment and carefully designed layout facilitated accurate and efficient data collection. Figure 3 shows the overall layout of the barn.

Surveillance system. For cattle surveillance, we used a HeimVision HM243 camera system kit consisting of four wireless cameras recording at 1080pixeis resolution, with a 110° angle of field and a night vision range of 50 ft. The Network Video Recorder (NVR) had a 12-inch monitor with a 500 GB hard drive for recording video scenes (Fig. 4). The cameras were set up to capture cattle behavior from different angles and record it 24 hours a day. Every camera generated a video file each hour and the NVR device saved it in the imbedded hard drive.

Accelerometer sensors. The data collection devices attached to the collars were mounted very tightly to the necks of the cows to ensure proper functioning of the accelerometers. Additionally, a counterweight was incorporated to guarantee the stability of the accelerometer. The data collection devices with three-axis accelerometers were fixed to the left side of the neck (Fig. 5). The X-axis sensed vertical (down-up) movement, the Y-axis detected horizontal (left-right) motion, and the Z-axis perceived forward-backward motion. The collars were worn by six cows for five days, with the tri-axial accelerometer set recording data at 10 Hz, 10 data points per second.

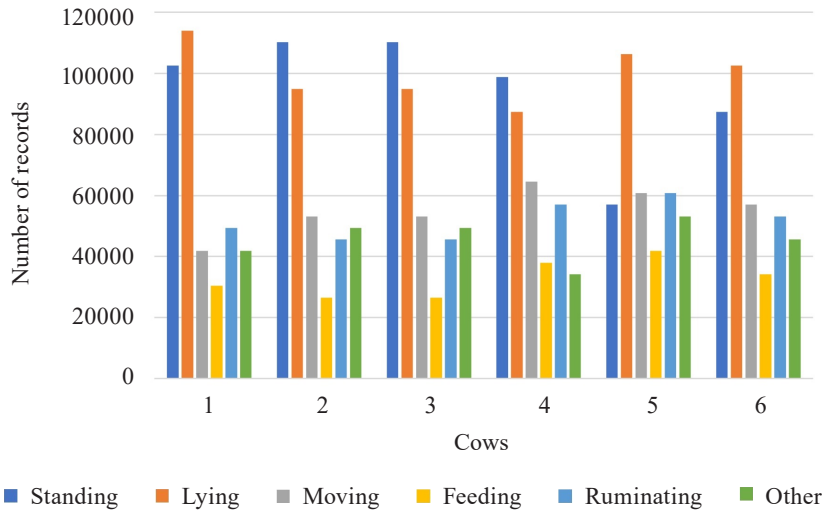

Figure 6 The frequency of recorded behaviors for each cow

Data labeling. The data was collected from the accelerometer sensors for five days (120 h per animal). Then, we selected 10 hours per each animal from 9 a.m. to 7 p.m. on those days when the cows displayed high activity and multiple behaviors. Our observations were meticulously recorded for each individual animal using the surveillance camera system. After retrieving the collars and uploading the data at the end of the trial, we used these recorded observations to label the corresponding accelerometer data.

For annotating the data, six observers were responsible for documenting the behaviors of the cows. Each observer was assigned to monitor one cow throughout the specified period, and the cows were observed sequentially. Five distinct behaviors were recorded: feeding, lying, standing, moving, and ruminating. Any behaviors not falling within these predefined categories (such as drinking, grooming, scratching, defecating, and urinating) were categorized as "other".

The labeling process presented certain challenges and was a labor-intensive task. Particularly, identifying rare behaviors could prove challenging, as they occurred infrequently and might easily be overlooked even by experienced observers. Additionally, distinguishing between periods of resting and rumination was often difficult, as there were instances of short resting episodes occurring during rumination, and vice versa, which were not always distinctly discernible. Furthermore, during periods of resting or rumination, whether standing or lying, cattle would occasionally exhibit subtle movements, such as head motions, ear flicks, or muscle twitches, which we meticulously observed and categorized as "other" behavior.

Dataset. We created a labeled dataset to classify cattle behavior by using the labeled accelerometer data. Particularly, we recorded the acceleration data from the 3-axis MEMS accelerometer at 10 Hz, with 10 data points per second. Each labeled segment represented a continuous period during which the cattle displayed a specific behavior.

Table 1 The total number and percentage of records for each behavior class

Behavior	Records	Percentage, %
Standing	524334	23
Lying	615522	27
Moving	341958	15
Feeding	205176	9
Ruminating	319158	14
Other	273564	12

Table 2 Dataset CSV file columns

Column Name	Description
Timestamp	The recorded date and time of the data are provided in ISO 8601 format
X	The acceleration measured in the x-direction
Y	The acceleration measured in the y-direction
Z	The acceleration measured in the z-direction
Classification	Behavior classification as labeled based on video scenes

Our choice of a window size of 10 data points per second was primarily guided by existing literature and our experimentation with various window sizes. This particular window size appears adequate for highlighting subtle distinctions between the considered behavior classes. Figure 6 shows the frequency of recorded behaviors for each cow. The total number and percentage of records for each behavior class is shown Table 1.

Every animal was given a distinct identifier XX ranging from 01 to 06. The generated accelerometer data was stored in CSV format in separate files named data-XX.csv, where XX represented the specific animal identifier. Each file consisted of four columns organized as shown in Table 2.

Data preprocessing. Raw data can be noisy and contain artifacts that can interfere with the performance of the Convolutional Neural Networks (CNNs). Therefore, the raw accelerometer data was preprocessed to

eliminate noise, filter out outliers, and convert it into a format suitable for deep learning. The preprocessing steps included filtering, segmentation, normalization, data augmentation, and feature extraction.

Filtering is used to remove noise and other unwanted signals from the data. For example, a high-pass filter is used to remove low-frequency signals such as drift, while a low-pass filter is used to remove high-frequency noise. For this purpose, we chose a median filter. This type of filter is effective in removing noise while preserving the overall shape of the signal.

Segmentation is used to divide the data into smaller, more manageable chunks. It is helpful for CNN models, which are typically trained on batches of data. We applied sliding window segmentation that divides the data into overlapping windows of a fixed length. This is a common approach for time series data, as it allows the CNN model to learn from both the current data point and the previous data points.

Normalization is used to scale the data so that all the features have a similar range of values. This can help the CNN model to learn more effectively. For this reason, we chose standard score normalization. This type of normalization subtracts the mean from each data point and then divides it by the standard deviation.

We used a data augmentation technique called temporal jittering. This technique involves randomly shifting the data in time. It helps improve the robustness of the CNN model to noise and variations in the data.

Feature extraction is used to extract meaningful features from the data. This helps the CNN model to learn more complex patterns in the data. For that, we extracted both time domain and frequency domain features. Time domain features are calculated directly from the accelerometer data, such as the mean, standard deviation, as well as maximum and minimum values. Frequency domain features are calculated from the Fourier transform of the accelerometer data, such as the power spectral density and the dominant frequency.

Once the data was preprocessed, we fed it to the CNN model for classification purposes. The details on the data collection, labeling, preprocessing, and behavior classification phases are shown in Fig. 7.

Behavior classification. We developed an advanced Convolutional Neural Network (CNN) model architecture to classify cattle behavior (Table 3). The choice of an architecture for a particular application depends on the specific dataset and requirements. The kernel sizes and stride lengths can be adjusted to extract different levels of features from the accelerometer data. The number

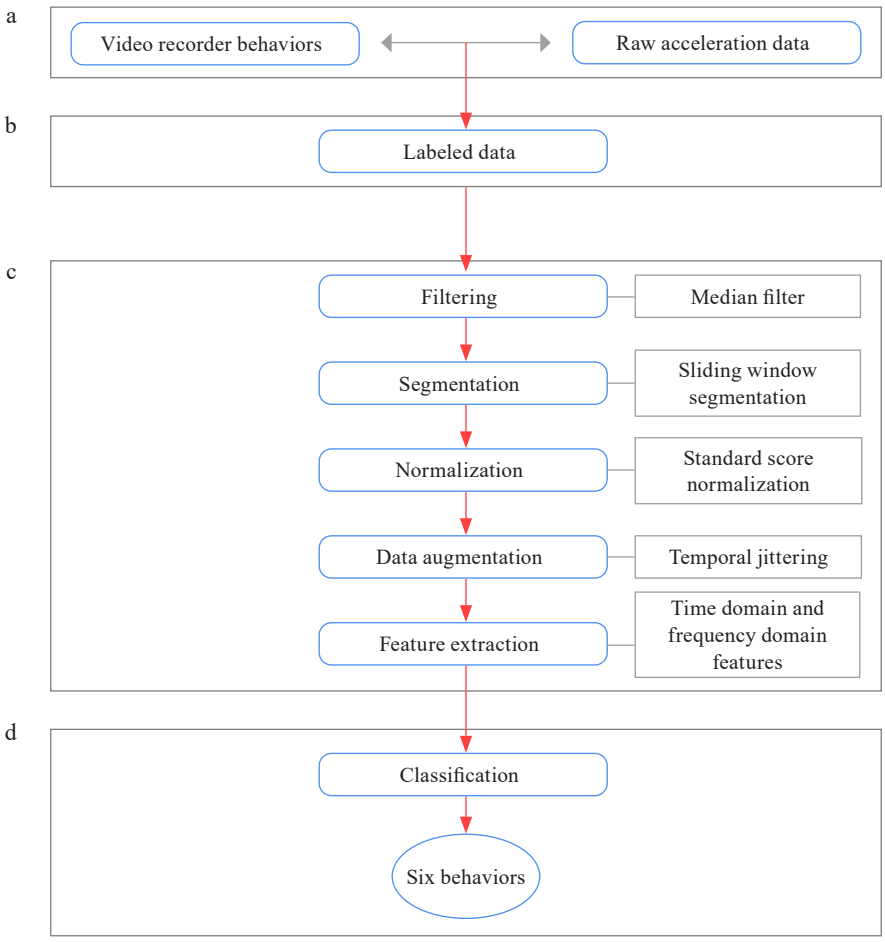

Figure 7 Data collection phase (a), data labeling phase (b), data preprocessing phase (c), and behavior classification phase (d) Segmentation

Table 3 CNN model architecture

Layer	Configuration	Output Shape
Input	(36000, 3)	(36000, 3)
Conv1D_1	filters: 320	(36000, 320)
BatchNorm_1		(36000, 320)
Activation_1	ReLU	(36000, 320)
MaxPooling1D_1	pool_size: 2	(18000, 320)
Conv1D_2	filters: 205, 120	(18000, 205, 120)
BatchNorm_2		(18000, 205, 120)
Activation_2	ReLU	(18000, 205, 120)
MaxPooling1D_2	pool_size: 2	(9000, 205, 120)
Flatten		(1846, 400)
Dense_1	units: 1024	1024
BatchNorm_3		1024
Activation_3	ReLU	1024
Dropout_1	dropout: 0.5	1024
Dense_2	units: 512	(512)
BatchNorm_4		(512)
Activation_4	ReLU	(512)
Dropout_2	dropout: 0.5	(512)
Output	units: 6	(6)

of convolutional layers and dense layers can also be adjusted to achieve the desired trade-off between accuracy and complexity. The dropout layers can be used to reduce overfitting. The Softmax activation function is used in the output layer to produce a probability distribution for each of the target classes.

Input represents the input layer with a shape (sequence_length, num_channels), where sequence length is the length of the time series data, and num channels is the number of channels in the input data. Conv1D is the convolutional layer with a specified number of filters. BatchNorm is a batch normalization layer to normalize the activations of the previous layer. Activation is the activation function, typically ReLU (Rectified Linear Unit). MaxPooling1D is the max pooling layer to down-sample the spatial dimensions. Flatten is used to flatten the input to a one-dimensional tensor. Dense is a fully connected layer with a specified number of units. Dropout is a dropout layer to prevent overfitting by randomly setting a fraction of input units to zero during training. Output is the output layer with the number of units equal to the number of classes for classification.

Performance evaluation. To evaluate the Convolutional Neural Network (CNN) model for cattle behavior classification, we used the Accuracy, Precision, Recall, and F1-score metrics, as defined in Table 4.

TP is the true positive, TN is the true negative, FP is the false positive, and FN is the false negative values.

In addition to the above metrics, we also tested our model using a confusion matrix. The confusion matrix shows the number of correct and incorrect predictions for each class. It can be used to identify any classes that the model is struggling to classify correctly.

RESULTS AND DISCUSSION

Our experiments demonstrated that deep neural networks, particularly Convolutional Neural Networks (CNNs), outperformed other algorithms in classifying cattle behavior [40]. Our CNN-based model achieved an overall accuracy of 97.99% in distinguishing different behaviors. Figure 8 shows the model performance during training and validation for 30 epochs.

Our results proved that the current model can be used as a real-time monitoring system that can process accelerometer data and provide instantaneous feedback on cattle behavior. This system can be integrated into the farm's infrastructure, enabling farmers to make informed decisions promptly. Table 5 shows the results of the evaluation metrics for each class.

According to the confusion matrix (Fig. 9), the model was good at classifying the cattle that were lying, moving, or standing. However, it was more likely to misclassify the cattle that were ruminating or feeding. This might be because these behaviors are more similar to each other than they are to the other behaviors.

The use of AI-driven approaches, specifically CNNs, to classify cattle behaviors based on accelerometer data presents a significant advancement in the field of precision livestock farming. Our results indicate a high level of accuracy indistinguishing between distinct behaviors such as standing, lying, moving, feeding, ruminating, and others, showcasing the potential of this technology for real-time monitoring of cattle activities in a barn environment.

The success of our CNN-based model in accurately classifying cattle behaviors is a testament to the robustness of deep learning algorithms in capturing complex patterns inherent in accelerometer data. The model's ability to differentiate these fundamental behaviors is crucial for understanding the daily activities and well-being of cattle, providing valuable insights for herd management and animal welfare.

However, a notable challenge emerged in the classification of feeding and ruminating behaviors. The model demonstrated a higher likelihood of misclassifying these behaviors, which can be attributed to the inherent similarities between them. Feeding and ruminating share common movement patterns and postures, making it more challenging for the algorithm to distinguish between

Table 4 Evaluation metrics

Evaluation metric	**Definition**	Equation
Accuracy	The percentage of predictions that are correct.	(TP + TN) / (TP + TN + FP + FN)
Precision	The percentage of positive predictions that are correct.	TP / (TP + FP)
Recall	The percentage of all positive cases that are correctly identified.	TP / (TP + FN)
F1 score	A harmonic mean of precision and recall.	2* (Precision * Recall) / (Precision + Recall)

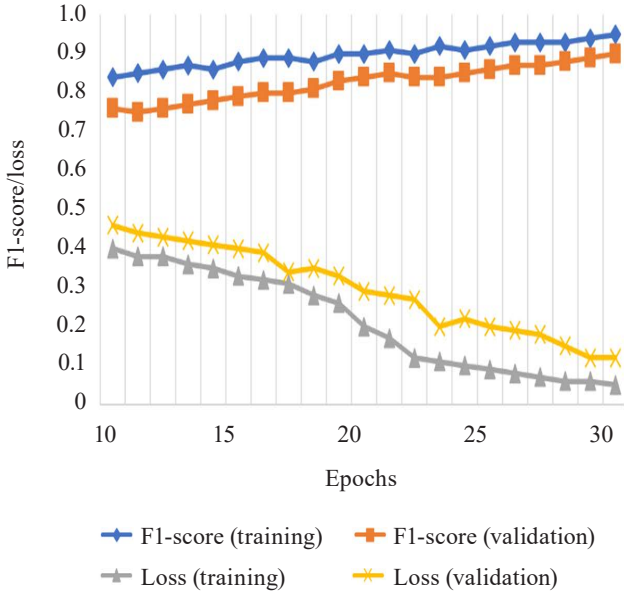

Figure 8 Model performance during training and validation

Table 5 Model performance indicators

Class	Accuracy, %	Precision, %	Recall, %	F1 score, %
Standing	99.20	99.50	99.00	99.91
Lying	99.30	99.80	99.91	96.98
Moving	99.00	99.10	96.14	99.86
Feeding	94.03	94.10	94.30	94.36
Ruminating	97.05	97.30	97.42	97.53
Other	99.35	96.55	99.22	99.83

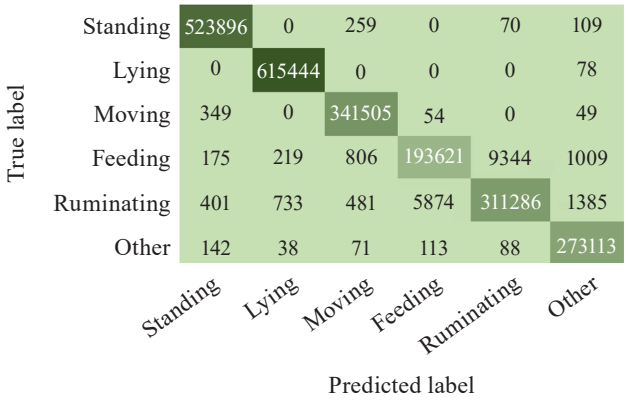

Figure 9 Confusion matrix

them accurately. This suggests that further refinement of the model may be necessary, potentially incorporating additional features or fine-tuning the network architecture to enhance the discrimination between these closely related behaviors.

One potential avenue for improvement could involve incorporating temporal information into the model. By considering the sequential nature of cattle behaviors, the model may gain a better understanding of the transitions between feeding and ruminating, improving its ability to discern subtle differences. Additionally, a larger and more diverse dataset, including variations in feeding and ruminating behaviors, could contribute to a more comprehensive training of the model, potentially addressing the observed misclassification.

Despite the challenges encountered in specific behavior classifications, our study highlights the overall efficiency of AI-powered approaches in cattle behavior monitoring. The implementation of wearable accelerometer devices offers a non-invasive and continuous monitoring solution, providing farmers and researchers with valuable insights into the daily activities and health status of individual animals within a herd. These devices are much better than video cameras, which require continuous monitoring, use a large bandwidth, and need a lot of processing power.

Deep learning models enable continuous monitoring of animal behavior, providing a comprehensive understanding of activity patterns and potential changes. This eliminates the need for manual observation and reduces subjectivity in data collection.

AI-based solutions can be easily scaled to monitor large herds of cattle, which makes them ideal for commercial farms and large-scale operations.

By continuously tracking behavior patterns, AI models can identify subtle changes indicative of health problems or stress. This enables early intervention and treatment, potentially improving animal welfare and preventing significant losses.

Insights gained from behavior analysis can be used to optimize feeding schedules, housing conditions, and other management practices. This can ultimately improve production efficiency and food security in addition to animal well-being.

Overall, our findings underscore the potential of AI-powered classification using wearable accelerometer devices in enhancing the understanding of cattle behaviors. While the model excels in distinguishing between certain activities, addressing the challenges associated with subtle behavioral nuances, such as feeding and ruminating, remains an area for future research and refinement. As technology continues to evolve, the integration of advanced machine learning techniques holds promise for revolutionizing precision livestock farming and promoting the welfare of cattle in agricultural settings. The ability to monitor cattle behavior in real-time not only enhances animal welfare but also increases the farm's efficiency. This technology can aid in detecting health issues, optimizing feeding schedules, and reducing labor costs.

CONCLUSION

In this study, we presented an innovative approach to classifying cattle behavior based on accelerometer data collected from the collars equipped with specialized sensors. Machine learning techniques, particularly deep neural networks, proved to be highly effective in accurately classifying different behaviors. These techni-

ques have significant potential for real-time monitoring and decision support in cattle farming. As we continue to refine and expand this technology, it promises to revolutionize the way cattle farming is conducted, benefitting both animals and farmers.

CONTRIBUTION

The authors were equally involved in writing the manuscript and are equally responsible for plagiarism.

CONFLICT OF INTEREST

The authors declare no conflict of interest regarding the publication of this article.

ACKNOWLEDGEMENTS

This study is an integral part of an ongoing research on digital agriculture conducted collaboratively by a team of experts affiliated with the LIMATI Laboratory at Sultan Moulay Slimane University in Morocco.

REFERENCES

1. Akhigbe BI, Munir K, Akinade O, Akanbi L, Oyedele LO. IoT Technologies for Livestock Management: A Review of Present Status, Opportunities, and Future Trends. Big Data and Cognitive Computing. 2021;5(1):10. https://doi.org/10.3390/bdcc5010010
2. Buller H, Blokhuis H, Lokhorst K, Silberberg M, Veissier I. Animal Welfare Management in a Digital World. Animals. 2020;10(10):1779. https://doi.org/10.3390/ani10101779
3. Sahu BK, Parganiha A, Pati AK. Behavior and foraging ecology of cattle: A review. Journal of Veterinary Behavior. 2020;40:50–74. https://doi.org/10.1016/j.jveb.2020.08.004
4. Džermeikaitė K, Bačėninaitė D, Antanaitis R. Innovations in Cattle Farming: Application of Innovative Technologies and Sensors in the Diagnosis of Diseases. Animals. 2023;13(5):780. https://doi.org/10.3390/ani13050780
5. Neethirajan S. Transforming the Adaptation Physiology of Farm Animals through Sensors. Animals. 2020;10(9):1512. https://doi.org/10.3390/ani10091512
6. Qiao Y, Kong H, Clark C, Lomax S, Su D, Eiffert S, *et al.* Intelligent Perception-Based Cattle Lameness Detection and Behaviour Recognition: A Review. Animals. 2021;11(11):3033. https://doi.org/10.3390/ani11113033
7. Neethirajan S, Kemp B. Digital Livestock Farming. Sensing and Bio-Sensing Research. 2021;32:100408. https://doi.org/10.1016/j.sbsr.2021.100408
8. Benaissa S, Tuyttens FAM, Plets D, Martens L,Vandaele L, Joseph W, *et al.* Improved cattle behaviour monitoring by combining Ultra-Wideband location and accelerometer data. Animal. 2023;17(4):100730. https://doi.org/10.1016/j.animal.2023.100730
9. Wagner N, Antoine V, Mialon M-M, Lardy R, Silberberg M, Koko J, *et al.* Machine learning to detect behavioural anomalies in dairy cows under subacute ruminal acidosis. Computers and Electronics in Agriculture. 2020;170:105233. https://doi.org/10.1016/j.compag.2020.105233
10. Balasso P, Marchesini G, Ughelini N, Serva L, Andrighetto I. Machine Learning to Detect Posture and Behavior in Dairy Cows: Information from an Accelerometer on the Animal's Left Flank. Animals. 2021;11(10):2972. https://doi.org/10.3390/ani11102972
11. Smith JE, Pinter-Wollman N. Observing the unwatchable: Integrating automated sensing, naturalistic observations and animal social network analysis in the age of big data. Journal of Animal Ecology. 2021;90(1):62–75. https://doi.org/10.1111/1365-2656.13362
12. Jabir B, Rabhi L, Falih N. RNN- and CNN-based weed detection for crop improvement: An overview. Foods and Raw Materials. 2021;9(2):387–396. https://doi.org/10.21603/2308-4057-2021-2-387-396
13. Arablouei R, Wang L, Currie L, Yates J, Alvarenga FAP, Bishop-Hurley GJ. Animal behavior classification via deep learning on embedded systems. Computers and Electronics in Agriculture. 2023;207:107707. https://doi.org/10.1016/j.compag.2023.107707
14. Allahbakhshi H, Conrow L, Naimi B, Weibel R. Using Accelerometer and GPS Data for Real-Life Physical Activity Type Detection. Sensors. 2020;20(3):588. https://doi.org/10.3390/s20030588
15. Heydarian H, Adam M, Burrows T, C Collins, Rollo ME. Assessing Eating Behaviour Using Upper Limb Mounted Motion Sensors: A Systematic Review. Nutrients. 2019;11(5):1168. https://doi.org/10.3390/nu11051168
16. Hassan M, Park J-H, Han M-H. Enhancing Livestock Management with IoT-based Wireless Sensor Networks: A Comprehensive Approach for Health Monitoring, Location Tracking, Behavior Analysis, and Environmental Optimization. Journal of Sustainable Urban Futures. 2023;13(6):34–46. https://neuralslate.com/index.php/Journal-of-Sustainable-Urban-Fut/article/view/18
17. Wang W-H, Hsu W-S. Integrating Artificial Intelligence and Wearable IoT System in Long-Term Care Environments. Sensors. 2023;23(13):5913. https://doi.org/10.3390/s23135913

18. Cao R, Tu W, Yang C, Li Q, Liu J, Zhu J, *et al.* Deep learning-based remote and social sensing data fusion for urban region function recognition. ISPRS Journal of Photogrammetry and Remote Sensing. 2020;163:82–97. https://doi.org/10.1016/j.isprsjprs.2020.02.014
19. Cabezas J, Yubero R, Visitación B, Navarro-García J, Algar MJ, Cano EL, *et al.* Analysis of Accelerometer and GPS Data for Cattle Behaviour Identification and Anomalous Events Detection. Entropy. 2022;24(3):336. https://doi.org/10.3390/e24030336
20. Monteiro A, Santos S, Gonçalves P. Precision Agriculture for Crop and Livestock Farming – Brief Review. Animals. 2021;11(8):2345. https://doi.org/10.3390/ani11082345
21. Liu Y, Pu H, Sun D-W. Efficient extraction of deep image features using convolutional neural network (CNN) for applications in detecting and analysing complex food matrices. Trends in Food Science and Technology. 2021;113:193–204. https://doi.org/10.1016/j.tifs.2021.04.042
22. Chen C, Zhu W, Norton T. Behaviour recognition of pigs and cattle: Journey from computer vision to deep learning. Computers and Electronics in Agriculture. 2021;187:106255. https://doi.org/10.1016/j.compag.2021.106255
23. Tan HX, Aung NN, Tian J, Chua MCH, Yang YO. Time series classification using a modified LSTM approach from accelerometer-based data: A comparative study for gait cycle detection. Gait and Posture. 2019;74:128–134. https://doi.org/10.1016/j.gaitpost.2019.09.007
24. Dávila-Montero S, Dana-Lê JA, Bente G, Hall AT, Mason AJ. Review and Challenges of Technologies for Real-Time Human Behavior Monitoring. IEEE Transactions on Biomedical Circuits and Systems. 2021;15(1):2–28. https://doi.org/10.1109/TBCAS.2021.3060617
25. Lemmens L, Schod K, Fuerst-Walt B, Schwarzenbacher H, Egger-Danner C, Linke K, *et al.* The Combined Use of Automated Milking System and Sensor Data to Improve Detection of Mild Lameness in Dairy Cattle. Animals. 2023;13(7):1180. https://doi.org/10.3390/ani13071180
26. Volkmann N, Kulig B, Hoppe S, Stracke J, Hensel O, Kemper N. On-farm detection of claw lesions in dairy cows based on acoustic analyses and machine learning. Journal of Dairy Science. Journal of Dairy Science. 2021;104(5):5921–5931. https://doi.org/10.3168/jds.2020-19206
27. Daneault J-F, Vergara-Diaz G, Parisi F, Admati C, Alfonso C, Bertoli M, *et al.* Accelerometer data collected with a minimum set of wearable sensors from subjects with Parkinson's disease. Scientific Data. 2021;8:48. https://doi.org/10.1038/s41597-021-00830-0
28. Qiu S, Zhao H, Jiang N, Wang Z, Liu L, An Y, *et al.* Multi-sensor information fusion based on machine learning for real applications in human activity recognition: State-of-the-art and research challenges. Information Fusion. 2022;80:241–265. https://doi.org/10.1016/j.inffus.2021.11.006
29. Rashamo VP, Sejian V, Pragna P, Lees AM, Bagath M, Krishnan G, *et al.* Prediction models, assessment methodologies and biotechnological tools to quantify heat stress response in ruminant livestock. International Journal of Biometeorology. 2019;63:1265–1281. https://doi.org/10.1007/s00484-019-01735-9
30. El Moutaouakil K, Jdi H, Jabir B, Falih N. Digital Farming: A Survey on IoT-based Cattle Monitoring Systems and Dashboards. AGRIS on-line Papers in Economics and Informatics. 2023;15(2):31–39. https://doi.org/10.7160/aol.2023.150203
31. El Moutaouakil K, Falih N. A design of a smart farm system for cattle monitoring. Indonesian Journal of Electrical Engineering and Computer Science. 2023;32(2):857–864. https://doi.org/10.11591/ijeecs.v32.i2.pp857-864
32. Farooq MS, Sohail OO, Abid A, Rasheed S. A Survey on the Role of IoT in Agriculture for the Implementation of Smart Livestock Environment. IEEE Access. 2022;10:9483–9505. https://doi.org/10.1109/ACCESS.2022.3142848
33. Cabrera VE, Fadul-Pacheco L. Future of dairy farming from the Dairy Brain perspective: Data integration, analytics, and applications. International Dairy Journal. 2021;121:105069. https://doi.org/10.1016/j.idairyj.2021.105069
34. Herlin A, Brunberg E, Hultgren J, Högberg N, Rydberg A, Skarin A. Animal Welfare Implications of Digital Tools for Monitoring and Management of Cattle and Sheep on Pasture. Animals. 2021;11(3):829. https://doi.org/10.3390/ani11030829
35. Rial C, Laplacette A,Caixeta L, Florentino C, Peña-Mosca F, Giordano JO. Metabolic-digestive clinical disorders of lactating dairy cows were associated with alterations of rumination, physical activity, and lying behavior monitored by an ear-attached sensor. Journal of Dairy Science. 2023;106(12):9323–9344. https://doi.org/10.3168/jds.2022-23156
36. Fan B, Bryant R, Greer A. Behavioral Fingerprinting: Acceleration Sensors for Identifying Changes in Livestock Health. Multidisciplinary Scientific Journal. 2022;5(4):435–454. https://doi.org/10.3390/j5040030
37. Tran D-N, Nguyen TN, Khanh PCP, Tran D-T. An IoT-Based Design Using Accelerometers in Animal Behavior Recognition Systems. IEEE Sensors Journal. 2022;22(18):17515–17528. https://doi.org/10.1109/JSEN.2021.3051194

38. Chapa JM, Maschat K, Iwersen M, Baumgartner J, Drillich M. Accelerometer systems as tools for health and welfare assessment in cattle and pigs – A review. Behavioural Processes. 2020;181:104262. https://doi.org/10.1016/j.beproc.2020.104262
39. Danso-Abbeam G, Dagunga G, Ehiakpor DS, Ogundeji AA, Setsoafia ED, Awuni JA. Crop–livestock diversification in the mixed farming systems: implication on food security in Northern Ghana. Agriculture and Food Security. 2021;10:35. https://doi.org/10.1186/s40066-021-00319-4
40. Borges Oliveira DA, Ribeiro Pereira LG, Bresolin T, Pontes Ferreira RE, Reboucas Dorea JR. A review of deep learning algorithms for computer vision systems in livestock. Livestock Science. 2021;253:104700. https://doi.org/10.1016/j.livsci.2021.104700

ORCID IDs
Khalid El Moutaouakil https://orcid.org/0000-0003-2589-5616
Noureddine Falih https://orcid.org/0000-0002-1418-3173
Karim Doumi https://orcid.org/0000-0003-0792-7338

Foods and Raw Materials. 2026;14(1)

ISSN 2308-4057 (Print)
ISSN 2310-9599 (Online)

Research Article
Open Access

Available online at http://jfrm.ru/en
https://doi.org/10.21603/2308-4057-2026-1-655
https://elibrary.ru/YEKYYG

Enhancing lowland rice physiology with integrated nitrogen nutrient sources in Nigeria's derived savannah

Olumayowa Joseph Iyanda[1,*], Akeem Abdulai Oyekanmi[2], Mufutau Olaoye Atayese[2], Christopher Adejuyigbe[2], Ayomide Afolabi[2]

[1] Afe Babalola University, Ado-Ekiti, Nigeria
[2] Federal University of Agriculture, Abeokuta, Nigeria

* e-mail: iyandamayojo@abuad.edu.ng

Received 29.11.2023; Revised 27.05.2024; Accepted 04.06.2024; Published online 30.01.2025

Abstract:
Nitrogen is an essential nutrient for optimal rice growth and yield. Many Nigerian rice fields encounter difficulties in their production process because of insufficient nitrogen in the soil leading to reduced crop yields. However, the sole reliance on expensive inorganic nitrogen fertilizers is economically challenging for small farmers in Nigeria's derived savannah. Therefore, integrated approaches to nutrient management have been put into practice to reduce the adverse effects of climate change and improve crop productivity in lowland rice cultivation. We aimed to investigate the impact of integrated nutrient inputs on the performance of NERICA L-34 and ARICA 3 rice varieties during the years 2017, 2018, and 2019.

Various treatments were administered, namely 100 kg of nitrogen/ha (NPK), 75 kg/ha (NPK) + 25 kg/ha (manure), 50 kg/ha (NPK) + 50 kg/ha (manure), 25 kg/ha (NPK) + 75 kg/ha (manure), and 100 kg/ha (manure). A control group was samples without fertilizers. Key physiological parameters were assessed, including partial factor productivity, nitrogen uptake, nitrogen utilization efficiency, nitrogen internal utilization efficiency, physiological efficiency, recovery efficiency, total leaf area index, chlorophyll content, as well as root fresh and dry weights. Our research followed a randomized complete block design with a split-plot arrangement, replicated three times. The data underwent analysis of variance and the Duncan multiple range test (with a significance level set at $p \leq 0.05$), and GENSTAT was used to compare the physiological traits of the rice varieties.

Our findings revealed that the combination of 75 kg/ha (NPK, inorganic) and 25 kg/ha (manure, organic) significantly enhanced nutrient recovery and uptake in the NERICA L-34 rice variety, resulting in improved nitrogen absorption. While the ARICA 3 variety consistently exhibited higher chlorophyll content, especially with the application of 100 kg nitrogen/ha (organic), NERICA L-34 displayed superior overall nutrient absorption, recovery, and nitrogen utilization. Therefore, we recommend that rice farmers prioritize cultivating NERICA L-34 for its high productivity and potential for sustainable rice farming.

Our findings can also guide farmers towards feasible integrated soil fertility management practices to enhance nutrient utilization efficiency, reduce environmental impact, and contribute to sustainable rice production in the derived savannah region of Nigeria.

Keywords: Physiology, lowland, rice productivity, rice varieties, climate change, fertilizers

Please cite this article in press at: Iyanda OJ, Oyekanmi AA, Atayese MO, Adejuyigbe C, Afolabi A. Enhancing lowland rice physiology with integrated nitrogen nutrient sources in Nigeria's derived savannah. Foods and Raw Materials. 2026;14(1):37–51. https://doi.org/10.21603/2308-4057-2026-1-655

A preprint of the manuscript for this article was published on the SSRN. See a preprint at https://ssrn.com/abstract=4517620 or https://doi.org/10.2139/ssrn.4517620

INTRODUCTION

In Nigeria, rice productivity is hindered by low nitrogen availability in soils, impacting the farmers' livelihoods and food security [1]. Climate change exacerbates these challenges, calling for sustainable solutions to enhance crop resilience and productivity [2]. The integration of nutrient management approaches, which involve a combination of synthetic fertilizers and organic compost, holds promise for enhancing nutrient absorption and rice growth [3]. The physiology of lowland rice varieties is closely linked to nitrogen supply, which influences their growth and yield [4]. Efficient nitrogen utilization and uptake systems are vital for optimal grain output [5]. Such factors as water availability

Copyright © 2025, Iyanda *et al.* This is an open access article distributed under the terms of the Creative Commons Attribution 4.0 International License (https://creativecommons.org/licenses/by/4.0/), allowing third parties to copy and redistribute the material in any medium or format and to remix, transform, and build upon the material for any purpose, even commercially, provided the original work is properly cited and states its license.

and nitrogen levels affect the nutrient uptake by the rice plant [6]. Understanding these dynamics is crucial for devising effective strategies to address food security concerns [7]. The enhancement of soil structure through the use of organic compost creates a more favorable setting for root growth and the soil's ability to retain water [8]. This study aimed to evaluate how combined sources of nitrogen nutrients influence the physiological characteristics of lowland rice varieties. We sought to compare how these varieties perform under various nutrient management approaches and, subsequently, to offer valuable knowledge and practical suggestions for promoting sustainable rice cultivation and food security in Nigeria's derived savannah environment.

The influence of fertilizers on physiological parameters. The application of chemical fertilizers, particularly nitrogen, stimulates vigorous vegetative growth in rice plants; however, their excessive usage may result in diminished grain production [9]. Split nitrogen application based on crop needs can mitigate this effect [6]. However, overusing chemical fertilizers raises concerns about soil toxicity [10]. Root morphology and soil pH play crucial roles in nutrient uptake and rice growth [6]. Organic manure application over time improves rice yield and soil health [11]. Nutrient release synchronization by organic fertilizers reduces the need for inorganic fertilizers and enhances nitrogen use efficiency [12]. Nutritional physiology research, which uses the SPAD meter, shows that organic and inorganic fertilizers outperform chemical fertilizers [13]. Rice growth and yield are influenced by such factors as leaf area, nitrogen availability, and integrated nutrient management [14]. Root characteristics affect water and nutrient uptake [15]. Better root development leads to increased nutrient absorption and carbohydrate translocation [16]. Root systems are vital for nutrient and water uptake, as well as plant anchorage [17].

The system of rice intensification. The System of Rice Intensification (SRI) provides valuable insights into how rice plants respond to different soil conditions and adapt their roots. It has the potential to enhance crop production by boosting root and rhizosphere activity [18]. SRI-grown plants exhibit stronger stems, flood-resistant roots, and increased drought resistance due to better root establishment and reduced transplanting shock, leading to earlier maturity [19]. Direct measurements confirm that SRI practices result in greater and deeper root growth, facilitating enhanced nutrient uptake throughout the crop cycle compared to traditional flooding methods [20]. SRI management practices also promote larger root systems, making plants more resilient to both biotic and abiotic stresses, and creating favorable conditions for beneficial soil microorganisms [21]. The use of organic fertilizers further boosts root growth, nutrient uptake, and stress resistance in SRI-grown rice [22].

Nitrogen use efficiency in lowland rice varieties. Rice possesses two distinct uptake systems for nitrate (NO_3^-) and ammonium (NH_4^+), consisting of a high-affinity transport system (HATS) and a low-affinity transport system (LATS) [23]. Additionally, rice can absorb NO_3^- and NH_4^+ resulting from ammonium oxidation in the rhizosphere, facilitated by oxygen release from root aerenchyma [24]. This increased nutrient availability and improved growth conditions lead to enhanced physiological development and grain yield [25]. In modern agriculture, the application of nitrogen fertilizers is crucial for achieving high crop yields [26]. However, it often leads to the loss of excess reactive nitrogen to the environment, posing risks to air and water quality, as well as ecosystems. Nitrate (NO_3^-) losses through leaching can contaminate drinking water and contribute to eutrophication in freshwater and marine ecosystems, particularly during periods of high drainage rates [27]. Rice roots have two Casparian strips on the exodermis and endodermis, along with aerenchyma forming in mature root zones [28]. The establishment of a large root system early in the growth period is critical for effective nitrogen uptake [29]. Direct seeding of rice results in more panicles per square meter, attributed to smaller leaf size, increased root activity, and nutritional status at the initiation of panicles [30].

STUDY OBJECTS AND METHODS

Three field experiments were conducted in the wet seasons of 2017, 2018, and 2019 within the inland valley, specifically in the Teaching and Research Farms of the Federal University of Agriculture, Abeokuta (FUNAAB). The study area had a tropical climate with an average annual rainfall of over 1300 mm and an elevation of 83.10 meters above sea level. The region experienced two distinct rainy seasons, providing sufficient moisture for crop growth in the early stages of the growing season.

The research primarily focused on two specific lowland rice varieties: ARICA-3 (WAB 2076-WAC 1-TGR 1-B) and NERICA L-34 (FARO 61). These varieties were chosen due to their higher yield and productivity in comparison with upland rice types. ARICA-3 showed exceptional attributes, including a reduced cooking time, superior grain quality, heightened milling recovery, and diminished chalkiness. These qualities contributed to a 30% yield growth as opposed to NERICA L-19 (FARO 60). The necessary fertilizers, including an inorganic type (NPK 15:15:15), were provided by the Department of Plant Physiology and Crop Production. Furthermore, an organic fertilizer in the form of well-processed poultry manure was obtained from the College of Animal and Livestock Management (COLANIM) at FUNAAB. The incorporation of the cured poultry manure into the soil occurred two weeks before transplanting the rice seedlings, an approach adopted to enhance soil fertility. Soil samples from the topmost layer (0–15 cm deep) were collected randomly and subsequently analyzed in the laboratory to evaluate the soil's physical and chemical characteristics. The rice seeds, specifically ARICA 3 and NERICA L-34, were initially immersed in water for 24 hours. Subsequently, they were incubated for 48 hours to ensure consistent germination and early establish-

ment. After germination, the seeds were planted in the nursery using the drilling technique, with a spacing of 20×20 cm between each seedling. This was carried out on a 4×8 m bed of fertile soil that had been effectively cleared manually.

The study employed a randomized complete block arrangement with a split-plot design, replicated three times. The main plot consisted of two rice varieties: 1) ARICA 3, a rain-fed lowland variety with short grain, high yield, and superior grain quality, and 2) NERICA L-34, a rain-fed lowland variety with long grain, early maturity, resistance to lodging and pests, and higher protein content. In the sub-plot, different nutrient sources of nitrogen were applied: 100 kg of nitrogen/ha (NPK), 75 kg/ha (NPK) + 25 kg/ha (manure), 50 kg/ha (NPK) + 50 kg/ha (manure), 25 kg/ha (NPK) + 75 kg/ha (manure), and 100 kg/ha (manure). A control sample was without fertilizers.

Data collection

Partial factor of productivity, kg/kg = Crop yield with applied nutrient, kg/ha / Amount of nutrient applied;

Nitrogen uptake, kg/kg = (Nutrient concentration, % × Dry weight, kg) / 100;

Nitrogen uptake in grain, kg/ha = (Nitrogen content in grain, % × Yield, kg/ha) / 100;

Nitrogen uptake in straw, kg/ha = (Nitrogen content in straw, % × Yield, kg/ha) / 100;

Total nitrogen uptake, kg/ha = Nitrogen uptake in grain, kg/ha + Nitrogen uptake in straw, kg/ha;

Nitrogen utilization efficiency = (Nitrogen uptake in grain, kg/ha × 100) / Total nitrogen uptake, kg/ha.

$$\text{Internal utilization efficiency} = \frac{Y}{U}$$

$$\text{Physiological efficiency} = \frac{Y - Y_0}{U - U_0}$$

$$\text{Recovery efficiency} = \frac{U - U_0}{F}$$

where Y is the crop yield with applied nutrient, kg/ha; U is the total plant nutrient uptake above ground biomass, kg/ha, in a plant that received fertilizer; Y_0 is the crop yield without nutrient, kg/ha; U_0 is the total nutrient uptake in above-ground biomass, kg/ha, in a plot that received no fertilizer; and F is the amount of nutrient applied.

The total leaf area index was divided by feeding area, cm^2, and the average was determined.

Chlorophyll content, %, of the tagged plant was obtained by using a chlorophyll meter (at LEAF CHL PLUS).

Root fresh and dry weight, g, was determined after oven-drying the samples using a sensitive scale.

Data analysis. The collected data was subjected to a mixed model of Analysis of Variance (ANOVA), and the treatment means that exhibited statistical significance were further evaluated through Duncan's Multiple Range Test (DMRT) at a significance level of 5% ($p \leq 0.05$). GenStat 12th edition software was employed for these statistical analyses.

RESULTS AND DISCUSSION

We studied the effects of integrated nitrogen nutrient sources on the physiological traits of two lowland rice varieties, ARICA 3 and NERICA L-34, in the derived savannah region of Nigeria. Effective nutrient management plays a pivotal role in elevating rice crop performance and overall agricultural productivity [31]. We also considered environmental conditions for optimizing crop performance, although it is essential to recognize that our findings are region-specific [32]. Furthermore, higher rice yields depend on the physiological characteristics of rice, including translocation, assimilate production, stomatal opening, and leaf area [13]. Our study highlighted that integrated nutrient management (INM) practices contribute to superior growth and yield parameters compared to the control methods [9]. Therefore, INM strategies need to be employed to enhance crop productivity and sustainability [33].

Physiological efficiency and recovery efficiency of applied nutrient. In 2017, physiological efficiency, kg/kg, was significantly impacted by integrated nitrogen nutrient sources. The physiological efficiency of 100 kg nitrogen/ha (organic) was 10.34 kg/kg, while the physiological efficiency of 50 kg/ha (organic) + 50 kg/ha was 0.300 kg/kg. The choice of nitrogen source (organic vs. inorganic) significantly affects the physiological efficiency of applied nutrients and their utilization by the rice plants [34, 35]. The application of inorganic fertilizers enhanced the activity of beneficial microbes and mycorrhizal fungal colonization in lowland rice. These microbes and fungi are important in mobilizing nutrients and improving nutrient availability, which in turn facilitates the plant's uptake and results in higher nitrogen use efficiency. Similar observations were made by earlier studies of variations in nutrient supplies and nitrogen levels [36–39].

The variety had a significant impact on recovery efficiency, kg/kg, in 2017 ($p \leq 0.05$). The nutrient recovery efficiency of NERICA L-34's (0.243 kg/kg) was higher than that of ARICA 3 (0.004 kg/kg), as shown in Table 1. Notably, NERICA L-34 consistently surpassed ARICA 3 in various growth-related aspects, suggesting that farmers should consider cultivating NERICA L-34 for its superior productivity and resilience [40].

Nitrogen uptake. Table 2 shows that integrated nitrogen nutrient sources had a significant ($p \leq 0.05$) effect on nitrogen uptake, kg/kg, in 2019. The highest nitrogen uptake (0.5237 kg/kg) was obtained when 75 kg/ha (inorganic) + 25 kg/ha (organic) of nitrogen was applied in 2019, while the lowest nitrogen uptake (0.4602 kg/kg) was obtained when neither organic nor inorganic fertilizer was applied. Specifically, the blend of 75 kg/ha (inorganic) and 25 kg/ha (organic) had remarkable effectiveness in boosting nitrogen uptake [41]. This indicated that specific nutrient combinations can optimize nutrient uptake, vital for plant growth and yield [42]. The study revealed that different combinations of integrated nutrient sources exerted a significant influence on nitrogen uptake by rice plants [43]. The data clearly showed that,

Table 1 Effects of integrated nutrient sources of nitrogen-on-nitrogen internal utilization efficiency, physiological efficiency, and recovery efficiency of applied nutrient for lowland rice varieties in a derived savannah

Treatment	Nitrogen internal utilization efficiency, kg/kg			Physiological efficiency, kg/kg			Recovery efficiency of applied nutrient, kg/kg		
Varieties (V)	2017	2018	2019	2017	2018	2019	2017	2018	2019
ARICA 3	1.51	1.20	1.34	4.19	0.15	5.70	0.0040^{b}	0.0030	0.10
NERICA L-34	1.52	1.42	2.25	2.31	1.35	–16.50	0.2430^{a}	0.0020	0.63
SED ± ($p \leq 0.05$)	n.s.	n.s.	n.s.	n.s.	n.s.	n.s.	0.3938*	n.s.	n.s.
Nutrient sources of nitrogen (N)									
100 kg/ha (inorganic)	1.48	1.28	1.62	10.34^{a}	2.18	–7.30	0.0360	0.0010	0.28
75 kg/ha (inorganic) + 25 kg/ha (organic)	1.53	1.33	2.23	1.80^{c}	–0.35	–1.00	0.1780	0.0014	0.92
50 kg/ha (inorganic) + 50 kg/ha (organic)	1.49	1.32	1.41	0.30^{f}	0.28	–49.40	0.1440	0.0038	0.08
25 kg/ha (inorganic) + 75 kg/ha (organic)	1.51	1.27	1.79	4.61^{b}	–1.17	4.50	0.1100	0.0033	0.57
100 kg/ha (organic)	1.55	1.30	1.82	1.06^{e}	–0.41	5.80	0.1330	0.0029	0.45
Control (no organic; no inorganic)	1.53	1.36	1.89	1.37^{ed}	3.97	15.20	0.1390	0.0026	–0.10
SED ± ($p \leq 0.05$)	n.s.	n.s.	n.s.	0.11**	n.s.	n.s.	n.s.	n.s.	n.s.
V × N ($p \leq 0.05$)	n.s.	n.s.	n.s.	n.s.	n.s.	n.s.	n.s.	n.s.	n.s.

SED ± – standard error of difference, WAP – weeks after planting, * – significant at $p \leq 0.05$, ** – significant at $p \leq 0.01$, n.s. – not significant. Means with the same letter in the same column are not significantly different at $p \leq 0.05$

Table 2 Effects of integrated nutrient sources of nitrogen-on-nitrogen uptake, partial factor productivity, and nitrogen utilization efficiency of lowland rice varieties in a derived savannah

Treatment	Nitrogen uptake, kg/kg			Partial factor productivity, kg/kg			Nitrogen utilization efficiency, kg/kg		
Varieties (V)	2017	2018	2019	2017	2018	2019	2017	2018	2019
ARICA 3	6.65	1.19	0.49	4.80	0.93	9.56	15.37^{b}	15.39^{b}	62.20
NERICA L-34	6.61	0.52	0.48	6.67	1.27	8.18	21.57^{a}	21.57^{a}	47.90
SED ± ($p \leq 0.05$)	n.s.	n.s.	n.s.	n.s.	n.s.	n.s.	5.64*	5.70*	n.s.
Nutrient sources of nitrogen (N)									
100 kg/ha (inorganic)	6.78	0.90	0.50^{ab}	4.66^{b}	1.22	9.79	17.59	17.58	64.60
75 kg/ha (inorganic) + 25 kg/ha (organic)	6.58	0.83	0.52^{a}	4.67^{b}	0.66	10.54	18.76	18.75	65.30
50 kg/ha (inorganic) + 50 kg/ha (organic)	6.75	1.12	0.49^{ab}	5.13^{b}	1.02	8.82	18.91	18.93	57.40
25 kg/ha (inorganic) + 75 kg/ha (organic)	6.62	0.85	0.47^{b}	5.28^{b}	0.84	6.44	18.03	18.03	48.30
100 kg/ha (organic)	6.48	0.76	0.47^{b}	10.28^{a}	1.24	10.88	18.82	18.83	59.20
Control (no organic; no inorganic)	6.55	0.69	0.46^{b}	4.39^{b}	1.61	6.75	18.74	18.75	35.50
SED ± ($p \leq 0.05$)	n.s.	n.s.	0.02*	1.82*	n.s.	n.s.	n.s.	n.s.	n.s.
V × N ($p \leq 0.05$)	n.s.	n.s.	n.s.	n.s.	n.s.	n.s.	n.s.	n.s.	n.s.

SED ± – standard error of difference, WAP – weeks after planting, * – significant at $p \leq 0.05$, n.s.– not significant. Means with the same letter in the same column are not significantly different at $p \leq 0.05$

in comparison with other treatments, those containing a larger amount of inorganic nitrogen facilitated greater nutritional absorption. This might be because there was enough nitrogen available from both organic and inorganic sources for a long time, which eventually increased nitrogen uptake [44]. Our results are consistent with the works of Vishwanathan and Singaravel [45], Mohan Rao *et al.* [46], Kumar *et al.* [47], Ganguly *et al.* [48], and Shultana *et al.* [49].

Partial factor of productivity. In 2017, the partial factor of productivity was significantly ($p \leq 0.05$) affected by integrated nitrogen nutrient sources. The organic nitrogen application of 100 kg/ha produced the highest partial factor productivity (10.28 kg/kg), while the control sample (without fertilizers) produced the lowest (4.39 kg/kg), as shown in Table 2. This indicated better economic output and use of fertilizers, as well as better utilization of all the nutrients under treatment. An estimate of the economic production of the use of all nutrition sources is given by the partial factor productivity of applied nutrients. Better crop management techniques, more fertilizer application, and higher nutrient conversion ratios of the plant systems all contribute to the partial factor productivity [50]. A balanced application of N, P, and K (NPK) also optimized nutrient utilization efficiency, as reported by Korneeva [51]. This underscores the critical importance of striking the right balance between nutrient sources to achieve optimal productivity in rice cultivation [52].

Nitrogen utilization efficiency. In 2017 and 2018, the varieties had a significant effect ($p \leq 0.05$) on nitrogen utilization efficiency, kg/kg. In particular, the nitrogen

utilization efficiencies of NERICA L-34 in 2017 and 2108 were higher (21.57 and 21.57 kg/kg, respectively) than those of ARICA 3 (15.37 and 15.39 kg/kg, respectively), as shown in Table 2. This can assist farmers in selecting those rice varieties which make more efficient use of nitrogen resources [33]. The research underscores the advantages of merging organic and inorganic fertilizers to enhance nitrogen utilization efficiency in rice farming [53].

Leaf area index. Our findings showed significant effects of the integrated nutrient sources on the leaf area index at different time after planting in 2017, 2018, and 2019. At 4 weeks after planting in 2018, the application of 50 kg/ha (inorganic) + 50 kg/ha (organic) resulted in the highest leaf area index, while the control sample led to the lowest leaf area index. At 6 weeks, various combinations of the integrated nutrient sources influenced the leaf area index differently, with different optimal combinations for each year. At 8 weeks, the integrated nutrient sources had a highly significant effect on the leaf area index, with the highest leaf area index varying between the years. 10 weeks after planting affected the leaf area index, with different combinations leading to variations in this index. At 12 weeks in 2017 and 2018, the integrated nutrient sources had a highly significant effect on the leaf area index. Different nutrient combinations influenced the leaf area index differently. 14 weeks after planting in 2017 demonstrated a significant effect on the leaf area index, with a nitrogen application of 75 kg/ha (inorganic) + 25 kg/ha (organic) resulting in the highest index (Tables 3 and 4).

In a study of Ikkonen *et al.*, integrated nutrient sources had a substantial influence on the leaf area index at

Table 3 Effects of integrated nutrient sources of nitrogen on the leaf area index of lowland rice varieties after planting in a derived savannah

Treatment	Leaf area index								
	4 weeks			6 weeks			8 weeks		
Varieties (V)	2017	2018	2019	2017	2018	2019	2017	2018	2019
ARICA 3	0.111	0.173	0.167	0.138	0.217	0.217	0.168	0.250	0.231
NERICA L-34	0.071	0.164	0.178	0.087	0.164	0.147	0.091	0.219	0.186
SED ± ($p \leq 0.05$)	n.s.	n.s.	n.s.	n.s.	n.s.	n.s.	n.s.	n.s.	n.s.
Nutrient sources of nitrogen (N)									
100 kg/ha (inorganic)	0.097	0.167^{a}	0.162	0.109^{a}	0.190^{a}	0.170^{bc}	0.121a	0.213^{ab}	0.207^{bc}
75 kg/ha (inorganic) + 25 kg/ha (organic)	0.089	0.182^{a}	0.166	0.118^{a}	0.203^{a}	0.192^{abc}	0.141^{a}	0.218^{a}	0.211^{ab}
50 kg/ha (inorganic) + 50 kg/ha (organic)	0.095	0.187^{a}	0.214	0.106^{a}	0.192^{a}	0.219^{a}	0.122^{a}	0.202^{abc}	0.228^{a}
25 kg/ha (inorganic) + 75 kg/ha (organic)	0.097	0.180^{a}	0.164	0.108^{a}	0.211^{a}	0.198^{ab}	0.125^{ab}	0.204^{ab}	0.208^{ab}
100 kg/ha (organic)	0.090	0.163^{a}	0.164	0.130^{a}	0.187^{b}	0.171^{abc}	0.132^{c}	0.193^{bc}	0.207^{bc}
Control (no organic; no inorganic)	0.079	0.090^{b}	0.138	0.101^{b}	0.113^{c}	0.143^{c}	0.104d	0.146^{c}	0.147^{c}
SED ± ($p \leq 0.05$)	n.s.	0.0044**	n.s.	0.018**	0.064*	0.039*	0.023**	0.077*	0.080**
V × N ($p \leq 0.05$)	n.s.	n.s.	n.s.	n.s.	n.s.	n.s.	n.s.	n.s.	n.s.

SED ± – standard error of difference, * – significant at $p \leq 0.05$, ** – significant at $p \leq 0.01$, n.s. – not significant. Means with the same letter in the same column are not significantly different at $p \leq 0.05$

Table 4 Effects of integrated nutrient sources of nitrogen on the leaf area index of lowland rice varieties after planting and maturity in a derived savannah

Treatment	Leaf area index											
	10 weeks			12 weeks			14 weeks			Maturity		
Varieties (V)	2017	2018	2019	2017	2018	2019	2017	2018	2019	2017	2018	2019
ARICA 3	0.46	0.30	0.45	0.32	0.29	0.46^{a}	0.17	0.33	0.46	0.29	0.20	0.29
NERICA L-34	0.67	0.17	0.24	0.31	0.14	0.23^{b}	0.23	0.13	0.22	0.18	0.10	0.18
SED ± ($p \leq 0.05$)	n.s.	n.s.	n.s.	n.s.	n.s.	0.07*	n.s.	n.s.	n.s.	n.s.	n.s.	n.s.
Nutrient sources of nitrogen (N)												
100 kg/ha (inorganic)	0.74^{a}	0.33^{a}	0.35	0.52^{a}	0.28^{ab}	0.39	0.21^{ab}	0.30	0.34	0.22	0.33	0.28
75 kg/ha (inorganic) + 25 kg/ha (organic)	0.70^{a}	0.31^{a}	0.35	0.27c	0.23^{b}	0.38	0.26^{a}	0.24	0.36	0.32	0.13	0.31
50 kg/ha (inorganic) + 50 kg/ha (organic)	0.71^{a}	0.18^{a}	0.48	0.41^{ab}	0.14^{bc}	0.46	0.22^{ab}	0.21	0.48	0.28	0.14	0.28
25 kg/ha (inorganic) + 75 kg/ha (organic)	0.69^{a}	0.37^{a}	0.39	0.32c	0.41^{a}	0.37	0.16^{ab}	0.39	0.37	0.14	0.20	0.17
100 kg/ha (organic)	0.41^{ab}	0.19^{ab}	0.39	0.25^{c}	0.20^{b}	0.34	0.19^{ab}	0.18	0.31	0.20	0.09	0.24
Control (no organic; no inorganic)	0.12^{c}	0.04^{b}	0.12	0.09^{d}	0.03^{c}	0.15	0.15^{c}	0.04	0.18	0.12	0.03	0.12
SED ± ($p \leq 0.05$)	0.16**	0.10*	n.s.	0.08**	0.08**	n.s.	0.04*	n.s.	n.s.	n.s.	n.s.	n.s.
V × N ($p \leq 0.05$)	n.s.	n.s.	n.s.	n.s.	n.s.	n.s	n.s.	n.s.	n.s.	n.s.	n.s.	5.02*

SED ± – standard error of difference, * – significant at $p \leq 0.05$, ** – significant at $p \leq 0.01$, n.s. – not significant. Means with the same letter in the same column are not significantly different at $p \leq 0.05$

various stages of rice growth [54]. Nitrogen causes vegetative growth through an increased leaf area. Therefore, more nitrogen available to plants can increase the leaf area. This highlights the capacity of nutrient management to affect the development of leaf area, which is pivotal for photosynthesis and overall plant health [55].

Effects of variety and integrated sources of nitrogen on the leaf area index at maturity in 2019. The interaction between the lowland rice varieties and the integrated nutrient sources of nitrogen had a significant effect ($p \leq 0.05$) on the leaf area index at maturity in 2019. ARICA 3 had the highest leaf area index (0.424) when 75 kg/ha (inorganic) + 25 kg/ha (organic) f nitrogen was applied at maturity. However, applying the control sample (no fertilizer) to ARICA 3 produced the lowest leaf area index (0.074) at maturity in 2019 (Fig. 1).

Chlorophyll content. At 4 weeks after planting, the highest chlorophyll content was observed with the nitrogen application of 100 kg/ha (inorganic) in 2018 and 100 kg/ha (organic) in 2019. 6 weeks after planting in 2017 showed a significant effect on the chlorophyll content, with NERICA L-34 exhibiting a higher content than ARICA 3. At 8 weeks in 2017 and 2018, the highest chlorophyll content was observed with the nitrogen application of 100 kg/ha (inorganic) in 2017 and 75 kg/ha (inorganic) + 25 kg/ha (organic) in 2018. At 10 WAP in 2017 and 2018, the integrated nutrient sources had a significant effect on the chlorophyll content, with different optimal combinations leading to its variations. At 12 WAP in 2019, the rice varieties had a highly significant effect on the chlorophyll content, with NERICA L-34 exhibiting a higher content than ARICA 3. At 14 WAP in 2017

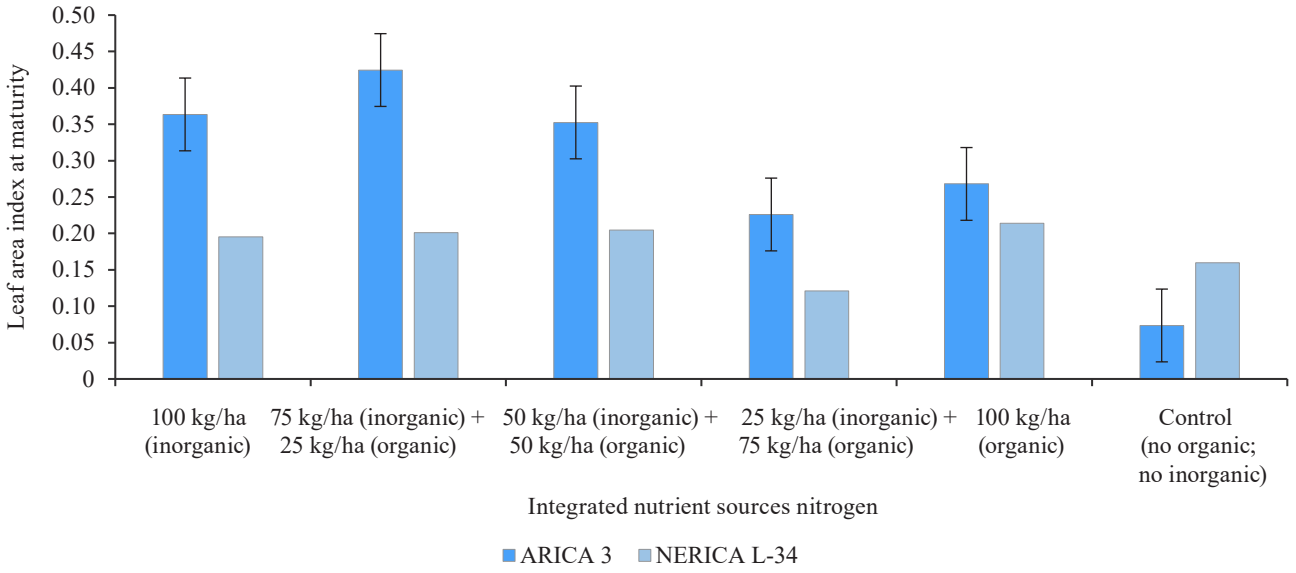

I – Standard error of difference at $p \leq 0.05$

Figure 1 Effects of rice variety and integrated nutrient sources of nitrogen on leaf area index at maturity in 2019

Table 5 Effects of integrated nutrient sources of nitrogen on chlorophyll content of lowland rice varieties after planting in a derived savannah

Treatment	Chlorophyll content, %								
	4 weeks			6 weeks			8 weeks		
Varieties (V)	2017	2018	2019	2017	2018	2019	2017	2018	2019
ARICA 3	31.54	32.77	37.87	37.11^{b}	40.54	43.10	38.31	39.37	41.47
NERICA L-34	31.98	30.61	35.69	37.82^{a}	35.88	41.34	36.57	37.84	39.05
SED ± ($p \leq 0.05$)	n.s.	n.s.	n.s.	0.09*	n.s.	n.s.	n.s.	n.s.	n.s.
Nutrient Sources (N)									
100 kg/ha (inorganic)	31.37	34.59^{a}	37.39^{ab}	35.46	39.80	42.82	39.97^{a}	39.40^{ab}	41.02
75 kg/ha (inorganic) + 25 kg/ha (organic)	31.10	34.43^{a}	33.54^{c}	37.11	39.16	43.13	38.86^{a}	41.71^{a}	40.03
50 kg/ha (inorganic) + 50 kg/ha (organic)	32.80	32.52^{a}	34.86^{bc}	37.75	38.67	42.32	37.62^{ab}	37.55^{b}	40.25
25 kg/ha (inorganic) + 75 kg/ha (organic)	33.48	32.05^{a}	37.25^{ab}	38.54	38.91	42.42	37.37^{ab}	39.01^{ab}	39.87
100 kg/ha (organic)	32.14	31.16^{a}	38.93^{a}	38.38	37.68	42.44	37.31^{ab}	38.25^{ab}	42.22
Control (no organic; no inorganic)	29.70	25.38^{b}	38.70^{a}	37.52	35.05	40.22	33.52^{c}	35.71^{b}	38.16
SED ± ($p \leq 0.05$)	n.s.	2.18**	1.46**	n.s.	n.s.	n.s.	1.88*	1.63*	n.s.
V×N ($p \leq 0.05$)	n.s.	n.s.	n.s.	n.s.	n.s.	n.s.	n.s.	n.s.	n.s.

SED ± – standard error of difference, * – significant at $p \leq 0.05$, ** – significant at $p \leq 0.01$, n.s. – not significant. Means with the same letter in the same column are not significantly different at $p \leq 0.05$

Table 6 Effects of integrated nutrient sources of nitrogen on chlorophyll content of lowland rice varieties after planting and maturity in a derived savannah

Treatment	Chlorophyll content, %											
	10 weeks			12 weeks			14 weeks			Maturity		
Varieties (V)	2017	2018	2019	2017	2018	2019	2017	2018	2019	2017	2018	2019
ARICA 3	40.57	38.03	42.39	42.61	39.58	39.01^{b}	41.16	42.21	42.06	29.14	32.46	31.64
NERICA L-34	38.46	36.57	37.93	42.23	37.95	43.53^{a}	40.46	36.63	42.85	29.14	32.24	30.32
SED ± ($p \leq 0.05$)	n.s.	n.s.	n.s.	n.s.	n.s.	2.19**	n.s.	n.s.	n.s.	n.s.	n.s.	n.s.
Nutrient Sources (N)												
100 kg/ha (inorganic)	39.76^{a}	38.01^{a}	39.61	43.62	39.03	41.51	41.33^{ab}	41.99^{ab}	42.56	31.23	32.98	30.80
75 kg/ha (inorganic) + 25 kg/ha (organic)	39.96^{a}	37.69^{a}	41.33	42.53	39.35	43.08	42.84^{a}	43.39^{a}	42.48	30.03	30.46	31.34
50 kg/ha (inorganic) + 50 kg/ha (organic)	41.22^{a}	37.72^{a}	39.37	42.3	37.58	39.70	40.42^{bc}	38.95^{ab}	42.85	31.06	32.55	29.66
25 kg/ha (inorganic) + 75 kg/ha (organic)	39.35^{ab}	37.98^{a}	42.01	42.78	40.03	39.26	39.03^{d}	33.83^{c}	41.44	28.01	32.81	31.79
100 kg/ha (organic)	39.56^{ab}	38.03^{a}	39.88	43.81	39.71	42.32	40.39^{bc}	42.27^{ab}	43.88	28.83	34.44	31.35
Control (no organic; no inorganic)	37.26^{c}	34.35^{b}	38.76	39.47	36.87	41.75	40.88^{abc}	36.10^{bc}	41.52	25.69	30.87	30.96
SED ± ($p \leq 0.05$)	1.06*	0.88**	n.s.	n.s.	n.s.	n.s.	0.96*	2.92*	n.s.	n.s.	n.s.	n.s.
V×N ($p \leq 0.05$)	n.s.	n.s.	n.s.	n.s.	n.s.	n.s.	n.s.	n.s.	n.s.	n.s.	n.s.	2.59**

SED ± – standard error of difference, * – significant at $p \leq 0.05$, ** – significant at $p \leq 0.01$, n.s. – not significant. Means with the same letter in the same column are not significantly different at $p \leq 0.05$

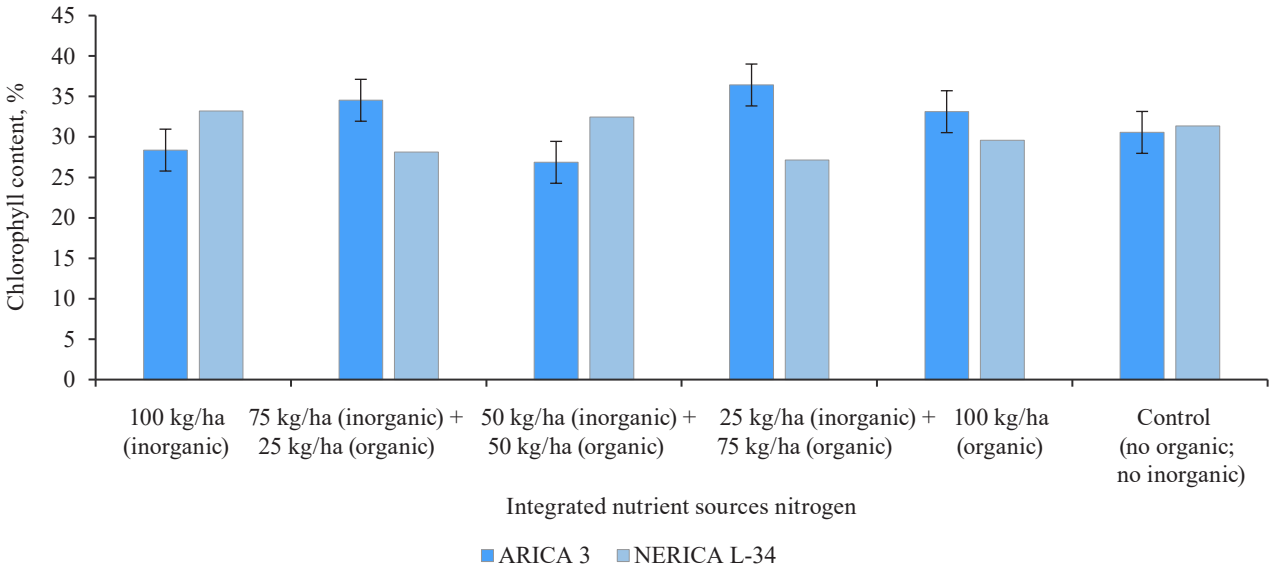

I – Standard error of difference at $p \leq 0.05$

Figure 2 Effects of rice variety and integrated nutrient sources of nitrogen on chlorophyll content at maturity in 2019

and 2018, the nitrogen combination of 75 kg/ha (inorganic) + 25 kg/ha (organic) resulted in the highest chlorophyll content in both years (Tables 5 and 6).

The chlorophyll content, a crucial indicator of plant health and photosynthetic capacity, is significantly affected by nutrient sources, with various sources yielding varying results [56]. This underscores the importance of nutrient management in optimizing photosynthetic activity in rice plants [54].

Effects of variety and integrated sources of nitrogen on chlorophyll content at maturity in 2019. The interaction between the lowland rice varieties and the integrated nutrient sources of nitrogen had a significant effect ($p \leq 0.05$) on the chlorophyll content, %, at maturity in 2019. ARICA 3 had the highest content (36.42%) at 25 kg/ha (inorganic) + 75 kg/ha (organic) of nitrogen was applied, while NERICA L-34 had the lowest content (27.16%), as shown in Figure 2.

Root fresh weight. At 4 weeks after planting in 2019, a combination of 50 kg/ha (inorganic) + 50 kg/ha (organic) resulted in the heaviest roots. At 6 weeks in 2017 and 2018, a combination of 50 kg/ha (inorganic) + 50 kg/ha (organic) produced the heaviest roots in both years. 8 weeks in 2017 demonstrated a significant effect on the root fresh weight, with ARICA 3 having heavier roots than NERICA L-34. The integrated nutrient

sources also had a significant effect, with the nitrogen application of 100 kg/ha (inorganic) resulting in the heaviest roots. The varieties also had a significant effect on the root fresh weight at 10 weeks after planting in 2018, while the integrated nutrient sources had a significant effect on this indicator in 2017 and 2019 (Tables 7 and 8).

Effects of variety and integrated sources of nitrogen on root fresh weight. At 12 weeks after planting in 2017, ARICA 3 exhibited the heaviest root fresh weight (93.6 g) when 100 kg/ha of nitrogen (inorganic) was applied, while the sample without fertilizers resulted in the lightest roots (64.5 g). At 14 weeks in 2017, ARICA 3 also had the heaviest root fresh weight (267 g) when 25 kg/ha (inorganic) + 75 kg/ha (organic) was applied. However, NERICA L-34 had the lightest roots (67 g) when 75 kg/ha (inorganic) + 25 kg/ha (organic) was used. At maturity in 2017, ARICA 3 had the heaviest root fresh weight (283 g) at 100 kg/ha (organic), whereas NERICA L-34 had the lightest root fresh weight (62 g) when no organic or inorganic nutrients were applied (control sample). 14 weeks after planting in 2019, ARICA 3 again exhibited the heaviest roots (92.1 g) at 25 kg/ha (inorganic) + 75 kg/ha (organic), while NERICA L-34 had the lightest roots (34 g) when the control sample was applied (Figs 3 and 4).

Table 7 Effects of integrated nutrient sources of nitrogen on root fresh weight of lowland rice varieties after planting in a derived savannah

Treatment	Root fresh weight, g								
	4 weeks			6 weeks			8 weeks		
Varieties (V)	2017	2018	2019	2017	2018	2019	2017	2018	2019
ARICA 3	1.78	3.51	0.20	25.90	13.48	2.54	40.30^{a}	39.50	5.96
NERICA L-34	1.65	2.86	0.16	15.20	14.02	3.40	29.00^{b}	48.40	7.28
SED ± ($p \leq 0.05$)	n.s.	n.s.	n.s.	n.s.	n.s.	n.s.	6.30*	n.s.	n.s.
Nutrient Sources (N)									
100 kg/ha (inorganic)	1.70	2.57	0.15^{b}	30.10^{a}	13.13^{ab}	2.89	52.00^{a}	40.90	7.42
75 kg/ha (inorganic) + 25 kg/ha (organic)	2.00	4.03	0.17^{b}	13.80^{c}	17.21^{a}	2.92	30.60^{c}	40.10	6.35
50 kg/ha (inorganic) + 50 kg/ha (organic)	2.01	4.25	0.27^{a}	30.40^{a}	15.38^{a}	2.99	38.40^{ab}	68.90	8.03
25 kg/ha (inorganic) + 75 kg/ha (organic)	1.23	3.14	0.18^{b}	12.80^{c}	11.77^{ab}	3.43	31.20^{c}	37.10	6.72
100 kg/ha (organic)	1.85	1.66	0.18^{b}	20.20^{ab}	18.24^{a}	2.91	28.90^{c}	47.30	6.17
Control (no organic; no inorganic)	1.51	3.47	0.13^{b}	15.90^{ab}	6.81^{b}	2.68	27.00^{c}	29.20	5.02
SED ± ($p \leq 0.05$)	n.s.	n.s.	0.04*	6.85*	3.30**	n.s.	6.84*	n.s.	n.s.
V×N ($p \leq 0.05$)	n.s.	n.s.	n.s.	n.s.	n.s.	n.s.	n.s.	n.s.	n.s.

SED ± – standard error of difference, * – significant at $p \leq 0.05$, ** – significant at $p \leq 0.01$, n.s. – not significant. Means with the same letter in the same column are not significantly different at $p \leq 0.05$

Table 8 Effects of integrated nutrient sources of nitrogen on root fresh weight of lowland rice varieties after planting and maturity in a derived savannah

Treatment	Root fresh weight, g											
	10 weeks			12 weeks			14 weeks			Maturity		
Varieties (V)	2017	2018	2019	2017	2018	2019	2017	2018	2019	2017	2018	2019
ARICA 3	86.40	107.90^{a}	60.70	85.70	114.10	41.80	172.00	223.00	58.90	150.00a	214.00	48.90
NERICA L-34	67.50	85.10^{b}	70.28	95.90	81.60	33.00	86.00	59.00	43.60	101.00b	101.00	30.60
SED ± ($p \leq 0.05$)	n.s.	17.98*	n.s.	n.s.	n.s.	n.s.	n.s.	n.s.	n.s.	7.69**	n.s.	n.s.
Nutrient Sources (N)												
100 kg/ha (inorganic)	80.70^{ab}	84.80	68.83^{a}	93.30	100.40^{a}	34.50	141.00	164.00	51.30^{ab}	112.00^{ab}	179.00	38.20
75 kg/ha (inorganic) + 25 kg/ha (organic)	80.50^{ab}	85.40	68.83^{a}	88.80	120.10^{a}	40.40	104.00	187.00	44.50^{b}	137.00^{ab}	97.00	41.30
50 kg/ha (inorganic) + 50 kg/ha (organic)	76.10^{ab}	107.10	66.13^{ab}	86.70	89.40^{ab}	42.80	120.00	86.00	51.30^{ab}	131.00^{ab}	278.00	35.10
25 kg/ha (inorganic) + 75 kg/ha (organic)	93.00^{a}	130.20	62.23^{b}	108.90	99.20^{a}	35.20	176.00	101.00	66.30^{a}	102.00^{ab}	166.00	54.50
100 kg/ha (organic)	61.40^{c}	97.70	65.49^{ab}	107.90	136.30^{a}	28.70	136.00	179.00	52.30^{ab}	189.00^{a}	160.00	38.10
Control (no organic; no inorganic)	69.90^{c}	73.60	61.43^{b}	59.10	41.90^{b}	43.00	96.00	130.00	41.50^{b}	81.00^{c}	65.00	31.20
SED ± ($p \leq 0.05$)	9.01*	n.s.	2.64*	n.s.	24.91*	n.s.	n.s.	n.s.	7.36*	4.35**	n.s.	n.s.
V×N ($p \leq 0.05$)	n.s.	n.s.	n.s.	12.26*	n.s.	n.s.	n.s.	n.s.	13.53*	5.89**	n.s.	n.s.

SED ± – standard error of difference, * – significant at $p \leq 0.05$, ** – significant at $p \leq 0.01$, n.s. – not significant. Means with the same letter in the same column are not significantly different at $p \leq 0.05$

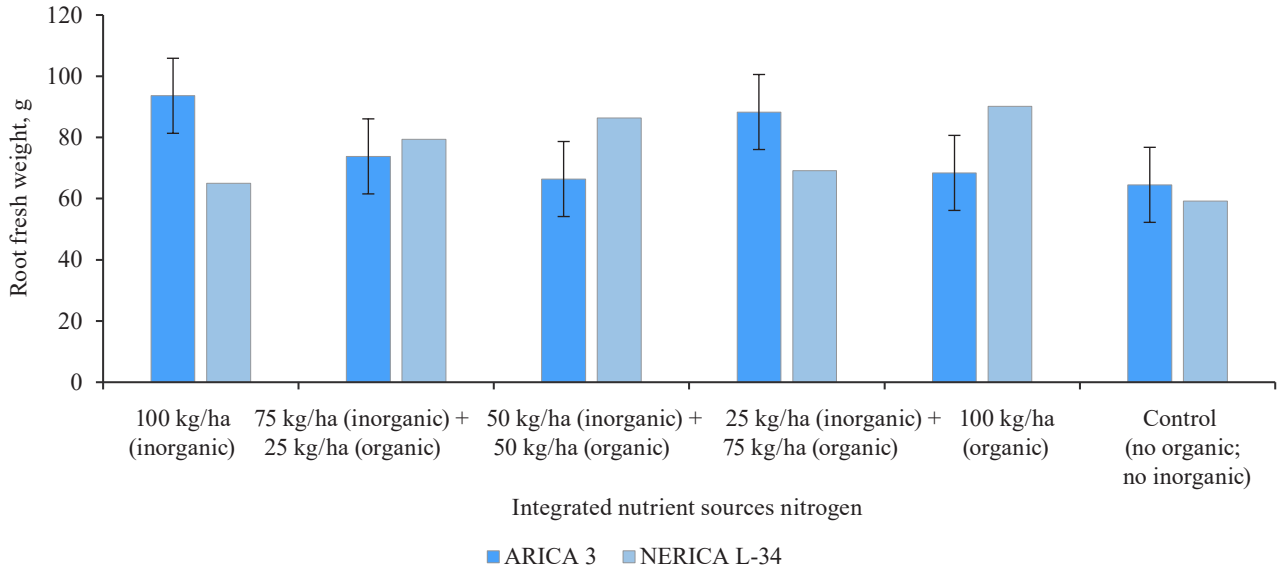

I – Standard error of difference at $p \leq 0.05$

Figure 3 Effects of rice variety and integrated nutrient sources of nitrogen on root fresh weight at 12 weeks after planting in 2017

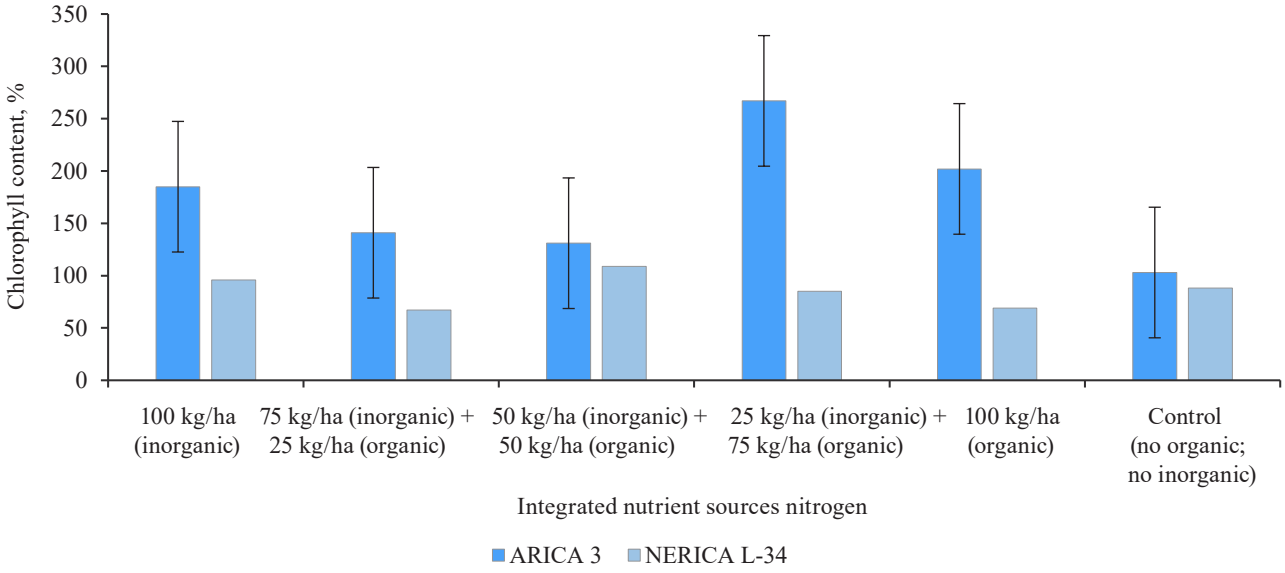

I – Standard error of difference at $p \leq 0.05$

Figure 4 Effects of rice variety and integrated nutrient sources of nitrogen on root fresh weight at 14 weeks after planting in 2017

Root dry weight. 4 weeks after planting in 2018, ARICA 3 had heavier roots (1.19 g) compared to NERICA L-34 (0.80 g). 100 kg nitrogen/ha (inorganic) resulted in the heaviest root dry weight (1.39 g), while the control sample produced the lightest root dry weight (0.71 g). 6 weeks after planting in 2018, NERICA L-34 had heavier roots (5.01 g) compared to ARICA 3 (3.81 g). At 8 weeks in 2018, NERICA L-34 again had heavier roots (11.9 g) compared to ARICA 3 (8.6 g). At 10 weeks in both 2018 and 2019, the varieties had a significant effect on the root dry weight, with NERICA L-34 consistently having heavier roots compared to ARICA 3. In 2019, the integrated nutrient sources of nitrogen had a highly significant effect on the root dry weight at 10 weeks after planting, with 75 kg/ha (inorganic) + 25 kg/ha (organic) resulting in the heaviest roots (18.66 g). 12 weeks in 2018 demonstrated that ARICA 3 had heavier roots (36.3 g) compared to NERICA L-34 (28 g). 100 kg nitrogen/ha (organic) produced the heaviest root dry weight (56.2 g). At maturity in both 2018 and 2019, the varieties had a significant effect on the root dry weight, with ARICA 3 consistently having heavier roots compared to NERICA L-34 (Tables 9 and 10).

Effects of variety and integrated sources of nitrogen on root dry weight. At 10 weeks after planting in 2019, the interaction between the rice varieties and the integrated nutrient sources of nitrogen had a highly significant effect on the root dry weight. NERICA L-34 recorded

Table 9 Effects of integrated nutrient sources of nitrogen on root dry weight of lowland rice varieties after planting in a derived savannah

Treatment	Root dry weight, g								
	4 weeks			6 weeks			8 weeks		
Varieties (V)	2017	2018	2019	2017	2018	2019	2017	2018	2019
ARICA 3	0.95	1.19[a]	0.06	6.74	3.81[b]	0.76	23.80	8.60[b]	1.58
NERICA L-34	0.84	0.80[b]	0.05	4.76	5.01[a]	0.66	21.20	11.90[a]	2.81
SED ± ($p \leq 0.05$)	n.s.	0.38*	n.s.	n.s.	0.81*	n.s.	n.s.	2.46*	n.s.
Nutrient Sources (N)									
100 kg/ha (inorganic)	0.90	1.39[a]	0.04	9.14	5.36	0.87	32.90	9.60	3.20
75 kg/ha (inorganic) + 25 kg/ha (organic)	1.02	0.94[ab]	0.06	3.91	4.47	0.59	17.80	12.30	1.90
50 kg/ha (inorganic) + 50 kg/ha (organic)	1.10	0.73[b]	0.06	7.77	4.66	0.87	33.70	13.80	2.70
25 kg/ha (inorganic) + 75 kg/ha (organic)	0.61	1.14[ab]	0.06	3.44	3.86	0.71	20.10	8.40	1.99
100 kg/ha (organic)	1.09	1.08[ab]	0.05	6.24	5.67	0.74	17.00	12.70	1.93
Control (no organic; no inorganic)	0.66	0.71[b]	0.04	3.98	2.45	0.49	13.70	4.50	1.46
SED ± ($p \leq 0.05$)	n.s.	0.21*	n.s.	n.s.	n.s.	n.s.	n.s.	n.s.	n.s.
V×N ($p \leq 0.05$)	n.s.	n.s.	n.s.	n.s.	n.s.	n.s.	n.s.	n.s.	n.s.

SED ± – standard error of difference, * – significant at $p \leq 0.05$, n.s. – not significant. Means with the same letter in the same column are not significantly different at $p \leq 0.05$

Table 10 Effects of integrated nutrient sources of nitrogen on root dry weight of lowland rice varieties after planting and maturity

Treatment	Root dry weight (g)											
	10 weeks			12 weeks			14 weeks			Maturity		
Varieties (V)	2017	2018	2019	2017	2018	2019	2017	2018	2019	2017	2018	2019
ARICA 3	34.00	8.60[b]	16.00[b]	26.51	36.30[a]	11.70	73.80[a]	69.80	21.00	67.70	63.20[a]	14.48[a]
NERICA L-34	32.40	11.90[a]	18.57[a]	24.80	28.00[b]	11.70	31.40[b]	18.20	15.80	48.30	28.40[b]	12.36[b]
SED ± ($p \leq 0.05$)	n.s.	2.46*	1.91*	n.s.	6.43*	n.s.	43.26*	n.s.	n.s.	n.s.	4.88*	1.40*
Nutrient Sources (N)												
100 kg/ha (inorganic)	29.30	9.60	18.45[a]	30.76[a]	34.80[ab]	14.00	58.80	51.70	20.70	50.00	54.80	14.76
75 kg/ha (inorganic) + 25 kg/ha (organic)	36.70	12.30	18.66[a]	25.97[ab]	33.20[ab]	9.70	47.80	64.80	15.00	65.50	38.00	14.77
50 kg/ha (inorganic) + 50 kg/ha (organic)	34.20	13.80	17.23[ab]	25.08[ab]	24.70[b]	15.00	41.60	29.60	16.10	55.40	63.50	13.00
25 kg/ha (inorganic) + 75 kg/ha (organic)	51.10	8.40	16.33[b]	25.71[ab]	32.00[ab]	10.50	79.30	30.30	23.00	52.00	44.20	13.10
100 kg/ha (organic)	26.00	12.70	16.83[b]	27.26[a]	56.20[a]	11.00	52.30	49.10	19.50	81.50	45.20	13.08
Control (no organic; no inorganic)	21.80	4.50	16.23[b]	19.17[c]	11.90[b]	10.20	36.00	38.40	16.00	43.80	29.20	11.82
SED ± ($p \leq 0.05$)	n.s.	n.s.	0.72**	3.26*	11.24*	n.s.	n.s.	n.s.	n.s.	n.s.	n.s.	n.s.
V×N ($p \leq 0.05$)	n.s.	n.s.	1.03*	4.65**	n.s.	n.s.	n.s.	n.s.	8.31*	n.s.	n.s.	n.s.

SED ± – standard error of difference, * – significant at $p \leq 0.05$, ** – significant at $p \leq 0.01$, n.s. – not significant. Means with the same letter in the same column are not significantly different at $p \leq 0.05$

the heaviest roots (21.01 g) when 75 kg nitrogen/ha (inorganic) + 25 kg/ha (organic) was applied. ARICA-3 had the lightest roots (15.07 g) at 50 kg/ha (inorganic) + 50 kg/ha (organic) of nitrogen. At 14 weeks in 2019, ARICA 3 had the heaviest roots (34.4 g) at 25 kg/ha (inorganic) + 75 kg/ha (organic) of nitrogen. NERICA L-34 had the lightest roots (11.6 g) when 25 kg/ha (inorganic) + 75 kg/ha (organic) was applied (Figures 5, 6, and 7).

The weight of roots, a critical indicator of plant health and nutrient uptake, is substantially influenced by both integrated nutrient sources and rice varieties [57]. These findings can provide valuable guidance for decisions regarding nutrient management and variety selection to promote root development and nutrient uptake [58].

The interaction between rice varieties and integrated nutrient sources yields significant effects on several parameters, including the leaf area index, chlorophyll content, root dry weight, and root fresh weight. This suggests that the choice of a rice variety should be considered alongside nutrient management practices to maximize crop performance [59].

CONCLUSION

In conclusion, our results highlighted the significance of integrated nitrogen nutrient sources in influencing the physiological parameters of lowland rice varieties, ARICA 3 and NERICA L-34, in Nigeria's derived savannah. Nutrient management strategies play

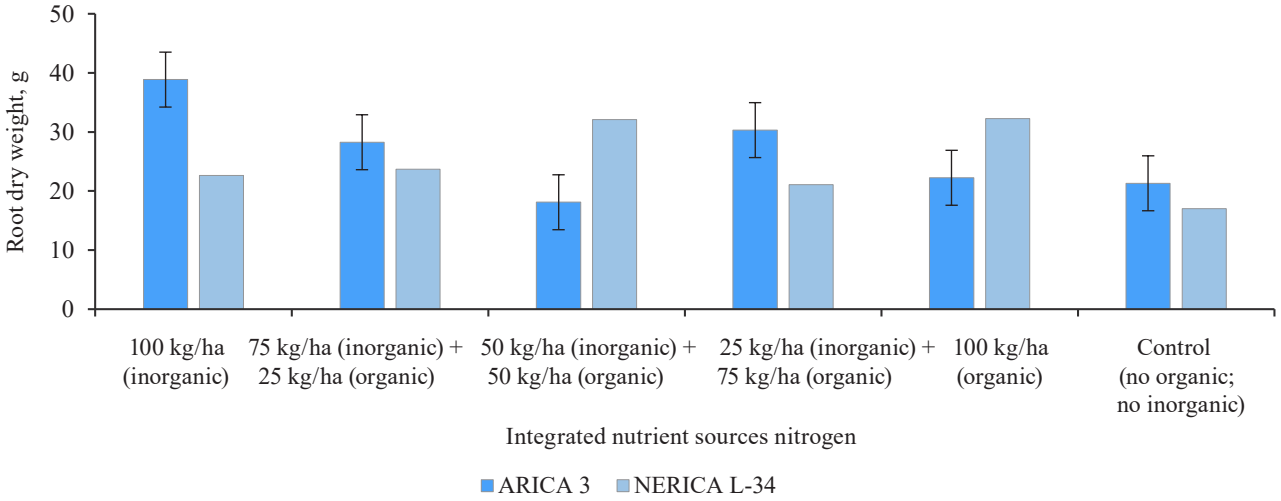

I – Standard error of difference at $p \leq 0.05$

Figure 5 Effects of rice variety and integrated nutrient sources of nitrogen on root dry weight at 12 weeks after planting in 2017

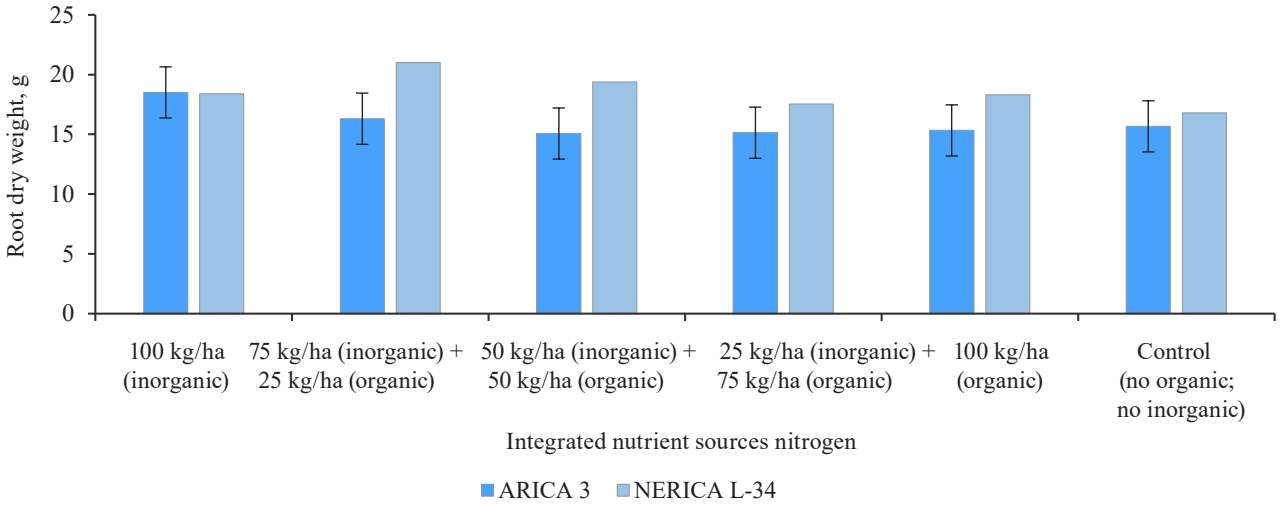

I – Standard error of difference at $p \leq 0.05$

Figure 6 Effects of rice variety and integrated nutrient sources of nitrogen on root dry weight at 10 weeks after planting in 2019

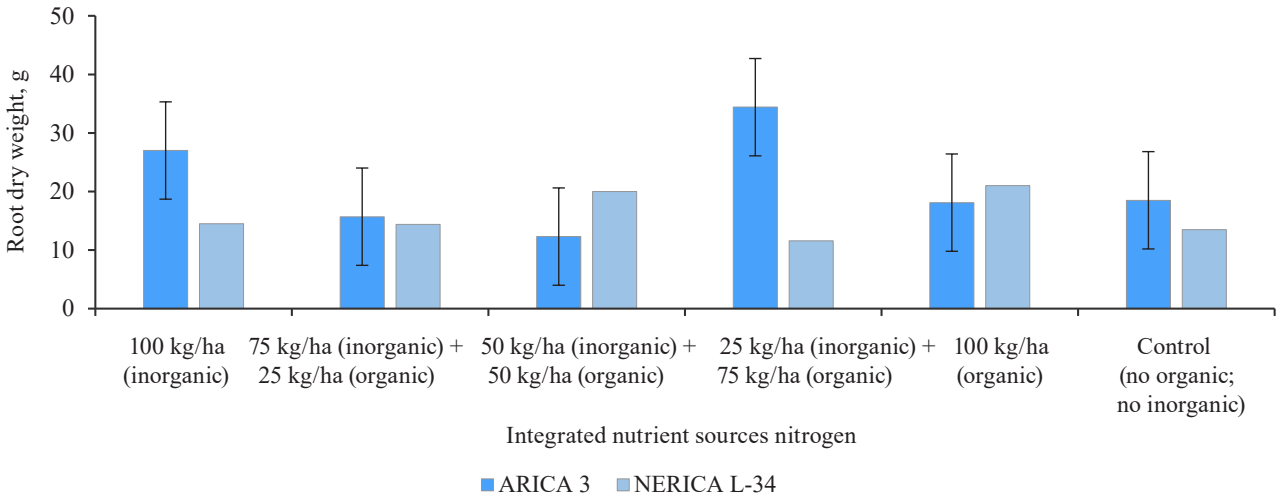

I – Standard error of difference at $p \leq 0.05$

Figure 7 Effects of rice variety and integrated nutrient sources of nitrogen on root dry weight at 14 weeks after planting in 2019

a critical role in enhancing rice crop performance and overall agricultural productivity in the region. Specific combinations of integrated nutrients, such as 75 kg nitrogen/ha (inorganic) + 25 kg/ha (organic) in 2019, proved effective in promoting nutrient absorption by the rice plants. Our study underscores the importance of varietal selection, with NERICA L-34 consistently outperforming ARICA 3 in applied nutrient recovery efficiency and nitrogen utilization efficiency.

In 2017, 2018, and 2019, the chlorophyll content was higher in the rice plants of ARICA 3 than in those of NERICA L-34. Furthermore, 100 kg nitrogen/ha (organic) produced the highest chlorophyll content in 2017, 2018, and 2019 compared to the other levels of nitrogen nutrient sources applied.

RECOMMENDATIONS

Based on our findings, we recommend that the rice plant NERICA L-34 should be adopted and cultivated by rice farmers. We also support the Integrated Nutrient Management approaches, which entail combining both organic and inorganic fertilizers to enhance the soil's nutrient content. In our study, specific combinations of nutrients, such as 75 kg/ha (inorganic) + 25 kg/ha (organic), improved nutrient absorption by the rice plants. NERICA L-34 demonstrated its superior performance in applied nutrient recovery efficiency and nitrogen utilization efficiency, as compared to ARICA 3. Considering environmental factors in nutrient management is crucial for optimizing crop performance and promoting sustainability. Further research in diverse ecological zones is needed to validate our findings and develop location-specific nutrient management recommendations. Education and awareness programs should be promoted to encourage farmers to adopt proper nutrient management practices and varietal selection. Conducting long-term studies on integrated nutrient sources can provide deeper insights into their sustainability. Governmental support in providing access to quality fertilizers, training, and extension services is vital for successful implementation. By following these recommendations, rice farmers can enhance productivity, ensure food security, and build a resilient agricultural sector for the nation's future.

CONTRIBUTION

All the authors were equally involved in conducting the research and writing the manuscript.

CONFLICT OF INTEREST

The authors declare no conflict of interest regarding the publication of this article.

REFERENCES

1. Kim D-G, Grieco E, Bombelli A, Hickman JE, Sanz-Cobena A. Challenges and opportunities for enhancing food security and greenhouse gas mitigation in smallholder farming in sub-Saharan Africa. A review. Food Security. 2021;13:457–476. https://doi.org/10.1007/s12571-021-01149-9
2. Anser MK, Hina T, Hameed S, Nasir MH, Ahmad I, ur Rehman Naseer MA. Modeling Adaptation Strategies against Climate Change Impacts in Integrated Rice-Wheat Agricultural Production System of Pakistan. International Journal of Environmental Research and Public Health. 2020;17(7):2522. https://doi.org/10.3390/ijerph17072522
3. Afolabi A, Iyanda O, Dayo-Olagbende O, Olasuyi K, Oyekanmi A. Response of lowland rice varieties to integrated nutrient management in a derived Savannah agro-ecology. Journal of Plant Nutrition. 2023;46(16):3894–3904. https://doi.org/10.1080/01904167.2023.2220705
4. Anas M, Liao F, Verma KK, Sarwar MA, Mahmood A, Chen Z-L, *et al.* Fate of nitrogen in agriculture and environment: agronomic, eco-physiological and molecular approaches to improve nitrogen use efficiency. Biological Research. 2020;53:47. https://doi.org/10.1186/s40659-020-00312-4
5. Waqas MA, Li Y, Smith P, Wang X, Ashraf MN, Noor M, *et al.* The influence of nutrient management on soil organic carbon storage, crop production, and yield stability varies under different climates. Journal of Cleaner Production. 2020;268:121922. https://doi.org/10.1016/j.jclepro.2020.121922
6. Iqbal A, He L, Ali I, Ullah S, Khan A, Khan A, *et al.* Manure combined with chemical fertilizer increases rice productivity by improving soil health, post-anthesis biomass yield, and nitrogen metabolism. PLoS ONE. 2020;15(10):e0238934. https://doi.org/10.1371/journal.pone.0238934
7. Ali I, Zhao Q, Wu K, Ullah S, Iqbal A, Liang H, *et al.* Biochar in Combination with Nitrogen Fertilizer is a Technique: To Enhance Physiological and Morphological Traits of Rice (*Oryza sativa* L.) by Improving Soil Physio-biochemical Properties. Journal of Plant Growth Regulation. 2022;41:2406–2420. https://doi.org/10.1007/s00344-021-10454-8
8. Ojo TO, Baiyegunhi LJS. Climate change perception and its impact on net farm income of smallholder rice farmers in South-West, Nigeria. Journal of Cleaner Production. 2021;310:127373. https://doi.org/10.1016/j.jclepro.2021.127373
9. Yu K, Fang X, Zhang Y, Miao Y, Liu S, Zou J. Low greenhouse gases emissions associated with high nitrogen use efficiency under optimized fertilization regimes in double-rice cropping systems. Applied Soil Ecology. 2021;160:103846. https://doi.org/10.1016/j.apsoil.2020.103846

10. Bhardwaj AK, Rajwar D, Basak N, Bhardwaj N, Chaudhari SK, Bhaskar S, *et al.* Nitrogen Mineralization and Availability at Critical Stages of Rice (*Oryza sativa*) Crop, and Its Relation to Soil Biological Activity and Crop Productivity Under Major Nutrient Management Systems. Journal of Soil Science and Plant Nutrition. 2020;20:1238–1248. https://doi.org/10.1007/s42729-020-00208-y
11. Nazish T, Arshad M, Jan SU, Javaid A, Khan MH, Naeem MA, *et al.* Transporters and transcription factors gene families involved in improving nitrogen use efficiency (NUE) and assimilation in rice (*Oryza sativa* L.). Transgenic Research. 2022;31:23–42. https://doi.org/10.1007/s11248-021-00284-5
12. Tang H, Li C, Xiao X, Shi L, Cheng K, Wen L, *et al.* Effects of short-term manure nitrogen input on soil microbial community structure and diversity in a double-cropping paddy field of southern China. Scientific Reports. 2020; 10:13540. https://doi.org/10.1038/s41598-020-70612-y
13. Xu A, Li L, Xie J, Wang X, Coulter JA, Liu C, *et al.* Effect of Long-Term Nitrogen Addition on Wheat Yield, Nitrogen Use Efficiency, and Residual Soil Nitrate in a Semiarid Area of the Loess Plateau of China. Sustainability. 2020;12(5):1735. https://doi.org/10.3390/su12051735
14. Feng H, Li Y, Yan Y, Wei X, Yang Y, Zhang L, *et al.* Nitrogen Regulates the Grain Yield, Antioxidant Attributes, and Nitrogen Metabolism in Fragrant Rice Grown Under Lead-Contaminated Soil. Journal of Soil Science and Plant Nutrition. 2020;20:2099–2111. https://doi.org/10.1007/s42729-020-00278-y
15. Yang S, Hao D, Jin M, Li Y, Liu Z, Huang Y, *et al.* Internal ammonium excess induces ROS-mediated reactions and causes carbon scarcity in rice. BMC Plant Biology. 2020;20:143. https://doi.org/10.1186/s12870-020-02363-x
16. Dai X, Song D, Zhou W, Guangrong L, Liang G, He P, *et al.* Partial substitution of chemical nitrogen with organic nitrogen improves rice yield, soil biochemical indictors and microbial composition in a double rice cropping system in south China. Soil and Tillage Research. 2021;205:104753. https://doi.org/10.1016/j.still.2020.104753
17. Khan Z, Khan MN, Luo T, Zhang K, Zhu K, Rana MS, *et al.* Compensation of high nitrogen toxicity and nitrogen deficiency with biochar amendment through enhancement of soil fertility and nitrogen use efficiency promoted rice growth and yield. GCB Bioenergy. 2021;13(11):1765–1784. https://doi.org/10.1111/gcbb.12884
18. Ouyang W, Yin X, Yang J, Struik P. Comparisons with wheat reveal root anatomical and histochemical constraints of rice under water-deficit stress. Plant and Soil. 2020;452:547–568. https://doi.org/10.1007/s11104-020-04581-6
19. Ding Y, Wang Z, Mo S, Liu J, Xing Y, Wang Y, *et al*. Mechanism of Low Phosphorus Inducing the Main Root Lengthening of Rice. Journal of Plant Growth Regulation. 2021;40:1032–1043. https://doi.org/10.1007/s00344-020-10161-w
20. Kitomi Y, Hanzawa E, Kuya N, Inoue H, Hara N, Kawai S, *et al.* Root angle modifications by the DRO1 homolog improve rice yields in saline paddy fields. Proceedings of the National Academy of Sciences. 2020;117(35):21242–21250. https://doi.org/10.1073/pnas.2005911117
21. Ajmera I, Henry A, Radanielson AM, Klein PS, Ianevski A, Bennett MJ, *et al.* Integrated root phenotypes for improved rice performance under low nitrogen availability. Plant, Cell and Environment. 2022;45(3):805–822. https://doi.org/10.1111/pce.14284
22. He S, Wang X, Wu X, Yin Y, Ma LQ. Using rice as a remediating plant to deplete bioavailable arsenic from paddy soils. Environment International. 2020;141:105799. https://doi.org/10.1016/j.envint.2020.105799
23. Huang S, Ma JF. Silicon suppresses zinc uptake through down-regulating zinc transporter gene in rice. Physiologia Plantarum. 2020;170(4):508–591. https://doi.org/10.1111/ppl.13196
24. Konishi N, Ma JF. Three polarly localized ammonium transporter 1 members are cooperatively responsible for ammonium uptake in rice under low ammonium condition. The New Phytologist. 2021;232(4):1778–1792. https://doi.org/10.1111/nph.17679
25. Wang B, Zhu X, Guo X, Qi X, Feng F, Zhang Y, *et al.* Nitrate Modulates Lateral Root Formation by Regulating the Auxin Response and Transport in Rice. Genes. 2021;12(6):850. https://doi.org/10.3390/genes12060850
26. Zhu Y, Qi B, Hao Y, Liu H, Sun G, Chen R, *et al.* Appropriate NH_4^+/NO_3^- Ratio Triggers Plant Growth and Nutrient Uptake of Flowering Chinese Cabbage by Optimizing the pH Value of Nutrient Solution. Frontiers in Plant Science. 2021;12:656144. https://doi.org/10.3389/fpls.2021.656144
27. Ma H, Zhao J, Feng S, Qiao K, Gong S, Wang J, *et al.* Heterologous Expression of Nitrate Assimilation Related-Protein DsNAR2.1/NRT3.1 Affects Uptake of Nitrate and Ammonium in Nitrogen-Starved Arabidopsis. International Journal of Molecular Sciences. 2020;21(11):4027. https://doi.org/10.3390/ijms21114027
28. Ullah S, Ali I, Liang H, Zhao Q, Wei S, Muhammad I, *et al.* An approach to sustainable agriculture by untangling the fate of contrasting nitrogen sources in double-season rice grown with and without biochar. GCB Bioenergy. 2021;13(3):382–392. https://doi.org/10.1111/gcbb.12789
29. Nojiri Y, Kaneko Y, Azegami Y, Shiratori Y, Ohte N, Senoo K, *et al.* Dissimilatory Nitrate Reduction to Ammonium and Responsible Microbes in Japanese Rice Paddy Soil. Microbes and Environments. 2020;35(4):ME20069. https://doi.org/10.1264/jsme2.ME20069

30. Li Y, Zhou J, Hao D, Yang S, Su Y. *Arabidopsis* under ammonium over-supply: Characteristics of ammonium toxicity in relation to the activity of ammonium transporters. Pedosphere. 2020;30(3):314–325. https://doi.org/10.1016/s1002-0160(20)60011-x
31. Iqbal A, Xie H, He L, Ahmad S, Hussain I, Raza H, *et al.* Partial substitution of organic nitrogen with synthetic nitrogen enhances rice yield, grain starch metabolism and related genes expression under the dual cropping system. Saudi Journal of Biological Sciences. 2021;28(1):1283–1296. https://doi.org/10.1016/j.sjbs.2020.11.039
32. Salam M, Sarker NI, Sharmin S. Do organic fertilizer impact on yield and efficiency of rice farms? Empirical evidence from Bangladesh. Heliyon. 2021;7(8):e07731. https://doi.org/10.1016/j.heliyon.2021.e07731
33. Lyu Y, Yang X, Pan H, Zhang X, Cao H, Ulgiati S, *et al.* Impact of fertilization schemes with different ratios of urea to controlled release nitrogen fertilizer on environmental sustainability, nitrogen use efficiency and economic benefit of rice production: A study case from Southwest China. Journal of Cleaner Production. 2021;293:126198. https://doi.org/10.1016/J.JCLEPRO.2021.126198
34. Farzadfar S, Knight J, Congreves K. Soil organic nitrogen: an overlooked but potentially significant contribution to crop nutrition. Plant and Soil. 2021;462:7–23. https://doi.org/10.1007/s11104-021-04860-w
35. Liu L, Li C, Zhu S, Xu Y, Li H, Zheng X, *et al.* Combined Application of Organic and Inorganic Nitrogen Fertilizers Affects Soil Prokaryotic Communities Compositions. Agronomy. 2020;10(1):132. https://doi.org/10.3390/agronomy10010132
36. Nasiyev B, Vassilina T, Zhylkybay A, Shibaikin V, Salykova A. Physicochemical and biological indicators of soils in an organic farming system. The Scientific World Journal. 2021;2021(1):9970957. https://doi.org/10.1155/2021/9970957
37. Jiang P, Xie X, Huang M, Zhou X, Zhang R, Chen J, *et al.* Characterizing N uptake and use efficiency in rice as influenced by environments. Plant Production Science. 2016;19(1):96–104. https://doi.org/10.1080/1343943X.2015.1128103
38. Hameed F, Xu J, Rahim SF, Wei Q, ur Rehman Khalil A, Liao Q. Optimizing nitrogen options for improving nitrogen use efficiency of rice under different water regimes. Agronomy. 2019;9(1):39. https://doi.org/10.3390/agronomy9010039
39. Shankar T, Malik GC, Banerjee M. Effect of nutrient management on yield attributes and yields in rice-based cropping system. International Journal of Bio-Resource, Environment and Agricultural Sciences. 2018;4(2):704–708. https://sbear.in/2_Tanmoy.pdf
40. Gweyi-Onyango JP, Ntinyari W, OgollaEgesa A, Mose R, Njinju S, Giweta M, *et al.* Differences in seasons and rice varieties provide opportunities for improving nitrogen use efficiency and management in irrigated rice in Kenya. Environmental Research Letters. 2021;16:075003. https://doi.org/10.1088/1748-9326/ac03dd
41. Makarov MI. The role of mycorrhiza in transformation of nitrogen compounds in soil and nitrogen nutrition of plants: a review. Eurasian Soil Science. 2019;52:193–205. https://doi.org/10.1134/S1064229319020108
42. Zhou G, Cao W, Bai J, Xu C, Zeng N, Gao S, *et al.* Co-incorporation of rice straw and leguminous green manure can increase soil available nitrogen (N) and reduce carbon and N losses: An incubation study. Pedosphere. 2020;30(5):661–670. https://doi.org/10.1016/s1002-0160(19)60845-3
43. Ali S, Ghosh B, Osmani AG, Hossain E, Fogarassy C. Farmers' Climate Change Adaptation Strategies for Reducing the Risk of Rice Production: Evidence from Rajshahi District in Bangladesh. Agronomy. 2021;11(3):600. https://doi.org/10.3390/AGRONOMY11030600
44. Dixit K, Gupta BR. Effect of farmyard manure, chemical and biofertilizers on yield and quality of rice (*Oryza sativa* L.) and soil properties. Journal of the Indian Society of Soil Science. 2000;48:773–780.
45. Vishwanathan K, Singaravel R. Effect of clay and organic amendments on yield and nutrient uptake of rice in coastal sandy soil. Crop Research. 2016;51(1-3):24–27.
46. Puli MR, Prasad PRK, Jayalakshmi M, Rao SB. Effect of organic and inorganic sources of nutrients on NPK uptake by rice crop at various growth periods. Research Journal of Agricultural Sciences. 2017;8(1):20–24.
47. Kumar K, Sridhara CJ, Nandini KM. Effect of integrated use of organic and inorganic fertilizers on soil fertility and uptake of nutrients in aerobic rice (*Oryza sativa* L.). International Journal of Chemical Studies. 2018;6(4):417–421.
48. Ganguly B, Imayavaramban V, Murugan G. Effect of integrated nutrient management on rice yield parameter's and nutrient uptake. Journal of Pharmacognosy and Phytochemistry. 2019;8:3910–3912.
49. Shultana R, Othman R, Zuan ATK, Yusop MR. Evaluation of growth and nutrient uptake of rice genotypes under different levels of salinity. Research on Crops. 2019;20(1):1–9. https://doi.org/10.31830/2348-7542.2019.001
50. Jat ML, Saharawat YS, Gupta R. Conservation agriculture in cereal systems of South Asia: nutrient management perspectives. Karnataka Journal of Agricultural Sciences. 2011;24(1):100–105.
51. Korneeva EA. Economic evaluation of ecological restoration of degraded lands through protective afforestation in the south of the Russian plain. Forests. 2021;12(10):1317. https://doi.org/10.3390/f12101317
52. Kiryushin VI. The management of soil fertility and productivity of agrocenoses in adaptive-landscape farming systems. Eurasian Soil Science. 2019;52:1137–1145. https://doi.org/10.1134/S1064229319070068

53. Ma X, Li H, Xu Y, Liu C. Effects of organic fertilizers via quick artificial decomposition on crop growth. Scientific Reports. 2021;11:3900. https://doi.org/10.1038/s41598-021-83576-4

54. Ikkonen E, Chazhengina S, Jurkevich M. Photosynthetic nutrient and water use efficiency of *Cucumis sativus* under contrasting soil nutrient and lignosulfonate levels. Plants. 2021;10(2):340. https://doi.org/10.3390/plants10020340

55. Kanash EV, Sinyavina NG, Rusakov DV, Egorova KV, Panova GG, Chesnokov YV, Morpho-Physiological, Chlorophyll Fluorescence, and Diffuse Reflectance Spectra Characteristics of Lettuce under the Main Macronutrient Deficiency. Horticulturae. 2023;9(11):1185. https://doi.org/10.3390/horticulturae9111185

56. Tarakanov IG, Kosobryukhov AA, Tovstyko DA, Anisimov AA, Shulgina AA, Sleptsov NN, *et al.* Effects of light spectral quality on the micropropagated raspberry plants during ex vitro adaptation. Plants. 2021;10(10):2071. https://doi.org/10.3390/plants10102071

57. Loskutov IG, Khlestkina EK. Wheat, barley, and oat breeding for health benefit components in grain. Plants. 2021;10(1):86. https://doi.org/10.3390/plants10010086

58. Ptushenko VV, Avercheva OV, Bassarskaya EM, Berkovich YuA, Erokhin AN, Smolyanina SO, *et al.* Possible reasons of a decline in growth of Chinese cabbage under a combined narrowband red and blue light in comparison with illumination by high-pressure sodium lamp. Scientia Horticulturae. 2015;194:267–277. https://doi.org/10.1016/j.scienta.2015.08.021

59. Shrestha J, Kandel M, Subedi S, Shah K. Role of nutrients in rice (*Oryza sativa* L.): A review. Agrica. 2020;9(1):53–62. https://doi.org/10.5958/2394-448x.2020.00008.5

ORCID IDs
Olumayowa Joseph Iyanda https://orcid.org/0000-0002-5340-9884
Akeem Abdulai Oyekanmi https://orcid.org/0000-0001-7704-1634
Mufutau Olaoye Atayese https://orcid.org/0000-0001-8363-6677
Ayomide Afolabi https://orcid.org/0000-0002-5171-886X

Foods and Raw Materials. 2026;14(1)

ISSN 2308-4057 (Print)
ISSN 2310-9599 (Online)

Research Article
Open Access

Available online at http://jfrm.ru/en
https://doi.org/10.21603/2308-4057-2026-1-659
https://elibrary.ru/CRGXJK

3D bioprinting of hybrid cultured meat from rabbit cells and sunflower protein

Sergey N. Golovin[1,*], Evgeniya Yu. Kirichenko[1], Maxim M. Khanukaev[1], Alexander K. Logvinov[2]

[1] Don State Technical University, Rostov-on-Don, Russia
[2] Southern Federal University, Rostov-on-Don, Russia

* e-mail: labbiobez@yandex.ru

Received 01.02.2024; Revised 11.07.2024; Accepted 06.08.2024; Published online 30.01.2025

Abstract:
A quarter of the world's population has no access to safe foods of high quality due to the inability of traditional agriculture to meet the growing needs. Therefore, cultivated meat produced from a large mass of animal cells in a laboratory is becoming a promising alternative to animal products. In this study, we aimed to develop a technology for obtaining a hybrid cultured meat product from rabbit cells, sodium alginate, and sunflower protein, as well as to analyze its morphological and functional characteristics.

We used rabbit stem cells isolated from the greater omentum and exposed to lipogenic and myogenic differentiation, as well as rabbit skin fibroblasts. The cells were placed in a hydrogel of sodium alginate and sunflower protein and cultured for 72 h to biofabricate tissue constructs by using 3D bioprinting. Confocal and transmission electron microscopy was applied to analyze the morphological and functional characteristics of the cells in the constructs.

Using 3D bioprinting, we obtained tissue constructs of 30×40×3 mm from rabbit cells, sodium alginate, and sunflower protein. According to confocal microscopy, the cells in the tissue constructs remained viable for at least 72 h. Transmission electron microscopy showed that the cells formed tight junctions and were metabolically active for at least 72 h, with fibroblasts secreting procollagen and lipoblasts secreting lipid droplets.

The resulting cellular meat was obtained from a combination of fibroblasts, lipocytes, and myogenic cells, as well as two ink components. The cellular meat product was safe and ready for consumption.

Keywords: Cultured meat, tissue construct, 3D bioprinting, stem cells, rabbit, vegetable protein

Funding: This study was funded by the Priority 2030 Program of the Don State Technical University and the BlueSky Research-2023 Competition of the St. Petersburg Foundation for the Support of Innovations and Youth Initiatives.

Please cite this article in press at: Golovin SN, Kirichenko EYu, Khanukaev MM, Logvinov AK. 3D bioprinting of hybrid cultured meat from rabbit cells and sunflower protein. Foods and Raw Materials. 2026;14(1):52–60. https://doi.org/10.21603/2308-4057-2026-1-659

INTRODUCTION

Over the last 200 years, the world's population has increased eightfold to reach about 8 billion people in 2022. By the end of the 21st century, this figure may grow to 10 billion [1].

According to the UN, about 690 million people worldwide (8.9% of the world population) currently suffer from hunger, and about 2 billion people do not have access to safe and good-quality food [2].

Meat is an essential part of a balanced human diet. Due to its properties, meat has played a decisive role in human evolution and contributed to the development of many economic sectors [3]. Today's animal husbandry, for example, boasts 1.4 billion cattle, 1.1 billion sheep, and 18.6 billion chickens. Farm animals are dominant among all terrestrial vertebrates in terms of their numbers and biomass [4]. However, instead of eliminating hunger, their increasing production leads to a number of global problems. These include higher greenhouse gas emissions, unsustainable use of land and water, antibiotic resistance, and a negative impact on biodiversity [5]. Moreover, animal husbandry is also associated with

Copyright © 2025, Golovin *et al.* This is an open access article distributed under the terms of the Creative Commons Attribution 4.0 International License (https://creativecommons.org/licenses/by/4.0/), allowing third parties to copy and redistribute the material in any medium or format and to remix, transform, and build upon the material for any purpose, even commercially, provided the original work is properly cited and states its license.

some ethical problems, such as inhumane euthanasia, mistreatment of animals, and hard, low-paid manual labor under unsatisfactory conditions [6]. These problems contradict modern principles of sustainable development [7].

In response to these global challenges, food scientists are developing technologies to produce alternative food products that can replace animal protein. They include products based on textured plant protein. Originating in the mid-20th century, they have now taken a significant share of the world market [8]. There are also techniques for producing alternative protein from microalgae [9] or insects, which are part of traditional cuisine in some parts of the world [10]. A relatively new idea is to obtain protein from bacteria, mold, and yeast-like fungi, including fermentation of waste from plant and animal products [11].

However, according to surveys and sensory evaluations, alternative protein products are not yet seen as a complete meat substitute. Despite many years of marketing, their consumption is still insignificant compared to the increasing consumption of meat [12–14].

Cultured meat is a technology that could potentially overcome this misbalance. Put forward by different scientists at different times, this technology was systematically developed by Mark Post, who also proposed its practical implementation [15, 16]. The idea is based on modern achievements in stem cell technology and tissue engineering. In particular, it involves growing edible tissues from donor animal cells under laboratory conditions. Within ten years of the first tasting, 55 companies in 19 countries started to produce cultured meat [17]. Scientists working in cell technologies aim to optimize standard laboratory procedures for the industrial production of cell mass. They replace fetal bovine serum in cell culture media with synthetic or plant analogues and develop methods for giving the cell mass a dense texture that is sensorily similar to that of traditional meat [13, 14, 16, 17].

Since it is technologically difficult to create a dense texture, most cultured meat produced today is minced [13, 16]. Despite its wide use in the food industry, minced meat is mainly used in various convenience foods, which also contain large amounts of fat, salt, and sugar. Such components and flavors are added to improve the taste of cultured meat, which is still inferior to that of traditional meat. This goes against the principles of healthy eating. Therefore, the nutritional profile of cultured meat products needs to be optimized, for example, by using plant protein.

Protein from plant processing waste (e.g., legumes or sunflower) is a cheap source of essential nutrients [18–20]. Since high cost is one of the main obstacles for a widespread use of cultured meat [21, 22], using plant protein can significantly reduce the cost of hybrid meat products.

The 3D layer-by-layer printing technology is increasingly used in various fields. It can create complex three-dimensional structures with high accuracy and reproducibility based on a digital template. This is one of the leading methods in tissue engineering, where it is known as 3D bioprinting [23]. It can be used to create three-dimensional cellular and tissue constructs and simple organs [24]. The use of 3D printing in the food industry is referred to as foodprinting [25]. Potentially, a combination of foodprinting and 3D bioprinting can create meat products with a texture as close as possible to that of meat. This can reduce sensory differences between cultured minced meat from cellular mass, plant protein, and traditional meat [26]. 3D printing also allows for customizing the shape of the final product and varying the ratio of cellular and plant protein mass, which opens up opportunities for a personalized approach [27]. Cellular meat is produced from cultures of multipotent mesenchymal stem cells (MMSCs) and fibroblasts. They are usually obtained from a donor animal by means of a lifetime tissue biopsy. MMSCs are differentiated into myoblasts and adipocytes, followed by cell culturing until the required mass is obtained [28].

In this study, we aimed to develop a technology for producing a hybrid cultured cell product from rabbit cells, sodium alginate, and sunflower protein, as well as to conduct its morphological and functional analysis. To achieve this aim, we set a number of objectives (Fig. 1), namely to: 1) select a donor animal; 2) isolate stable cultures of MMSCs and fibroblasts from the donor, and conduct the myogenic and adipogenic differentiation of MMSCs; 3) manufacture a hydrogel based on sodium alginate and sunflower protein; 4) biofabricate a three-dimensional construct using 3D bioprinting with bio-ink made from the hydrogel and cells; 5) cultivate the resulting construct in a culture medium for 72 h; and 6) conduct a morphological and functional analysis of the cells in the printed construct using confocal laser scanning microscopy and transmission electron microscopy.

STUDY OBJECTS AND METHODS

Obtaining tissue from a donor animal. An adult male rabbit *Oryctolagus cuniculus domesticus* of the Soviet Chinchilla breed was used as a donor animal. The animal was kept in a vivarium in accordance with the internal regulations of the local ethical committee of Don State Technical University and the laws of the Russian Federation. To isolate multipotent mesenchymal stem cells (MMSCs), 2-g fragments of adipose tissue were obtained from the greater omentum by laparoscopic biopsy. Fibroblasts were isolated from the abdominal skin biopsy samples.

Isolating and cultivating MMSCs. MMSCs were isolated from a fragment of adipose tissue of the greater omentum under sterile conditions in a biological safety box. For this, we followed the protocol proposed by Bunnel *et al.* [29]. First, we incubated the biopsy samples in a 0.2% solution of collagenase from crab hepatopancreas (Biolot, Russia) in Dulbecco's phosphate-buffered saline (DPBS) (Biolot, Russia) for 60 min at 37°C and constant shaking. Then, we filtered the resulting suspension through a cell sieve and allowed the cells to sediment by centrifugation.

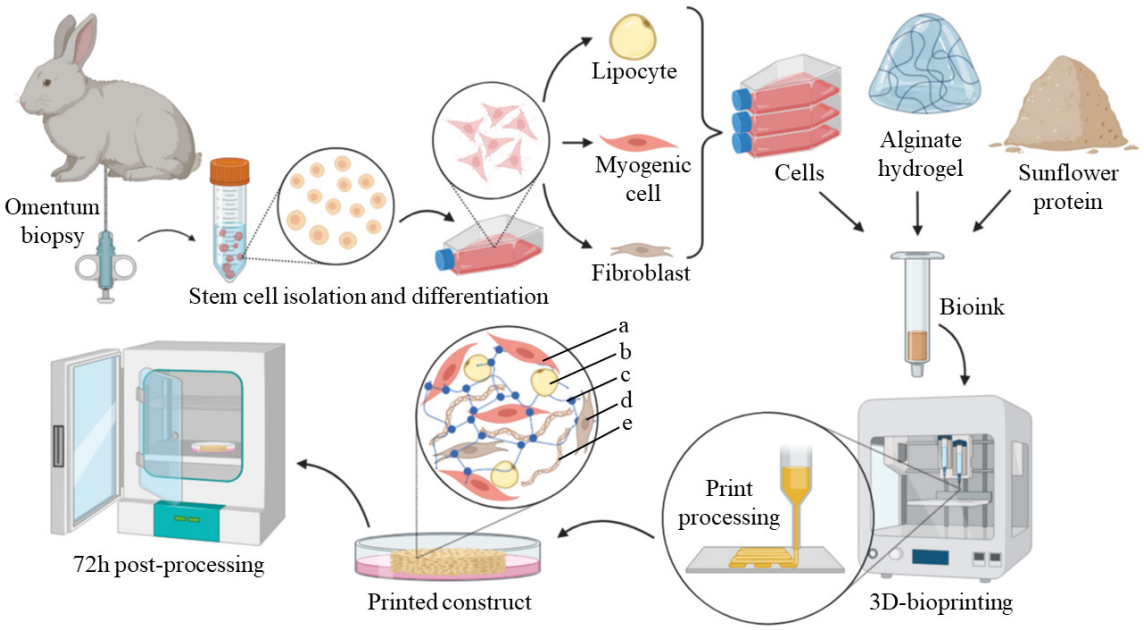

Figure 1 The main stages of production of a hybrid cultured meat product (a – myogenic cell, b – lipocyte, c – Ca^{2+} ionic crosslinked alginate, d – fibroblast, and e – sunflower protein)

Then, we placed the resulting cell mass into culture flasks with the DMEM/F12 medium (Biolot, Russia) and added 10% fetal bovine serum (Biolot, Russia) and 1 ng/mL recombinant basic human fibroblast growth factor (FGF2, Sigma-Aldrich, USA). After 48 h, the medium was changed to remove non-adherent cells. The resulting cell culture was maintained for five passages. Antibiotics and antimycotics were not used during cell cultivation. A 0.25% trypsin-Versene (1:1) solution (Biolot, Russia) was used for cell disaggregation during the passages.

Differentiating MMSCs. To induce adipogenic differentiation, we used a DMEM medium with a high glucose content and stable L-glutamine (Biolot, Russia), 10% fetal bovine serum (Biolot, Russia), 0.1 µmol dexamethasone (D4902 Sigma-Aldrich, USA), 0.45 µmol isobutylmethylxanthine (I5879 Sigma-Aldrich, USA), 170 nmol insulin (I5500 Sigma-Aldrich, USA), and 0.2 µmol indomethacin (I7378 Sigma-Aldrich, USA) [30]. On the 10th day of cultivation, the medium was replaced with a complete DMEM medium for further use. The MMSC culture cultivated in a complete DMEM medium without any inducers was used as a differentiation control.

Lipid droplets detected in the cell cytoplasm during microscopy were taken as a specific differentiation marker [30].

To induce myogenic differentiation, we used a DMEM medium with a high glucose content and stable L-glutamine (Biolot, Russia), 10% fetal bovine serum (Biolot LLC, Russia), 10 mM 5-azacytidine (Sisco Research Laboratories, India), and 50 µmol hydrocortisone (H6909 Sigma-Aldrich, USA) [31]. On the 15th day of cultivation, the medium was replaced with a complete DMEM medium for further use. The MMSC culture cultivated in a complete DMEM medium without any inducers was used as a differentiation control.

Cell fusion with the formation of multinucleated myotubes detected by microscopy was taken as a specific differentiation marker [32].

Isolating fibroblasts. Fibroblasts were isolated from the skin biopsy samples under sterile conditions in a biosafety box according to the protocol proposed by Abade dos Santos [33]. To prevent microbial contamination, the tissue fragments were washed five times in a DMEM medium with a solution of antibiotics and antimycotics (200 units/mL penicillin, 200 µg/mL streptomycin, 0.5 µg/mL amphotericin B, and 50 µg/mL gentamicin) with vigorous shaking. The medium was changed every 5 min.

The tissue fragments were sterilely cut with scissors, placed in a trypsin solution preheated to 37°C for dissociation, and incubated at 37°C for 10 min. After that, the solution was centrifuged at 150 g for 10 min. The sedimented cells were resuspended in a DMEM medium with 10% fetal bovine serum and a solution of antibiotics and antimycotics (100 units/mL penicillin, 100 µg/mL streptomycin, 0.5 µg/mL amphotericin B (Gibco, USA), and 25 µg/mL gentamicin (Biolot, Russia)). Then, the suspension was transferred into culture flasks and incubated at 37°C with 5% CO_2 for 4 h, after which the flasks were washed for a new portion of the medium to be added. After 2 h, washing was repeated and the medium was changed. Subcultivation was carried out when the density of the cell layer reached 90%, with no antibiotics or antimycotics used in the further passages.

Sunflower protein. Dry sunflower protein concentrate with a protein content of 840 g/kg (Kjeldahl method) was provided by MEZ YUG RUSI, Russia.

Bioink preparation. A mixture of sodium alginate and sunflower protein concentrate was used to prepare the bioink. The components were sterilized under ultraviolet light in a biosafety box for 30 min. Then, the components were dissolved in a Dulbecco's phosphate-buffered saline (DPBS) solution without calcium and magnesium (Gibco, China). First, 30 mg/mL of sodium alginate (Sigma-Aldrich, Germany) was dissolved in the DPBS solution on a rotary shaker at room temperature for 1 h. Then, sunflower protein concentrate was added to the solution at a concentrate:alginate ratio of 3:1 dry weight basis. The mixture was homogenized and kept for 2 h at room temperature. Then, a 5-mL syringe was filled with 3 mL of hydrogel and centrifuged for 3 min at 3000 rpm to remove air bubbles.

Immediately before printing, fibroblasts, lipocytes, and myosatellite cells (1:1:1) were pelleted by centrifugation and resuspended in the hydrogel (2×10^6 cells/g) by mixing between two syringes connected by an adapter. Finally, the hydrogel with cells was transferred into the injector, which was placed in the bioprinter head for printing to begin.

3D bioprinting and bioprinter characteristics. For 3D bioprinting, we developed a hydraulically driven print head in the form of a peristaltic pump and a stepper motor. It was installed on an Anet A8 FDM printer. Such a drive allowed us to keep the extrusion speed and the speed of the printer actuators in accordance to each other, as well as to implement a bioink retract procedure at the end of each layer to improve the print quality. Slic3r in the Repitier Host 3D printer control software package (Hot-world GmbH and Co, Germany) was used as a slicer with the following parameters: object's dimensions – 30×40×3 mm, layer height – 0.2 mm, number of perimeters – 0, number of solid layers at the bottom – 0, number of solid layers at the top – 0, filling – 8%, filling type – rectilinear, filling angle – 90°, filling printing speed – 10 mm/s, 25 G nozzle diameter – 0.2 mm, filament diameter – 1.2 mm, extruder feed multiplier – 1.3.

Printing was performed in laminar flow in a biosafety box, and all procedures were conducted at room temperature. Material strands were deposited in 60-mm Petri dishes using air as a plotting medium. After plotting, the scaffolds were transferred into 100 mg/mL of $CaCl_2$ solution and incubated for 10 min to crosslink the alginate component. After crosslinking, the printed construct was transferred to Petri dishes with a DMEM medium and placed in a CO_2 incubator at 37°C for 72 h.

Confocal laser scanning microscopy. Fragments of tissue constructs were incubated in a solution with Sytox Green Stain dye (ThermoFisher Scientific, USA, dilution 1:1000), washed in phosphate buffer, embedded in a medium that prevents signal fading (Abberior, Germany), covered with a cover glass, and viewed in an Abberior Facility Line inverted confocal laser scanning microscope (Abberior Instruments GmbH, Germany). To visualize a 3D object, it was scanned along the Z-axis with a step of 200 nm at a pixel size of 40 nm. The 3D model was constructed using the ImageJ program.

Transmission electron microscopy. Fragments of tissue constructs were fixed in 2.5% glutaraldehyde (Aurion, USA), washed in phosphate buffer, and additionally postfixed in a 1% OsO_4 solution in phosphate buffer for 1.5 h. Then, the cells were dehydrated in alcohols of increasing concentration and absolute ethanol, treated in three changes of propylene oxide, and embedded in epoxy resin based on Epon-812. Semi-thin and ultrathin sections were made using an EM UC 7 ultramicrotome (Leica, Germany) and an ultra 45° diamond knife (Diatome, Switzerland). Semi-thin sections were stained with methylene blue and viewed under a Leica 6000 light-optical microscope (Leica, Germany). Ultra-thin sections were contrasted with uranyl acetate and lead citrate and viewed in a Jem-1011 electron microscope (Jeol, Japan) with an accelerating voltage of 80 kV.

RESULTS AND DISCUSSION

We chose the rabbit as a cell donor because this animal is commonly used in both meat farming and scientific research. Biopsy allowed us to save the life of the donor animal, which is one of the most important principles in the concept of cultured meat. However, we should also consider restrictions that some religions impose on the consumption of certain parts of a living animal. In Islam or Judaism, for example, an animal has to be slaughtered in a ritual for the product to be kosher or halal [34, 35]. This is an important issue for a large number of potential consumers of cultured meat. Noteworthily, the use of a rabbit as a cell donor makes the resulting product non-kosher [36]. Yet, Judaism allows the consumption of cultured meat produced from the cells of kosher animals slaughtered in a ritual manner [35].

The protocols used for cell isolation and differentiation allowed us to obtain stable cell cultures (Fig. 2), which were subcultured during 25 passages for fibroblasts and lipocytes and 12 passages for myogenic cells.

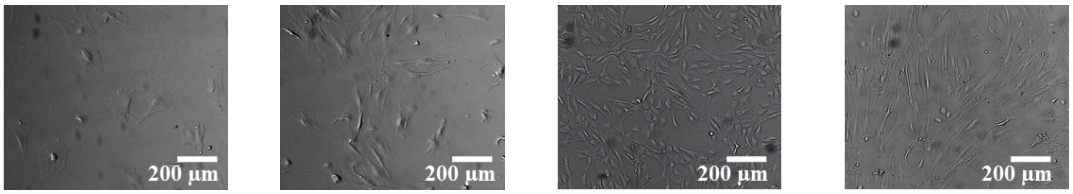

Figure 2 Cell cultures used in this study: (a) MMSCs; (b) fibroblasts; (c) lipocyte; and (d) myogenic cells

Sodium alginate is a standard component of bioink in 3D bioprinting. It is widely available and its hydrogels have acceptable characteristics for cell growth in 3D printed constructs. Due to its ability to cross-link in the presence of calcium ions, sodium alginate contributes to stable constructs [37, 38]. It is a registered food additive (E401) that can be used not only as a thickener and stabilizer, but also as a functional component in nutrition [39, 40].

Sunflower protein concentrate is a second component of bioink. It is non-toxic to cells, has acceptable printability (Fig. 3a), and is widely used in the food industry. In addition, due to its texture and density, plant protein can give the final product familiar sensory properties expected from meat [41].

The color of a product is an important sensory parameter. Although it is not a reliable indicator of safety or quality, consumers often associate the meat's color with its healthiness, which affects their purchasing decision [42]. The technology we used in this study did not allow us to obtain a large amount of myoglobin, which is mainly responsible for the meat's color. Therefore, we used raw beet juice to give the final product a "meaty" color without affecting its structure and integrity. Particularly, the constructs were immersed in raw beet juice for 5 min after post-processing (Fig. 3b).

For sensory evaluation, the samples were fried on both sides in an open frying pan using refined and deodorized vegetable oil at 200 °C for 4 min, without adding spices or flavorings. During frying, the product's color changed from red to yellowish-brown as a result of the Maillard reaction. The panelists described the taste, aroma, and texture of the product as "similar to a meat product".

In semi-thin section preparations stained with methylene blue, fragments of the construct (after 72h of post-processing) consisted of spindle-shaped cells with elongated outgrowths, with moderately stained cytoplasm distributed around the nucleus (Fig. 4a). The cells were arranged in the form of rounded rosettes and clusters visibly contacting one another. The nuclei were oval and round, with finely dispersed chromatin, mostly large and small (Fig. 4b). Some fragments had outwardly empty lumens and others were filled with cytoplasmic outgrowths of the surrounding cells.

Thus, the cells of the constructs under study had the features of young fibroblasts and lipoblasts actively synthesizing proteins – cell growth and differentiation factors or intercellular components (collagen, elastin, glycosaminoglycans, proteoglycans, and multi-adhesive glycoproteins).

Immunofluorescence images of tissue construct fragments were obtained to determine if the cell nuclei were damaged. The samples prepared for immunofluorescence had nuclear rounded groupings resembling a spheroid. The nucleus of such cell groupings looked like a conglomerate of several dozens of cells circling as a crown around the center (Fig. 4c). The nuclei of such cells had an oval, slightly elongated shape with clear contours and uniform intranuclear distribution of nucleic acids (Fig. 4d).

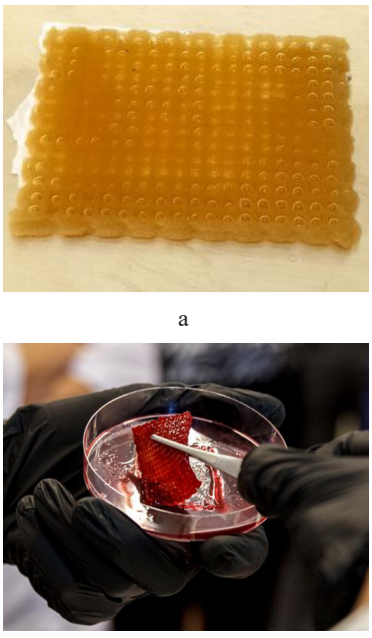

a

b

Figure 3 The printed product: immediately after printing (a); after 72 h of post-processing (b). The product is colored with beetroot juice to look more familiar and is ready to cook

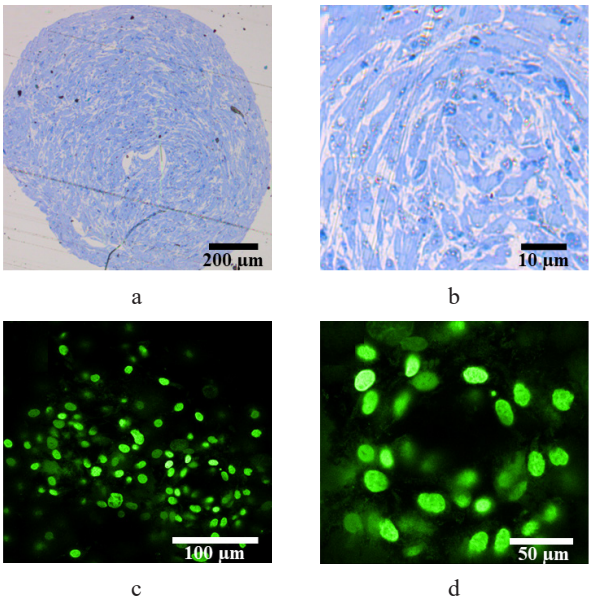

a b c d

Figure 4 Light and confocal laser microscopy of the printed construct cells after 72 h of postprocessing: (a) transverse semi-thin section of the fragment stained with methylene blue (100× magnification); (b) a conglomeration of cells inside the construct (400× magnification); (c) cell nuclei inside the construct stained with Sytox Green (400× magnification); and (d) enlarged section C, with a circular growth of cell nuclei of an oval regular shape with uniform non-condensed chromatin (600× magnification)

According to the immunofluorescence and confocal microscopy, the cell nuclei were fragmentated and transformed, rather than damaged (Fig. 5).

The ultrastructural examination showed that the cells with ultrastructural features of fibroblasts and lipoblasts had spindle-shaped, elongated, and triangular bodies with branched thin outgrowths alongside, as well as small irregular cytoplasmic outgrowths. The cells were densely adjacent to each other, with fragments of direct contact between the membranes of the bodies and the outgrowths (Fig. 6).

Both fibroblasts and lipoblasts contained oval nuclei with finely dispersed chromatin. Almost every cell had one or two large nucleoli, which indicated fibroblast activity. In some cases, the cell nuclei had a curved shape due to invaginations and bulging of the karyolemma. The cytoplasm of fibroblasts was sufficiently saturated with organelles, indicating a high level of intracellular metabolism. Also visible were small oval and round mitochondria in large numbers, rough endoplasmic reticulum (RER), Golgi complexes, lysosomes, centrioles, and multi-vesicular bodies. The lipoblasts had multiple inclusions of round homogeneous osmiophilic lipid droplets of various diameters.

The developed network of the endoplasmic reticulum (rough or granular) and the Golgi complexes indicated an active synthesis of proteins, such as collagen. The endoplasmic reticulum occupied most of the cytoplasm. It looked like stacks of parallel-packed and twisted tubes, as well as rounded and elongated membrane cisterns with signs of expansion, which were dotted with ribosomes on the side facing the cytoplasm. The cytoplasm itself was saturated with individual ribosomes that were not attached to the membrane.

High magnifications also showed the activity of the Golgi complexes involved in the procollagen synthesis (Fig. 7a). Clearly distinguishable were both dictyosomes (transport vesicles) and spherical expansions limited by the membrane and having a smooth surface. Some expanded cisterns of the Golgi complex contained osmiophilic dense material, which might be procollagen molecules (tangled threads). Then the contents of the cylindrical vesicles condensed and turned into secretory granules and vacuoles. They contained the secreted product in concentrated form on the side facing the plasma membrane of the cell. The presence of a large number of Golgi complexes was also a sign of high secretory activity of the cells.

Specialized intercellular tight junctions detected in the cultured meat prototype were an important indicator of intercellular interaction (Fig. 7a, b). A tight junction formed between two dense osmiophilic areas where two cell membranes contacted with each other. At a certain plane of section, osmiophilic stripes were interrupted by a narrow, light intercellular gap that was parallel to them. Such contacts act as highly specialized selective barriers that provide direct contact between the proteins of two adjacent plasma membranes and allow groups of cells to function as structural units. In our prototype of cellular meat, tight junctions were detected between the cells of the same phenotype: fibroblast cells (fibroblast/fibroblast) and lipoblast cells (lipoblast/lipoblast) (Fig. 7a, b).

We managed to reduce the cost of our product by adding sunflower protein and sodium alginate to replace up to 60% of the cell mass, the most expensive component in this technology. At the time of the study, our product cost us $400/100 g. However, it cannot be considered the final cost since we only aimed to demonstrate a possibility of producing a cultured product from rabbit cells in laboratory conditions. According to our estimates, scaling this technology up by using bioreactors and serum-free media for cell cultivation will allow us to reach a cost of $60/kg for the final product at the current level of technological development.

Noteworthily, the technology of cultured meat is only beginning to enter the market, with only the USA and Singapore officially approving its sale [44]. However, since 2013, as much as $3.1 billion has been invested in the companies developing the cultured meat technology, their number reaching 174 in 2023 [45]. This shows high potential of this technology.

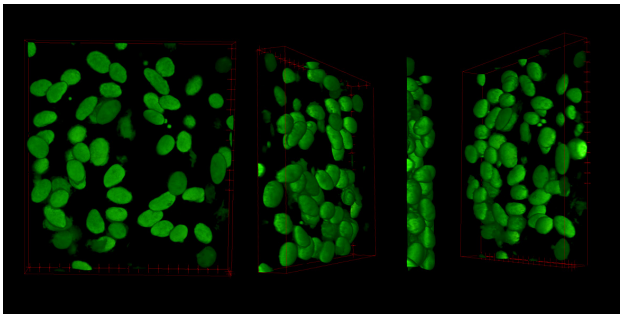

Figure 5 Confocal laser scanning microscopy of the construct's fragment stained with Sytox Green (3D reconstruction in ImageJ [43])

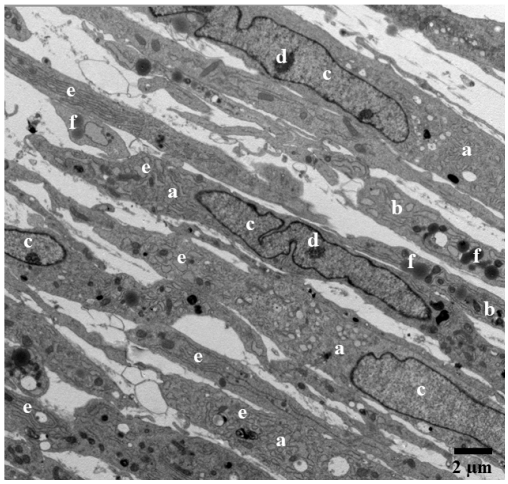

Figure 6 Transmission electron microscopy of the construct cells: a – fibroblast; b – lipoblast; c – nucleus; d – nucleolus; e – rough endoplasmic reticulum; and f – lipid droplets. 10 000× magnification

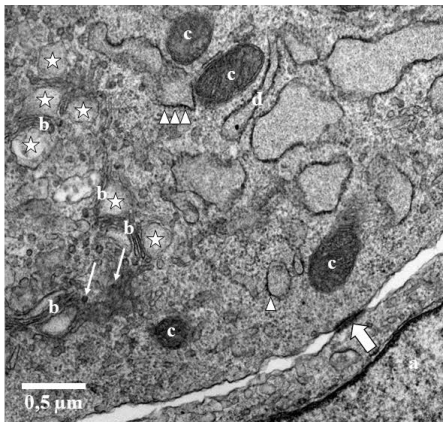

Legends: a – nucleus; b – Golgi complex;
c – mitochondrion; d – rough endoplasmic reticulum.

a

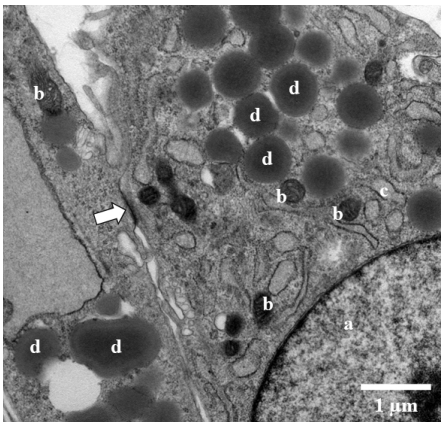

Legends: a – nucleus; b – mitochondrion;
c – rough endoplasmic reticulum; d – lipid droplet.

b

Figure 7 Transmission electron microscopy showing cell proliferation within the printed construct during postprocessing:
(a) the ultrastructure of an active fibroblast region (80 000× magnification). The Golgi complex is in the center of the micrograph, with spherical expansions (asterisks) in addition to the Golgi stacks. Some dilated Golgi cisternae contain osmiophilic dense material in the form of tangled filaments, which may be procollagen molecules. The content of the cylindrical vesicles condenses and is subsequently converted into secretory granules (thin arrows). Two fibroblasts are connected by a tight junction (thick arrow). Ribosomes (triangles) are attached to the rough endoplasmic reticulum.
(b) the ultrastructure of two lipoblasts connected by a tight junction (arrow) (40 000× magnification)

We believe that 3D printing is hardly promising for commercial production due to its technical complexity. We see further development of the hybrid cultured meat technology in producing a cell mass cultivated on microcarriers in a bioreactor. Texturates of plant proteins, such as sunflower, can be used as microcarriers. This way we can obtain a product that resembles minced meat and, in the future, produce ready-to-eat products from it. However, 3D bioprinting can be used to produce cultured meat products for personalized nutrition.

CONCLUSION

In this study, we bioengineered a construct consisting of differentiated rabbit cells, alginate hydrogel, and sunflower protein by using 3D bioprinting. We showed a possibility of producing a cellular meat product from a selected combination of fibroblasts, lipocytes, and myogenic cells, as well as two ink components. According to confocal laser microscopy and electron microscopy, the cells in the construct remained viable, functionally active, and dividing for more than 72 h.

The product developed in our study is safe and ready to eat. We proved that cultured meat can be created from rabbit cells and biofabrication techniques can make the product's structure close to that of traditional meat.

Using components such as alginate and sunflower protein can reduce the cost of the final product and vary its nutritional properties and sensory qualities.

CONTRIBUTION

S.N. Golovin developed the study concept and design and was involved in the cell isolation and cultivation, bioink preparation, 3D bioprinting, and writing the manuscript (drafting, reviewing, and editing). E.Yu. Kirichenko managed the project, developed the study concept and design, prepared the samples for confocal laser scanning microscopy, imaging, and transmission electron microscopy, as well as contributed to writing the manuscript (drafting, reviewing, and editing). M.M. Khanukaev assembled the 3D bioprinter and was involved in 3D bioprinting and writing the manuscript (drafting, reviewing, and editing). A.K. Logvinov prepared the samples for transmission electron microscopy and contributed to writing the manuscript (drafting, reviewing, and editing).

CONFLICT OF INTEREST

The authors declare that there is no conflict of interest regarding this publication.

REFERENCES

1. Pison G, Couppié E, Caporali A. Tous les pays du monde. Population and Sociétés. 2022;(603):1–8. https://doi.org/10.3917/popsoc.603.0001
2. Sustainable Development Goals. Goal 2: Zero Hunger [Internet]. [cited 2024 Mar 20]. Available from: https://www.un.org/sustainabledevelopment/hunger/

3. de Castro Cardoso Pereira PM, dos Reis Baltazar Vicente AF. Meat nutritional composition and nutritive role in the human diet. Meat Science. 2013;93(3):586–592. https://doi.org/10.1016/j.meatsci.2012.09.018
4. Groombridge B, Jenkins M. World Atlas of Biodiversity: Earth's Living Resources in the 21st Century. California: University of California Press; 2002. 340 p.
5. Broom DM. Animal welfare complementing or conflicting with other sustainability issues. Applied Animal Behaviour Science. 2019;219:104829. https://doi.org/10.1016/j.applanim.2019.06.010
6. Losada-Espinosa N, Miranda-De la Lama GC, Estévez-Moreno LX. Stockpeople and Animal Welfare: Compatibilities, Contradictions, and Unresolved Ethical Dilemmas. Journal of Agricultural and Environmental Ethics. 2020;33:71–92. https://doi.org/10.1007/s10806-019-09813-z
7. Stavins R, Wagner AF, Wagner G. Interpreting Sustainability in Economic Terms: Dynamic Efficiency Plus Intergenerational Equity. Economics Letters. 2003;79(3):339–343. https://doi.org/10.1016/S0165-1765(03)00036-3
8. Sha L, Xiong YL. Plant protein-based alternatives of reconstructed meat: Science, technology, and challenges. Trends in Food Science and Technology. 2020;102:51–61. https://doi.org/10.1016/j.tifs.2020.05.022
9. Koyande AK, Chew KW, Rambabu K, Tao Y, Chu DT, Show PL. Microalgae: A potential alternative to health supplementation for humans. Food Science and Human Wellness. 2019;8(1):16–24. https://doi.org/10.1016/j.fshw.2019.03.001
10. Liceaga AM, Aguilar-Toalá JE, Vallejo-Cordoba B, González-Córdova AF, Hernández-Mendoza A. Insects as an alternative protein source. Annual Review of Food Science and Technology. 2022;13:19–34. https://doi.org/10.1146/annurev-food-052720-112443
11. Molfetta M, Morais EG, Barreira L, Bruno GL, Porcelli F, Dugat-Bony E, *et al.* Protein sources alternative to meat: state of the art and involvement of fermentation. Foods. 2022;11(14):2065. https://doi.org/10.3390/foods11142065
12. Macdiarmid J. The food system and climate change: Are plant-based diets becoming unhealthy and less environmentally sustainable? Proceedings of the Nutrition Society. 2022;81(2):162–167. https://doi.org/10.1017/S0029665121003712
13. Siegrist M, Hartmann C. Why alternative proteins will not disrupt the meat industry. Meat Science. 2023;203:109223. https://doi.org/10.1016/j.meatsci.2023.109223
14. Onwezen MC, Bouwman EP, Reinders MJ, Dagevos H. A systematic review on consumer acceptance of alternative proteins: Pulses, algae, insects, plant-based meat alternatives, and cultured meat. Appetite. 2020;159:105058. https://doi.org/10.1016/j.appet.2020.105058
15. Post MJ. Cultured meat from stem cells: Challenges and prospects. Meat Science. 2012;92(3):297–301. https://doi.org/10.1016/j.meatsci.2012.04.008
16. Post MJ, Levenberg S, Kaplan DL, Genovese N, Fu J, Bryant CJ, *et al.* Scientific, sustainability and regulatory challenges of cultured meat. Nature Food. 2020;1:403–415. https://doi.org/10.1038/s43016-020-0112-z
17. Chen L, Guttieres D, Koenigsberg A, Barone PW, Sinskey AJ, Springs SL. Large-scale cultured meat production: Trends, challenges and promising biomanufacturing technologies. Biomaterials. 2022;280:121274. https://doi.org/10.1016/j.biomaterials.2021.121274
18. Ganesh KS, Sridhar A, Vishali S. Utilization of fruit and vegetable waste to produce value-added products: Conventional utilization and emerging opportunities-A review. Chemosphere. 2022;287(3):132221. https://doi.org/10.1016/j.chemosphere.2021.132221
19. Tassoni A, Tedeschi T, Zurlini C, Cigognini IM, Petrusan J-I, Rodríguez Ó, *et al.* State-of-the-Art Production Chains for Peas, Beans and Chickpeas–Valorization of Agro-Industrial Residues and Applications of Derived Extracts. Molecules. 2020;25(6):1383. https://doi.org/10.3390/molecules25061383
20. de Oliveira Filho JG, Egea MB. Sunflower seed byproduct and its fractions for food application: An attempt to improve the sustainability of the oil process. Journal of Food Science. 2021;86(5):1497–1510. https://doi.org/10.1111/1750-3841.15719
21. Nezlek JB, Forestell CA. Meat substitutes: current status, potential benefits, and remaining challenges. Current Opinion in Food Science. 2022;47:100890. https://doi.org/10.1016/j.cofs.2022.100890
22. Grasso S, Asioli D, Smith R. Consumer co-creation of hybrid meat products: A cross-country European survey. Food Quality and Preference. 2022;100:104586. https://doi.org/10.1016/j.foodqual.2022.104586
23. Ovsianikov A, Yoo J, Mironov V. 3D printing and biofabrication. ACM Digital Library: Springer Publishing Company; 2018. 563 p.
24. Dey M, Ozbolat IT. 3D bioprinting of cells, tissues and organs. Scientific Reports. 2020;10:14023. https://doi.org/10.1038/s41598-020-70086-y
25. Nachal N, Moses JA, Karthik P, Anandharamakrishnan C. Applications of 3D Printing in Food Processing. Food Engineering Reviews. 2019;11:123–141. https://doi.org/10.1007/s12393-019-09199-8

26. Seo J W, Jung WK, Park YH, Bae H. Development of cultivable alginate fibers for an ideal cell-cultivated meat scaffold and production of hybrid cultured meat. Carbohydrate Polymers. 2023;321:121287. https://doi.org/10.1016/j.carbpol.2023.121287
27. Chen Y, Zhang M, Bhandari B. 3D Printing of Steak-like Foods Based on Textured Soybean Protein. Foods. 2021;10(9):2011. https://doi.org/10.3390/foods10092011
28. Srutee R, Sowmya RS, Annapure US. Clean meat: techniques for meat production and its upcoming challenges. Animal Biotechnology. 2022;33(7):1721–1729. https://doi.org/10.1080/10495398.2021.1911810
29. Bunnell BA, Flaat M, Gagliardi C, Patel B, Ripoll C. Adipose-derived stem cells: isolation, expansion and differentiation. Methods. 2008;45(2):115–120. https://doi.org/10.1016/j.ymeth.2008.03.006
30. Lund P, Pilgaard L, Duroux M, Fink T, Zachar V. Effect of growth media and serum replacements on the proliferation and differentiation of adipose-derived stem cells. Cytotherapy. 2009;11(2):189–197. https://doi.org/10.1080/14653240902736266
31. Meligy FY, Shigemura K, Behnsawy HM, Fujisawa M, Kawabata M, Shirakawa T. The efficiency of in vitro isolation and myogenic differentiation of MSCs derived from adipose connective tissue, bone marrow, and skeletal muscle tissue. In Vitro Cellular and Developmental Biology – Animal. 2012;48:203–215. https://doi.org/10.1007/s11626-012-9488-x
32. Freshney RI. Culture of Animal Cells: A Manual of Basic Technique and Specialized Applications. Hoboken, New Jersey: John Wiley and Sons; 2015. pp.383–401
33. Abade dos Santos FA, Carvalho CL, Almeida I, Fagulha T, Rammos F, Barros SC, *et al.* Simple Method for Establishing Primary Leporidae Skin Fibroblast Cultures. Cells. 2021;10(8):2100. https://doi.org/10.3390/cells10082100
34. Regenstein JM, Chaudry MM, Regenstein CE. The kosher and halal food laws. Comprehensive reviews in food science and food safety. 2003;2(3):111–127. https://doi.org/10.1111/j.1541-4337.2003.tb00018.x
35. Kenigsberg JA, Zivotofsky AZ. A Jewish Religious Perspective on Cellular Agriculture. Frontiers in Sustainable. Food Systems. 2019;3:128. https://doi.org/10.3389/fsufs.2019.00128
36. Farouk MM, Regenstein JM, Pirie MR, Najm R, Bekhit AED, Knowles SO. Spiritual aspects of meat and nutritional security: Perspectives and responsibilities of the Abrahamic faiths. Food Research International. 2015;76: 882–895. https://doi.org/10.1016/j.foodres.2015.05.028
37. Axpe E, Oyen ML. Applications of alginate-based bioinks in 3D bioprinting. International Journal of Molecular Sciences. 2016;17(12):1976. https://doi.org/10.3390/ijms17121976
38. Gao Q, Kim BS, Gao G. Advanced strategies for 3D bioprinting of tissue and organ analogs using alginate hydrogel bioinks. Marine Drugs. 2021;19(12):708. https://doi.org/10.3390/md19120708
39. Qin Y, Jiang J, Zhao L, Zhang J, Wang F. Applications of Alginate as a Functional Food Ingredient. In: Grumezescu AM, Holban AM. Biopolymers for Food Design. Academic Press; 2018. pp. 409–429. https://doi.org/10.1016/b978-0-12-811449-0.00013-x
40. Puscaselu GR, Lobiuc A, Dimian M, Covasa M. Alginate: From Food Industry to Biomedical Applications and Management of Metabolic Disorders. Polymers. 2020;12(10):2417. https://doi.org/10.3390/polym12102417
41. Joo ST, Choi JS, Hur SJ, Kim GD, Kim CJ, Lee EY, *et al.* A comparative study on the taste characteristics of satellite cell cultured meat derived from chicken and cattle muscles. Food Science of Animal Resources. 2022;42(1):175–185. https://doi.org/10.5851/kosfa.2021.e72
42. Tomasevic I, Djekic I, Font-i-Furnols M, Terjung N, Lorenzo JM. Recent advances in meat color research. Current Opinion in Food Science. 2021;41:81–87. https://doi.org/10.1016/j.cofs.2021.02.012
43. Rasband W. ImageJ User Guide. (1997–2018). National Institutes of Health, Bethesda, Maryland, USA. https://imagej.net/ij/
44. Santos ACA, Camarena DEM, Roncoli Reigado G, Chambergo FS, Nunes VA, Trindade MA, *et al.* Tissue Engineering Challenges for Cultivated Meat to Meet the Real Demand of a Global Market. International Journal of Molecular Sciences. 2023;24(7):6033. https://doi.org/10.3390/ijms24076033
45. Battle M, Bomkamp C, Carter M, Colley Clarke J, Fathman L, Gertner D, *et al.* 2023 State of the industry report: Cultivated meat and seafood. Washington DC: The Good Food Institute; 2023. 74 p. https://gfi.org/wp-content/uploads/2024/04/2023-State-of-the-Industry-Report-Cultivated-meat-and-seafood.pdf

ORCID IDs
Sergey N. Golovin https://orcid.org/0000-0002-1929-6345
Evgeniya Yu. Kirichenko https://orcid.org/0000-0003-4703-1616
Maxim M. Khanukaev https://orcid.org/0009-0002-3127-3389
Alexander K. Logvinov https://orcid.org/0000-0002-8873-3625

Foods and Raw Materials. 2026;14(1)

ISSN 2308-4057 (Print)
ISSN 2310-9599 (Online)

Research Article
Open Access

Available online at http://jfrm.ru/en
https://doi.org/10.21603/2308-4057-2026-1-654
https://elibrary.ru/XIKVIS

Fiber supplements from agro-industrial waste: Effect on valproic acid hepatotoxicity in rats

Maria R. Ramirez[1,2,*], Debora Manuale[1,3], Juan C. Yori[1,3]

[1] National Scientific and Technical Research Council, Buenos Aires, Argentina
[2] University Institute of Medical Sciences – Hector A. Barceló Foundation, Buenos Aires, Argentina
[3] National University of Littoral, Santa Fe, Argentina

* e-mail: mr.ramirez@conicet.gov.ar

Received 27.03.2024; Revised 23.05.2024; Accepted 04.06.2024; Published online 14.02.2025

Abstract:
The agro-industrial sector is one of the biggest organic waste producers. Instead of being discarded into the environment, fruit and vegetable waste could be processed to obtain added value. This article introduces pomace fiber powder made from agro-industrial waste of fruits and vegetables. Its protective potential against hepatotoxicity induced by valproic acid was studied in Wistar rats, both as preventive and curative treatments.

In the preventive test, valproic acid (250 mg/kg/day) was administered orally together with the pomace fiber powder (0.3 and 0.15 mg/kg/day) for 14 days. In the curative test, the rats received valproic acid for 14 days, followed by pomace fiber powder another 14 days, at the same amounts. Physicochemical analysis revealed that the experimental pomace fiber powder contained 15.2 ± 0.5% and 22.0 ± 1.2% of insoluble and soluble dietary fiber, respectively. This ratio made it possible to classify the new supplement as functional. The rats administered with valproic acid gained body weight and demonstrated a significant increase in serum enzyme activities, alanine aminotransferase, and alkaline phosphatase ($p < 0.05$).

These results were confirmed by histopathological examination. In both preventive and curative treatments, the supplementation normalized body weight, improved liver biomarkers, and attenuated the hepatic injury induced in rats by valproic acid. The new pomace fiber powder made of agro-industrial waste proved to be an effective raw material that attenuates the side effects associated with prolonged valproic acid administration.

Keywords: Food waste, waste minimization, pomace, sustainable production, bioeconomy, fiber, hepatotoxicity

Funding: This work was supported by the National Agency for the Promotion of Research, Technological Development and Innovation (ANPCyT), PICT-2020-SERIE A-03055, and the National Scientific Research Council of the Argentina government (CONICET), PIP Project N° 11220200103171CO and PIP No. 11220200100054.

Please cite this article in press as: Ramirez MR, Manuale D, Yori JC. Fiber supplements from agro-industrial waste: Effect on valproic acid hepatotoxicity in rats. Foods and Raw Materials. 2026;14(1):61–70. https://doi.org/10.21603/2308-4057-2026-1-654

INTRODUCTION

Industrial production of fruits and vegetables offers a number of economic benefits: it extends the shelf-life of products while facilitating its transportation and storage. However, the sorting procedure has to follow consumer demands; as a result, it produces a lot of waste that generates contamination. Fruits and vegetables that do not meet consumer requirements are discarded or used as livestock feed [1]. Horticulture waste causes serious environmental problems such as unpleasant odors or proliferation of insects and rodents. For example, the central market of Santa Fe, Argentina, is one of the largest waste generators in the city. Every month, it sends about 150 tons of unsorted organic (food) and inorganic (plastic, paper, wood, cardboard) wastes to the landfill. The environmental costs are not the only costs associated with the final disposal of agro-industrial waste: it also includes the missed profit associated with the food waste, the costs of transportation to the landfill, the fee for its overturn, etc.

Other large market hubs face a similar situation, as do companies that wash and package fruits and vegetables. Argentina needs new technologies that would provide sustainable economic solutions since industrial fruit production is one of its fundamental industries.

Copyright © 2025, Ramirez *et al.* This is an open access article distributed under the terms of the Creative Commons Attribution 4.0 International License (https://creativecommons.org/licenses/by/4.0/), allowing third parties to copy and redistribute the material in any medium or format and to remix, transform, and build upon the material for any purpose, even commercially, provided the original work is properly cited and states its license.

Although fruit waste possesses economic value, it is currently undervalued [2]. An optimized system for treating fruit and vegetable waste could turn it into a high-quality and low-cost source of fiber and bioactive compounds. Fruit and vegetable waste could even be revalued as raw materials with good prospects in the food industry and medicine, where it could be used as a source of food additives [3]. In particular, dietary fiber and phytocompounds play a key role in the prevention and modulation of host response to certain diseases, infections, and adverse drug reactions [4–6]. Drug-induced adverse reactions account for about 6% of hospital admissions [7]. Valproic acid is a medical preparation that is usually well-tolerated in humans. However, its chronic use may lead to adverse reactions, ranging from increased body weight and asymptomatic elevation of liver enzymes (transaminases) to microvesicular steatosis with diffuse necrosis [6, 8].

This effect seems to be related to carnitine depletion, with the consequent mitochondrial alteration. Consequently, concomitant administration of L-carnitine is recommended as a preventive treatment of hepatotoxicity given decompensation in carnitine shuttle during fatty acid metabolism following the accumulation of valproic acid metabolites [8]. In turn, animal models of valproic acid toxicity show an alteration of fatty acid metabolism associated with accumulation of hepatic lipid content within 2-4 h after valproic acid administration. Molecular studies suggest that hepatic accumulation of 4-en-valproic acid and its b-oxidation products trigger a cascade of reactions culminating in liver injury [8]. Histopathological and biochemical assays also revealed that valproic acid causes inflammation, oxidative stress, and hepatocyte damage in rats [8, 9]. Another research focused on supplementation with such antioxidants as postbiotic butyrate. It is a short-chain fatty acid produced by intestinal bacterial fermentation of dietary fibers. It normalized liver biomarkers, improved fatty acid metabolism, and reduced inflammation and fibrosis induced by valproic acid [10]. Ellagic acid, polyunsaturated fatty acid, and ω-3 docosahexaenoic acid also prevent hepatotoxicity associated with valproic acid [10, 11].

However, no attempt has been made so far to mitigate the toxicity of valproic acid through the intake of natural fiber. Dietary fiber is known for its numerous health benefits against various diseases [12]. Fiber consumption was reported to improve liver biochemistry in cases of necroinflammatory and fibrotic changes associated with steatohepatitis [13]. This study was designed to reuse fruit and vegetable discards in order to investigate whether the administration of the raw material obtained would attenuate adverse effects induced by valproic acid in rats.

STUDY OBJECTS AND METHODS

Raw materials. The possibility of recovering a waste material depends on its composition and availability over time. The first step was to quantify waste by type to define an appropriate processing strategy. In this study, fruit and vegetable discards were obtained from the Fruit and Vegetable Concentrator Market in Santa Fe, Argentina. The wastes were sorted into three groups. Group 1 included carrots, pumpkins, tomatoes, grapes, watermelons, pink grapefruits, peppers, etc. Group 2 included potatoes, sweet potatoes, cassava, zucchini, squash, peas, corn, beans, bananas, apples, etc. Group 3 included artichoke, chard, celery, cauliflower, asparagus, chicory, lettuce, broccoli, cucumbers, beans, cabbage, garlic, etc.

Figure 1 shows the temporal distribution of the wastes in April 2023. Group 1 and, to a lesser extent, Group 2 were the main contributors to waste production throughout the year. Group 3, on average, represented less than 10% of the total waste and became significant only during November. This study focused on the valorization of Group 1 discards generated on a sales day in April 2023. Regarding handling and storage, the discards were subjected to visual inspection: the parts affected by microorganisms were extracted and stored at 4°C until use.

Preparing pomace fiber powder from fruit and vegetable waste. Group 1 wastes were processed in a JU655 juice extractor to obtain pomace and juice, which were separated by filtration. Then, the pomace was dried in a stove at 110°C overnight and milled in a micronizer into a fine powder (Fig. 2).

Analytical methods. We used standard methods 934.01, 942.05, 922.06, and 991.43, as recommended by the Association of Official Analytical Chemists, to determine the moisture, ash, fats, and total dietary fiber (soluble and insoluble), respectively. The nitrogen content was determined by the Kjeldahl method 2001.11 [14]. The protein content was estimated as the nitrogen content multiplied by 6.25. The concentration of total sugar was measured by the 3.5-dinitrosalicylic acid (DNS) method after acid hydrolysis with 1.2 M HCl at 65°C for 15 min and neutralization with 1 M NaOH [3]. To define the contents of phosphorus, iron, and heavy metals (Hg, Pb, As, Cd), we appealed to the inductively coupled plasma-optical emission spectroscopy (ICP-OES, Perkin Elmer, Optima 2100 DV). This procedure was preceded by the digestion in a nitric and perchloric acid solution (1:5, v/v).

The water- and oil-holding capacities were determined in line with the methodology described in [3]. The fiber density was determined by measuring the volume and weight of a representative sample of the fiber and combining these values to calculate density.

The microbiological profile of the pomace was described using the manufacturer's instructions for a bacteriological diagnostic kit, ZT Lab, Argentina. It involved total plate count, total coliforms, and Salmonella [15].

Quantifying total flavonoids. We used spectrophotometry to define the total flavonoids as described in [4]. The aluminum chloride colorimetric method was used to determine the flavonoid content in the waste extract: absorption readings were taken at 425 nm after 30 min of incubation in the dark. With the standard curve of quercetin, the total flavonoid contents were expressed as milligram quercetin equivalent per gram of extract, mg QE/g.

Animal treatments. The Wistar male rats (155 and 160 g) were acquired from the biotherium of the Veterinary Medicine Department, National University of Santa Fe, Argentina. The experimental animals lived in an animal house in a room with controlled temperature and humidity, with a constant 12:12 h light and dark cycle and free access to water and food of Ganave brand, Argentina.

Ethical approval. This work was approved by the Ethics Committee of the Medical Department, National University of the Northeast (UNNE, Corrientes), Permit Number: Res N° 0017 CICUAL 23.

Experimental procedures. After a week of clinical observation, the rats were randomly divided into eight groups of four rats in each. During the first seven days of the trial, they followed a control diet. The rats that passed this acclimatization and quarantine period were randomly divided into four groups, four rats in each. For 14 days, they received food according to the scheme described below. All in all, the animals underwent two trials, a preventive and a curative one:

During preventive trial, the animals were subjected to preventive treatment to induce hepatotoxicity and evaluate the protection potential of the fiber from fruit and vegetables waste during valproic acid (TEVA-Argentina) treatment.

This stage included the following groups of experimental animals:

– control group animals that received distilled water (Group I);
– animals that received 250 mg/kg body weight of valproic acid orally for 14 days to induce hepatotoxicity (Group II);
– control group that received orally 0.3 mg/kg body weight of experimental fiber (Group III);
– animals administered concomitantly with valproic acid and fiber at a low dose of 0.15 mg/kg body weight for 14 days (Group IV); and
– animals administered concomitantly with valproic acid and fiber at a high dose of 0.3 mg/kg body weight for 14 days (Group V).

During curative trial, the animals were assessed for possible reversal of hepatotoxicity.

This stage included the following groups of experimental animals:

– rats that received 250 mg/kg body weight of valproic acid for 14 days to induce hepatotoxicity before being sacrificed 14 days after the end of the valproic acid treatment (Group VI);
– rats administered with valproic acid for 14 days, then supplemented with fiber at a low dose of 0.15 mg/kg body weight (Group VII); and
– rats administered with valproic acid for 14 days, then supplemented with fiber at a high dose of 0.3 mg/kg body weight (Group VIII).

The bioavailability of orally administered drugs depends on the absorption and plasma clearance processes that can be affected by some dietary components in the gastrointestinal tract. Thus, food can decrease, delay, increase, or accelerate the absorption of different drugs. However, these studies are scarce, and their results are variable. An *in-vivo* study in healthy individuals evaluated the influence of citrus pectin (14 g) on the pharmacokinetics of valproic acid (500 mg; single dose) [16]: the fiber affected neither the absorption rate nor the amount of drug absorbed.

However, it is not easy to assess the extent to which they contribute to changes in drug bioavailability, therapeutic failures, and toxicity. For this reason, in this study, the administration of valproic acid was carried out in the morning (8 a.m.); and the pomace fiber was given in the late afternoon (6 p.m.), that is, with a difference of 10 h between the administrations. The doses of fiber supplemented were in line with our previous research [3]. In the case of valproic acid, the dose and time of administration came from Abdelkader *et al*. [10].

Biochemical Assay. At the end of each experimental period, four rats from each group were weighed and then anaesthetized after fasting for 8 h. We collected heart, livers, kidneys, and blood samples in heparinized tubes by cardiac puncture. The blood was centrifuged immediately after collection at 4°C and 4000 g for 15 min. The plasma obtained was processed in a spectrophotometer (Biotraza), using colorimetric and kinetic techniques distributed by Wiener Laboratories (Santa Fe, Argentina). The parameters assessed in each of them included total cholesterol, high-density lipoprotein cholesterol, low-density lipoprotein cholesterol, triglycerides, aspartate amino transferase, alanine amino transferase, and alkaline phosphatase [3, 4].

Total cholesterol. Through the action of the enzyme cholesteryl esterase, cholesterol esters broke down to free cholesterol and fatty acids. In turn, the enzyme cholesterol oxidase catalyzed the oxidation of cholesterol to form cholest-4-ene-3-one and hydrogen peroxide. In the presence of peroxidase, the hydrogen peroxide caused the oxidative coupling of phenol and 4-aminoantipyrine to form a red quinoneimine dye. The intensity of the dye was proportional to the concentration of cholesterol, which was measured by the absorbance increase at 512 nm.

High-density lipoprotein cholesterol (HDLC). The test relied on the adsorption of synthetic polyanions on the lipoprotein surface. The combined action of the polyanions and the detergent solubilized the high-density lipoprotein cholesterol. In the presence of peroxidase, the hydrogen peroxide formed reacts with N, N-bis(4-sulphobutyl)-m-toluidine and 4-aminoantipyrine to produce a quinoneimine red dye. Its intensity was proportional to the high-density lipoprotein cholesterol concentration, which was determined by the absorbance increase at 552 nm.

Low-density lipoprotein cholesterol (LDLC). In this method, high-density lipoprotein cholesterol, very low-density lipoprotein cholesterol, and chylomicrons were hydrolyzed with Detergent 1. Consequently, cholesterol from these lipoproteins was affected by the enzymatic action of cholesteryl esterase and cholesterol

oxidase enzymes to generate hydrogen peroxide. The latter was then consumed by peroxidase in the presence of 4-aminoantipyrine, thus generating a colorless product. Detergent 2 added together with N,N-bis(4-sulphobutyl)-m-toluidine as a conjugating agent released cholesterol from the low-density lipoprotein cholesterol particles to produce a colored compound. Its intensity was proportional to the concentration of low-density lipoprotein cholesterol, which was determined by measuring the absorbance increase at 552 nm.

Triglycerides. Lipoprotein lipase hydrolyzed triglycerides to fatty acids and glycerol. The resulting molecule was phosphorylated to glycerol-3-phosphate by adenosine triphosphate in a reaction catalyzed by glycerol kinase. Glycerol phosphate oxidase catalyzed oxidation of glycerol-3-phosphate to form dihydroxyacetone phosphate and hydrogen peroxide. In the presence of peroxidase enzyme activity, hydrogen peroxide carried out the oxidative coupling of 4-chlorophenol and 4-aminophenazone and formed a quinoneimine red dye, which was measured at 512 nm. The increase in absorbance was proportional to the concentration of triglycerides in the sample.

Aspartate aminotransferase. This enzyme catalyzed the transfer of an amino group between L-aspartate and 2-oxoglutarate to obtain oxaloacetate and L-glutamate. In the presence of malate dehydrogenase, oxaloacetate reacted with nicotinamide adenine dinucleotide + hidrogen (NADH) to form its oxidized and reduced form NAD+. The rate of NADH oxidation was proportional to the catalytic activity of aspartate aminotransferase assessed by measuring the absorbance decrease at 340 nm.

Alkaline phosphatase. In the presence of magnesium and zinc ions, phosphatases cleaved p-nitrophenylphosphate into phosphate and p-nitrophenol.

Alanine aminotransferase. This enzyme catalyzed the reaction between L-alanine and 2-oxoglutarate. Pyruvate formed was reduced by NADH in a reaction catalyzed by lactate dehydrogenase to form L-lactate and NAD+. Thus, the rate of NADH oxidation was proportional to the catalytic activity of alanine aminotransferase determined by the absorbance decrease at 340 nm.

Histopathological examination. After sacrifice, the hearts, livers, and kidneys were dissected, examined for color changes, and weighed to obtain a relative weight. After fixing liver and kidney samples in 10% buffered formalin for 24 h, they were dehydrated in isopropyl alcohol of increasing strength, rinsed with xylol, and embedded in paraffin. After being cut with a microtome, the histological sections were deparaffinized and stained with hematoxylin/eosin to evaluate histopathological alterations in each experimental group [3, 4]. The stained tissue sections underwent optical microscopy to obtain digital images.

Statistical analysis. The data were expressed as mean ± standard deviation, and the significance of the data between groups was tested by Infostat scientific software, Argentina. Statistical analyses relied on Tuckey's test. In all cases, we took the probability level of 95% as significant.

RESULTS AND DISCUSSION

Figure 1 describes the selection and temporal classification of the original fruit and vegetable waste obtained from the central market in Santa Fe, Argentina. The research featured colored fruits and vegetables discarded in April 2023.

The discards yielded a light brown fiber-rich powder of neutral flavor (Fig. 2).

Table 1 shows the chemical composition of the experimental pomace powder. The moisture content proved adequate for long shelf-life under suitable conditions. The total dietary fiber content was 37.20 ± 0.22% solids, where 15.20 ± 0.50% corresponded to insoluble dietary fiber and the remaining 22.0 ± 1.20% corresponded to soluble dietary fiber. The ratio made it possible to classify the pomace powder as a functional supplement [3].

The ash content was in agreement with the values reported by other researchers who studied similar fruit and vegetable wastes [17]. It can be associated with the presence of iron and phosphorus, both bio-elements

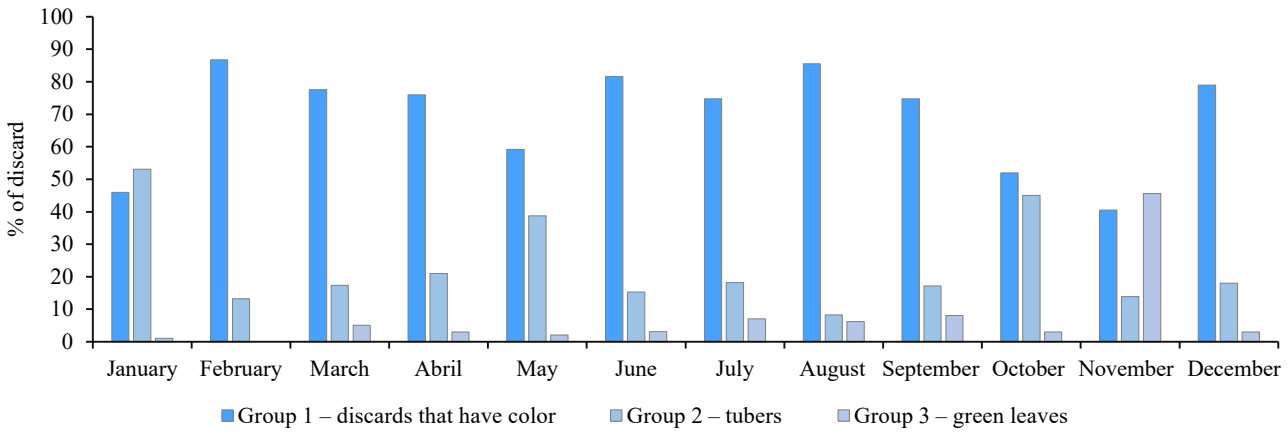

Figure 1 Fruit and vegetable waste discarded on the central market of Santa Fe, by month



Figure 2 Experimental fiber-rich powder obtained from agro-industrial waste pomace

Table 1 Chemical composition of pomace fiber powder obtained from fruit and vegetable waste

Compound	Value
Water, %	12.0 ± 0.10
Sugars, %	18.60 ± 0.15
Soluble fiber, %	22.00 ± 1.20
Insoluble fiber, %	15.20 ± 0.50
Total fiber, %	37.20 ± 0.22
Proteins, %	8.70 ± 0.25
Fats, %	5.20 ± 0.02
Ash, %	4.70 ± 0.30
Iron, ppm	13.00 ± 0.50
Phosphorus, ppm	176.00 ± 0.50
Heavy metals, ppm	< 10

Values are represented as means ± standard deviations (n = 3). Some results were expressed as % solids

Table 2 Physical composition of pomace fiber powder obtained from fruit and vegetable waste

Indicator	Value
Water-holding capacity, g/g	3.30 ± 0.40
Oil-holding capacity, g/g	1.30 ± 0.25
Density, g/cm^3	350.0 ± 10.0

Values are represented as means ± standard deviations (n=3)

Table 3 Microbiological analysis of pomace fiber powder obtained from fruit and vegetable waste

Indicator	Value
Total plate count, UFC/g	< 1000
Salmonella	not detected
Total coliforms, UFC/g	< 10

Values are means ± standard deviations (n = 3)

being important for human and animal nutrition. The heavy metal content was low, indicating that the pomace fiber powder was not toxic to humans. Insoluble dietary fiber absorbs and retains water. Water-holding capacity is the amount of water that binds to fiber without any external force but gravity and atmospheric pressure [3]. Our pomace fiber powder had a water-holding capacity value of 3.30 ± 0.40 g/g, which is relatively low compared to other natural fibers with lower amounts of fermentable sugars (Table 2). The oil holding capacity was 1.30 ± 0.25 g fat/g.

The microbiological analyses proved that the method of production guaranteed the safety of the experimental product, rendering it suitable for human and animal consumption (Table 3).

The *in-vivo* assays showed that valproic acid administration resulted in a large increase in body weight (Tables 4 and 5) and a significant decrease in the relative weights of both the liver and kidneys compared to the control group (Table 6) [17]. Table 4 shows the results of the preventive study.

Previous clinical and experimental studies reported a dietary inverse correlation between fiber intake and body weight, body fat and changes in body mass index [18]. In our research, the experimental pomace fiber powder in rats' diet reversed body weight gain to normal values, in both preventive and curative studies. The mechanism by which fiber reduces body weight is a subject of different hypotheses, e.g., that it increases satiety, decreases energy intake, and/or slows down nutrient absorption. Table 5 shows the results of the curative study.

In this study, periodic observations demonstrated no major change in habitual energy intake or behavioral patterns during the entire test period. These findings suggest that the experimental pomace powder had an effect on fat oxidation and storage, as reported in other publications. However, other certain factors might be considered, e.g., hormonal control and the effects of fiber in the intestines [6, 13, 18]. Similarly, the animals that received the pomace fiber powder had a lower liver weight relative to the group that received valproic acid only. The effect was probably due to the loss of white adipose tissue [19].

The relative kidney weight was lower than in the animals that received valproic acid, but this result could not be related to a possible biological significance (data not shown). The macroscopic and microscopic examinations clearly showed that neither valproic acid

Table 4 Body weight after treatment with valproic acid and pomace fiber powder during preventive study

Groups	Initial body weight, g	Final body weight, g
Group I: control (distilled water)	165.15 ± 4.60	197.09 ± 6.52^a
Group II: valproic acid	166.54 ± 7.01	242.06 ± 6.97^b
Group III: control + pomace powder	168.46 ± 6.56	200.03 ± 6.72^a
Group IV: valproic acid + pomace powder 0.15 mg/kg body weight	162.66 ± 5.13	220.47 ± 7.14^a
Group V: valproic acid + pomace powder 0.3 mg/kg body weight	167.01 ± 6.28	221.53 ± 7.08^a

Mean ± standard deviation with different superscripts in the column differ from each other ($p < 0.05$)

Table 5 Body weight after treatment with valproic acid and pomace fiber powder during curative study

Groups	Initial body weight, g	Final body weight, g
Group I: control (distilled water)	202.06 ± 7.63	220.88 ± 6.08[a]
Group VI: valproic acid	244.32 ± 5.47	256.95 ± 7.72[b]
Group VII: valproic acid + pomace powder 0.15 mg/kg body weight	236.73 ± 5.52	223.41 ± 7.75[a]
Group VIII: valproic acid + pomace powder 0.3 mg/kg body weight	234.76 ± 6.29	219.72 ± 8.03[a]

Mean ±standard deviation followed by different letters in the column differ from each other ($p < 0.05$)

Table 6 Relative organ weight from rats after treatment with valproic acid and pomace fiber powder

Groups	Heart, g	Liver, g	Kidney, g
Group I: control (distilled water)	0.37 ± 0.02[a]	3.88 ± 0.14[a]	0.91 ± 0.09[a]
Group II / VI: valproic acid	0.28 ± 0.03[b]	3.21 ± 0,09[b]	0.77 ± 0.07[b]
Group III: control + pomace powder	0.37 ± 0.03[a]	3.83 ± 0.11[a]	0.92 ± 0.10[a]
Group IV / VII: valproic acid + pomace powder 0.15 mg/kg body weight	0.39 ± 0.05[a]	3.55 ± 0.14[a]	0.93 ± 0.11[a]
Group V / VIII: valproic acid + pomace powder 0.3 mg/kg body weight	0.38 ± 0.06[a]	3.45 ± 0.12[a]	0.94 ± 0.12[a]

Mean ± standard deviation followed by different superscripts in the column differ from each other by Tukey's test, with 95% confidence (n = 4)

Table 7 Effects of valproic acid and pomace fiber powder on blood biochemistry in rats during preventive study

Variable	Group I: control	Group II: valproic acid	Group III: pomace powder	Group IV: valproic acid + 0.15 mg/kg body weight, pomace powder	Group V: valproic acid + 0.3 mg/kg body weight, pomace powder
Total colesterol, mg/dL	61.23 ± 3.37[a]	92.33 ± 4.64[b]	83.13 ± 4.89[a]	78.43 ± 3.37[a]	55.11 ± 5.03[a]
High-density lipoprotein cholesterol, mg/dL	30.41 ± 1.88[a]	19.03 ± 1.91[b]	23.25 ± 2.31[b]	19.63 ± 2.92[b]	33.93 ± 3.20[a]
Low-density lipoprotein cholesterol, mg/dL	20.81 ± 2.49[a]	35.01 ± 2.98[b]	16.07 ± 2.08[a]	32.13 ± 4.27[b]	14.14 ± 3.67[a]
Triglycerides, mg/dL	142.67 ± 14.25[a]	222.40 ± 16.75[b]	109.12 ± 15.57[a]	99.57 ± 17.40[a]	104.27 ± 16.01[a]
Aspartate aminotransferase, U/mL	73.33 ± 21.46[a]	85.41 ± 24.30[b]	69.93 ± 22.20[a]	60.43 ± 19.47[a]	52.14 ± 15.09[a]
Alanine aminotransferase, U/mL	36.71 ± 11.97[a]	104.17 ± 34.40[b]	34.55 ± 10.91[a]	39.86 ± 12.56[a]	42.57 ± 10.62[a]
Alkaline phosphatase, U/mL	322.57 ± 89.40[a]	468.23 ± 104.16[b]	329.12 ± 81.50[a]	282.37 ± 75.21[a]	288.79 ± 60.46[a]

Mean ± standard deviation followed by different superscripts in the column differ from each other ($p < 0.05$)

(250 mg/kg/day) nor the high dose (0.3 mg/kg/day) of experimental pomace fiber alone could cause obvious morphological changes in the kidney tissue [8]. In addition, the administration of valproic acid caused a significant increase in total cholesterol, low-density lipoprotein cholesterol, and triglycerides in plasma after treatment (Table 7) [20]. On the other hand, the healthy animals supplemented with the pomace fiber powder demonstrated an increase in total cholesterol while the values of low-density lipoprotein cholesterol and triglycerides went down. The increase in total cholesterol was probably due to the fact that the time elapsed between the beginning of the study and the sacrifice of the healthy animals was not long enough for the healthy rats to adapt to the supplementation, or that the effect depended on the physiological state of the animal [12, 21].

A reduction in triglycerides and total cholesterol was detected in the rats administered with valproic acid and supplemented with both doses of pomace powder (Tables 7). The animals supplemented with the high dose of pomace powder demonstrated lower low-density lipoprotein cholesterol and higher high-density lipoprotein cholesterol. Results similar to ours were reported for other types of fiber, which showed that daily intake of soluble fiber significantly reduced serum concentrations of total cholesterol and low-density lipoprotein cholesterol in rodents and humans [12, 18, 22]. The reduction in cholesterol levels was probably due to the soluble fiber fraction in the pomace fiber powder, in particular fermentable pectins and hemicelluloses [6, 18]. In contrast, our results were inconsistent with those of other studies, probably, due to the differences in processing techniques, molecular weight, viscosity, and administration method. According to the scientific literature, this finding could be due to the effect of pomace fiber powder on the expression of HMG-CoA reductase, which reduces cholesterol synthesis and increases cholesterol excretion in bile [22, 23]. It is also possible that the fermentation of pomace powder by the intestinal microflora modified the production of short-chain fatty acids, thus reducing

Table 8 Effects of valproic acid and pomace fiber powder on blood biochemical parameters in rats during curative study

Variable	Group I: control	Group VI: valproic acid	Group VII: valproic acid + 0.15 mg/kg body weight, pomace powder	Group VIII: valproic acid + 0.3 mg/kg body weight, pomace powder
Total cholesterol, mg/dL	75.11 ± 4.53[a]	99.51 ± 3.40[b]	92.79 ± 3.43[b]	94.16 ± 4.73[b]
High-density lipoprotein cholesterol, mg/dL	33.07 ± 3.03[a]	21.44 ± 2.76[b]	21.44 ± 2.63[b]	26.63 ± 2.13[a]
Low-density lipoprotein cholesterol, mg/dL	20.27 ± 3.25[a]	20.50 ± 2.05[a]	12.87 ± 3.23[b]	16.20 ± 2.61[b]
Triglycerides, mg/dL	155.01 ± 18.02[a]	230.13 ± 15.36[b]	178.72 ± 18.50[a]	144.41 ± 17.10[a]
Aspartate aminotransferase, U/mL	76.22 ± 23.21[a]	78.59 ± 29.78[a]	52.25 ± 16.97[b]	51.43 ± 19.52[b]
Alanine aminotransferase, U/mL	45.04 ± 13.89[a]	79.96 ± 24.89[b]	33.01 ± 11.37[a]	37.60 ± 13.49[a]
Alkaline phosphatase, U/mL	357.68 ± 62.54[a]	396.70 ± 63.77[a]	293.33 ± 59.74[b]	305.14 ± 57.18[b]

Mean ± standard deviation followed by different superscripts in the column differ from each other ($p < 0.05$)

acetate production and increasing propionate synthesis. Consequently, endogenous synthesis of cholesterol, fatty acids, and low-density lipoproteins went down [22, 24].

In animals exposed to the curative study and supplemented with the experimental pomace fiber powder, plasma concentrations of low-density lipoprotein cholesterol and triglycerides decreased significantly and those of high-density lipoprotein cholesterol increased with respect to the group that received valproic acid (Table 8). This finding was consistent with the results of previous reports on the cholesterol-reducing effects of dietary fiber [3, 23]. Interestingly, both doses of pomace fiber powder significantly decreased total plasma triglyceride concentrations in both assays, i.e., preventive and curative, and, at basal level, in healthy animals supplemented with pomace powder only. This seems to indicate that the experimental fiber supplement was effective in reducing triglycerides in plasma and that its effect depended on the physiological state of the animal [21]. The reason for this finding is not fully established at present. Probably, the reduction in serum triglyceride levels is the result of decreased fat absorption in the small intestine, as well as preservation of the gastrointestinal tract due to the prebiotic activity of the fibers [12, 21, 24]. In the present work, the cytosolic integrity was estimated from the concentrations of aspartate aminotransferase, alanine aminotransferase, and alkaline phosphatase in the different mice groups under study. The results showed a significant increase in alanine aminotransferase and alkaline phosphatase activity in the plasma of animals administered with valproic acid compared to the control animals (Table 7). This increase was evident in both preventive and curative trials (Table 8). The alterations could be related to oxidative stress caused by toxic metabolites of valproic acid that damaged liver cells and consequently released these enzymes into the systemic circulation [20].

In both preventive and curative studies, the experimental pomace fiber powder affected the concentration of aspartate aminotransferase, alanine aminotransferase, and alkaline phosphatase with respect to the group that received valproic acid. These results suggest that the supplement reduced hepatotoxicity induced by valproic acid. The pomace fiber powder was obtained from its original vegetable source, which was processed to obtain the fibers, i.e., it contained other bioactive substances, e.g., flavonoids, which also prevent degenerative diseases [4, 5]. The analysis of the pomace fiber powder composition showed that the extract contained 30 mg/100 g of total flavonoids (quercitrin equivalents, dry weight). Therefore, these antioxidants were likely to be able to stabilize the plasma membrane in liver cells, thus protecting them from the stress caused by valproic acid [4, 10]. The reduction in aspartate aminotransferase, alanine aminotransferase, and alkaline phosphatase observed in our research (Tables 7 and 8) was in agreement with some previous studies [23]. On the other hand, the liver histology of the experimental rats showed under an optical microscope that the control group rats maintained intact hepatic lobular architecture. Figure 3a illustrates sinusoids and portal channels in rat liver. These findings were similar to those observed in the group supplemented with pomace fiber powder only (Fig. 3b). Thus, both groups showed normal hepatic lobular architecture.

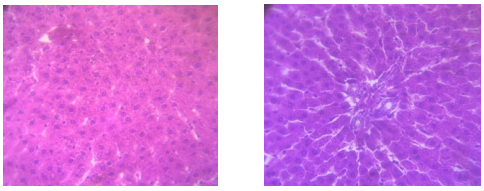

a b

Figure 3 Photomicrographs of liver sections: (a) control group; (b) rats fed with experimental pomace powder. 40× magnification

However, the livers removed from the rats that received valproic acid were paler than normal at necropsy (data not shown). As with previous reports, the liver sections stained with hematoxylin-eosin revealed numerous optically clear or cloudy empty vacuoles in periportal hepatocytes (Fig. 4). The lobular architecture was distorted compared with the control group. Moreover, these histological changes were accompanied by moderate inflammatory cell infiltration [9–11]. These features persisted up to 14 days after the rats stopped receiving valproic acid.

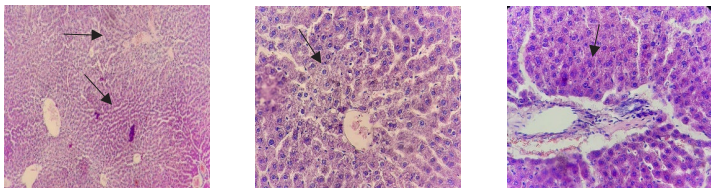

a b c

Figure 4 Photomicrographs of liver histology from rats treated with valproic acid: (a and b) after 14 days of treatment with valproic acid; (c) 14 days after final treatment with valproic acid. 10 and 40× magnification. Black arrows point at signs of distorted hepatic lobules associated with inflammatory cells infiltration

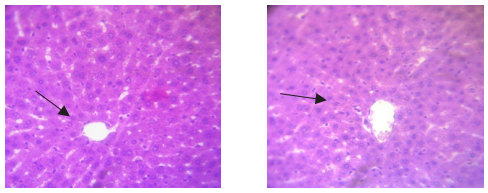

a b

Figure 5 Photomicrographs of liver sections from rats administered with valproic acid and concomitantly supplemented with: (a) 0.3 mg/kg body weight; (b) 0.15 mg/kg body weight of pomace fiber powder during preventive study. 40× magnification. Black arrows point at histological structure preservation sites

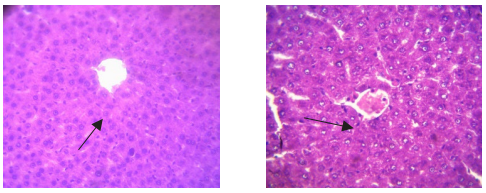

a b

Figure 6 Photomicrographs of liver sections from rats administered with valproic acid and concomitantly supplemented with (a) 0.3 mg/kg body weight; (b) 0.15 mg/kg body weight of pomace fiber powder during curative study. 40× magnification. Black arrows point at histological restoration sites

In contrast, Figs 5 and 6 clearly show that the experimental pomace fiber powder attenuated and restored the histological abnormalities induced by valproic acid. In the current study, the histopathological examination of rats treated with valproic acid and supplemented with the experimental pomace fiber powder showed well-preserved liver architecture and absence of inflammatory processes, both in the preventive (Fig. 5a, b) and curative study (Fig. 6a, b).

Therefore, the experimental pomace fiber powder obtained from fruit and vegetable waste counteracted histopathological liver alterations related to prolonged treatment with valproic acid. This finding could be related to the anti-inflammatory and lipotropic effects of flavonoids and fibers present in the pomace powder, respectively [12, 25]. This study did not feature the pharmacokinetic parameters of valproic acid generated in the presence and absence of pomace powder. In addition, the administration of valproic acid and pomace fiber powder was performed in opposite periods and separated by about 10 h, thus ruling out any interaction between the two. Treatment with valproic acid often results in gastrointestinal side effects, e.g., constipation [26]. In this regard, previous studies reported that fiber was fermented by intestinal microorganisms to produce short-chain fatty acids (propionic acid, butyric acid, etc.), which regulated hepatic lipid metabolism [24, 25]. These components were less fermentable and could contribute significantly to fecal bulk and stool frequency, thus reducing the symptoms of constipation. This effect, probably, favors the excretion of toxic metabolites derived from valproic acid, in particular, valproyl-CoA, which is not metabolized and inhibits the hepatic carnitine palmitoyltransferase 1A [8, 20]. This enzyme regulates β-oxidation of mitochondrial fatty acids. In addition, it is associated with drug-induced hepatotoxic mechanisms and weight gain, commonly observed in patients or animals administered with valproic acid [8–10]. However, further studies might corroborate this hypothesis.

CONCLUSION

This research re-evaluated fruit and vegetable wastes as a potential source of fiber supplements, as well as defined its main components and bioactivity. The experimental pomace fiber powder administered orally to rats protected liver tissue from valproic acid toxicity by normalizing the level of hepatic biomarkers and preserving the hepatic architecture. In view of the results obtained, complementary studies might explain the mechanisms involved in the effect of pomace fiber powder on the different pathways involved in valproic acid toxicity.

CONTRIBUTION

Conceptualization, M.R. Ramirez; methodology, M.R. Ramirez and J.C. Yori; software, M.R. Ramirez; validation, M.R. Ramirez, D. Manuale and J.C. Yori; formal analysis, M.R. Ramirez, and J.C. Yori; investigation, M.R. Ramirez; D. Manuale and J.C. Yori; resources, M.R. Ramirez and J.C. Yori; data curation, M.R. Ramirez and J.C. Yori.; writing-original draft preparation, M.R. Ramirez; writing-review and editing, M.R. Ramirez and J.C. Yori; visualization, M.R. Ramirez and; supervision, M.R. Ramirez project administration, M.R. Ramirez

and J.C. Yori. All authors have read and approved the final version of the manuscript.

CONFLICT OF INTEREST

No conflict of interest was disclosed by the authors.

ACKNOWLEDGMENTS

The authors would like to express their gratitude to their CONICET research colleagues Dr. Ignacio Rintoul and Jorge Oyhenart for their collaboration, as well as to the Barceló foundation.

REFERENCES

1. Clementz A, Torresi PA, Molli JS, Cardell D, Mammarella E, Yori JC. Novel method for valorization of by-products from carrot discards. LWT. 2019;100:374–380. https://doi.org/10.1016/j.lwt.2018.10.085
2. Lucarini M, Durazzo A, Bernini R, Campo M, Vita C, Souto EB, *et al.* Fruit Wastes as a Valuable Source of Value-Added Compounds: A Collaborative Perspective. Molecules. 2021;26(21):6338. https://doi.org/10.3390/molecules26216338
3. Ramirez MR, Manuale D, Yori JC. Assessment of effectiveness of oral supplementation of isolated fiber of carrot on metabolic parameters in mature rats. Food Science and Human Wellness. 2023;12(6):2022–2028. https://doi.org/10.1016/j.fshw.2023.03.016
4. Ramirez MR, Rintoul I, Leiva M, Molli JS, Yori JC. Oral supplementation of *Ilex paraguariensis* extract and eggshell membrane exhibit beneficial effects on the skin of mature male rats. Journal of Pharmacy and Pharmacognosy Research. 2023;11(2):216–228. https://doi.org/10.56499/jppres22.1509_11.2.216
5. Okpoghono J, Ukperegbulem JK, Igue UB. Anti-lipidemic and protein restoration potential of *Monodora myristica* (Gaertn.) in rats fed with cassava containing crude oil. Foods and Raw Materials. 2024;12(2):249–255. https://doi.org/10.21603/2308-4057-2024-2-602
6. Pouwels S, Sakran N, Graham Y, Leal A, Pintar T, Yang W, *et al.* Non-alcoholic fatty liver disease (NAFLD): a review of pathophysiology, clinical management and effects of weight loss. BMC Endocrine Disorders. 2022;22(1):63. https://doi.org/10.1186/s12902-022-00980-1
7. Walter SR, Day RO, Gallego B, Westbrook JI. The impact of serious adverse drug reactions: a population-based study of a decade of hospital admissions in New South Wales, Australia. British Journal of Clinical Pharmacology. 2017;83:416–426. https://doi.org/10.1111/bcp.13124
8. Shnayder NA, Grechkina VV, Khasanova AK, Bochanova EN, Dontceva EA, Petrova MM, *et al.* Therapeutic and Toxic Effects of Valproic Acid Metabolites. Metabolites. 2023;13(1):134. https://doi.org/10.3390/metabo13010134
9. Pirozzi C, Lama A, Annunziata C, Cavaliere G, De Caro C, Citraro R, *et al.* Butyrate prevents valproate-induced liver injury: In vitro and in vivo evidence. FASEB Journal. 2020;34(1):676–690. https://doi.org/10.1096/fj.201900927RR
10. Abdelkader NF, Elyamany M, Gad AM, Assaf N, Fawzy HM, Elesawy WH. Ellagic acid attenuates liver toxicity induced by valproic acid in rats. Journal of Pharmacological Science. 2020;143(1):23–29. https://doi.org/10.1016/j.jphs.2020.01.007
11. Abdel-Dayem MA, Elmarakby AA, Abdel-Aziz AA, Pye C, Said SA, El-Mowafy AM. Valproate-induced liver injury: Modulation by the omega-3 fatty acid DHA proposes a novel anticonvulsant regimen. Drugs in R and D. 2014;14(2):85–94. https://doi.org/10.1007/s40268-014-0042-z
12. Liu X, Yang W, Petrick JL, Liao LM, Wang W, He N, *et al*. Higher intake of whole grains and dietary fiber are associated with lower risk of liver cancer and chronic liver disease mortality. Nature Communication. 2021;12:6388. https://doi.org/10.1038/s41467-021-26448-9
13. Zhao H, Yang A, Mao L, Quan Y, Cui J, Sun Y. Association Between Dietary Fiber Intake and Non-alcoholic Fatty Liver Disease in Adults. Frontiers in Nutrition. 2020;7:593735. https://doi.org/10.3389/fnut.2020.593735
14. Official methods of analysis AOAC, 17th ed. Gaithersburg, MD, USA. The Association of Official Analytical Chemists; 2000.
15. Parra-Orobio BA, Rotavisky-Sinisterra MP, Pérez-Vidal A, Marmollejo-Revellon LF, Torres-Lozada P. Physicochemical, microbiological characterization and phytotoxicity of digestates produced on single-stage and two-stage anaerobic digestion of food waste. Sustainable Environment Research. 2021;31:11. https://doi.org/10.1186/s42834-021-00085-9
16. Issy AM, Lanchote VL, de Carvalho D, Silva HC. Lack of kinetic interaction between valproic acid and citrus pectin. Therapeutic Drug Monitoring. 1997;19(5):516–520. https://doi.org/10.1097/00007691-199710000-00005
17. Ramirez MR, Mohamad L, Alarcon-Segovia LC, Rintoul I. Effect of Processing on the Nutritional Quality of *Ilex paraguariensis*. Applied Sciences. 2022;12(5):2487. https://doi.org/10.3390/app12052487
18. Cantero I, Abete I, Monreal JI, Martinez JA, Zulet MA. Fruit Fiber Consumption Specifically Improves Liver Health Status in Obese Subjects under Energy Restriction. Nutrients. 2017;9(7):667. https://doi.org/10.3390/nu9070667

19. Caroline W, Martin H, Katarzyna L, Robert W, Norbert S, Jürgen M. Potential effects of reduced red meat compared with increased fiber intake on glucose metabolism and liver fat content: a randomized and controlled dietary intervention study. The American Journal of Clinical Nutrition. 2019;109(2):288–296. https://doi.org/10.1093/ajcn/nqy307
20. Xu S, Chen Y, Ma Y, Liu T, Zhao M, Wang Z, *et al.* Lipidomic Profiling Reveals Disruption of Lipid Metabolism in Valproic Acid-Induced Hepatotoxicity. Frontiers in Pharmacology. 2019;10:819. https://doi.org/10.3389/fphar.2019.00819
21. Hannon BA, Thompson SV, Edwards CG, Skinner SK, Niemiro GM, Burd NA, *et al.* Dietary Fiber Is Independently Related to Blood Triglycerides Among Adults with Overweight and Obesity. Current Development in Nutrition. 2019;3(2):nzy094. https://doi.org/10.1093/cdn/nzy094
22. He J, Zhang P, Shen L, Niu L, Tan Y, Chen L, *et al*. Short-Chain Fatty Acids and Their Association with Signalling Pathways in Inflammation, Glucose and Lipid Metabolism. International Journal of Molecular Sciences. 2020;21(17):6356. https://doi.org/10.3390/ijms21176356
23. Chen J, Huang Y, Xie H, Bai H, Lin G, Dong Y, *et al.* Impact of a low-carbohydrate and high-fiber diet on nonalcoholic fatty liver disease. Asia Pacific Journal of Clinical Nutrition. 2020;29(3):483–490. https://doi.org/10.6133/apjcn.202009_29(3).0006
24. Pérez-Montes de Oca A, Julián MT, Ramos A, Puig-Domingo M, Alonso N. Microbiota, Fiber, and NAFLD: Is There Any Connection? Nutrients. 2020;12(10):3100. https://doi.org/10.3390/nu12103100
25. Maciejewska-Markiewicz D, Drozd A, Palma J, Ryterska K, Hawryłkowicz V, Zał ̨eska P, *et al.* Fatty Acids and Eicosanoids Change during High-Fiber Diet in NAFLD Patients—Randomized Control Trials (RCT). Nutrients. 2022;14(20):4310. https://doi.org/10.3390/nu14204310
26. Jahromi SR, Togha M, Fesharaki SH, Najafi M, Moghadam NB, Kheradmand JA, *et al.* Gastrointestinal adverse effects of antiepileptic drugs in intractable epileptic patients. Seizure. 2011;20:343–346. https://doi.org/10.1016/j.seizure.2010.12.011

ORCID IDs
Maria R. Ramirez https://orcid.org/0000-0001-9989-7978
Debora Manuale https://orcid.org/0000-0003-2523-6530
Juan C. Yori https://orcid.org/0000-0001-8874-6242

Foods and Raw Materials. 2026;14(1)

ISSN 2308-4057 (Print)
ISSN 2310-9599 (Online)

Research Article
Open Access

Available online at http://jfrm.ru/en
https://doi.org/10.21603/2308-4057-2026-1-656
https://elibrary.ru/HJPDZE

Kelulut stingless bee honey stored under different thermal conditions: Non-destructive assessment

Yee Mun Chin, Lejaniya Abdul Kalam Saleena, Lee Ying Lim, Liew Phing Pui*, Mahmud Iwan Solihin

UCSI University, Kuala Lumpur, Malaysia

* e-mail: puilp@ucsiuniversity.edu.my

Received 01.04.2024; Revised 25.06.2024; Accepted 02.07.2024; Puplished online 14.02.2025

Abstract:
Kelulut honey (*Heterotrigona itama* Cockerell, 1918) is gaining popularity, which makes its quality assessment an important issue. We employed the method of near-infrared spectroscopy to perform a non-destructive quality assessment of refrigerated and non-refrigerated postharvest Kelulut honey. The research objective was to define the physical and chemical properties of Kelulut honey stored for 0, 1, 2, 7, and 14 days, as well as to establish effective prediction models based on the methods of principal component regression and partial least squares.

The Brix value, moisture content, and sugar content exhibited no significant differences ($p > 0.05$) for the entire storage time. However, the Brix value and sugar content decreased as the moisture increased during storage. pH values decreased while the hydroxymethylfurfural content increased across the entire storage time. Significant differences ($p > 0.05$) were observed between the pH and hydroxymethylfurfural values for honey stored at different temperatures. The prediction model of sugar content based on principal component regression demonstrated acceptable accuracy ($R^2 = 0.7$) and low mean squared error. After pre-processing and partial least squares regression, the method of near-infrared spectroscopy proved accurate and effective in defining the quality of Kelulut honey.

Keywords: *Heterotrigona itama*, near-infrared spectroscopy (NIRS), physicochemical properties, prediction model, storage

Funding: The authors would like to express their gratitude to the Centre of Excellence for Research, Value Innovation, and Entrepreneurship (CERVIE) – UCSI University, for supporting this project under the PSIF project code: Proj-2019-In-FETBE-063. Besides that, the authors would also like to thank Melipoly Sdn. Bhd. for providing honey.

Please cite this article in press as: Chin YM, Saleena LAK, Lim LY, Pui LP, Solihin MI. Kelulut stingless bee honey stored under different thermal conditions: Non-destructive assessment. Foods and Raw Materials. 2026;14(1):71–83. https://doi.org/10.21603/2308-4057-2026-1-656

INTRODUCTION

Honey is a viscous and supersaturated natural solution derived from nectar gathered and modified by honeybees, *Apis mellifera* L. [1]. It can be used as food and medicinal products for humans and animals [2]. In Malaysia, stingless bee farming activity is increasing in the honey industry. Stingless bee honey is also known as Kelulut honey, with *Heterotrigona itama* Cockerell, 1918 as the main commercial cultivated bee species [3].

Kelulut honey has some storage problems as it undergoes rapid alcoholic fermentation once harvested due to its high moisture content, which exceeds 30%, and osmophilic yeasts. Alcoholic fermentation produces ethanol and carbon dioxide substances. As a result, honey becomes off-flavored and acquires a more acidic taste and unpleasant appearance. Since honey is unavoidably contaminated with osmophilic yeast and fungi at the stage of nectar collection, it has to undergo special treatment to avoid fermentation during storage.

The quality of honey is evaluated by physicochemical analysis of its destructive constituents. The analysis includes such variables as moisture, color, ash, electrical conductivity, pH, hydroxymethylfurfural, Brix value, sugar, total solids-free acidity, and diastase activity [4–6]. Nowadays, near-infrared spectroscopy (NIRS) is a popular non-destructive assessment of honey quality. It provides a rapid determination of organic components [7].

Near-infrared spectroscopy is a spectroscopic method that measures electromagnetic radiation absorption, including wavelengths of 750–2500 nm [8]. The

Copyright © 2025, Chin *et al.* This is an open access article distributed under the terms of the Creative Commons Attribution 4.0 International License (https://creativecommons.org/licenses/by/4.0/), allowing third parties to copy and redistribute the material in any medium or format and to remix, transform, and build upon the material for any purpose, even commercially, provided the original work is properly cited and states its license.

absorptions measured by near-infrared spectroscopy often correspond to overtones and combinations of vibrational modes, involving chemical bonds C–H, O–H, and N–H [9]. The method has recently been adapted to verification of authenticity and fraud detection in the honey industry [10].

This study assessed the physical and chemical profile of Kelulut honey to collect data for prediction models using near-infrared spectroscopy. The quality of Kelulut honey was assessed on days 0, 1, 2, 7, and 14. The spectral data were collected with a handheld near-infrared spectrometer and used to build the prediction model and evaluate its accuracy.

STADY OBJECTS AND METHODS

Preparing samples and storage. This study involved stingless bee (*Heterotrigona Itama* Cockerell, 1918) honey, pure Kelulut honey, and H and B honey (bee farm Malacca) produced in Malaysia. Equal quantities of Kelulut honey samples were placed into six containers, divided into two groups, and stored at room and chilled temperature for 0, 1, 2, 7, and 14 days. The samples were stored in clean, dry and sealed food-grade containers and kept in a chiller (0 to 4°C).

Physical analysis. ***The color*** of samples after storage was determined by using a Hunter Lab visible spectrometer (Hunter Associate Laboratory Inc., USA) [11]. Kelulut honey was poured into a sample glass to measure its reflectance spectrum and determine its color parameter. The L^*, a^*, and b^* values made it possible to describe the color in lightness, red-green intensity, and yellow-blue intensity, respectively. The color index (ΔE) expresses the total color differences between samples, as in the equation below:

$$\Delta E = \sqrt{(\Delta L^*)^2 + (\Delta a^*)^2 + (\Delta b^*)^2} \quad (1)$$

where ΔL^*, Δa^*, and Δb^* are the color differences between the samples after different storage times and the control sample of fresh Kelulut honey.

The pH of Kelulut honey after different storage times was determined using a digital pH meter (Mettler-Toledo, China). The procedure involved dissolving 10 g of Kelulut honey in 75 mL of distilled water in a 250 mL beaker. The solution was then stirred in a magnetic stirrer. After that, the pH electrode was immersed in the solution to record pH [12].

The moisture content in Kelulut honey after different storage times was determined using the refractometric method. After being homogenized again, the honey samples were put in a flask, which was subjected to water bath at 50°C until all crystals dissolved. Then, the solution was cooled down to room temperature and stirred. We tested each honey sample three times to obtain the mean value. The corresponding moisture content was calculated using the equation below [12]:

$$W = \frac{1.73190 - log(RI - 1)}{0.002243} \quad (2)$$

where W is the water content per 100 g honey, and RI is the refractive index.

Chemical analysis. ***The reducing sugar content*** in Kelulut honey after different storage times was determined using the Nelson-Somogyi method [13]. First, we diluted ≈ 1 mL of honey with ≤ 10 mL of water. Second, we further diluted 1 mL of each sample with 9 mL of distilled water. Approximately 1 mL of each diluted sample was mixed with the Nelson reagent (A+B ratio of 25:1) and heated at 100°C for 20 min. After cooling, the samples were mixed and shaken with 1 mL of arsenomolybdate reagent and 7 mL of distilled water to measure absorbance at 510 nm. The procedure involved a standard curve with different concentrations of standard glucose solution.

The content of hydroxymethylfurfural was determined according to Malaysian Standards [12]. We poured ≈ 5 g of honey and 25 mL of distilled water into a 50 mL volumetric flask for 0.5 mL of Carrez solution I to be added and mixed. Then, we added ≈ 0.5 mL of Carrez solution II and mixed thoroughly. After filling the flask with distilled water up to the mark, we added a drop of alcohol to suppress the surface foam. Having filtered the solution through paper, we discarded the first 10 mL of the filtrate. Approximately 5 mL of the filtrate was pipetted into two sets of test tubes: ≈ 5 mL of distilled water served as a sample and 0.5 mL of 0.20% bisulfite served as a reference. The two solutions were mixed well in a vortex mixer. Using a spectrophotometer, we measured the absorbance of the test samples against the reference at 284 nm and 336 nm. The content of hydroxymethylfurfural (HMF) was calculated as in the equation below:

$$\text{HMF} = \frac{(A_{284} - A_{336}) \times 149.7 \times 5 \times D}{W} \quad (3)$$

where A_{284} is the absorbance at 284 nm, A_{336} is the absorbance at 336 nm, D is the dilution factor, and W is the weight of honey sample.

Statistical analysis. The experiments were carried out in triplicates (n = 3), with three samples for each storage time. Statistical results were expressed in mean and standard deviations. A one-way ANOVA test made it possible to identify the data with a significant difference of $p \leq 0.05$. The final data interpretation involved SPSS Statistics 26 (IBM, Chicago).

Near-infrared spectroscopy analysis. ***Spectral collection.*** Five Kelulut honey samples with different storage times were prepared to be scanned in a DLP® NIRscan™ Nano EVM evaluation module (Texas Instruments®, USA). The samples were poured into cuvettes and wrapped with aluminum foil to reflect spectra. The wavelength range was 900–1700 nm. The data obtained were analyzed using the multivariate analysis and machine learning. The procedure involved Orange v 3.18 software (Bioinformatics Lab, University of Ljubljana, Slovenia). The results made it possible to define the effect of storage time on the quality of Kelulut honey [14].

Pre-processing of spectra. Spectral pre-processing can improve the predictive model by reducing the spectra-to-noise ratio. The pre-processing techniques included cut (keep) filter, Gaussian smoothing, Savitzky-Golay (SG) smoothing, multiplicative scatter correction (MSC), and standard normal variate (SNV). The software involved was Orange v 3.18 developed by the Bioinformatics Lab, University of Ljubljana, Slovenia.

RESULTS AND DISCUSSION

Physical and chemical analysis. ***Color.*** Table 1 shows that the *L** values at room temperature increased from 6.60 ± 0.21 to 7.43 ± 0.29 as the storage time proceeded from day 0 to day 1. Subsequently, the *L** values of honey stored at room temperature demonstrated a decreasing trend from day 2 to day 14, which means that the samples became darker. The sample stored under room temperature for 14 days had the darkest shade. The *L** values of refrigerated honey decreased from 6.92 ± 0.10 to 6.77 ± 0.06 on day 1 and increased from 6.77 ± 0.06 to 6.90 ± 0.06 on day 2. The *L** values tended to decrease between storage days 2 and 14, which means that the honey darkened during this period. On storage day 14, the samples stored under both thermal conditions demonstrated the darkest color in the set.

The *a** value decreased from –0.99 ± 0.11 to –1.08 ± 0.04 after honey was stored at room temperature for one day. Table 1 shows an increasing trend in *a** values when honey was stored under room temperature from day 1 to day 14. The honey stored under room temperature turned red on day 2. The *a** values of the samples stored under chilling temperature also increased from –1.20 ± 0.06 to –0.89 ± 0.09 after being stored for one day and dropped to –1.24 ± 0.06 after being stored for another day. The *a** values tended to increase in the samples stored under both room and chilling temperature between days 2 and 14.

The *b** values of the honey stored under room temperature dropped from 1.02 ± 0.21 to –0.33 ± 0.16 on day 1 and reached 1.18 ± 0.10 after being stored for another day. Between days 2 and 7, the *b** values of the samples stored at room temperature tended to decrease. No significant difference ($p > 0.05$) was detected between days 7 and 14. While the *b** values of the refrigerated honey showed the same trend, it went down from 1.26 ± 0.20 to –0.35 ± 0.11 after one day of storage and went up to 1.46 ± 0.09 after another day of storage. The *b** value decreased again and dropped to 0.09 ± 0.06 on day 7. However, it reached 0.22 ± 0.10 on day 14 under chilling temperature. As for the color change (ΔE), the honey stored at room temperature for two days showed the lowest ΔE value of 0.53 ± 0.10. The honey stored under chilling temperature for 14 days also had the greatest ΔE value, 2.87 ± 0.24, compared with day 0.

The color of honey is the first quality appearance decision that affects customer perception [15]. The honey color could be affected by the floral origin or source of the plant, minerals, phenolic content, storage time, and storage temperature [16]. All pure honey gradually darkens in color due to various non-enzymatic browning reactions, also known as Maillard reactions [15]. The darkening is attributed to the breakdown of volatile compounds, sugar caramelization, and brown melanoidins [6].

In our case, the darkening of honey color could be due to the degradation of volatile compounds. The higher the storage temperature, the faster the degradation of volatile compounds [17]. Under room temperature, the honey color darkened faster than in the fridge (Table 1). Our results were in agreement with Visquert *et.al.* [18], where the color of honey darkened as storage time and temperature increased. Turkmen *et al*. [19] reported that the color of honey changed dramatically when the temperature rose. Yap *et al*. [17] also reported that the *a** value of honey increased with prolonged storage. In a study of Piotraszewska-Pająk and Gliszczyńska-Świgło [20], the *b** value of honey also increased with storage time. The longer the storage time and the higher the storage temperature, the stronger the honey color [15]. The intensive coloration after long storage may be due to the degradation of volatile compounds in the honey [17, 18].

Brix, moisture, and sugar. Table 1 shows that Brix values of the honey samples stored at room temperature remained unchanged from day 0 to day 14. The Brix values of the refrigerated honey also remained the same from day 0 to day 2. However, day 7 showed an immediate increase to 74.11 ± 3.97% in the refrigerated samples. It was followed by a drop to 70.80 ± 0.46% on day 14, with no statistical significance.

The moisture content in the honey stored under room temperature remained unchanged during the entire experiment time (Table 1). On the other hand, the moisture content in the refrigerated honey stayed the same on days 0, 1, and 2 but dropped from 28.20 ± 0.18 to 24.34 ± 4.05% on day 7 to rise to 27.73 ± 0.46% on day 14. It means that room temperature provided better honey storage.

The sugar content in the samples stored under room and chilling temperature complied with the Malaysian Standard requirements for Kelulut honey (Table 1). The sugar content of the honey stored at room temperature did not change on day 1. However, it rose from $5.23\times10^{-8} \pm 0.05\times10^{-8}$ g/100g to $7.60\times10^{-8} \pm 0.32\times10^{-8}$ g/100g after being stored at room temperature for another day. Then, it showed a decreasing trend between days 7 and 14. The sugar content in the samples stored under chilling temperature also remained unchanged after one day of storage. It immediately changed from $5.20\times10^{-8} \pm 0.09\times10^{-8}$ g/100g to $7.77\times10^{-8} \pm 0.61\times10^{-8}$ g/100g after another day of storage. On day 7, the sugar content dropped to $6.80\times10^{-8} \pm 0.21\times10^{-8}$ g/100g and remained the same for another seven days.

The Brix value describes the soluble solid value, which highly correlates with the moisture and sugar content. Therefore, it is an important parameter that affects the honey quality [21]. Based on Majid *et al*. [22], stingless bee honey has a higher moisture content than that obtained from stinging bees. Water content is known to

correlate with botanical sources, although this parameter can be affected by soil, climatic conditions, collection time, and processing aspects [22]. Differences in the Brix value depend on the bee species and the regional biodiversity.

In our research, the honey content complied with the Malaysian Standard [12], which indicates that honey should have good quality after 14 days of storage. Other findings also report that moisture, ash, and electrical conductivity change little over time and do not depend on storage temperature [23]. Humid climate may increase the moisture content, which is the most important honey characteristic as it affects viscosity, basic weight, maturation, crystallization, and taste [24]. A high moisture content in honey exhibits a higher probability of fermenting upon storage, which affects the shelf-life [25]. The water activity of honey was reported to correlate linearly with the moisture content of honey [6].

Honey is a concentrated reduction solution, with fructose and glucose representing the largest proportion of its composition [26]. The sugar content of honey highly correlates with the Brix value and moisture content. Table 1 shows that the Brix values of the room temperature samples and the refrigerated samples demonstrated no significant difference on days 0, 1, 2, and 14 ($p > 0.05$). Therefore, we recorded no significant differences between the storage temperatures for moisture and sugar content. This finding indicates that the storage temperature did not affect the Brix value, moisture, and sugar content. Our results confirmed those reported by Batu *et al*. [27] and Fuad *et al*. [28], who detected no significant changes in the Brix value and moisture content, respectively, when the samples were stored at different temperatures.

pH and hydroxymethylfurfural. In our research, pH values of both honey samples stored under room and chilling temperatures met the standard requirements for raw Kelulut honey (pH 2.5–3.8) (Table 1). The pH values of the honey stored under room temperature had no significant difference ($p > 0.05$) on days 0, 1, 2, and 7 with a range of 3.42–3.56. Day 14 of room temperature storage demonstrated a decrease from 3.42 ± 0.02 to 3.18 ± 0.02. The pH value of the honey stored under chilling temperature decreased from 3.57 ± 0.04 to 3.47 ± 0.01 on day 1 and further decreased from 3.45 ± 0.01 on day 7 to 3.45 ± 0.01 on day 14.

Table 1 shows that the hydroxymethylfurfural content in the honey stored under room temperature had a significant increasing trend on days 2, 7, and 14. The hydroxymethylfurfural content in the refrigerated honey also increased significantly on days 1, 2, 7, and 14. This result was in agreement with that reported by Chuttong *et al*. [23]. The longer storage time and the higher temperature, the greater the hydroxymethylfurfural content honey contains.

Table 1 shows no significant difference ($p > 0.05$) for the pH value between the storage temperatures on days 0, 1, 2, and 7. The pH value decreased from day 7 to day 14 with different storage temperatures. At room temperature, the pH decreased from 3.42 ± 0.02 to 3.18 ± 0.02 between storage days 7 and 14. On the other hand, the pH of the refrigerated honey samples decreased from 3.45 ± 0.01 to 3.18 ± 0.02 between storage days 7 and 14. The hydroxymethylfurfural content demonstrated no significant difference ($p > 0.05$) between the storage temperatures on days 0 and 2. From day 2 to day 14, the samples stored under different thermal conditions demonstrated significant changes, indicating that storage temperature may affect the formation of hydroxymethylfurfural content in honey. The hydroxymethylfurfural value significantly increased during both room temperature and refrigerated storage.

Kelulut honey has a lower pH value than other honey types, which contributes to its unique sour taste. The low pH of honey inhibits the presence and development of microorganisms. During the extraction and storage, the pH parameter is important because pH affects texture, stability, and shelf-life [16]. In our research (Table 1), the pH range (3.18–3.57) was similar to the studies performed in Thailand by Chuttong *et al*. [23] and in Brazil by Nascimento *et al*. [24]. Low pH prevents microorganisms from developing, thus protecting honey from contamination [24]. According to Sousa *et al*. [29], hydroxymethylfurfural is a generally recognized parameter of honey freshness and consistency. Hydroxymethylfurfural is a six-carbon heterocyclic organic compound that contains functional aldehyde and alcohol (hydroxymethyl) produced by sugar degradation via the Maillard reaction (a non-enzymatic browning reaction). Because it is associated with honey aging and overheating, hydroxymethylfurfural is frequently utilized as a quality evaluation parameter for honey [6].

Hydroxymethylfurfural also depends on climate. After a long thermal exposure, samples from tropical regions can develop hydroxymethylfurfural. According to the Malaysian Standard for Kelulut honey, the hydroxymethylfurfural content does not exceed 30.0 mg/kg. In our study, the hydroxymethylfurfural content met the standard requirement, indicating that the honey was of good quality even after 14 days of storage at different temperatures.

Correlation coefficient. Pearson's correlation is used to determine the independence of the variable. Table 2 shows the relationship between color parameyters (L^*, a^*, b^*) of Kelulut honey. The L^* value positively correlated with the pH value and moisture content but had a high negative correlation with hydroxymethylfurfural. The L^* value indicated light intensity. Low L^* suggested darkening; the honey became acidic and had a lower moisture content. The Brix value positively correlated with the sugar content, which agrees with some previous studies on honey [21].

The content of honey produced by stingless bees of various species varies greatly, depending primarily on floral sources and geographical conditions. However, the true element controlling its characteristics could not be identified. The higher the Brix value, the greater the sugar content in honey. The moisture content had a

Table 1 Color, color change, %Brix, moisture, sugar, pH, and hydroxymethylfurfural in honey stored under room (RT) and chilled (C) temperatures for different storage times

Day	*L**		*a**		*b**		ΔE		Brix, %		Moisture, %		Sugar, $\times 10^{-8}$ g/100g		pH		Hydroxymethyl-furfural, mg/kg	
	RT	C	RT	C	RT	C	RT	C	RT	C	RT	C	RT	C	RT	C	RT	C
0	6.60 ± 0.21^{dA}	6.92 ± 0.10^{dA}	–0.99 ± 0.11^{aA}	–1.20 ± 0.06^{aB}	1.02 ± 0.21^{cA}	1.26 ± 0.20^{cB}	0.00 ± 0.00^{aA}	0.00 ± 0.00^{aA}	69.42 ± 0.72^{aA}	70.01 ± 0.24^{aA}	29.13 ± 0.73^{aB}	28.53 ± 0.24^{bA}	5.23 ± 0.05^{aA}	5.17 ± 0.10^{aA}	3.56 ± 0.02^{bA}	3.57 ± 0.04^{cA}	14.64 ± 0.23^{aA}	14.70 ± 0.42^{aA}
1	7.43 ± 0.29^{eB}	6.77 ± 0.06^{cA}	–1.08 ± 0.04^{aB}	–0.89 ± 0.09^{bA}	–0.33 ± 0.16^{aA}	–0.35 ± 0.11^{aA}	1.67 ± 0.06^{cA}	1.65 ± 0.27^{cA}	70.01 ± 0.77^{aA}	70.28 ± 0.10^{aA}	28.53 ± 0.78^{aA}	28.26 ± 0.10^{bA}	5.23 ± 0.05^{aA}	5.20 ± 0.09^{aA}	3.47 ± 0.02^{bA}	3.47 ± 0.01^{bA}	15.50 ± 0.78^{aB}	14.60 ± 0.24^{aA}
2	6.24 ± 0.10^{cA}	6.90 ± 0.06^{dA}	–1.04 ± 0.08^{aA}	–1.24 ± 0.06^{aB}	1.18 ± 0.10^{cA}	1.46 ± 0.09^{dB}	0.53 ± 0.10^{bB}	0.31 ± 0.15^{bA}	70.52 ± 0.26^{aA}	70.33 ± 0.18^{aA}	28.01 ± 0.26^{aA}	28.20 ± 0.18^{bA}	7.60 ± 0.32^{cA}	7.77 ± 0.61^{cA}	3.54 ± 0.35^{bA}	3.44 ± 0.02^{bA}	15.80 ± 0.25^{aA}	15.44 ± 0.26^{bA}
7	5.59 ± 0.04^{bB}	4.88 ± 0.04^{bA}	–0.67 ± 0.53^{bA}	–0.64 ± 0.08^{cA}	0.35 ± 0.06^{bB}	0.09 ± 0.06^{bA}	1.23 ± 0.26^{cA}	2.43 ± 0.21^{dB}	70.04 ± 2.79^{aA}	74.11 ± 3.97^{bB}	28.34 ± 2.93^{aB}	24.34 ± 4.05^{aA}	6.71 ± 0.18^{bA}	6.80 ± 0.21^{bA}	3.42 ± 0.02^{bA}	3.45 ± 0.01^{bA}	20.44 ± 2.89^{bB}	15.59 ± 0.32^{bcA}
14	4.5 5± 0.05^{aA}	4.30 ± 0.06^{aA}	–0.58 ± 0.07^{bA}	–0.55 ± 0.06^{cA}	0.28 ± 0.57^{bA}	0.22 ± 0.10^{bA}	2.22 ± 0.26^{cA}	2.87 ± 0.24^{eB}	70.63 ± 1.43^{aA}	70.80 ± 0.46^{aA}	27.90 ± 1.45^{aA}	27.73 ± 0.46^{bA}	6.58 ± 0.08^{bA}	6.80 ± 0.09^{bA}	3.18 ± 0.02^{aA}	3.31 ± 0.01^{aB}	24.00 ± 1.74^{cB}	16.07 ± 0.60^{cA}

All values were expressed as triplicate in mean ± standard deviation.

Different superscripts within the same column indicate significant differences at $p \leq 0.05$, according to Tukey's test.

Letters $^{a–e}$ indicate different storage times.

Letters $^{A–B}$ indicate different storage temperatures.

Table 2 Pearson's correlation between physical and chemical properties of honey stored under room (RT) and chilled (C) temperatures for different storage times

	*L**	*a**	*b**	pH	Brix, %	Moisture	Hydroxymethylfurfural	Sugar
*L**	1	–0.62**	–0.09	0.55**	–0.16	0.16	–0.81**	–0.52**
*a**	–0.62**	1	–0.16	–0.40**	0.25	–0.25	0.51**	0.18
*b**	–0.09	–0.16	1	0.31*	–0.00	0.01	–0.26	0.42**
pH	0.55**	–0.40**	0.31*	1	– 0.14	0.14	–0.55**	–0.06
Brix, %	–0.16	0.25	–0.00	–0.14	1	–0.99**	–0.10	0.19
Moisture	0.16	–0.25	0.01	0.14	–0.99**	1	0.09	–0.19
Hydroxymethylfurfural	–0.81**	0.51**	–0.26	–0.55**	–0.10	0.09	1	0.37*
Sugar	–0.52**	0.18	0.42**	–0.06	0.19	–0.19	0.37*	1

** Indicates significant correlation ($p \leq 0.01$)

* Indicates significant correlation ($p \leq 0.05$)

positive correlation with pH and sugar. The water activity in honey decreased; the sugar content increased due to water loss during storage. The correlation between moisture and sugar agreed with a previous study on honey properties [26].

Near-infrared spectroscopy analysis. ***Spectral data.*** The absorbance of honey spectral data gathered from the honey samples ranged from 900 to 1700 nm. Figure 1 illustrates 90 spectral data for the combined wavelength patterns of the honey samples stored under various temperatures for 0, 1, 2, 7, and 14 days. Figure 1 makes it hard to distinguish between the honey samples stored under different temperature conditions and storage times: the absorbances in different honey samples look almost the same.

Spectral pre-processing. Figure 2 shows a smooth spectra line after the pre-processing stage, which involved five pre-processing techniques: cutting (keep) filter, standard normal variate (SNV), multiplicative scatter correction (MSC), Savitzky-Golay smoothing, and Gaussian smoothing. The cut (keep) filter made it possible to remove unnecessary spectra.

Predictive model. Figure 3a shows graphs of predicted and actual values of L^* with principal component regression and partial least squares predictive models. Both graphs revealed a slope of ≈ 45°, which indicated that the predicted value was approximating the actual value. Figure 3b shows the a^* graphs with another slope of about 45°. The predicted a^* value was also very near to the actual one. Figure 3c demonstrates the b^* value: the slope that was near to the horizontal line indicated that the predicted value was far from the actual one. Figures 4a and 4b show the graphs of the Brix value and moisture content, respectively, which had slopes similar to Fig. 3c. Figures 4c and 4d illustrate the sugar content and pH value, respectively, with slopes of approximately 45°. Figure 5 shows the hydroxymethylfurfural content: the slope line was better than that of the b^* value, Brix value, and moisture content. The L^* value, a^* value, sugar content, and pH demonstrated predicted values closest to the actual physicochemical data. The figures below show that the predictive model based on principal component regression was more accurate than that based on partial least squares due to higher R^2 values.

Table 3 shows the predicted values of parameters of the honey samples stored under room temperature using the predictive model based on principal component regression. The values of the predicted color parameter had the same trend as the actual ones. No significant difference ($p > 0.05$) was detected between the actual and predicted values of L^* for days 0 and 2. For the a^* value, no significant difference ($p > 0.05$) was detected

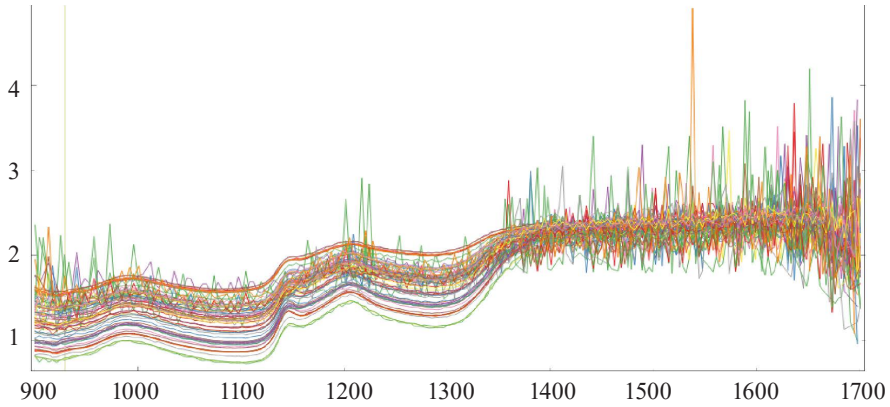

Figure 1 Spectral data collected from honey samples: overall spectra for all samples

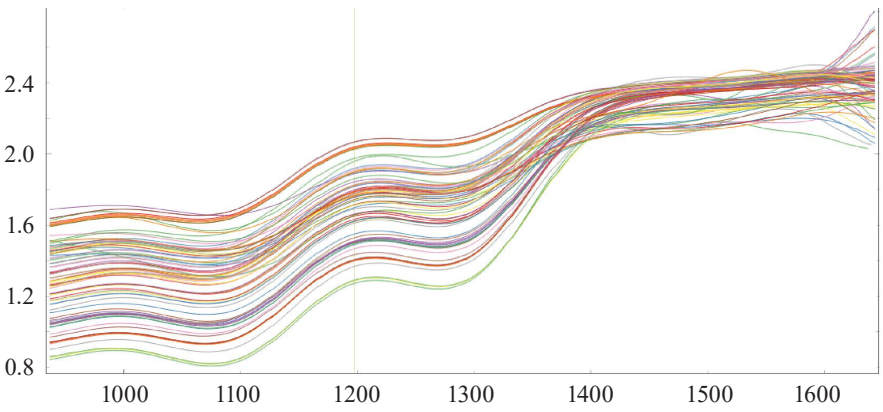

Figure 2 Pre-processed spectra

between days 0 and 7. The *b** value demonstrated no significant difference ($p > 0.05$) on days 1, 7, and 14. These patterns indicate that the predicted values were close to the actual ones. The ΔE value revealed a significant difference, suggesting that it was far from the actual value. The predicted values proved to be inaccurate.

The predicted Brix values did not differ significantly ($p > 0.05$) from the actual ones under room temperature during the entire storage time. Therefore, the prediction of the Brix value based on principal component regression was highly accurate for the honey stored under room temperature. We revealed no significant difference ($p > 0.05$) between the predicted and actual value of moisture content on day 1 and day 14. The predicted sugar content had no significant difference ($p > 0.05$) with the actual value on days 0, 1, 2, and 14. Therefore, the prediction of the sugar content was more accurate than that of the moisture content.

The predicted pH value showed a decreasing trend, complying with the actual pH value. In addition, the predicted pH value did not differ ($p > 0.05$) from the actual value for the entire storage time. Thus, the pH value prediction was the most accurate one among all the physicochemical variables. The predicted hydroxymethylfurfural content showed an increasing trend, similar to the actual values. However, we detected no significant difference ($p > 0.05$) on days 2 and 7. According to Malaysian guidelines for hydroxymethylfurfural in refrigerated and non-refrigerated honey, our samples were within the safe threshold values for consumption.

Table 4 shows the predicted values of parameters of the honey samples stored under chilled temperature using the predictive model based on principal component regression. The values of the predicted color parameter had the same trend as the actual values. The predicted and actual values at chilled temperature reflected the same phenomena as the honey at room temperature. We detected no significant difference ($p > 0.05$) between the actual and predicted values of *L** for day 0 and day 2. For the *a** value, no significant difference ($p > 0.05$) was registered between days 0 and 7. The *b** value showed no significant difference ($p > 0.05$) on days 1, 7, and 14.

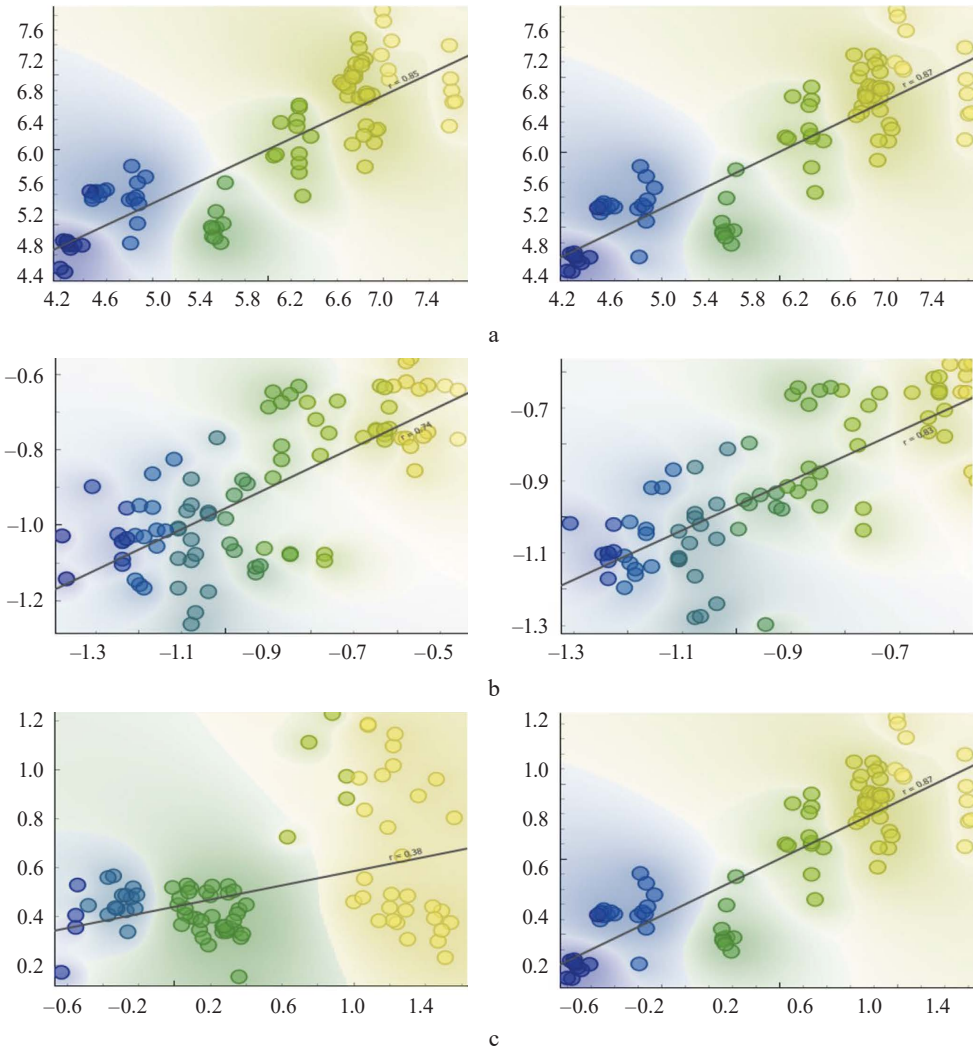

Figure 3 Actual vs. predicted values of honey variables: *L** (a), *a** (b), *b** (c) with partial least squares (PLS) predictive model (left) and principal component regression (PCR) predictive model (right)

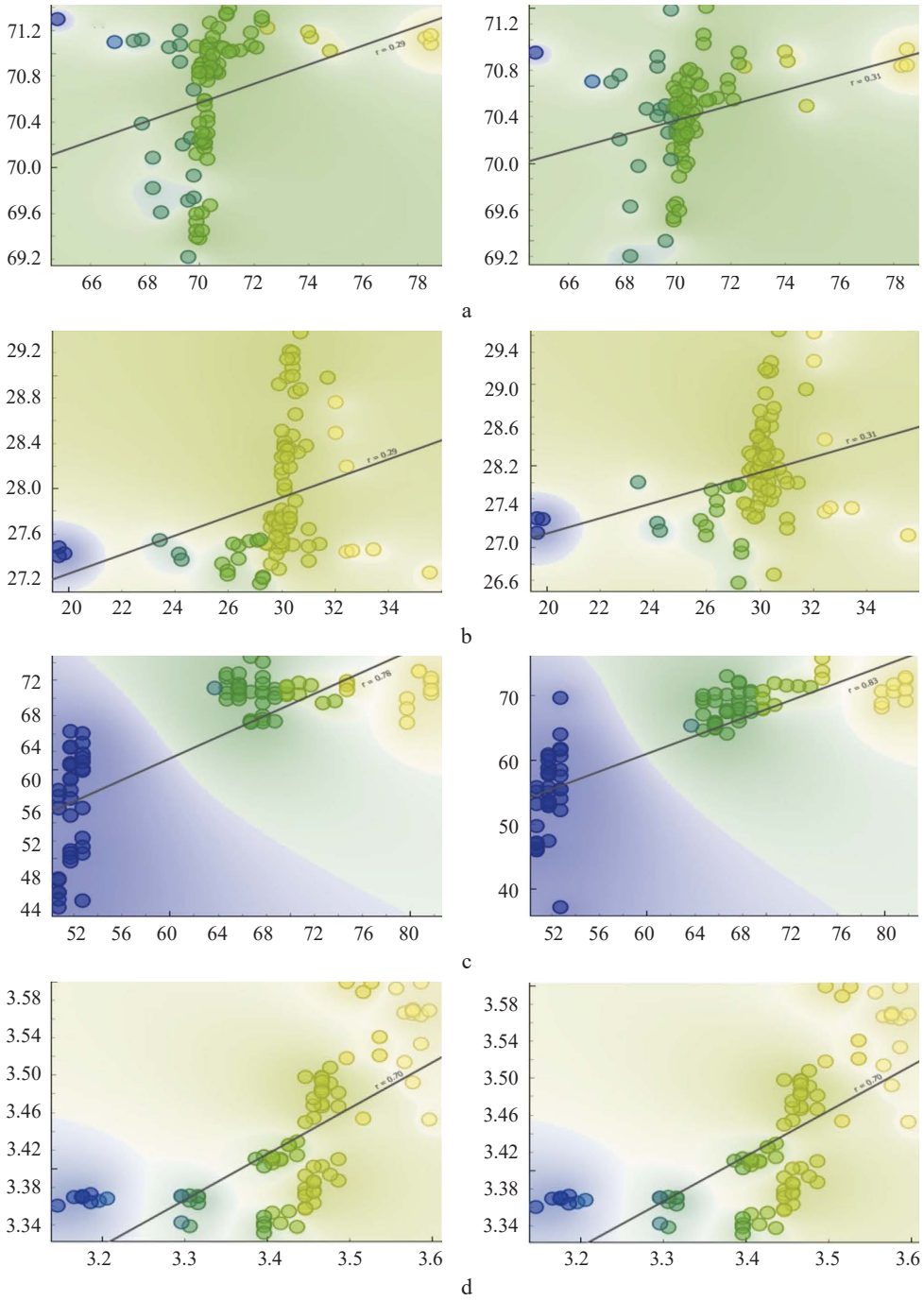

Figure 4 Actual vs. predicted values of honey variables: %Brix (a), moisture (b), sugar (c), and pH (d) with partial least squares (PLS) predictive model (left) and principal component regression (PCR) predictive model (right)

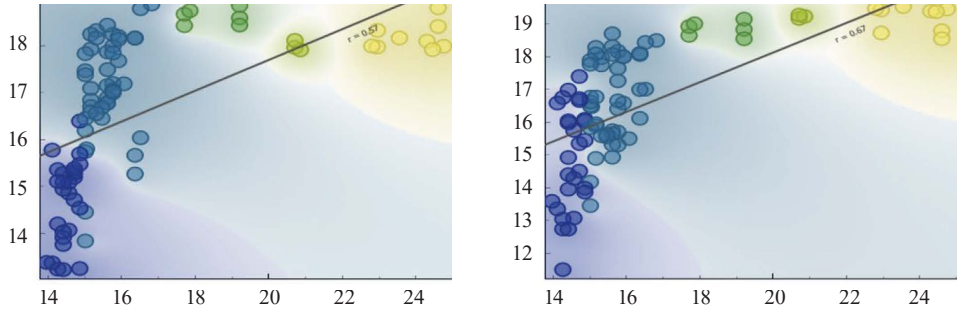

Figure 5 Actual vs. predicted values of hydroxymethylfurfural with partial least squares (PLS) predictive model (left) and principal component regression (PCR) predictive model (right)

Table 3 Values predicted by near-infrared spectroscopy: color, color change, Brix, moisture, sugar, pH, and hydroxymethylfurfural of honey stored at room temperature

Day	*L**		*a**		*b**		Δ*E*		Brix, %		Moisture, %		Sugar, $\times 10^{-8}$ g/100 g		pH		Hydroxymethylfurfural, mg/kg	
	Actual	Predicted	Actual	Predicted	Actual	Predicted	Actual	Predicted	Actual	Predicted	Actual	Predicted	Actual	Predicted	Actual	Predicted	Actual	Predicted
0	6.60 ± 0.21^{dA}	6.68 ± 0.41^{bcA}	–0.99 ± 0.11^{aA}	–1.05 ± 0.14^{aA}	1.02 ± 0.21^{cA}	1.18 ± 0.56^{cB}	0.00 ± 0.00^{aA}	0.00 ± 0.00^{aA}	69.42± 0.72^{aA}	69.91 ± 0.70^{aA}	29.13 ± 0.73^{aB}	28.62 ± 0.63^{aA}	5.23 ± 0.05^{aA}	5.59 ± 0.65^{aA}	3.56 ± 0.02^{bA}	3.58 ± 0.05^{dA}	14.64 ± 0.23^{aB}	13.77 ± 1.33^{aA}
1	7.43 ± 0.29^{eB}	7.04 ± 0.63^{cA}	–1.08 ± 0.04^{aA}	–1.08 ± 0.16^{aA}	–0.33 ± 0.16^{aA}	0.31 ± 0.28^{bA}	1.67 ± 0.06^{dB}	1.10 ± 0.45^{bA}	70.01± 0.77^{aA}	70.29 ± 0.15^{abA}	28.53 ± 0.78^{aA}	28.27 ± 0.16^{aA}	5.23 ± 0.05^{aA}	5.90 ± 0.21^{aA}	3.47 ± 0.02^{bA}	3.45 ± 0.05^{cA}	15.50 ± 0.78^{aA}	15.89 ± 1.11^{bA}
2	6.24 ± 0.10^{cA}	6.27 ± 0.47^{bA}	–1.04 ± 0.08^{aA}	–1.00 ± 0.11^{aA}	1.18 ± 0.10^{cB}	0.88 ± 0.15^{cA}	0.53 ± 0.10^{bA}	0.91 ± 0.45^{bB}	70.52± 0.26^{aA}	70.67 ± 0.22^{bcA}	28.01 ± 0.26^{aA}	29.01 ± 3.31^{aB}	7.60 ± 0.32^{cA}	7.12 ± 0.23^{cA}	3.54 ± 0.35^{bA}	3.43 ± 0.02^{cA}	15.80 ± 0.25^{aA}	15.80 ± 0.25^{bA}
7	5.59 ± 0.04^{bB}	5.04 ± 0.31^{aA}	–0.67 ± 0.53^{bA}	–0.70 ± 0.07^{bA}	0.35 ± 0.06^{bA}	0.38 ± 0.10^{bA}	1.23 ± 0.26^{cA}	1.91 ± 0.52^{cB}	70.04± 2.79^{aA}	71.38 ± 0.31^{dA}	28.34 ± 2.93^{aB}	27.13 ± 0.29^{aA}	6.71 ± 0.18^{bA}	7.21 ± 0.65^{cB}	3.42 ± 0.02^{bA}	3.36 ± 0.03^{bA}	20.44 ± 2.89^{bB}	18.72 ± 0.20^{cA}
14	4.55 ± 0.05^{aA}	5.24 ± 0.04^{aB}	–0.58 ± 0.07^{bA}	–0.67 ± 0.01^{bB}	0.28 ± 0.57^{bA}	-0.11 ± 0.04^{aA}	2.22 ± 0.26^{eB}	2.01 ± 0.57^{cA}	70.63± 1.43^{aA}	70.98 ± 0.16^{cdA}	27.90 ± 1.45^{aA}	27.52 ± 0.13^{aA}	6.58 ± 0.08^{bA}	6.50 ± 0.07^{bA}	3.18 ± 0.02^{aA}	3.31 ± 0.01^{aA}	24.00 ± 1.74^{cB}	19.29 ± 0.13^{cA}

Values were expressed as triplicate in mean ± standard deviation

Different superscripts within the same column indicate significant differences at $p \leq 0.05$ according to Tukey's test

Letters $^{a–e}$ indicate different storage times

Letters $^{A–B}$ indicate actual and predicted values

Table 4 Values predicted by near-infrared spectroscopy: color, color change, Brix, moisture, sugar, pH, and hydroxymethylfurfural of honey stored at chilled temperature

Day	*L**		*a**		*b**		Δ*E*		Brix, %		Moisture, %		Sugar, $\times 10^{-8}$ g/100g		pH		Hydroxymethylfurfural mg/kg	
	Actual	Predicted	Actual	Predicted	Actual	Predicted	Actual	Predicted	Actual	Predicted	Actual	Predicted	Actual	Predicted	Actual	Predicted	Actual	Predicted
0	6.92 ± 0.10^{dA}	6.95 ± 0.38^{cA}	–1.20 ± 0.06^{aA}	–1.14 ± 0.06^{aA}	1.26 ± 0.20^{cB}	0.91 ± 0.23^{cA}	0.00 ± 0.00^{aA}	0.00 ± 0.00^{aA}	70.01 ± 0.24^{aA}	70.00 ± 0.94^{aA}	28.53 ± 0.24^{bA}	28.56 ± 0.96^{cA}	5.23 ± 0.05^{aB}	4.82 ± 0.66^{aA}	3.57 ± 0.04^{cA}	3.57 ± 0.03^{dA}	14.70 ± 0.42^{aA}	14.20 ± 1.61^{aA}
1	6.77 ± 0.06^{cA}	6.57 ± 0.30^{cA}	–0.89 ± 0.09^{bA}	–0.96 ± 0.07^{bA}	–0.35 ± 0.11^{aB}	0.03 ± 0.14^{aA}	1.10 ± 0.45^{bA}	1.65 ± 0.27^{cB}	70.28 ± 0.10^{aA}	70.32 ± 0.23^{abA}	28.26 ± 0.10^{bA}	28.25 ± 0.21^{bcA}	5.23 ± 0.05^{aA}	5.52 ± 0.25^{bA}	3.47 ± 0.01^{bA}	3.42 ± 0.01^{cA}	14.60 ± 0.24^{aA}	16.31 ± 0.44^{bB}
2	6.90 ± 0.06^{dA}	6.57 ± 0.27^{cA}	–1.24 ± 0.06^{aA}	–1.08 ± 0.04^{aA}	1.46 ± 0.09^{dB}	0.81 ± 0.07^{cA}	0.91 ± 0.45^{bB}	0.31 ± 0.15^{bA}	70.33 ± 0.18^{aA}	70.62 ± 0.31^{abcA}	28.20 ± 0.18^{bB}	27.87 ± 0.25^{abA}	7.60 ± 0.32^{cA}	7.11 ± 0.13^{cA}	3.44 ± 0.02^{bA}	3.44 ± 0.02^{cA}	15.44 ± 0.26^{bA}	15.94 ± 0.51^{bA}
7	4.88 ± 0.04^{bA}	5.29 ± 0.35^{bB}	–0.64 ± 0.08^{cA}	–0.77 ± 0.10^{cA}	0.09 ± 0.06^{bA}	0.44 ± 0.14^{bB}	1.91 ± 0.52^{cA}	2.43 ± 0.21^{dB}	74.11 ± 3.97^{bB}	71.14 ± 0.29^{cA}	24.34 ± 4.05^{aA}	27.37 ± 0.24^{aB}	6.71 ± 0.18^{bA}	6.80 ± 0.14^{cA}	3.45 ± 0.01^{bA}	3.39 ± 0.03^{bA}	15.59 ± 0.32^{bcA}	17.93 ± 0.43^{cB}
14	4.30 ± 0.06^{aA}	4.53 ± 0.09^{aA}	–0.55 ± 0.06^{cA}	–0.61 ± 0.02^{dA}	0.22 ± 0.10^{bA}	0.43 ± 0.05^{bB}	2.01 ± 0.57^{cA}	2.87 ± 0.24^{eB}	70.80 ± 0.46^{aA}	70.90 ± 0.17^{bcA}	27.73 ± 0.46^{bA}	27.64 ± 0.16^{abA}	6.58 ± 0.08^{bA}	6.80 ± 0.12^{cA}	3.31 ± 0.01^{aA}	3.34 ± 0.01^{aA}	16.07 ± 0.60^{cA}	18.02 ± 0.23^{cB}

Values were expressed as triplicate in mean ± standard deviation

Different superscripts within the same column indicate significant differences at $p \leq 0.05$ according to Tukey's test

Letters $^{a–e}$ indicate different storage times

Letters $^{A–B}$ indicate actual and predicted values

The anticipated color values followed the same pattern as the actual ones.

The predicted Brix values did not differ ($p > 0.05$) from the actual ones on days 0, 1, 2, and 14. We detected no significant difference ($p > 0.05$) between the predicted and actual moisture contents on days 0, 1, and 14. The predicted sugar content value also had no significant difference ($p > 0.05$) between days 1 and 14. Therefore, the predicted sugar content value in the refrigerated honey was more accurate than the moisture content and Brix while the predicted Brix value was more accurate than the moisture content.

The predicted pH decreased together with the actual value, and the predicted hydroxymethylfurfural content increased together with the actual values. We detected no significant differences ($p > 0.05$) between the predicted and actual pH values for the entire storage time. The prediction of pH value for the refrigerated honey also proved highly accurate. The predicted hydroxymethylfurfural content did not differ ($p > 0.05$) from the actual values on days 0 and 2. The predicted values of %Brix and pH were closest to the actual values among all the physicochemical variables. Both had no significant difference ($p > 0.05$) between the predicted and actual values for the samples stored under room and chilled temperatures for the entire storage time. The predicted hydroxymethylfurfural appeared to be the furthest from the actual value among all the physicochemical variables. Probably, it was because this parameter had no significant difference ($p > 0.05$) only between predicted and actual values for two storage times.

Model evaluation. According to Table 5, the R^2 value of *L** (0.755) in the predictive model based on principal component regression was higher than in the predictive model based on partial least squares (0.722), which indicates that the principal component regression predictive model had a high accuracy prediction. The prediction of *L** had the highest R^2 value in the predictive model compared to other physiochemical variables. The prediction of *a** had a slightly lower accuracy than that of *L**. The accuracy of *a** in the predictive model based on partial least squares (0.544) was lower than the *a** in the predictive model based on principal component regression (0.682). The accuracy of prediction of *b** in the predictive model based on partial least squares was very low (0.146). However, the *b** in the predictive model based on principal component regression had a higher R^2 value (0.460), indicating a higher prediction accuracy. The accuracy of prediction for %Brix and moisture in the predictive model based on partial least squares appeared to be the lowest among all variables (0.84).

The accuracy of the predictive model based on principal component regression for %Brix and moisture was slightly higher, i.e., 0.97 and 0.93, respectively. The accuracy of prediction for sugar content in the predictive model based on principal component regression (0.689) was higher than that in the predictive model based on partial least squares (0.605), and it also demonstrated a very low root mean square error (0.000). The pH and hydroxymethylfurfural were also more accurate in the predictive model based on principal component regression (0.673 and 0.453, respectively) than in the predictive model based on partial least squares (0.490 and 0.329, respectively). When compared with other physicochemical variables, the predictive model based on principal component regression demonstrated a more accurate prediction. The values of *L**, *a**, sugar, and pH had higher accuracy ($R^2 > 50\%$) among all the variables.

Figure 1 illustrates the near-infrared transmittance spectra of Kelulut honey samples. Light scattering often provides unnecessary background information, resulting in spectra with unsmooth lines. Hence, we conducted a pre-processing stage before constructing the prediction models. Pre-processing is an important stage that improves the accuracy and calibration of the prediction model. Pre-processing eliminates physical phenomena from the continuum to enhance subsequent qualitative or quantitative analysis [30]. The spectral data collected may contain unnecessary noise and background information caused by light scattering. The noise and background information may affect the calibration and classification model. Therefore, pre-processing is needed to remove the unwanted noise and unnecessary background information before the prediction stage. Figure 2 shows that we removed the ranges with a wavelength of about 900 and 1700. The Gaussian smoothing soothed false edges and enhanced edge detection [31]. The complicating effect induced by the physical properties were separated and removed using Standard normal variate [30].

We used the partial least square regression and principal component regression to construct predictive models [32] and acquire information about the physicochemical properties of Kelulut honey hidden in the spectral data. Both methods regressed with actual measured value (X-axis) and predicted value from spectra data (Y-axis). The difference between the projected and the actual values for the honey samples stored at chilly temperatures was the same as that for the samples stored at room temperature. The determinant coefficient (R^2) and root mean square error evaluated the performance of the predictive model [33]. R^2 reflected the percentages in the dataset of the explained variance of the result [34]. We used root mean square error to calculate the prediction error for each model. If the coefficient of determination was high, the prediction output was higher while the root means square error was low [33]. We compared the R^2 and root means square error of the predictive model constructs using the partial least square regression and principal component regression to evaluate the accuracy of the two methods [34].

Table 5 shows that hydroxymethylfurfural had the highest prediction error while sugar content had the lowest model prediction error. The higher the root means square error, the greater the error of the predictive model. Thus, the sugar content demonstrated the highest accuracy and the lowest error for both models. All the physicochemical properties in the predictive model based on

Table 5 Regression results of physiochemical properties of honey based on principal component regression (PCR) and partial least square regression (PLS)

Properties	Regression method	R^2	Root means square error
*L**	PLS	0.722	0.560
	PCR	0.755	0.525
*a**	PLS	0.544	0.168
	PCR	0.682	0.141
*b**	PLS	0.146	0.350
	PCR	0.460	0.471
%Brix	PLS	0.084	1.890
	PCR	0.097	1.877
Moisture	PLS	0.084	1.925
	PCR	0.093	1.915
Sugar	PLS	0.605	0.000
	PCR	0.689	0.000
pH	PLS	0.490	0.078
	PCR	0.673	0.063
Hydroxymethylfurfural	PLS	0.329	2.337
	PCR	0.453	2.110

principal component regression had a lower prediction model error than the model based on partial least square regression. In Table 5, sugar content and pH had the highest accuracy and the lowest error for all the physiochemical properties in the model based on principal component regression compared with the model based on partial least square regression. The comparison between the two models showed that the method of principal component regression was more accurate and suitable for quantification. In contrast, the method of partial least square regression was more suitable for classification.

CONCLUSION

In this study, we used near-infrared spectroscopy to assesses the quality of Kelulut honey. Pre-processing and partial square regression provided excellent accuracy. Near-infrared spectroscopy analysis of honey samples, spanning 900 to 1700 nm, showed indistinguishable absorbance patterns across different storage conditions. Preprocessing techniques, such as standard normal variate (SNV) and Gaussian smoothing, improved the data quality. The predictive model based on principal component regression proved more accurate for various physicochemical properties, outperforming the models based on partial least square regression. The physical and chemical properties of Kelulut honey made it possible to build its physicochemical profile. Such parameters as moisture, sugar, pH, and hydroxymethylfurfural complied with the Malaysian Standard even after being stored under room and chilling temperature for 14 days. The color of honey darkened as the storage time increased. The hydroxymemethylfurfural content also increased after long storage due to the chemical reaction that occurred in honey. These phenomena require further research. The formation of hydroxymethylfurfural in honey during storage depended on a number of variables.

The physicochemical parameters (pH, total acidity, mineral content) of honey were connected with the floral source, humidity, and thermal and/or photochemical stress. The pH value of honey decreased with storage time. When comparing room temperature storage to refrigerated storage, several physicochemical parameters revealed distinct positive and negative associations. The Brix value, sugar content, pH, and hydroxymethylfurfural content strongly correlated with the storage temperature. The pre-processing of spectral data improved the prediction model. The sugar content and pH values proved to be the best attributes to determine the quality of Kelulut honey with acceptable accuracy ($R^2 > 0.6$). The predictive model based on principal component regression proved more effective to assess the quality of Kelulut honey.

CONTRIBUTION

Y.M. Chin collected the data, performed the analysis, and wrote the paper; L.A.K. Saleena contributed data and analysis tools, as well as wrote the paper; L.Y. Lim contributed data and analysis tools; L.P. Pui conceived and designed the analysis; M.I. Solihin conceived and designed the analysis.

CONFLICT OF INTEREST

The authors declared no conflict of interests regarding the publication of this paper.

REFERENCES

1. Jull AB, Cullum N, Dumville JC, Westby MJ, Deshpande S, Walker N. Honey as a topical treatment for wounds. Cochrane Database of Systematic Reviews. 2015;(3):CD005083. https://doi.org/10.1002/14651858.CD005083.pub4
2. Adadi P, Obeng AK. Assessment of bacterial quality of honey produced in Tamale metropolis (Ghana). Journal of Food and Drug Analysis. 2017;25(2):369–373. https://doi.org/10.1016/j.jfda.2016.07.005
3. Md Dan PNS, Omar S, Ismail WIW. Physicochemical Analysis of Several Natural Malaysian Honeys and Adulterated Honey. IOP Conference Series: Materials Science and Engineering. 2018;440:012049. https://doi.org/10.1088/1757-899X/440/1/012049
4. Juan-Borrás M, Domenech E, Conchado A, Escriche I. Physicochemical quality parameters at the reception of the honey packaging process: Influence of type of honey, year of harvest, and beekeeper. Journal of Chemistry. 2015;2015(1):929658. https://doi.org/10.1155/2015/929658

5. Pascual-Maté A, Osés SM, Fernández-Muiño MA, Sancho MT. Methods of analysis of honey. Journal of Apicultural Research. 2018;57(1):38–74. https://doi.org/10.1080/00218839.2017.1411178
6. Zawawi N, Zhang J, Hungerford NL, Yates HSA, Webber DC, Farrell M, *et al.* Unique physicochemical properties and rare reducing sugar trehalulose mandate new international regulation for stingless bee honey. Food Chemistry. 2022;373:131566. https://doi.org/10.1016/j.foodchem.2021.131566
7. García-Sánchez F, Galvez-Sola L, Martínez-Nicolás JJ, Muelas-Domingo R, Nieves M. Using Near-Infrared Spectroscopy in Agricultural Systems. In: Kyprianidis KG, Skvaril J, editors. Developments in Near-Infrared Spectroscopy. 2017. p. 92–127. https://doi.org/10.5772/67236
8. Porep JU, Kammerer DR, Carle R. On-line application of near infrared (NIR) spectroscopy in food production. Trends in Food Science and Technology. 2015;46(2):211–230. https://doi.org/10.1016/j.tifs.2015.10.002
9. Prieto N, Pawluczyk O, Dugan MER, Aalhus JL. A Review of the principles and applications of near-infrared spectroscopy to characterize meat, fat, and meat products. Applied Spectroscopy. 2017;71(7):1403–1426. https://doi.org/10.1177/0003702817709299
10. Guelpa A, Marini F, du Plessis A, Slabbert R, Manley M. Verification of authenticity and fraud detection in South African honey using NIR spectroscopy. Food Control. 2017;73:1388–1396. https://doi.org/10.1016/j.foodcont.2016.11.002
11. Pui LP, Karim R, Yusof YA, Wong CW, Ghazali HM. Physicochemical and sensory properties of selected 'cempedak' (*Artocarpus integer* L.) fruit varieties. International Food Research Journal. 2018;25(2):861–869
12. Malaysian Standards MS 2683:2017. Kelulut (Stingless bee) honey – Specification. Malaysia: Department of Malaysian Standards, 2017. 33 p. https://www.brizy.cloud/customfile/7512f96ecef15ae5d649ccb4015712b9.pdf
13. Sadasivam S. Biochemical Methods. New Age International Publisher. New Delhi; 1996. pp. 124–126.
14. Woodcock T, Downey G, O'Donnell CP. Confirmation of declared provenance of European extra virgin olive oil samples by NIR spectroscopy. Journal of Agricultural and Food Chemistry. 2008;56(23):11520–11525. https://doi.org/10.1021/jf802792d
15. Can Z, Yildiz O, Sahin H, Turumtay EA, Silici S, Kolayli S. An investigation of Turkish honeys: Their physico-chemical properties, antioxidant capacities and phenolic profiles. Food Chemistry. 2015;180:133–141. https://doi.org/10.1016/j.foodchem.2015.02.024
16. Kek SP, Chin NL, Yusof YA, Tan SW, Chua LS. Classification of entomological origin of honey based on its physicochemical and antioxidant properties. International Journal of Food Properties. 2017;(S3):S2723–S2738. https://doi.org/10.1080/10942912.2017.1359185
17. Yap SK, Chin NL, Yusof YA, Chong KY. Quality characteristics of dehydrated raw Kelulut honey. International Journal of Food Properties. 2019;22(1):556–571. https://doi.org/10.1080/10942912.2019.1590398
18. Visquert M, Vargas M, Escriche I. Effect of postharvest storage conditions on the colour and freshness parameters of raw honey. International Journal of Food Science and Technology. 2014;49(1):181–187. https://doi.org/10.1111/ijfs.12296
19. Turkmen N, Sari F, Poyrazoglu ES, Velioglu YS. Effects of prolonged heating on antioxidant activity and colour of honey Food Chemistry. 2006;95(4):653–657. https://doi.org/10.1016/j.foodchem.2005.02.004
20. Piotraszewska-Pająk A, Gliszczyńska-Świgło A. Directions of colour changes of nectar honeys depending on honey type and storage conditions. Journal of Apicultural Science. 2015;59(2):51–61. https://doi.org/10.1515/jas-2015-0019
21. Biluca FC, Braghini F, Gonzaga LV, Costa ACO, Fett R. Physicochemical profiles, minerals and bioactive compounds of stingless bee honey (*Meliponinae*). Journal of Food Composition and Analysis. 2016;50:61–69. https://doi.org/10.1016/j.jfca.2016.05.007
22. Majid YM, Fadzelly Abu Bakar M, Mian Z, Esa F, Kok Yeow Y. Variations of physicochemical properties of stingless bee honey from different botanical origin in state of Johor, Malaysia. IOP Conference Series: Earth and Environmental Science. 2019;269:012028. https://doi.org/10.1088/1755-1315/269/1/012028
23. Chuttong B, Chanbang Y, Sringarm K, Burgett M. Effects of long-term storage on stingless bee (Hymenoptera: Apidae: Meliponini) honey. Journal of Apicultural Research. 2015;54(4):441–451. https://doi.org/10.1080/00218839.2016.1186404
24. do Nascimento AS, Marchini LC, de Carvalho CAL, Araújo DFD, de Olinda RA, da Silveira TA. Physical-Chemical Parameters of Honey of Stingless Bee (Hymenoptera: Apidae). Chemical Science International Journal. 2015;7(3):139–149. https://doi.org/10.9734/ACSJ/2015/17547
25. Bogdanov S. Books of Honey, physical properties of honey. Bee Product Science. Zhejiang; 2011.
26. Ávila S, Beux MR, Ribani RH, Zambiazi RC. Stingless bee honey: Quality parameters, bioactive compounds, health-promotion properties and modification detection strategies. Trends in Food Science and Technology. 2018;81:37–50. https://doi.org/10.1016/j.tifs.2018.09.002

27. Batu A, Aydoğmuş RE, Bayrambaş K, Eroğlu A, Karakavuk E, Eroğlu Z. Changes in Brix, pH and total antioxidants and polyphenols of various honeys stored in different temperatures. Journal of Food, Agriculture and Environment. 2014;12(2):281–285.
28. Fuad AMA, Zakaria AJ, Shahidan N, Zakaria Z. Physicochemical characteristics of Malaysian honeys influenced by storage time and temperature. International Journal of Fundamental and Applied sciences. 2017;9(2S):841–851. https://doi.org/10.4314/jfas.v9i2s.52
29. de Sousa JMB, de Souza EL, Marques G, de Toledo Benassi M, Gullón B, Pintado MM, *et al.* Sugar profile, physicochemical and sensory aspects of monofloral honeys produced by different stingless bee species in Brazilian semi-arid region. LWT. 2016;65:645–651. https://doi.org/10.1016/j.lwt.2015.08.058
30. Dotto AC, Dalmolin RSD, ten Caten A, Grunwald S. A systematic study on the application of scatter-corrective and spectral-derivative preprocessing for multivariate prediction of soil organic carbon by Vis-NIR spectra. Geoderma. 2018;314:262–274. https://doi.org/10.1016/j.geoderma.2017.11.006
31. Khorbotly S, Hassan F. A modified approximation of 2D Gaussian smoothing filters for fixed-point platforms. 2011 IEEE 43rd Southeastern Symposium on System Theory. 2011;151–159. https://doi.org/10.1109/SSST.2011.5753797
32. Wentzell PD, Montoto LV. Comparison of principal components regression and partial least squares regression through generic simulations of complex mixtures. Chemometrics and Intelligent Laboratory Systems. 2003;65(2):257–279. https://doi.org/10.1016/S0169-7439(02)00138-7
33. Chai T, Draxler RR. Root mean square error (RMSE) or mean absolute error (MAE)? – Arguments against avoiding RMSE in the literature. Geoscientific Model Development. 2014;7:1247–1250. https://doi.org/10.5194/gmd-7-1247-2014
34. Curcio D, Ciraolo G, D'Asaro F, Minacapilli M. Prediction of Soil Texture Distributions Using VNIR-SWIR Reflectance Spectroscopy. Procedia Environmental Sciences. 2013;19:494–503. https://doi.org/10.1016/j.proenv.2013.06.056

ORCID IDs
Yee Mun Chin https://orcid.org/0000-0001-6073-7205
Lejaniya Abdul Kalam Saleena https://orcid.org/0000-0001-7852-8073
Liew Phing Pui https://orcid.org/0000-0001-5305-4334
Mahmud Iwan Solihin https://orcid.org/0000-0002-5293-7466

Foods and Raw Materials. 2026;14(1)

ISSN 2308-4057 (Print)
ISSN 2310-9599 (Online)

Review Article
Open Access

Available online at http://jfrm.ru/en
https://doi.org/10.21603/2308-4057-2026-1-660
https://elibrary.ru/TYXMAN

Functional attributes and bio-prospects of fruit peel waste

Himanshu[1], Nishant Kumar[2], Ishu Khangwal[1,*]

[1] Baba Mastnath University, Rohtak, India
[2] National Institute of Food Technology Entrepreneurship and Management, Sonipat, India

* e-mail: ishukhanagwal.35@gmail.com

Received 22.02.2024; Revised 08.07.2024; Accepted 06.08.2024; Published online 14.02.2025

Abstract:
The fruit processing industry generates a considerable amount of waste, which leads to significant nutritional and economic losses. The most common waste materials include pomace, peels, rind, and seeds. They contain valuable natural bioactive compounds, such as carotenoids, polysaccharides, dietary fibers, enzymes, polyphenols, oils, and vitamins. These compounds can be recovered by using suitable conventional or non-conventional methods. Conventional methods include Soxhlet extraction, hydro-distillation, and maceration. Non-conventional methods include enzyme-assisted, ultrasound-assisted, microwave-assisted, solid-liquid, and solvent extractions, as well as pulsed electric field. Fruit peels can be used to synthesize metallic nanoparticles, edible packaging, single-cell proteins, biosorbents, biochar, carbon dots, and biofertilizers. Furthermore, their bioactive compounds have a significant pharmacological potential. In particular, they can be utilized as antioxidant, anti-inflammatory, antimicrobial, antiviral, and anti-neoplastic agents.
Fruit peels are also a cost-effective solution that can mitigate various environmental problems and aid in reducing nutritional loss. In this article, we reviewed different extraction techniques employed to retrieve bioactive compounds from fruit peel waste, along with their industrial, biotechnological, and pharmacological applications.

Keywords: Bioactive compounds, nanoparticles, carbon dots, biochar, biofertilizers, edible packaging, single-cell protein, biosorbents

Please cite this article in press as: Himanshu, Kumar N, Khangwa I. Functional attributes and bio-prospects of fruit peel waste. Foods and Raw Materials. 2026;14(1):84–103. https://doi.org/10.21603/2308-4057-2026-1-660

INTRODUCTION

Around the world, 931 million metric tons of fruit and vegetable waste is produced each year, with China producing the most at 91.65 million tons, followed by Nigeria and India at 68.76 and 37.94 million tons, respectively [1]. Fruit and vegetable processing generates a significant amount of by-products, such as pulp, seeds, peels, and stones, with waste peels accounting for approximately 25–30% [2]. Fruit peels contain essential bioactive functional constituents, such as polyphenols, vitamins, enzymes, dietary fibers, oils, carotenoids, polysaccharides, and other beneficial compounds. These bioactive compounds exhibit antibacterial, antioxidant, anti-carcinogenic, anti-phlogistic, and antidiabetic properties [3, 4].

Bioactive compounds can be recovered and recycled by suitable techniques, such as solvent extraction, mechanical expelling, supercritical extraction, and microwave extraction. Conventional extraction has time limitations, low extraction efficiency, low yield, and solvent requirements. Ultrasound-assisted extraction (UAE), by contrast, is an efficient extraction technique that can recover bioactive components from plants with less energy and solvent. It extracts valuable components, such as polyphenols, carotenoids, aromas, and polysaccharides, from both plants and their by-products at low temperatures while retaining their functionality. To optimize the UAE process, a number of variables need to be understood and optimized for each by-product, including frequency, power, duty cycle, temperature, time, solvent type, and liquid-solid ratio [5].

In recent years, there has been a notable shift in the perspective towards fruit and vegetable by-products. Studies have indicated that these by-products can exhibit higher concentrations of bioactive compounds in comparison to the edible portions of the fruit. For instance, the peels of lemons, grapes, and oranges, as well as the seeds of avocado, jackfruit, and mangoes, have been shown to contain 15% more phenolic compounds than the pulpy parts of the fruits. These findings suggest that fruit and vegetable by-products may possess greater

Copyright © 2025, Himanshu *et al.* This is an open access article distributed under the terms of the Creative Commons Attribution 4.0 International License (https://creativecommons.org/licenses/by/4.0/), allowing third parties to copy and redistribute the material in any medium or format and to remix, transform, and build upon the material for any purpose, even commercially, provided the original work is properly cited and states its license.

health benefits than previously thought and warrant further investigation [6]. Using fruit peels to recover and recycle bioactive compounds has emerged as a cost-effective and eco-friendly solution to environmental challenges while also providing numerous health benefits [7].

Studies of fruit waste have uncovered such bioactive compounds as polyphenols, dietary fiber, enzymes, polysaccharides, proteins, and olfactory components. These beneficial nutrients are responsible for a number of health benefits. The use of fruit peels in nutrient supplementation depends on their chemical composition. Studies have shown that *Punica granatum* L. peels, typically inedible, contain such essential phytochemical constituents as gallic acid, ellagic acid, punicalins, and punicalagin. These compounds have multiple pharmacological properties, such as immune modulation, humectancy, as well as antibacterial, antioxidant, and anti-atherosclerotic effects [8]. Similarly, the phytochemical profile of *Mangifera indica* L. peels reveals that they contain phenols (14.85–127.6 mg/g dry weight), ascorbic acid, fibers (26–78 g/100g dry weight), as well as tocopherols and carotenoids (0.1–51 mg/g dry weight) [9]. Previous research has identified a group of phenolic compounds (*p*-coumaric, caffeic, ferulic, and sinapic acids), polyethoxylated flavones (tangeretin and nobiletin), and flavanones (hesperidin and naringin) responsible for certain peels' antioxidative properties [10]. The peels of *Ananas comosus* L. were found to contain ferulic acid (19.50 mg/100 g), catechin (58.51 mg/100 g dry extracts), gallic acid (31.76 mg/100 g), and epicatechin (50.00 mg/100 g) [11]. *Musa sapientum* L. peels contain crude fat (5.93 ± 0.13%), crude proteins (1.95 ± 0.14%), and saccharides (11.82 ± 2.17%), as well as phosphorus, iron, calcium, magnesium, and sodium. They also have low concentrations of copper, zinc, potassium, and manganese [12]. Further, a comparative analysis of various fruit peels has shown that orange peels have the highest DPPH radical scavenging activity, total anthocyanin composition, and total phenol content, compared to kiwi, pineapple, apple, and banana peels.

The fruit peels, often discarded as waste, not only pose significant environmental issues but also represent an enormous loss of nutrients with high bioactive properties. These bioactive compounds have been recently shown to exhibit multiple pharmacological properties, such as antidiabetic, anticancerous, anti-glycemic, neuroprotective, antimutagenic, antibacterial, and anti-inflammatory effects [13]. In addition, these compounds can be used directly as nutraceuticals due to their potential health benefits or can be utilized as raw materials by various industries, including pharmaceuticals, cosmetics, and food industries. This idea has captured the interest of developing nations that seek to optimize eco-friendly methods and ensure food security [14]. Bioactive compounds derived from fruit peels are also being explored for their biotechnological properties which can be used in the production of biodegradable plastics and biofuels.

Our study aimed to suggest a way of minimizing fruit peel waste. We explored a possibility of using selected fruit peel wastes for therapeutic purposes to combat a wide range of multidrug-resistant microorganisms. We also sought to review various innovative approaches to extracting bioactive compounds from fruit peels. The study explored their diverse applications, including synthesizing metallic nanoparticles, edible packaging, carbon dots, biofertilizers, biochar, and more. Additionally, we briefly discussed the diverse pharmacological activities that fruit peels exhibit, underscoring the need for further research in this area.

METHODS FOR EXTRACTING BIOACTIVE COMPOUNDS

The methods for extracting bioactive compounds can be classified as conventional and unconventional techniques (Fig. 1). Some of the conventional methods are Soxhlet extraction, maceration, and hydro-distillation. Unconventional methods include ultrasound-assisted, supercritical fluid, pressurized liquid extraction, microwave-assisted extraction, and others.

1. Conventional methods

Conventional methods have been in use for a long time and are known as traditional approaches. These methods rely on the solvent extraction capacity or energy delivered, or both [5].

1.1. Soxhlet extraction

Soxhlet extraction is a conventional technique used to extract bioactive compounds from plants. This method involves a continuous cycle of boiling and condensation

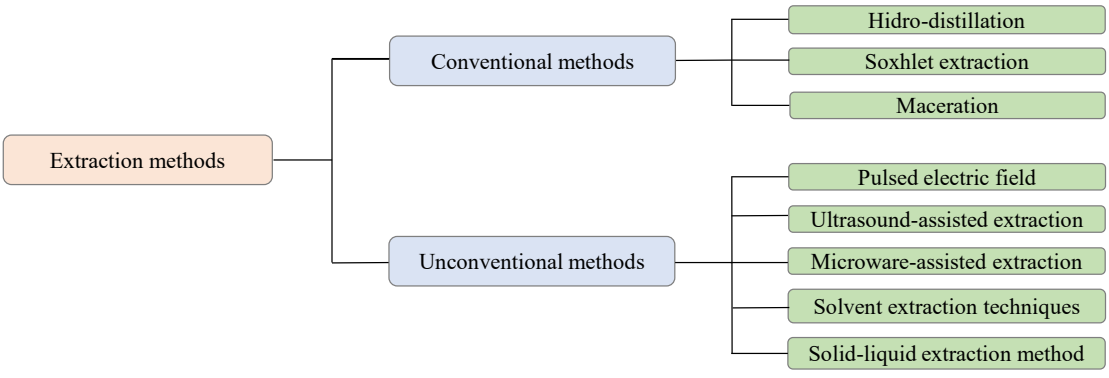

Figure 1 Methods for extracting bioactive compounds from plant sources [15, 16]

that enables efficient extraction of desired components. A small dry material is placed in a thimble, and a beaker is filled with a preferred solvent. The solvent is repeatedly added to the plant material while the extracted solute remains in a distillation flask [15]. For example, Rezvankhah *et al*. [17] effectively extracted fatty acids from hemp seeds at 70°C for eight hours and phenolic compounds from hemp leaves for two hours using 60% ethanol.

1.2. Hydro-distillation

Hydro-distillation is an approved method used to extract essential oil. Fragrant plant material is boiled with water in a still or added to live steam to release oil glands. Oil is separated from distillate water in a separator [18]. Azmat *et al*. [19] compared supercritical fluid extraction with hydro-distillation used to extract essential oil constituents from pomegranate peel. They found that supercritical extraction provided a higher yield (1.18%, v/w) compared to hydro-distillation (0.21%, v/w).

1.3. Maceration

Maceration is a standard method for extracting medicinal herbs typically used in galenical medicines. The fundamental principles and procedures involved in maceration, percolation, and infusion for obtaining crude drug extracts are similar to those used in leaching, which involves extracting soluble elements from solid substances using a solvent. The extraction process is influenced by such factors as the speed at which the solvent enters the mass, the rate at which the soluble elements dissolve in the solvent, and the rate at which the solution exits the insoluble material. Low efficiency and long duration are the major disadvantages of this extraction method [15]. A number of studies used maceration to extract flavonoids from turmeric rhizomes (non-ionic surfactant Triton X-100, neutral pH, 35°C), from *Arbutus unedo* L. fruits (79.6°C, 3.7% diluted ethanol), and from the leaves of *Ficus carica* and *Euphorbia neriifolia* (75% concentrated ethanol, room temperature) [20–22].

2. Unconventional methods

Various novel methods that can extract bioactive substances from agricultural waste include enzyme-assisted extraction, solvent extraction, solid-liquid extraction, pulsed electric field, microwave-assisted extraction, subcritical water extraction, ultrasound-assisted extraction, and supercritical fluid extraction.

2.1. Solid-liquid extraction and solvent extraction techniques

Phenolic compounds can be extracted from agri-food residues using organic solvents, but they can be expensive, time-consuming, and environmentally harmful. On the other hand, water seems an ideal solvent for polar and hydrophilic compounds [23]. Deep eutectic solvent extraction is an eco-friendly and cost-effective method that can recover phenolic compounds [24]. The Naviglio extractor is a new solid-liquid extractor that can extract bioactive compounds by depleting the solid matrix [25]. Its benefits include performing extractions at room temperature, reducing thermal stress, and improving extraction accuracy [15].

Previous studies have reported that potato phenolic compounds extracted using solid CO_2 cryomaceration and solid-liquid extraction with 10% ethanol/water showed efficient antioxidant activity, which could help maintain the quality of fresh-cut apples. The studies also highlighted the potential use of natural deep eutectic solvents (NADES) to avoid the use of chemicals in food applications [26, 27].

Solvent extraction is an effective way to extract complex soluble components and extra flavorings from raw materials. The choice of a solvent impacts the effectiveness of extraction. Smaller particles improve the solvent's ability to penetrate, but the filtering procedure becomes challenging if they are too small. Commonly used solvents are alcohols, acetone, and acetonitrile. However, with hazardous solvents, this approach needs an evaporation/concentration phase for retrieval, enormous volumes of solvent, as well as a lengthy time frame. Other technologies, such as ultrasonic, microwave-assisted, Soxhlet, or supercritical fluid extractions, have increased solvent extraction yields [15].

2.2. Enzyme-assisted extraction

Enzymes can extract bioactive substances from food waste by breaking down plant cell wall polysaccharides such as pectin, hemicellulose, and cellulose. This allows associated compounds to be released. Enzyme-aided extraction is an eco-friendly method that uses water instead of organic solvents. Based on the enzymes' ability to catalyze interactions in aqueous media under moderate process conditions, it can replace traditional solvent extraction methods [28]. Enzyme-assisted extraction is highly effective for extracting phenolic compounds from citrus peels at 20–60°C [29].

2.3. Pulsed electric field

Pulsed electric field is a new method to obtain valuable molecules from fruit leftovers. It uses high-voltage microsecond pulses on a material sandwiched between two electrodes. Pulsed electric field improves recovery rates of chemicals without affecting the grade of retrieved substances. It is a non-thermal method that improves recovery when used as a pre-treatment over heat-based pre-treatment. The critical process variables are the electric field strength and processing time. The energy needed is modest and does not affect the general architecture of the cell [30, 31]. Pulsed electric field serves as an effective method for valorizing by-products, e.g., for extracting phenolic compounds from plum, grapes, and citrus peels [23].

2.4. Microwave-assisted extraction

Microwave-assisted extraction generates heat within the material to rupture cell walls and extract bioactive compounds. This method allows for shorter extraction and has been used to recover various bioactive substances. Different processes occur during microwave-assisted extraction, including solvent penetration, component solubility or dissolution, and transfer of solubilized chemicals. Microwave-assisted extraction can be carried out in sealed or exposed vessels. Recently, devices operating in a vacuum or nitrogen atmosphere have

been developed [32]. Several studies have reported that oil from curcuma can decompose during traditional Soxhlet extraction. However, it was successfully extracted using microwave-assisted extraction under the best conditions of 29.99 minutes extraction time, 160 watts power, and a curcuma powder-to-ethanol ratio of 1:20 (w/v), resulting in an optimal yield of 10.32% [33]. Thus, microwave-assisted extraction is a highly versatile and user-friendly technique that enables extraction of volatile compounds in significantly reduced time frames [34].

2.5. Ultrasound-assisted extraction

Ultrasound-assisted extraction uses ultrasound energy and solvents to extract target compounds from plant matrices. It uses high-frequency mechanical waves that induce cavitation bubbles, which grow and collapse, creating hot spots and extreme local conditions. The collapsing cavitation bubbles generate shockwaves and accelerate inter-particle collision, causing fragmentation in cellular structures and leading to the solubilization of bioactive components in the solvent. Ultrasound-assisted extraction also induces erosion, sonoporation, and shear force, resulting in the release of bioactive compounds. This method increases the plant tissue matrix's water absorption and swelling indexes, which helps in the desorption and diffusion of solutes, resulting in increased extraction. Ultrasound-assisted extraction can be performed in an ultrasonic bath or a probe-based system. While both systems are economical and easy to handle, probe-based systems are commonly preferred due to higher ultrasonic intensity and efficient cavitation effect [5]. Several studies have reported extraction of polyphenols from *Punica granatum* L. peels at 50–60°C and 37 kHz [35].

INDUSTRIAL APPLICATIONS OF FRUIT PEELS

1. Edible coatings

Edible coatings are thin coats that are applied to prolong the shelf life of food products. It is a cost-effective method to maintain the properties, quality, functions, and effects of the food material [36]. Edible coatings have the potential to prevent the damage resulting from microbial attacks. Several studies have reported the use of edible coatings as a carrier matrix for specific antimicrobial agents [37]. Packaging materials can incorporate natural bioactive compounds such as essential oils, α-tocopherol, and polyphenols, which can replace chemical preservatives and increase food longevity [38].

According to previous studies, pomegranate peel waste is rich in functional bioactive constituents and natural antioxidants which can be used to prepare edible films based on biopolymers to enhance their bio-functionality. However, its bitter taste is a limitation that can be addressed by using encapsulation strategies, such as biopolymers/edible matrices. Encapsulated forms of pomegranate peel extracts can have customizable wall thickness to mask their bitter taste and determine their release effect over time. Incorporating pomegranate peel extract in an edible matrix can improve the interaction between the matrix and the particles. This can result in enhanced mechanical, biochemical, and structural features such as phenolic composition, as well as antioxidant and antimicrobial potential.

Pomegranate peel extract can also prevent lipid oxidation, natural pigment retardation, and microbial contamination, thereby enhancing the shelf life of food products [39]. Additionally, an edible coating based on a combination of mango kernel seed starch and lemongrass essential oil can extend the storage life of guava fruit. It can also maintain its physiochemical characteristics, including acidity, total soluble solids, textural properties, and phenolic contents [40]. To prepare edible biofilms, several other fruit peels are employed (Table 1).

2. Fruit peel-derived metallic nanoparticles

Bioactive functional components in fruit peels, such as polyphenols, enzymes, amino acids, proteins, alkaloids, tannins, carbohydrates, saponins, and vitamins, can act as reducing agents during the synthesis of metallic nanoparticles [45]. Some of these components can also serve as capping agents preventing nanoparticle agglomeration, while others can act as modeling agents allowing particles to grow in a specific direction [46]. Different fruit peel extracts with high efficacy have been utilized to develop metallic nanoparticles, such as silver, gold, iron, palladium, titanium, and zinc oxide. Silver and gold nanoparticles have shown promising antimicrobial action against a wide range of pathogenic microbes. These nanoparticles can be synthesized through hydrothermal, electrochemical, microwave, and green chemistry methods [47, 48]. For example, polyphenolic-rich *Punica granatum* waste has been utilized to synthesize silver nanoparticles with antiviral, antioxidant, anticancerous, and antimicrobial activities. The antioxidant and antimicrobial potential of pomegranate silver nanoparticles allows citrus fruit to be stored in the cold for a long period [49]. Nano-bacterial cellulose has been made from citrus waste such as pomace and peel, using *Komagataeibacter xylinus*, which has distinct physicochemical characteristics and potential applications in various pharmacological and biomedicine sectors [50].

Using fruit peels to synthesize metallic nanoparticles is an eco-friendly and non-toxic alternative to toxic solvents, which benefits the environment and human health. This green method reduces the use of hazardous organic solvents, toxic reagents, or non-biodegradable stabilizing agents. In addition, it does not need expensive instruments to control the chemical reduction process, which results in a more environmentally-friendly process. Researchers have evaluated various plants and plant-based materials as substrates for synthesizing metallic oxide nanoparticles due to their reduction potentiality and simple scale-up process [49]. Several other fruit peels can be utilized to synthesize nanoparticles (Table 2).

3. Fruit peel-derived carbon dots

"Carbon dots" are minute fluorescent carbon nanoparticles below 10 nm in size which exhibit photoluminescent behavior. Carbon dots are produced by two methods, namely bottom-up and top-down synthetic routes (Fig. 2). The top-down approach involves breaking down

Table 1 Fruit peels as a source of edible coatings

Common name	Scientific name	Matrix	Food item	Technique	Effects	References
Apple	*Malus domestica*	Carboxymethyl-cellulose	Fresh beef patties	Micro-fluidization	Totally reduced lipid oxidation and effectively inhibited microbial development on uncooked beef patties. No impact on the sensory qualities of beef patties, either raw or cooked	[41]
Pomegranate	*Punica granatum*	Chitosan/ gelatine	n.d.	Film	Improved rheological, antioxidant, and antibacterial qualities	[39]
		Mung bean protein	n.s.	n.d.	Increased total phenolic content, antioxidant activity, and antibacterial capacity in pomegranate peel-enriched films compared to the control mung bean protein film	[44]
		20% glycerol	Bread	Film as wrapping material	Substantially reduced microbial load and bread weight loss during storage	[39]
Orange	*Citrus sinensis*	Chitosan film	Deepwater pink shrimp	Casting	The shelf life of fresh shrimp extended to 15 days by chitosan film with 2% orange peel essential oil	[42]
		Pectin coating	Fresh-cut orange	n.d.	The shelf life of orange slices extended by nanoemulsion-based edible coatings enriched with orange peel essential oil, with no adverse effects on sensory qualities	[43]

n.d. – not detected

n.s. – not specified

Table 2 Fruit peels as a source of nanoparticles

Common name	Scientific name	Type of nano-particle	Reaction time	Morphology	Size	Applications	References
Orange	*Citrus sinensis*	Silver	10 min	Sphere	47–53 nm	Photocatalytic activity against methylene blue	[51]
Cavendish banana	*Musa acuminata*	Silver	30 min	Sphere	55 nm	Antimicrobial activity against *S. aureus, E. coli, Bacillus subtilis* and *K. pneumoniae;* antioxidant activity (DPPH); 2,2'-azino-bis (3-ethylbenzothiazoline-6)	[52]
Banana	*Musa paradisiaca*	Silver	1 h	Sphere	23.7 nm	Antibacterial efficacy against *E. coli, S. aureus, P. aeruginosa,* and *Bacillus subtilis*; antifungal activity against *C. albicans*	[53]
Orange, banana	*Citrus sinensis*, *Musa*	Silver	1 h	Sphere	n.d.	Antibacterial activity against *Proteus vulgaris* and *Staphylococcus aureus*	[54]
Orange, banana, apple	*Citrus sinensis*, *Musa*, *Malus domestica*	Silver	2 min	Sphere	25 nm	Antibacterial activity against *Aeromonas hydrophila*, *Pseudomonas spc, E. coli*, and *Salmonella spc*; antifungal action against *Fuarium spc.*; antioxidant activity and cytotoxicity (DPPH) against human breast cancer cells MCF-7	[55]
Orange	*Citrus sinensis*	Zinc oxide	1 h	Hexagonal	12.55 nm	Photocatalytic activity against methylene blue	[56]
Grapefruit	*Citrus paradise*	Zinc oxide	1 h	Hexagonal	19.6 nm	Photocatalytic activity against methylene blue	[56]

n.d. – not detected

complex carbon structures using electrooxidation, acid-assisted chemical oxidation, or laser ablation. On the other hand, the bottom-up approach uses plants and their by-products instead of chemical substances. This method is more cost-effective, with cheaper precursors and simpler experimental setups [57]. In particular, it involves selecting suitable carbon precursors, such as carbohydrates, citrate, and polymer-silica nano-compo-

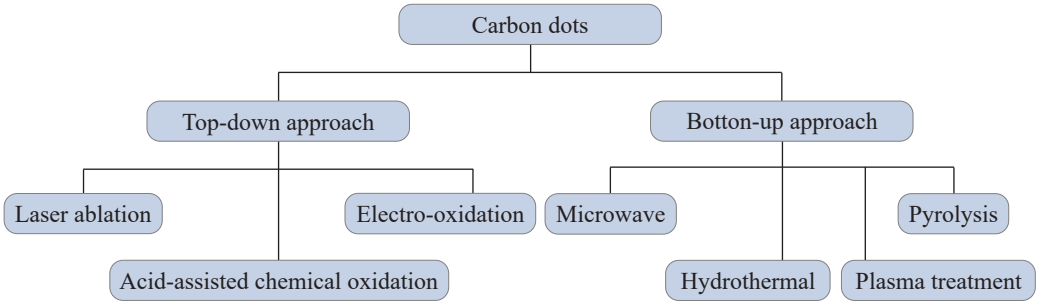

Figure 2 Approaches for synthesizing nanostructured materials (carbon dots) [57]

Table 3 Carbon dots derived from different fruit peels

Common name	Scientific name	Conditions	Heavy metals detection limit	Applications	References
Sweet lime	*Citrus limetta*	Hydrothermal/180°C/3 h	n.a.	Breast cancer detection, gene therapy	[61]
Grapefruit	*Citrus paradisi*	Hydrothermal/190°C/12 h	n.a.	Photoluminescence immunoassay	[62]
Pomelo	*Citrus maxima*	Hydrothermal/200°C/3 h	0.23 nM	Hg^{2+} sensing	[63]
Pomegranate	*Punica granatum*	Hydrothermal/180°C/36 h	n.a.	Recovering latent prints	[64]
Banana	*Musa acuminata*	Microwave-assisted/ 500 W/20 min	n.a.	Determination of colitoxin DNA	[65]
Mango	*Mangifera indica*	Hydrothermal/300°C/2 h	1.2 µM	Detection of iron ions (Fe^{2+}) using cellular labelling	[66]
Watermelon	*Citrullus lanatus*	Hydrothermal/220°C/2 h	n.a.	Imaging probe	[67]

n.a. – not assessed

sites. These precursors are then carbonized and purified to remove any impurities. The resulting nanoscale carbon structures are assembled through chemical processes. Carbon precursors with functional groups such as hydroxyl or carboxyl are suitable for this process. Carbon quantum dots (CQDs) can be synthesized through various methods, including microwave irradiation, thermal decomposition, hydrothermal treatment, template-based routes, and plasma treatment.

The use of green material as a carbon source for CQD synthesis (hydrothermal and microwave synthesis, carbonization) has attracted scientific interest due to its eco-friendliness. The raw materials and methods used for CQD synthesis affect the size, crystallinity, functional groups, colloidal stability, fluorescence properties, quantum yield, and compatibility of the resulting CQDs. Hydrothermal synthesis is the dominant method for synthesizing biomass-based CQDs compared to other chemical methods. Recently, many studies have focused on synthesizing environmentally friendly biomass-based CQDs from common biomasses using various hydrothermal synthesis conditions [58].

Researchers are looking into various carbon sources, including agricultural by-products, biomass, and food waste, to establish environmentally friendly and low-cost routes to produce CQDs. These carbon sources are plentiful, renewable, and less expensive, which makes them appealing alternatives to traditional sources. CQDs have the potential to be used in a variety of fields, including bioimaging, optoelectronics, and sensing. Heavy metals, including iron, chromium, copper, and aluminum, are nutritionally essential elements needed by various organisms to sustain their lives. These elements have a higher density than water and are the most common toxic and non-biodegradable contaminants. Their increased employment in various fields has led to an increase in environmental pollution. Eco-friendly, feasible, and efficient sensors are required to identify the presence of heavy metals and prevent their negative consequences [58].

Several studies have employed the peels of *Mangifera indica* and *Ananas comosus*. They are highly effective for developing carbon dots due to a variety of functional bioactive constituents, such as dietary fibers, gallic acid, polyphenols, and flavonoids [59]. Additionally, *Citrus maxima* can detect 0.23 nM heavy metals and Hg^{2+}, while *Citrus sinensis* can be used for sensing ferric ions and tartrazine, as well as for cell imaging. Fruit peels serve as a potential source of carbon dots due to low toxicity, photostability, biocompatibility, and innocuousness [60] (Table 3).

BIOTECHNOLOGICAL APPLICATIONS OF FRUIT PEELS

1. Fruit peel-derived biosorbents

Rapid industrialization and population increase have resulted in serious environmental challenges such as heavy metal poisoning of wastewater, which harms people's health. The primary sources of water pollution include the discharge of untreated sanitary and toxic industrial wastes, dumping of industrial effluent, and run-off from agricultural fields. In recent years, various toxic

chemicals (e.g., micropollutants, personal care products, endocrine-disrupting compounds, pesticides, inorganic anions, etc.) have been detected at dangerous amounts in drinking waters in many parts of the world [68]. Various health risks due to water pollution have been reported in the literature. These heavy metals are commonly classified as hazardous and non-destructible pollutants. When agglomerated in living tissues, they cause various infectious diseases and disorders via food chain biomagnification [69]. In view of severe problems for human health caused by elevated concentrations of toxic pollutants, there is an urgent need to develop robust, economically feasible, and environmentally friendly processes to remove them from water and safeguard the health of affected populations.

Various treatment technologies are available, with varying degrees of success, to control or minimize water pollution. However, the shortcomings of most of these methods are high operational and maintenance costs, generation of toxic sludge, and complicated procedures involved in the treatment. Comparatively, the adsorption process is considered a better alternative to water treatment because of its convenience, ease of operation, and simplicity of design. Further, this process has a broader applicability in water pollution control since it can remove or minimize different types of pollutants.

Activated carbon is undoubtedly considered a universal adsorbent for effluent treatment and is commonly used to remove various pollutants from water. However, its widespread use in wastewater treatment is sometimes restricted due to its higher cost. A large variety of low-cost adsorbents have been examined for their ability to remove various types of pollutants from water and wastewater. Generally, an adsorbent can be assumed to be “low cost” if it requires little processing, is abundant in nature, or is a by-product or waste material from the industry. Various low-cost adsorbents of different origin have been found to show little or poor adsorption potential for the removal of aquatic pollutants, as compared to commercial activated carbon.

Recently, numerous approaches have been studied to develop cheaper and more effective adsorbents containing natural biopolymers. These biopolymers are an attractive alternative as adsorbents because of their particular structure, physicochemical characteristics, chemical stability, high reactivity, and excellent selectivity toward aromatic compounds and metals. This results from the presence of chemically reactive groups (hydroxyl, acetamido, or amino functions) in polymer chains.

Various bio-based/biopolymer materials have been examined for the removal of diverse types of pollutants from water. Agricultural waste materials are economical and eco-friendly due to their unique chemical composition. Their abundance, renewable nature, and low cost make them viable options for remediating aquatic pollutants [70]. There are numerous methods to remove heavy metals, one of which is using fruit peels as a natural sorbent. They are of low cost and have good absorbent properties attributed to various organic acids, tannins, lignin, protein, and mineral constituents [71]. Diverse functional groups associated with the biosorbent surface, such as sulfhydryl, carbonyl, hydroxyl, amine, amide, phenolic, phosphate, and sulfonate groups, are responsible for attracting and sequestering pollutants [72]. As renewable agro-industrial waste, fruit peels are a promising resource for environmental technology if applied in water and wastewater treatment [73]. Several studies have focused on the use of *Hylocereus undatus* L. and *Malus domestica* L. fruit peels to remove methylene blue dye from aqueous solutions [60]. These fruit peels can be used as a raw material for synthesizing biosorbent, biochar, nanoparticles, etc. (Fig. 3).

2. Fruit peel-derived single-cell protein

Single-cell proteins, also known as microbial proteins, are dead, dry microbial cells or complete proteins that are separated from a pure microbial cell culture and are created utilizing a variety of microorganisms such as bacteria, fungi, and algae [75]. Citrus waste, which has wide applications in various functional foods, can also be used to produce single-cell proteins. These single-cell proteins are regarded as the bulk of dried cells produced through the action of microbes, yeast, bacteria, fungi, etc. They are referred to as bio-proteins, microbial proteins, or biomass [76]. Single-cell proteins can be an excellent alternative to vegetable protein sources since they do not have high land or water requirements for production [77]. The cost of their production can be reduced by selecting cheap substrates or biodegradable agricultural and food industry waste as a nutrient source for microorganisms to grow and yield large amounts of protein. Various substrates have been used for this purpose. Some of the most common substrates are orange peels, apple pomace, yam pulp, citrus pulp, potato pulp, pineapple waste, papaya waste, and more [78].

Several studies have investigated the production of single-cell proteins using fruit waste [79]. For example, single-cell proteins have been synthesized from orange and cucumber peels by submerged fermentation using *Saccharomyces cerevisiae*. According to the results, the products obtained from biotransformation of agricultural waste are cost-effective and rich in protein [76].

The fruit peels are an excellent starting material for synthesizing single-cell proteins. For their production, a unique chemical technique converts the cellulose component into more easily accessible sugar [77]. Single-cell proteins can be produced from orange peels using *Aspergillus niger* and *S. cerevisiae* [80]. Several studies have looked into developing fungal single-cell proteins by using *Rhizopus oligosporus* on fruit waste [77]. Another study synthesized single-cell proteins from pineapple peels by using *S. cerevisiae* NCDC 364 [81].

3. Fruit peel-derived biochar

Biochar is a stable carbon-rich solid formed under high temperatures and anaerobic conditions as a result of thermo-chemical decomposition followed by pyrolysis of organic materials [82]. Biochar is utilized to remove heavy metals and impurities from contaminated water [83]. Biochar has garnered significant attention

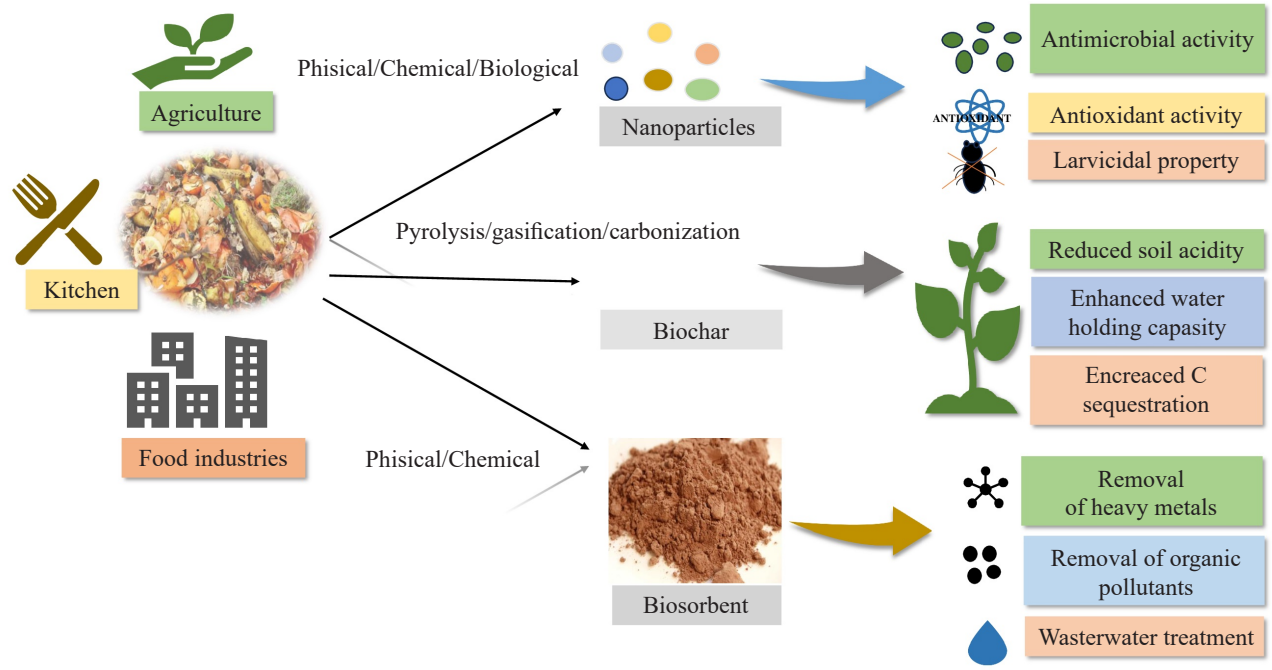

Figure 3 Extraction and application of fruit peels as valuable products [49, 55, 71–75]

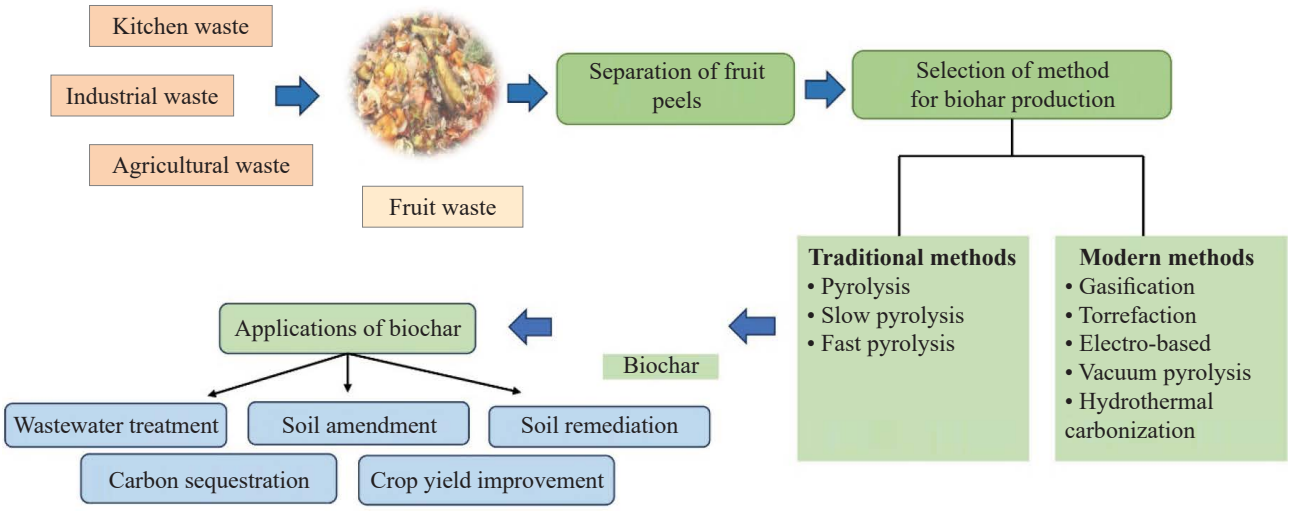

Figure 4 Fruit peel waste utilization for producing biochar and its applications [75, 84]

recently for its versatility in various agricultural and industrial applications.

The physicochemical characteristics of biochar play a crucial role in determining its suitability for different purposes. Recent studies have shown that the raw material and process parameters significantly affect biochar properties, including elemental ingredient concentrations, density, porosity, and pH [84].

Biochar is used in industrial waste treatment to eliminate organic and inorganic pollutants, dyes, and pigments from textiles. In agriculture, it helps improve the soil quality and nutrient retention. Additionally, biochar's high carbon content makes it a suitable fuel for power generation. The primary biomass sources for biochar production include agricultural and animal wastes, algae biomass, crop residues, activated sludge, energy crops, and digestate. Various physical, thermochemical, and biochemical methods can convert biomass into high-value products. Thermochemical conversion techniques, such as pyrolysis, gasification, torrefaction, and hydrothermal carbonization, produce biochar by heating carbonaceous biomass at temperatures ranging from 300 to 900°C in limited oxygen conditions. Biochar's physical, chemical, and mechanical characteristics vary depending on the raw material and pyrolysis conditions. Therefore, choosing an appropriate locally available feedstock is essential to minimize transportation costs and CO_2 emissions [85]. Furthermore, numerous fruit by-products are used to create these stabilized carbon-rich solid substances with diverse physiochemical properties (Fig.4) [86].

Ananas comosus, Citrus limetta, and *Citrus maxima* peels are used to create biochar that eliminates hexavalent chromium from aqueous solutions [55]. Some authors have also shown that biochar is generated by using rambutan and pomegranate peel to remove copper (II) ions from soil and aquatic systems [87]. For instance, biochar derived from orange and banana peels through pyrolysis at 400–500°C yields approximately 30.7–47.7 wt%. Biochar is durable against various chemical reactions, including oxidation, and has a hard texture, no sulfur, and a volatile composition. As a result, pyrolysis is the preferred method for converting fruit peels into biochar, which acts as an excellent adsorbent [88]. Producing biochar from different fruit peels with suitable methods is illustrated in Table 4.

4. Fruit peel-derived biofertilizers

Fertilizers are a most vital input for enhancing the agricultural yield. Due to their immediate action and low cost, farmers employ higher dosages of chemical fertilizers than the recommended level to enhance crop production. As a result, they not only accelerate the soil acidification but also introduce contaminants in water and the environment. Thus, there is an urgent need for developing biofertilizers that satisfy both nutritional value and crop yield [94]. The synthesis of biofertilizers from fruit peels is illustrated in Fig. 5.

Citrus waste can be used as a biofertilizer to improve soil fertility as it contains such essential micronutrients as carbon, nitrogen, and potassium. This biofertilizer has antimicrobial properties because of its high pH and

Table 4 Fruit peels as a source of biochar

Common name	Scientific name	Conditions	Applications	References
Banana	*Musa*	Pyrolysis at 500°C for 10 min	Reducing biological and chemical oxygen demands, total suspended solids, and palm oil mill effluent to an acceptable level below the discharge	[88]
Pineapple	*Ananas comosus*	Pyrolysis at 750°C for 2 h	Adsorbing hexavalent chromium at 7.44 mg/g	[89]
Litchi	*Litchi chinensis*	Hydrothermal carbonization at 180°C for 12 h	Adsorbing malachite green and congo red at 2468 and 404.4 mg/g, respectively	[90]
Orange	*Citrus sinensis*	Pyrolysis at 500°C for 10 min	Reducing biological and chemical oxygen demands, total suspended solids, and palm oil mill effluent to an acceptable level below the discharge	[88]
Pomegranate	*Punica granatum*	Pyrolysis at 300°C for 2 h	Adsorbing Cu (II) at 52 mg/g	[91]
Rambutan	*Nephelium lappaceum*	Pyrolysis at 600°C for 3 h	Removing copper ion Cu(II) from aqueous solutions of 50 and 100 mg/L at 0.2 and 0.4 g/L adsorbent dosages, respectively	[92]
Pomelo	*Citrus maxima*	Pyrolysis at 450°C for 1 h	Adsorbing methyl orange dye (1 g of biochar adsorbing 150 mg/L of methyl orange dye)	[93]

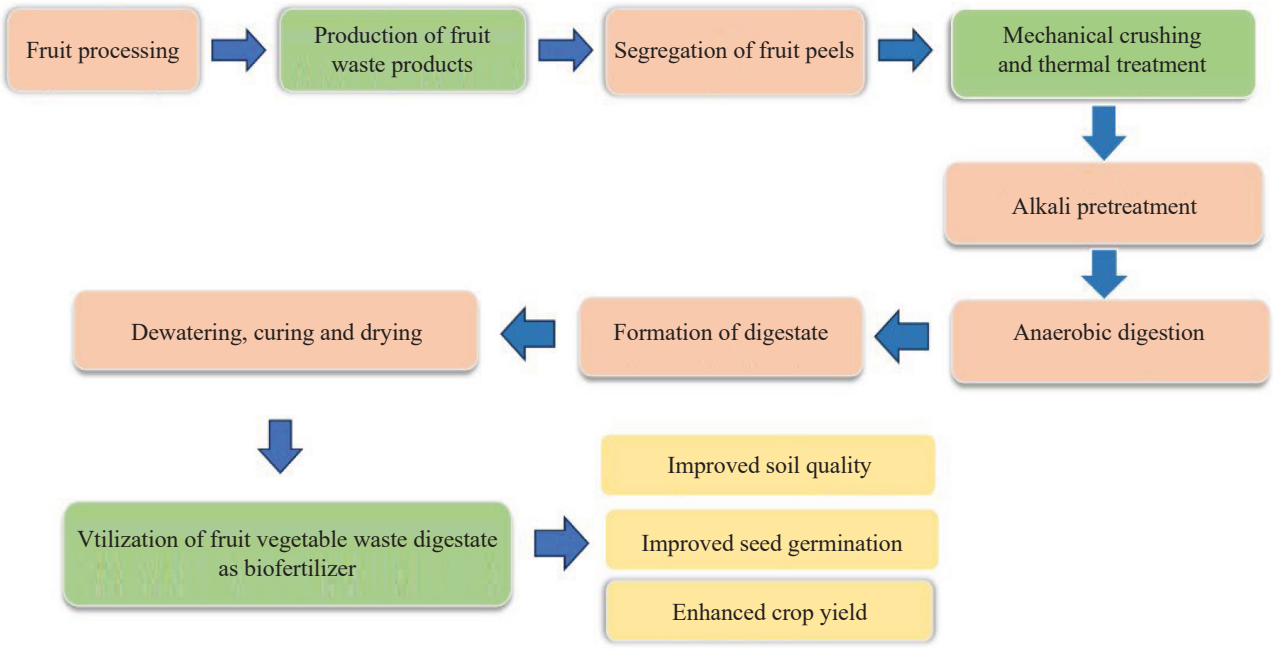

Figure 5 Fruit peel waste utilization for developing biofertilizers [93, 94]

lignocellulose, and it can remove toxic heavy metals from soil [96]. Citrus pulp waste can be used as a biofertilizer as well as to produce biogas [97]. A combination of maize silage, animal manure, and citrus pulp waste was found to be a better substrate for biogas development. The residual digestate, rich in antioxidants, can also be used as a biofertilizer. The peels of orange, sweet lime, and pomegranate can serve as a low-cost source of lactic acid bacteria, which makes them an excellent biofertilizer [98–99]. Several studies have looked into the synthesis of biofertilizers from papaya peels to enhance the nutritional value of crops [95]. Other researchers have identified beneficial bacteria such as *Azospirillum* in food waste which can enhance plant growth [100]. Thus, probiotic farming can be an alternative to chemical fertilizers for long-term benefits. Enriching the organic matter composition and soil morphology, fruit peel by-products can help maintain the soil's pH, nutritional content, seed germination, and fertility. By promoting the growth of soil microbiota, they can protect the plants from insects, fungi, and pathogenic attacks [101].

PHARMACOLOGICAL APPLICATIONS OF FRUIT PEELS

1. Antidiabetic agent

Diabetes is a disease characterized by excessive blood glucose levels as a result of the body cells' improper reaction to insulin. Insulin is a hormone that allows human cells to receive and convert glucose into energy. If the body cannot absorb glucose, it builds up in the bloodstream (hyperglycemia), which causes a number of health problems. Diabetes mellitus can cause diverse organ failure, as well as typical symptoms such as polyuria, weight loss, blurred vision, and metabolic imbalance, which worsens with age and requires natural medication [102]. α-glucosidase facilitates the breakdown of starch and dietary carbohydrates into glucose, thereby elevating blood glucose levels. Its inhibition lowers postprandial hyperglycemia and delays absorption of glucose in diabetics.

An *in vitro* investigation has demonstrated that the ethanolic pomegranate peel extract contains phenolic compounds and flavonoids that suppress α-glucosidase [103]. Furthermore, *C. limetta* peel has been found to exhibit hypoglycemic activity (in vitro) and have a postprandial glycemic effect (in vivo), lowering blood sugar levels [104]. The peel of red dragon fruit (*Hylocereus polyrhizus*) can also be used as an antidiabetic medication. It is rich in flavonoids, polyphenolic, anthocyanins, isorhamnetin glucoside, rutin, quercetin hexoside, kaempferol glucorhamnoside, isorhamnetin, and galloylglucoside [105].

Another example includes the Citrus maxima peel extract, which effectively reduced blood glucose levels by 70.17% ($p = 0.05$). Further, the extract (600 mg) increased high-density lipoprotein cholesterol by 4.43%, while lowering total cholesterol (30.86%), triglycerides (10.58%), and low-density lipoprotein cholesterol (10.20%). The control groups' liver enzyme activity increased dramatically, whereas the treated groups exhibited no significant changes. Thus, fruit peels are associated with multiple pharmacological activities (Table 5).

2. Anti-microbial agent

Anti-microbials are substances that kill or inhibit the growth of microorganisms such as bacteria, fungi, and protozoa. Disinfectants are antibacterial compounds that are utilized on non-living items. Herbal medicines have a long history of being effectively used to treat infectious diseases. Most natural medicines are made from

Table 5 Pharmacological properties of different fruit peels

Common name	Fruit peels	Phytochemicals	Pharmacological applications	References
Apple	*Malus domestica*	Polyphenols, flavonoids, quercetin, procyanidin, chlorogenic acid, anthocyanins, and hydroxycinnamic acid	Antidiabetic, anti-inflammatory, anti-proliferative, and anti-hypertensive	[106]
Kiwi fruit	*Actinidia deliciosa*	Gallic acid, catechin, syringic acid, caffeic acid, chrysin acid, and quercetin	Anticancerous, antimicrobial, and antioxidant	[107]
Pineapple	*Ananas comosus*	Phenols, flavonoids, terpenoids, carotenoids, saponin, coumarins, lignin, ascorbic acid, myricetin, gallic acid, catechin, epicatechin, and ferulic acid	Antimicrobial, anti-inflammatory, antioxidative, anticarcinogenic, anti-hypertensive, and hypoglycaemic	[108]
Mango	*Mangifera indica*	Mangiferin, *p*-coumaric acid, epicatechin, ferulic acid, rutin, tannic acid, kaempferol, ellagic acid, quercetin, and homogentisic acid	Immunomodulatory, anti-inflammatory, antimicrobial, and antioxidant	[109]
Custard apple	*Annona squamosa*	Alkaloids, steroids, saponins, tannins, and polyphenols	Anti-thrombotic, anti-inflammatory, anthelmintic, anticarcinogenic, and antidiabetic	[110]
Banana	*Musa acuminata*	Carotenoids, biogenic amines, polyphenols, phytosterols, and antioxidants	Antioxidant, antimicrobial, anti-inflammatory, and anticancerous	[111]
Melon	*Cucumis melo*	Flavones, hydroxybenzoic and hydroxycinnamic acids, β-carotene, lutein, β-cryptoxanthin, and violaxanthin	Antimicrobial, anticancerous, antioxidant, and antidiabetic	[112]

plant materials, including leaves, flowers, fruits, and stems. These materials can be used to create new antimicrobial compounds with different chemical structures and mechanisms of action to fight against multidrug-resistant microorganisms. A previous study found that banana peel extracts had antimicrobial properties that were effective against *Staphylococcus aureus*, *Bacillus subtilis*, *Bacillus cereus, Salmonella enteritidis*, and *Escherichia coli* [113]. Several studies have shown that *M. paradisiaca cv. Puttabale* and *M. acuminata cv. Grand naine* ethanol extracts have broad-spectrum antibacterial activity against *P. vulgaris* and *S. paratyphi*.

Bioactive compounds such as glycosides, flavonoids, terpenoids, and tannins were also discovered through phytochemical analysis. These derivatives may be used to treat clinical pathogenic bacteria. A study [114] showed that the *Musa acuminata* peel methanolic extract (300 mg/mL) has varying inhibitory activity against *E. coli* (ATCC 25922), *S. aureus* (ATCC 25923), *Lactobacillus casei, Bacillus spp., Pseudomonas aeruginosa,* and *Saccharomyces cerevisiae* [114]. Meanwhile, several other studies have reported that the oil from this methanolic peel extract (30 mg/mL) has high antibacterial potential against several bacterial species. This finding is attributed to 2-methyl-5-(1-methylethyl) phenol, a potent antimicrobial compound present in the peel. Tannins have also demonstrated antimicrobial activity against *E. coli, S. aureus, and P. aeruginosa* [114].

Punica granatum peel extracts are best against foodborne pathogens, including *E. coli, Fusarium sambucinum, Penicillium italicum*, and *B. subtilis.* These extracts also suppressed Gram-positive *S. aureus* and Gram-negative *Salmonella* growth in one of the tests [115]. Several studies have stated that the extraction procedures highly influence the antibacterial potential of pomegranate peels. Banana peels contain vitamin A, vitamin C, gallocatechin, dopamine, vitamin E, vitamin B6, â-sitosterol, malic acid, succinic acid, palmitic acid, magnesium, phosphorus, potassium, fiber, and iron as major constituents. Fatty acids found in banana peels are responsible for their antimicrobial action [116].

3. Anticancerous agent

Cancer is one of the primary causes of high mortality in humans. Drug development for cancer intervention has advanced significantly in recent decades, but the existing medications show many limitations in terms of their applicability and efficacy. They are sometimes associated with major side effects that can further degrade the patients' quality of life. Fruit peels are a rich source of bioactive chemicals which act as antioxidants and anticancerous agents in the treatment of colon, prostate, and breast cancers [117, 118].

Fruits are nutritious plant-based foods that contain vitamins, minerals, fiber, antioxidants, and bioactive compounds. Therefore, their daily consumption may help prevent cancer. Eating more fruits and vegetables is associated with a lower risk of cancer in various body parts. Combined phytochemical constituents in fruits and vegetables are more effective in preventing cancer than individual components. Edible phytochemicals offer a suitable and accessible basis for cancer control and management.

A study by Mondal *et al.* demonstrated that the aqueous methanolic extract of Nendran banana peel had significant cytotoxic activity against MCF-7 breast cell lines [119]. Additionally, banana peel crude extract could be used to synthesize gold nanoparticles that were cytotoxic to human lung cancer cells and inhibited the biofilm formation of Gram-positive bacteria *Enterococcus faecalis.* The researchers postulated that the flavonoids present in the banana peel contributed to its anticancer properties. They could inhibit ROS-scavenging enzyme activities, inducing apoptosis, arresting the cell cycle and suppressing tumor growth [114].

Zaini *et al.* and Phacharapiyangkul *et al.* discovered that ferulic acid, which is highly identified in Sucrier banana peel, potentially acts as anti-melanogenesis agent by regulating the growth factor of vascular endothelial expression [114, 120]. This acid initiates nitric oxide synthase and acts as a suppressor gene of the tumor. Previous studies have shown that the banana peel extract prepared from hexane solvent exhibited the highest toxicity towards HCT-116 (colorectal carcinoma cell line from humans), with 64.02% inhibition of cell proliferation [114]. Similarly, citrus peels and related extracts have shown remarkable efficacy against many malignancies, mainly due to high flavonoid contents in them. Various biological features crucial to health and illness have been identified [121].

4. Source of dietary fiber

Dietary fiber is an essential constituent of a balanced diet, and the scientific community has established its good association with human health [122]. Oligosaccharides, lignin, resistant starch, tannins, and other plant components are all found in dietary fibers. Dietary fibers are classified into two categories based on their water solubility: soluble (pectin, gums, mucilage, and some hemicelluloses) and insoluble (cellulose, other forms of hemicelluloses, and lignin). Several authors have stated the benefits of appropriate fiber intake, including intestinal transit management and the prevention or treatment of diabetes, cardiovascular disease, and colon cancer [123]. Further, dietary fibers lower the risk of hyperlipidemia, hypercholesterolemia, and hyperglycemia by modulating food consumption and influencing nutrient digestion, absorption, and metabolism [124].

The leading cause of death in patients with diabetes is cardiovascular disease, which increases mortality two to four times. Doctors advise most diabetic patients to avoid or limit their intake of highly nutritious fruits, such as bananas, as they can lead to hyperglycemia and weight gain. However, recent studies have shown that banana fruit has potential antidiabetic properties, leading to further exploration of its antihyperglycemic effect. Starch hydrolysis in the pulp (about 20%) during maturation results in sucrose, glucose, and fructose accumulation, making it sweeter and more palatable. On the other hand, the unripe peels contain only about 3% of starch, leading to a less sweet taste even after ripening.

Studies have indicated that dietary fiber intake is associated with lower levels of total and low-density lipoprotein cholesterol [125]. Interestingly, soluble dietary fiber from *Musa paradisiaca* in tested dosages (50–250 mg of dietary fiber) is more effective in reducing cholesterol absorption than insoluble dietary fiber [126]. Oxidized low-density lipoprotein increases the expression of pro-inflammatory genes that cause monocyte recruitment into the vascular endothelial cells of a dysfunctional blood vessel wall. Oxidized low-density lipoprotein is destroyed by generating free radicals, making it crucial to inhibit its oxidation in managing cardiovascular disease and atherosclerosis. The methanol and ethyl acetate extracts of *M. paradisiaca* effectively prevented low-density lipoprotein oxidation, with IC_{50} values of 169.52 and 217.45 μg/mL, respectively. Angiotensin-I-converting enzyme is an enzyme that transforms angiotensin I into angiotensin II, a potent vasoconstrictor that plays a crucial role in blood pressure regulation. Angiotensin II has been associated with insulin resistance and the progression of vascular complications in diabetes. Therefore, inhibiting the angiotensin-I-converting enzyme is a clinical approach to treating diabetes. Several studies have demonstrated that *M. paradisiaca* extracts have an inhibitory effect on this enzyme comparable to the positive control, captopril (100–200 μg/mL) [114].

Peel is a prominent by-product of citrus fruit processing and is considered a good source of dietary fiber. It contains approximately 25.71–80.41% of total dietary fiber in a variety of foods [127]. Orange peel contains 57% of total dietary fiber, 47.6% of which is insoluble and 9.41% of which is soluble. Mango contains 51.2% of total dietary fiber [128]. Banana peel is a fruit residue that accounts for 30–40% of the entire fruit weight and contains considerable amounts of carbohydrates, proteins, and fiber [129].

5. Anti-oxidant agent

Free radicals, also known as reactive oxygen species, are by-products of normal metabolic activities. Free radicals are also produced as a result of exposure to air pollution, cigarette smoking, industrial chemicals, ozone, and X-rays. The exposure to free radicals causes damage to various macromolecules such as nucleic acids, lipids, and protein. This damage is responsible for several pathogenic disorders, such as cancer, as well as inflammatory, respiratory, cardiovascular, neurodegenerative, and digestive-tract diseases [130]. According to previous research, dietary antioxidants lower the prevalence of diseases such as cancer, cardiovascular disease, and diabetes associated with oxidative stress [131]. Dietary antioxidants may help prevent and treat certain diseases by scavenging free radicals and lowering oxidative stress. They can also protect food from oxidation, making them a potentially safer alternative to synthetic antioxidants [132].

Because of the low cost and vast quantities of plant biowastes produced, their usage in the food sector can be broadened to include antioxidants for developing novel functional foods. Phenolics are significant secondary metabolites found in banana peels at high levels compared to other fruits. Banana peel contains several phenolic compounds, including catechin, anthocyanin, tannins, epicatechin, and gallic acid [133]. Furthermore, gallocatechin levels in banana peel are five times greater than in banana pulp, making banana peel a rich source of antioxidant chemicals [134]. More than 40 compounds from banana peel have been discovered based on individual phenolics, totaling 47 mg of gallic acid equivalent/g dry matter. These phenolic chemicals can be further classified into four subgroups: flavonols, hydroxycinnamic acids, flavan-3-ols, and catecholamines [114].

Citrus fruit also decreases homocysteine levels and prevents free radical formation. It has anti-carcinogenic, antidiabetic, anti-inflammatory, and anti-arthritic characteristics [135]. Citrus peel contains the highest concentration of natural antioxidants, compared to any other fruit part. They include natural flavonoids, phenolics, ascorbic acid, carotenoids, and reducing sugar. Citrus peel extracts demonstrated the highest antioxidant activity, compared to citrus pulp and seeds [136].

CONCLUSION

The modern fruit processing industry is producing a variety of food products to meet consumers' increasing daily demand, which unavoidably generates a high quantity of fruit peel by-products. Fruit peels that are thrown away possess beneficial bioactive compounds, which makes them a highly efficacious material for the synthesis of edible packaging, biochar, single-cell proteins, carbon dots, nanoparticles, etc. Researchers are getting more interested in mixing nanoparticles with other substances to produce smart biofertilizers for agriculture due to their rapid outcomes. However, very few studies have been conducted in this area. With several articles describing the formation of nano-biofertilizers, there has been no extensive investigation into the mechanism of their action for plant growth. Thus, there is a need to create nano-biofertilizers by correctly combining nanoparticles with biofertilizers.

Our study indicated that fruit peels are a rich source of probiotics that can be employed as biofertilizers to improve the quality and quantity of food crops in agricultural fields. Studies have indicated that fruit peels not only contribute to improved nutritional status and supply of essential antioxidant compounds for disease prevention, but they may also have potential applications in the treatment of cancer and diabetes. Firstly, peels benefit the environment since they are secondary processing materials. Secondly, they provide a new perspective for consumers and producers about value-added food products. Furthermore, employing different methods, such as transcriptomics, proteomics, and metabolomics, can offer a comprehensive understanding of the molecular processes that underpin the health-promoting properties of fruit peels, thereby improving our knowledge of fruit peel phytochemicals as functional ingredients. Yet, there is a need for more advanced research into the applicability of peel waste-based edible packaging material.

CONFLICT OF INTEREST

The authors declare that there is no conflict of interest regarding this article.

ACKNOWLEDGMENT

The authors acknowledge Baba Mast Nath University, Rohtak for providing its infrastructure and lab facilities.

REFERENCES

1. Adamu H, Bello U, Yuguda AU, Tafida UI, Jalam AM, Sabo A, *et al.* Production processes, techno-economic and policy challenges of bioenergy production from fruit and vegetable wastes. Renewable and Sustainable Energy Reviews. 2023;186:113686. https://doi.org/10.1016/j.rser.2023.113686
2. Bisht B, Gururani P, Aman J, Vlaskin MS, Kurbatova AI, Adarchenko IA, *et al.* A review on holistic approaches for fruits and vegetables biowastes valorization. Materials Today: Proceedings. 2023;73:54–63. https://doi.org/10.1016/j.matpr.2022.09.168
3. Lekhuleni IL, Shabalala A, Maluleke MK. Quality aspects of marula (*Sclerocarya birrea*) fruit, nutritional composition, and the formation of value-added products for human nutrition: a review. Discover Food. 2024;4:35. https://doi.org/10.1007/s44187-024-00108-5
4. Hussain A, Kausar T, Sehar S, Sarwar A, Ashraf AH, Jamil MA, *et al.* A Comprehensive review of functional ingredients, especially bioactive compounds present in pumpkin peel, flesh and seeds, and their health benefits. Food Chemistry Advances. 2022;1:100067. https://doi.org/10.1016/j.focha.2022.100067
5. Shen L, Pang S, Zhong M, Sun Y, Qayum A, Liu Y, *et al*. A comprehensive review of ultrasonic assisted extraction (UAE) for bioactive components: Principles, advantages, equipment, and combined technologies. Ultrasonics Sonochemistry. 2023;101:106646. https://doi.org/10.1016/j.ultsonch.2023.106646
6. Choudhury AG, Roy P, Kumari S, Singh VK. Utility of Fruit-Based Industry Waste. In: Baskar C, Ramakrishna S, Baskar S, Sharma R, Chinnappan A, Sehrawat R, editors. Handbook of Solid Waste Management: Sustainability through Circular Economy. Singapore: Springer; 2022. pp. 757–784. https://doi.org/10.1007/978-981-16-4230-2_38
7. Sarangi PK, Mishra S, Mohanty P, Singh PK, Srivastava RK, Pattnaik R, *et al*. Food and fruit waste valorisation for pectin recovery: Recent process technologies and future prospects. International Journal of Biological Macromolecules. 2023;235:123929. https://doi.org/10.1016/j.ijbiomac.2023.123929
8. Laaraj N, Bouhrim M, Kharchoufa L, Tiji S, Bendaha H, Addi M, *et al.* Phytochemical analysis, α-Glucosidase and α-Amylase inhibitory activities and acute toxicity studies of extracts from pomegranate (*Punica granatum*) bark, a valuable agro-industrial by-product. Foods. 2022;11(9):1353. https://doi.org/10.3390/foods11091353
9. Marcal S, Pintado M. Mango peels as food ingredient/additive: Nutritional value, processing, safety and applications. Trends in Food Science and Technology. 2021;114:472–489. https://doi.org/10.1016/j.tifs.2021.06.012
10. Singh B, Singh JP, Kaur A, Singh N. Phenolic composition, antioxidant potential and health benefits of citrus peel. Food Research International. 2020;132:109114. https://doi.org/10.1016/j.foodres.2020.109114
11. Li T, Shen P, Liu W, Liu C, Liang R, Yan N, *et al.* Major polyphenolics in pineapple peels and their antioxidant interactions. International Journal of Food Properties. 2014;17(8):1805–1817. https://doi.org/10.1080/10942912.2012.732168
12. Hikal WM, Said-Al Ahl HAH, Bratovcic A, Tkachenko KG, Sharifi-Rad J, Kačániová M, *et al*. Banana peels: A waste treasure for human being. Evidence-Based Complementary and Alternative Medicine. 2022;2022(1):7616452. https://doi.org/10.1155/2022/7616452
13. Afsharnezhad M, Shahangian SS, Panahi E, Sariri R. Evaluation of the antioxidant activity of extracts from some fruit peels. Caspian Journal of Environmental Sciences. 2017;15(3):213–222. https://doi.org/10.22124/cjes.2017.2463
14. Ritika, Rizwana, Shukla S, Sondhi A, Tripathi AD, Lee J-K, *et al.* Valorisation of fruit waste for harnessing the bioactive compounds and its therapeutic application. Trends in Food Science and Technology. 2024;144:104302. https://doi.org/10.1016/j.tifs.2023.104302
15. Jha AK, Sit N. Extraction of bioactive compounds from plant materials using combination of various novel methods: A review. Trends in Food Science and Technology. 2022;119:579–591. https://doi.org/10.1016/j.tifs.2021.11.019
16. Pai S, Hebbar A, Selvaraj S. A critical look at challenges and future scopes of bioactive compounds and their incorporations in the food, energy, and pharmaceutical sector. Environmental Science and Pollution Research. 2022;29:35518–35541. https://doi.org/10.1007/s11356-022-19423-4
17. Rezvankhah A, Emam-Djomeh Z, Safari M, Askari G, Salami M. Microwave-assisted extraction of hempseed oil: Studying and comparing of fatty acid composition, antioxidant activity, physiochemical and thermal properties with Soxhlet extraction. Journal of Food Science and Technology. 2019;56:4198–4210. https://doi.org/10.1007/s13197-019-03890-8

18. Mohamad N, Ramli N, Abd-Aziz S, Ibrahim MF. Comparison of hydro-distillation, hydro-distillation with enzyme-assisted and supercritical fluid for the extraction of essential oil from pineapple peels. 3 Biotech. 2019;9:1–9. https://doi.org/10.1007/s13205-019-1767-8

19. Azmat F, Safdar M, Ahmad H, Khan MRJ, Abid J, Naseer MS, *et al.* Phytochemical profile, nutritional composition of pomegranate peel and peel extract as a potential source of nutraceutical: A comprehensive review. Food Science and Nutrition. 2024;12(2):661–674. https://doi.org/10.1002/fsn3.3777

20. Albuquerque BR, Prieto MA, Barreiro MF, Rodrigues A, Curran TP, Barros L, *et al.* Catechin-based extract optimization obtained from *Arbutus unedo* L. fruits using maceration/microwave/ultrasound extraction techniques. Industrial Crops and Products. 2017;95:404–415. https://doi.org/10.1016/j.indcrop.2016.10.050

21. Trifunschi SI, Ardelean DG. Flavonoid extraction from Ficus carica leaves using different techniques and solvents. Zbornik Matice srpske za prirodne nauke. 2013;(125):81–86. https://doi.org/10.2298/ZMSPN1325081T

22. Sharma V, Janmeda P. Extraction, isolation and identification of flavonoid from *Euphorbia neriifolia* leaves. Arabian Journal of Chemistry. 2017;10(4):509–514. https://doi.org/10.1016/j.arabjc.2014.08.019

23. Gil-Martín E, Forbes-Hernández T, Romero A, Cianciosi D, Giampieri F, Battino M. Influence of the extraction method on the recovery of bioactive phenolic compounds from food industry by-products. Food Chemistry. 2022;378:131918. https://doi.org/10.1016/j.foodchem.2021.131918

24. del Contreras-Gámez MM, Galán-Martín Á, Seixas N, da Costa Lopes AM, Silvestre A, Castro E. Deep eutectic solvents for improved biomass pretreatment: Current status and future prospective towards sustainable processes. Bioresource Technology. 2023;369:128396. https://doi.org/10.1016/j.biortech.2022.128396

25. Arun KB, Madhavan A, Sindhu R, Binod P, Pandey A, Reshmy R, *et al*. Remodeling agro-industrial and food wastes into value-added bioactives and biopolymers. Industrial Crops and Products. 2020;154:112621. https://doi.org/10.1016/j.indcrop.2020.112621

26. Jimenez-Champi D, Romero-Orejon FL, Moran-Reyes A, Muñoz AM, Ramos-Escuder F. Bioactive compounds in potato peels, extraction methods, and their applications in the food industry: a review. CyTA-Journal Food. 2023;21(1):418–432. https://doi.org/10.1080/19476337.2023.2213746

27. Cabrera L, Xavier L, Zecchi B. Extraction of phenolic compounds with antioxidant activity from olive pomace using natural deep eutectic solvents: modelling and optimization by response surface methodology. Discover Food. 2024;4:29. https://doi.org/10.1007/s44187-024-00100-z

28. Alexandre EMC, Silva S, Santos SAO, Silvestre AJD, Duarte MF, Saraiva JA, *et al.* Antimicrobial activity of pomegranate peel extracts performed by high pressure and enzymatic assisted extraction. Food Research International. 2019;115:167–176. https://doi.org/10.1016/j.foodres.2018.08.044

29. Li BB, Smith B, Hossain MM. Extraction of phenolics from citrus peels: I. Solvent extraction method. Separation and Purification Technology. 2006;48(2):182–188. https://doi.org/10.1016/j.seppur.2005.07.005

30. Rajha HN, Abi-Khattar A-M, El Kantar S, Boussetta N, Lebovka N, Maroun RG, *et al.* Comparison of aqueous extraction efficiency and biological activities of polyphenols from pomegranate peels assisted by infrared, ultrasound, pulsed electric fields and high-voltage electrical discharges. Innovative Food Science and Emerging Technologies. 2019;58:102212. https://doi.org/10.1016/j.ifset.2019.102212

31. Jadhav HB, Choudhary P. Emerging techniques for the processing of food to ensure higher food safety with enhanced food quality: a review. Discover Food. 2024;4:20. https://doi.org/10.1007/s44187-024-00089-5

32. Pimentel-Moral S, Borrás-Linares I, Lozano-Sánchez J, Arráez-Román D, Martínez-Férez A, Segura-Carretero A. Microwave-assisted extraction for *Hibiscus sabdariffa* bioactive compounds. Journal of Pharmaceutical and Biomedical Analysis. 2018;156:313–322. https://doi.org/10.1016/j.jpba.2018.04.050

33. Fernández-Marín R, Fernandes SCM, Andrés MA, Labidi J. Microwave-assisted extraction of *Curcuma longa* L. Oil: Optimization, chemical structure and composition, antioxidant activity and comparison with conventional soxhlet extraction. Molecules. 2021;26(6):1516. https://doi.org/10.3390/molecules26061516

34. Xu K, Gao X, Chi M, Chen K, Zhang Y, Kong W, *et al.* Microwave-assisted extraction coupled with mass spectrometry for determining five volatile compounds from soy sauces. Journal of Analytical Methods in Chemistry. 2021;2021(1):6625929. https://doi.org/10.1155/2021/6625929

35. da Machado APF, Sumere BR, Mekaru C, Martinez J, Bezerra RMN, Rostagno MA. Extraction of polyphenols and antioxidants from pomegranate peel using ultrasound: influence of temperature, frequency and operation mode. International Journal of Food Science and Technology. 2019;54:2792–2801. https://doi.org/10.1111/ijfs.14194

36. Kouhi M, Prabhakaran MP, Ramakrishna S. Edible polymers: An insight into its application in food, biomedicine and cosmetics. Trends in Food Science and Technology. 2020;103:248–263. https://doi.org/10.1016/j.tifs.2020.05.025

37. Kaur J, Singh J, Rasane P, Gupta P, Kaur S, Sharma N, *et al.* Natural additives as active components in edible films and coatings. Food Bioscience. 2023;53:102689. https://doi.org/10.1016/j.fbio.2023.102689

38. Mezhoudi M, Salem A, Abdelhedi O, Fakhfakh N, Mabrouk M, Khorchani T, *et al.* Development of active edible coatings based on fish gelatin enriched with *Moringa oleifera* extract: Application in fish (*Mustelus mustelus*) fillet preservation. Food Science and Nutrition. 2022;10(11):3979–3992. https://doi.org/10.1002/fsn3.2993

39. Kumar N, Daniloski D, Pratibha, Neeraj, D'Cunha NM, Naumovski N, *et al.* Pomegranate peel extract–A natural bioactive addition to novel active edible packaging. Food Research International. 2022;156:111378. https://doi.org/10.1016/j.foodres.2022.111378

40. Yadav A, Kumar N, Upadhyay A, Anuraget RK, Pandiselvam R, *et al.* Effect of mango kernel seed starch-based active edible coating functionalized with lemongrass essential oil on the shelf-life of guava fruit. Quality Assurance and Safety of Crops and Foods. 2022;14(3):103–115. https://doi.org/10.15586/qas.v14i3.1094

41. Shin S-H, Chang Y, Lacroix M, Han J. Control of microbial growth and lipid oxidation on beef product using an apple peel-based edible coating treatment. LWT. 2017;84:183–188. https://doi.org/10.1016/j.lwt.2017.05.054

42. Alparslan Y, Baygar T. Effect of chitosan film coating combined with orange peel essential oil on the shelf life of deepwater pink shrimp. Food and Bioprocess Technology. 2017;10:842–853. https://doi.org/10.1007/s11947-017-1862-y

43. Radi M, Akhavan-Darabi S, Akhavan H-R, Amiri S. The use of orange peel essential oil microemulsion and nanoemulsion in pectin-based coating to extend the shelf life of fresh-cut orange. Journal of Food Processing and Preservation. 2018;42(2):e13441. https://doi.org/10.1111/jfpp.13441

44. Moghadam M, Salami M, Mohammadian M, Khodadadi M, Emam-Djomeh Z. Development of antioxidant edible films based on mung bean protein enriched with pomegranate peel. Food Hydrocolloids. 2020;104:105735. https://doi.org/10.1016/j.foodhyd.2020.105735

45. Salem MZM, EL-Hefny M, Ali HM, Abdel-Megeed A, El-Settawy AAA, Böhm M, *et al.* Plants-derived bioactives: Novel utilization as antimicrobial, antioxidant and phytoreducing agents for the biosynthesis of metallic nanoparticles. Microbial Pathogenesis. 2021;158:105107. https://doi.org/10.1016/j.micpath.2021.105107

46. Ahmad NM, Mohamed AH, Hasan N, Zainal-Abidin N, Nawahwi MZ, Azzeme AM, *et al.* Effect of optimisation variable and the role of plant extract in the synthesis of nanoparticles using plant-mediated synthesis approaches. Inorganic Chemistry Communications. 2024;161:111839. https://doi.org/10.1016/j.inoche.2023.111839

47. Suhag R, Kumar R, Dhiman A, Sharma A, Prabhakar PK, Gopalakrishnan K, *et al*. Fruit peel bioactives, valorisation into nanoparticles and potential applications: A review. Critical Reviews in Food Science and Nutrition. 2023;63(24):6757–6776. https://doi.org/10.1080/10408398.2022.2043237

48. Mohammad ZH, Ahmad F, Ibrahim SA, Zaidi S. Application of nanotechnology in different aspects of the food industry. Discover Food. 2022;2:12. https://doi.org/10.1007/s44187-022-00013-9

49. Alharbi AA, Alghamdi AM, Al-Goul ST, Allohibi A, Baty RS, Qahl SH, *et al.* Valorizing pomegranate wastes by producing functional silver nanoparticles with antioxidant, anticancer, antiviral, and antimicrobial activities and its potential in food preservation. Saudi Journal of Biological Sciences. 2024;31(1):103880. https://doi.org/10.1016/j.sjbs.2023.103880

50. Aswathi VP, Meera S, Maria CGA, Nidhin M. Green synthesis of nanoparticles from biodegradable waste extracts and their applications: a critical review. Nanotechnology for Environmental Engineering. 2023;8:377–397. https://doi.org/10.1007/s41204-022-00276-8

51. Skiba MI, Vorobyova VI. Synthesis of Silver Nanoparticles Using Orange Peel Extract Prepared by Plasmochemical Extraction Method and Degradation of Methylene Blue under Solar Irradiation. Advances in Materials Science and Engineering. 2019;2019:8306015. https://doi.org/10.1155/2019/8306015

52. Kokila T, Ramesh PS, Geetha D. Biosynthesis of silver nanoparticles from Cavendish banana peel extract and its antibacterial and free radical scavenging assay: a novel biological approach. Applied Nanoscience. 2015;5:911–920. https://doi.org/10.1007/s13204-015-0401-2

53. Ibrahim HMM. Green synthesis and characterization of silver nanoparticles using banana peel extract and their antimicrobial activity against representative microorganisms. Journal of Radiation Research and Applied Sciences. 2015;8(3):265–275. https://doi.org/10.1016/j.jrras.2015.01.007

54. Shet AR, Tantri S, Bennal A. Economical biosynthesis of silver nanoparticles using fruit waste. Journal of Chemical and Pharmaceutical Sciences. 2016;9(3):2306–2311.

55. Kumar H, Bhardwaj K, Sharma R, Nepovimova E, Kuča K, Dhanjal DS, *et al.* Fruit and vegetable peels: Utilization of high value horticultural waste in novel industrial applications. Molecules. 2020;25(12):2812. https://doi.org/10.3390/molecules25122812

56. Nava OJ, Soto-Robles CA, Gómez-Gutiérrez CM, Vilchis-Nestor AR, Castro-Beltrán A, Olivas A, *et al.* Fruit peel extract mediated green synthesis of zinc oxide nanoparticles. Journal of Molecular Structure. 2017;1147:1–6. https://doi.org/10.1016/j.molstruc.2017.06.078

57. Jamaludin N, Rashid SA, Tan T. Natural biomass as carbon sources for the synthesis of photoluminescent carbon dots. In: Rashid SA, Othman RNIR, Hussein MZ, editors. Synthesis, Technology and Applications of Carbon Nanomaterials. Elsevier; 2019. pp. 109–134. https://doi.org/10.1016/B978-0-12-815757-2.00005-X

58. Dhariwal J, Rao GK, Vaya D. Recent advancements towards the green synthesis of carbon quantum dots as an innovative and eco-friendly solution for metal ion sensing and monitoring. RSC Sustainability. 2024;2:11–36. https://doi.org/10.1039/D3SU00375B

59. Bhardwaj K, Najda A, Sharma R, Nurzyńska-Wierdak R, Dhanjal DS, Sharma R, Manickam S, *et al.* Fruit and vegetable peel-enriched functional foods: potential avenues and health perspectives. Evidence-Based Complementary and Alternative Medicine. 2022;2022(1):8543881. https://doi.org/10.1155/2022/8543881

60. Kumar H, Bhardwaj K, Dhanjal DS, Sharma R, Nepovimova E, Verma R, *et al.* Fruit and Vegetable Peel Waste: Applications in Food and Environmental Industries. In: Ray RC, editor. Fruits and Vegetable Wastes: Valorization to Bioproducts and Platform Chemicals. Singapore: Springer; 2022. pp. 259–287. https://doi.org/10.1007/978-981-16-9527-8_11

61. Ghosh S, Ghosal K, Mohammad SA, Sarkar K. Dendrimer functionalized carbon quantum dot for selective detection of breast cancer and gene therapy. Chemical Engineering Journal. 2019;373:468–484. https://doi.org/10.1016/j.cej.2019.05.023

62. Xiao P, Ke Y, Lu J, Huang Z, Zhu X, Wei B, *et al.* Photoluminescence immunoassay based on grapefruit peel-extracted carbon quantum dots encapsulated into silica nanospheres for p53 protein. Biochemical Engineering Journal. 2018;139:109–116. https://doi.org/10.1016/j.bej.2018.08.012

63. Lu W, Qin X, Liu S, Chang G, Zhang Y, Luo Y, *et al.* Economical, green synthesis of fluorescent carbon nanoparticles and their use as probes for sensitive and selective detection of mercury (II) ions. Analytical Chemistry. 2012;84(12):5351–5357. https://doi.org/10.1021/ac3007939

64. Amith Yadav HJ, Eraiah B, Basavaraj RB, Nagabhushana H, Darshan GP, Sharma SC, *et al*. Rapid synthesis of C-dot@ TiO2 core-shell composite labeling agent: Probing of complex fingerprints recovery in fresh water. Journal of Alloys and Compounds. 2018;742:1006–1018. https://doi.org/10.1016/j.jallcom.2017.12.251

65. Huang Q, Lin X, Zhu J-J, Tong Q-X. Pd-Au@ carbon dots nanocomposite: Facile synthesis and application as an ultrasensitive electrochemical biosensor for determination of *colitoxin* DNA in human serum. Biosensors and Bioelectronics. 2017;94:507–512. https://doi.org/10.1016/j.bios.2017.03.048

66. Jiao X-Y, Li L-S, Qin S, Zhang Y, Huang K, Xu L. The synthesis of fluorescent carbon dots from mango peel and their multiple applications. Colloids and Surfaces A: Physicochemical and Engineering Aspects. 2019;577:306–314. https://doi.org/10.1016/j.colsurfa.2019.05.073

67. Zhou J, Sheng Z, Han H, Zou M, Li C. Facile synthesis of fluorescent carbon dots using watermelon peel as a carbon source. Materials Letters. 2012;66(1):222–224. https://doi.org/10.1016/j.matlet.2011.08.081

68. Karri RR, Ravindran G, Dehghani MH. Wastewater – sources, toxicity, and their consequences to human health. In: Karri RR, Ravindran G, Dehghani MH, editors. Soft computing techniques in solid waste and wastewater management. Elsevier; 2021. pp 3–33. https://doi.org/10.1016/B978-0-12-824463-0.00001-X

69. Mitra S, Chakraborty AJ, Tareq AM, Emran TB, Nainu F, Khusro A, *et al.* Impact of heavy metals on the environment and human health: Novel therapeutic insights to counter the toxicity. Journal of King Saud University–Science. 2022;34(3):101865. https://doi.org/10.1016/j.jksus.2022.101865

70. Bhatnagar A, Sillanpää M, Witek-Krowiak A. Agricultural waste peels as versatile biomass for water purification–A review. Chemical Engineering Journal. 2015;270:244–271. https://doi.org/10.1016/j.cej.2015.01.135

71. Syeda HI, Sultan I, Razavi KS, Yap P-S. Biosorption of heavy metals from aqueous solution by various chemically modified agricultural wastes: A review. Journal of Water Process Engineering. 2022;46:102446. https://doi.org/10.1016/j.jwpe.2021.102446

72. Dey S, Veerendra GTN, Manoj AVP, Padavala SSAB. Removal of chlorides and hardness from contaminated water by using various biosorbents: A comprehensive review. Water-Energy Nexus. 2024;7:39–76. https://doi.org/10.1016/j.wen.2024.01.003

73. Freitas LC, Barbosa JR, da Costa ALC, Bezerra FWF, Pinto RHH, de Carvalho Junior RN. From waste to sustainable industry: How can agro-industrial wastes help in the development of new products? Resources, Conservation and Recycling. 2021;169:105466. https://doi.org/10.1016/j.resconrec.2021.105466

74. Velu K, Elumalai D, Hemalatha P, Janaki A, Babu M, Hemavathi M, *et al.* Evaluation of silver nanoparticles toxicity of *Arachis hypogaea* peel extracts and its larvicidal activity against malaria and dengue vectors. Environmental Science and Pollution Research. 2015;22:17769–17779. https://doi.org/10.1007/s11356-015-4919-3

75. Sultana S, Ali ME, Ahamad MNU. Gelatine, collagen, and single cell proteins as a natural and newly emerging food ingredients. In: Ali E, Nizar NNA, editors. Preparation and processing of religious and cultural foods. Elsevier; 2018. pp. 215–239. https://doi.org/10.1016/B978-0-08-101892-7.00011-0

76. Suri S, Singh A, Nema PK. Current applications of citrus fruit processing waste: A scientific outlook. Applied Food Research. 2022;2(1):100050. https://doi.org/10.1016/j.afres.2022.100050

77. Koukoumaki DI, Tsouko E, Papanikolaou S, Ioannou Z, Diamantopoulou P, Sarris D. Recent advances in the production of single cell protein from renewable resources and applications. Carbon Resources Conversion. 2024;7(2):100195. https://doi.org/10.1016/j.crcon.2023.07.004

78. Banerjee S, Arora A. Microbes as Bio-Factories for the Valorization of Fruit and Vegetable Processing Wastes. In: Chhikara N, Panghal A, Chaudhary G, editors. Microbes in the Food Industry. Scrivener Publishing; 2023. pp. 321–353. https://doi.org/10.1002/9781119776406.ch8

79. Kumar R, Raj T, Næss G, Sørensen M, Dhawan V. Opportunities and challenges in single-cell protein production using lignocellulosic material. Biofuels, Bioproducts and Biorefining. 2024;18(1):310–321. https://doi.org/10.1002/bbb.2563

80. Azam S, Khan Z, Ahmad B, Khan I, Ali J. Production of single cell protein from orange peels using *Aspergillus niger* and *Saccharomyces cerevisiae*. Global Journal of Biotechnology and Biochemistry. 2014;9(1):14–18. https://doi.org/10.5829/idosi.gjbb.2014.9.1.82314

81. Umesh M, Thazeem B, Preethi K. Valorization of pineapple peels through single cell protein production using Saccharomyces cerevisiae NCDC 364. Applied Food Biotechnology. 2019;6(4):255–263. https://doi.org/10.22037/afb.v6i4.25906

82. Khalid ZB, Siddique NI, Nayeem A, Adyel TM, Ismail SB, Ibrahim MZ. Biochar application as sustainable precursors for enhanced anaerobic digestion: A systematic review. Journal of Environmental Chemical Engineering. 2021;9(4):105489. https://doi.org/10.1016/j.jece.2021.105489

83. Gupta S, Sireesha S, Sreedhar I, Patel CM, Anitha KL. Latest trends in heavy metal removal from wastewater by biocharbased sorbents. Journal of Water Process Engineering. 2020;38:101561. https://doi.org/10.1016/j.jwpe.2020.101561

84. F Amalina, ASA Razak, S Krishnan, H Sulaiman, AW Zularisam, M Nasrullah. Biochar production techniques utilizing biomass waste-derived materials and environmental applications–A review. Journal of Hazardous Materials Advances. 2022;7:100134. https://doi.org/10.1016/j.hazadv.2022.100134

85. Chormare R, Moradeeya PG,Sahoo TP, Seenuvasan M, Baskar G, Saravaia HT, *et al.* Conversion of solid wastes and natural biomass for deciphering the valorization of biochar in pollution abatement: A review on the thermo-chemical processes. Chemosphere. 2023;339:139760. https://doi.org/10.1016/j.chemosphere.2023.139760

86. Seow YX, Tan YH, Mubarak NM, Kansedo J, Khalid M, Ibrahim ML, *et al.* A review on biochar production from different biomass wastes by recent carbonization technologies and its sustainable applications. Journal of Environmental Chemical Engineering. 2022;10(1):107017. https://doi.org/10.1016/j.jece.2021.107017

87. Ahmed MM, Badawy MT, Ahmed FK, Kalia A, Abd-Elsalam KA. Fruit peel waste-to-wealth: Bionanomaterials production and their applications in agroecosystems. In: Abd-Elsalam KA, Periakaruppan R, Rajeshkumar S, editors. Agri-Waste and Microbes for Production of Sustainable Nanomaterials. Elsevier; 2022. pp. 231–257. https://doi.org/10.1016/B978-0-12-823575-1.00001-9

88. Lam SS, Liew RK, Cheng CK, Rasit N, Ooi CK, Ma NL, *et al.* Pyrolysis production of fruit peel biochar for potential use in treatment of palm oil mill effluent. Journal of Environmental Management. 2018;213:400–408. https://doi.org/10.1016/j.jenvman.2018.02.092

89. Wang C, Gu L, Liu X, Zhang X, Cao L, Hu X. Sorption behavior of Cr (VI) on pineapple-peel-derived biochar and the influence of coexisting pyrene. International Biodeterioration and Biodegradation. 2016;111:78–84. https://doi.org/10.1016/j.ibiod.2016.04.029

90. Wu J, Yang J, Feng P, Huang G, Xu C, Lin B. High-efficiency removal of dyes from wastewater by fully recycling litchi peel biochar. Chemosphere. 2020;246:125734. https://doi.org/10.1016/j.chemosphere.2019.125734

91. Cao Q, Huang Z, Liu S, Wu Y. Potential of *Punica granatum* biochar to adsorb Cu (II) in soil. Scientific Reports. 2019;9:11116. https://doi.org/10.1038/s41598-019-46983-2

92. Selvanathan M, Yann KT, Chung CH, Selvarajoo A, Arumugasamy SK, Sethu V. Adsorption of copper (II) ion from aqueous solution using biochar derived from rambutan (*Nephelium lappaceum*) peel: feedforward neural network modelling study. Water, Air, Soil Pollution. 2017;228:299. https://doi.org/10.1007/s11270-017-3472-8

93. Wu Y, Cha L, Fan Y, Fang P, Ming Z, Sha H. Activated biochar prepared by pomelo peel using H_3PO_4 for the adsorption of hexavalent chromium: performance and mechanism. Water, Air, Soil Pollution. 2017;228:405. https://doi.org/10.1007/s11270-017-3587-y

94. Wu P, Wu Q, Huang H, Xie L, An H, Zhao X, *et al.* Global meta-analysis and three-year field experiment shows that deep placement of fertilizer can enhance crop productivity and decrease gaseous nitrogen losses. Field Crops Research. 2024;307:109263. https://doi.org/10.1016/j.fcr.2024.109263

95. Dahunsi SO, Oranusi S, Efeovbokhan VE, Adesulu-Dahunsi AT, Ogunwole JO. Crop performance and soil fertility improvement using organic fertilizer produced from valorization of *Carica papaya* fruit peel. Scientific Reports. 2021;11:4696. https://doi.org/10.1038/s41598-021-84206-9

96. Saharia M, Dey G, Kumar V. Vermiremediation of plant agro waste to recover residual nutrients and improve crop productivity. In: Huang K, Li F, Bhat SA, Kumar V, editors. Earthworm Technology in Organic Waste Management. Elsevier; 2024. pp. 79–113. https://doi.org/10.1016/B978-0-443-16050-9.00008-6

97. Akbay HEG. Anaerobic mono and co-digestion of agro-industrial waste and municipal sewage sludge: Biogas production potential, kinetic modelling, and digestate characteristics. Fuel. 2024;355:129468. https://doi.org/10.1016/j.fuel.2023.129468

98. Andey A, Daim W, Lim SA. Food Waste to Bio-Products: Recent Opportunities and Challenges to Promote Bio-Circular-Green. In: Ramakrishna Y, Wahab SN, editors. Handbook of Research on Designing Sustainable Supply Chains to Achieve a Circular Economy. Global Scientific Publishing; 2023. pp. 306–331. https://doi.org/10.4018/978-1-6684-7664-2.ch015

99. Krithika R, Raajeswari PA. Characterization of selected fruit peel as biofertilizer. Sustainability, Agri, Food and Environmental Research. 2024;12(2):art82. https://doi.org/10.7770/safer-V13N1-art82

100. Mahmud MS, Chong KP. Formulation of biofertilizers from oil palm empty fruit bunches and plant growth-promoting microbes: A comprehensive and novel approach towards plant health. Journal of King Saud University–Science. 2021;33(8):101647. https://doi.org/10.1016/j.jksus.2021.101647

101. Alasa JJ, Bashir AU, Mustapha M, Mohammed B. Experimental study on the use of banana and pineapple peel waste as biofertilizers, tested on *Hibiscus sabdariffa* plant: Promoting sustainable agriculture and environmental sanitation. Arid Zone Journal of Engineering, Technology and Environment. 2021;17(4):547–554.

102. Rathor S, Singh S, Sharma N, Zahoor I, Bhyan B. Understanding the role of angiogenesis, inflammation and oxidative stress in diabetes mellitus: Insights into the past, present and future trends. In: Behl T, Singh S, Sharma N, editors. Targeting Angiogenesis, Inflammation, and Oxidative Stress in Chronic Diseases. Elsevier; 2024. pp. 1–25. https://doi.org/10.1016/B978-0-443-13587-3.00012-6

103. Mayasankaravalli C, Deepika K, Lydia DE, Agada R, Thagriki D, Govindasamy C, *et al.* Profiling the phyto-constituents of *Punica granatum* fruits peel extract and accessing its in-vitro antioxidant, anti-diabetic, anti-obesity, and angiotensin-converting enzyme inhibitory properties. Saudi Journal of Biological Sciences. 2020;27(12):3228–3234. https://doi.org/10.1016/j.sjbs.2020.09.046

104. Animish A, Jayasri MA. A retrospective review of marine algae and the strategies employed for prospective diabetes management. Algal Research. 2023;74:103209. https://doi.org/10.1016/j.algal.2023.103209

105. Saenjum C, Pattananandecha T, Nakagawa K. Antioxidative and anti-inflammatory phytochemicals and related stable paramagnetic species in different parts of dragon fruit. Molecules. 2021;26(12):3565. https://doi.org/10.3390/molecules26123565

106. Vasile M, Bunea A, Ioan CR, Ioan BC, Socaci S, Viorel M. Phytochemical content and antioxidant activity of *Malus domestica* Borkh peel extracts. Molecules. 2021;26(24):7636. https://doi.org/10.3390/molecules26247636

107. Zeinab SA, Aboul-Enein AM, Gaafar AA, Abou-Elella F, Hanan F A, Mohsen SA, *et al.* Active Constituents of Kiwi (*Actinidia Deliciosa Planch*) Peels and Their Biological Activities as Antioxidant, Antimicrobial and Anticancer. Research Journal of Chemistry and Environment. 2018;22(9):52–59.

108. Soni S, Noor U, Gupta E. *Ananas comosus* peel waste, a novel substrate of therapeutic potential: Evidences and prospects. Indian Journal of Natural Products and Resources. 2022;13(2):129–143. https://doi.org/10.56042/ijnpr.v13i2.37958

109. Huang C-Y, Kuo C-H, Wu C-H, Kuan A-W, Guo H-R, Lin Y-H, *et al.* Free radical-scavenging, anti-inflammatory, and antibacterial activities of water and ethanol extracts prepared from compressional-puffing pretreated mango (*Mangifera indica* L.) peels. Journal of Food Quality. 20218;2018:1025387. https://doi.org/10.1155/2018/1025387

110. Roy N, Sasikala S. Influence of Pre-treatment on Secondary Metabolites and Hypo-Glycemic Activity of Custard Apple (*Annona squamosa*) Peel. Malaysian Journal of Nutrition. 2016;22(3):433–442

111. Bhavani M, Morya S, Saxena D, Awuchi CG. Bioactive, antioxidant, industrial, and nutraceutical applications of banana peel. International Journal of Food Properties. 2023;26(1):1277–1289. https://doi.org/10.1080/10942912.2023.2209701

112. Gómez-García R, Campos DA, Oliveira A, Aguilar CN, Madureira AR, Pintado M. A chemical valorisation of melon peels towards functional food ingredients: Bioactives profile and antioxidant properties. Food Chemistry. 2021;335:127579. https://doi.org/10.1016/j.foodchem.2020.127579

113. Goh HT, Cheok CY, Yeap SP. Green synthesis of silver nanoparticles using banana peel extract and application on banana preservation. Food Frontiers. 2023;4(1):283–288. https://doi.org/10.1002/fft2.206

114. Zaini HM, Roslan J, Saallah S, Munsu E, Sulaiman NS, Pindi W. Banana peels as a bioactive ingredient and its potential application in the food industry. Journal of Functional Foods. 2022;92:105054. https://doi.org/10.1016/j.jff.2022.105054

115. Salim A, Deiana P, Fancello F, Molinu MG, Santona M, Zara S. Antimicrobial and antibiofilm activities of pomegranate peel phenolic compounds: Varietal screening through a multivariate approach. Journal of Bioresources and Bioproducts. 2023;8(2):146–161. https://doi.org/10.1016/j.jobab.2023.01.006

116. Teshome E, Forsido SF, Rupasinghe HP, Keyata EO. Potentials of natural preservatives to enhance food safety and shelf life: A review. The Scientific World Journal. 2022;2022(1):9901018. https://doi.org/10.1155/2022/9901018

117. Ain HBU, Tufail T, Bashir S, Ijaz N, Hussain M, Ikram A, *et al.* Nutritional importance and industrial uses of pomegranate peel: A critical review. Food Science and Nutrition. 2023;11(6):2589–2598. https://doi.org/10.1002/fsn3.3320

118. Jain E, Tripathi AD, Agarwal A, Mauraya KK, Rai DC, Mishra R, *et al.* Anticancerous compounds in fruits, their extraction, and relevance to food. In: Singh RB, Watanabe S, Isaza AA, editors. Functional Foods and Nutraceuticals in Metabolic and Non-Communicable Diseases. Academic Press; 2022. pp. 517–532. https://doi.org/10.1016/B978-0-12-819815-5.00022-7

119. Mondal A, Banerjee S, Bose S, Das PP, Sandberg EN, *et al.* Cancer preventive and therapeutic potential of banana and its bioactive constituents: a systematic, comprehensive, and mechanistic review. Frontiers in Oncology. 2021;11:697143. https://doi.org/10.3389/fonc.2021.697143

120. Phacharapiyangkul N, Thirapanmethee K, Sa-Ngiamsuntorn K, Panich U, Lee C-H, Chomnawang MT. Effect of sucrier banana peel extracts on inhibition of melanogenesis through the ERK signaling pathway. International Journal of Medical Sciences. 2019;16(4):602–606. https://doi.org/10.7150/ijms.32137

121. Nirmal NP, Khanashyam AC, Mundanat AS, Shah K, Babu KS, Thorakkattu P, *et al.* Valorization of Fruit Waste for Bioactive Compounds and Their Applications in the Food Industry. Foods. 2023;12(3):556. https://doi.org/10.3390/foods12030556

122. Khorasaniha R, Olof H, Voisin A, Armstrong K,Wine E, Vasanthan T, *et al.* Diversity of fibers in common foods: Key to advancing dietary research. Food Hydrocolloids. 2023;139:108495. https://doi.org/10.1016/j.foodhyd.2023.108495

123. Ioniță-Mîndrican C-B, Ziani K, Mititelu M, Oprea E, Neacșu SM, Moroșan E, *et al.* Therapeutic benefits and dietary restrictions of fiber intake: A state of the art review. Nutrients. 2022;14(13):2641. https://doi.org/10.3390/nu14132641

124. Xie L, Alam MJ, Marques FZ, Mackay CR. A major mechanism for immunomodulation: Dietary fibres and acid metabolites. Seminars in Immunology. 2023;66:101737. https://doi.org/10.1016/j.smim.2023.101737

125. Jabbari M, Eini-Zinab H, Safaei E, Poursoleiman F, Amini B, Babashahi M, *et al.* Determination of the level of evidence for the association between different food groups/items and dietary fiber intake and the risk of cardiovascular diseases and hypertension: An umbrella review. Nutrition Research. 2023;111:1–13. https://doi.org/10.1016/j.nutres.2022.12.011

126. Youssef EA, Shaltout OE, Abouel-Yazeed AM. Chemical and nutritional evaluation of banana peels and their potential use in improving the egyptian balady bread. Journal of the Advances in Agricultural Researches. 2024;29(1):107–115. https://doi.org/10.21608/jalexu.2024.263293.1187

127. Rout S, Gupta RK, Jadhav HB, Srivastav PP, Annapure U. Understanding the role of dietary fibers on gluten-free pasta's functional quality aspects. In: Gull A, Nayik GA, Brennan C, editors. Development of Gluten-Free Pasta. Academic Press; 2024. pp. 157–178. https://doi.org/10.1016/B978-0-443-13238-4.00012-5

128. Martins R, Sales H, Pontes R, Nunes J, Gouveia I. Food Wastes and Microalgae as Sources of Bioactive Compounds and Pigments in a Modern Biorefinery: A Review. Antioxidants. 2023;12(2):328. https://doi.org/10.3390/antiox12020328

129. de la Rosa O, Cano-Gonzalez CN, Peña-Lucio EM, Aguilar CN. Fermentable sugars from agricultural wastes. In: Ong HC, Fattah IR, Indra Mahlia TM, editors. Waste Valorization for Bioenergy and Bioproducts. Woodhead Publishing; 2024. pp. 189–205. https://doi.org/10.1016/B978-0-443-19171-8.00009-2

130. Martemucci G, Costagliola C, Mariano M, D'Andrea L, Napolitano P, D'Alessandro AG. Free radical properties, source and targets, antioxidant consumption and health. Oxygen. 2022;2(2):48–78. https://doi.org/10.3390/oxygen2020006

131. Naliyadhara N, Kumar A, Gangwar SK, Devanarayanan TN, Hegde M, Alqahtani MS, *et al.* Interplay of dietary antioxidants and gut microbiome in human health: What has been learnt thus far? Journal of Functional Foods. 2023;100:105365. https://doi.org/10.1016/j.jff.2022.105365

132. Feng J, Zheng Y, Guo M, Ares I, Martínez M, Lopez-Torres B, *et al.* Oxidative stress, the blood–brain barrier and neurodegenerative diseases: The critical beneficial role of dietary antioxidants. Acta Pharmaceutica Sinica B. 2023;13(10):3988–4024. https://doi.org/10.1016/j.apsb.2023.07.010

133. Shanker MA, Krishnan R, Kumar GS, Mohammed T, Hymavathi AS, Rosamma, *et al.* Insights on the astringency of non-alcoholic beverages: Fruit, vegetable & plantation-based perspective. Food Chemistry Advances. 2024;4:100630. https://doi.org/10.1016/j.focha.2024.100630

134. Maseko KH, Regnier T, Meiring B, Wokadala OC, Anyasi TA. *Musa* species variation, production, and the application of its processed flour: A review. Scientia Horticulturae. 2024;325:112688. https://doi.org/10.1016/j.scienta.2023.112688

135. Jain N, Radhakrishnan A, Kuppusamy G. Review on nutraceuticals: phase transition from preventive to protective care. Journal of Complementary and Integrative Medicine. 2022;19(3):553–570. https://doi.org/10.1515/jcim-2022-0026

136. Costanzo G, Vitale E, Iesce MR, Naviglio D, Amoresano A, Fontanarosa C, *et al.* Antioxidant properties of pulp, peel and seeds of phlegrean mandarin (*Citrus reticulata* Blanco) at different stages of fruit ripening. Antioxidants. 2022;11(2):187. https://doi.org/10.3390/antiox11020187

ORCID IDs
Himanshu https://orcid.org/0009-0007-7219-8270
Nishant Kumar https://orcid.org/0000-0003-0187-7544
Ishu Khangwal https://orcid.org/0000-0001-7880-4840

Foods and Raw Materials. 2026;14(1)

ISSN 2308-4057 (Print)
ISSN 2310-9599 (Online)

Review Article
Open Access

Available online at http://jfrm.ru/en
https://doi.org/10.21603/2308-4057-2026-1-661
https://elibrary.ru/EQYVWR

Derivation of hazardous wastes: Pharmaceutical and food applications

Manoj Kumar Sharma[1,2], Anupama Diwan[1], Satish Sardana[2,*], Kapil Kumar[3,]**

[1] Apeejay Stya University, Gurugram, India
[2] Amity University, Gurugram, India
[3] University of Petroleum and Energy Studies, Dehradun, India

* e-mail: ssardana@ggn.amity.edu
** e-mail: kapil.py@gmail.com

Received 01.04.2024; Revised 06.10.2024; Accepted 05.11.2024; Published online 25.02.2025

Abstract:
Around the globe, solid waste generation rates are reaching 2.01 billion tons, resulting in a footprint of 0.78 kg per person per day as of 2020. It is expected to escalate by 70% and reach approximately 3.42 billion tons by the end of 2050, indicating that waste generating and its disposal are a relevant issue worldwide. Waste can be a source of various useful pharmaceutical and food raw materials, which partially solves the global waste problem.
This comprehensive review paper focuses on different types of wastes that can yield carbohydrate polymers for pharmaceutical or food purposes. It covers systemic documentation and summarizes numerous scientific articles published in 2004–2022.
The review demonstrates a great perspective for waste re-utilization as an alternative source of pharmaceutical and food materials. It provides a complete insight into the responsible approach to hazardous waste recycling, thus promoting research in bio-waste remediation, novel raw materials, and natural sustainability.

Keywords: Agricultural waste, macromolecules, carbohydrate polymers, excipients, raw material, environment, waste generating

Funding: The research was supported by the Haryana State Council for Science, Innovation, and Technology (HSCSIT), Government of Haryana, India (Grant No. HSCSIT/R&D/2022/2976).

Please cite this article in press as: Sharma MK, Diwan A, Sardana S, Kumar K. Derivation of hazardous wastes: Pharmaceutical and food applications. Foods and Raw Materials. 2026;14(1):104–116. https://doi.org/10.21603/2308-4057-2026-1-661

INTRODUCTION

The European Union Waste Framework Directive 2008/98/EC, Art. 3, defines waste as "an object that the holder discards, intends to discard, or is required to discard" [1]. Waste generation is divided into the urban areas in developed or developing countries, with metropolitan regions of developing countries generating less garbage compared to the urban areas of developed or industrialized countries (Table 1) [2].

Waste can be classified based on its origin and type. The Union Ministry of Environment, Forests, and Climate Change of India issued a new set of Solid Waste Management Rules in 2016. The document highlights such major issues as waste segregation at place, disposal of hygienic waste, waste-to-energy methods, waste management in mountain regions, etc. [3].

Misclassification of waste leads to inappropriate handling and thus to hazards for environment or human health. This review examines the current research and methodologies that look into the source of harmful waste materials and assess their potential for repurposing as raw materials for new waste derivatives that promote sustainable practices and reduce waste burden.

STUDY OBJECTS AND METHODS

This review focuses on unsafe agricultural, municipal, industrial, farming, and biological wastes that could be used again in the food industry and healthcare. It covers influential publications registered in PubMed, Scopus, WoS, and eLIBRARY.RU within the past three decades. The information obtained was categorized based on key metrics and then subjected to a detailed comparative analysis.

Copyright © 2025, Sharma *et al.* This is an open access article distributed under the terms of the Creative Commons Attribution 4.0 International License (https://creativecommons.org/licenses/by/4.0/), allowing third parties to copy and redistribute the material in any medium or format and to remix, transform, and build upon the material for any purpose, even commercially, provided the original work is properly cited and states its license.

Table 1 Classification of waste by its origin

Type of waste	Description
Domestic/municipal/commercial	Generated by such routine household activities as cooking, cleaning, repairing, painting, etc.
Construction/industrial	Generated by construction sites as a result of demolition, repair, construction processes, e.g., bricks, stones, cement, sand, plumbing material, electric materials, etc.
E-waste	Electronic appliances approaching the end of their useful life; hazardous to health due to presence of harmful components, e.g., heavy metals.
Biodegradable	Organic waste, e.g., fruits, vegetables, food, paper, cardboard, etc., generated by offices, schools, commercial buildings, etc. Includes such agricultural and industrial wastes as cotton, wool, leaves, timber, etc.
Non-biodegradable	Metal, plastic, steel, glass, etc.
Derelict vehicles/hazardous waste	Trucks, cars, or any other automobiles with metal scrape value that are abandoned on the roads or elsewhere
Farm/agricultural	Generated by agricultural activities, e.g., planting, harvesting, cutting, weeding, dairy production, animal slaughter, etc.

RESUITS AND DISCUSSION

Pharmaceutically valuable excipients from agricultural waste. Materials obtained by processing various agricultural waste include cellulose polymer, microcrystalline cellulose, starch, silica, chitosan, enzymes, etc.

Cellulose from agricultural waste. The unique fiber shape of cellulose is responsible for its biological function and diverse applications. Fibrils and microfibrillar bands make up its morphological hierarchy [4].

Cellulose from cotton stalk. Science knows numerous biochemical ways to extract cellulose and its derived nano-materials by breaching the hydrogen bonds between fibrils. The traditional methods include hydrolysis by chemicals or enzymes, defibrillation by mortar and pestle, and oxidation by 2,2,6,6-tetramethylpyperidine-1-oxyl (TEMPO). The TEMPO-facilitated oxidation trailed by mechanical breakdown yields cellulose nanofibrils of a uniform size. Cellulose nanofibrils are used in modified coatings in medicines, food packing or containers, nano-paper, absorbents, and nano-composites. Degumming of cotton bark is a pre-treatment for cellulose nanofibril extraction. The dried films of cellulose nanofibrils are usually examined for their yields, morphologies, crystalline structures, thermal characteristics, natural charge, and various properties. Miao *et al*. [5] reported that the resulting yield, which was as high as 20%, had a better crystallinity than the original material. The starting materials included sulfuric acid (98%), hydrogen peroxide (30%), DMSO, TEMPO (98%), sodium hydroxide (97%), sodium bromide (99.6%), sodium hypochlorite (12%), and sodium carbonate [5].

Cellulose from corn husk. Sodium carboxymethyl cellulose is a chemically altered polymer synthesized from cellulose by treating it with a water-soluble base and an organochlorine compound, e.g., monochloroacetic acid, using an organic reaction medium under heterogeneous condition. The chemicals employed are sodium hydroxide, chloroacetic acid, silver nitrate, ethanol, methanol, glacial acetic acid, benzene, ammonium oxalate, sodium chlorite, sulfuric acid, etc. [6].

Cellulose from orange peel. Cellulose can be obtained from orange peel by pulping sulfite with sodium sulfite and sodium metabisulphite. Orange peel is heated in liquid with sodium sulfate (Na_2O_3S). The final cellulose has good yield, luster, whiteness, and water retention, as well as stable molecular weight, high purity, and low crystallinity [7]. Cellulose and carboxy methyl cellulose can also be obtained from orange peel by alkali treatment [8].

Cellulose from oil palm empty fruit bunch fiber. Containing 42% of α-cellulose, empty fruit bunch fiber is a potential origin of cellulose. It is extracted by a multistep process based on a combination of alkaline treatment and bleaching. Two foremost factors affect the isolation and lightening of palm tree cellulose. First, empty fruits have 17.2% of lignin, 70% holocellulose, 42% α-cellulose, 17.2% sodium-hydroxide-soluble materials, 2.8% hot water-soluble materials, and 0.7% ash content. Second, empty fruit bunch fiber is more subtle to alkaline. After the alkaline treatment, the fibers are oxidatively bleached with a peracid/hydrogen peroxide mix to remove non-cellulosic components and increase thread hydrophilicity and approachability. Al-Hoqbani *et al*. [9] reported 30 mmol of potassium bromate, 30 mmol thiourea dioxide, and 150 g simplest unsaturated carboxylic acid as the best conditions for additional grafting (per 100 g cellulose).

Cellulose from balloon bellflower peel. In China and Korea, balloon bellflower (*Platycodon grandiflorum* A. DC) is used to cure cough, rhinitis, sore throat, hyperlipidemia, high blood pressure, and hyperglycemia. Cellulose could be recovered from this source material by chlorination and alkaline extraction [10].

Cellulose from wheat straw and soy hull. Other probable sources of cellulose nanofibrils include wheat straw and soy hull. The current application of soy hull is feeding cattle as a source of fibers while wheat straw is usually discarded as waste. In this case, cellulose extraction relies on the chemical-mechanical technique. Cellulose nanofibrils possess good thermal characteristics, with thermal breakdown temperatures up to 45%, which makes them good candidates for thermoplastic composites. Wheat straw cellulose nanofibers have prospective utility in aerospace, automotive, and medical bio-composites. Due to their shorter length, soy hull nanofibers were

reported to have a better utility in low-to-medium-grade composite applications, such as commodities and building items [11].

Cellulose from soyabean straw. Soybean straw technical fibers have a high cellulose content (85%) but poor crystallinity (47%). Although they have low crystallinity, the cellulose crystals are well aligned along the fiber axis. The breaking tenacity and elongation of technical fibers are higher than those of ordinary bast fibers, e.g., linen or kenaf, but lower than those of cotton. The breaking tenacity (2.7 g/den) and breaking elongation (4%) are higher in technical fibers than in wheat straw and sorghum stalk and leaf fibers, but lower than in cotton fibers. The nature and qualities of technical fibers of soybean straw indicate that they could be used in textiles, composites, and other industrial applications. Soybean straw reduces reliance on non-renewable petroleum resources for fibers like nylon or polyester [12].

Cellulose from sorghum leaves and stems. Sorghum leaves and stems are mainly discarded as by-products. However, their chemical profile includes cellulose, hemicellulose, and such polymeric substance as lignin, which are of no economic value. The process of cellulose extraction involves alkali treatment followed by acid treatment. The resulting breaking toughness and elongation were reported as comparable to those demonstrated by natural fibers [13].

Cellulose from banana waste. To isolate cellulose fibers, banana fibers have to be separated from lignin, hemicellulose, and pectin by applying an alkaline solution and bleaching. Elanthikkal *et al.* solubilized pectin and hemicelluloses using an alkaline solution procedure [14]. The washing with deionized water removed solubilized components. The bleaching technique was used to whiten the pulp by breaking down phenolic compounds or molecules with chromophoric groups found in lignin. The by-products of that breakdown also had to be removed by treating banana fibers with 5% sodium hypochlorite at 30°C for 3 h.

Cellulose from grape skin. Grape beverage production leaves 50 million tons of pomace per year. Grape pomace is known to impede germination by immobilizing plant nutrients and raising the biological and chemical oxygen requirements. A procedure comprising organic extraction, acid and base dissolutions, basic and acidic oxidation, and bleaching produced 16.4% of pure cellulose from chardonnay grape skins. 54.9% of the extracted cellulose had a crystalline and microfibrillar structure, as revealed by Fourier-transform infrared spectroscopy (FTIR), thermal analysis, and X-ray diffraction (XDR). To create cellulose nanocrystals, the extracted grape cellulose was further hydrolyzed using an atypical sulfuric acid hydrolysis process (8.75 mL/g, 65% sulfuric acid, 45°C, 30 min) [15].

Cellulose from coconut coir fibers. Coconut coir is an available in sufficiency and recyclable plant dry matter generated out of outer casing husk of *Cocos nucifera*. Coir fibers have a considerably higher lignin content than cotton stalks. Lignin could be removed using a blend of mechanical and chemical treatments. After washing, coir fibers were milled, powdered, sieved to 100–150 mesh in a milling machine, and dewaxed. The pulverized coir strands were processed in a basic liquid at high temperature with air condenser and heating. The pulping was carried out using 6% sodium hydroxide at a ratio of 15–25 mL/g of coir threads. The pulp was rinsed in deionized water and dissolved in demineralized water with urea. Then, it was sonicated for 30 min and dispersed in a solution of NaOH, NH_2CONH_2, and H_2O. After the removal of sodium-lignin outgrowth, the

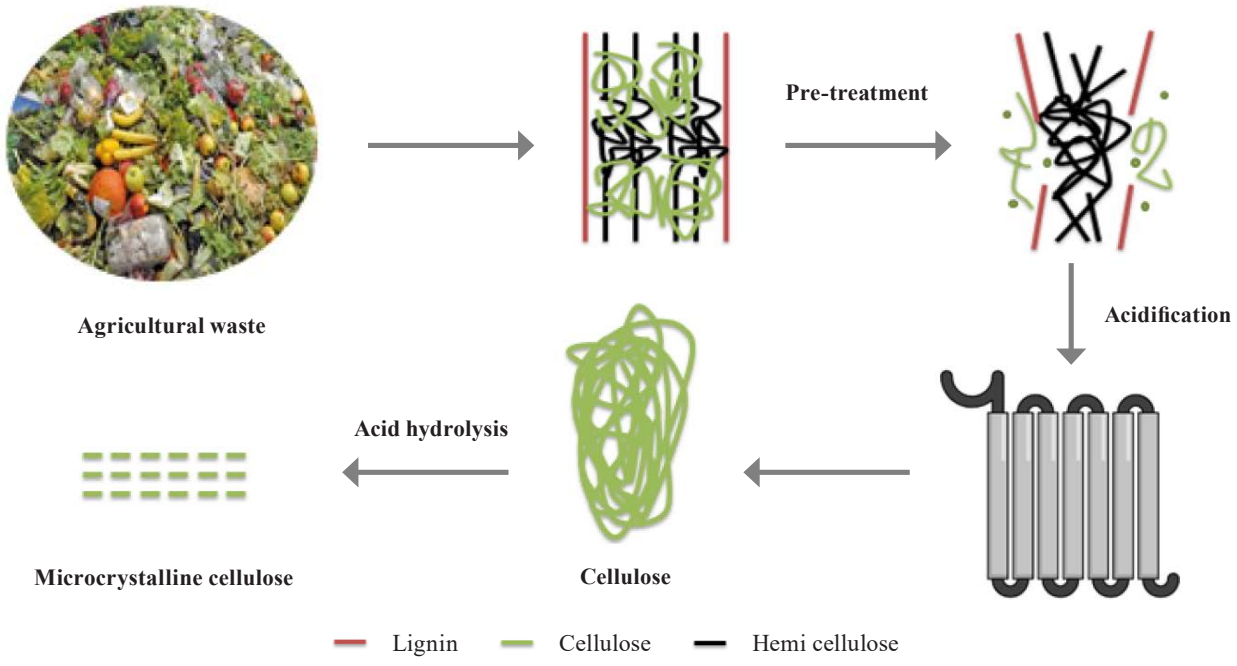

Figure 1 Obtaining microcrystalline cellulose from agricultural waste

reaction mix served as a raw material for cellulose and its derivates, e.g., aerogels [16].

Microcrystalline cellulose from agricultural waste. Microcrystalline cellulose is safe, renewable, and biocompatible. Its high natural strength, huge superficial area, and low bulk have drawn considerable scientific interest during the last twenty years. Microcrystalline cellulose is used as binders and fillers in food products and medicines. More specifically, it serves as a reinforcing agent in the formation of polymers. Besides, microcrystalline cellulose is also a suspension stabilizer, water-holding agent, viscosity maintainer, and emulsifier in pastes and creams. Traditionally, pulpwood and pure *Gossypium herbaceum* fibers were the main cellulose sources serving as an important feedstock for microcrystalline cellulose production. Figure 1 shows a diagrammatic representation of production of microcrystalline cellulose from agricultural waste.

However, new sources of microcrystalline cellulose are reported every day.

Microcrystalline cellulose from tea waste. Deep-processing produces a huge portion of tea waste. Tea leftovers are disposed of by composting, incineration, or dumping. Unfortunately, tea waste is difficult to break down, which puts a stress on the environment, not to mention a severe loss of important components. Controlled acid hydrolysis with good thermal stability is a novel way to extract microcrystalline cellulose from tea waste. Its efficiency depends on hydrochloric acid concentration, acid-to-material ratio, heat, and processing time. An orthogonal experiment design involved the degree of polymerization and tea waste yield as dependent variables. The resulting microcrystalline cellulose had smaller fibers with rough surface morphology and several surface pores [17].

Microcrystalline cellulose from fodder grass. Setaria glauca (L) P. Beauv proved to be another potential source of microcrystalline cellulose [18]. The first stage was to remove lignin and hemicellulose from the dehydrated grass with sodium hydroxide. It was followed by applying bleaching chemicals, i.e., sodium hypochlorite and hydrogen peroxide, in an equal ratio, to remove any traces of lignin and hemicellulose. After that, 10 g cellulose was acid-hydrolyzed with hydrochloric acid (2.5 N) at 100°C for 30 min. The obtained microcrystalline cellulose was properly rinsed with water to remove any traces of acid.

Microcrystalline cellulose from banana fibers. A combination of fermentation and acid hydrolysis yields microcrystalline cellulose from banana fibers. This method is economical and environmentally-safe [19].

Microcrystalline cellulose from sisal fibers. Extraction of microcrystalline cellulose from sisal fibers involves the Soxhlet extraction followed by acid hydrolysis with mineral acid treatment and bleaching. Bhimte and Tayade [20] described a three-stage bleaching procedure:

Stage 1: bleaching with water, buffer solution, and sodium chloride;

Stage 2: bleaching with buffer solution and sodium chloride solution 30 min after Stage 1; and

Stage 3: bleaching with buffer solution and sodium chloride solution 30 min after Stage 2.

The physiochemical analysis of the resulting microcrystalline cellulose showed long thread-like fibers.

Microcrystalline cellulose from mango kernel. Mango kernel is an abundant and accessible agricultural type of waste. Hydrochloric acid hydrolysis of α-cellulose obtained from the mango kernel was reported to produce microcrystalline cellulose with a compact structure and rough surface with 50% crystallinity, as evidenced by a scanning electron microscope. Its physicochemical profile demonstrated excellent flow and compression characteristics [21].

Microcrystalline cellulose from orange peel. Ejikeme obtained microcrystalline cellulose from orange mesocarp extracted after epicarp and endocarp were removed from oranges [22]. The moisture content of the dried mesocarp was 8.3%. With the α-cellulose share in the orange mesocarp being 62.5%, the yield of microcrystalline cellulose was 25.3%. Orange mesocarp underwent acid hydrolysis, and the isolated cellulose was acid-hydrolyzed with dilute mineral acid, which caused partial depolymerization. This strategy could lower the cost of microcrystalline cellulose production in areas where orange peel is easily available.

Microcrystalline cellulose from sugarcane stem pulp. In this case, the isolated cellulose was similarly acid-hydrolyzed with dilute mineral acid to cause partial depolymerization [23].

Microcrystalline cellulose from peanut shell. Peanut shell subjected to acid hydrolysis is another potential source of microcrystalline cellulose. Like in the previous cases, the resulting cellulose has to be acid-hydrolyzed with dilute mineral acid for partial depolymerization [24].

Microcrystalline cellulose from palm oil biomass. Oil palm empty fruit bunch pulp is a common source of biomass in Malaysia. The resulting cellulose has to be hydrolyzed with dilute mineral acid for partial depolymerization to yield microcrystalline cellulose. The Fourier-transform infrared spectroscopy (FTIR) confirmed that acid hydrolysis had no effect on the chemical structure of cellulose fragments. According to the scanning electron microscopy analysis (SEM), the microcrystalline cellulose obtained from oil palm empty fruit bunch had a rough and compact structure. Atomic force microscopy (AFM) revealed spherical particles. The crystallinity index was high, indicating that acid hydrolysis had no effect on the crystal building of the pulp cellulose I allomorph [25].

Starch from agricultural waste. The list of methods for obtaining starch from agricultural waste keeps growing as new research data are published.

Starch from pineapple stem waste. Pineapple properties make it an ideal source of resistant starch or thermoplastic starch in food and non-food applications, respectively. Its physiochemical examination was reported to consist of 34.4% amylose. The amylose content is the most significant factor in defining the valuable assets of type III resistant starch. As a result, pineapple starch

can be used as resistant starch in functional foods for anti-diabetic diets [26].

Starch from banana peels. Catering generates high amounts of banana peel, which is an emerging source of starch as it contains 50% of starch. The technique of extraction (generally wet extraction) includes oxidation with ascorbic acid followed by grinding, filtration, and washing. The washing water waste can be processed by employing clotting + flocculation + transferring with aluminum salts, namely Al_2O_3 and $Al_2(SO_4)_3$ (10 000 ppm solution, 15 mL/L) in order to reduce turbidness and carbon-based amount prior to discarding. The yield reported under these conditions was 29% while the purity approached 70% [27].

Starch from turmeric waste. Turmeric rhizomes are rich in starch. The crop is a popular dietary food ingredient. Turmeric waste is an alternative source of starch extraction. Santana *et al*. claimed 50% of starch in turmeric waste [28]. They used supercritical extraction and pressurized fluid extraction to obtain 80% in the final product.

Starch from avocado seed. Avocado seeds (*Persea americana* Miller) are a waste by-product from fruit processing that causes ecological and environmental issues, contributing to the spread of vermin, e.g., flies or rats. Avocado seeds can be an alternative supply of starch as they contain 29% of starch. The two methods reported for starch isolation from avocado seeds are those by enzyme and by sulfite reagent. The amylose content was reported as 16% while the gelatinization temperature fluctuated from 56 to 74°C, peaking at 65.7°C; the transition enthalpy ranged from 11.4 to 11.6 J/g. At 90°C, the water solubility was 19–20% [29].

Starch from jackfruit seed. Jackfruit farming is a rapidly growing sector. Dumping jackfruit seeds is a waste of useful resources and a threat to the environment. Jackfruit seed starch remains understudied; the extraction procedure involves using protease enzyme as a potential supply of starch. After pre-treatments, the obtained product is further processed and purified to remove residues [30].

Silica from agricultural waste. Silicon dioxide is also known as silica. It is a derivative form of silicon obtained from fused quartz, flint, and agate. These methods are costly and hazardous, which indicates an urgent need for an alternative source. Today, silica is extracted from sugarcane bagasse, rice husk, peanut shell, bamboo leaves, etc.

Silica from rice husk. Rice husk is an important agricultural by-product. Its global annual output exceeds 80 million tons. Rice husk yields 72–98% of silica with a particle size of 40–50 nm [31]. Silica is a result of rice husk carbonization, which indicates that a silica amount is a temperature-dependent variable [32]. Other methods include hydrothermal crystallization, sonochemical synthesis, sol-gel technique, and pyrolysis [33–35].

Silica from peanut shell, bamboo leaves, and sugar cane bagasse. Silica can be obtained from peanut (*Arachis hypogaea* L.) shell, bamboo (*Bambusa vulgaris* L.) leaves, and sugarcane (*Saccharum officinarum* L.) bagasse. Large quantities of these waste materials pose a grave ecological threat. In line with the dissolution and precipitation approach, waste materials are dehumidified in a hot plate before being sintered at 900°C for 7 h. The powder is treated first with 1M sodium hydroxide to make sodium silicate, then with 6M sulfuric acid to synthesize silica. Vaibhav *et al*. reported high purity of silicon dioxide (98%, wt.) from rice husk, sugarcane bagasse, and bamboo leaves, with yields of 78, 71, and 52%, respectively [36]. The silica powders were analyzed by such modern analytical instrumentations as Fourier-transforminfrared spectroscopy (FTIR), X-ray diffraction (XRD), and energy dispersive X-ray analysis (SEM-EDAX). All the sources but peanut shell yielded pure silica. The peanut samples generated magnesium-substituted silica, which needed additional procedures to obtain silica.

Chitosan from agricultural waste (mushrooms). Chitosan is a bioactive polysaccharide derived from chitin, a natural polymer used in the food industry and biomedicine. Currently, almost all commercial chitosan is derived from crustacean shellfish, e.g., shrimps and crabs. Vegetarianism, allergy, and religious beliefs prevent many people from consuming fruits and vegetables coated with animal-sourced chitosan. Mushrooms are consumed as food or added as taste modifiers all over the world. In this regard, mushroom waste may become a source of chitosan because cell walls in mushrooms are made up of chitin. Chitosan can be obtained from mushroom waste by a combination of alkalinization, oxidation, and acidification. The thickness of chitosan-based coatings was measured to be 25 μm by a laser scanning confocal microscope [37]. Another technique for procurement of chitosan is deacetylation, where chitin is isolated from mushroom waste and transformed into chitosan by *N*-deacetylation. The density, porosity, and water vapor barrier of mushroom chitosan films were similar to those of animal chitosan [38].

Enzymes from waste. Agricultural waste is a source of cellulase, amylase, protease, tannase, xylanase, etc. Microbes become a solution to the major problem of agricultural waste disposal. The enzymes obtained by microbes are more stable than those of animal or plant origin. Enzymes are basically obtained by fermentation.

Amylase from agricultural waste. Wheat bran, rice husk, and coconut oil cake are alternative sources of amylase. In case of wheat bran, the fermentation involved *Gibberella fujikuroi*, followed by enzyme extraction with acetate buffer filtration. Rice husk was fermented with *Bacillus subtilis* and extracted by phosphate buffer filtration. Coconut oil cake is a by-product of oil extraction from dried copra; it was fermented with *Aspergillus oryzae*, extracted with distilled water containing Tween 80 polysorbate, and centrifuged. Amylase production often relies on solid state fermentation because of its simplicity, minimal capital asset, low wastewater output, minimal end-product inhibition, improved product retrieval, and high-quality production. As a result, solid state fermentation is usually preferred over submerged fermentation [39–41].

Cellulase from agricultural waste. Cellulase is a plant-produced enzyme that contributes to the breakdown of polymer cellulose. Potato peels could be fermented with bacteria *Aspergillus niger* to produce cellulase. Paddy straw, sugarcane bagasse, sugarcane *barbojo*, grass powder, sorghum husks, and corn straw were fermented with *Klebsiella* sp. [42, 43].

Tannase from agricultural waste. This enzyme belongs to the hydrolase family, which includes enzymes that act on carboxylic ester bonds. Tannin acylhydrolase is the scientific name for this enzyme class. Tannase is an enzyme that aids in the breakdown of gallotannins, which are a form of hydrolysable tannin. Tannase is found in many microbes, including rumen bacteria. Effective tannin utilization requires solid state fermentation technology with non-pathogenic microorganisms that can generate hydrolytic enzymes, i.e., tannase.

Tannase was isolated from palm kernel cake and powdered tamarind seed by solid state fermentation using *A. niger*; the yield was 13.03 IU/g dry solids from palm kernel and 6.44 IU/g dry solids from tamarind seed powder. Coffee pulp is a by-product of coffee processing that accounts for 30% of coffee fruit dry solids. Coffee pulp provides tannase using *Penicillium verrucosum*. Coffee pulp was used as the only carbon source for solid state fermentation, yielding 28.173 ± 1.4 U/g dry solids of tannase. A 3.93-fold increase in tannase production (115.995 U/g dry solids) was also achieved utilizing a statistical approach called central composite rotatable design. Various wastes were fermented with *Aspergillus terreus* to produce tannase, including red gramme husk, green gramme husk, ground nut waste, cotton seed waste, wheat bran, rice bran, coffee husk, tamarind seed powder, cashew apple bagasse, coconut powder, and corn powder [44–46].

Xylanase from agricultural waste. Xylanase comes from various sources, e.g., wheat bran, rice straw, sugarcane bagasse, and soyabean hull. In some studies, it was obtained by fermenting with *A. terreus* strain 5 and *A. niger* strain 44. Wheat bran showed the maximal yield, with the bacterial strain producing less by-product cellulose. Hemicellulose fractions were selectively separated during the saccharification of lignocellulosic substrates, enhancing the commercial viability of xylanase production. Other sources included sorghum straw fermented by *Thermomyces lanuginosus*. In submerged culture using corncobs as carbon source, a thermophilic fungus was reported to produce large amounts of cellulase-free xylanase. This process yielded 11 855 U/g of xylanase free from cellulase and hemicellulose [47, 48].

Protease from agricultural waste. Proteolytic enzymes make up about 60% of the industrial enzyme market. They are used in the food industry for cheese ripening, meat tenderizing, protein hydrolysate manufacturing, and bread making. Protease could be produced using such cheap substrate as defatted soybean cake by solid-state fermentation; it was found suitable for industrial use as a commercial detergent. Defatted soya cake produced protease using *Penicillium* sp. The fermentation of coffee pulp and corn cob involved *Bacillus* sp. and showed a maximal yield (920 U/mL) with the BT MASC 3 strain. Such variables as pH, incubation time, coffee pulp waste, and corncob substrate content could be optimized using the Box-Behnken design [49, 50].

Pharmaceutically useful excipients from industrial waste. Various industrial wastes may yield such pharmaceutically demanding excipients as cellulose, chitosan, and gelatin [51].

Cellulose from industrial waste. One of the major sources of cellulose is the leather and garment industry. Other sources include foods, beer, fabrics, and cotton.

Cellulose from cotton fabric. The global fiber output for textiles exceeds 70.5 million tons per year, with cotton fiber accounting for 40% and polyester fiber accounting for 45.2%. Cellulose is obtained from waste cotton fabrics by acetylation with 1-allyl-3-methylimidazolium chloride (AMIMCl) as a catalyst. It disintegrates cotton-based fabrics before enzymatic hydrolysis. Acid hydrolysis was used to grow *Gluconacetobacter xylinus*, which then produced biopolymer-cellulose pellicle. The resulting cellulose demonstrated satisfactory toughness, dry mass, and moisture holding capacity [52]. Cellulose acetate is a form of cellulose that can be obtained by using ionic liquid *N*-methyl-imidazoliumbisulfate [Hmim]. The yield of cellulose acetate was reported as 49.3%, with the conversion to cellulose at the rate of 84. Waste cotton cloth was utilized to make cellulose nanocrystals with degreasing cotton as control. Cellulose was removed by alkali and bleaching treatments, and cellulose nanocrystals were isolated by controlled acid solution hydrolysis. Cellulose nanocrystals produced from discarded cotton material had a strong crystalline phase index of 55.76 ± 7.82%, indicating that they were more thermostable [53].

Cellulose from rice husk. Rice husk is the most available cellulosic source in global agricultural crop waste. The temperature of 45°C was reported as optimal for acid hydrolysis because it was comparatively low and controllable. The hydrolysis lasted for 30 and 45 min, producing cellulose nanocrystals CNC30 and CNC45, respectively. The yields for CNC30 and CNC45 decreased as the length of hydrolysis increased, amounting 6.43 and 4.83%, respectively. Both CNC30 and CNC45 appeared on individual isotropic transmission electron microscopy (TEM) images as distributed rod-like crystals formed by air-drying dilute suspension of cellulose nanocrystals [54–57].

Cellulose from citrus peel. Citrus peel is another potential source of cellulose. Fan *et al.* produced bacterial cellulose by fermentation using *Komagataeibacter xylinus* CICC No. 10529 [58]. They used Fourier transform infrared spectroscopy (FTIR), scanning electron microscopy (SEM), X-ray diffraction (XRD), and differential scanning calorimetry (DSC) to analyze its properties. The steam explosion technique, which involved sodium hydroxide, a bleaching reagent, and subsequent hydrothermal compressing, proved to be the most effective preparation for plant fibers based on incomplete lignin and hemicellulose separation. *Xanthomonas axonopodis pv.*

citri (strain 306) was able to produce cellulose from citrus waste biomass, which demonstrated a good potential for important nano biomaterials, e.g., nanofibers [59].

Cellulose from beer waste. Beer waste is an alternative potential source of nanocellulose, which is obtained by alkaline treatment, bleaching with sodium chlorite, and controlled acid hydrolyzation. Shahabi-Ghahfarrokhi *et al*. [60] described the visual, thermal, and physical properties of the final product, which was crystalline in nature.

Chitosan from industrial waste. Chitin and its metabolite chitosan are one of the most popular of all carbohydrate natural polymers. Chitosan is a linear polysaccharide obtained mainly form animal sources, with chitin as a basic exoskeleton building block. Chemically, chitosan consists of 2-amino-2-deoxy-D-glucose (deacetylated, D-unit) and *β*-(1-4)-linked *N*-acetyl-2-amino-2-deoxy-D-glucose (acetylated, A-unit). Chitin has different concentrations of A- and D-units. The amount of A-unit exceeds that of D-unit, resulting in water insolubility. In chitosan, the high amount of D-unit makes it water soluble. Chitosan is the key module of the outer shell in crustaceans and other species. Fish factories discard crustacean and shrimp shells as waste, thus losing a potential source of chitosan.

Chitosan from crustacean waste. Crustacean waste is a traditional source of chitosan, which is obtained by demineralization, deproteinization, and deacetylation [61].

Chitosan from shrimp waste. Microbiological fermentation is a good option for chitin production. Demineralization and deproteinization are the two main processes of chitin extraction. Shrimp waste undergoes lactic acid fermentation and is utilized for chitosan isolation by *Pseudomonas aeruginosa.* Lactic acid ($C_3H_6O_3$) is formed in the process of glucose degradation. As a result, exoskeletons shells yield calcium carbonate in a water-soluble form and various minerals. Enzymes or proteases found in biowaste break down crustacean shell proteins into water-soluble protein hydrolysates. Sedaghat *et al*. studied the effect of three parameters on demineralization and deproteinization of crustacean biowaste, i.e., glucose content, inoculation volume, and fermentation time [62]. They produced chitosan by microwave, autoclave, and conventional methods. The autoclave method yielded 87% of chitosan. Fermentation proved to be a simple and effective method for chitosan isolation from shrimp waste.

Chitosan from squid bone plate. Chitosan can be obtained from squid bone plates both chemically and by fermentation. The procedure involves demineralization and deproteination, followed by decarboxylation to form chitosan. Nwe *et al*. [63] obtained chitosan of various qualities by treating chitin with strong sodium hydroxide under various circumstances. The demineralization process of squid bone plate required only 3 h with 3M sodium hydroxide at room temperature.

Chitosan from lobster waste. Chitin was extracted by protease-assisted extraction from Norway lobster (*Nephrops norvegicus* L.). Sayari *et al*. produced chitosan by deacetylating chitin and described its antibacterial, antiproliferative, and physicochemical properties [64].

Chitosan from blue crab waste. Deacetylation of chitin derived from blue crab (*Callinectes sapidus* L.) waste also was reported to yield chitosan. Carapace, hooks, chest, legs, guts, and eggs made up 80% of the raw matter. Baron *et al*. defined the deacetylation amount and the viscos metric of chitosan, as well as described the properties of chitosan film, i.e., opacity, gloss, color parameter, water vapor permeability, moisture content, thickness, and swelling [65].

Gelatin from industrial waste. Gelatin is the key component of pharmaceutical capsules. This hydrocolloid is a popular non-carbohydrate gelling agent in foods, pharmacy, and skincare products.

Gelatin from meat waste. Gelatin usually comes from the tendons of slain cattle (*Flexor digitorum*, *Flexor digitorum profundus*, and *Extensor communis*). Acid or alkaline treatment of collagen prior to water extraction was reported to facilitate gelatine production. Gelatin obtained from short tendons was processed by enzymatic refinement and acidic treatment followed by extraction. The reported Bloom strength was 360–410°C with a yield of 55–60% [66].

Gelatin from pollock skin. Fish skin is composed of collagen, which can be turned into gelatin through mild heat denaturation. Cindy *et al*. dehydrated, pre-treated, and dissolved pollock skin in water to obtain gelatin solution [67]. This solution was cast to form gelatin film; its physicochemical profile included gel strength, tensile strength, physical and mechanical properties, molecular weight, and amino acid content.

Gelatin from fish skin. Gelatin can also be produced from fish skin with the 71.8–97% gelatin purity and 78.1–98.8% yield. Boran and Regenstein [68] studied such properties as protein recovery, gelatin recovery, viscosity, gel strength, etc. Although other processing elements such as acid strength had an impact on the gelatin quality, extraction temperature and pre-treatment time appeared to be the most important variables. However, the extraction temperature and pre-treatment method also affected the quality and strength of the fish skin gelatin.

Pharmaceutically useful materials from municipal waste. Co-combustion with electricity generation by coal represent a unique method of municipal waste disposal.

Silica from municipal waste. Different grades of silica are used in thin layer chromatography and column chromatography. Other applications involve a lubricant for granules, desiccant, etc.

Silica from incinerated municipal waste. The alkaline fusion method is commonly used for silica extraction. The obtained silica demonstrated high porosity with a pore size of 2–3.8 nm. Mining ash and municipal incinerator ash undergo hydrothermal or fusing processes to produce a variety of zeolites. Zeolites have ion exchange capabilities and selective adsorption capacities, which makes it possible to use them as molecular sieves [69, 70].

Cellulose from municipal waste. Municipal waste includes a lot of newspaper and corrugated boxes that can be used as a source of cellulose.

Cellulose from newspaper. Newspaper waste yields pure cellulose of good fiber uniformity [71].

Cellulose from corrugated boxes. Enzymatic hydrolysis proved successful in increasing the yield of cellulose nanocrystals following phosphoric acid hydrolysis, which would significantly improve the industrial production. The crystallinity and thermal stability of cellulose nanocrystals improved after enzymatic treatment. Tang *et al*. [72] reported the particle size, rheological properties, and thermal stability of cellulose nanocrystals obtained from corrugated boxes.

Pharmaceutically useful materials from waste recycling. Isolation of pharmaceutically useful material from waste is an alternative to traditional waste management. Waste recycling for pharmaceutical materials should be encouraged only based on the applicability of the obtained material and the rationality of the method. Recycling produces ethanol, lactic acid, acetic acid, etc.

Ethanol from waste recycling. Ethanol serves as a solvent and co-solvent in the pharmaceutical industry, both as a solubility enhancer and as a vehicle. Due to its bactericidal activity, ethanol is also used as a tropical disinfectant. Traditionally, ethanol was obtained from grape juice fermentation or by fermenting any other sugar-containing substrate.

Ethanol from fiber waste recycling. Ethanol was successfully obtained from fiber waste using enzymatic treatment followed by fermentation with *Saccharomyces cerevisiae.* With a high dry weight concentration of fiber sludge, fermentation with *S. cerevisiae* was conducted as simultaneous saccharification and fermentation [73].

Ethanol from food waste recycling. Developing nations are responsible for a greater proportion of food waste in the total municipal solid waste. Enzymatic treatment, flocculation, and biological fermentation employ food waste fermentation to make ethanol. Ethanol production is increased continuously with the increasing cycles of reflux fermentation; the maximal yield was obtained at cycle five [74].

Lactic acid from waste recycling. Lactic acid fermentation employs renewable carbohydrates as a carbon source.

Lactic acid from food stillage. Ma *et al*. developed the protocol for lactic acid production by employing ethanol fermentation stillage from food waste [75]. Suspended particles can be eliminated by centrifugation and ultrafiltration during pre-treatment, which is followed by electrodialysis. The membranes of electrodialysis have fairly low contamination retention; therefore, stillage pretreatment is necessary before electrodialysis. The maximal lactic acid recovery rate from stillage was 71.2%.

Lactic acid from food waste. Diet food production results in waste with a high biological content, e.g., sugars, which can be used to produce lactic acid by fermentation. Kim *et al*. utilized a native mixed culture to obtain lactic acid from food waste by gradually raising the temperature up to 50°C [76]. The methodology involved fermentation and nanofiltration, followed by electrodialysis. The final fermented broth contained lactic acid of high purity.

Lactic acid from grass silage. Danner *et al*. rationalized the method of recovering lactic acid from grass silage by testing a variety of silages with various levels of organic acids [77]. They used the method of mono-polar electrodialysis to purify the crude liquid extract after it had been pre-treated with ultra-filtration membranes to yield lactic acid from silage preparations. The unrefined lactic acid extract was isolated from the remaining solid pulp by filtration. The press-filtering of the moistened silage produced a fairly unrefined extract with plant mucilage. Lactic acid was eventually recovered by centrifugation, ultrafiltration, and electrodialysis.

Acetic acid from waste recycling. Acetic acid is generally utilized as a starting material for pure terephthalic acid, vinyl acetate monomer, and acetic anhydride. Acetic acid is usually obtained from discarded liquid crystal displays, which are extensively used in TVs, computer monitors, and other devices due to its benefits of good light quality, compact size, and low power consumption. Wang *et al.* presented an ecologically friendly method of recycling organic materials before indium recovery [78]. The method reduces the consumption of fossil fuels. Acetic acid was obtained from expired liquid crystal panels by sub/supercritical fluid extraction, which involves supercritical water. The methods of gas chromatography-mass spectrometry (GC-MS) and high-performance liquid chromatography (HPLC) yielded a comprehensive qualitative and quantitative analysis of the resulting product: 78.23% acetic acid was gained at 400°C and 23 MPa.

CONCLUSION

Wastes of various kind are responsible for environmental pollution worldwide. However, they contain useful excipients. Sustainable recovery of these excipients and materials reduces the environmental burden, thus providing a cleaner and safer environment. The derivation of harmful wastes for food or pharmaceutical applications solves a multifaceted challenge that intersects environmental science, public health, and regulatory compliance. By understanding the sources and types of harmful wastes and their implications, the food and pharmaceutical industries can develop more sustainable practices to minimize environmental and health hazards while maintaining the essential advancements.

Based on our interest in pharmaceutical sciences, we reviewed a significant number of publications that described methods of obtaining various pharmaceutically important excipients from different types of waste [79–87]. Waste proved to be a potential source of pharmaceutically useful components. The final products complied with the standards applicable for the pharmaceutical materials while the novel and sustainable methods proved more economical than traditional ones. The yield of the final product was mentioned in most studies as an imperative criterion in the selection of the waste as raw material.

CONTRIBUTION

All the authors participated in developing the concept and writing of the manuscript.

CONFLICT OF INTEREST

The authors declared no conflict of interests regarding the publication of this article.

REFERENCES

1. European Commission [Internet]. [cited 2024 Feb 10]. Available from: https://commission.europa.eu/index_en
2. Ribic B, Voca N, Ilakovac B. Concept of sustainable waste management in the city of Zagreb: Towards the implementation of circular economy approach. Journal of the Air and Waste Management Association. 2017;67(2):241–259. https://doi.org/10.1080/10962247.2016.1229700
3. Government of India. Solid Waste Management Handeling Rules. 2000.
4. Klemm D, Heublein B, Fink H-P, Bohn A. Cellulose: Fascinating biopolymer and sustainable raw material. Angewandte Chemie International Edition. 2005;44(22):3358–3393. https://doi.org/10.1002/anie.200460587
5. Miao X, Lin J, Tian F, Li X, Bian F, Wang J. Cellulose nanofibrils extracted from the byproduct of cotton plant. Carbohydrate Polymers. 2016;136:841–850. https://doi.org/10.1016/j.carbpol.2015.09.056
6. Yeasmin MS, Mondal MIH. Synthesis of highly substituted carboxymethyl cellulose depending on cellulose particle size. International Journal of Biological Macromolecules. 2015;80:725–731. https://doi.org/10.1016/j.ijbiomac.2015.07.040
7. Bicu I, Mustata F. Cellulose extraction from orange peel using sulfite digestion reagents. Bioresource Technology. 2011;102(21):10013–10019. https://doi.org/10.1016/j.biortech.2011.08.041
8. Yaşar F, Toğrul H, Arslan N. Flow properties of cellulose and carboxymethyl cellulose from orange peel. Journal of Food Engineering. 2007;81(1):187–199. https://doi.org/10.1016/j.jfoodeng.2006.10.022
9. Al-Hoqbani AA, Abdel-Halim ES, Al-Deyab SS. Extraction of palm tree cellulose and its functionalization via graft copolymerization. International Journal of Biological Macromolecules. 2014;70:275–283. https://doi.org/10.1016/j.ijbiomac.2014.07.009
10. Qiu H-W, Zhou Q-C, Geng J. Pyrolytic and kinetic characteristics of *Platycodon grandiflorum* peel and its cellulose extract. Carbohydrate Polymers. 2015;117:644–649. https://doi.org/10.1016/j.carbpol.2014.09.034
11. Alemdar A, Sain M. Isolation and characterization of nanofibers from agricultural residues – Wheat straw and soy hulls. Bioresource Technology. 2008;99(6):1664–1671. https://doi.org/10.1016/j.biortech.2007.04.029
12. Reddy N, Yang Y. Natural cellulose fibers from soybean straw. Bioresource Technology. 2009;100(14):3593–3598. https://doi.org/10.1016/j.biortech.2008.09.063
13. Reddy N, Yiqi Y. Structure and properties of natural cellulose fibers obtained from sorghum leaves and stems. Journal of Agricultural and Food Chemistry. 2007;55(14):5569–5574. https://doi.org/10.1021/jf0707379
14. Elanthikkal S, Gopalakrishnapanicker U, Varghese S, Guthrie JT. Cellulose microfibres produced from banana plant wastes: Isolation and characterization. Carbohydrate Polymers. 2010;80(3):852–859. https://doi.org/10.1016/j.carbpol.2009.12.043
15. Lu P, Hsieh Y-L. Cellulose isolation and core-shell nanostructures of cellulose nanocrystals from chardonnay grape skins. Carbohydrate Polymers. 2012;87(4):2546–2553. https://doi.org/10.1016/j.carbpol.2011.11.023
16. Fauziyah M, Widiyastuti W, Balgis R, Setyawan H. Production of cellulose aerogels from coir fibers via an alkali-urea method for sorption applications. Cellulose. 2019;26:9583–9598. https://doi.org/10.1007/s10570-019-02753-x
17. Amarasinghe BMWPK, Williams RA. Tea waste as a low cost adsorbent for the removal of Cu and Pb from waste water. Chemical Engineering Journal. 2007;132(1–3):299–309. https://doi.org/10.1016/j.cej.2007.01.016
18. Kalita RD, Nath Y, Ochubiojo ME, Buragohain AK. Extraction and characterization of microcrystalline cellulose from fodder grass; *Setaria glauca* (L) P. Beauv and its potential as a drug delivery vehicle for isoniazid, a first line antituberculosis drug. Colloids and Surfaces B: Biointerfaces. 2013;108:85–89. https://doi.org/10.1016/j.colsurfb.2013.02.016
19. Shanmugam N, Nagarkar RD, Kurhade M. Microcrystalline cellulose powder from banana pseudostem fibres using bio-chemical route. Indian Journal of Natural Products and Resources. 2015;6(1):42–50.
20. Bhimte NA, Tayade PT. Evaluation of microcrystalline cellulose prepared from sisal fibers as a tablet excipient: A technical note. AAPS PharmSciTech. 2007;8(1):8. https://doi.org/10.1208/pt0801008
21. Nwadiogb JO, Igwe AA, Okoye NH, Chime CC. Extraction and characterization of microcrystalline cellulose from mango kernel: A waste management approach. Der Pharma Chemica. 2015;7(11):1–7.
22. Ejikeme PM. Investigation of the physicochemical properties of microcrystalline cellulose from agricultural wastes I: orange mesocarp. Cellulose. 2008;15:141–147. https://doi.org/10.1007/s10570-007-9147-7

23. Nwachukwu N, Ugoeze KC, Okoye AC, Chinaka CN. Application of microcrystalline cellulose from Saccharum officinarum as dry binder in ciprofloxacin tablet formulation. Journal of Pharmacy and Bioresources. 2018;15(1):48–55. https://doi.org/10.4314/jpb.v15i1.6

24. Azubuike CP, Odulaja JO, Okhamafe AO. Physicotechnical, spectroscopic and thermogravimetric properties of powdered cellulose and microcrystalline cellulose derived from groundnut shells. Journal of Excipients and Food Chemicals. 2012;3(3):106–115.

25. Haafiz MKM, Eichhorn SJ, Hassan A, Jawaid M. Isolation and characterization of microcrystalline cellulose from oil palm biomass residue. Carbohydrate Polymers. 2013;93(2):628–634. https://doi.org/10.1016/j.carbpol.2013.01.035

26. Nakthong N, Wongsagonsup R, Amornsakchai T. Characteristics and potential utilizations of starch from pineapple stem waste. Industrial Crops and Products. 2017;105:74–82. https://doi.org/10.1016/j.indcrop.2017.04.048

27. Suhartini S, Hidayat N, Rosaliana E. Influence of powdered *Moringa oleifera* seeds and natural filter media on the characteristics of tapioca starch wastewater. International Journal of Recycling of Organic Waste in Agriculture. 2013:2:12. https://doi.org/10.1186/2251-7715-2-12

28. Santana ÁL, Zabot GL, Osorio-Tobón JF, Johner JCF, Coelho AS, Schmiele M, *et al.* Starch recovery from turmeric wastes using supercritical technology. Journal of Food Engineering. 2017;214:266–276. https://doi.org/10.1016/j.jfoodeng.2017.07.010

29. Chel-Guerrero L, Barbosa-Martín E, Martínez-Antonio A, González-Mondragón E, Betancur-Ancona D. Some physicochemical and rheological properties of starch isolated from avocado seeds. International Journal of Biological Macromolecules. 2016;86:302–308. https://doi.org/10.1016/j.ijbiomac.2016.01.052

30. Zhang Y, Zhang Y, Li B, Wang X, Xu F, Zhu K, *et al. In vitro* hydrolysis and estimated glycemic index of jackfruit seed starch prepared by improved extrusion cooking technology. International Journal of Biological Macromolecules. 2019;121:1109–1117. https://doi.org/10.1016/j.ijbiomac.2018.10.075

31. Liu Y, Guo Y, Zhu Y, An D, Gao W, Wang Z, *et al.* A sustainable route for the preparation of activated carbon and silica from rice husk ash. Journal of Hazardous Materials. 2011;186(2–3):1314–1319. https://doi.org/10.1016/j.jhazmat.2010.12.007

32. Li T, Wang T. Preparation of silica aerogel from rice hull ash by drying at atmospheric pressure. Materials Chemistry and Physics. 2008;112(2):398–401. https://doi.org/10.1016/j.matchemphys.2008.05.066

33. Prasetyoko D, Ramli Z, Endud S, Hamdan H, Sulikowski B. Conversion of rice husk ash to zeolite beta. Waste Management. 2006;26(10):1173–1179. https://doi.org/10.1016/j.wasman.2005.09.009

34. Salavati-Niasari M, Javidi J. Sonochemical synthesis of silica and silica sulfuric acid nanoparticles from rice husk ash: A new and recyclable catalyst for the acetylation of alcohols and phenols under heterogeneous conditions. Combinatorial Chemistry and High Throughput Screening. 2012;15(9):705–712. https://doi.org/10.2174/138620712803519743

35. Palanivelu R, Padmanaban P, Sutha S, Rajendran V. Inexpensive approach for production of high-surface-area silica nanoparticles from rice hulls biomass. IET Nanobiotechnology. 2014;8(4):290–294. https://doi.org/10.1049/iet-nbt.2013.0057

36. Vaibhav V, Vijayalakshmi U, Roopan SM. Agricultural waste as a source for the production of silica nanoparticles. Spectrochimica Acta Part A: Molecular and Biomolecular Spectroscopy. 2015;139:515–520. https://doi.org/10.1016/j.saa.2014.12.083

37. Poverenov E, Arnon-Rips H, Zaitsev Ya, Bar V, Danay O, Horev B, *et al.* Potential of chitosan from mushroom waste to enhance quality and storability of fresh-cut melons. Food Chemistry. 2018;268:233–241. https://doi.org/10.1016/j.foodchem.2018.06.045

38. Bilbao-Sainz C, Chiou B-S, Williams T, Wood D, Du W-X, Sedej I, *et al.* Vitamin D-fortified chitosan films from mushroom waste. Carbohydrate Polymers. 2017;167:97–104. https://doi.org/10.1016/j.carbpol.2017.03.010

39. Mulimani VH, Ramalingam GNP. ***α***-Amylase production by solid state fermentation: A new practical approach to biotechnology courses. Biochemical Education. 2000;28(3):161–163. https://doi.org/10.1016/S0307-4412(99)00145-4

40. Baysal Z, Uyar F, Aytekin Ç. Solid state fermentation for production of α-amylase by a thermotolerant *Bacillus subtilis* from hot-spring water. Process Biochemistry. 2003;38(12):1665–1668. https://doi.org/10.1016/S0032-9592(02)00150-4

41. Ramachandran S, Patel AK, Nampoothiri KM, Francis F, Nagy V, Szakacs G, *et al.* Coconut oil cake – a potential raw material for the production of **α**-amylase. Bioresource Technology. 2004;93(2):169–174. https://doi.org/10.1016/j.biortech.2003.10.021

42. dos Santos TC, Gomes DPP, Bonomo RCF, Franco M. Optimisation of solid state fermentation of potato peel for the production of cellulolytic enzymes. Food Chemistry. 2012;133(4):1299–1304. https://doi.org/10.1016/j.foodchem.2011.11.115

43. Waghmare PR, Kshirsagar SD, Saratale RG, Govindwar SP, Saratale GD. Production and characterization of cellulolytic enzymes by isolated Klebsiella sp. PRW-1 using agricultural waste biomass. Emirates Journal of Food and Agriculture. 2014;26(1):44–59. https://doi.org/10.9755/ejfa.v26i1.15296

44. Sabu A, Pandey A, Jaafar Daud M, Szakacs G. Tamarind seed powder and palm kernel cake: two novel agro residues for the production of tannase under solid state fermentation by *Aspergillus niger* ATCC 16620. Bioresource Technology. 2005;96(11):1223–1228. https://doi.org/10.1016/j.biortech.2004.11.002

45. Bhoite RN, Murthy PS. Biodegradation of coffee pulp tannin by *Penicillium verrucosum* for production of tannase, statistical optimization and its application. Food and Bioproducts Processing. 2015;94:727–735. https://doi.org/10.1016/j.fbp.2014.10.007

46. Malgireddy NR, Nimma LNR. Optimal conditions for production of Tannase from newly isolated Aspergillus terrus under solid state fermentation. European Journal of Biotechnology and Bioscience. 2015;3(2):56–64.

47. Gawande PV, Kamat MY. Production of *Aspergillus* xylanase by lignocellulosic waste fermentation and its application. Journal of Applied Microbiology. 1999;87(4):511–519. https://doi.org/10.1046/j.1365-2672.1999.00843.x

48. Sonia KG, Chadha BS, Saini HS. Sorghum straw for xylanase hyper-production by *Thermomyces lanuginosus* (D_2W_3) under solid-state fermentation. Bioresource Technology. 2005;96(14):1561–1569. https://doi.org/10.1016/j.biortech.2004.12.037

49. Germano S, Pandey A, Osaku CA, Rocha SN, Soccol CR. Characterization and stability of proteases from *Penicillium* sp. produced by solid-state fermentation. Enzyme and Microbial Technology. 2003;32(2):246–251. https://doi.org/10.1016/S0141-0229(02)00283-1

50. Kandasamy S, Muthusamy G, Balakrishnan S, Duraisamy S, Thangasamy S, Seralathan K-K, *et al.* Optimization of protease production from surface-modified coffee pulp waste and corncobs using *Bacillus* sp. by SSF. 3 Biotech. 2016;6:167. https://doi.org/10.1007/s13205-016-0481-z

51. Aivalioti M, Cossu R, Gidarakos E. New opportunities in industrial waste management. Waste Management. 2014;34(10):1737–1738. https://doi.org/10.1016/j.wasman.2014.07.006

52. Hong F, Guo X, Zhang S, Han S, Yang G, Jönsson LJ. Bacterial cellulose production from cotton-based waste textiles: Enzymatic saccharification enhanced by ionic liquid pretreatment. Bioresource Technology. 2012;104:503–508. https://doi.org/10.1016/j.biortech.2011.11.028

53. Sun X, Lu C, Zhang W, Tian D, Zhang X. Acetone-soluble cellulose acetate extracted from waste blended fabrics via ionic liquid catalyzed acetylation. Carbohydrate Polymers. 2013;98(1):405–411. https://doi.org/10.1016/j.carbpol.2013.05.089

54. Wang Z, Yao Z, Zhou J, Zhang Y. Reuse of waste cotton cloth for the extraction of cellulose nanocrystals. Carbohydrate Polymers. 2017;157:945–952. https://doi.org/10.1016/j.carbpol.2016.10.044

55. Lu P, Hsieh Y-L. Preparation and characterization of cellulose nanocrystals from rice straw. Carbohydrate Polymers. 2012;87(1):564–573. https://doi.org/10.1016/j.carbpol.2011.08.022

56. Yadav N, Diwan A, Sharma MK, Ajmal G, Kumawat MK. Biological activity of rice straw-derived materials: An overview. Uttar Pradesh Journal of Zoology. 2021;42(24):1256–1264. https://doi.org/10.56557/upjoz/2021/v42i243243

57. Yadav N, Rani S, Sharma MK, Kumawat MK, Diwan A. Pharmaceutical applications of RS: An overview. Uttar Pradesh Journal of Zoology. 2021;42(24):1335–1343. https://doi.org/10.56557/upjoz/2021/v42i243258

58. Fan X, Gao Y, He W, Hu H, Tian M, Wang K, *et al.* Production of nano bacterial cellulose from beverage industrial waste of citrus peel and pomace using *Komagataeibacter xylinus*. Carbohydrate Polymers. 2016;151:1068–1072. https://doi.org/10.1016/j.carbpol.2016.06.062

59. Mariño M, da Silva LL, Durán N, Tasic L. Enhanced materials from nature: Nanocellulose from citrus waste. Molecules. 2015;20(4):5908–5923. https://doi.org/10.3390/molecules20045908

60. Shahabi-Ghahfarrokhi I, Khodaiyan F, Mousavi M, Yousefi H. Green bionanocomposite based on kefiran and cellulose nanocrystals produced from beer industrial residues. International Journal of Biological Macromolecules. 2015;77:85–91. https://doi.org/10.1016/j.ijbiomac.2015.02.055

61. Kaur S, Dhillon GS. The versatile biopolymer chitosan: Potential sources, evaluation of extraction methods and applications. Critical Reviews in Microbiology. 2014;40(2):155–175. https://doi.org/10.3109/1040841X.2013.770385

62. Sedaghat F, Yousefzadi M, Toiserkani H, Najafipour S. Bioconversion of shrimp waste *Penaeus merguiensis* using lactic acid fermentation: An alternative procedure for chemical extraction of chitin and chitosan. International Journal of Biological Macromolecules. 2017;104:883–888. https://doi.org/10.1016/j.ijbiomac.2017.06.099

63. Nwe N, Furuike T, Tamura H. Isolation and characterization of chitin and chitosan from marine origin. Advances in Food and Nutrition Research. 2014;72:1–15. https://doi.org/10.1016/B978-0-12-800269-8.00001-4

64. Sayari N, Sila A, Abdelmalek BE, Abdallah RB, Ellouz-Chaabouni S, Bougatef A, *et al.* Chitin and chitosan from the Norway lobster by-products: Antimicrobial and anti-proliferative activities. International Journal of Biological Macromolecules. 2016;87:163–171. https://doi.org/10.1016/j.ijbiomac.2016.02.057

65. Baron RD, Pérez LL, Salced JM, Córdoba LP, Sobral PJA. Production and characterization of films based on blends of chitosan from blue crab (*Callinectes sapidus*) waste and pectin from Orange (*Citrus sinensis Osbeck*) peel. International Journal of Biological Macromolecules. 2017;98:676–683. https://doi.org/10.1016/j.ijbiomac.2017.02.004

66. Mokrejs P, Langmaier F, Mladek M, Janacova D, Kolomaznik K, Vasek V. Extraction of collagen and gelatine from meat industry by-products for food and non food uses. Waste Managementnd a Research. 2009;27(1):31–37. https://doi.org/10.1177/0734242X07081483

67. Bower CK, Avena-Bustillos RJ, Hietala KA, Bilbao-Sainz C, Olsen CW, McHugh TH. Dehydration of pollock skin prior to gelatin production. Journal of Food Science. 2010;75(4):C317–C321. https://doi.org/10.1111/j.1750-3841.2010.01596.x

68. Boran G, Regenstein JM. Optimization of gelatin extraction from silver carp skin. Journal of Food Science. 2009;74(8):E432–E441. https://doi.org/10.1111/j.1750-3841.2009.01328.x

69. Liu Z-S, Li W-K, Huang C-Y. Synthesis of mesoporous silica materials from municipal solid waste incinerator bottom ash. Waste Management. 2014;34(5):893–900. https://doi.org/10.1016/j.wasman.2014.02.016

70. Fan Y, Zhang F-S, Zhu J, Liu Z. Effective utilization of waste ash from MSW and coal co-combustion power plant – Zeolite synthesis. Journal of Hazardous Materials. 2008;153(1–2):382–388. https://doi.org/10.1016/j.jhazmat.2007.08.061

71. Srasri K, Thongroj M, Chaijiraaree P, Thiangtham S, Manuspiya H, Pisitsak P, *et al.* Recovery potential of cellulose fiber from newspaper waste: An approach on magnetic cellulose aerogel for dye adsorption material. International Journal of Biological Macromolecules. 2018;119:662–668. https://doi.org/10.1016/j.ijbiomac.2018.07.123

72. Tang Y, Shen X, Zhang J, Guo D, Kong F, Zhang N. Extraction of cellulose nano-crystals from old corrugated container fiber using phosphoric acid and enzymatic hydrolysis followed by sonication. Carbohydrate Polymers. 2015;125:360–366. https://doi.org/10.1016/j.carbpol.2015.02.063

73. Cavka A, Alriksson B, Rose SH, van Zyl WH, Jonsson LJ. Production of cellulosic ethanol and enzyme from waste fiber sludge using SSF, recycling of hydrolytic enzymes and yeast and recombinant cellulase-producing *Aspergillus niger*. Journal of Industrial Microbiology and Biotechnology. 2014;41(8):1191–1200. https://doi.org/10.1007/s10295-014-1457-9

74. Ma H, Yang J, Jia Y, Wang Q, Tashiro Y, Sonomoto K. Stillage reflux in food waste ethanol fermentation and its by-product accumulation. Bioresource Technology. 2016;209:254–258. https://doi.org/10.1016/j.biortech.2016.02.127

75. Ma H, Yue S, Li H, Wang Q, Tu M. Recovery of lactic acid and other organic acids from food waste ethanol fermentation stillage: Feasibility and effects of substrates. Separation and Purification Technology. 2019;209:223–228. https://doi.org/10.1016/j.seppur.2018.07.031

76. Kim M-S, Na J-G, Lee M-K, Ryu H, Chang Y-K, Triolo JM, *et al.* More value from food waste: Lactic acid and biogas recovery. Water Research. 2016;96:208–216.

77. Danner H, Madzingaidzo L, Holzer M, Mayrhuber L, Braun R. Extraction and purification of lactic acid from silages. Bioresource Technology. 2000;75(3):181–187. https://doi.org/10.1016/S0960-8524(00)00068-7

78. Wang R, Chen Y, Xu Z. Recycling acetic acid from polarizing film of waste liquid crystal display panels by sub/supercritical water treatments. Environmental Science and Technology. 2015;49(10):5999–6008. https://doi.org/10.1021/acs.est.5b00104

79. Pawar S, Kumar K, Gupta MK, Rawal RK. Synthetic and medicinal perspective of fused-thiazoles as anticancer agents. Anti-Cancer Agents in Medicinal Chemistry. 2021;21(11):1379–1402. https://doi.org/10.2174/1871520620666200728133017

80. Konar D, Maru S, Kar S, Kumar K. Synthesis and clinical development of palbociclib: An overview. Medicinal Chemistry. 2022;18(1):2–25. https://doi.org/10.2174/1573406417666201204161243

81. Yadav N, Sharma MK, Diwan A. Rice straw-based biomaterials for tablet coating and a method thereof. Indian patent application no 202211031062. 2022.

82. Kumar K, Rawal RK. CuI/DBU-mediated MBH reaction of isatins: A convenient synthesis of 3-substituted-3-hydroxy-2-oxindole. ChemistrySelect. 2020;5(10):3048–3051. https://doi.org/10.1002/slct.201903703

83. Kumawat MK, Sharma MK, Tewatia S. 4-aminoquinoline derivatives as antimalarial agents: molecular docking studi. Uttar Pradesh Journal of Zoology. 2021;42(24):1286–1292. https://doi.org/10.56557/upjoz/2021/v42i243248

84. Kumawat MK, Sharma MK, Yadav N, Singh B. 4-Aminoquinolines as antimalarial agents: A review of a medicinal chemistry perspective. International Journal of Life science and Pharma Research. 2022;13(1):P83–P97. https://doi.org/10.22376/ijlpr.2023.13.SP1.P83-P97

85. Sharma MK, Yadav N, Kumawat MK, Iqbal MR. The significance of urotensin-II receptor in cardiovascular diseases. Uttar Pradesh Journal of Zoology. 2021;42(24):1438–1447. https://doi.org/10.56557/upjoz/2021/v42i243282

86. Kumar N, Sharma MK, Kumawat MK. Molecular docking study of selected phytochemicals with COVID-19 main protease. Uttar Pradesh Journal of Zoology. 2021;42(24):1265–1285. https://doi.org/10.56557/upjoz/2021/v42i243244

87. Ajmal G, Yadav N, Kumawat MK, Sharma MK, Iqbal MR. Application of electrospun nanofiber in wound healing: trends and recent patents analysis. International Journal of Life science and Pharma Research. 2022;13(1):L37–L47. https://doi.org/10.22376/ijlpr.2023.13.SP1.L37-47

ORCID IDs
Manoj Kumar Sharma https://orcid.org/0000-0003-4872-1651
Anupama Diwan https://orcid.org/0000-0002-7734-7147
Satish Sardana https://orcid.org/0000-0002-0436-9716
Kapil Kumar https://orcid.org/0000-0003-2875-2119

Foods and Raw Materials. 2026;14(1)

ISSN 2308-4057 (Print)
ISSN 2310-9599 (Online)

Short Communication
Open Access

Available online at http://jfrm.ru/en
https://doi.org/10.21603/2308-4057-2026-1-662
https://elibrary.ru/USAXXS

Sunflower press-cake and its protein extract for food applications: Effects of sonication on functional properties

Francesca Girotto

University of Milan, Milan, Italy

e-mail: francesca.girotto@unimi.it

Received 07.02.2025; Revised 27.02.2025; Accepted 04.03.2025; Published online 27.03.2025

Abstract:
Oilseed press-cakes, a by-product of the oil industry, are currently utilized primarily as animal feed. However, their high protein content and nutritional value make them a promising and sustainable alternative protein source for human nutrition. Their utilization aligns with the principles of circular economy and resource upcycling, promoting a more efficient use of agro-industrial by-products in the food sector.

This research featured industrial dehulled sunflower press-cake with the protein content of 44.4% and the total phenolic content of 33.8 mg GAE/g total solids. The functional properties of the micronized press-cake and its protein extract were investigated, with a focus on the impact of ultrasound treatment.

Sonication notably enhanced the water-holding capacity by 25% and the oil-holding capacity by 48% in the micronized press-cake improving its suitability for applications that require moisture and lipid retention, such as baked goods and snacks. In the extracted protein fraction (72.6% protein), the ultrasound treatment improved the emulsifying capacity by 8.5% and the emulsifying stability by 17%, reinforcing its potential for protein-fortified beverages, sauces, and other emulsified foods.

In this research, sonication emerged as a promising processing step worthy of further optimization, given its ability to enhance key functional properties of sunflower materials. Targeted micronization, protein extraction, and sonication made it possible to upcycle sunflower press-cake as a nutritionally valuable and sustainable ingredient in the food industry, either in its micronized form or as a concentrated protein extract.

Keywords: Oilseed cake, protein-rich ingredients, alternative protein sources, upcycling, ultrasound treatment, sonication

Funding: The project was supported under the National Recovery and Resilience Plan (NRRP) (Mission 4, Component 2, Investment 1.3; Call for tender no. 341, March 15, 2022) of Italian Ministry of University and Research and funded by the European Union – NextGenerationEU (Project code PE00000003, Concession Decree no. 1550, October 11, 2022; adopted by the Italian Ministry of University and Research, CUP D93C22000890001, Project title: ON Foods – Research and Innovation Network on Food and Nutrition Sustainability, Safety, and Security – Working ON Foods).

Please cite this article in press as: Girotto F. Sunflower press-cake and its protein extract for food applications: Effects of sonication on functional properties. Foods and Raw Materials. 2026;14(1):117–122. https://doi.org/10.21603/2308-4057-2026-1-662

INTRODUCTION

With the rapid growth of the global population and the rising consumer awareness of sustainability and environmental concerns, the search for alternative and sustainable protein sources has become increasingly crucial. The food industry is under pressure to reduce its reliance on conventional animal-based proteins, shifting toward more sustainable, plant-based alternatives. Oilseed cake, a by-product of oil extraction, is currently predominantly used in the animal feed sector [1] and, to a lesser extent, as a natural fertilizer. Yet, its high protein content, typically ranging from 27 to 53% [2], positions it as a promising ingredient for human nutrition. Valorizing this by-product aligns with the principles of circular economy and resource upcycling, promoting a more sustainable use of agricultural materials.

Among oilseed cakes, sunflower press-cake stands out due to its substantial global trade volumes, which indicates its economic significance. According to the World Integrated Trade Solution (WITS) software, the leading exporters of sunflower press-cake are Ukraine ($761.8 million, 3.28 billion kg), the European Union

Copyright © 2025, Girotto. This is an open access article distributed under the terms of the Creative Commons Attribution 4.0 International License (https://creativecommons.org/licenses/by/4.0/), allowing third parties to copy and redistribute the material in any medium or format and to remix, transform, and build upon the material for any purpose, even commercially, provided the original work is properly cited and states its license.

($361.3 million, 1.01 billion kg), Bulgaria ($323.7 million, 906.5 million kg), Hungary ($182.7 million, 526.4 million kg), and Argentina ($150.4 million, 590.5 million kg). The primary importers include China ($956.6 million, 2.33 billion kg), the European Union ($859.5 million, 2.76 billion kg), France ($234.2 million, 641.9 million kg), Italy ($232.9 million, 722.2 million kg), and Turkey ($221.8 million, 682 million kg).

Although scientific literature extensively discusses the use of sunflower seeds in the food industry and the potential of press-cakes as a protein source [3], publications that focus on the direct application of whole sunflower press-cake in food formulations remain scarce. This is likely due to its high content of insoluble fibers, which can impact texture, processing properties, and digestibility. However, this limitation can be addressed through a preliminary dehulling step before oil extraction [4, 5]. Dehulling has increasingly gained attention as a key processing strategy [6, 7], and the Italian oil industry is actively working to optimize the method of mechanical oil extraction following the achene removal, based on the varying characteristics of seeds.

This study explored the valorization of industrial dehulled sunflower press-cake as a protein-rich ingredient for food applications, both in its raw form and after protein extraction. Micronization was applied with a dual purpose: breaking down plant cell walls to improve access to intracellular proteins for extraction [8] and potentially enhancing dispersibility, thus contributing to a smoother, creamier texture while reducing the perception of grittiness or roughness in formulations [9].

The functional properties of sunflower press-cake are critical physicochemical parameters that determine its behavior in food matrices. Such key properties as water-holding capacity, oil-holding capacity, foaming capacity, and emulsifying capacity shape the texture, stability, and sensory attributes of food products. These properties arise from the intricate interactions between structural and molecular components; they affect the formulation, processing, and final product quality [10].

To further assess the functional potential of sunflower press-cake, we also examined the impact of ultrasound treatment as a means of optimizing the technological and functional properties needed for food applications. Sonication is known to modify protein structures and solubility, which improves the functional properties of the material, rendering ultrasound treatment a promising technique for food ingredient development [11]. By demonstrating the feasibility of sunflower press-cake as a functional and sustainable ingredient, this study contributes to the development of novel plant-based protein alternatives, supporting a more circular and resource-efficient food system.

STUDY OBJECTS AND METHODS

Dehulled sunflower press-cake was provided by Savi Italo Srl (Fiorenzuola d'Arda, Italy). It was obtained after cold pressing oil from dehulled seeds using a single helix screw press and stored under vacuum at room temperature. All chemicals were purchased from Sigma-Aldrich (USA) and Merck KGaA (Germany).

Micronization and protein extraction. The micronization of the dehulled sunflower press-cake involved a KMX-500 ultra-fine mill (Separ Microsystem, Italy) operating at a frequency of 70 Hz. This process produced a micronized flour with particle sizes below 700 μm. Sunflower proteins were chemically extracted at their isoelectric point (pH 4) [12], neutralized to pH 7 with 1N NaOH, and freeze-dried for 72 h using a LIO-5PDGT lyophilizer (5pascal S.r.l., Italy), then stored under vacuum at room temperature.

Chemical and physicochemical analyses. The total solids, ash, and protein contents in the micronized dehulled sunflower press-cake and its protein extract were determined according to the specific methods outlined by the Association of Official Analytical Chemists [13]. The protein quantification involved the Kjeldahl method with a nitrogen-to-protein conversion factor of 5.6 [14]. The total phenolic content was measured using the Folin-Ciocalteu assay as described by Dewanto *et al*. [15], with few modifications.

The color profile was defined with a tristimulus colorimeter (Chroma Meter II Reflectance, Konica-Minolta, Japan), calibrated with a Konica Minolta ceramic white pad (99%), and expressed using the CIE $L^*a^*b^*$ space [12].

Functional properties. The functional properties of the micronized dehulled sunflower press-cake and its protein concentrate included water-holding capacity, oil-holding capacity, foaming capacity, emulsifying capacity, and emulsifying stability. The analyses relied on the methodologies adapted from Girotto *et al*. [5] for water- and oil-holding capacity, Siddiq *et al*. [16] for emulsifying capacity and stability, and Waghmare *et al*. [17] for foaming capacity. The analyses were conducted on both the micronized dehulled sunflower press-cake and its protein extract, with and without ultrasound treatment.

Ultrasound treatment. The ultrasound treatment involved a sonicator (Fisherbrand, FB505EUK-220, USA) equipped with a three-millimeter diameter probe. The sonicator operated at an ultrasonic frequency of 20 kHz and an amplitude of 45% (~100 μm) for 5 min (20 s on, 10 s off). The samples remained in an ice bath to prevent any temperature variation exceeding 2°C.

Statistical analysis. The data represented the mean of three replicates ± their standard deviation. The JMP 5.0 software (SAS Institute Cary NC, USA) provided a one-way analysis of variance (ANOVA) with Tukey-Kramer honestly significant difference $p < 0.05$.

RESULTS AND DISCUSSION

Through isoelectric point precipitation, the sunflower proteins obtained from the micronized dehulled sunflower press-cake were concentrated into an extract (72.6 g protein per 100 g), representing an approximate 64% increase compared to the protein content in the raw press-cake (44.4 g protein per 100 g) (Table 1).

The total solids concentration was significantly higher in the protein extract (99.58 ± 0.17%) due to the

Table 1 Physicochemical analysis of micronized dehulled sunflower press-cake and its protein extract

Chemical component	Micronized dehulled sunflower press-cake	Protein extract
Total solids, %	92.84 ± 0.16[a]	99.58 ± 0.17[b]
Ash, %	7.00 ± 0.02[a]	3.85 ± 0.09[b]
Proteins, %	44.35 ± 0.50[a]	72.61 ± 0.66[b]
Total phenolics, mg GAE/g total solids	33.75 ± 0.33[a]	35.20 ± 1.11[a]

Values within a row with different superscripts are significantly different ($p < 0.05$)

Table 2 Color characteristics of micronized dehulled sunflower press-cake and its protein extract

Color	Micronized dehulled sunflower press-cake	Protein extract
*L**	65.4 ± 0.4[a]	47.2 ± 0.6[b]
*a**	0.8 ± 0.2[a]	–18.9 ± 0.4[b]
*b**	13.5 ± 0.5[a]	–1.6 ± 0.5[b]

Values within a row with different superscripts are significantly different ($p < 0.05$)

Table 3 Functional properties of micronized dehulled sunflower press-cake and its protein extract

Functional properties	Micronized dehulled sunflower press-cake	Protein extract
Water-holding capacity, g H_2O/g total solids	1.12 ± 0.17[a]	0.92 ± 0.01[a]
Oil-holding capacity, g oil/g total solids	1.20 ± 0.02[a]	1.57 ± 0.01[b]
Foaming capacity, %	21.0 ± 1.1[a]	77.0 ± 4.9[b]
Emulsifying capacity, %	54.2 ± 7.2[a]	58.8 ± 1.8[a]
Emulsifying stability, %	26.7 ± 2.9[a]	37.0 ± 0.6[b]

Values within a row with different superscripts are significantly different ($p < 0.05$)

optimal lyophilization performance, compared to the press-cake (92.84 ± 0.16%). However, the ash content, which represented the mineral component, was higher in the dehulled sunflower press-cake (7.00 ± 0.02%). The high total phenolic content was observed both in the dehulled sunflower press-cake (33.75 ± 0.33 mg GAE/g total solids) and in the sunflower protein concentrate (35.20 ± 1.11 mg GAE/g total solids). According to our previous study, chlorogenic acid was detected as the main phenolic compound sunflower press-cake [5]. The significant presence of phenolic compounds in sunflower kernels and shells, previously reported by Weisz *et al*. [18], offers a valuable opportunity to improve the nutritional profile and health-promoting properties of food formulations.

The dehulled sunflower press-cake and its protein extract differed in color (Table 2).

The protein concentrate exhibited a strong green component ($a^* = –18.9 ± 0.4$) and a slight blue component ($b^* = –1.6 ± 0.5$), whereas the press-cake had a pronounced yellowness ($b^* = 13.5 ± 0.5$). The green coloration resulted from the interactions between chlorogenic acid and proteins [19], which presents a unique opportunity for industrial formulators. The distinct natural hue of the extracted sunflower proteins could be particularly appealing to consumers looking for innovative and eco-friendly beverage options [20].

Table 3 presents the functional properties of micronized dehulled sunflower press-cake and its protein concentrate, which are essential for predicting their suitability as protein-rich ingredients for the food industry. A better understanding water-holding, oil-holding, foaming, and emulsifying capacities enables manufacturers to predict how these ingredients will behave in various processing conditions and food applications.

Significant differences were highlighted. Despite the similar water-holding capacity, the protein extract showed a significantly higher oil-holding capacity (1.57 ± 0.01 g oil/g total solids) than the micronized press-cake (1.20 ± 0.02 g oil/g total solids). This result could be attributed to the greater affinity of concentrated proteins for lipids, facilitated by their purer and more specific molecular structure. The reduced amount of fiber and complex carbohydrates in the extract, compared to the press-cake, allowed proteins to interact with lipids more effectively, thus enhancing the oil absorption capacity. Indeed, non-polar side chains of amino acids are known to form hydrophobic interactions with the hydrocarbon chains of lipids [21].

The foaming capacity is another parameter that showed a significant difference, with the protein extract reaching a much higher value (77 ± 4.9%) compared to the press-cake (21 ± 1.1%). The higher solubility and structural flexibility of the concentrated proteins probably allowed them to stabilize entrapped air more effectively than the less refined proteins present in the press-cake, which was rich in polysaccharides, e.g., dietary fibers.

Despite the similar emulsifying capacity, the emulsifying stability was significantly higher in the protein extract (37 ± 0.6%) than in the press-cake (26.7 ± 2.9%). The greater homogeneity and purity of the protein extract, free from coarse components, allowed for a better emulsion stability and reduced the phase separation.

Overall, the protein extract emerged as a more suitable matrix for applications requiring high performance in terms of protein ingredient purity, lipid interaction capacity, and emulsifying properties. These characteristics suggest the potential application of the protein extract in protein beverages, sauces, dressings, creams, and glazes.

The potential of sunflower press-cake becomes evident when comparing its functional properties with those of other plant-based protein-rich ingredients popular in the food sector. For instance, lentil flour exhibits a water-holding capacity of 1.33 ± 0.02 g H_2O/g total solids, while chickpea flour reaches 1.19 ± 0.01 g H_2O/g total solids [22], both of which are comparable to the values observed in this research for the dehulled sunflower

press-cake. In terms of emulsifying capacity, lentil and chickpea flours achieve 65.75 ± 0.11 and 61.1 4 ± 0.61%, respectively, which are nearly matched by those calculated for sunflower protein concentrate in this research.

Effect of sonication on functional properties. Sonication is a physical treatment that uses high-frequency sound waves to induce physical and chemical phenomena within food matrices. Ultrasound waves with frequencies ≥20 kHz generate high-intensity vibrations that cause cavitation phenomena, leading to the formation of vapor microbubbles that undergo alternating compression and expansion phases, growing until they implode. This implosion releases shock energy that impacts the surface under treatment. The collapse of the bubbles causes a shock that generates intense mechanical forces and localized temperatures. They alter the physical structure, e.g., cell wall rupture, and chemical composition of the matrices, thus modifying their functional properties [23]. In protein matrices, ultrasound primarily alters the three-dimensional structure of proteins, causing denaturation, solubilization, and fragmentation [24].

In this study, the ultrasound treatment had a serious impact on the functional properties of both the micronized sunflower press-cake and its protein extract, inducing relevant structural modifications in both matrices and producing significant functional variations (Table 4). As for the water-holding capacity, the ultrasound treatment increased the value for the press-cake from 1.12 ± 0.17 to 1.40 ± 0.02 g H_2O/g total solids. This effect seems attributable to the formation of micro-channels within the press-cake structure generated by the ultrasound action. These micro-channels facilitate water penetration and retention [25]. Conversely, the water-holding capacity of the protein extract decreased from 0.92 ± 0.01 to 0.78 ± 0.09 g H_2O/g total solids. It happened as a result of increased protein solubility, which reduced the ability to absorb and retain water within the modified protein matrix.

The ultrasound treatment significantly improved the oil-holding capacity of the press-cake, which grew from 1.20 ± 0.02 to 1.78 ± 0.04 g oil/g total solids. This increase could again be due to the greater porosity of the press-cake structure, which facilitated the interaction and oil retention. For the protein extract, the oil-holding capacity decreased from 1.57 ± 0.01 to 1.35 ± 0.04 g oil/g total solids. Apparently, the ultrasound treatment reduced the lipid affinity of the matrix, possibly due to the changes in protein conformation, which altered its fat-binding efficiency.

The foaming capacity went down in both matrices, dropping from 21.0 ± 1.1 to 13.0 ± 0.1% in the dehulled sunflower press-cake and from 77.0 ± 4.9 to 48.0 ± 2.9% in the protein extract. This reduction could be attributed to protein denaturation, which impairs the ability of the matrix to form and stabilize air bubbles, thus reducing the foaming capacity and, consequently, foaming stability.

The sonication had a differentiated effect on the emulsifying capacity. In the press-cake, the emulsifying capacity dropped down from 54.2 ± 7.2 to 38.3 ± 1.4%. Conversely, in the protein extract, the emulsifying capacity increased from 58.8 ± 1.8 to 63.8 ± 1.8%, suggesting that ultrasound-modified proteins had a stronger stabilizing effect on the emulsions. This improvement was likely due to the increased conformational flexibility and reduced particle size, both of which enhanced molecular interactions at the oil-water interface.

While the emulsifying stability remained unchanged in the dehulled sunflower press-cake, it increased from 37.0 ± 0.6 to 43.4 ± 0.7% in the protein extract. The result could be attributed to the improved adsorption of smaller protein aggregates onto the interface, which reinforced the emulsion stability [26].

In summary, the ultrasound treatment had different effects on the functional properties of the sunflower press-cake and its protein extract, making them more suitable for specific applications. The sonicated sunflower press-cake with its good water- and oil-holding capacities could be used in bakery products that benefit from moisture retention and a soft texture (e.g., cakes and muffins) and in formulations requiring sufficient fat-holding ability (e.g., sweet and savory snacks). On the other hand, the sonicated protein extract with its enhanced emulsifying capacity and stability demonstrated good prospects for formulations that require stable emulsions (e.g., salad dressings or mayonnaise-like sauces). However, the low foaming capacity in both matrices may limit their use in aerated products, e.g., whipped or leavened ones.

Ultrasound treatment offers significant advantages over traditional physical treatment methods, particularly by avoiding thermal damage. This study provided important insights into the functional properties of the sonicated micronized dehulled sunflower press-cake and its protein concentrate. However, the research had some limitations that could affect the interpretation and generalization of the results. Since the effectiveness of sonication hinges on the precise regulation of key parameters, such as exposure time and intensity, different treatment conditions should be further investigated to understand the outcomes and optimize the setting parameters according to specific formulation objectives. Additionally, it would be useful to examine other functional characte-

Table 4 Functional properties of sonicated micronized dehulled sunflower press-cake and its protein extract

Functional properties after sonication	Micronized dehulled sunflower press-cake	Protein extract
Water-holding capacity, g H_2O/g total solids	1.40 ± 0.02[a]	0.78 ± 0.09[b]
Oil-holding capacity, g oil/g total solids	1.78 ± 0.04[a]	1.35 ± 0.04[b]
Foaming capacity, %	13.0 ± 0.1[a]	48.0 ± 2.9[b]
Emulsifying capacity, %	38.3 ± 1.4[a]	63.8 ± 1.8[b]
Emulsifying stability, %	20.0 ± 4.3[a]	43.4 ± 0.7[b]

Means within a row with different superscripts are significantly different ($p < 0.05$)

ristics, such as protein solubility, gelling capacity, or dispersion viscosity, which may be affected by ultrasound treatment and could impact food applications.

CONCLUSION

This study explored the potential of micronized dehulled sunflower press-cake as an alternative protein source in the food industry, emphasizing the importance of upcycled by-products in the agro-industrial sector. It revealed the functional properties of micronized sunflower press-cake and its protein extract with and without ultrasound treatment. The micronized dehulled sunflower press-cake demonstrated good water and oil absorption capacities (1.12 g H_2O/g total solids; 1.20 g oil/g total solids), both of which could be enhanced through sonication (1.40 g H_2O/g total solids; 1.78 g oil/g total solids). As a result, the press-cake showed a strong potential for applications in baked goods, as well as in sweet and savory snacks. Meanwhile, the protein extract (72.6% protein) had superior emulsifying capacity (58.8%) and stability (37%), particularly when sonicated (63.8 and 43.4%, respectively). It proved to be an ideal ingredient for formulations that require effective fat integration and prolonged stability of both oil and aqueous phases. Its applications are promising for sauces, dressings, protein beverages, and creams. However, neither the press-cake nor its protein concentrate could be used in formulations that need a strong foaming capacity.

This study represents a significant step toward the integration of sunflower press-cake and its protein concentrate in the food industry. Sonication proved to be an important technological step that enhances their functional properties and expands application prospects. Additional research is needed to optimize the ultrasound treatment conditions and explore other types of oilseed meals, fostering the development of more sustainable and innovative plant-based protein-rich food alternatives.

CONFLICT OF INTEREST

The author declared no conflict of interests regarding the publication of this article.

REFERENCES

1. Rakita S, Kokić B, Manoni M, Mazzoleni S, Lin P, *et al*. Cold-pressed oilseed cakes as alternative and sustainable feed ingredients: A review. Foods. 2023;12(3):432. https://doi.org/10.3390/foods12030432
2. Arrutia F, Binner E, Williams P, Waldron KW. Oilseeds beyond oil: Press cakes and meals supplying global protein requirements. Trends in Food Science and Technology. 2020;100:88–102. https://doi.org/10.1016/j.tifs.2020.03.044
3. Petraru A, Ursachi F, Amariei S. Nutritional characteristics assessment of sunflower seeds, oil and cake. Perspective of using sunflower oilcakes as a functional ingredient. Plants. 2021;10(11):2487. https://doi.org/10.3390/plants10112487
4. Grasso S, Omoarukhe E, Wen X, Papoutsis K, Methven L. The use of upcycled defatted sunflower seed flour as a functional ingredient in biscuits. Foods. 2019;8(8):305. https://doi.org/10.3390/foods8080305
5. Girotto F, Merlino M, Giovanelli G, Condurso C, Piazza L. Unveiling the potential of micronized dehulled sunflower press-cake: A breakthrough in sustainable plant-based protein-rich sport beverages. International Journal of Food Science and Technology. 2024;59(7):4784–4796. https://doi.org/10.1111/ijfs.17208
6. Lazaro E, Benjamin Y, Robert M. The effects of dehulling on physicochemical properties of seed oil and cake quality of sunflower. Tanzania Journal of Agricultural Sciences. 2014;13(1):41–47.
7. Chang L, Shi R, Dai F, Zhao W, Zhao Y, *et al*. Current Flaxseed Dehulling Technology in China. Agriculture. 2024;14(4):632. https://doi.org/10.3390/agriculture14040632
8. Rommi K, Holopainen U, Pohjola S, Hakala TK, Lantto R, *et al*. Impact of particle size reduction and carbohydrate-hydrolyzing enzyme treatment on protein recovery from rapeseed (*Brassica rapa* L.) press cake. Food and Bioprocess Technology. 2015;8:2392–2399. https://doi.org/10.1007/s11947-015-1587-8
9. Dhiman A, Prabhakar PK. Micronization in food processing: A comprehensive review of mechanistic approach, physicochemical, functional properties and self-stability of micronized food materials. Journal of Food Engineering. 2021;292:110248. https://doi.org/10.1016/j.jfoodeng.2020.110248
10. Singh R, Langyan S, Sangwan S, Rohtagi B, Khandelwal A, *et al*. Protein for human consumption from oilseed cakes: A review. Frontiers in Sustainable Food Systems. 2022;6:856401. https://doi.org/10.3389/fsufs.2022.856401
11. Higuera-Barraza OA, Del Toro-Sanchez CL, Ruiz-Cruz S, Márquez-Ríos E. Effects of high-energy ultrasound on the functional properties of proteins. Ultrasonics Sonochemistry. 2016;31:558–562. https://doi.org/10.1016/j.ultsonch.2016.02.007
12. Girotto F, Ceccanti C, Narra F, Piazza L. Investigating the suitability of sunflower press-cake proteins in formulated sport beverages. Food & Function. 2025;16:1992. https://doi.org/10.1039/d4fo04530k
13. AOAC. Official methods of analysis of the association of official analytical chemists international. Methods: 934.01, 923.03, 920.39, 954.01. 22nd Edition. Rockville: AOAC International; 2023.

14. Slabi SA, Mathe C, Basselin M, Framboisier X, Ndiaye M, *et al*. Multi-objective optimization of solid/liquid extraction of total sunflower proteins from cold press meal. Food Chemistry. 2020;317:126423. https://doi.org/10.1016/j.foodchem.2020.126423
15. Dewanto V, Wu X, Adom KK, Liu RH. Thermal processing enhances the nutritional value of tomatoes by increasing total antioxidant activity. Journal of Agricultural and Food Chemistry. 2002;50(10):3010–3014. https://doi.org/10.1021/jf0115589
16. Siddiq M, Nasir M, Ravi R, Dolan KD, Butt MS. Effect of defatted maize germ addition on the functional and textural properties of wheat flour. International Journal of Food Properties. 2009;12(4):860–870. https://doi.org/10.1080/10942910802103028
17. Waghmare AG, Salve MK, LeBlanc JG, Arya SS. Concentration and characterization of microalgae proteins from *Chlorella pyrenoidosa*. Bioresources and Bioprocessing. 2016;3:16. https://doi.org/10.1186/s40643-016-0094-8
18. Weisz GM, Kammerer DR, Carle R. Identification and quantification of phenolic compounds from sunflower (*Helianthus annuus* L.) kernels and shells by HPLC-DAD/ESI-MS^n. Food chemistry. 2009;115(2):758–765. https://doi.org/10.1016/j.foodchem.2008.12.074
19. Wildermuth SR, Young EE, Were LM. Chlorogenic acid oxidation and its reaction with sunflower proteins to form green-colored complexes. Comprehensive Reviews in Food Science and Food Safety. 2016;15(5):829–843. https://doi.org/10.1111/1541-4337.12213
20. Vermeir I, Roose G. Visual design cues impacting food choice: A review and future research agenda. Foods. 2020;9(10):1495. https://doi.org/10.3390/foods9101495
21. Biswas KM, DeVido DR, Dorsey JG. Evaluation of methods for measuring amino acid hydrophobicities and interactions. Journal of Chromatography A. 2003;1000(1–2):637–655. https://doi.org/10.1016/S0021-9673(03)00182-1
22. Du S, Jiang H, Yu X, Jane J. Physicochemical and functional properties of whole legume flour. LWT – Food Science and Technology. 2013;55(1):308–313. https://doi.org/10.1016/j.lwt.2013.06.001
23. Arruda TR, Vieira P, Silva BM, Freitas TD, do Amaral AJB, *et al*. What are the prospects for ultrasound technology in food processing? An update on the main effects on different food matrices, drawbacks, and applications. Journal of Food Process Engineering. 2021;44(11):e13872. https://doi.org/10.1111/jfpe.13872
24. Chen J, Chen X, Zhou G, Xu X. Ultrasound: A reliable method for regulating food component interactions in protein-based food matrices. Trends in food science and technology. 2022;128:316–330. https://doi.org/10.1016/j.tifs.2022.08.014
25. Umaña M, Calahorro M, Eim V, Rosselló C, Simal S. Measurement of microstructural changes promoted by ultrasound application on plant materials with different porosity. Ultrasonics Sonochemistry. 2022;88:106087. https://doi.org/10.1016/j.ultsonch.2022.106087
26. Wang T, Wang N, Li N, Ji X, Zhang H, *et al*. Effect of high-intensity ultrasound on the physicochemical properties, microstructure, and stability of soy protein isolate-pectin emulsion. Ultrasonics sonochemistry. 2022;82:105871. https://doi.org/10.1016/j.ultsonch.2021.105871

ORCID IDs
Francesca Girotto https://orcid.org/0000-0002-1217-0918

Foods and Raw Materials. 2026;14(1)

ISSN 2308-4057 (Print)
ISSN 2310-9599 (Online)

Review Article
Open Access

Available online at http://jfrm.ru/en
https://doi.org/10.21603/2308-4057-2026-1-663
https://elibrary.ru/SNBQLV

Antioxidant and anti-inflammatory activities of the Black Bean (*Phaseolus vulgaris* L.): A systematic review

Durga R. Priyadarshini, Annette D. Beatrice*, Tinhoithem Haokip

Women's Christian College, University of Madras, Chennai, India

* e-mail: annettebeatrice@wcc.edu.in

Received 22.06.2024; Revised 22.08.2024; Accepted 03.09.2024; Published online 15.04.2025

Abstract:
The black bean (*Phaseolus vulgaris* L.), a nutrient-dense legume containing bioactive compounds, has proven to have excellent antioxidant and anti-inflammatory effects. However, the available literature data are diverse and needs summarizing. Therefore, we aimed to systematically review the studies on the antioxidant and anti-inflammatory activities of the black bean.
A literature search following the PRISMA guidelines was carried out for *in vitro*, *in vivo*, and human studies assessing the antioxidant and anti-inflammatory effects of the black bean. For this, we used Boolean operators in the following databases: PUBMED, DOAJ, Google Scholar, and WHO's International Clinical Trials Registry Platform. A total of 411 articles was screened, with 28 duplicate articles removed. Among the remaining 383 articles, only 38 matched the inclusion criteria. The risks of bias were evaluated using the QUIN tool for the *in vitro* studies and the OHAT tool for the *in vivo* and human studies.
The seed coat of the black bean exhibited the strongest antioxidant and anti-inflammatory activities compared to the other parts of the seed. While thermal processing negatively impacted the beneficial effects, the retention of the cooking water improved the beans' antioxidant and anti-inflammatory activities. Germinated and fermented black beans had higher potential than raw and cooked beans. Thus, the black bean can exert a protective effect against inflammatory cytokines.
The antioxidant and anti-inflammatory activities of the black bean depend on which parts of the bean are used and how they are processed. There is a need for further studies and clinical trials to focus on the beneficial role of germinated and fermented black beans in human health.

Keywords: Beans, legumes, oxidative stress, inflammation, bioactive compounds, therapeutic application

Please cite this article in press as: Priyadarshini DR, Beatrice AD, Haokip T. Antioxidant and anti-inflammatory activities of the Black Bean (*Phaseolus vulgaris* L.): A systematic review. Foods and Raw Materials. 2026;14(1):123–137. https://doi.org/10.21603/2308-4057-2026-1-663

INTRODUCTION

Chronic diseases such as diabetes, cardiovascular diseases, and cancer are a significant threat to global health, as they contribute to higher incidence of premature mortality [1]. According to the Global Burden of Disease Study 2021, 529 million people have diabetes worldwide and their number is expected to increase to more than 1.31 billion by the year 2050 [2]. Similarly, the incidence of cardiovascular diseases nearly doubled from 271 million cases in 1990 to 523 million cases in 2019 [3]. Moreover, 10.8 million people died prematurely in 2021 from causes associated with cardiovascular diseases [4]. According to the GLOBOCAN online database, new cancer cases amounted to 20 million in 2022 and their number is expected to reach 35 million by 2050 [5].

The origin of chronic diseases is multifactorial. Oxidative stress, which is considered a common denominator, plays a pivotal role in pathogenesis [6]. Oxidative stress results from the imbalance between production and accumulation of reactive oxygen species in the body [7]. This triggers a chain of adverse events leading to the disruption in cell metabolism and normal functioning of the body. Oxidative stress facilitates the generation of cytokines, thereby causing vascular endothelial activation. Moreover, it promotes the development of defective pancreatic β-cells and inflammation, eventually leading to the onset of chronic diseases [8]. Inflammation is primarily a defense mechanism of the immune system against harmful stimuli and is vital to health. Acute or chronic inflammatory responses in various organ systems perpetuate tissue or organ damage. This leads to oxidative stress, which eventually results

Copyright © 2025, Priyadarshini *et al.* This is an open access article distributed under the terms of the Creative Commons Attribution 4.0 International License (https://creativecommons.org/licenses/by/4.0/), allowing third parties to copy and redistribute the material in any medium or format and to remix, transform, and build upon the material for any purpose, even commercially, provided the original work is properly cited and states its license.

in the onset or aggravation of chronic diseases, becoming a vicious circle [9].

Evidence shows that plant-based dietary patterns are linked with a protective effect against oxidative stress and inflammation [10]. Alongside with that, the rising prevalence of chronic diseases has also led to a surge in societal interest towards the consumption of healthy foods in recent years [11]. Legumes are a main source of plant-based foods, comprising essential nutrients required for maintaining human health [12]. Due to their high protein content, they are considered as a cheap, healthy, and climate-friendly alternative source of proteins rich in micronutrients. The consumption of legumes has numerous health benefits, including the prevention and management of chronic diseases [13–15]. These benefits are more pronounced in varieties with a darker seed coat color such as black, as they contain higher levels of polyphenols and flavonoids, especially anthocyanins [16].

The black bean (*Phaseolus vulgaris* L.) is an important variety of the common bean belonging to the *Fabaceae* family [17]. Black beans are small kidney-shaped seeds with a black coat and a small white spot [18]. They are a rich source of complex carbohydrates with about 50% of total starch and 4.65% of resistant starch [19]. The protein contents in raw and cooked black beans are reported to be 21.6 and 8.86 g/100 g, respectively. They contain all essential amino acids with large amounts of leucine and lysine [20]. The black bean is naturally low in fats and rich in polyunsaturated fatty acids, important for the heart's health [20]. It is also an excellent source of dietary fiber (69.2%), with soluble fiber accounting for only 7.8% [21]. The black bean has a low glycemic index due to its contents of complex carbohydrates, resistant starch, and dietary fiber [14, 22]. With respect to micronutrients, the black bean is a good source of folate and minerals such as calcium, potassium, phosphorus, magnesium, zinc, and iron [20]. Finally, the black bean contains a variety of bioactive compounds, including phenols, flavonoids (anthocyanins), saponins, and phytosterols, which exert antioxidant and anti-inflammatory effects [23–25].

Several studies have explored the antioxidant and anti-inflammatory activities of black beans. However, the diverse literature available on this topic has not been systematized or summarized. Therefore, we aimed to systematically review and summarize the literature on the antioxidant and anti-inflammatory properties of the black bean, seeking to provide valuable insights for clinical applications and future research.

STUDY OBJECTS AND METHODS

Our systematic review followed the Preferred Reporting Items for Systematic Review and Meta-Analysis (PRISMA) guidelines.

Search strategy. An electronic literature search was performed on PubMed, the Directory of Open Access Journals (DOAJ), Google Scholar databases, and the WHO's International Clinical Trial registry platform to find *in vitro*, *in vivo*, and human studies evaluating the antioxidant and anti-inflammatory activities of black beans. The articles published in English before June, 12th, 2024 were filtered using the following Boolean operators: "black bean AND antioxidant activity" and "black bean AND anti-inflammatory activity". Following the recommendation by Bramer *et al.* [26], only the first 200 articles obtained in the Google Scholar search results as per relevance ranking were checked for eligibility.

Eligibility criteria. The research articles were included based on the following inclusion and exclusion criteria. We included full text *in vitro* or *in vivo* studies and human studies, namely randomized controlled trials, non-randomized clinical trials, cross-sectional studies, and cohort studies written in English and assessing the antioxidant and anti-inflammatory activities of the black bean. We excluded the review articles, editorials, or articles written in languages other than English.

Study selection. The literature search yielded 411 research articles. Of them, 28 articles were found to be duplicates and therefore excluded before the screening phase. Some 383 studies were screened, of which only 38 studies matched the inclusion criteria. The numbers of studies identified, screened, and included in the study are presented in a flow chart adapted from PRISMA (Fig. 1).

Quality assessment of included studies. The risk of bias was evaluated using the Quality Assessment Tool for *In Vitro* Studies (QUIN tool) and the Office of Health Assessment and Translation (OHAT) tool for *in vivo* and human studies. Briefly, the QUIN tool uses 12 criteria, namely: 1) clearly stated aims/objectives, 2) detailed explanation of sample size calculation, 3) detailed explanation of sampling technique, 4) details of comparison groups, 5) detailed explanation of methodology, 6) operator details, 7) randomization, 8) method of outcome measurement, 9) outcome assessor details, 10) blinding, 11) statistical analysis, and 12) presentation of results [27]. A score of 2 was given to the articles with adequately specified criteria. A score of 1 was given to the articles that did not specify the criteria adequately. A score of 0 was given to the articles with no specification or with inapplicable criteria. A final score was obtained using the formula [(Total score × 100) / (2 × number of applicable criteria)] for each study to grade their risk of bias as low (> 70%), medium (50–70%), or high (< 50%).

The OHAT tool is a domain-based tool that is used to assess the risk of bias in *in vivo* and human studies [28]. It asks the following questions to identify the following biases:

– *Selection bias*: Was administered dose or exposure level adequately randomized? Was allocation to study groups adequately concealed? Did selection of study participants result in appropriate comparison groups?
– *Confounding bias*: Did the study design or analysis account for important confounding and modifying variables?
– *Performance bias*: Were experimental conditions identical across study groups? Were the research personnel and human subjects blinded to the study group during the study?

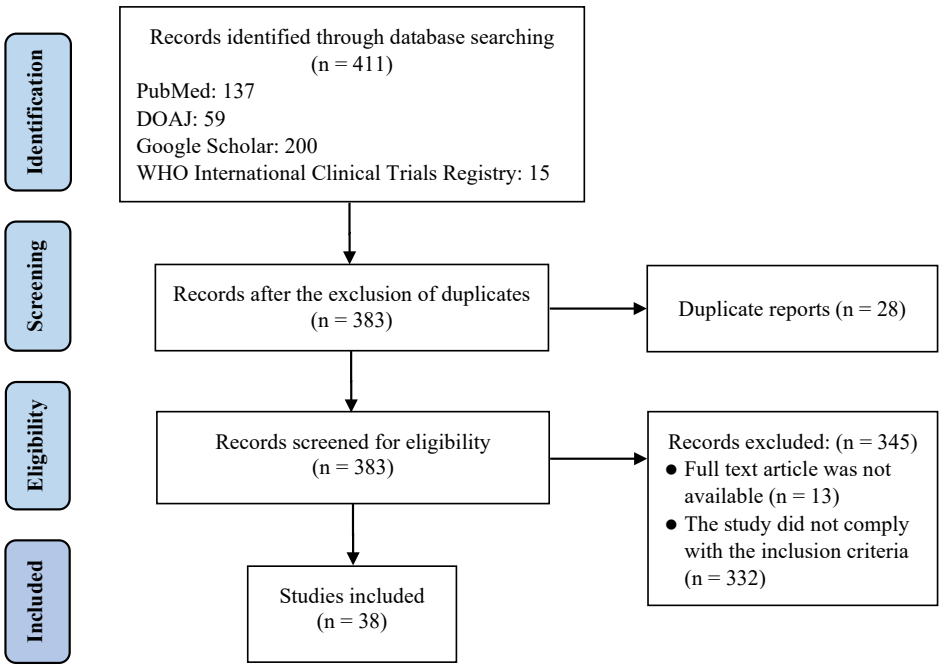

Figure 1 Search strategy flow chart for articles included in this systematic review

– *Attrition/Exclusion bias*: Were outcome data complete without attrition or exclusion from analysis?
– *Detection bias:* Can we be confident in the exposure characterization? Can we be confident in the outcome assessment?
– *Selective reporting bias*: Were all measured outcomes reported?
– *Other bias*: Were there no other potential threats to internal validity (e.g., statistical methods were appropriate and researchers adhered to the study protocol)?

For each question, the risk of bias was rated as "definitely high", "probably high", "probably low", and "definitely low".

RESULTS AND DISCUSSION

Study characteristics. Thirty-eight studies were included in this systematic review, with 32 *in vitro* studies, 5 *in vivo* studies, and 1 human study. Most of these studies were carried out using black beans from Mexico (12 studies), followed by the USA (8 studies), China (4 studies), Canada (3 studies), Portugal and Africa (2 studies each), as well as India, Brazil, Spain, Czech Republic, Malaysia, and France (1 study each).

Risk of bias. Assessing the risk of bias is a crucial component of a systematic review that helps present the quality of included studies and endorses transparency. The QUIN tool used for the *in vitro* studies showed a high risk of bias for 7 studies, a medium risk for 24 studies, and a low risk for 1 study (Table 1). The OHAT tool used for the *in vivo* and human studies showed a low risk of bias, except for 2 studies with a high risk of selection bias (Table 2).

Antioxidant activity. The antioxidant activity of black beans was explored by all 32 *in vitro* studies (Table 3) and one human study (Table 4). Among the *in vitro* studies, 23 studies used whole black bean seeds, 6 used seed coats, 3 used protein hydrolysates, and one study used black bean flour. Black beans were mainly used in the raw form (28 studies), followed by the cooked (boiled – 6 studies, pressure cooked – 5 studies, steamed – 4 studies), germinated (4 studies), and fermented (2 studies) forms. Two studies assessed the impact of retaining or draining the cooking water on the antioxidant activity, while 1 study involved cooking beans without soaking.

According to the results, the black bean demonstrated antioxidant potential regardless of the parts of seed used or the type of processing. Among the bean parts, the seed coat had higher antioxidant activity due to its dark black color [37]. It is a reservoir of bioactive compounds, mainly, anthocyanins, flavonoids, flavonols, and tannins [63], which could have attributed to the stronger antioxidant activity. The proteins extracted from the black bean seeds and subsequently hydrolyzed exhibited significant antioxidant activity against DPPH radicals [29].

With regard to processing techniques, thermal processing of black beans such as boiling, pressure cooking and steaming was found to negatively affect the bioactive compounds and their antioxidant activities, compared to raw beans [43, 47, 56]. However, Teixeira-Guedes *et al.* [64] reported that the retention of cooking water led to increased antioxidant activity. Cooking water, especially boiling water, contains a greater quantity of total polyphenols, as well as higher DPPH and ORAC values [65], so its retention could have contributed to higher antioxidant activity. Confirming this, a recent study by Acito *et al.* [66] found that cooking water had remarkable antioxidant activity against DPPH radical in both boiled and pressure-cooked samples.

Table 1 Risk of bias assessment of *in vitro* studies

Reference	Clearly stated aim/objectives	Detailed explanation of sample size calculation	Detailed explanation of sampling technique	Details of comparison group	Detailed methodology	Operator details	Randomization	Methods of measurement of outcome	Outcome assessor details	Blinding	Statistical analysis	Presentation of results	Total score	Final score/Bias evaluation
[23]	2	0	0	2	2	2	0	2	2	0	2	2	16	66.67% Medium
[25]	2	0	0	2	2	0	0	2	0	0	2	2	12	50.00% Medium
[24]	2	0	0	2	2	0	0	2	0	0	1	2	11	45.83% High
[29]	2	0	0	2	2	2	0	2	2	0	2	2	16	66.67% Medium
[30]	2	0	0	2	2	0	0	2	0	0	0	2	10	41.67% High
[31]	2	0	0	2	2	2	0	2	2	0	2	2	16	66.67% Medium
[32]	2	0	0	2	2	2	0	2	2	0	2	2	16	66.67% Medium
[33]	2	0	0	2	2	0	0	2	0	0	2	2	12	50.00% Medium
[34]	2	0	0	2	2	2	2	2	2	0	2	2	18	75.00% Low
[35]	2	0	0	2	2	2	0	2	2	0	2	2	16	66.67% Medium
[36]	2	0	0	2	2	0	0	2	0	0	2	2	12	50.00% Medium
[37]	2	0	0	2	2	2	0	2	2	0	2	2	16	66.67% Medium
[38]	2	0	0	2	2	2	0	2	2	0	2	2	16	66.67% Medium
[39]	2	0	0	2	2	0	0	2	0	0	2	2	12	50.00% Medium
[40]	2	0	0	2	2	0	0	2	0	0	2	2	12	50.00% Medium
[41]	2	0	0	2	2	0	0	2	0	0	2	2	12	50.00% Medium
[42]	2	0	0	2	2	2	0	2	2	0	2	2	16	66.67% Medium
[43]	2	0	2	2	2	0	0	2	0	0	2	2	14	58.33% Medium
[44]	0	0	0	2	2	0	0	2	0	0	2	2	10	41.67% High
[45]	2	0	0	2	2	0	0	2	0	0	2	2	12	50.00% Medium
[46]	2	0	0	2	2	0	0	2	0	0	2	2	12	50.00% Medium
[47]	2	0	0	2	2	0	0	2	0	0	2	2	12	50.00% Medium
[48]	2	0	2	2	2	0	0	2	0	0	2	2	14	58.33% Medium
[49]	2	0	0	2	2	0	0	2	0	0	2	2	12	50.00% Medium
[50]	2	0	0	2	2	0	0	2	0	0	2	2	12	50.00% Medium
[51]	0	0	0	2	2	0	0	2	0	0	2	2	10	41.67% High
[52]	0	0	0	2	2	0	0	2	0	0	2	2	10	41.67% High
[53]	2	0	0	2	2	0	0	2	0	0	2	2	12	50.00% Medium
[54]	2	0	0	2	2	0	0	2	0	0	2	2	12	50.00% Medium
[55]	0	0	0	2	2	0	0	2	0	0	2	2	10	41.67% High
[56]	2	0	2	2	2	0	0	2	0	0	2	2	14	58.33% Medium
[57]	2	0	0	2	2	0	0	2	0	0	0	2	10	41.67% High

Table 2 Risk of bias assessment of *in vivo* studies and human study

Bias domains	[58]	[19]	[59]	[60]	[61]	[62]
Selection bias						
1 Was administered dose or exposure level adequately randomized?	++	++	++	--	--	++
2) Was allocation to study groups adequately concealed?	--	--	--	--	--	--
3) Did selection of study participants result in appropriate comparison groups?	n.a.	n.a.	n.a.	n.a.	n.a.	n.a.
Confounding bias						
4) Did the study design or analysis account for important confounding and modifying variables?	n.a.	n.a.	n.a.	n.a.	n.a.	n.a.
Performance bias						
5) Were experimental conditions identical across study groups?	++	++	++	++	++	n.a.
6) Were the research personnel and human subjects blinded to the study group during the study?	--	--	--	--	--	--
Attrition/Exclusion bias						
7) Were outcome data complete without attrition or exclusion from analysis?	++	++	--	++	++	--
Detection bias						
8) Can we be confident in the exposure characterization?	++	++	++	++	++	++
9) Can we be confident in the outcome assessment?	++	++	++	++	++	++
Selective reporting bias						
10) Were all measured outcomes reported?	++	++	++	++	++	++
Other bias						
11) Were there no other potential threats to internal validity (e.g., statistical methods were appropriate and researchers adhered to the study protocol)?	++	++	++	++	++	++

n.a. – not applicable; n.r. – not reported; "++" – definitely low; "+" – probably low; "- -" – definitely high; "-" – probably high.

Table 3 *In vitro* studies – antioxidant and anti-inflammatory activities of black beans

Bean sample	Location	Solvent/Extraction	Processing/Part(s)	Bioactive compound(s)	Cell line/ Enzyme/Assay	IC_{50} /Effect/EC_{50}	Main outcomes	References
Black Bean cv. Negro de vaina morada	Mexico	Ethanol/Water	Raw seeds and fractions	Total phenols, total anthocyanins	DPPH ABTS Nitric Oxide iNOS COX-1 COX-2	5.0–120 mg C3GE/L 0.5–150 mg C3GE/L 0.3–147.9 mg C3GE/L 3.34–5.02 mg C3GE/L 0.17–0.82 mg C3GE/L 0.04–1.35 mg C3GE/L	– Raw and raw extract fraction 2 had the strongest antioxidant potential – Raw and purified extract had the highest inhibition against iNOS, while purified extract fraction 2 had the highest inhibition against COX-1 and COX-2	[23]
Black Bean	India	Ethanol, microwave-assisted extraction (MAE) and conventional solvent extraction (CSE)	Raw bean seed hull	Total phenols, flavonoids, anthocyanins	DPPH ABTS	93.51 ± 0.01% (MAE) 85.69 ± 0.03% (CSE) 91.37 ± 0.01% (MAE) 87.74 ± 0.01% (CSE)	MAE had higher antioxidant activity than CSE	[25]
Black Bean cv. San Luis	Mexico	Spray-dried microencapsulation of bean coat flour	Raw bean seed coat flour	Total phenols, flavonoids, and monomeric anthocyanins	ABTS DPPH	31.6 ± .03 mg TE/g 35.1 ± .02 mg GAE/g	– Significant antioxidant activity retained in microcapsules with spray-dried black bean seed coat flour – Lower drying temperature led to greater retention of bioactive compounds	[24]
Black Bean	China	Hexane (Black bean protein hydrolysate – BPH, BPH > 10 kDa, BPH 3–10 kDa BPH < 3 kDa)	Raw bean protein hydrolysate and fractions	Protein hydrolysates	 DPPH ABTS FRAP	Highest activity 67.78 µg/mL (BPH < 3 kDa) 160.03 µg/mL (BPH < 3 kDa) 46.85 µg/mL (BPH 3–10 kDa)	– Black bean protein and its peptide fractions exhibited antioxidant activity – Peptide fraction BPH < 3 kDa had the highest DPPH and ABTS antioxidant activity, while BPH 3–10 kDa had the strongest FRAP activity	[29]
Black Bean	China	Ethanol	Steamed beans fermented with *Cordyceps militaris* (solid state fermentation – SSF)	Total phenols, flavonoids	DPPH ABTS FRAP	4.59 to 25.56% At 4 mg/mL: 91.83% On day 30 of fermentation: 2.81 mM/mL	– Antioxidant activity increased with longer fermentation time	[23]
Black Bean	USA	– Acidified ethanol for phenolic compound extraction – Protein hydrolyses: simulated gastrointestinal digestion assay	Raw, pressure cooked, fermented (SSF: *Bacillus subtilis*) beans protein hydrolysates and phenolic compounds	Protein hydrolysates, total polyphenols (flavonoids, anthocyanins, tannins)	ABTS ROS inhibition	*Protein hydrolysate extract*: 5.7 mg/mL (raw) 27.14 mg/mL (cooked) 10.68 mg/mL (SSF, 48 h) 11.30 mg/mL (SSF, 96 h) *Phenolic compound extract*: 0.322 mg/mL (raw) 0.249 mg/mL (cooked) 0.256 mg/mL (SSF, 48 h) 0.719 mg/mL (SSF, 96 h) *Protein hydrolysate extract*: 3.45 mg/mL (raw) 9.01 mg/mL (cooked) 1.16 mg/mL (SSF, 48 h) 0.63 mg/mL (SSF, 96 h) *Phenolic compound extract*: 2.94 mg/mL (raw) 2.96 mg/mL (cooked) 3.78 mg/mL (SSF, 48 h) not detected (SSF, 96 h)	– SSF protein hydrolysates had higher antioxidant activity (ABTS radical scavenging) than cooked bean and higher ability to inhibit ROS than raw and cooked beans – All phenolic extracts had the ability to scavenge the ABTS radical and inhibit ROS (except for SSF 98 h), with no significant difference between the extracts	[31]

Continuation of Table 3

Bean sample	Location	Solvent/Extraction	Processing/Part(s)	Bioactive compound(s)	Cell line/ Enzyme/Assay	IC_{50} /Effect/EC_{50}	Main outcomes	References
Black Bean var. Turtle	Nigeria, Africa	Water, ethanol, dichloromethane, ethyl acetate, hexane	Raw bean seeds	Total phenols, flavonoids, and anthocyanins	DPPH FRAP ABTS	12.54 ± 2.30 – 26.12 ± 4.94 mg/mL 80.78 ± 0.60 – 789.87 ± 4.30 mg/mL 5.69 ± 2.86 – 13.24 ± 3.60 mg/mL	– Ethanol extract showed the strongest inhibition against DPPH radical and the highest reducing capacity (FRAP), while dichloromethane extract exhibited the strongest inhibition against ABTS radical	[32]
Black Bean cv. Negro Jamapa	Mexico	Methanol	Raw and cooked (boiled) seeds	Total polyphenols	TEAC & ABTS Murine macrophages	Two-fold increase after cooking Decreased expression of IL6 by 20% at 100 µg/mL Decreased expression of IL1β by 16% and iNOS by 35% at 100 µg/mL	– Stronger antioxidant activity after cooking – Moderate anti-inflammatory activity after cooking	[33]
Black Bean	Spain	Aqueous, Methanol extract	Raw bean seeds	Total phenols, flavonoids, monomeric anthocyanins	FRAP DPPH PAOXI	42.3 ± 11.3 µmol Fe (II)/g 17.4 ± 5.1 µmol TE/g 18.1 ± 2.7	Stronger antioxidant activity correlated with total phenolic content	[34]
Black Bean	Mexico	Supercritical fluid (SFE), leaching extract	Raw bean seed coat	Total phenols, anthocyanins	DPPH ABTS	0.32 mg GAE/g coat 0.40 mg GAE/g coat	Purified SFE had stronger inhibitory potential against DPPH and ABTS radical than pure leached extract	[35]
Black Bean	Czech Republic	Hydrogen peroxide	Raw beans and Germinated beans seed flakes	Methionine and phytic acid	DPPH FRAP	16.6 ± 6.1%/100g (raw) 6.3 ± 0.6%/100g (germinated) 11.4 ± 0.2%/100g (raw) 6.0 ± 0.3%/100g (germinated)	Thermal exposure during flaking process led to lowered antioxidant activity in germinated bean flakes than raw beans	[36]
Black Bean	Portugal	Methanol:water extract	Raw bean flour	Total phenols, ortho-diphenols, flavonoids, tannins, phytic acid	DPPH ABTS FRAP	9.37–10.47 µmol TE/g 13.99–20.72 µmol TE/g 13.33–20.97 µmol TE/g	Significantly higher antioxidant activity due to black seed coat color	[37]
Black Bean cv. San Luis	Mexico	Ethanol:distilled water, leaching process (LEA), pressurized-liquid extraction (PLE), supercritical CO_2 extraction (SFE)	Raw seeds	Anthocyanins, non-colored phenols, total phenols	DPPH ABTS	0.078 ± 0.010 mg C3GE/g coat 0.161 ± 0.030 mg C3GE/g coat	SFE extract exhibited stronger antioxidant activity than other extracts	[38]
Black Bean	Portugal	Methanol:Water extract	Raw, boiled, boiled/drained, pressure cooked, pressure cooked/drained	Total phenols, flavonoids, ortho-diphenols	DPPH ABTS FRAP	2.29–8.88 µmol TEq/g dw 0.63–2.22 µmol TEq/g dw 4.24–15.70 µmol TEq/g dw	Retention of cooking water led to increased antioxidant activity	[39]
Black Bean	Cameroon, Africa	Hexane	Raw	Amino acids	FRAP DPPH Hydroxyl free radical	23.12 ± 0.10 mg Fe (II)/100g 10.76 ± 1.50 mg/mL 2.04 ± 0.10 mg/mL	Excellent antioxidant activity	[40]

Bean sample	Location	Solvent/Extraction	Processing/Part(s)	Bioactive compound(s)	Cell line/ Enzyme/Assay	IC_{50} /Effect/EC_{50}	Main outcomes	References
Black Bean var. Turtle	USA	Aqueous	Raw, cooked (steamed) beans and their fractions	Total phenols, flavonoids, condensed tannins	DPPH	12.1 ± 0.3 – 4259.8 ± 20.1 µmol TE/g (raw and fractions) 18.4 ± 1.1 – 4343.8 ± 7.3 µmol TE/g (cooked and fractions) 67.9 ± 1.7 – 7355.2 ± 146.6 µmol TE/g (raw and fractions)	– In raw samples, seed and fraction 1 extracts had the highest inhibition against DPPH radical, while seed and crude extracts had thestrongest antioxidant activity (ORAC value) – In cooked samples, seed and crude extracts had the strongest antioxidant activity (DPPH and ORAC)	[41]
					ORAC	42.0 ± 1.1 – 6864.2 ± 34.5 µmol TE/g (cooked and fractions)		
Black Bean	Mexico	80% Methanol	Raw seeds	Total phenols, flavonoids and anthocyanins	DPPH FRAP	40% (approx.) 0.12%	Black beans had lower radical scavenging capacity and medium reducing antioxidant power, compared to other bean varieties (Flor de mayo, Bayo, Frijola, Patola, Navy Bean, Flor de junio, Reata Bean, and Japanese Bean)	[42]
Black Bean (Organic and inorganic beans)	Malaysia	Ethanol extract	Raw, cooked without soaking, cooked after soaking	Total phenols	Effect DPPH ABTS FRAP	 411.41–1965.03 µmol TE/100 g 1206.84–3923.68 µmol TE/100 g 457.53–2945.09 µmol TE/100 g	– Cooking beans after soaking led to greater reduction in antioxidant capacity compared to beans cooked without soaking – No difference in organic and inorganic beans for antioxidant capacity – Total phenolic content showed significant correlation with antioxidant activity	[43]
Black Bean cv. San Luis	Mexico	Enzymatic digestion and hydrolysis (h)	Raw and germinated beans cotyledons	Protein hydrolysates	ORAC	1769 µmol TE/g (raw) 1604 µmol TE/g (germinated) 1383 µmol TE/g (raw-h) 1451 µmol TE/g (germinated -h) > 60 units for all extracts	– ORAC: Raw and germinated (day 1) extracts had higher antioxidant activity than hydrolyzed extracts – CAA: No significant differences between extracts; germinated hydrolysate had the highest CAA at 120 min – Nitric oxide: Significant inhibition by germinated and hydrolysate extracts	[44]
					CAA	23% at 120 min, 34% at 180 min (raw) 55% at 120 min, 73% at 180 min (germinated)		
					Nitric oxide	90% at 60 min (germinated-h)		
Black Bean	Brazil	Protein extraction (BBPC) Protein hydrolysis for 120 min by pepsin (BBPHP) and by alcalase (BBPHA)	Raw seeds – protein hydrolysates	Protein hydrolysates	DPPH	BBPC – 39.45 ± 0.77 BBPHP – 45.15 ± 0.93 BBPHA – 37.15 ± 0.27	BBPHA showed stronger DPPH radical scavenging potential, while BBPHP had higher potential to inhibit ABTS radical	[45]
					ABTS	BBPC – 55.32 ± 0.08 BBPHP – 47.04 ± 0.46 BBPHA – 63.56 ± 0.44		
Black Bean	China	Acetone extract	Germinated seeds	Total phenols, total flavonoids	Total reducing power	133.3%	Strong antioxidant activity with major contribution from the total phenols and flavonoids contents	[46]
					Hydroxyl radical scavenging	62.5% (approx.)		
					Relative DPPH	78.6%		
					ABTS	90.1%		

Bean sample	Location	Solvent/Extraction	Processing/Part(s)	Bioactive compound(s)	Cell line/ Enzyme/Assay	IC_{50} /Effect/EC_{50}	Main outcomes	References
Black Bean	France	Acetone extract	Raw and cooked (pressure) bean seeds	Total polyphenols, flavonoids, anthocanins	DPPH PAOXI	EC_{50} 4.346–14.528 mg/mL 10.709–23.003	Black bean had excellent antioxidant capacity; marginal reduction in antioxidant activity after cooking	[47]
Black Bean	Mexico	Methanol and ethanol extract	Raw bean seed coat	Total phenols, tannins, flavonoids, anthocyanins, non-colored phenols	ORAC Nitric oxide radical scavenging assay	215–223.4 µmol TE/g 52.83–53.08 /g coat	Excellent antioxidant capacity	[48]
Black Bean cv. San Luis	Mexico	80% aqueous methanol	Raw, soaked and germinated sprouts, cotyledons and seed coat	Total phenols, flavonoids, and saponins	ORAC	9.7–27.0 µmol TE/g (sprouts) 11.1–95.8 µmol TE/g (cotyledons) 132.4–580.0 µmol TE/g (seed coat)	– Sprouts: Soaking/germination did not affect antioxidant capacity – Cotyledons: Reduced antioxidant capacity after germination – Seed coat: The strongest antioxidant capacity after germination with maximum value on day 3	[49]
Black Bean cv. Turtle eclipse	USA	Acetone:water:acetic acid	Raw seeds	Total phenols, procyanidin, saponin, phytic acid	DPPH ORAC Peroxyl radical scavenging Cellular antioxidant	19.4 µmol TE/g 92.7 µmol TE/g 67.9 µmol TE/g 0.64 mg/mL	Excellent antioxidant potential	[50]
Black Bean	USA	Methanol	Raw seed	Total anthocyanins, total polyphenols	DPPH	Percentage 17.09–32.79%	Antioxidant activity attributed to high anthocyanin and polyphenol contents	[51]
Black Bean	USA	Acetone:water:acetic acid	Raw, regular boiling, regular steaming, pressure boiling and pressure steaming seeds	Total phenols, saponins, phytic acid	Cellular antioxidant	0.63 mg/mL	Cellular antioxidant activity of cooked beans reduced due to thermal processing	[52]
Black Bean cv. Cotaxtla	Mexico	Lyophilization with cooking broth and its total indigestible fraction	Cooked (boiling) seeds	Non-digestible fraction, condensed tannins, total phenols	Radical scavenging	Effect (µmol/L TE/g dry sample) 13.2 ± 0.0 (cooked) 6.6 ± 0.1 (indigestible fraction)	Indigestible fraction exhibited stronger antioxidant potential than cooked seeds	[53]
Black Bean cv. Cotaxtla	Mexico	Methanol	Cooked (boiling) seeds	Polyphenols, anthocyanins	DPPH	15–20% within 60 min	Excellent antioxidant activity	[54]
Black Bean ac. Violet	Canada	Aqueous, acetone – bean hull extract	Raw bean hulls	Phenolic compounds	ORAC COX LOX enzyme inhibition	18.14–282.25 mg/g IC_{50} COX1: 1.2–52.7 µg/mL COX2: 38–188.5 µg/mL COX1/COX2: 0.03–0.28 IC_{50} 186.9 µg/mL	Bean hulls had stronger antioxidant and anti-inflammatory capacity	[55]

Bean sample	Location	Solvent/Extraction	Processing/Part(s)	Bioactive compound(s)	Cell line/ Enzyme/Assay	IC_{50} /Effect/EC_{50}	Main outcomes	References
Black Bean var. Turtle Eclipse	USA	Acetone: water: acetic acid extract Raw, regular boiling, pressure boiling, regular steaming, pressure steaming processing	Raw, regular boiling, regular steaming, pressure boiling and pressure steaming of seeds	Total phenols, flavonoids, total condensed tannins, monomeric anthocyanins	DPPH FRAP ORAC	Boiling reduced antioxidant activity by 46% Boiling reduced antioxidant activity by 72% Boiling reduced antioxidant activity by 70–82%; Steaming preserved antioxidant activities at $p < 0.05$	Thermal processing affected bioactive compounds and their antioxidant activities	[56]
Black Bean	USA	Acetone	Raw seed coat	Triterpenoids, phenols, and flavonoids	Peroxyl radical scavenging	8.11–6.11 μM	Raw seed coats of black beans exhibited significant antioxidant activity	[57]

DPPH radical scavenging assay (DPPH); ABTS radical scavenging assay (ABTS); Ferric Reducing Antioxidant Power assay (FRAP); Nitric Oxide inhibition assay (Nitric Oxide); Trolox Equivalent Antioxidant Capacity (TEAC); Oxygen Radical Absorbance Capacity (ORAC); Cellular Antioxidant Activity (CAA); Cyclooxygenase isoenzymes (COX); Inducible Nitric Oxide Synthase (iNOS).

Table 4 Human study – antioxidant and anti-inflammatory activities of black beans

Bean sample	Participant characteristics			Study design	Study setting	Intervention		Parameters	Main outcomes	References
	Gender	Age	Sample Size			Form	Duration			
Black Bean	Male, Female	18 and above	12 with metabolic syndrome	Randomized controlled crossover trial	USA	Black bean meals (BB) Fiber matched meals (FM) Antioxidant matched meals (AM)	3 study days with 1-week washout period between meals	Metabolic syndrome criteria (AHA, 2014), food record, BMI, serum lipids (TG, TC), hsCRP, IL-6, IL-1β, sICAM 1, sVCAM1, serum glucose, serum insulin, HOMA IR, HOMA βcell, Quantitative IS check index, G:I ratio, OxLDL, total ORAC	– Significant decrease in insulin after BB meals compared to others – Significant meal time interaction for plasma antioxidant capacity – AM > BM > FM – Increased TG, increased IL-6 at $p < 0.0001$ after all meals – Lower trend of OxLDL after BB and AM meals	[62]

Table 5 *In vivo* studies – antioxidant and anti-inflammatory activities of black beans

Bean sample	Location	Animal characteristics			Intervention			Main outcomes	References
		Type	Gender	Age	Sample size	Diet	Duration	Parameters/Analysis	
Black Bean var. Turtle	USA	C57BL/6J	Male	NA	n = 24 (8 in each group)	High fat diet (HF) – 46% energy from fat; HF + cooked black turtle bean (HFB) –20%; Low fat diet (LF) – 16% energy from fat	6 weeks	Inflammatory cytokines (IL-2, IL-4, IL-5, IL-12, GM-CSF, IFN-g and TNFα) and IL-10	Reduction in all inflammatory and anti-inflammatory cytokine after HFB diet	[58]
Black Bean	Mexico	Wistar rats	Male	6 weeks	n = 36 (6 in each diet group)	Casein (C); Black bean protein concentrate (BPC); Whole cooked black bean flour (WCB); C + high fat sucrose (HFS at 5% sucrose); BPC + HFS; WCB + HFS	10 weeks	Body composition, energy expenditure, glucose tolerance, insulin, liver cholesterol and triglyceride levels, histological analysis, gene expression analysis (SREBP 1c, FAS, PPARα, CPT-1, TNFα), western blot analysis	– BPC/WCB reduced body weight and body fat, even with HFS diet – Increased energy expenditure, lower glucose, insulin and lipogenic genes. Normal glucose tolerance – BPC + HFS: reduced SREBP 1c by 63%, FAS by 80% and TNFα by 49%; increased PPARα by 58% and CPT-1 by 110% – WCB + HFS: decreased SREBP 1c 2-fold, FAS 5.7-fold and TNFα by 61.1%; increased PPARα 1.5-fold and CPT-1 1.9-fold	[19]
Black Bean, Navy Bean	Canada	C57BL/ 6 mice	Male	4 weeks	n = 36 (12 in each diet group)	AIN-93G diet with soybean oil and 7% cellulose – Basal diet (BD); BD + BB (20%); BD + NB (20%)	3 weeks	Colon histology and immunohistochemistry, colon mRNA expression, colon cytokine and chemokine analysis, colon transcription factor activation and GTPase activity assay, body weight, food intake, water intake	Colon priming potential, both beans reduced colitis induced inflammation and prevented colitis-associated epithelial damage, no significant difference in body weight, food intake, water intake	[59]
Black Bean Peal (BBE), Pomegranate Peal (PPE)	China	Kunming mice	Male	NA	n = 35 (control diabetes mellitus (DM) – 8; BBE – 6, PPE – 6; BBE + PPE – 6; normal control mice (NS) – 9)	DM – 1% CMC solution; BBE (40% anthocyanins); PPE (40% total polyphenols); BBE+PPE; NS – 1% CMC	4 weeks	GSH levels and total antioxidant capacity (T-AOC) using FRAP assay of plasma	GSH levels and T-AOC levels increased in all three treatment groups, while BBE+PPE had the highest antioxidant activity	[60]
Black Bean, Navy Bean	Canada	C57BL/6 mice	Male	5 weeks	n = 52 (BD-26, BB-13, NB-13)	Isoenergetic BD; BD + BB (20%); BD + NB (20%)	3 weeks	Inflammatory cytokines, Il-10, chemokines (C-X-C motif) ligand 1 (Cxcl1) and Cxcl5, Toll-like receptor 4 (Tlr4) and Fas ligand (FasL)	– Lowered mRNA expression of IL-6, IL-9, IFN-γ, IL-17A, IL-1 β, TNFα, and chemokines after both beans diet – Increased expression of IL-10, IL-8, Tlr4, and FasL was upregulated after both beans diet	[61]

Carboxymethyl Cellulose (CMC); Sterol Regulatory Element-Binding Protein (SREBP 1c); Fatty Acid Synthase (FAS); Peroxisome Proliferator-Activated Receptor (PPARα); Carnitine Palmitoyl Transferase-1 (CPT-1), Tumor Necrosis Factor – TNFα.

The antioxidant activity of germinated black beans was found to vary depending on different parts of the seed. Guajardo-Flores *et al.* [49] reported that the germinated seed coats had stronger antioxidant capacity than the germinated cotyledons. In another study by Lopez-Barrios *et al.* [44], the cotyledons germinated for 1 day had higher antioxidant capacity (ORAC, cellular antioxidant activity and nitric oxide inhibition) than those germinated for longer duration (day 2 to day 5). This stronger activity can be attributed to increased total phenols and flavonoids resulting from germination [46]. By contrast, Viktorinova *et al.* [36] found lower antioxidant activity in germinated black bean flakes. This could be because the thermal exposure during the flaking process lowered bioactive compounds and subsequently reduced the antioxidant activity. Fermentation, on the other hand, was reported to be effective in increasing the antioxidant capacity of black beans [31]. Liu *et al.* [30] found that the antioxidant activity increased with longer fermentation time. Toor *et al.* [67] noted that fermentation increased total phenols in legumes, leading to better antioxidant activity.

In adults with metabolic syndrome, the consumption of black bean meal was reported to cause significant plasma antioxidant activity [62]. This potential of black beans is primarily attributed to their rich bioactive compounds, namely phenols, flavonoids, condensed tannins, phytic acid, and saponins [23–25, 37, 50]. These compounds are involved in such mechanisms as hydrogen atom transfer, single electron transfer, sequential proton loss electron transfer, and chelation of transition metals. They can also decrease enzymatic activity of oxidases (such as xanthine oxidase) and stimulate enzymes (such as superoxide dismutase, glutathione peroxidase, and catalase), thereby eventually reducing free radicals and oxidants [68].

Anti-inflammatory activity. The anti-inflammatory activity of black beans was explored by three *in vitro* studies (Table 3), all five *in vivo* studies (Table 5), and one human study (Table 4). Among the *in vitro* studies, two used whole black bean seeds and one used the seed coats. The form was raw in two *in vitro* studies and cooked (boiled) in one study. The *in vivo* studies used C57BL/6 mice (three studies), Kunming mice (one study) and Wistar rats (one study). Three studies used whole cooked black beans at different amounts, one study administered black bean protein concentrate, and one study used black bean peel extract with 40% anthocyanins. The duration of the *in vivo* studies ranged between 3 to 10 weeks.

As for the *in vitro* studies, Oomah *et al.* [55] reported excellent inhibitory potential of black beans (*Phaseolus vulgaris* L.) whose anti-inflammatory activity was investigated via the Cox and Cox enzyme inhibition assay. A recent study by Contreras *et al.* [23] also found that the raw and purified black bean extracts showed the highest inhibition against the enzymes related to inflammation, namely iNOS, COX-1, and COX-2. Perez-Hernandez *et al.* [33] reported that the raw and boiled extracts of black bean seeds decreased the expression of IL6 by 20% and IL1β by 35% at 100 µg/mL in murine macrophages, thereby exhibiting moderate anti-inflammatory activity.

The *in vivo* studies also showed the anti-inflammatory activity of black beans [19, 58–61]. According to Monk *et al.* [59], male C57 BL/6 mice that had consumed a black bean diet for 3 weeks showed lower colitisinduced inflammation and no colitis-associated epithelial tissue damage, which highlighted the anti-inflammatory and colon priming potential of black beans. In another study by Sanchez-Tapia *et al.* [69], male Wistar rats had lower NF-kB protein in the colon after a black bean diet. This transcription factor is the central mediator of inflammation, so its reduction is beneficial. A recent study by Tan *et al.* [58] also reported a significant reduction in all inflammatory and anti-inflammatory cytokines in C57BL/6J male mice whose high fat diet was supplemented with black beans (20%).

The beneficial antiinflammatory effect of black beans is attributed to the polyphenols that improve inflammation-induced intestinal barrier dysfunction [70]. Besides, Rivera-Jimenez *et al.* [71] stated that peptides and protein hydrolysates also contribute to the anti-inflammatory effects.

However, the human-randomized, control, crossover trial showed no significant increase in the pleiotropic proinflammatory cytokine IL-6 (Interleukin-6) after a single black bean meal [62]. Further long-term studies are needed to extensively explore the black bean as an anti-inflammatory agent and to shed a clear light on the reported association.

CONCLUSION

Black beans evidently exhibit excellent antioxidant and anti-inflammatory activities due to their rich and diverse bioactive compounds.

Future studies should focus on assessing the long-term effects of black beans on adults with, or at risk of, diabetes, cardiovascular diseases, or cancer. More research is needed to explore the potential of germinated and fermented black beans.

CONFLICT OF INTEREST

The authors declare that there is no conflict of interest related to this publication.

CONTRIBUTION

D. R. Priyadarshini conceptualized the research, designed the study methods, and wrote the manuscript. A. D. Beatrice was involved in the conceptualization, visualization, reviewing, supervision, and editing of the manuscript. T. Haokip designed the study methods and performed the reviewing.

ACKNOWLEDGMENT

The authors would like to thank the Principal of Women's Christian College, Chennai, India for her constant support and encouragement.

REFERENCES

1. Malta DC, Duncan BB, Schmidt MI, Teixeira R, Ribeiro ALP, Felisbino-Mendes MS, *et al.* Trends in mortality due to non-communicable diseases in the Brazilian adult population: National and subnational estimates and projections for 2030. Population Health Metrics. 2020;18:16. https://doi.org/10.1186/s12963-020-00216-1
2. Global, regional, and national burden of diabetes from 1990 to 2021, with projections of prevalence to 2050: A systematic analysis for the Global Burden of Disease Study 2021. The Lancet. 2023;402(10397):203–234. https://doi.org/10.1016/S0140-6736(23)01301-6
3. Roth GA, Mensah GA, Johnson CO, Addolorato G, Ammirati E, Baddour LM, *et al.* Global burden of cardiovascular diseases and risk factors, 1990-2019: Update from the GBD 2019 study. Journal of the American College of Cardiology. 2020;76(25):2982–3021. https://doi.org/10.1016/j.jacc.2020.11.010
4. Vaduganathan M, Mensah GA, Turco JV, Fuster V, Roth GA. The global burden of cardiovascular diseases and risk: A compass for future health. Journal of the American College of Cardiology. 2022;80(25):2361–2371. https://doi.org/10.1016/j.jacc.2022.11.005
5. Bray F, Laversanne M, Sung H, Ferlay J, Siegel RL, Soerjomataram I, *et al.* Global cancer statistics 2022: GLOBOCAN estimates of incidence and mortality worldwide for 36 cancers in 185 countries. CA: A Cancer Journal for Clinicians. 2024;74(3):229–263. https://doi.org/10.3322/caac.21834
6. Jomova K, Raptova R, Alomar SY, Alwasel SH, Nepovimova E, Kuca K, *et al.* Reactive oxygen species, toxicity, oxidative stress, and antioxidants: Chronic diseases and aging. Archives of Toxicology. 2023;97:2499–2574. https://doi.org/10.1007/s00204-023-03562-9
7. Pizzino G, Irrera N, Cucinotta M, Pallio G, Mannino F, Arcoraci V, *et al.* Oxidative stress: Harms and benefits for human health. Oxidative Medicine and Cellular Longevity. 2017;2017(1). https://doi.org/10.1155/2017/8416763
8. Leyane TS, Jere SW, Houreld NN. Oxidative stress in ageing and chronic degenerative pathologies: Molecular mechanisms involved in counteracting oxidative stress and chronic inflammation. International Journal of Molecular Sciences. 2022;23(13):7273. https://doi.org/10.3390/ijms23137273
9. Furman D, Campisi J, Verdin E, Carrera-Bastos P, Targ S, Franceschi C, *et al.* Chronic inflammation in the etiology of disease across the life span. Nature Medicine. 2019;25:1822–1832. https://doi.org/10.1038/s41591-019-0675-0
10. Aleksandrova K, Koelman L, Rodrigues CE. Dietary patterns and biomarkers of oxidative stress and inflammation: A systematic review of observational and intervention studies. Redox Biology. 2021;42:101869. https://doi.org/10.1016/j.redox.2021.101869
11. Baker MT, Lu P, Parrella JA, Leggette HR. Consumer acceptance toward functional foods: A scoping review. International Journal of Environmental Research and Public Health. 2022;19(3):1217. https://doi.org/10.3390/ijerph19031217
12. Ding Y, Ban Q, Wu Y, Sun Y, Zhou Z, Wang Q, *et al.* Effect of high hydrostatic pressure on the edible quality, health and safety attributes of plant-based foods represented by cereals and legumes: A review. Critical Reviews in Food Science and Nutrition. 2023;63(20):4636–4654. https://doi.org/10.1080/10408398.2021.2005531
13. Sharif HR, Williams PA, Sharif MK, Abbas S, Majeed H, Masamba KG, *et al.* Current progress in the utilization of native and modified legume proteins as emulsifiers and encapsulants – A review. Food Hydrocolloids. 2018;76:2–16. https://doi.org/10.1016/j.foodhyd.2017.01.002
14. Lukus PK, Doma KM, Duncan AM. The role of pulses in cardiovascular disease risk for adults with diabetes. American Journal of Lifestyle Medicine. 2020;14(6):571–584. https://doi.org/10.1177/1559827620916698
15. Angeles JGC, Villanueva JC, Uy LYC, Mercado SMQ, Tsuchiya MCL, Lado JP, *et al.* Legumes as functional food for cardiovascular disease. Applied Sciences. 2021;11(12):5475. https://doi.org/10.3390/app11125475
16. Jaiswal SK, Dakora FD. Seed-coat pigmentation plays a crucial role in partner selection and N_2 fixation in legume-root–microbe associations in african soils. Plants. 2024;13(11):1464. https://doi.org/10.3390/plants13111464
17. Meenu M, Chen P, Mradula M, Chang SKC, Xu B. New insights into chemical compositions and health-promoting effects of black beans (*Phaseolus vulgaris* L.). Food Frontiers. 2023;4(3):1019–1038. https://doi.org/10.1002/fft2.246
18. Melini F, Lisciani S, Camilli E, Marconi S, Melini V. Effect of cooking on phenolic compound content and in vitro bioaccessibility in sustainable foods: A case study on black beans. Sustainability. 2024;16(1):279. https://doi.org/10.3390/su16010279
19. Hernandez-Velazquez I, Sanchez-Tapia M, Ordaz-Nava G, Torres N, Tovar AR, Galvez A. Black bean protein concentrate ameliorates hepatic steatosis by decreasing lipogenesis and increasing fatty acid oxidation in rats fed a high fat-sucrose diet. Food and Function. 2020;11:10341–10350. https://doi.org/10.1039/d0fo02258f
20. Beans, black turtle, mature seeds, raw [Internet]. [cited 2024 May 3]. Available from: https://fdc.nal.usda.gov/fdc-app.html#/food-details/175186/nutrients

21. Feng Z, Dou W, Alaxi S, Niu Y, Yu L. Modified soluble dietary fiber from black bean coats with its rheological and bile acid binding properties. Food Hydrocolloids. 2017;62:94–101. https://doi.org/10.1016/j.foodhyd.2016.07.032
22. Thompson SV, Winham DM, Hutchins AM. Traditional bean and rice meals reduce postprandial glycemia in adults with type 2 diabetes: A cross-over study. Nutrition Journal. 2012;11:23. https://doi.org/10.1186/1475-2891-11-23
23. Contreras J, Alcázar-Valle M, Lugo-Cervantes E, Luna-Vital DA, Mojica L. Mexican native black bean anthocyanin-rich extracts modulate biological markers associated with inflammation. Pharmaceuticals. 2023;16(6):874. https://doi.org/10.3390/ph16060874
24. Cruz-Bravo RK, Guajardo-Flores D, Gómez-Aldapa CA, Castro-Rosas J, Navarro-Cortez RO, Díaz-Batalla L, *et al.* Spray-dried microencapsulation of bean coat flour (*Phaselus vulgaris*, L.) bioactive compounds: optimization, functional activity, and storage. CYTA – Journal of Food. 2023;21(1):493–501. https://doi.org/10.1080/19476337.2023.2226186
25. Mali PS, Kumar P. Optimization of microwave assisted extraction of bioactive compounds from black bean waste and evaluation of its antioxidant and antidiabetic potential in vitro. Food Chemistry Advances. 2023;3:100543. https://doi.org/10.1016/j.focha.2023.100543
26. Bramer WM, Rethlefsen ML, Kleijnen J, Franco OH. Optimal database combinations for literature searches in systematic reviews: A prospective exploratory study. Systematic Reviews. 2017;6:245. https://doi.org/10.1186/s13643-017-0644-y
27. Sheth VH, Shah NP, Jain R, Bhanushali N, Bhatnagar V. Development and validation of a risk-of-bias tool for assessing in vitro studies conducted in dentistry: The QUIN. The Journal of Prosthetic Dentistry. 2024;131(6):1038–1042. https://doi.org/10.1016/j.prosdent.2022.05.019
28. Handbook for conducting a literature-based health assessment using ohat approach for systematic review and evidence integration [Internet]. [cited 2024 May 3]. Available from: https://ntp.niehs.nih.gov/whatwestudy/assessments/noncancer/handbook/index.html
29. Chen Y, Zheng Z, Ai Z, Zhang Y, Tan CP, Liu Y. Exploring the antioxidant and structural properties of black bean protein hydrolysate and its peptide fractions. Frontiers in Nutrition. 2022;9:884537. https://doi.org/10.3389/fnut.2022.884537
30. Liu W, Dun M, Liu X, Zhang G, Ling J. Effects on total phenolic and flavonoid content, antioxidant properties, and angiotensin I-converting enzyme inhibitory activity of beans by solid-state fermentation with *Cordyceps militaris*. International Journal of Food Properties. 2022;25(1):477–491. https://doi.org/10.3389/fnut.2022.884537
31. Flores-Medellín SA, Camacho-Ruiz RM, Guízar-González C, Rivera-Leon EA, Llamas-Covarrubias IM, Mojica L. Protein hydrolysates and phenolic compounds from fermented black beans inhibit markers related to obesity and type-2 diabetes. Legume Science. 2021;3(1):e64. https://doi.org/10.1002/leg3.64
32. Abdulrahman BO, Bala M, Bello OM. Evaluation of *in vitro* antioxidant and antidiabetic potential of extracts from *Phaseolus vulgaris* L. seeds (Black turtle beans). Functional Food Science. 2021;1(9):23–38. https://doi.org/10.31989/ffs.v1i9.821
33. Perez-Hernandez LM, Hernández-Álvarez AJ, Morgan M, Boesch C, Orfila C. Polyphenol bioaccessibility and anti-inflammatory activity of Mexican common beans (*Phaseolus vulgaris* L.) with diverse seed colour. CYTA – Journal of Food. 2021;19(1):682–690. https://doi.org/10.1080/19476337.2021.1965660
34. Rodriguez Madrera R, Campa Negrillo A, Suárez Valles B, Ferreira Fernández JJ. Phenolic content and antioxidant activity in seeds of common bean (*Phaseolus vulgaris* L.). Foods. 2021;10(4):864. https://doi.org/10.3390/foods10040864
35. Hernandez DF, Orozco-Avila I, Lugo-Cervantes E, Mojica L. Black bean (Phaseolus vulgaris L.) phenolic extract exhibits antioxidant and anti-aging potential. Current Developments in Nutrition. 2020;4. https://doi.org/10.1093/cdn/nzaa040_024
36. Viktorinová K, Petřeková K, Šimek J, Hartman I, Hertel V. Nutrition and sensory evaluation of germinated legumes. Kvasny Prumysl. 2020;66(3):270–276. https://doi.org/10.18832/kp2019.66.270
37. Carbas B, Machado N, Oppolzer D, Ferreira L, Queiroz M, Brites C, *et al.* Nutrients, antinutrients, phenolic composition, and antioxidant activity of common bean cultivars and their potential for food applications. Antioxidants. 2020;9(2):186. https://doi.org/10.3390/antiox9020186
38. Hsieh-Lo M, Castillo-Herrera G, Mojica L. Black bean anthocyanin-rich extract from supercritical and pressurized extraction increased *in vitro* antidiabetic potential, while having similar storage stability. Foods. 2020;9(5):655. https://doi.org/10.3390/foods9050655
39. Teixeira JE, Bragada JA, Bragada JP, Coelho JP, Pinto IG, Reis LP, *et al.* Structural equation modelling for predicting the relative contribution of each component in the metabolic syndrome status change. International Journal of Environmental Research and Public Health. 2022;19(6):3384. https://doi.org/10.3390/ijerph19063384

40. Nkenmeni DC, Kotue TC, Kumar P, Djouhou FM, Ngo SF, Pieme AC, *et al.* HPLC profiling, *in vitro* antisickling and antioxidant activities of phenolic compound extracts from black bean seeds (*Phaseolus vulgarus* L.) used in the management of sickle cell disease in the West Region of Cameroon. International Journal of Food and Nutrition Research. 2019;3:30. https://doi.org/10.28933/ijfnr-2019-08-0105

41. Zhang Y, Pechan T, Chang SKC. Antioxidant and angiotensin-I converting enzyme inhibitory activities of phenolic extracts and fractions derived from three phenolic-rich legume varieties. Journal of Functional Foods. 2018;42:289–297. https://doi.org/10.1016/j.jff.2017.12.060

42. Herrera-Hernández IM, Armendáriz-Fernández KV, Muñoz-Márquez E, Sida-Arreola JP, Sánchez E. Characterization of bioactive compounds, mineral content and antioxidant capacity in bean varieties grown in semi-arid conditions in Zacatecas, Mexico. Foods. 2018;7(12):199. https://doi.org/10.3390/foods7120199

43. Mastura YH, Hasnah H, Dang TN. Total phenolic content and antioxidant capacity of beans: Organic vs inorganic. International Food Research Journal. 2017;24(2):510–517.

44. López-Barrios L, Antunes-Ricardo M, Gutiérrez-Uribe JA. Changes in antioxidant and antiinflammatory activity of black bean (*Phaseolus vulgaris* L.) protein isolates due to germination and enzymatic digestion. Food Chemistry. 2016;203:417–424. https://doi.org/10.1016/j.foodchem.2016.02.048

45. do Evangelho JA, Berrios JJ, Pinto VZ, Antunes MD, Vanier NL, Zavareze ER. Antioxidant activity of black bean (*Phaseolus vulgaris* L.) protein hydrolysates. Food Science and Technology. 2016;36:23–27. https://doi.org/10.1590/1678-457X.0047

46. Xue Z, Wang C, Zhai L, Yu W, Chang H, Kou X, *et al.* Bioactive compounds and antioxidant activity of mung bean (*Vigna radiata* L.), soybean (*Glycine max* L.) and black bean (*Phaseolus vulgaris* L.) during the germination process. Czech Journal of Food Sciences. 2016;34(1):68–78. https://doi.org/10.17221/434/2015-CJFS

47. Ombra MN, d'Acierno A, Nazzaro F, Riccardi R, Spigno P, Zaccardelli M, *et al.* Phenolic composition and antioxidant and antiproliferative activities of the extracts of twelve common bean (*Phaseolus vulgaris* L.) endemic ecotypes of southern italy before and after cooking. Oxidative Medicine and Cellular Longevity. 2016;2016(1):1398298. https://doi.org/10.1155/2016/1398298

48. Mojica L, Meyer A, Berhow MA, de Mejía EG. Bean cultivars (*Phaseolus vulgaris* L.) have similar high antioxidant capacity, *in vitro* inhibition of α-amylase and α-glucosidase while diverse phenolic composition and concentration. Food Research International. 2015;69:38–48. https://doi.org/10.1016/j.foodres.2014.12.007

49. Guajardo-Flores D, Serna-Saldívar SO, Gutiérrez-Uribe JA. Evaluation of the antioxidant and antiproliferative activities of extracted saponins and flavonols from germinated black beans (*Phaseolus vulgaris* L.). Food Chemistry. 2013;141(2):1497–1503. https://doi.org/10.1016/j.foodchem.2013.04.010

50. Xu B, Chang SKC. Comparative study on antiproliferation properties and cellular antioxidant activities of commonly consumed food legumes against nine human cancer cell lines. Food Chemistry. 2012;134(3):1287–1296. https://doi.org/10.1016/j.foodchem.2012.02.212

51. Golam Masum Akond ASM, Khandaker L, Berthold J, Gates L, Peters K, Delong H, *et al.* Anthocyanin, total polyphenols and antioxidant activity of common bean. American Journal of Food Technology. 2011;6(5):385–394. https://doi.org/10.3923/ajft.2011.385.394

52. Xu B, Chang SKC. Reduction of antiproliferative capacities, cell-based antioxidant capacities and phytochemical contents of common beans and soybeans upon thermal processing. Food Chemistry. 2011;129(3):974–981. https://doi.org/10.1016/j.foodchem.2011.05.057

53. Hernández-Salazar M, Osorio-Diaz P, Loarca-Piña G, Reynoso-Camacho R, Tovar J, Bello-Pérez LA. *In vitro* fermentability and antioxidant capacity of the indigestible fraction of cooked black beans (*Phaseolus vulgaris* L.), lentils (*Lens culinaris* L.) and chickpeas (*Cicer arietinum* L.). Journal of the Science of Food and Agriculture. 2010;90(9):1417–1422. https://doi.org/10.1002/jsfa.3954

54. Silva-Cristobal L, Osorio-Díaz P, Tovar J, Bello-Pérez LA. Chemical composition, carbohydrate digestibility, and antioxidant capacity of cooked black bean, chickpea, and lentil Mexican varieties. CYTA – Journal of Food. 2010;8(1):7–14. https://doi.org/10.1080/19476330903119218

55. Oomah BD, Corbé A, Balasubramanian P. Antioxidant and anti-inflammatory activities of bean (*Phaseolus vulgaris* L.) hulls. Journal of Agricultural and Food Chemistry. 2010;58(14):8225–8230. https://doi.org/10.1021/jf1011193

56. Xu B, Chang SKC. Total phenolic, phenolic acid, anthocyanin, flavan-3-ol, and flavonol profiles and antioxidant properties of pinto and black beans (*Phaseolus vulgaris* L.) as affected by thermal processing. Journal of Agricultural and Food Chemistry. 2009;57(11):4754–4764. https://doi.org/10.1021/jf900695s

57. Dong M, He X, Rui HL. Phytochemicals of black bean seed coats: Isolation, structure elucidation, and their antiproliferative and antioxidative activities. Journal of Agricultural and Food Chemistry. 2007;55(15):6044–6051. https://doi.org/10.1021/jf070706d

58. Tan Y, Tam CC, Meng S, Zhang Y, Alves P, Yokoyama W. Cooked black turtle beans ameliorate insulin resistance and restore gut microbiota in C57BL/6J mice on high-fat diets. Foods. 2021;10(8):1691. https://doi.org/10.3390/foods10081691

59. Monk JM, Wu W, Hutchinson AL, Pauls P, Robinson LE, Power KA. Navy and black bean supplementation attenuates colitis-associated inflammation and colonic epithelial damage. The Journal of Nutritional Biochemistry. 2018;56:215–223. https://doi.org/10.1016/j.jnutbio.2018.02.013

60. Wang J-Y, Zhu C, Qian T-W, Guo H, Wang D-D, Zhang F, *et al.* Extracts of black bean peel and pomegranate peel ameliorate oxidative stress-induced hyperglycemia in mice. Experimental and Therapeutic Medicine. 2015;9(1):43–48. https://doi.org/10.3892/etm.2014.2040

61. Zhang C, Monk JM, Lu JT, Zarepoor L, Wu W, Liu R, *et al.* Cooked navy and black bean diets improve biomarkers of colon health and reduce inflammation during colitis. British Journal of Nutrition. 2014;111(9):1549–1563. https://doi.org/10.1017/S0007114513004352

62. Reverri EJ, Randolph JM, Steinberg FM, Tissa Kappagoda C, Edirisinghe I, Burton-Freeman BM. Black beans, fiber, and antioxidant capacity pilot study: Examination of whole foods vs. functional components on postprandial metabolic, oxidative stress, and inflammation in adults with metabolic syndrome. Nutrients. 2015;7(8):6139–6154. https://doi.org/10.3390/nu7085273

63. Abdulrahman BO, Bala M, Bello OM. Bioactive compounds of black bean (*Phaseolus vulgaris* L.). In: Murthy HN, Paek K-Y, editors. Bioactive compounds in underutilized vegetables and legumes. Cham: Springer; 2020. https://doi.org/10.1007/978-3-030-44578-2_38-1

64. Teixeira-Guedes CI, Oppolzer D, Barros AI, Pereira-Wilson C. Impact of cooking method on phenolic composition and antioxidant potential of four varieties of *Phaseolus vulgaris* L. and *Glycine max* L. LWT. 2019;103:238–246. https://doi.org/10.1016/j.lwt.2019.01.010

65. Xu B, Chang SKC. Effect of soaking, boiling, and steaming on total phenolic contentand antioxidant activities of cool season food legumes. Food Chemistry. 2008;110(1):1–13. https://doi.org/10.1016/j.foodchem.2008.01.045

66. Acito M, Fatigoni C, Villarini M, Moretti M. Effect of cooking and domestic storage on the antioxidant activity of Lenticchia di Castelluccio di Norcia, an Italian PGI lentil landrace. International Journal of Environmental Research and Public Health. 2023;20(3):2585. https://doi.org/10.3390/ijerph20032585

67. Toor BS, Kaur A, Sahota PP, Kaur J. Antioxidant potential, antinutrients, mineral composition and FTIR spectra of legumes fermented with *Rhizopus oligosporus*. Food Technology and Biotechnology. 2021;59(4):530–542. https://doi.org/10.17113/ftb.59.04.21.7319

68. Tsao R. Chemistry and biochemistry of dietary polyphenols. Nutrients. 2010;2(12):1231–1246. https://doi.org/10.3390/nu2121231

69. Sánchez-Tapia M, Hernández-Velázquez I, Pichardo-Ontiveros E, Granados-Portillo O, Gálvez A, Tovar AR, *et al.* Consumption of cooked black beans stimulates a cluster of some clostridia class bacteria decreasing inflammatory response and improving insulin sensitivity. Nutrients. 2020;12(4):1182. https://doi.org/10.3390/nu12041182

70. Peng L, Guo F, Pei M, Tsao R, Wang X, Jiang L, *et al.* Anti-inflammatory effect of lentil hull (*Lens culinaris*) extract via MAPK/NF-κB signaling pathways and effects of digestive products on intestinal barrier and inflammation in Caco-2 and Raw264.7 co-culture. Journal of Functional Foods. 2022;92:105044. https://doi.org/10.1016/j.jff.2022.105044

71. Rivera-Jiménez J, Berraquero-García C, Pérez-Gálvez R, García-Moreno PJ, Espejo-Carpio FJ, Guadix A, *et al.* Peptides and protein hydrolysates exhibiting anti-inflammatory activity: sources, structural features and modulation mechanisms. Food and Function. 2022;13(24):12510–12540. https://doi.org/10.1039/D2FO02223K

ORCID IDs
Durga R. Priyadarshini https://orcid.org/0000-0002-8177-4889
Annette D. Beatrice https://orcid.org/0000-0002-2969-737X
Tinhoithem Haokip https://orcid.org/0009-0002-0856-0144

Foods and Raw Materials. 2026;14(1)

ISSN 2308-4057 (Print)
ISSN 2310-9599 (Online)

Research Article
Open Access

Available online at http://jfrm.ru/en
https://doi.org/10.21603/2308-4057-2026-1-664
https://elibrary.ru/TEQFHT

Antilithiasic and antioxidant activities of propolis and bee pollen extracts: *In vitro* and *in silico* studies

Safia Ali Haimoud[1,*], Fatiha Arioui[1], Meriem Medjekane[2], Leila Ali Haimoud[3], Khelifa Bahri[1], Asma Cheikh[1], Saadia Ghiboub[1], Hanane Benabed[1], Ikram Boudali[1], Besma Ayache[1], Chaima Beskri[1]

[1] Hassiba Benbouali University of Chlef, Ouled Fares, Algeria
[2] University Center Nour Bachir, El Bayadh, Algeria
[3] Public Hospital, Chlef, Algeria

* e-mail: s.alihaimoud@univ-chlef.dz

Received 24.05.2024; Revised 10.10.2024; Accepted 05.11.2024; Published online 15.04.2025

Abstract:
Urolithiasis is a wide-spread condition with no efficient pharmacological treatments. It causes the formation of renal stones.
The article describes the antioxidant and anti-lithiasis potencies of extracts of Algerian propolis and bee pollen. Their inhibiting effect on calcium oxalate crystallization was assessed against citric acid using UV-Visible spectrophotometry at 620 nm. The effect of rutin and liquiritin on xanthine dehydrogenase was analyzed in silico.
The highest levels ($p < 0.05$) of total phenols (129.28 ± 1.51 mg GAE/g) and flavonoids (77.58 ± 1.95 mg QEQ/g) belonged to the bee pollen ethanolic extract. The same extract had the strongest ($p < 0.05$) DPPH scavenging capacity (9.420 ± 0.002 µg/mL). The ethanolic extract of propolis possessed the highest antioxidant potency (63.05 ± 3.49%) according to the β-carotene assay. Crystal nucleation in the presence of 16 mg/mL extracts was the same as in the samples tested with citric acid. The propolis ethanolic extract (82.83 ± 0.83%) demonstrated the maximal inhibition of crystal growth at 16 mg/mL, compared with citric acid (91.90 ± 0.26%). Based on the binding free energy (ΔG) and root mean square deviation, the ligands were efficient inhibitors of xanthine dehydrogenase.
Bee pollen and propolis proved to contain bioactive components that can make them an alternative to traditional methods of urolithiasis prevention and treatment.

Keywords: Bee products, calcium oxalate, crystallization, extracts, DPPH method, antilithiasic activity, xanthine dehydrogenase

Please cite this article in press as: Ali Haimoud S, Arioui F, Medjekane M, Ali Haimoud L, Bahri K, Cheikh A, *et al.* Antilithiasic and antioxidant activities of propolis and bee pollen extracts: *In vitro* and *in silico* studies. Foods and Raw Materials. 2026;14(1):138–147. https://doi.org/10.21603/2308-4057-2026-1-664

INTRODUCTION

Urolithiasis is a common disorder that arises from the formation of renal stones and has no efficient pharmacological treatment [1]. Some forms are recurrent; severe cases may lead to kidney disorders, causing pain, bleeding, and urinary tract infections. The stone formation encompasses all processes within the urinary tract and is divided into two primary stages, i.e., nucleation and crystallization. Crystals develop from substances originally dissolved in urine. This stage is not inherently pathological as these crystals can aggregate and grow at various points within the urinary system [1]. Infection appears to facilitate stone formation by inducing physical and chemical changes in urine, including acidification [2]. Urolithiasis depends on health conditions, eating habits, and lifestyle [3]. The most common clinical symptom of this kidney pathology is nephritic colic, which is characterized by severe and sudden pain in the renal region. Urolithiasis affects around 10% of population in non-industrialized regions [4, 5].

Urolithiasis exacerbates the oxidative stress, which is a cytotoxic condition implicated in the development of such pathologies as cancer, cardiovascular disease, hypertension, autoimmune disease, diabetes, multiple sclerosis, and arthritis [6]. Xanthine dehydrogenase facilitates purine metabolism by generating reactive oxygen species, such as superoxide anions (O_2^-) and hydrogen peroxide (H_2O_2). Xanthine oxidoreductase exists in

Copyright © 2025, Ali Haimoud *et al.* This is an open access article distributed under the terms of the Creative Commons Attribution 4.0 International License (https://creativecommons.org/licenses/by/4.0/), allowing third parties to copy and redistribute the material in any medium or format and to remix, transform, and build upon the material for any purpose, even commercially, provided the original work is properly cited and states its license.

two interchangeable forms, i.e., xanthine dehydrogenase and xanthine oxidase. The dehydrogenase form transitions to the oxidase form, which then produces hydrogen peroxide and superoxide. This transformation happens through the oxidation of sulfhydryl groups or via stimulated proteolysis. Both forms of the enzyme can cause the oxidation of nicotinamide adenine dinucleotide hydrogen (NADH) while simultaneously producing reactive oxygen species. Because the xanthine oxidase reaction produces reactive oxygen species and uric acid, this enzyme is considered to be a major source of reactive oxygen species in the bloodstream [7].

Bees produce beeswax, royal jelly, bee pollen, and propolis. The importance of bee pollen comes from its rich complex composition. It includes vitamins (C, E, B-group vitamins), mineral salts (phosphorus, calcium, magnesium, copper, zinc, iron), essential amino acids, and phenolic compounds known for their numerous biological properties [8].

Propolis is a natural resinous substance gathered by bees (*Apis mellifera*). It contains more than 300 constituents, including volatile aromatic compounds, minerals (iron, calcium, zinc, copper, manganese), vitamins (C, E, B-group), aliphatic fatty acids, esters, amino acids, phenolic acids, and flavonoids [9–12].

Bee by-products and their chemical composition receive a lot of scientific attention due to their phenolic components [13]. However, their biological effects remain understudied. For instance, no reliable scientific data are available on the antilithiatic effect of propolis and bee pollen extracts on the crystallization of calcium oxalate monohydrate. This research examined the antioxidant and inhibiting effects of Algerian native propolis and bee pollen on the crystallization of calcium oxalate. The research objective was to unravel possible new applications in medicine as antilithiatic agents, as well as to determine the interaction of rutin and liquiritin with xanthine dehydrogenase *in silico*.

STUDY OBJECTS AND METHODS

Ingredients and chemicals. The chemicals used in this work were of analytical grade. The list of solvents included methanol, ethanol, chloroform, sodium bicarbonate, 2,2-diphenyl-1-picrylhydrazyl (DPPH) radical, calcium chloride, sodium oxalate, hydrochlorid acid, and butylated hydroxytoluene. They were supplied from Sigma-Aldrich GmbH (Germany). The Folin-Ciocalteu reagent, *β*-carotene, sodium hydroxide, gallic acid, quercetin, linoleic acid, and Tween 40 were obtained from Sigma Chemical (USA). The sodium nitrite and aluminum chloride were supplied by Fluka (Germany).

Beehive by-products. In this research, the by-products of bees were represented by bee pollen and propolis. They were harvested from the Chlef Region, Western Algeria, in February 2020 and 2021, respectively. Bee pollen is bright yellow round grains; propolis is a dark brown substance with a pungent flavor and sweet fragrance. The samples were stored in a freezer at –20°C for further analysis (Fig. 1).

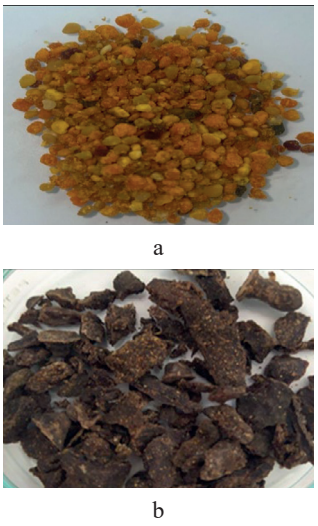

Figure 1 *Apis mellifera*'s beehive by-products: (a) bee pollen, (b) propolis

Preparing the extracts. To obtain crude methanolic extracts, 2.5 g of propolis and bee pollen were separately added to 25 mL of methanol. The resulting mix was filtered and concentrated using a rotary vacuum evaporator (Büchi, Switzerland) [13]. After that, 10 g of pollen and propolis grain powder were separately added to 100 mL of ethanol. The preparations were stirred magnetically for 30 min. After 24 h, the macerates were filtered and concentrated under vacuum [10].

Bioactive content. ***Total phenolic content.*** To determine the total phenolic content, we shook 200 µL of each extract with 1.5 mL of the Folin-Ciocalteu reagent (1:10) and 1.5 mL of sodium bicarbonate (60 g/L). After 90 min, the absorbance was measured spectrophotometrically at 725 nm using an Optizen 2120 device (Mecasys, South Korea). The total phenolic content was given as 1 mg gallic acid equivalent per 1 g extract (mg GAE/g) [14].

Total flavonoid content. To determine the total flavonoid content, we mixed 1 mL of each extract, 4 mL of distilled water, and 0.3 mL of sodium nitrite (5%). After 5 min, we added 0.3 mL of aluminum chloride (10%), 2 mL sodium hydroxide (4%), and 2.4 mL distilled water. After another 5 min, we measured the optical density at 510 nm. The total flavonoid content was given as 1 mg quercetin equivalent per 1 g extract (mg QEQ/g) [15].

Antioxidant potencies *in vitro. β-Carotene-linoleic assay.* We mixed 1 mL of *β*-carotene (3 mg) dissolved in 30 mL chloroform with 40 mg of linoleic acid and 400 mg of Tween 40. Upon removing chloroform at 40°C, we added 100 mL of distilled water. After that, we added 3 mL of the resulting emulsion to 50 µL of the test sample (20 mg/mL); 10 µg/mL butylated hydroxytoluene served as comparison. The optical density was recorded at 470 nm. The antiradical activity (AA, %) of the test sample was calculated by the following Eq. (1):

$$AA = \frac{A_{t0} - A_{t60}}{A_{t0}} \times 100 \quad (1)$$

where A_{t0} and A_{t60} were the initial absorbance and the absorbance measured after 60 min of incubation for the extracts and the blank, respectively [16].

DPPH radical-scavenging. We incubated the mixes of 2.7 mL extract concentrations of propolis and bee pollen with 0.3 mL of a DPPH (2,2-diphenyl-1-picrylhydrazyl) solution (0.004%) for 30 min. The discoloration was recorded at 517 nm; butylated hydroxytoluene served as comparison. The inhibition activity (I, %) was calculated using the following Eq. (2):

$$I = \frac{A_0 - A_1}{A_0} \times 100 \quad (2)$$

where A_0 and A_1 were the absorbance values of the blank (DPPH solution) and the sample extracts, respectively.

The antiradical potency was expressed in term of IC_{50} (μg/mL), i.e., the scavenging of 50% of DPPH radical [17].

Inhibiting effect in vitro on calcium oxalate crystallization. After mixing 1 mL of calcium chloride solution (5 mmol/L) with 1 mL of distilled water to read the blank, we added 1 mL of sodium oxalate solution (7.5 mmol/L) to trigger crystallization. The optical density of the solution was measured at 620 nm for 10 min.

To determine the *in-vitro* effect of the propolis and bee pollen extracts on calcium oxalate formation, we mixed 1 mL of calcium chloride solution with 1 mL of each extract at 2, 4, 8, and 16 mg/mL. After adding 1 mL of sodium oxalate solution, the procedure was repeated with citric acid at 6 mM as a positive control [18]. The absorbance was recorded at 620 nm. The inhibition percentage (I, %) was calculated by the Eq. (3):

$$I = \frac{N_{Ss} - N_{Si}}{N_{Ss}} \times 100 \quad (3)$$

where N_{Si} and N_{Ss} were the nucleation slope test results with and without the inhibitor, respectively [18].

Interaction of xanthine dehydrogenase and phenolic compounds *in silico*. We used the *in-silico* method to study the interaction between xanthine dehydrogenase with rutin and liquiritin as the major phenolic compounds in the propolis and bee pollen extracts.

Protein preparation. The structure of xanthine dehydrogenase (ID: 1N5X at a resolution of 2.80 Å) was obtained from the Protein Data Bank at www.pdb.org. The Gasteiger-type atomic charges and hydrogen atoms were added to the xanthine dehydrogenase structure using the AutoDockTools (ADT) software. The modified protein structures were saved in the PDBQT format for subsequent docking studies.

Ligand preparation. Rutin and liquiritin were downloaded from the PubChem database in the SDF format and converted to the PDB format using the PyMOL software. To evaluate the energy of the system and facilitate the ligand binding, the protein receptor was enclosed in a three-dimensional grid encompassing the active site. The grid box allowed a free rotation of the ligand and was centered on the ligand with dimensions adjusted to fit all the ligands under study. The grid spacing was fixed at 1 Å.

Root mean square deviation. The AutoDock Vina software was used to determine the interactions between xanthine dehydrogenase and the phenolic ligands. The reliability of the docking program was assessed by calculating the root mean square deviation (RMSD) between the predicted ligand conformations and the experimental complex conformations. The maximal allowable difference in the root mean square deviation was 2 Å to ensure accuracy. Discovery Studio 4.0 made it possible to validate the accuracy of the docking predictions and the visual analysis.

Statistical analysis. The results were given as mean ± standard deviation (SD). The statistical analysis involved the SPSS software. The analysis of variance (ANOVA) revealed differences in mean values. The Tukey test highlighted statistically significant differences ($p < 0.05$).

RESULTS AND DISCUSSION

Bioactive content. The total phenolic content of the extracts under study varied from 41.25 ± 0.93 to 129.28 ± 1.51 mg GAE/g. The ethanolic extract of bee pollen had the highest total phenolic content (129.28 ± 1.51 mg GAE/g) ($p < 0.05$) followed by the methanolic extract of propolis (93.50 ± 2.65 mg GAE/g) and the ethanolic extract of propolis (93.16 ± 2.49 mg GAE/g). The lowest total phenolic content (41.25 ± 0.93 mg GAE/g) belonged to the methanolic extract of pollen ($p < 0.05$) (Table 1).

The statistical analysis revealed that the ethanolic extract of bee pollen had the maximal total flavonoid content (77.58 ± 1.95 mg QEQ/g) followed by the ethanolic extract of propolis (34.91 ± 3.25 mg QEQ/g). The lowest total flavonoid fraction was detected in the methanolic extract of bee pollen (10.54 ± 1.45 mg QEQ/g) (Table 1).

Nieva Moreno *et al.*, who studied the total phenolic and flavonoid contents of bee pollen extracts from different regions of Argentine, reported them as 19.28–48.90 mg GAE/g and 13.39–42 mg CEQ/g, respectively [19]. Ahn *et al.* reported that the total phenolic content of Chinese propolis varied from 85 ± 2 to 228 ± 8 mg GAE/g [12]. Moreira *et al.* defined the total phenolic content of methanolic propolis extract as ranging from 151.00 ± 0.01 to 329.00 ± 0.01 mg GAE/g [20]. Our results were much higher compared to those reported by Mohammadzadeh, who found that the total phenolic

Table 1 Bioactive content of propolis and bee pollen extracts

Extracts	Total phenolic content, mg GAE/g	Total flavonoid content, mg QEQ/g
Methanolic extract of propolis	93.50 ± 2.65^{b}	14.36 ± 1.82^{c}
Ethanolic extract of propolis	93.16 ± 2.49^{b}	34.91 ± 3.25^{b}
Methanolic extract of bee pollen	41.25 ± 0.93^{c}	10.54 ± 1.45^{d}
Ethanolic extract of bee pollen	129.28 ± 1.51^{a}	77.58 ± 1.95^{a}

Different letters in the same raw are significantly different ($p < 0.05$); mg GAE/g = 1 mg gallic acid equivalent per 1 g; mg CEQ/g = 1 mg catechin equivalent per 1 g

content of Iranian propolis extracts varied from 3.08 ± 0.02 to 8.46 ± 0.03 mg EAG/g [21]. Our results were also much higher than those published by Asem *et al.*, in whose study the total phenolic and flavonoid contents of Malaysian bee propolis extracts varied from 135.93 ± 5.95 to 326.10 ± 4.94 μM EAG/g and 28.57 ± 3.17 to 55.16 ± 7.52 μM QEQ/g, respectively [22].

Our findings were in accordance with those reported by Carpes *et al.*, who studied the total flavonoid content of Brazilian bee pollen (2.10–28.33 mg CEQ/g) [23]. According to Ahn *et al.*, the total flavonoid contents of Korean propolis extract ranged between 15.90 and 135.20 mg CEQ/g [24]. A recent study with 13 types of Anzer pollens from Turkey reported that the flavonoid contents ranged from 44.07 to 124.10 mg CEQ/g. The observed differences may be associated with the extraction conditions, the local vegetation, and the species of stingless bees [25].

High performance liquid chromatography (HPLC) showed the following list of major phenolic compounds: caffeic, syringic, ellagic, hydroxybenzoic, vanillic, as well as ferulic and o'coumaric acids [26–28]. Shi *et al.* and Rzepecka-Stojko *et al.* described gallic, benzoic, cinnamic, and phenylacetic acids as the dominant phenolic compounds in bee pollen [29, 30]. Luteolin, quercetin, rutin, formononectin, and liquiritin were the major flavonoids in Brazilian propolis [31, 32]. Apigenin, rutin, catechin, epicatechin, luteolin, quercetin, kaempferol, and naringenin were identified in bee pollen, and some of them could be antioxidant components [33, 34].

In-vitro* antioxidant potencies. *β-carotene-linoleic assay. Table 2 shows that the highest antioxidant capacity ($p < 0.05$) belonged to the ethanolic extract of propolis (63.05 ± 3.49%), whereas the ethanolic extract of bee pollen had the lowest antioxidant capacity (16.67 ± 1.08%). Based on a *β*-carotene bleaching assay, the order of antiradical capacity of the propolis and bee pollen extracts was as follows: bee pollen ethanolic extract < bee pollen methanolic extract < propolis methanolic extract < propolis ethanolic extract. None of the test samples exceeded the potency of butylated hydroxytoluene (96.35 ± 1.29%).

DPPH radical-scavenging. The ethanolic extract of bee pollen showed the highest level of antiradical efficiency (9.42 ± 0.0028 μg/mL) while the methanolic extract of bee pollen had the lowest one (33.56 ± 0.012 μg/mL). Based on the DPPH method, the order of antioxidant activity of extracts was as follows: bee pollen methanolic extract < propolis methanolic extract < propolis ethanolic extract < bee pollen ethanolic extract. No significant difference ($p > 0.05$) was detected between the antioxidant potencies of butylated hydroxytoluene and the ethanolic extract of bee pollen (Table 2).

A combination of more than one method is necessary to cover different mechanisms of antioxidant action, e.g., synergistic interactions. In this research, each extract was tested for its antioxidant activity by two complementary and universally methods, namely the *β*-carotenelinoleic acid system and the DPPH assay. Carpes *et al.* reported that ethanolic extracts of Brazilian bee pollen exhibited potent antioxidant activity by bleaching the *β*-carotene assay: the inhibition percentage varied from 40 to 90% [23]. According to Zhang *et al.*, caffeoylquinic acids and artepillin C were the major effective metabolites for quality control of Brazilian propolis due to their high antiradical capacity [34]. The ethanol extracts of propolis from different regions of Argentine showed antiradical capacity against DPPH, which varied from 20.00 ± 1.10 to 67.5 ± 2.3% at 20 μg/mL [16]. Gulcin *et al.*, who studied lyophilized aqueous extracts of Turkish propolis with the DPPH test, reported an IC_{50} of 31.81 μg/mL [35]. Khider *et al.* tested the antioxidant potency of the methanolic extracts of Egyptian bee pollen from maize, clover, and date palm using the DPPH assay [36]. The respective values of IC_{50} were 0.6, 0.8 and 0.7 μg/mL.

Table 2 Antioxidant activities of propolis and bee pollen extracts

Extracts	*β*-carotene bleaching assay, %	IC_{50} DPPH, μg/mL
Methanolic extract of propolis	20.35 ± 2.62[c]	11.80 ± 0.0043[b]
Ethanolic extract of propolis	63.05 ± 3.49[b]	10.95 ± 0.0068[b]
Methanolic extract of bee pollen	17.18 ± 1.90[c]	33.56 ± 0.012[a]
Ethanolic extract of bee pollen	16.67 ± 1.08[c]	9.42 ± 0.0028[c]
Butylated hydroxytoluene	96.35 ± 1.29[a]	4.59 ± 0.00086[c]

Different letters in the same raw are significantly different ($p < 0.05$)

Therefore, the antioxidant capacity of such bee by-products as propolis and bee pollen depends on their phenolic content.

Boeing *et al.* proved that phenolic components were responsible for the antioxidant activity of berry extracts [37]. In their case, methanol was the most efficient extraction solvent, followed by water and ethanol. This result could have been due to better solvation of antioxidant compounds present in fruits as a result of interactions (hydrogen bonds) between the polar sites of the antioxidant molecules and the solvent.

Antilithiasic potency of propolis and pollen extracts. *Crystallization kinetics of calcium oxalate.* The crystallization was significant ($p < 0.001$) in the presence of citric acid at 6 mM, compared to that of the blank, which contained no extract. The crystallization kinetics in the presence of the propolis and bee pollen ethanolic extracts at 8 and 16 mg/mL and in the presence of citric acid were not significantly different ($p > 0.05$). The absorbance values of citric acid proved to be significantly different ($p < 0.05$), compared to those of different concentrations of propolis and pollen ethanolic extracts (2, 4, 8, and 16 mg/mL). A significant difference ($p < 0.001$) was recorded between the absorbance of citric acid and those of the ethanolic extracts of propolis and bee pollen at 2 and 4 mg/mL (Figs. 2 and 3).

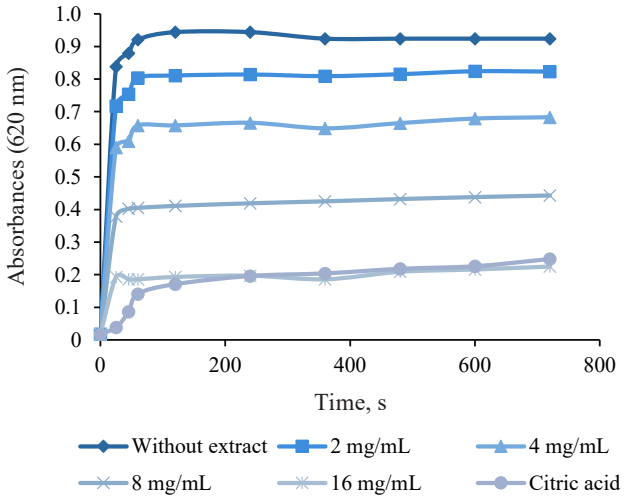

Figure 2 Inhibiting effect of ethanolic bee pollen extract on calcium oxalate crystallization

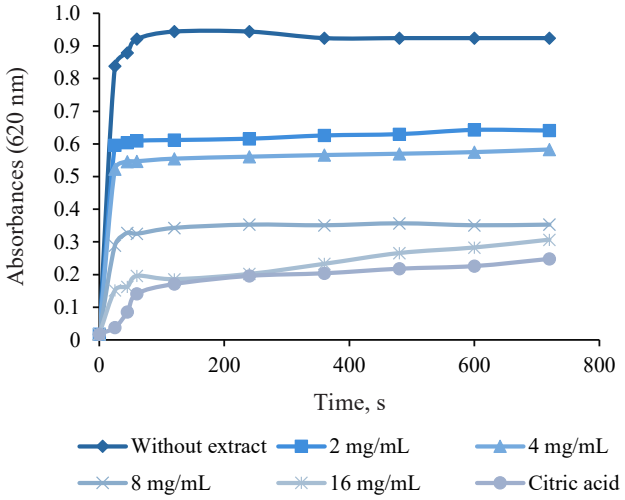

Figure 3 Inhibiting effect of methanolic bee pollen extract on calcium oxalate crystallization

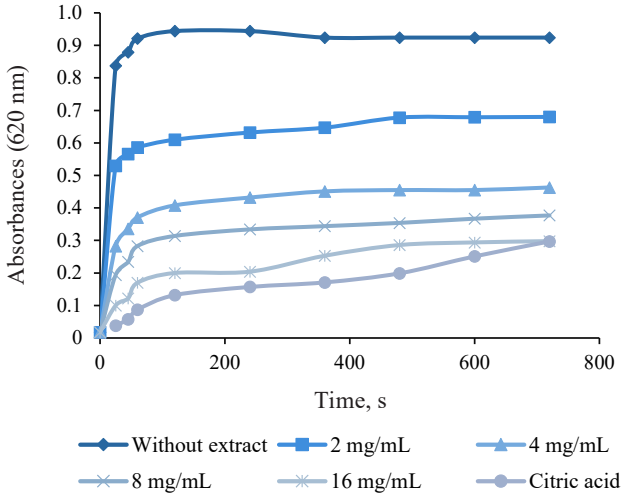

Figure 4 Inhibiting effect of ethanolic propolis extract on calcium oxalate crystallization

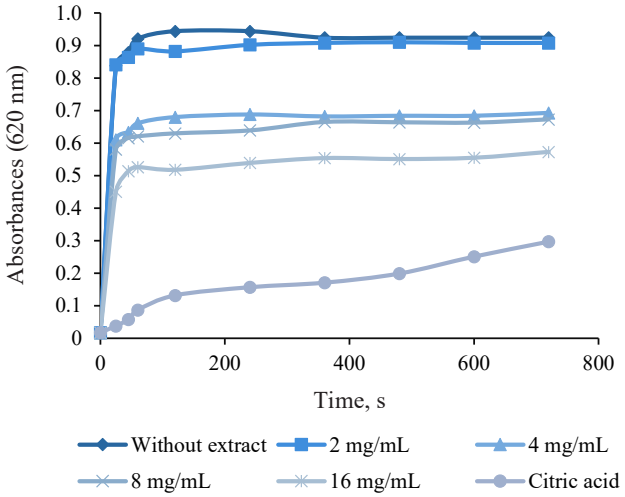

Figure 5 Inhibiting effect of methanolic propolis extract on calcium oxalate crystallization

The crystallization kinetics in the presence of the methanolic extract of pollen at 16 mg/mL did not differ significantly ($p > 0.05$) from that obtained in the presence of citric acid. However, a significant difference ($p < 0.05$) was recorded between the absorbance of citric acid ($p < 0.05$) and those of the methanolic extracts of propolis and pollen at 2, 4, 8, and 16 mg/mL. A very significant difference ($p < 0.01$) was recorded between the absorbances of citric acid and that of the methanolic extract of pollen at 2, 4, 8, and 16 mg/mL. The crystallization kinetics in the presence of citric acid at 6 mM proved to be very significant ($p < 0.001$), compared to that observed in the blank (without extract) (Figs. 4 and 5).

Inhibition percentage of calcium oxalate crystallization. The inhibition percentage (I, %) was calculated from turbidity slopes with and without propolis and bee pollen extracts. The inhibition percentage of the extracts was lower than that observed in citric acid (91.90 ± 0.26%). The latter showed significant antilithiasis activity ($p < 0.001$), compared to the ethanolic extract of propolis and the methanolic extract of pollen at 2, 4, 8, and 16 mg/mL. The inhibition percentage of citric acid crystallization was highly significant ($p < 0.01$), compared to those of the ethanolic propolis extract (82.83 ± 0.84%), the methanolic pollen extract (80.480 ± 0.021%), and the ethanolic pollen extract (80.480 ± 0.021%) at 16 mg/mL (Fig. 6).

Many studies report various effects of medicinal plant extracts on lithogenesis. Plants inhibit calcium oxalate crystallization under different protocols *in vivo* and *in vitro*. However, according to our knowledge, no scientific research ever evaluated the anti-lithiasic activity of propolis and bee pollen extracts. We compared our results with data on extracts from different plants reported by other authors.

Kachkoul *et al.* found a potent antilithiasic effect of *Ammi visnaga* L. and *Punica granatum* L., the respective inhibition percentages being 97.80 ± 0.12 and 73.25 ± 0.81%

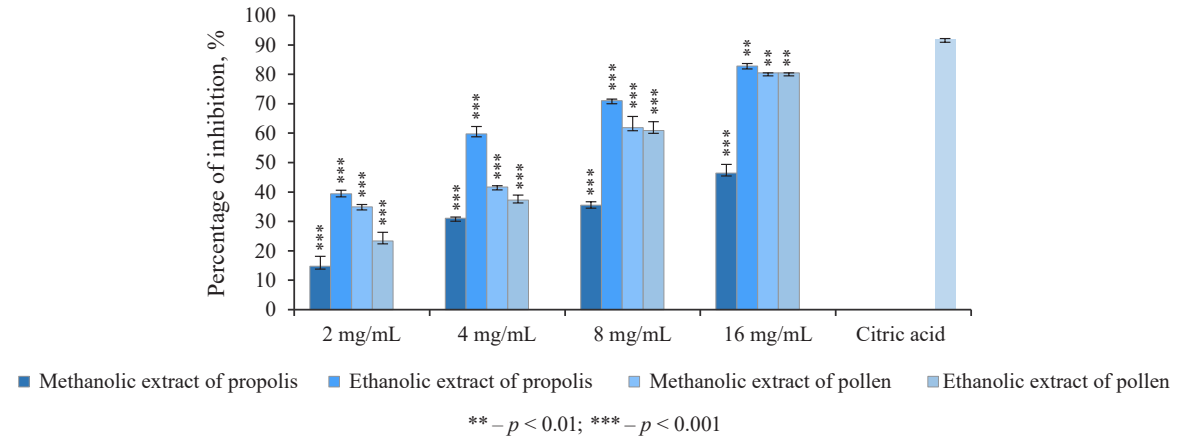

Figure 6 Percentage of crystallization inhibition in presence of extracts

Table 3 Binding free energy (ΔG), AutoDock Vina code

Ligands	Binding free energy (ΔG), kcal/mol
Rutin	–9.3
Liquiritin	–9.2

during nucleation and 83.46 ± 1.34 and 59.44 ± 3.30% during aggregation, respectively [38]. This inhibiting effect could be attributed to the abundance of bioactive molecules in these plants, e.g., polyphenols and flavonoids, which probably worked via their capacity to form soluble species to reduce the formation of oxalate stones.

The aqueous extract of *Cynodon dactylon* (L.) Pers. showed an antilithiasic effect with inhibition percentages of 60% at 1 mg/mL. Flavonoids exhibited an inhibitory effect on crystal growth by changing the crystal state and degree of hydration of calcium oxalate from the insoluble monohydrate form to poorly soluble dihydrate form and a decrease in numbers and sizes of aggregates [39]. Li *et al.* reported citrate as a potent inhibitor of the formation and crystallization of oxalate stones [40]. In their case, the presence of citric acid could modulate the water content of nucleated amorphous precipitates and hence promoted the formation of different calcium oxalate hydrates. Gallic acid altered the nucleation and the formation of calcium oxalate hydrates.

Khan *et al.* described the effect of *A. visnaga* seeds on kidney stones: the anti-calcination was mainly due to the strong diuretic activity and attenuation of hypersecretion and hyperbilirubinemia exerted by visnaga seeds [41].

Benalia *et al.* conducted an *in-vitro* study on dissolution of cystine stones using four traditional plant extracts and a saline control solution [42]. They subjected the calcinations to magnetic agitation for eight weeks. The plants examined were *Arenaria ammophila* L. (leaves and stems), *Parietaria officinalis* L. (leaves and flowers separately), and *Paronychia argentea* L. (flowers).

Interaction of xanthine dehydrogenase and phenolic compounds *in silico*. *Energy.* Rutin formed the most stable complex with xanthine dehydrogenase with a binding free energy (ΔG) of –9.3 kcal/mol, followed by liquiritin with –9.2 kcal/mol (Table 3).

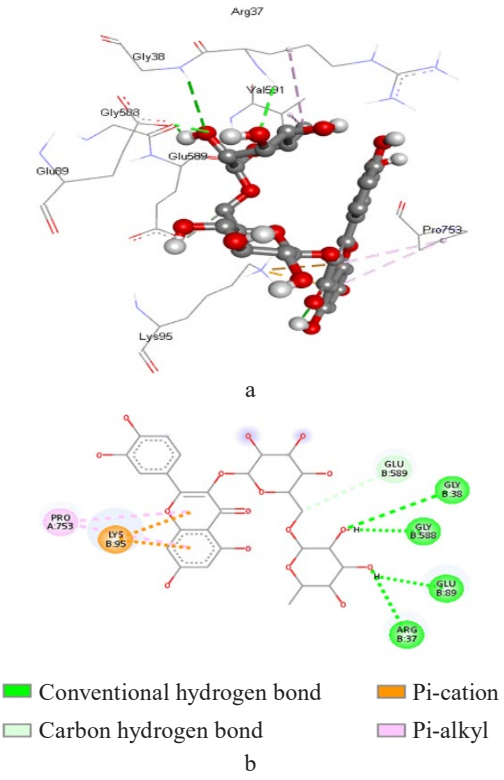

Figure 7 Three-dimensional (a) and dimensional (b) visualization of interactions between the active site of xanthine dehydrogenase and rutin

Interaction of ligands and xanthine dehydrogenase. *Interaction of rutin and xanthine dehydrogenase.* A three-dimensional visualization of the interactions between the active site of xanthine dehydrogenase and rutin showed that the interaction involved lysine 95, proline 753, glutamate 89, glycine 588, glycine 38, and glutamate 589 (Fig. 7).

According to the visualization (Discovery Studio), rutin penetrated well into the active site of xanthine dehydrogenase by forming different Pi-cation, Pi-alkyl, hydrogen, Pi-anion, and hydrogen carbon interactions (Table 4).

Interaction of liquiritin and xanthine dehydrogenase. A three-dimensional visualization of the interactions

Table 4 Interactions between rutin and xanthine dehydrogenase

Residue	Type of interaction	Distance (Å)
Lysine 95	Pi-cation	3.35
Proline 753	Pi-alkyl	5.50
Glutamate 89	Hydrogen	2.12
Glycine 588	Hydrogen	1.9
Glycine 38	Hydrogen	3.07
Glutamate 589	Carbon hydrogen bond	3.36

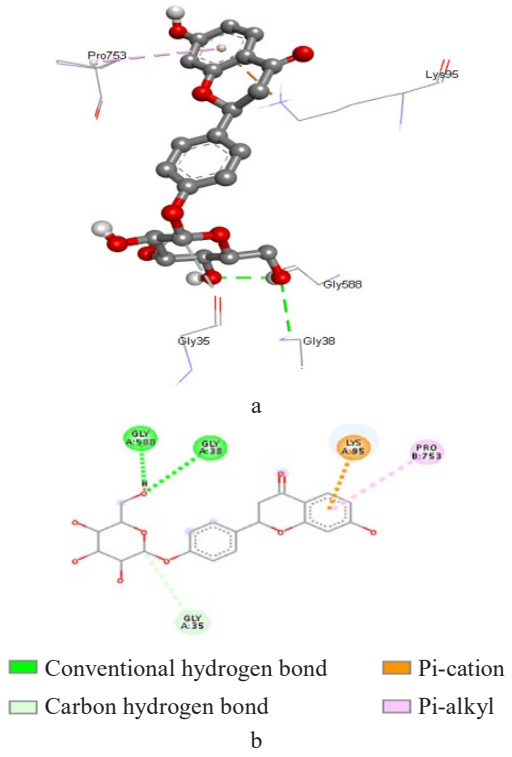

Figure 8 Three-dimensional (a) and dimensional (b) visualization of interactions between the active site of xanthine dehydrogenase and liquiritin

Table 5 Interactions between liquiritin and xanthine dehydrogenase

Residue	Type of interaction	Distance (Å)
Glycine 38, 588	Hydrogen	2.96
Glycine 588	Hydrogen	1.76
Lysine 95	Pi-cation	3.81
Proline 753	Pi-alkyl	5.34
Glycine 35	Carbon hydrogen bond	3.71

between the active site of xanthine dehydrogenase and liquiritin showed that the interaction involved glycine 38, glycine 588, glycine 35, lysine 95, and proline 753 (Fig. 8).

According to the visualization (Discovery Studio), liquiritin penetrated well into the active site of xanthine dehydrogenase by forming different Pi-cation, Pi-alkyl, hydrogen, Pi-anion, and hydrogen carbon interactions (Table 5).

Reliability testing of the molecular docking program. ***Root Mean Square Deviation.*** To predict the interaction between the ligands and the enzyme, we determined the exact position of each ligand in relation to its receptor. The root mean square deviation program compared the model and the structure of the reference ligand (co-crystallized). A root mean square deviation of ≤ 2 Å was considered acceptable [43]. In this study, xanthine dehydrogenase was the enzyme complex under analysis (PDB: 1n5x). After extracting the co-crystallized ligand from the target and repositioning it through docking in the active site, we calculated the root mean square deviation of the best position of the reference ligand after docking and compared it to its crystallographic binding mode before docking. The root mean square deviation value of hydroxytyrosol in the software-generated model stayed below 2 Å (Table 6).

Table 6 Root mean square deviation values of ligand interaction with xanthine dehydrogenase

Ligands	Root mean square deviation (Å)
Rutin	1.257
Liquiritin	1.839

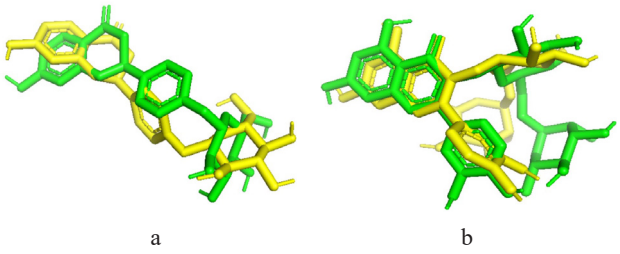

Figure 9 Superposition of inhibitors by Pymol to calculate root mean square deviation: (a) rutin, (b) liquiritin

Visual analysis plays a crucial role in complementing the numerical root mean square deviation values. When we examined the selected complexes of xanthine dehydrogenase (PDB: 1n5x) and ligands using PyMOL, the ligands predicted by AutoDock-Vina aligned well with the reference ligand. The visual confirmation substantiated the previously obtained values for root mean square deviation (Fig. 9).

Xanthine oxidase forms through the oxidation and/or proteolytic conversion of xanthine dehydrogenase. This enzyme occurs vascular cells, circulates in plasma, and binds to the extracellular matrix of endothelial cells. It facilitates the metabolism of nicotinamide adenine dinucleotide hydrogen (NADH), molecular oxygen, hypoxanthine, and xanthine, resulting in the production of O and HO, which makes it a significant source of reactive oxygen species [44]. Inhibiting this enzyme can protect against diabetic kidney disease and endometrial hyperplasia by reducing oxidative stress and improving uterine-reduced glutathione and superoxide dismutase, as well as inhibiting the expression of phosphatidylinositol-3-kinase (PI3K), Akt, and vascular endothelial growth factor (VEGF) [45, 46]. Antioxidants, such as phenolic acids and flavonoids, can inhibit xanthine oxidase activity. The method was validated by attaching

the inhibitory ligand to xanthine oxidase, with root mean square deviation values ranging from 1.019 to 2.35 [45]. Cinnamon phenolic acid inhibited xanthine dehydrogenase and oxidase [47]. Serrano *et al.* studied the inhibition mechanisms of eight structurally diverse phenolic compounds in fruits, i.e., quercetin, quercetin-3-rhamnoside, 4,5-O-dicaffeoylquinic acid, 3,5-O-dicaffeoylquinic acid, 3,4-O-dicaffeoylquinic acid, 4-O-caffeoylquinic acid, 3-O-caffeoylquinic acid, and caffeic acid [48]. They used the methods of 1H NMR spectroscopy, atomic force microscopy, and computational techniques to prove that these biomolecules were potent inhibitors of the enzyme. Amraoui *et al.* studied hydroxytyrosol as major phenolic compounds in *Olea europaea* L. leaves and revealed an effective xanthine dehydrogenase inhibition *in silico* [49].

The abovementioned studies prove that inhibiting xanthine oxidase with phenolic compounds can help prevent various diseases.

CONCLUSION

The research demonstrated appreciable levels of total phenolic and flavonoid contents in the ethanolic extract of such apicultural products as bee pollen and propolis. These natural compounds could be recommended as functional supplements in the treatment of various diseases, as well as natural sources of antioxidants in foods.

In our study, the ethanolic extract of propolis had notable inhibitory effects on the crystallization of calcium oxalate monohydrate. Based on the energy and root mean square deviations, the selected ligands were able to inhibit xanthine dehydrogenase. Bee pollen and propolis proved to contain components that can be used as a natural alternative to other methods of pharmaceutical prevention and treatment of kidney stones.

CONTRIBUTION

S. Ali Haimoud, A. Cheikh, S. Ghiboub, L. Ali Haimoud, K. Bahri, H. Benabed, B. Ayache, C. Beskri, and I. Boudali conceived and designed the analysis. S. Ali Haimoud, A. Cheikh, and S. Ghiboub collected the data. S. Ali Haimoud contributed data and analysis tools. L. Ali Haimoud, F. Arioui, and M. Medjekane performed the analysis. Ali Haimoud wrote the manuscript.

CONFLICT OF INTEREST

The authors declare that there is no conflict of interests related to the publication of this article.

ACKNOWLEDGEMENTS

The authors express their gratitude to Mr. Benghalia Mhamed for his help in harvesting the beehive by products.

REFERENCES

1. de Bellis R, Piacentini MP, Meli MA, Mattioli M, Menotta M, Mari M, *et al. In vitro* effects on calcium oxalate crystallization kinetics and crystal morphology of an aqueous extract from *Ceterach officinarum*: Analysis of a potential antilithiatic mechanism. PLoS ONE. 2019;14(6):e0218734. https://doi.org/10.1371/journal.pone.0218734
2. Adhikari A, Bhattacharya S, Bose S, Ray M, Indu R, Banerjee S. Prospective experimental studies of some herbs used in urinary disorders in Unani medicine. Advances in Traditional Medicine. 2023;23:753–775. https://doi.org/10.1007/s13596-022-00639-1
3. Bensatal A, Ouahrani M. Inhibition of crystallization of calcium oxalate by the extraction of *Tamarix gallica* L. Urological Research. 2008;36:283–287. https://doi.org/10.1007/s00240-008-0157-1
4. Cunningham P, Noble H, Al-Modhefer A, Walsh I. Kidney stones: pathophysiology, diagnosis and management. British Journal of Nursing. 2016;25(20):1112–1116. https://doi.org/10.12968/bjon.2016.25.20.1112
5. Li X, Li B, Meng Y, Yang L, Wu G, Jing H, *et al.* Treatment of recurrent renal transplant lithiasis: analysis of our experience and review of the relevant literature. BMC Nephrology. 2020;21:238. https://doi.org/10.1186/s12882-020-01896-5
6. Burits M, Bucar F. Antioxidant activity of *Nigella sativa* essential oil. Phytotherapy Research. 2000;14(5):323–328. https://doi.org/10.1002/1099-1573(200008)14:5%3C323::AID-PTR621%3E3.0.CO;2-Q
7. Veljković A, Hadži-Dokić J, Sokolović D, Bašić D, Veličković-Janković L, Stojanović M, *et al.* Xanthine oxidase/dehydrogenase activity as a source of oxidative stress in prostate cancer tissue. Diagnostics. 2020;10(9):668. https://doi.org/10.3390/diagnostics10090668
8. Campos MGR, Frigerio C, Lopes J, Bogdanov S. What is the future of Bee-Pollen? Journal of ApiProduct ApiMedical Science. 2010;2(4):131–144. https://doi.org/10.3896/IBRA.4.02.4.01
9. Sime D, Atlabachew M, Abshiro MR, Zewde T. Total phenols and antioxidant activities of natural honeys and propolis collected from different geographical regions of Ethiopia. Bulletin of the Chemical Society of Ethiopia. 2015;29(2):163–172. https://doi.org/10.4314/bcse.v29i2.1
10. Afrouzan H, Tahghighi A, Zakeri S, Es-haghi A. Chemical composition and antimicrobial activities of Iranian propolis. Iranian Biomedical Journal. 2018;22(1):50–65. https://doi.org/10.22034/ibj.22.1.50
11. Eroglu N, Akkus S, Yaman M, Asci B, Silici S. Amino acid and vitamin content of propolis collected by native Caucasican honey bees. Journal of Apicultural Science.2016;60(2):101–110. https://doi.org/10.1515/jas-2016-0021

12. Ahn M-R, Kumazawa S, Hamasaka T, Bang K-S, Nakayama T. Antioxidant activity and constituents of propolis collected in various areas of Korea. Journal of Agricultural and Food Chemistry. 2004;52(24):7286–7292. https://doi.org/10.1021/jf048726s
13. Falleh H, Ksouri R, Chaieb K, Karray-Bouraoui N, Trabelsi N, Boulaaba M, *et al.* Phenolic composition of *Cynara cardunculus* L. organs, and their biological activities. Comptes Rendus Biologies. 2008;331(5):372–379. https://doi.org/10.1016/j.crvi.2008.02.008
14. Kamazawa S, Tanguchi M, Suzuki Y, Shimara M, Kwon M-S, Nakayama T. Antioxidant activity of polyphenols in carob pods. Journal of Agricultural and Food Chemistry. 2002;50(2):373–377. https://doi.org/10.1021/jf010938r
15. Biglari F, Alkarkhi AFM, Easa AM. Antioxidant activity and phenolic content of various date palm (*Phoenix dactylifera*) fruits from Iran. Food Chemistry. 2008;107(4):1636–1641. https://doi.org/10.1016/j.foodchem.2007.10.033
16. Mikami I, Yamaguchi M, Shinmoto H, Tsushida T. Development and validation of a microplate-based β-carotene bleaching assay and comparison of antioxidant activity (AOA) in several crops measured by β-carotene bleaching, DPPH and ORAC assays. Food Science and Technology Research. 2009;15(2):171–178. https://doi.org/10.3136/fstr.15.171
17. Okada Y, Okada M. Scavening effect of water soluble proteins in broad beans on free radicals and active oxygen species. Journal of Agricultural and Food Chemistry. 1998;46(2):401–406. https://doi.org/10.1021/jf9704701
18. Elhadri I, Baddade L, Berkani M. Antioxidant activity and Inhibitory effects of *Cydonia oblonga Miller.* leaves extracts against calcium oxalate stones. Urolithiasis. 2024;52:62. https://doi.org/10.1007/s00240-024-01532-z
19. Nieva Moreno MI, Isla MI, Sampietro AR, Vattuone MA. Comparison of the free radical-scavenging activity of propolis from several regions of Argentine. Journal of Ethnopharmacology. 2000;71(1–2):109–114. https://doi.org/10.1016/S0378-8741(99)00189-0
20. Moreira L, Dias LG, Pereira JA, Estevinho L. Antioxidant properties, total phenols and pollen analysis of propolis samples from Portugal. Food and Chemical Toxicology. 2008;46(11):3482–3485. https://doi.org/10.1016/j.fct.2008.08.025
21. Mohammadzadeh S, Sharriatpanahi M, Hamedi M, Amanzadeh Y, Ebrahimi SES, Ostad SN. Antioxydant power of Iranian extract. Food Chemistry. 2007;103(3):729–733. https://doi.org/10.1016/j.foodchem.2006.09.014
22. Asem N, Gapar NAA, Hapit NNA, Omar EA. Correlation between total phenolic and flavonoid contents with antioxidant activity of Malaysian stingless bee propolis extract. Journal of Apicultural Research. 2020;59(4):437–442. https://doi.org/10.1080/00218839.2019.1684050
23. Carpes ST, Mourao GB, de Alencar SM, Masson ML. Chemical composition and free radical scavenging activity of Apis mellifera bee pollen from Southern Brazil. Brazilian Journal of Food Technology. 2009;12(3):220–229. https://doi.org/10.4260/BJFT2009800900016
24. Ahn M-R, Kumazawa S, Usu Y, Nakamura J, Matsuka M, Zhu F, *et al.* Antioxidant activity and constituents of propolis collected in various areas of China. Food Chemistry. 2007;101(4):1383–1392. https://doi.org/10.1016/j.foodchem.2006.03.045
25. Ulusoy E, Kolayli S. Phenolic composition and antioxidant properties of Anzer bee pollen. Journal of Food Biochemistry. 2020;38(1):73–82. https://doi.org/10.1111/jfbc.12027
26. Miorin PL, Levy Junior NC, Custodio AR, Bretz WA, Marcucci MC. Antibacterial activity of honey and propolis from *Apis mellifera* and *Tetragonisca angustula* against *Staphylococcus aureus*. Journal of Applied Microbiology. 2003;95(5):913–920. https://doi.org/10.1046/j.1365-2672.2003.02050.x
27. Christov R, Trusheva B, Popova M, Bankova V, Bertrand M. Chemical composition of propolis from Canada, its antiradical activity and plant origin. Natural Product Research. 2006;20(6):531–536. https://doi.org/10.1080/14786410500056918
28. Popova M, Silici S, Kaftanoglu O, Bankova V. Antibacterial activity of Turkish propolis and its qualitative and quantitative chemical composition. Phytomedcine. 2005;12(3):221–228. https://doi.org/10.1016/j.phymed.2003.09.007
29. Shi H, Yang H, Zhang X, Yu L. Identification and quantification of phytochemical composition and anti-inflammatory and radical scavenging properties of methanolic extracts of Chinese propolis. Journal of Agricultural and Food Chemistry. 2012;60(50):12403–12410. https://doi.org/10.1021/jf3042775
30. Rzepecka-Stojko A, Stojko J, Kurek-Gorecka A, Górecki M, Kabała-Dzik A, Kubina R, *et al.* Polyphenols from bee pollen: structure, absorption, metabolism and biological activity. Molecules. 2015;20(12):21732–21749. https://doi.org/10.3390/molecules201219800
31. Daugsch A, Moraes CS, Fort P, Par YK. Brazilian red propolis – Chemical composition and botanical origin. Evidence-Based Complementary and Alternative Medicine. 2008;5(4):435–441. https://doi.org/10.1093/ecam/nem057
32. Salatino A, Salatino MLF. Brazilian red propolis: Legitimate name of the plant resin source. MOJ Food Processing and Technology. 2018;6(1):21–22. https://doi.org/10.15406/mojfpt.2018.06.00139

33. Mohdaly AAA, Mhmoud AA, Roby MHH, Smetanska IS, Ramadan MF. Phenolic extract from propolis and bee pollen: composition, antioxidant and antibacterial activities. Journal of Food Biochemistry. 2015;39(5):538–547. https://doi.org/10.1111/jfbc.12160
34. Zhang C, Shen X, Chen J, Jiang X, Hu F. Identification of free radical scavengers from Brazilian green propolis using off-line HPLC-DPPH assay and LC-MS. Journal of Food Science. 2017;82(7):1602–1607. https://doi.org/10.1111/1750-3841.13730
35. Gulcin I, Bursal E, Şehitoglu MH, Bilsel M, Gorend AC. Polyphenol contents and antioxidant activity of lyophilized aqueous extract of propolis from Erzurum, Turkey. Food and Chemical Toxicology. 2010;48(8–9):2227–2238. https://doi.org/10.1016/j.fct.2010.05.053
36. Khider M, Elbanna K, Mahmoud A, Owayss AA. Egyptian honeybee pollen as antimicrobial, antioxidant agents, and dietary food supplements. Food Science and Biotechnology. 2013;22:1–9. https://doi.org/10.1007/s10068-013-0238-y
37. Boeing JS, Barizão ÉO, e Silva BC, Montanher PF, Almeida V, Visentainer JV. Evaluation of solvent effect on the extraction of phenolic compounds and antioxidant capacities from the berries: application of principal component analysis. Chemistry Central Journal. 2014;8:48. https://doi.org/10.1186/s13065-014-0048-1
38. Kachkoul R, Sqalli Houssaini T, Miyah Y, Mohim M, El Habbani R, Lahrichi A. The study of the inhibitory effect of calcium oxalate monohydrate's crystallization by two medicinal and aromatic plants: *Ammi visnaga* and *Punica granatum*. Progress in Urology. 2018;28(3):156–165. https://doi.org/10.1016/j.purol.2017.12.003
39. Sekkoum K, Cheriti A, Taleb S, Belboukhari N, Djellouli HM. Inhibition effect of some Algerian Sahara medicinal plants on calcium oxalate crystallization. Asian Journal of Chemistry. 2012;22:2891–2897.
40. Li S, Tang W, Li M, Wang L, Yang Y, Gong G. Understanding the role of citric acid on the crystallization pathways of calcium oxalate hydrates. Crystal Growth and Design. 2019;19(6):3139–3147. https://doi.org/10.1021/acs.cgd.8b01305
41. Khan ZA, Assiri AM, Al-Afghani HMA, Magharbi TMA. Inhibition of oxalate nephrolithiasis with Ammi visnaga (Ai-Khillah). International Urology and Nephrology. 2001;33:605–608. https://doi.org/10.1023/a:1020526517097
42. Benalia H, Mahfoudi R, Djeridane A, Yousfi M. High antiurolithiatic capacities of isolated fractions of the hydromethanolic extract from Pituranthos scoparius roots. Phytothérapie, 2020;18(6):386–398.
43. Li S, Tang W, Shi P, Li M, Sun J, Gong J. A new perspective of gallic acid on calcium oxalate nucleation. Crystal Growth and Design. 2020;20(5):3173–3181. https://doi.org/10.1021/acs.cgd.0c00044
44. Yang K-J, Choi WJ, Chang Y-K, Park CW, Kim SY, Hong YA. Inhibition of xanthine oxidase protects against diabetic kidney disease through the amelioration of oxidative stress via VEGF/VEGFR axis and NOX-FoxO3a-eNOS signaling pathway. International Journal of Molecular Sciences. 2023;24(4):3807. https://doi.org/10.3390/ijms24043807
45. Mohamed MZ, Baky ME, Hassan OA, Mohammed HH, Abdel-Aziz AM. PTEN/PI3K/VEGF signaling pathway involved in the protective effect of xanthine oxidase inhibitor febuxostat against endometrial hyperplasia in rats. Human and Experimental Toxicology. 2020;39(9):1224–1234. https://doi.org/10.1177/0960327120914977
46. Ngoc TM, Khoi NM, Ha DT, Nhiem NX, Tai BH, Don DV, *et al.* Xanthine oxidase inhibitory activity of constituents of *Cinnamomum cassia* twigs. Bioorganic and Medicinal Chemistry Letters. 2012;22(14):4625–4628. https://doi.org/10.1016/j.bmcl.2012.05.051
47. Hendriani R, Nursamsiar N, Tjitraresmi A. *In vitro* and *in silico* evaluation of xanthine oxidase inhibitory activity of quercetin contained in *Sonchus arvensis* leaf extract. Asian Journal of Pharmaceutical and Clinical Research. 2017;10(14):50–53. https://doi.org/10.22159/ajpcr.2017.v10s2.19486
48. Serrano JL, Figueiredo J, Almeida P, Silvestre, S. From xanthine oxidase inhibition to *in vivo* hypouricemic effect: an integrated overview of *in vitro* and *in vivo* studies with focus on natural molecules and analogues. Evidence-Based Complementary and Alternative Medicine. 2020;2020(1):9531725. https://doi.org/10.1155/2020/9531725
49. Amraoui A, Djerrou Z, Ali Haimoud S, Zerouki K, Elmokli S. Antihyperlipidemic and antioxidant potential of *Olea europaea* L. leaves: An experimental study *in vivo*, *in vitro* and *in silico*. Foods and Raw Materials. 2025;13(1):35–45. https://doi.org/10.21603/2308-4057-2025-1-621

ORCID IDs
Safia Ali Haimoud https://orcid.org/0000-0002-6693-7942
Fatiha Arioui https://orcid.org/0000-0002-3160-5550
Meriem Medjekane https://orcid.org/0000-0002-7805-6499
Leila Ali Haimoud https://orcid.org/0009-0004-2819-9178
Khelifa Bahri https://orcid.org/0009-0003-0873-8632
Asma Cheikh https://orcid.org/0009-0004-0022-6322
Saadia Ghiboub https://orcid.org/0009-0008-3658-4948
Hanane Benabed https://orcid.org/0009-0008-1662-5765
Ikram Boudali https://orcid.org/0009-0003-6731-6894
Besma Ayache https://orcid.org/0009-0008-7483-6069
Chaima Beskri https://orcid.org/0009-0008-6906-5490

Foods and Raw Materials. 2026;14(1)

ISSN 2308-4057 (Print)
ISSN 2310-9599 (Online)

Research Article
Open Access

Available online at http://jfrm.ru/en
https://doi.org/10.21603/2308-4057-2026-1-665
https://elibrary.ru/TOLAUG

Irradiated sorghum grain: Phytochemical, physicochemical, and functional properties

Fidelis C.K. Ocloo[1,2], Joyce Agyei-Amponsah[1,2], Bernard T. Odai[1,2], Tahiru Mahami[1], Jonathan O. Armah[1], Ernestina A. Ayeh[1], Isaac Adjei[1], Jacob Basugilo[1], Sarah Asomaniwaa[1], Martin N.Y.H. Egblewogbe[2], Bernard Darfour[1,2,*]

[1] Ghana Atomic Energy Commission, Accra, Ghana
[2] University of Ghana, Accra, Ghana

* e-mail: yawdar4@yahoo.com

Received 23.08.2024; Revised 14.11.2024; Accepted 03.12.2024; Published online 15.04.2025

Abstract:
Sorghum (*Sorghum bicolor* L. Moench) grain is prone to microbial and insect infestation. This study evaluated some quality properties of sorghum grain irradiated with low energy electron beam (LEEB), high energy electron beam (HEEB), and gamma rays.

The experimental samples were sorghum grain irradiated at 2, 4, 6, 8, and 10 kGy, while the unirradiated sample served as a control. The experiments with LEEB and HEEB involved accelerators ILU-6 (250 keV) and ELEKTRONIKA 10-10 (9 MeV), respectively. A Chamber 5000 Co-60 device provided gamma irradiation. The phytochemical, physicochemical, and functional properties were defined by standard methods.

The study revealed significant ($p \leq 0.05$) reductions in the total phenolic, flavonoid, and tannin contents, although they were not dose-dependent. The total phenolic contents reduced from 6.15 (control) to 3.13 GAE/g (gamma rays), 2.74 (HEEB), and 3.47 GAE/g (LEEB). The total flavonoid content reduced from 3.55 (control) to 1.83 QE/g (gamma), 1.78 (HEEB), and 1.59 QE/g (LEEB). The tannin content reduced from 11.96 (control) to 5.19 TAE/g (gamma rays), 2.58 (HEEB), and 6.17 TAE/g (LEEB). The HEEB treatment and gamma rays reduced the pasting properties whereas the LEEB method caused no significant changes. Irradiation did not change the A-type starch crystals but affected its relative crystallinity. The bulk density, oil absorption capacity, solubility index, and swelling power changed significantly after irradiation.

The low energy electron beam treatment demonstrated a good potential as an alternative irradiation source for sorghum grain because it had no adverse effect on its physicochemical and functional properties.

Keywords: High energy electron beam, low energy electron beam, gamma rays, phytochemical profile, physicochemical profile, X-ray diffraction

Funding: The research was partially supported by the International Atomic Energy Agency (IAEA) Collaboration Research Project (CRP-D61025) and the Biotechnology and Nuclear Agriculture Research Institute (GHA/CRP/24367, Government of Ghana).

Please cite this article in press as: Ocloo FCK, Agyei-Amponsah J, Odai BT, Mahami T, Armah JO, Ayeh EA, *et al.* Irradiated sorghum grain: Phytochemical, physicochemical, and functional properties. Foods and Raw Materials. 2026;14(1):148–158. https://doi.org/10.21603/2308-4057-2026-1-665

INTRODUCTION

Sorghum (*Sorghum bicolor* L. Moench) is an ancient cereal grain that originated over 8000 years ago in Northern Africa [1]. Sorghum grain is stored in many different ways to reduce its susceptibility to microbial and insect-pest infestation. Chemicals are the most common disinfesting method. However, chemicals are expensive and unsustainable. Physical techniques offer a greener alternative. They include low gamma radiation, electron beams, and X-rays [2].

As a physical method of food decontamination, ionizing radiation has been accepted by *The Codex Alimentarius* and many countries globally [3]. The method relies on gamma rays from radionuclide sources rather than on electron beams or X-rays because gamma rays possess a higher penetration power [4]. However, the use

Copyright © 2025, Ocloo *et al.* This is an open access article distributed under the terms of the Creative Commons Attribution 4.0 International License (https://creativecommons.org/licenses/by/4.0/), allowing third parties to copy and redistribute the material in any medium or format and to remix, transform, and build upon the material for any purpose, even commercially, provided the original work is properly cited and states its license.

of gamma rays may become problematic in the future due to the increasing cobalt-60 prices, transportation risk, and license issues [4]. The food industry is looking for more sustainable solutions to enhance the safety and quality of food while reducing the environmental impact, i.e., carbon footprint, high energy consumption, inefficient use of water, chemical waste, etc. [5]. This approach results in a new method of food irradiation that involves low-energy beams. It requires relatively small devices that generate ionizing radiation with energies of hundreds keV [5]. This technology also makes it possible to relocate food irradiation processes to the production line in food factories or packing facilities because low-energy beams do not require heavy shielding [5].

Sugar content in Fuji apples and Niitaka pears was not affected by gamma ray and electron beam irradiation at a 0.2–1 kGy [6]. Gamma ray and electron beam irradiation (2–10 kGy) had no effect on the capsaicinoid content of pepper [7]. The extraction yield of polysaccharides from tamarind seed increased after gamma (0.5 kGy) and electron (10 kGy) irradiation [8]. Dried apricot and quince irradiated with gamma ray and electron beam maintained most of their physicochemical qualities and even enhanced their antioxidant potential [4].

One of our previous studies featured the effects of low energy electron beams, high energy electron beams, and gamma rays on the microbial load and aflatoxin levels in sorghum grain. The irradiation either significantly reduced or totally eliminated the microbial loads on sorghum grain [9]. However, the research did not cover the effects of these radiation sources on the physicochemical and functional properties of sorghum grain and powder. This study, therefore, sought to evaluate some quality properties of sorghum grain as affected by low and high energy electron irradiation in comparison with gamma rays (cobalt-60).

STUDY OBJECTS AND METHODS

Preparing the samples and irradiating the sorghum grain. Red sorghum grain (*Sorghum bicolor* L. Moench) was purchased on a local market in Ghana. The grain was thoroughly sorted to remove foreign materials and then kept in 13×21 cm zip-lock bags. The samples underwent standard irradiation at the Institute of Nuclear Chemistry and Technology, Warsaw, Poland [9]. The samples were separately irradiated with low energy electron beam, high energy electron beam, and gamma rays. The irradiation doses were 2, 4, 6, 8, and 10 kGy. Unirradiated sorghum grain served as a control.

The high energy electron beam irradiation experiment involved 300 g of sorghum grain and an ELEKTRONIKA 10-10 accelerator (9 MeV) with a dose rate of 10^3 Gy/s. The gamma irradiation was performed using a Gamma Chamber 5000 Co-60 at a dose rate of about 2 kGy/h. Alanine pellets (Aerial) were used to determine the delivered doses for the samples irradiated with high energy electron beam and gamma rays. They were measured at the INCT Laboratory for Measurements of Technological Doses, Poland (5% uncertainty). All the dose measurements were traceable to the NPL standard. The dose uniformity ratio (DUR) was evaluated as the ratio of maximal and minimal dose in the sample and equaled 1.1.

The low energy electron beam irradiation experiment involved 150 g of sorghum grain irradiated in a cylinder with an ILU-6 accelerator. The system for loose sample irradiation with low energy electron beam [10] provided a uniform dose distribution on each grain surface and made it possible to control the dose by the irradiation time. The dose rate to the grain surface was 2.5 kGy/min. The electrons had 250 keV energy; the layer under the surface of each grain was 150 μm thick. B3 dosimetric foil and the RISOSCAN software made it possible to determine the dose and penetration ability of electrons. The dose variability was 15% because of the irradiation conditions and the approximated dose measurements. All the experiments were triplicated, and the irradiated samples were sent back to Ghana for further analysis.

Powdering the irradiated and unirradiated sorghum grain. The irradiated and unirradiated sorghum samples were milled separately in a Waring CB15 blender (USA) and then sieved through a 500-μm sieve. The powder samples went to low-density zip-lock polyethylene bags to be analyzed within four weeks.

Determining the phytochemical properties. ***Preparing the extracts and determining the total phenolic content.*** The sorghum samples were subjected to extraction to measure the total phenolic content [11, 12]: 1 g of powder was extracted twice with water and methanol (40 mL) at a volume of 20:80 for 2 h. The supernatants were removed after centrifuging. The extracts were pooled, dried by evaporation at 50°C, and reconstituted in 10 mL of methanol to be refrigerated until further analysis.

The Folin-Ciocalteu spectrophotometric technique [13] made it possible to define the total phenolic content in the control and experimental sorghum grain. The test was conducted in triplicate using 10-mL test tubes. About 100 μL of diluted grain extract (1 mg/mL) was mixed with 50 μL of Folin-Ciocalteu's reagent (1M), followed by adding 1.85 mL of distilled water. After incubation in the dark at 25°C for 5 min, we added 1.0 mL of Na_2CO_3 (20% w/v) to the mix and shook it slowly with intermittent agitation. After 1 h, each seed extract underwent spectrophotometry using a Jasco V530 UV-VIS spectrophotometer (Japan) at a wavelength of 725 nm against the blank (without extracts) to check the absorbance value. The results were expressed as gallic acid equivalents (GAE) per 1 g of dry sample.

Preparing the extracts and determining the total flavonoid content. After adding 1 g of powder to the methanol/HCl (1%, v/v) solution, the mix was stirred in a water bath at 180 rpm for 120 min. The centrifugation of the supernatant lasted 5 min at 2790 g. Acidified methanol was added to the collected supernatants until a total volume of 20 mL. The extract was stored at –20°C until further use [14].

The colorimetric method [15] made it possible to quantify the total flavonoid content of the control and

irradiated sorghum grain. We mixed 250 µL of grain extract (1 mg/mL) with 100 µL of 10% $AlNO_3$ and 100 µL of potassium acetate (1M). After adding 4.3 mL of 80% ethanol to achieve a final volume of 5 mL, the mix was shaken and permitted to react for 10 min. A Jasco V530 UV-VIS spectrophotometer (Japan) measured the absorbance in triplicate at a wavelength of 410 nm. Quercetin served as the standard curve. The total flavonoid content of each extract was expressed in terms of quercetin equivalent (QE) per 1 g of dry sample.

Determining the tannin content. The tannin content was quantified as in [16]. Approximately 0.1 g of each sample was measured into Erlenmeyer flasks. After pipetting 10 mL of HCl (4%) in methanol, the flasks were sealed by parafilm, shaken for 20 min, and centrifuged at 4500 rpm for 10 min. The supernatants were transferred to 25-mL volumetric flasks, followed by the second extraction of residue using 1% HCl (5 mL) for 600 s. Both extracts (first and second) were combined and topped up to 25 mL using methanol.

The Folin-Denis reagent [17] made it possible to measure the tannin content. Using the standard calibration curve, we estimated the absorbance against the concentration of tannins at a specific wavelength as follows. Suitable aliquots of the tannin-containing extract (initially 0.05, 0.2, and 0.5 mL) were pipetted in test tubes. The volume was made up to 1.00 mL with distilled water, followed by adding 2.5 mL of sodium carbonate reagent. After shaking, the absorbance was read in a Jasco V530 UV-VIS spectrophotometer (Japan) at 725 nm after 40 min. Finally, we calculated the total phenolics as tannic acid equivalent from the standard curve and expressed it as mg/g.

Determining the physicochemical properties. ***Pasting profile.*** The pasting profile analysis involved a Brabender Viscograph-E (Germany). We prepared about 9.5% powder slurry by suspending 40 g (dry basis) powder in 420 mL of distilled water. The starch-containing suspension was thoroughly mixed and poured into a measuring bowl. The test mode had a 700 cmg measuring range at 75 rpm. The heating process started at 50°C at the rate of 3°C/min and continued until 92°C. After 15 min at 92°C, the samples were cooled down to 55°C at the rate of 3°C/min. This temperature remained constant for 15 min. The resulting pasting properties included time, temperature, and viscosity. The test was triplicated for each sample.

X-ray diffraction and relative crystallinity. The X-ray diffraction revealed the crystal patterns and the relative crystallinity of the sorghum grain in the sorghum powder. It involved a PAN analytical Empyrean diffractometer (Netherlands). The experimental conditions presupposed the 95% relative humidity and 22% glycerol solution [18]. The samples were equilibrated at 25°C for 5 days. The operating conditions were 45 kV, 40 m A, and Cu Kα1 (0.154 nm). The samples underwent scanning from 5° to 40° (2θ) at a step size of 0.20° and a step time of 10 s. By plotting relative intensity peaks against 2θ peaks, we calculated the relative crystallinity as the integrated area of crystalline peaks to the total integrated area above a straight baseline as a percentage [19].

pH. The pH test on sorghum powder was conducted in triplicate: 5 g of dry basis was mixed with 20 mL of distilled water, stirred for 5 min, and left to settle for 10 min. The pH of the water phase was measured using a calibrated Edge HI2002pH meter (Hanna Instruments) [20].

Titratable acidity. The procedure relied on the method described in [20]. We weighed 10 g of the powder sample in triplicate and mixed it with 100 mL of boiled distilled water at 25°C. The resulting suspension was stirred and allowed to digest for 30 min with frequent shaking. After 10 min of settling, the decanted supernatant was put in a 250-mL flask and immediately titrated with NaOH (0.1 N) using 0.3 mL of phenolphthalein. The lactic acid was calculated in %.

Functional properties. ***Bulk density.*** After weighing, an empty graduated tube was filled with powder to the 5-mL mark and tapped until the volume remained constant. After weighing the tube with its content, we divided the difference in weight (g) by the volume of the sample (5 mL) to obtain bulk density.

Water and oil absorption capacities. The water/oil absorption capacity of sorghum grain was determined as in [21, 22]. We mixed 1 g of powder with 10 mL of distilled water/oil in a centrifuge tube and allowed the mix to stand at ambient temperature (25 ± 2°C) for 1 h. After centrifuging in a Universal 320 centrifuge (Germany) at 2000 rpm for 30 min, we measured the volume of water/oil in the sediment. The water/oil absorption capacity was calculated as 1 mL of water/oil absorbed per 1 g of sorghum powder.

Solubility index and swelling power. The modified method described in [23] made it possible to estimate the solubility and swelling power of sorghum powder. We added 1 g of sorghum powder and 40 mL of distilled water into a centrifuge tube (50 mL) of pre-established weight. The suspension was gently stirred to prevent the starch granules in the powder from rapturing. An OLS200 Grant thermostatically controlled water bath (England) heated the suspension at 85°C for 30 min with constant stirring. Then, the tube was taken out of the water bath, wiped, and allowed to dry and cool to ambient temperature. After that, we poured the supernatant into a pre-weighed crucible and allowed it to dry at 105°C in a Gallenkamp oven (United Kingdom). The weight of the dried supernatant and the sediment paste measured after cooling made it possible to calculate the solubility and swelling power, respectively.

Data analysis. The mean values were compared using a one-way analysis of variance (ANOVA, Tukey-Kramer HSD, $p \leq 0.05$) and the Minitab 20 software.

RESULTS AND DISCUSSION

Phytochemical properties as affected by irradiation dose levels and radiation sources. Table 1 shows the total phenolic content. It decreased significantly ($p \leq 0.05$) after irradiation with gamma rays, low energy electron beam (LEEB), and high energy electron beam (HEEB).

Table 1 Effects of radiation source and dose on phytochemical properties of sorghum grain

Phytochemical property	Irradiation dose, kGy	Irradiation source		
		Gamma	High energy electron beam	Low energy electron beam
Total phenolic content, GAE/g	Control	6.15 ± 0.15^{Aa}	6.15 ± 0.15^{Aa}	6.15 ± 0.15^{Aa}
	2	3.13 ± 0.03^{Cb}	2.74 ± 0.04^{Dc}	5.96 ± 0.09^{Aa}
	4	4.61 ± 0.13^{Ba}	3.98 ± 0.01^{Cb}	4.60 ± 0.07^{Ca}
	6	4.42 ± 0.00^{Ba}	3.81 ± 0.01^{Cb}	3.47 ± 0.00^{Ec}
	8	3.28 ± 0.07^{Cb}	3.00 ± 0.03^{Dc}	3.96 ± 0.02^{Da}
	10	6.21 ± 0.21^{Aa}	4.29 ± 0.08^{Bc}	5.55 ± 0.09^{Bb}
Total flavonoid content, QE/g	Control	3.55 ± 0.05^{Aa}	3.55 ± 0.05^{Aa}	3.55 ± 0.05^{Aa}
	2	2.16 ± 0.04^{Eb}	1.78 ± 0.03^{Cc}	3.25 ± 0.02^{Ba}
	4	3.02 ± 0.04^{Ba}	2.35 ± 0.01^{Bb}	2.21 ± 0.01^{Dc}
	6	2.37 ± 0.05^{Da}	2.39 ± 0.02^{Ba}	1.82 ± 0.01^{Eb}
	8	2.61 ± 0.03^{Ca}	1.82 ± 0.02^{Cb}	1.59 ± 0.00^{Fc}
	10	1.83 ± 0.01^{Fc}	2.38 ± 0.01^{Bb}	2.81 ± 0.01^{Ca}
Tannin content, TAE/g	Control	11.96 ± 0.39^{Aa}	11.96 ± 0.39^{Aa}	11.96 ± 0.39^{Aa}
	2	11.74 ± 0.62^{Aa}	5.41 ± 0.08^{Bc}	9.07 ± 1.08^{Bb}
	4	8.36 ± 0.69^{Ba}	3.01 ± 0.62^{Cb}	7.48 ± 0.31^{BCDa}
	6	5.74 ± 0.39^{Ca}	4.54 ± 0.77^{BCa}	6.17 ± 0.23^{Da}
	8	5.19 ± 0.23^{Cb}	4.16 ± 0.46^{BCc}	6.39 ± 0.15^{CDa}
	10	5.58 ± 0.62^{Cb}	2.58 ± 0.62^{Cc}	8.41 ± 0.31^{BCa}

Means with different superscripts (lower case) in the same row that concern the irradiation source are significantly different ($p \leq 0.05$) from each other. Means with different superscript (upper case) in the same column that concern the dose of a particular irradiation type are significantly different ($p \leq 0.05$) from each other

The total phenolics reduced from 6.15 (control) to 3.13, 2.74, and 3.47 GAE/g for the samples treated with gamma rays, HEEB, and LEEB, respectively. However, at 10 kGy the total phenolic content was similar to that of the control for the gamma-irradiated sorghum grain. The reductions were not dose-dependent. The samples exposed to HEEB had the lowest values at each dose level in terms of total phenolics. The total phenolic content in the untreated samples exceeded the values reported in [24]. However, they stayed below the values reported in [13], which ranged from 8 to over 500 mg/g (8000 to 500 000 mg/kg) of total phenolics in other varieties.

Table 1 also shows the total flavonoid content of the control and experimental (irradiated) samples. It decreased significantly ($p \leq 0.05$) with irradiation across the sources and doses. The total flavonoid content reduced from 3.55 QE/g in the control sample to 1.83, 1.78, and 1.59 QE/g in the samples treated with gamma rays, HEEB, and LEEB, respectively. The decrease was not dose-dependent. Flavonoids are one of the several sources of natural antioxidants needed by humans and are mostly consumed as supplements [13]. In our case, the total flavonoid content was higher than the values reported in [13]. However, our total flavonoid content in the unirradiated sample (control) also exceeded some previous findings [25]. In addition, the values of some of the irradiated sorghum samples recorded in the present study compared favorably with those described in [25].

Table 1 summarizes the tannin (condensed tannin) contents of the unirradiated (control) and irradiated sorghum grain. Irradiation with gamma rays, LEEB, and HEEB reduced the tannin content in sorghum grain ($p \leq 0.05$) from 11.96 (control) to 5.19 (gamma rays), 2.58 (HEEB), and 6.17 TAE/g (LEEB). In terms of tannin content, the HEEB irradiated samples had the lowest values at each dose level. However, the reduction was not dose-dependent. The tannin contents recorded in the present study were lower than those reported in [25] but higher than in [26]. Tannins in food facilitate glucose uptake, as well as possess anticancer, anti-allergic, and anti-diabetic properties [27].

The total phenolic, flavonoid, and tannin contents that we observed in the unirradiated (control) sorghum samples differed from the values reported by other authors. The phenomenon could be attributed to the varietal differences, as well as some edaphic and climatic factors. Generally, irradiation dose and source had a significant effect on the phenolic, flavonoid, and tannin contents of sorghum grain. Some reports are quite conflicting, when it comes to the effect of gamma irradiation, as well as low and high energy electron beam treatments, on the total flavonoid, phenolic, and tannin contents of various crops [28]. Some authors reported that gamma irradiation increased the total flavonoid, phenolic, and tannin contents in some instances while reducing them under other conditions. In the present study, we observed a general reduction in the total flavonoid, phenolic, and tannin contents of sorghum grain, as previously reported in [29]. The reductions could be attributed to the degradation effect of gamma rays, LEEB, and HEEB on the components of total flavonoids, phenols, and tannins [29].

Physicochemical properties as affected by irradiation dose levels and radiation sources. ***Pasting profile.*** The pasting profile included such variables as pasting temperature, peak viscosity, viscosity at 92°C, setback

viscosity, and breakdown viscosity (Table 2). The general trend suggests that LEEB treatment did not alter the pasting parameters even at 10 kGy compared to the control. This observation was not different from those reported by other researchers: although the LEEB treatment was more energy efficient than HEEB or gamma rays, it was effective for surface decontamination without irradiating the bulk food [5, 10]. Gamma rays and HEEB irradiation caused significant changes in some pasting profiles ($p \leq 0.05$) (Table 2). With the exception of breakdown viscosity, which was not observed for both the irradiated and unirradiated grain, the other variables demonstrated some changes. Unlike LEEB, HEEB and gamma rays irradiated the bulk food [5], thus causing the abovementioned changes.

Below 6 kGy, gamma rays and HEEB treatment had no effect on the pasting temperature. However, the pasting temperature values decreased at 6–10 kGy, although not significantly. The pasting temperature of starch or flour is the temperature at which a sudden rise in viscosity first occurs with concurrent swelling. It indicates the minimal temperature for cooking starch [30]. High pasting temperature relates to a restricted swelling ability [30, 31]. The significant reduction in the pasting temperature of the sorghum grain irradiated at ≥ 6 kGy suggests that starch in the irradiated samples would cook faster than in the unirradiated samples. Kumar *et al*. [32] reported a decrease in the pasting temperature in gamma-irradiated brown rice starch.

In general, the peak viscosity and viscosity at 92°C for the sorghum grain powder decreased with increasing irradiation dose in the samples treated with gamma rays and HEEB. Despite the decreases, we recorded no significant ($p > 0.05$) changes in the peak viscosity and viscosity at 92°C across the samples exposed to doses ≥ 4 kGy. The effects of gamma rays and HEEB were not significant. Peak viscosity relates to the behavior of flour and starch paste under varying shear, temperature, and time [31]. The decrease in peak viscosity and viscosity at 92°C in the irradiated sorghum grain could be attributed to the depolymerization of sorghum starch molecules through chain scission [33]. Similar outcomes were reported for irradiated brown rice, lotus stem starch, and cowpeas [18, 32, 34].

At 4–10 kGy, gamma rays and HEEB affected the setback viscosity of sorghum grain, although both sources were not significantly different in effect. Gamma rays and HEEB treatments caused the setback viscosity to decrease at all the dose levels, especially at 4–10 kGy, where they had no significant differences. Setback viscosity indicates the inability of amylopectin to hold granules during water imbibition [18, 32]. It is mostly associated with polymerization of leached amylose and depolymerization of long linear amylopectin molecules [34]. They

Table 2 Effects of radiation source and dose on pasting properties of sorghum grain

Irradiation dose, kGy	Radiation source	pH	Titratable acidity, % lactic acid	Pasting parameters				
				Pasting temperature, °C	Peak viscosity, Brabender units	Viscosity at 92°C, Brabender units	Setback viscosity, Brabender units	Breakdown viscosity (Brabender units)
Control	Gamma	6.353 ± 0.006^{Ad}	0.021 ± 0.005^{Aa}	85.73 ± 2.40^{Aa}	122.33 ± 8.08^{Aa}	66.33 ± 11.59^{Aa}	195.00 ± 71.72^{Aa}	0
	LEEB	6.353 ± 0.006^{Ad}	0.021 ± 0.005^{Aa}	85.50 ± 0.86^{Aa}	124.50 ± 5.46^{Aa}	64.33 ± 10.58^{Aa}	151.67 ± 23.25^{Aa}	0
	HEEB	6.353 ± 0.006^{Ac}	0.021 ± 0.005^{Aa}	87.17 ± 1.67^{Aa}	100.00 ± 18.19^{Aa}	58.67 ± 2.16^{Aa}	152.33 ± 12.10^{Aa}	0
2	Gamma	6.433 ± 0.006^{ABa}	0.024 ± 0.005^{Aa}	86.53 ± 1.79^{Aa}	73.00 ± 36.59^{Bb}	44.00 ± 9.00^{Bb}	132.67 ± 129.00^{Ab}	0
	LEEB	6.437 ± 0.006^{Aab}	0.021 ± 0.005^{Aa}	85.33 ± 0.32^{Aa}	128.67 ± 7.23^{Aa}	60.67 ± 5.13^{Aa}	159.33 ± 7.51^{Aa}	0
	HEEB	6.423 ± 0.006^{Ba}	0.021 ± 0.005^{Aa}	87.27 ± 1.10^{Aa}	72.33 ± 32.62^{Bb}	46.33 ± 9.29^{Bb}	107.67 ± 35.01^{Ab}	0
4	Gamma	6.447 ± 0.012^{ABa}	0.018 ± 0.000^{Aa}	73.47 ± 20.38^{Aa}	31.00 ± 3.61^{Bc}	29.67 ± 3.78^{Bbc}	39.00 ± 12.29^{Bc}	0
	LEEB	6.443 ± 0.006^{Aab}	0.018 ± 0.000^{Aa}	85.60 ± 1.32^{Aa}	112.00 ± 12.49^{Aa}	57.33 ± 12.22^{Aa}	152.67 ± 8.08^{Aa}	0
	HEEB	6.420 ± 0.010^{Ba}	0.018 ± 0.000^{Aa}	88.47 ± 1.10^{Aa}	25.33 ± 7.23^{Bc}	24.33 ± 6.35^{Bc}	45.67 ± 14.15^{Bc}	0
6	Gamma	6.393 ± 0.006^{Bbc}	0.021 ± 0.005^{Aa}	50.17 ± 0.06^{Bb}	29.33 ± 0.58^{Bc}	24.00 ± 1.00^{Bc}	21.33 ± 0.58^{Bc}	0
	LEEB	6.437 ± 0.006^{Abc}	0.024 ± 0.005^{Aa}	86.03 ± 0.55^{Aa}	109.67 ± 15.89^{Aa}	60.00 ± 9.54^{Aa}	141.33 ± 22.37^{Aa}	0
	HEEB	6.380 ± 0.010^{Bb}	0.024 ± 0.005^{Aa}	50.17 ± 0.56^{Bb}	28.00 ± 1.00^{Bc}	24.33 ± 0.58^{Bc}	26.67 ± 3.79^{Bc}	0
8	Gamma	6.403 ± 0.006^{Bb}	0.024 ± 0.005^{Aa}	50.20 ± 0.00^{Bb}	30.33 ± 0.58^{Bc}	21.67 ± 0.58^{Bc}	15.33 ± 1.53^{Bc}	0
	LEEB	6.427 ± 0.006^{Ac}	0.024 ± 0.005^{Aa}	86.10 ± 0.79^{Aa}	91.33 ± 10.60^{Aa}	41.67 ± 14.57^{Aa}	135.00 ± 6.00^{Aa}	0
	HEEB	6.387 ± 0.006^{Cb}	0.021 ± 0.005^{Aa}	50.23 ± 0.06^{Bb}	28.00 ± 2.00^{Bc}	20.67 ± 1.16^{Bc}	14.67 ± 3.22^{Bc}	0
10	Gamma	6.380 ± 0.010^{Bc}	0.022 ± 0.000^{ABa}	50.23 ± 0.66^{Bb}	29.00 ± 0.00^{Bc}	19.00 ± 0.00^{Bc}	12.00 ± 1.00^{Bc}	0
	LEEB	6.457 ± 0.006^{Aa}	0.021 ± 0.005^{ABa}	85.60 ± 0.30^{Aa}	104.33 ± 6.11^{Aa}	55.33 ± 12.22^{Aa}	149.00 ± 7.21^{Aa}	0
	HEEB	6.377 ± 0.006^{Bb}	0.018 ± 0.000^{Ba}	52.30 ± 0.00^{Bb}	29.00 ± 1.00^{Bc}	20.00 ± 0.00^{Bc}	14.33 ± 0.58^{Bc}	0

Means with different superscripts (upper case) in the same column that concern the irradiation source are significantly different ($p \leq 0.05$) from each other. Means with different superscript (lower case) in the same column that concern the dose of a particular irradiation type are significantly different ($p \leq 0.05$) from each other

LEEB – low energy electron beam; HEEB – high energy electron beam

might have caused the decrease in the setback viscosity. The decrease in the setback viscosity at cooling might have resulted in a higher resistance to starch retrogradation [18], thus the inability of amylopectin to hold the granules during water imbibition. The current results agree with the earlier findings [18, 34] connected with irradiated cowpea and lotus stem starch, respectively.

Breakdown viscosity happens when the swelling granules rupture [34]. Zero breakdown viscosity indicates that the extent of swelling was extremely low before the disintegration. The breakdown viscosity value estimates the susceptibility of cooked starch to disintegration [35]; therefore, the zero values could be linked to the stability of the pastes during cooling [36].

pH and titratable acidity. Compared to the control, we detected a significant increase in pH values, although not in a dose-dependent manner, irrespective of the radiation sources at all the dose levels (Table 2). However, the titratable acidity values demonstrated no significant difference across the samples. Despite the appreciable increase in pH, the pH of the grain samples irradiated with gamma rays and HEEB, unlike those irradiated with LEEB, were significantly ($p \leq 0.05$) lower at all the dose levels, as compared to the control. At 6–10 kGy, gamma ray and HEEB treatments reduced the pH level but not significantly below that of the control. This trend of increased pH in the irradiated sorghum grain contradicts other findings. For instance, a certain reduction in pH after gamma irradiation was reported for chickpea starch [37] and exopolysaccharide [38]. The change in pH could be attributed to the formation of free radicals and the cleavage of large starch molecules during irradiation [39]. The reduction in pH in the samples irradiated with gamma rays and HEEB at 6–10 kGy could be associated with the cleavage of starch molecules, as well as with acetic, formic, glucuronic, and pyruvic acids formed during irradiation [38].

X-ray diffraction and relative crystallinity. Figure 1 and Table 3 illustrate the X-ray diffraction patterns and the relative crystallinity of powders obtained from sorghum grain irradiated with gamma, HEEB, and LEEB. Major diffraction peaks were observed at 2 Theta;

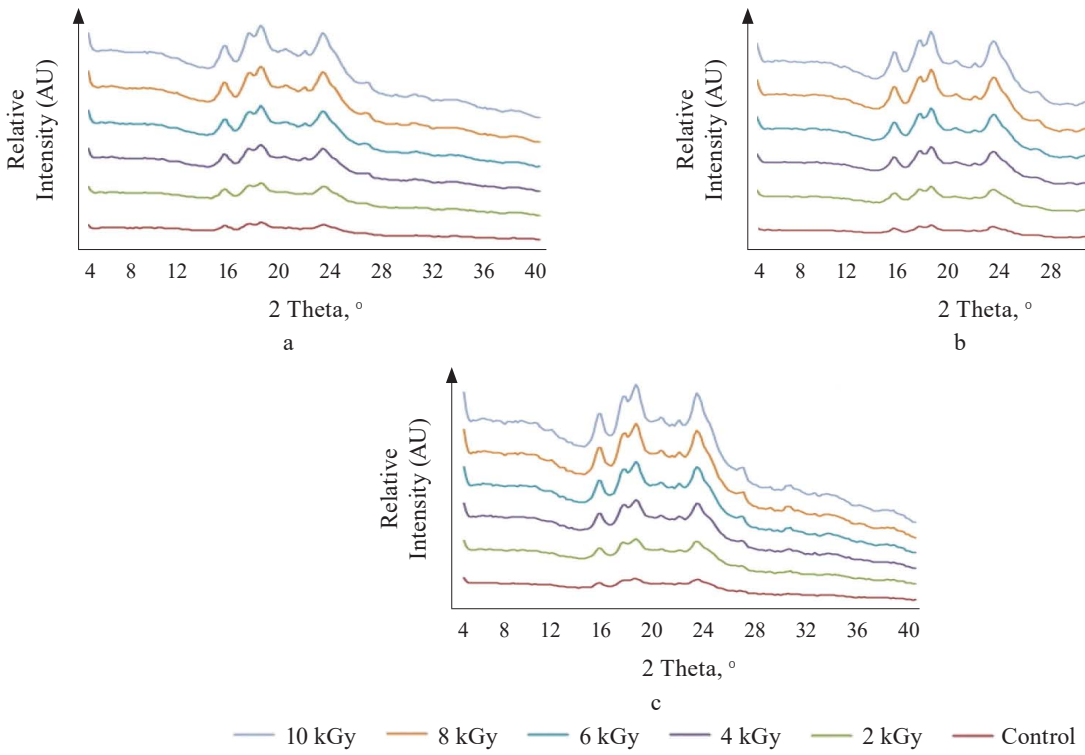

Figure 1 X-ray diffractograms of powder from sorghum grain irradiated with gamma rays (a), low energy electron beam (b), and high energy electron beam (c)

Table 3 Effects of radiation source and dose on relative crystallinity of sorghum grain

Irradiation source	Irradiation doses, kGy					
	0	2	4	6	8	10
Gamma rays	15.96 ± 0.00^{Ac}	16.31 ± 0.00^{Aa}	16.06 ± 0.00^{Bb}	15.93 ± 0.00^{Cd}	15.67 ± 0.00^{Ce}	14.69 ± 0.00^{Bf}
High energy electron beam	14.84 ± 0.05^{Ce}	15.43 ± 0.00^{Bd}	16.41 ± 0.00^{Ab}	18.28 ± 0.00^{Aa}	15.69 ± 0.00^{Bc}	14.55 ± 0.00^{Cf}
Low energy electron beam	15.64 ± 0.00^{Bc}	15.38 ± 0.00^{Ce}	14.95 ± 0.00^{Cf}	16.38 ± 0.00^{Ba}	16.11 ± 0.00^{Ab}	15.60 ± 0.00^{Ad}

Means with different superscripts (upper case) in the same column that concern the irradiation source are significantly different ($p \leq 0.05$) from each other. Means with different superscript (lower case) in the same row that concern the dose of a particular irradiation type are significantly different ($p \leq 0.05$) from each other

Table 4 Effects of radiation source and dose on some functional properties of sorghum grain

Parameters	Radiation source	Irradiation doses, kGy					
		0	2	4	6	8	10
Bulk density, g/mL	Gamma	0.841 ± 0.039^{Aa}	0.764 ± 0.042^{Aa}	0.812 ± 0.012^{Aa}	0.855 ± 0.037^{Aa}	0.776 ± 0.027^{Aa}	0.821 ± 0.041^{Aa}
	HEEB	0.806 ± 0.039^{Aa}	0.746 ± 0.024^{Aab}	0.682 ± 0.023^{Bb}	0.720 ± 0.057^{Bb}	0.703 ± 0.063^{Ab}	0.773 ± 0.004^{Aab}
	LEEB	0.841 ± 0.039^{Aa}	0.766 ± 0.048^{Aa}	0.759 ± 0.043^{Aa}	0.823 ± 0.017^{Aa}	0.775 ± 0.040^{Aa}	0.775 ± 0.009^{Aa}
Water absorption, mL/g	Gamma	1.720 ± 0.117^{Ab}	1.790 ± 0.007^{Aab}	1.794 ± 0.005^{Aab}	1.856 ± 0.110^{Aab}	1.924 ± 0.064^{Aab}	1.920 ± 0.114^{Aab}
	HEEB	1.720 ± 0.117^{Aa}	1.726 ± 0.111^{Aa}	1.860 ± 0.115^{Aa}	1.720 ± 0.114^{Aa}	1.918 ± 0.114^{Aa}	1.723 ± 0.111^{Aa}
	LEEB	1.720 ± 0.117^{Aa}	1.656 ± 0.120^{Aa}	1.728 ± 0.113^{Aa}	1.722 ± 0.110^{Aa}	1.721 ± 0.116^{Aa}	1.656 ± 0.116^{Aa}
Oil absorption, mL/g	Gamma	1.196 ± 0.002^{Ac}	1.592 ± 0.195^{Ab}	1.542 ± 0.115^{Ab}	1.660 ± 0.121^{Aa}	1.659 ± 0.121^{Aa}	1.661 ± 0.115^{Aa}
	HEEB	1.196 ± 0.002^{Ab}	1.658 ± 0.116^{Aa}	1.524 ± 0.117^{Aa}	1.726 ± 0.113^{Aa}	1.722 ± 0.112^{Aa}	1.723 ± 0.114^{Aa}
	LEEB	1.196 ± 0.002^{Ad}	1.388 ± 0.001^{Ac}	1.458 ± 0.115^{Abc}	1.488 ± 0.001^{Abc}	1.591 ± 0.002^{Aab}	1.720 ± 0.117^{Aa}
Solubility Index, %	Gamma	7.19 ± 0.08^{Af}	7.79 ± 0.02^{Ae}	8.35 ± 0.08^{Ad}	8.53 ± 0.31^{Bc}	9.40 ± 0.16^{Bb}	9.90 ± 0.31^{Ba}
	HEEB	7.21 ± 0.02^{Ac}	7.35 ± 0.01^{Bd}	7.16 ± 0.13^{Bf}	10.82 ± 0.18^{Ab}	10.77 ± 0.14^{Ac}	11.21 ± 0.33^{Aa}
	LEEB	7.28 ± 0.05^{Aa}	5.42 ± 0.02^{Cd}	6.22 ± 0.42^{Cc}	5.19 ± 0.12^{Cf}	6.53 ± 0.45^{Cb}	5.25 ± 0.65^{Ce}
Swelling power	Gamma	8.53 ± 0.01^{Aa}	7.03 ± 0.56^{Cb}	6.52 ± 0.08^{Cd}	5.59 ± 0.57^{Cf}	6.01 ± 0.39^{Ce}	6.62 ± 0.27^{Bc}
	HEEB	8.54 ± 0.01^{Aa}	7.58 ± 0.09^{Bb}	7.21 ± 0.05^{Bc}	5.86 ± 0.08^{Bf}	6.33 ± 0.32^{Be}	6.64 ± 0.41^{Bd}
	LEEB	8.53 ± 0.00^{Ac}	8.76 ± 0.15^{Ab}	8.51 ± 0.09^{Ac}	8.96 ± 0.06^{Aa}	8.13 ± 0.15^{Ad}	8.16 ± 0.05^{Ad}

Means with different superscripts (upper case) in the same column that concern the irradiation source are significantly different ($p \leq 0.05$) from each other. Means with different superscript (lower case) in the same row that concern the dose of a particular irradiation type are significantly different ($p \leq 0.05$) from each other

LEEB – low energy electron beam; HEEB – high energy electron beam

they approximately equaled 15, 17, 18, and 23° for both the unirradiated control sample and the powders from sorghum grain irradiated with gamma rays, LEEB, and HEEB (Fig. 1). These major peaks could be attributable to the presence of A-type crystal [33]. Similar patterns for sorghum powder from different sorghum hybrids cultivated in Argentina were reported in [40]. The X-ray diffraction patterns of the sorghum powder samples did not depend on the sources and doses. A similar finding was reported for rice [33].

The relative crystallinity values were significantly different across the samples (Table 3). Gamma irradiation doses from 6 to 10 kGy significantly decreased the relative crystallinity of the starch in the sorghum powder samples. However, a non-dose-dependent increase was recorded for 2 and 4 kGy. The effect of high and low energy electron irradiation had no pattern. Ocloo *et al.* [33] reported no significant difference in the relative crystallinity of some local rice cultivars after gamma irradiation doses of 0.25, 0.5, 0.75, 1.0, and 1.5 kGy.

Functional properties as affected by irradiation dose levels and radiation sources. Table 4 shows the bulk density, water absorption capacity, oil absorption capacity, solubility index, and swelling power of the sorghum grain samples under study. The bulk density decreased at 4 and 6 kGy in the samples subjected to high energy electron beam tretament. On the contrary, the samples irradiated with gamma ray and low energy electron beam retained the same bulk density from 2 to 10 kGy (Table 4). Compared with the control, gamma ray and LEEB did not significantly alter the bulk density. However, HEEB irradiation caused significant reductions in the bulk density at 4, 6, and 8 kGy. A previous study reported that gamma irradiation had no effect on the bulk density of cowpea flour [18]. Similarly, gamma irradiation had no significant effect on rice flour [33]. Bulk density is a function referred to the particle size of the samples. In the food industry, it is important for determining the packaging requirements, material handling, and application in wet processing [36]. The disparities in the bulk density values in the present study could be due to the differences in doses and radiation sources.

The water absorption capacity demonstrated no significant changes at all the dose levels across all irradiation sources (Table 4). Water absorption capacity explains the interaction between the product and water, with water being the limiting factor. Water absorption capacity helps preserve freshness and mouthfeel [41]. Other studies reported contrary findings. For instance, water absorption capacity increased in gamma-irradiated cowpea [18] and rice protein irradiated with high energy electron beam [41]. The fact that water absorption capacity remains the same after irradiation indicates that irradiation did not affect the freshness and mouthfeel.

The oil absorption capacity demonstrated no significant differences between the irradiation sources at 2–10 kGy (Table 4). However, oil absorption capacity increased in all the irradiated grain compared to the control. Greater increments in oil absorption capacity were observed at 6–10 kGy for the gamma-irradiated samples and at 10 kGy for the samples subjected to low energy electron beam treatment.

Oil absorption capacity is important in flavor retention, shelf-life improvement, and palatability [18]. Surface hydrophobicity, physical entrapment of oil, and macromolecule size could affect oil absorption capacity [41]. During irradiation, the partial unfolding of proteins causes the exposure of non-polar protein residues inside

the molecules, thus enhancing protein and oil interactions [41], which might result in the increment in oil absorption capacity. The outcomes of this study agree with a previous study that reported an increased oil absorption capacity of rice protein after irradiation with high energy electron beam [41]. Therefore, the increment in oil absorption capacity could improve shelf stability, palatability, and flavor.

The solubility index increased in the grain irradiated with gamma rays and HEEB. However, it decreased in the samples subjected to LEEB irradiation (Table 4). In the gamma-irradiated samples, the solubility index increased together with the dose. In the HEEB samples, the increase was not dose-dependent, and the highest solubility index was obtained at 10 kGy. In the LEEB samples, the decrease in solubility index did not depend on the dose either. The effect of radiation source on the solubility index was significant across the three sources, with LEEB being the lowest. At 2 and 4 kGy, the gamma-irradiated samples had a significantly higher solubility index than those irradiated with HEEB. However, a reverse trend was obtained at 6–10 kGy. Our results corresponded with the dose-dependent increase in solubility index reported for gamma-irradiated cowpea and potato starch [42].

An increase in the solubility of some rice cultivars with increasing irradiation dose was described in [33]. Solubility is mostly associated with the presence of soluble molecules, e.g., amylose, sugars, and albumins [35]. Irradiation could lead to depolymerization and breakdown of the polysaccharide (amylopectin), thus causing the formation of low molecular weight or shorter fragments [38], e.g., soluble molecules. The increase in solubility index could be related to the increased depolymerization of starch chains resulting in enhanced hydration of powder particles [2]. A comparative increase in solubility index renders irradiated sorghum grain the capabilities of a bio-thickener or stabilizing agent.

A reduction in the swelling power was observed in the grain samples irradiated with HEEB and gamma rays but it was not dose-dependent. In the LEEB irradiated grain, the swelling power increased at 2 and 6 kGy before decreasing at 8 and 10 kGy, as compared with the control. This trend shows the inconsistent effect of LEEB on swelling power. The three sources had significantly different effects on the swelling power.

At 2–8 kGy, the gamma-irradiated samples exhibited a lower swelling power followed by HEEB and then LEEB treatments, except at 10 kGy, where gamma rays and HEEB irradiation had a comparable effect. A similar decrease in swelling power was previously reported in the study of gamma-irradiated cowpea and potato starch [42]. Similarly, electronirradiated yam flour demonstrated a decrease in swelling power [43]. Ocloo *et al*. [33] also reported a decrease in the swelling power of some rice cultivars with increasing irradiation dose. Swelling is the ability of starch molecules (amylopectin) to trap and retain water within its structure [34]. In our case, the decrease in the swelling power in the irradiated samples could be linked to the reduced ability of starch (amylopectin) to imbibe water since the starch molecule might have been depolymerized by the irradiation.

CONCLUSION

In this study, the source of irradiation significantly ($p \leq 0.05$) affected the phytochemical parameters of sorghum grain. Irradiation with low energy electron beam (LEEB) had the least effect on most components, as compared with the other treatments. Except for LEEB, the irradiation sources had a different effect on most pasting parameters. The alteration (reduction) in the pasting parameters was not dose-dependent. The functional properties were significantly altered or remained unchanged after irradiation with gamma rays, high energy electron beam (HEEB), and LEEB. Different irradiation sources had different effects on some functional parameters, which usually depended on the increasing dose. The data obtained suggest that LEEB treatment proved to be an effective alternative to gamma rays and HEEB in sorghum grain production as the method had no significant effect on the physicochemical and functional properties of sorghum powder.

CONTRIBUTION

B. Darfour, J. Agyei-Amponsah, B.T. Odai, T. Mahami, J.O. Armah, E.A. Ayeh, I. Adjei, J. Basugilo, S. Asomaniwaa, and M.N.Y.H. Egblewogbe are responsible for the research, methodology, formal analysis, original draft, review, and proofreading. F.C.K. Ocloo developed the research concept and provided data curation and resources, as well as participated in the review and proofreading.

CONFLICT OF INTEREST

The authors declare that there is no conflict of interests related to the publication of this article.

ACKNOWLEDGEMENTS

The authors are grateful to the International Atomic Energy Agency, the Institute of Nuclear Chemistry and Technology, Poland, and the technologists at the XRD-laboratory at the University of Ghana for their diverse support.

REFERENCES

1. Dahlberg JA, Wasylikowa K. Image and statistical analyses of early sorghum remains (8000 B.P.) from the Nabta Playa archaeological site in the Western Desert, southern Egypt. Vegetation History and Archaeobotany. 1996;5: 293–299. https://doi.org/10.1007/BF00195297
2. Pan L, Xing J, Zhang H, Luo X, Chen Z. Electron beam irradiation as a tool for rice grain storage and its effects on the physicochemical properties of rice starch. International Journal of Biological Macromolecules. 2020;164:2915–2921. https://doi.org/10.1016/j.ijbiomac.2020.07.211

3. Chmielewski AG, Migdal W. Radiation decontamination of herbs and spices. Nukleonika. 2005;50(4):179–184.
4. Rather SA, Hussain PR, Suradkar PP, Ayob O, Sanyal B, Tillu A, *et al*. Comparison of gamma and electron beam irradiation for using phytosanitary treatment and improving physicochemical quality of dried apricot and quince. Journal of Radiation Research and Applied Sciences. 2019;12(1):245–259. https://doi.org/10.1080/16878507.2019.1650223
5. Innovation of irradiation technologies on surface treatment of food commodities. Report of a consultants meeting IAEA Headquarters, Vienna, Austria [Internet]. [cited 2024 July 3]. Available from: https://www-pub.iaea.org/MTCD/Publications/PDF/Newsletters/fep-23-1.pdf
6. Jung K, Go S-M, Moon B-G, Song B-S, Park J-H. Comparative study on the sensory properties of Fuji apples and Niitaka pears irradiated by gamma rays, electron beams or X-rays. Food Science and Technology Research. 2016;22(1):23–29. https://doi.org/10.3136/fstr.22.23
7. Jung K, Song B-S, Kim MJ, Moon B-G, Go S-M, Kim J-K, *et al*. Effect of X-ray, gamma ray and electron beam irradiation on the hygienic and physic-chemical qualities of red pepper powder. LWT – Food Science and Technology. 2015;63(2):846–851. https://doi.org/10.1016/j.lwt.2015.04.030
8. Choi J, Kim J-K, Srinivasan P, Kim J-H, Park H-J, Byun M-W, *et al*. Comparison of gamma ray and electron beam irradiation on extraction yield, morphological and antioxidant properties of polysaccharides from tamarind seed. Radiation Physics and Chemistry. 2009;78(7–8):605–609. https://doi.org/10.1016/j.radphyschem.2009.04.004
9. Ocloo FCK, Odai BT, Darfour B, Mahami T, Armah JO, Ayeh EA, *et al*. Microbial quality and aflatoxin levels of sorghum grains (*Sorghum bicolor*) irradiated with gamma rays, low energy electron beam (LEEB) and high energy electron beam (HEEB). Radiation Physics and Chemistry. 2024;216:111474. https://doi.org/10.1016/j.radphyschem.2023.111474
10. Gryczka U, Kamey H, Kimura K, Todoriki S, Migdała W, Bułka S. Efficacy of low energy electron beam on microbial decontamination of spices. Radiation Physics and Chemistry. 2020;170:108662. https://doi.org/10.1016/j.radphyschem.2019.108662
11. Wu L, Huang Z, Qin P, Ren G. Effects of processing on phytochemical profiles and biological activities for production of sorghum tea. Food Research International. 2013;53(2):678–685. https://doi.org/10.1016/j.foodres.2012.07.062
12. Van Hung P, Morita N. Distribution of phenolic compounds in the graded flours milled from whole buckwheat grains and their antioxidant capacities. Food Chemistry. 2008;109(2):325–331. https://doi.org/10.1016/j.foodchem.2007.12.060
13. Ghimire B-K, Seo J-W, Yu C-Y, Kim S-H, Chung I-M. Comparative study on seed characteristics, antioxidant activity, and total phenolic and flavonoid contents in accessions of *Sorghum bicolor* (L.) Moench. Molecules. 2021;26(13):3964. https://doi.org/10.3390/molecules26133964
14. Pinheiro SS, Anunciação PC, Cardoso LM, Della Lucia CM, de Carvalho CWP, Queiroz VAV, *et al.* Stability of B vitamins, vitamin E, xanthophylls and flavonoids during germination and maceration of sorghum (*Sorghum bicolor* L.). Food Chemistry. 2021;345:128775. https://doi.org/10.1016/j.foodchem.2020.128775
15. Moreno MIN, Isla MI, Sampietro AR, Vattuone MA. Comparison of the free radical-scavenging activity of propolis from several regions of Argentina. Journal of Ethnopharmacology. 2000;71(1–2):109–114. https://doi.org/10.1016/S0378-8741(99)00189-0
16. Dykes L, Rooney LW, Waniska RD, Rooney WL. Phenolic compounds and antioxidant activity of sorghum grains of varying genotypes. Journal of Agricultural and Food Chemistry. 2005;53(17):6813–6818. https://doi.org/10.1021/jf050419e
17. Makkar HPS, Blummel M, Borowy NK, Becker K. Gravimetric determination of tannins and their correlations with chemical and protein precipitation methods. Journal of the Science of Food and Agriculture. 1993;61(2):161–165. https://doi.org/10.1002/jsfa.2740610205
18. Darfour B, Wilson DD, Ofosu DO, Ocloo FCK. Physical, proximate, functional and pasting properties of flour produced from gamma-irradiated cowpea (*Vigna unguiculata, L.* Walp). Radiation Physics and Chemistry. 2012;81(4):450–457. https://doi.org/10.1016/j.radphyschem.2011.12.015
19. Cheetham NWH, Tao L. Variation in crystalline type with amylose content in maize starch granules: an X-ray powder diffraction study. Carbohydrate Polymers. 1998;36(4):277–284. https://doi.org/10.1016/S0144-8617(98)00007-1
20. Official methods of analysis. 15th Ed. Washington: Association of Official Analytical Chemists; 1990.
21. Sathe SK, Salunkhe DK. Functional properties of the great northern bean (*Phaseolus vulgaris* L.) proteins: emulsion, foaming, viscosity, and gelation properties. Journal of Food Science. 1981;46(1):71–81. https://doi.org/10.1111/j.1365-2621.1981.tb14533.x
22. Adebowale KO, Olu-Owolabi BI, Olawumi E, Lawal OS. Functional properties of native, physically, and chemically modified breadfruit (*Artocarpus artilis*) starch. Industrial Crops and Products. 2005;21(3):343–351. https://doi.org/10.1016/j.indcrop.2004.05.002

23. Leach HW, Mccowen LD, Schoch TJ. Structure of the starch granule. I. Swelling and solubility patterns of various starches. Cereal Chemistry. 1959;36(6):534–544.

24. Khalid W, Ali A, Arshad MS, Afzal F, Akram R, Siddeeg A, *et al*. Nutrients and bioactive compounds of *Sorghum bicolor* L. used to prepare functional foods: a review on the efficacy against different chronic disorders. International Journal of Food Properties. 2022;25(1):1045–1062. https://doi.org/10.1080/10942912.2022.2071293

25. Ofosu KF, Elahi F, Daliri EB-M, Yeon S-J, Ham HJ, Kim J-H, *et al*. Flavonoids in decorticated sorghum grains exert antioxidant, antidiabetic and antiobesity activities. Molecules. 2020;25(12):2854. https://doi.org/10.3390/molecules25122854

26. Pan L, Li W, Gu XM, Zhu WY. Comparative ileal digestibility of gross energy and amino acids in low and high tannin sorghum fed to growing pigs. Animal Feed Science and Technology. 2021;292:115419. https://doi.org/10.1016/j.anifeedsci.2022.115419

27. Sharma K, Kumar V, Kaur J, Tanwar B, Goyal A, Sharma R, *et al*. Health effects, sources and safety of tannins: a critical review. Toxin Reviews. 2019;40(4):432–444. https://doi.org/10.1080/15569543.2019.1662813

28. Gumul D, Berski W. The polyphenol profile and antioxidant potential of irradiated rye. International Journal of Food Science. 2021;2021(1):8870754. https://doi.org/10.1155/2021/8870754

29. Rodríguez-Núñez JR, Rodríguez-Félix A, Campa-Siqueiros PI, Val-Félix L, Madera-Santana TJ. Ionizing technology effects on bioactive compounds from food products. In: Shayanfar S, Pillai SD, editors. Ionizing radiation technologies: managing and extracting value from wastes. John Wiley & Sons Ltd; 2022. pp. 104–119. https://doi.org/10.1002/9781119488583.ch7

30. Hashimoto JM, Schmiele M, Nabeshima EH. Pasting properties of raw and extruded cowpea cotyledons flours. Brazilian Journal of Food Technology. 2020;23:e2019303. https://doi.org/10.1590/1981-6723.30319

31. Ayetigbo O, Latif S, Abass A, Müller J. Comparing characteristics of root, flour and starch of biofortified yellow-flesh and white-flesh cassava variants, and sustainability considerations: a review. Sustainability. 2018;10(9):3089. https://doi.org/10.3390/su10093089

32. Kumar P, Prakash KS, Jan K, Swer TL, Jan S, Verma R, *et al*. Effects of gamma irradiation on starch granule structure and physicochemical properties of brown rice starch. Journal of Cereal Science. 2017;77:194–200. https://doi.org/10.1016/j.jcs.2017.08.017

33. Ocloo FCK, Owureku-Asare M, Agyei-Amponsah J, Agbemavor WSK, Egblewogbe MNYH, Apea-Bah FB, *et al*. Effect of gamma irradiation on physicochemical, functional and pasting properties of some locally-produced rice (*Oryza* spp) cultivars in Ghana. Radiation Physics and Chemistry. 2017;130:196–201. https://doi.org/10.1016/j.radphyschem.2016.08.025

34. Gani A, Gazanfar T, Jan R, Wani SM, Masoodi FA. Effect of gamma irradiation on the physicochemical and morphological properties of starch extracted from lotus stem harvested from Dal Lake of Jammu and Kashmir, India. Journal of the Saudi Society of Agricultural Sciences. 2013;12(2):109–115. https://doi.org/10.1016/j.jssas.2012.08.004

35. Wani IA, Sogi DS, Gill BS. Physicochemical properties of acetylated starches from some Indian kidney bean (*Phaseolus vulgaris* L.) cultivars. International Journal of Food Science and Technology. 2012;47(9):1993–1999. https://doi.org/10.1111/j.1365-2621.2012.03062.x

36. Ocloo FCK, Bansa D, Boatin R, Adom T, Agbemavor WS. Physico-chemical, functional and pasting characteristics of flour produced from Jackfruits (*Artocarpus heterophyllus*) seeds. Agriculture and Biology Journal of North America. 2010;1(5):903–908. https://doi.org/10.5251/abjna.2010.1.5.903.908

37. Bashir M, Haripriya S. Physicochemical and structural evaluation of alkali extracted chickpea starch as affected by γ-irradiation. International Journal of Biological Macromolecules. 2016;89:279–286. https://doi.org/10.1016/j.ijbiomac.2016.04.080

38. Kavitake D, Techi M, Abid UK, Kandasamy S, Devi PB, Shetty PH. Effect of γ-irradiation on physico-chemical and antioxidant properties of galactan exopolysaccharide from *Weissella confusa* KR780676. Journal of Food Science and Technology. 2019;56:1766–1774. https://doi.org/10.1007/s13197-019-03608-w

39. Sabularse VC, Liuzzo JA, Rao RM, Grodner RM. Cooking quality of brown rice as influenced by gamma irradiation, variety and storage. Journal of Food Science. 1991;56(1):96–98. https://doi.org/10.1111/j.1365-2621.1991.tb07984.x

40. Palavecino PM, Penci MC, Calderón-Domínguez G, Ribotta PD. Chemical composition and physical properties of sorghum flour prepared from different sorghum hybrids grown in Argentina. Starch-Stärke. 2016;68(11–12):1055–1064. https://doi.org/10.1002/star.201600111

41. Zhang X, Wang L, Chen Z, Li Y, Luo X, Li Y. Effect of electron beam irradiation on the structural characteristics and functional properties of rice proteins. RSC Advances. 2019;9(24):13550–13560. https://doi.org/10.1039/C8RA10559F

42. Verma K, Jan K, Bashir K. γ irradiation of cowpea and potato starch: Effect on physicochemical functional and rheological properties. Journal of Food Processing and Technology. 2019;10(9):1000810. https://doi.org/10.35248/2157-7110.19.10.810

43. Wang G, Wang D, Qing C, Chen L, Gao P, Huang M. Impacts of electron-beam-irradiation on microstructure and physical properties of yam (*Dioscorea opposita Thunb.*) flour. LWT. 2022;163:113531. https://doi.org/10.1016/j.lwt.2022.113531

ORCID IDs
Fidelis C.K. Ocloo https://orcid.org/0000-0002-8926-4875
Joyce Agyei-Amponsah https://orcid.org/0000-0001-6576-3736
Bernard T. Odai https://orcid.org/0000-0001-8602-8976
Tahiru Mahami https://orcid.org/0000-0003-1672-3310
Jonathan O. Armah https://orcid.org/0009-0009-2549-2818
Ernestina A. Ayeh https://orcid.org/0009-0005-2918-1583
Isaac Adjei https://orcid.org/0009-0009-8437-6366
Jacob Basugilo https://orcid.org/0009-0004-4527-5945
Sarah Asomaniwaa https://orcid.org/0009-0003-6889-2068
Martin N.Y.H. Egblewogbe https://orcid.org/0000-0001-5921-4300
Bernard Darfour https://orcid.org/0000-0003-3321-0242

Foods and Raw Materials. 2026;14(1)

ISSN 2308-4057 (Print)
ISSN 2310-9599 (Online)

Research Article
Open Access

Available online at http://jfrm.ru/en
https://doi.org/10.21603/2308-4057-2026-1-667
https://elibrary.ru/PLSQQA

Polymer stoppers: Quality of alcohol beverages during storage

Larisa E. Chemisova*, Natalia M. Ageyeva, Olga N. Sheludko, Mikhail V. Antonenko, Yurii F. Yakuba

North Caucasian Federal Scientific Center of Horticulture, Viticulture, Wine-making, Krasnodar, Russia

* e-mail: nognichenko@mail.ru

Received 11.03.2024; Revised 27.08.2024; Accepted 03.09.2024; Published online 30.04.2025

Abstract:
Polymer stoppers are gaining popularity over traditional corks. However, their quality level remains understudied, as does their effect on commercial alcoholic beverages. This research featured the quality and safety indicators of polymer stoppers. The research objective was to assess their potential impact on the quality and safety of alcoholic drinks during storage.
The study focused on six types of polymer stoppers that differed in manufacturer, price, and material. Such aspects as appearance, geometry, impermeability, sensory profile, and polymer dust were determined based on State Standard 32626-2014. Toxic substances were assessed by gas chromatography while the migration of substances from the stopper surface was studied using direct microscopy. Sample preparation protocol followed Technical Regulation of Customs Union 005/2011 and State Standard 32626-2014.
Certain stoppers, mainly from the low-cost segment, failed to meet the impermeability requirements, especially in case of hot-process bottling. The experiment revealed such toxic and hazardous substances as dibutyl and dioctyl phthalates, acetone, ethyl acetate, hexane, heptane, methanol, propyl, butyl, and isobutyl. They penetrated into the model environment and deteriorated the sensory properties of the alcoholic beverages. The acceptable level of methanol migration was exceeded by ≥ 10 times. The concentration of propyl alcohol reached 0.435 mg/L, with its acceptable level being 0.100 mg/L. The concentration of ethyl acetate was 20 times as high as the standard.
The research confirmed phthalate migration from polymer stoppers into alcoholic beverages during storage. Their migration rate and concentration in the finished product correlated with the strength of the beverage and storage temperature. Apparently, winemakers should apply stricter sanitary, quality, and safety standards to the stoppers they use to bottle their produce.

Keywords: Polymer materials, bottling, corks, alcohol industry, safety, toxic elements, dioctyl phthalate, dimethyl phthalate

Funding: The research was supported by the Kuban Science Foundation as part of Innovative Research Project No. NIP-20.1/22.25.

Please cite this article in press as: Chemisova LE, Ageyeva NM, Sheludko ON, Antonenko MV, Yakuba YuF. Polymer stoppers: Quality of alcohol beverages during storage. Foods and Raw Materials. 2026;14(1):159–173. https://doi.org/10.21603/2308-4057-2026-1-667

INTRODUCTION

The wine and the stopper have been inseparable throughout human history. The stopper has been a key element of wine preservation during storage, from the epoch of amphorae to modern glass bottles. The earliest stoppers were made from any available materials, such as wood, bamboo, etc. Natural cork stoppers appeared in the IX century. Eventually, their production technology became as mechanized as that of glass bottles.

However, the cork tree and, subsequently, the cork itself are vulnerable to pests and various microorganisms. Their waste products may spoil the wine. Mold-induced polychlorophenols and polychloroanisoles cause a moldy taint and a number of other wine faults, even at low doses [1, 2]. Moreover, the cork tree has become a depletable resource that needs protection. To support the market for natural wine stoppers, the alcohol industry has introduced alternative variants. Polymer stoppers (Fig. 1) are a functional analogue to traditional corks. They are made of synthetic polymers treated with silicone or other similar substances. Since they entered the market in the late XX century, polymer stoppers have remained a popular cork alternative.

The current share of polymer stoppers is 16–20% of the global market for wine stoppers [3]. They are made by casting or coextrusion from food packaging polymers.

Copyright © 2025, Chemisova *et al.* This is an open access article distributed under the terms of the Creative Commons Attribution 4.0 International License (https://creativecommons.org/licenses/by/4.0/), allowing third parties to copy and redistribute the material in any medium or format and to remix, transform, and build upon the material for any purpose, even commercially, provided the original work is properly cited and states its license.

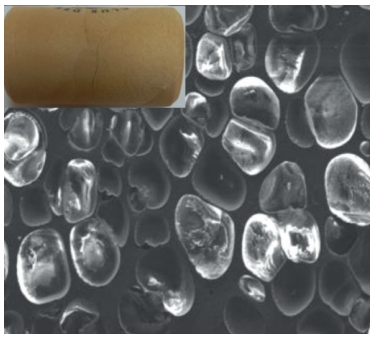

Figure 1 Polymer cork structure, scanning electron microscopy

Casting, or injection molding, involves pouring a mix of thermoplastic elastomers (styrene-butadiene-styrene and styrene-ethylene/butadiene-styrene) into a special mold cavity. Coextrusion is a two-step process. First, high-density polyethylene and talc are mixed, melted, and extruded as a long foam cylinder. Second, the resulting stopper is thermally bonded to the outer flexible shell made of thermoplastic elastomer based on high-density polyethylene [4, 5]. To satisfy consumers, synthetic stoppers are designed to imitate the properties of natural cork, but, unlike real cork, polymer stoppers are microbiologically inert [6].

Once wine is bottled, sealed, and labelled, it acquires a complex set of attributes that give it some extra concept: bottled wine is much more than the sensory properties of the beverage itself. Winemakers extend the range of brands and styles by designing new types of packaging: it is the bottle shape, glass color, label, and stopper that make a wine brand unique.

The type of stopper affects consumer perception of the wine, making the external attributes no less important and attractive than the internal ones, e.g., taste, bouquet, and overall wine quality [7]. In this case, consumers tend to exaggerate the quality properties of wine sealed with a natural cork.

A particular stopper can add wine immediate value by improving its appearance: consumers believe that it reflects the quality of the wine, which affects their purchasing decision [7]. Although most polymer stoppers are scientifically proved safe, consumers still prefer natural ones, presuming that natural cork preserves and even improves the quality of wine during storage. However, the quality of the cork itself remains beyond their concern, probably, as a result of inertia and resistance to change and innovation [8].

Other problems associated with cork stoppers include wine oxidation, discoloration, leakage, crumbling, etc. A natural cork stopper often falls apart during opening. Using low-quality natural cork eventually results in lost revenue, as consumers start to avoid the brand, attributing the poor quality of the product to the winemaker rather than the cork [9]. Consumer perception appears to be the main marketing factor for each type of wine stoppers.

Impermeability is the main function of stoppers, i.e., preventing leakage during storage. Permeability for oxygen is another important factor that affects the sensory profile of wine, including its color [10, 11].

Stoppers and their effect on wine aging have recently become a popular research issue [12–14]. However, it was Louis Pasteur who discovered that oxygen was both *a friend and a foe* to wine quality due to its ability to change the sensory properties and appearance of wine during aging [15]. Oxygen exposure improves the taste, preserves the color, and reduces the astringency of red wine [14, 16]. However, too much oxygen spoils white wine: it darkens, ages too fast, and acquires unwanted flavor and smell [12, 17]. Similarly, too little oxygen during aging promotes the formation of undesirable low molecular weight sulfur compounds, e.g., hydrogen sulfide or hydrosulfides. It suppresses some flavor compounds, as well as develops silicon and rubbery taints, also known as reductive aromas (reductive notes) [12, 17, 18].

Recent research [17, 19] shows that packaging materials, including stoppers, can have a negative impact on the appearance and other quality indicators of alcoholic beverages. Its effect on the quality and safety of wine is a matter of vigorous discussion [20]. Some experts insist that natural cork remains the best material while others claim that polymer analogues are better in preserving wine quality [21, 22].

Yet, polymer stoppers require a complex and labor-intensive production technology that employs materials of various nature, not to mention auxiliary agents. Moreover, polymer stoppers can lead to contamination with microplastics and plasticizers.

Phthalates are much more than a mere plasticizer responsible for flexibility and elasticity: they are high-boiling substances that provide polymers with resistance to thermal and thermal-oxidative degradation, water, and ultraviolet radiation. An effective material with high elasticity and wear resistance may contain as much plasticizer (phthalate) as the polymer itself [23]. Most industrial phthalates are used to plasticize polyvinyl chloride. The type of *o*-phthalic acid ester and its amount in polyvinyl chloride depend on the application of the final polymer product.

Phthalates are organic compounds, derivatives of benzene-1,2-dicarboxylic acid. They are formed when phthalic anhydride interacts with aromatic or aliphatic alcohols with 0 (1)-13 carbon atoms. The substituents can be symmetrical or asymmetrical. All phthalates are colorless low-polar oily high-boiling liquids that are highly soluble in most organic solvents and poorly soluble or even insoluble in water [24, 25].

Individual esters of *o*-phthalic acid are known for their pathogenic action. Modern phthalate studies focus on just a few of them, i.e., diethyl phthalate (DEP), dimethyl phthalate (DMP), dibutyl phthalate (DBP), and bis(2-ethylhexyl) phthalate (DEHP). Most researchers that used a number of homologues to study phthalate toxicology report their toxic effect as inversely proportional to the molecular weight of the ester radical [26].

Many countries have food safety requirements for phthalates. However, the existing standards seldom coincide for each individual homologue:

– EU Commission Regulation 10/2011 of January 14, 2011, on plastic materials and articles intended to come into contact with food fails to mention the acceptable amounts for diethyl phthalate and dimethyl phthalate;
– Russian Sanitary/Hygienic Rules and Standards 1.2.3685-21 on safety of environmental factors for people give the maximum allowable concentrations for diethyl phthalate, dibutyl phthalate, and bis(2-ethylhexyl) phthalate in an inverse correlation with concentration values of 3.0, 0.2, and 0.008 mg/L, respectively;
– European Directive 2008/105/CE of December 16, 2008, sets the maximum allowable concentration of bis(2-ethylhexyl) phthalate in water as 0.0013 mg/L;
– The USA have no restrictions on the acceptable content of diethyl phthalate and dimethyl phthalate in food products (Public Law 110-314-AUG. 14, 2008).

Russian food safety standards stipulate the content of such phthalates as dibutyl phthalate and dioctyl phthalate in polymer stoppers. For instance, dioctyl phthalate is banned from model environments that come into contact with bottle stoppers.

Dibutyl phthalate and dioctyl phthalate are orthophthalic acid esters. They have four hydrogen bond acceptors and bond with reducing agents.

The current scientific interest in food-package phthalates is due to their high pathogenic activity [27]. The content of phthalates is strictly regulated by Technical Regulations of Customs Union 055/2011 and Russian Sanitary/Hygienic Rules and Standards 1.2.3.685-21.

The Japanese Chemical Management Center and the US National Institute of Standards and Technology classify dibutyl phthalate and dioctyl phthalate as reproductive toxins and skin sensitizers that also disrupt the endocrine system and cause the so-called phthalate syndrome [28, 29]. However, these substances exhibit such toxicity only when heated [30]. Apparently, the storage conditions of wine sealed with a polymer stopper should exclude any chance of temperature increase.

Many research institutes study the kinetics of phthalate migration due to the wide application range of phthalate-containing materials and the high lability of phthalate molecules.

The rate at which plasticizer migrates from polymer depends on a number of physical factors. Such diffusion-related factors as temperature, pressure, humidity, nature, and solvent volume can be controlled while others cannot, e.g., polymer composition, nature, and content of plasticizer, distribution density of plasticizer in polymer, interaction with other additives, etc.

Lazakovich *et al*. [31] reported that wine can be contaminated with phthalates as early as at the production stage. In addition, time also contributes to contamination, i.e., the longer the production process, the higher the contamination risk.

The rate with which phthalates enter water-alcohol solutions depends on the alcohol concentration. The rate of natural extraction depends not so much on the alcohol content in the model as on the water content and the type of phthalate. In addition, the migration rate of phthalates into ethanol directly depends on temperature increase, which makes phthalate more soluble and mobile in supramolecular structures of the polymer (Fig. 2).

The migration rate increases together with the volume fraction of ethyl alcohol as the volume of water goes down. The extraction intensifies when the concentration exceeds 30% or the temperature goes beyond 20°C.

Russian winemaking industry is facing an acute shortage of wine stoppers because natural cork and most exported synthetic materials have fallen under sanctions.

The First Russian Winemaking Forum was organized by the Roscongress Foundation and the Federal Self-Regulatory Organization of Winegrowers and Winemakers of Russia in Moscow in November 2022. There it was announced that the capacity of the Russian market for alternative stoppers through 2033 would amount to 49 billion rubles (Fig. 3). As a result, the production of polymer wine stoppers is expected to grow.

Despite all these problems, the safety and quality assessment of polymer stoppers fall within the framework of the requirements established by the Eurasian Economic Union in the Technical Regulations of the Customs Union 005/2011 for safe food packaging and State Standard 32626-2014 that introduces general specifications for polymer stoppers.

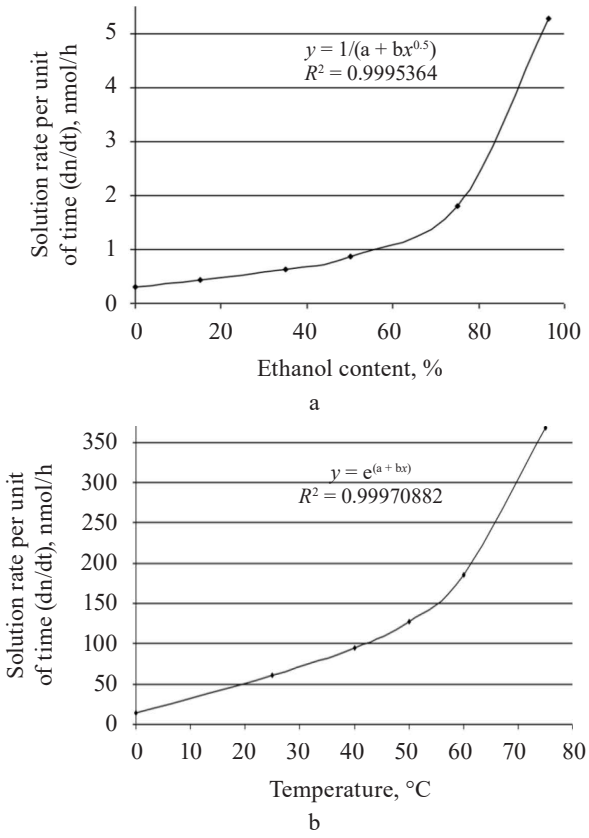

Figure 2 Migration rate of dibutyl phthalate from polyvinyl chloride throughout 7 h depending on ethyl concentration (a) and temperature (b)

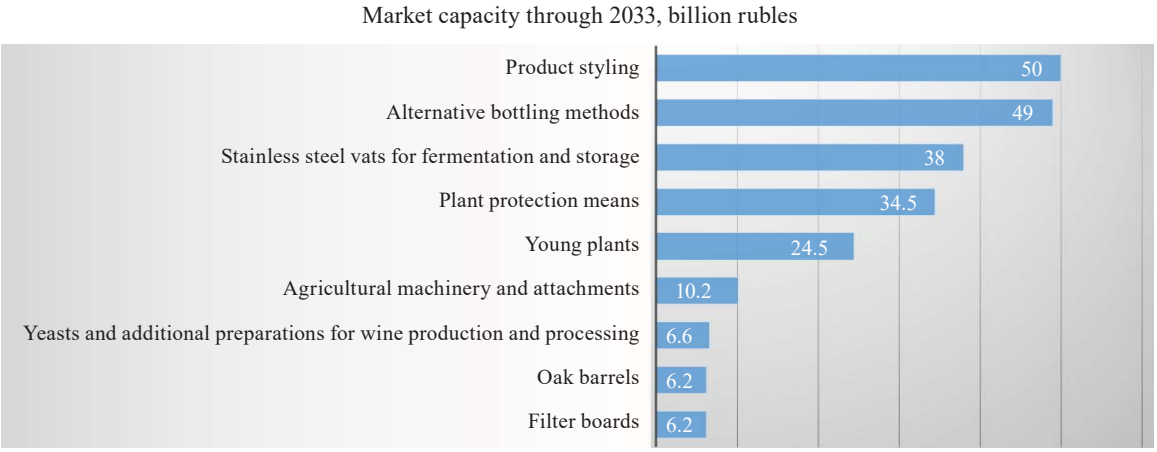

From the presentation of the General Director of JSC MOE VINO Arsen Karapetyan within the framework of the topic "Science, agriculture, and industry for the development of winemaking in Russia": https://xn--80aea0d.xn--p1ai/20221125/231909.html

Figure 3 Wine stopper market through 2033 as announced at the plenary session of The First Russian Winemaking Forum 2022

In Technical Regulations of the Customs Union 005/2011, safety is provided by a set of requirements for the materials that contact with food. These requirements cover sanitation, hygiene, impermeability, chemical inertness, safe opening, and physical and mechanical indicators. The sanitary and hygienic safety indicators for polymer stoppers in the food industry include the content of formaldehyde, ethyl acetate, hexane, heptane, acetone, styrene, methyl, propyl, isopropyl, butyl, isobutyl, and phthalates. The Eurasian Economic Union (EAEU) specifies permissible levels of their migration into the model environment. The list of phthalates to be controlled includes dioctyl phthalate and dibutyl while the presence of dibutyl phthalate in model environments is not allowed.

In terms of physical and mechanical properties and chemical inertness, polymer stoppers must provide impermeability under standard operating conditions and withstand internal pressure if they are intended for sparkling wines. In addition, the amount of polymer dust is strictly standardized. State Standard 32626-2014 also specifies the requirements for appearance, shape, and sensory profile.

This research assessed effects of polymer stoppers on the quality and safety of alcoholic beverages on the domestic market.

STUDY OBJECTS AND METHODS

The experiment involved 27 samples of polymer stoppers available on the Russian domestic market (Table 1).

The stoppers were classified by the production method (casting or coextrusion) and market value. The low-cost cast stoppers were ≤ 10 rubles per piece; the medium-price cast stoppers were ≥ 10 rubles per piece. Coextruded medium-cost stoppers were 20–50 rubles per piece while those of premium level were ≥ 50 rubles per piece (price per one piece may vary within 30%, depending on the batch volume). The final price classification consisted of three types: low, medium, and premium. The classification also included such extra features of production and appearance as color. In addition, the research covered some new types of T-shape cast polymer stoppers (Fig. 4).

Cognac and grape vodka were provided by winemakers to establish effects of polymer stoppers on the quality of these alcoholic beverages.

The appearance of the stoppers was assessed visually, without magnifying, by comparing them with the description in standards State Standard 32626-214 and 34257-2017.

The dimensions were checked with State Standard 32626-2014 by direct measurement with a 0.05 mm caliper (State Standard 166-89, ISO 3599-76). All the measurements were carried out in triplicate with error assessment.

The impermeability tests followed State Standard 32626-2014, Art. 9.5. The glass bottles were filled with the product to the nominal volume and sealed with the test stopper, 10 pieces for each sample group. After that, the bottles spent 48 h in a horizontal position on filter

Table 1 Types of polymer stoppers

Type and price																										
Cast stopper for sparkling wine			Still wines																							
			Cast stopper, low-cost			Cast stopper, medium-cost			Painted cast stopper, medium-cost			Coextruded stopper, premium									Coextruded stopper, medium-cost					
Sample																										
1	2	3	1	2	3	1	2	3	1	2	3	1	2	3	4	5	6	7	8	9	1	2	3	4	5	6



a b c d

Figure 4 T-shape polymer stoppers: (a) wooden flange, (b) wood-covered flange, (c) and (d) goldish and blue metal-covered flange

paper. The packaging was considered impermeable if the filter paper demonstrated no trace of liquid.

The amount of polymer dust was determined for six stoppers per each group using the standard methods described in State Standard 32626-2014, Art. 9.11.

The sensory profile was defined by tasting the water-alcohol extracts that had contacted with the experimental stopper samples. The panelists were recruited from the Winemaking Research Center, North-Caucasian Federal Scientific Center for Horticulture, Viticulture, and Winemaking.

The high-precision equipment tests were carried out at the Shared Use Center and the Testing Laboratory, North-Caucasian Federal Scientific Center for Horticulture, Viticulture, and Winemaking. The mass concentrations in the model environments were determined by gas chromatography in line with State Standard 34174-2017 for ethyl acetate, hexane, heptane, acetone, and styrene, as well as methyl, propyl, isopropyl, butyl, and isobutyl. The method involved a gas chromatographic analysis of the equilibrium vapor phase using a vapor dozer on two parallel-connected capillary columns and two flame ionization detectors. The quantitative analysis relied on the absolute calibration method, with the arithmetic mean of two parallel measurements as the final result. The content of formaldehyde in the model medium was determined by gas chromatography in line with State Standard 33446-2015. The method was based on the reaction between formaldehyde and 2,4-dinitrophenylhydrazine in an acidic medium. The resulting 2,4-dinitrophenylhydrazone of formaldehyde was extracted with toluene, and the toluene extract underwent chromatography on a device with an electron capture detector. The final result was a mean concentration value by two parallel calculations. The migration of dioctyl phthalate and dibutyl phthalate was studied in line with State Standard 33451-2015 by gas chromatography with an electron capture detector, as well as by measuring the concentrations in the model environment by toluene extraction. The final result was the arithmetic mean of two parallel measurements.

The potential migration of polymer and other dusts from the stopper surface into the model environment and finished products was studied by subjecting the sediment to microscopy. The sediment was isolated by centrifuging the water-alcohol extracts and finished products. The microscopy involved an Olympus microscope (Japan) and a webcam.

The samples were prepared in line with Technical Regulation of Customs Union 005/2011, Appendix 2. A 20% water-alcohol solution with 2% citric acid served as the model solution of wine. A 40% water-alcohol solution simulated grape vodkas and cognacs.

RESULTS AND DISCUSSION

We tested the samples for compliance with the requirements of State Standard 32626-2014, which covers appearance, geometry, impermeability, smell, flavor, color, and transparency changes, as well as the amount of polymer dust.

Foreign smells in the model environment proved to be the main non-compliance for most samples. Almost all samples (90–100%) of cast stoppers in all price segments introduced undesired smells into the model solution. This phenomenon resulted in rejecting 10–20% of coextruded stoppers of premium cost; however, the medium-cost coextruded stoppers of the same type did not give the final product any foreign smell.

The low-cost cast stoppers and the coextruded medium-cost stoppers violated the impermeability indicator. The proportion of rejected samples was 6–10% for the cast stoppers and 1–3% for the coextruded stoppers.

Other parameters demonstrated no violations.

Figures 5 and 6 visualize permeability that occurred after 10 min in the reclined position (Fig. 5). When the bottle was re-verticalized, some liquid accumulated on the stopper surface in the neck area (Fig. 6). In addition to product loss, such faulty stoppers may trigger bacterial development in the bottle neck, and microorganisms may eventually enter the finished product during storage.

The hot-process bottling test, when the beverage was heated to 40°C before bottling, revealed a two-fold increase in permeability, and the share of non-compliant

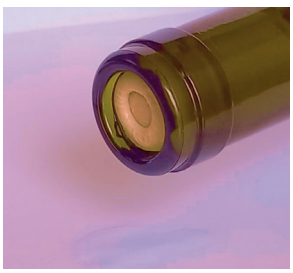

Figure 5 A permeable stopper

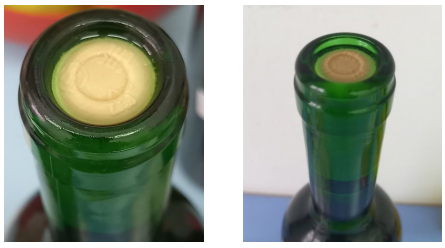

Figure 6 A faulty stopper

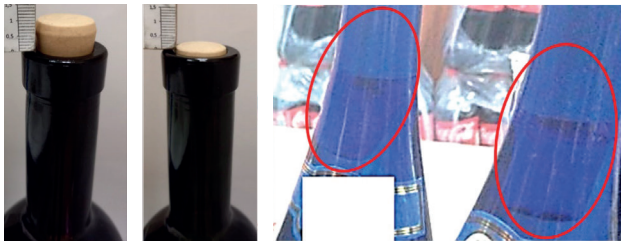

a b c

Figure 7 Permeability during hot-process bottling: (a) and (b) the stopper is sliding out, (c) the stopper is falling inside (the photos were taken in a retail chain shop)

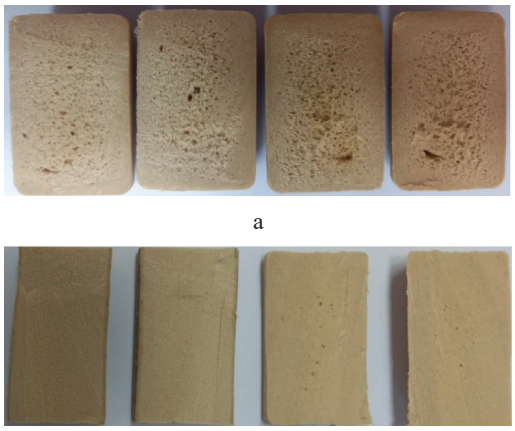

a

b

Figure 8 Internal structure of stopper samples: (a) faulty stoppers, (b) good-quality stoppers

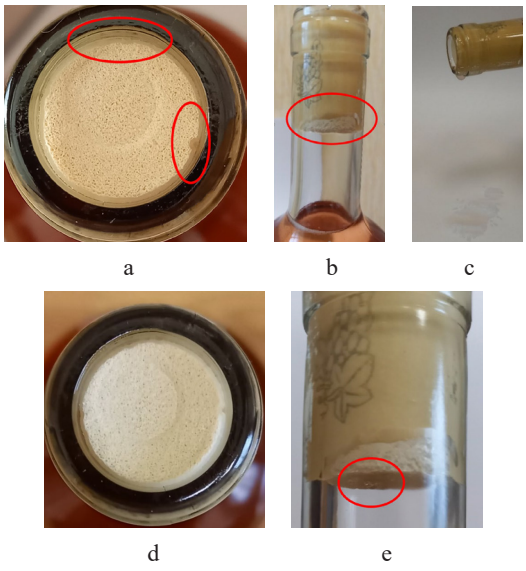

a b c

d e

Figure 9 Bottles withdrawn from the retail chain due to permeability: (a) the end of a coextruded stopper in the bottle neck with visible leakage, (b) horizontal leakage, (c) a loose stopper, (d) reverse leakage from the middle of the stopper to its lower end, and (e) leakage along the entire central part length

stoppers reached 20%. In addition, the stoppers could partially slide down the bottle neck (Figs. 7a and b) or even fall inside completely (Fig. 7c). Yet, the accompanying documents for the cast stopper allowed for hot-process bottling.

During the cut test, the rejected samples demonstrated a non-uniform porous structure in the middle, which got denser at the periphery (Fig. 8a). The stoppers of the same type and quality that met the impermeability requirements had a uniform internal structure (Fig. 8b).

Probably, the low impermeability index resulted from poor technological standards.

Figure 9 shows a coextruded medium-cost stopper in a bottle that was withdrawn from the retail network for permeability. The bottle neck was subjected to visual inspection after removing the heat-shrink capsule. The end surface of the stopper was intact, but it was loose at the circumference and some part of the side length (Figs. 9a and b). When reclined, the bottle immediately started leaking (Fig. 9c). When returned to the vertical position, the liquid accumulated in the bottle neck above the stopper (Fig. 9d). Unlike the cast stoppers, the coextruded ones resulted in the leakage not only at the points of contact with the bottle neck, but also along the entire length of the central part, as evidenced by the accumulation of liquid on the bottom end surface of the stopper (Fig. 9e). Apparently, the porous structure of the coextruded stopper did not guarantee impermeability as a result of procedural violation.

A set of safety tests (Technical Regulations of the Customs Union 005/2011) indicated various quantities of the substances under analysis in the model environments, depending on the type and quality of the stopper. Figures 10–14 show the mean values for mass concentrations for each substance and stopper type. The widest range and the largest quantity of toxic substances belonged to the low-cost cast samples intended for still wine. They contained 0.795–0.877 mg/L of acetone, 1.998–2.470 mg/L methyl alcohol, and 1.030–1.230 mg/L dioctyl phthalate. These substances are toxic and may cause irreversible defects in the wine.

At these concentrations, acetone gives wine a synthetic flavor. Also, it reacts with various wine components, thus boosting oxidation. Dioctyl phthalate also enhances synthetic or chemical taints, as well as develops amorphous inclusions that destroy the commercial appearance. Red wines are especially at risk since they contain phenolic components that bond with cork phthalates.

The premium coextruded stoppers also demonstrated a high migration rate of unwanted substances into the wine. These samples had the highest acetone content across all the stopper types (1.549 mg/L). The methyl alcohol content reached 2.082 mg/L. Therefore, premium polymer stoppers do not guarantee the wine quality.

The medium-cost and premium coextruded stoppers also increased the concentration of ethyl acetate in the model environment: 0.918–2.972 and ≤ 0.698 mg/L, respectively.

The premium coextruded stoppers also demonstrated an active dioctyl phthalate migration (1.412 mg/L). The concentration was 0.873–0.952 mg/L for the sparkling wine cast stoppers and 1.030–1.230 mg/L for still wine stoppers. In the model environments that contacted with medium-cost coextruded corks, the dioctyl phthalate contration stayed below 0.1 mg/L (Fig. 11). Unlike other substances, the level of dioctyl phthalate corresponded with the standard established by EAEU Technical Regulations of Customs Union 055/2011, Appendix 1 (≤ 2000 mg/L).

For instance, the amount of propyl alcohol (Fig. 12) that migrated from the stopper into the model environment was exceeded several times in almost all samples, reaching 0.168–0.435 mg/L, while the standard concentration is ≤ 0.100 mg/L. The cast samples for sparkling wine (0.054 mg/L) and the medium-cost stoppers for still wine (0.097 mg/L) were the only exceptions.

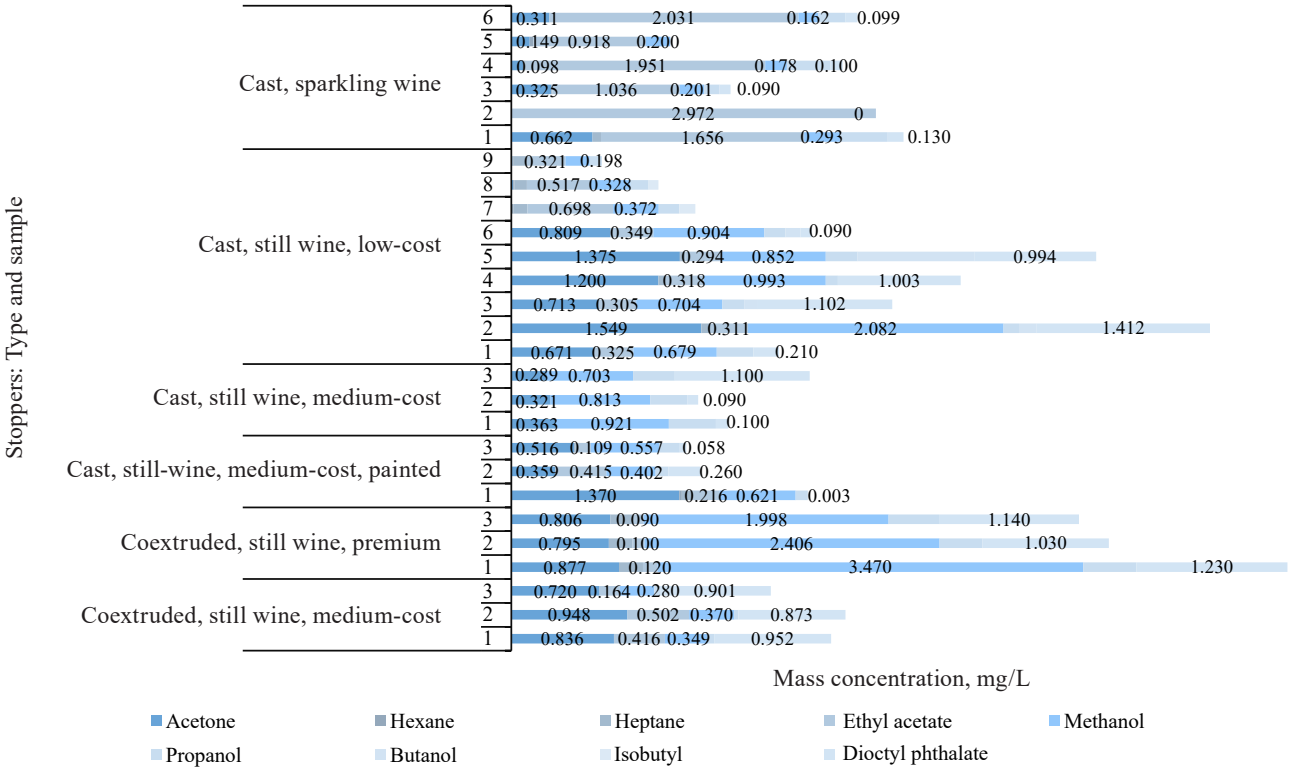

Figure 10 Mass concentration of substances released into the solution from various types of stoppers

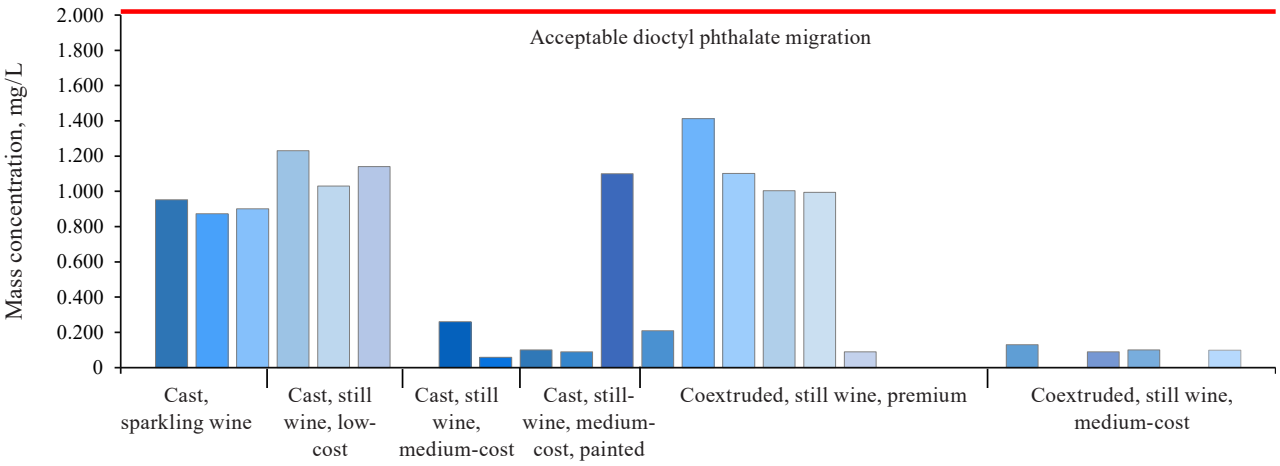

Figure 11 Dioctyl phthalate migration into model environments from various types of stoppers

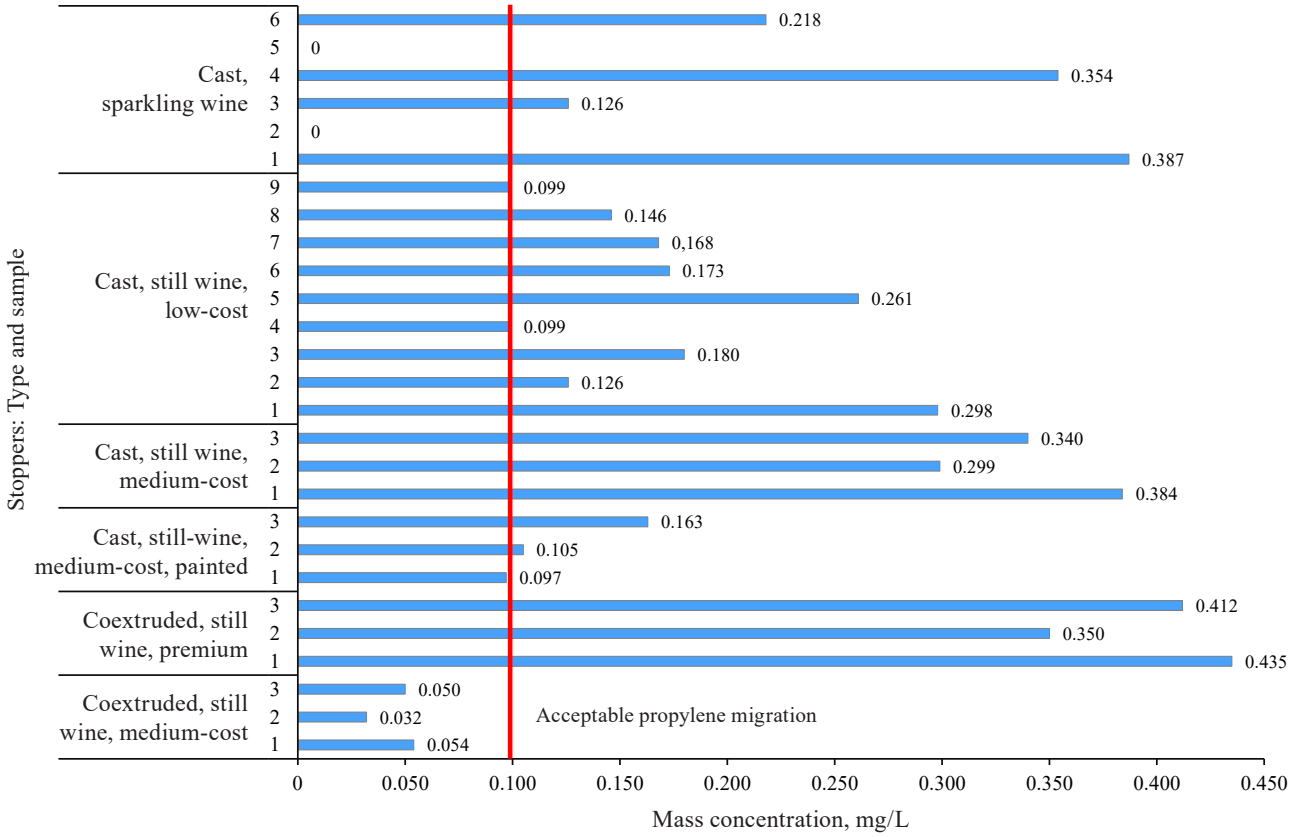

Figure 12 Propyl alcohol migration into model environments from various types of stoppers

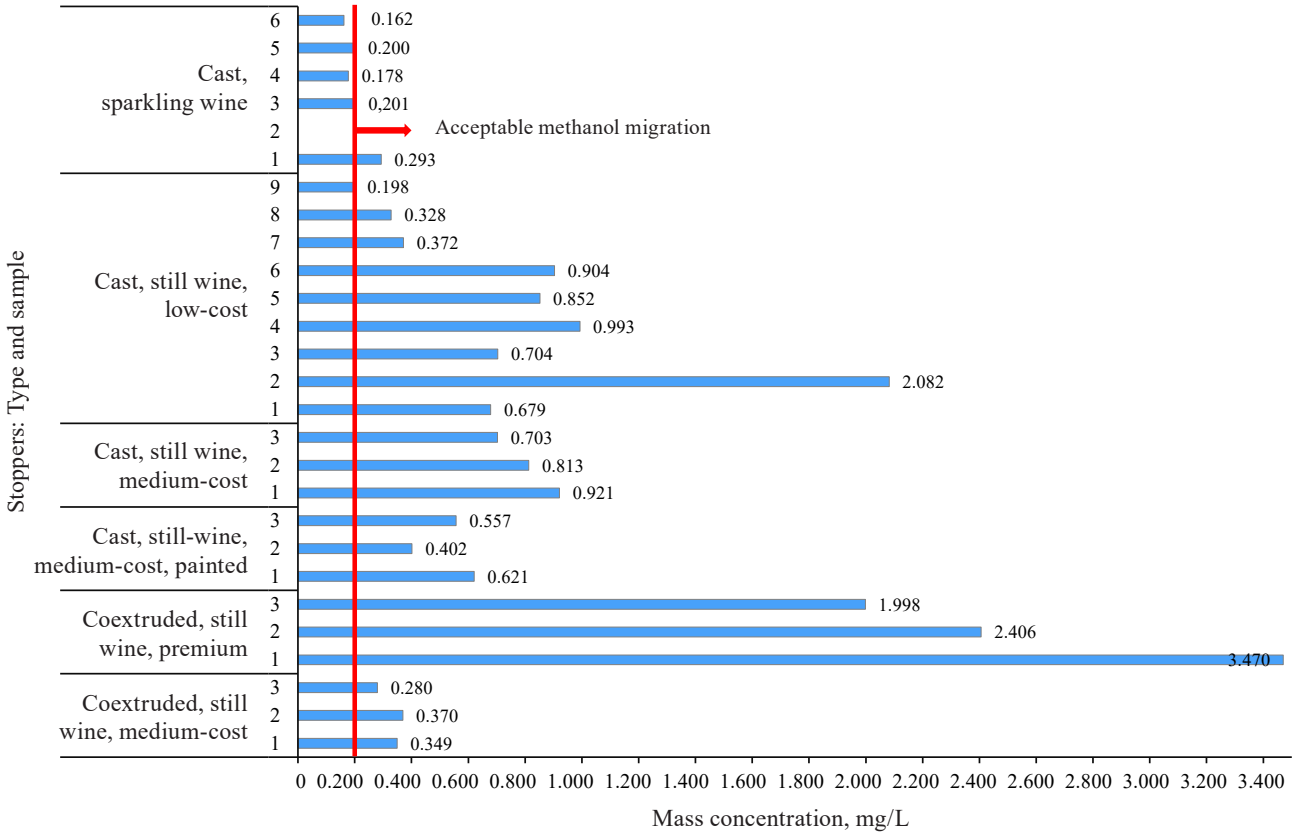

Figure 13 Methyl alcohol migration into model environments from various types of stoppers

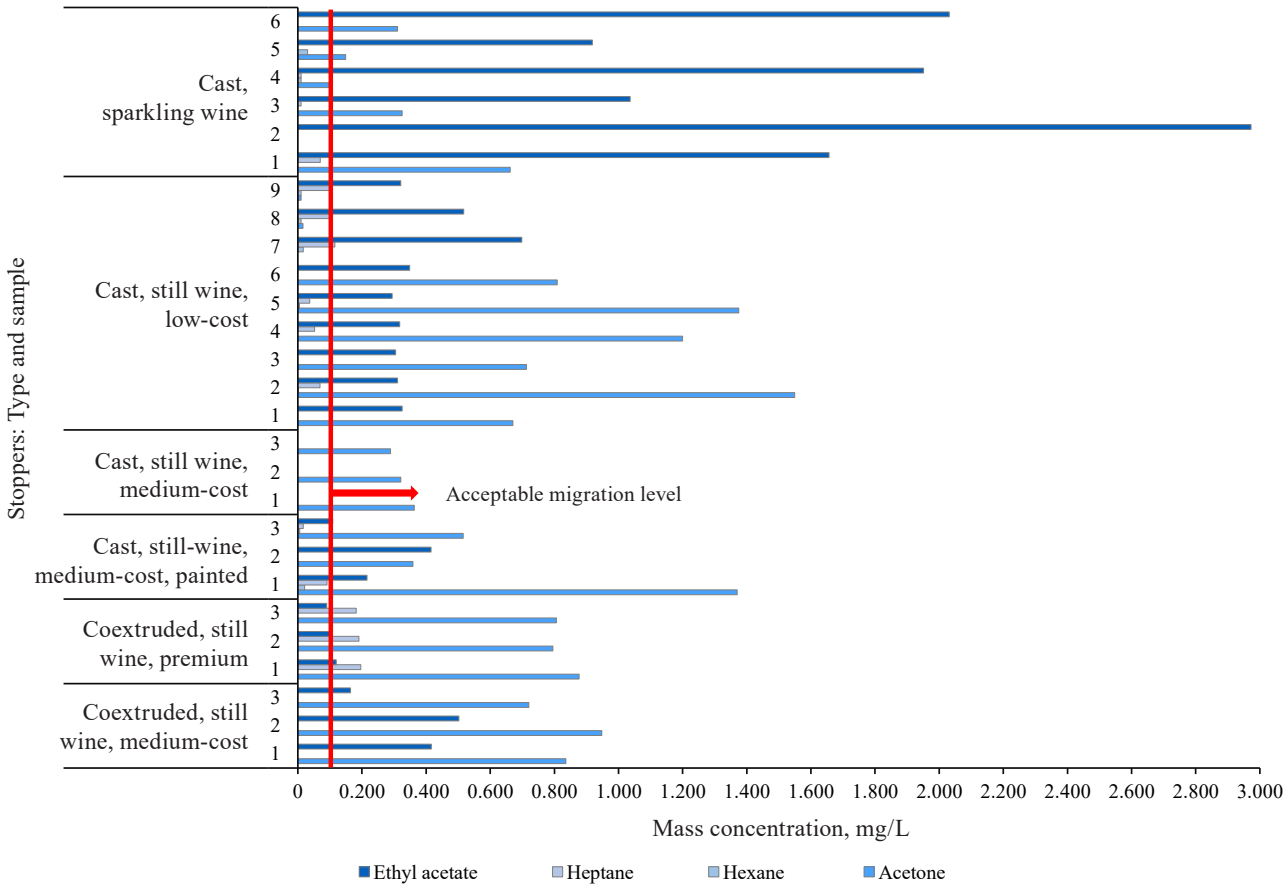

Figure 14 Mass concentration of substances released into the solution from various types of stoppers

The methyl alcohol migration far exceeded the standard (≤ 0.200 mg/L) (Fig. 13). The methanol level in the low-cost cast stoppers intended for still wine was by more than a tenfold higher (2.470 mg/L). The still wine premium coextruded stopper also extended a large amount of methyl alcohol into the model environment (2.082 mg/L).

Methanol is a common toxic pollutant that spoils alcoholic beverages. In distilled alcoholic drinks, the limits of methanol content are established in the regulatory documents for finished products (State Standards 31732-2014, 31728-2014, 31763-2012, 31493-2012, 55458-2013, 55459-2013, and 55461-2013). For example, the Interstate Standards for cognac and cognac distillates stipulate the mass concentration of methyl alcohol as ≤ 1.0 g/L; in wine distillates and wine alcohol, it is 2.0 g/L. In grape vodka, grape distillate, and grape alcohol, the national standards for methanol concentration are the same, i.e., ≤ 2.0 g/L.

Thus, the migration of methanol from the stopper increases its concentration in the drink, which may classify the product as hazardous when it is already in storage or on the shop shelves. Moreover, further storage increases methanol migration into the environment and, eventually, the toxicity of the drink.

Only some samples of premium coextruded stoppers demonstrated signs of butyl and isobutyl migration. Samples 7 and 8 were positive for isobutyl alcohol migration (0.08 and 0.13 mg/L, respectively). Samples 2, 3, 5, and 6 received 0.101–0.950 mg/L of butyl alcohol from of the same stopper type. Sample 5 violated the acceptable butanol migration level, i.e., ≤ 0.5 mg/L.

Butyl and isobutyl alcohols are always present in wine because they are secondary products of alcoholic fermentation. However, additional exposure to these alcohols violates the physical and chemical balance in the wine system, which has developed during production. It encourages butyl and isobutyl alcohols to react, and the wine esterifies in the bottle, resulting in unpleasant sharp alcoholic smell after opening.

Ethyl acetate was detected in large quantities in almost all the samples, except the painted medium-cost cast stopper for still wine (Fig. 14). This indicator was exceeded by more than a tenfold and reached 2.972 mg/L in the coextruded medium-cost stoppers. The premium coextruded stoppers rendered 0.294–0.698 mg/L of ethyl acetate into the solution, which also exceeded the threshold value of ≤ 0.100 mg/L. The low and medium-cost cast stoppers demonstrated a slight excess while no excess was detected for low-price samples 2 and 3. Ethyl acetate migration from the cast stoppers was 0.164–0.502 mg/L for sparkling wine, 0.09–0.12 mg/L for the low-cost cast stoppers for still wine, and 0.109–0.415 mg/L for the medium-cost cast corks.

Ethyl acetate is a potential source of unpleasant taint in alcoholic beverages [32]. It is the most common ester in

wines that changes its native sensory profile. Ethyl acetate migration from the stopper also affects the wine quality.

The content of heptane that exceeded the acceptable level of 0.100 mg/L was observed in the low-cost cast stoppers for still wine (0.182–0.196 mg/L) and the premium coextruded stoppers (0.115 and 0.102 mg/L in samples 7 and 8, respectively).

An insignificant amount of hexane that fell within the norm of ≤ 0.1 mg/L was detected in the model environments that contacted with the medium-cost cast stoppers for still wine (0.021 mg/L in sample 1; 0.006 mg/L in sample 3), the premium coextruded stoppers (0.01–0.017 mg/L), and the medium-cost coextruded stoppers (0.01–0.03 mg/L).

The acetone concentration exceeded the standard of 0.100 mg/L in almost all the samples and ranged from 0.149 to1.549 mg/L, namely 0.720–0.948 mg/L in the cast stoppers for sparkling wine, 0.795–0.877 mg/L in the low-cost cast corks for still wine, and 0.359–1.370 mg/L in the medium-cost cast stoppers for still wine. The lowest concentration belonged to the painted stoppers (0.289–0.363 mg/L). The solution that contacted with medium-cost coextruded sample 2 contained no acetone while other samples of the same group contained 0.098–0.662 mg/L of acetone. A similar situation was observed for the solutions that contacted with the premium coextruded stoppers. For example, sample 7 contained no acetone whereas sample 2 demonstrated the highest acetone content across the similar samples (1.549 mg/L).

The painted medium-cost cast stoppers for still wine promoted only acetone migration (0.289–0.363 mg/L) whereas ethyl acetate, heptane, and hexane were totally absent from the model solutions.

When swallowed, acetone is absorbed rather quickly, but the pharmacokinetics and the metabolic pathway depend on the dose. Although acetone is neither genotoxic nor mutagenic, it enhances the toxicity of other organic compounds [33].

Dibutyl phthalate and formaldehyde did not migrate into the model solutions.

These results clearly demonstrate that polymer stoppers affect the safety of alcoholic beverages. Moreover, in this research, neither type nor price correlated with the migration rate of toxic substances into the liquid environment.

When the abovementioned chemical components enter the finished products, they intensify the oxidation processes and subsequently reduce or entirely spoil the quality of the drink by changing their appearance and other sensory properties.

As synthetic polymer stoppers contact with reactive components in wine, their surface gets damaged, and the resulting substances migrate into the wine. Further reactions lead to formation of new compounds. Oxidation and sorption are the most active reactions triggered by polymer stopper components. The resulting opaqueness and foreign inclusions spoil the commercial appearance. Other consequences include poor sensory profile and safety violation.

The standards for commercial wine products are practically the same as those for all food products. However, alcoholic beverages contain a lot of ethanol, organic acids, and flavoring agents. As a result, they are subject to much stricter quality control. The primary quality assessment begins with a visual inspection for compliance with legislative and regulatory standards.

In line with State Standards P 55458-2013 and 31732-2014, bottled wine products must be transparent and free of foreign inclusions or sediment. Otherwise, the products are rejected and withdrawn from circulation for violation of cosmetic standards.

Phthalate migration depends on their solubility in water-alcohol solutions. Its rate directly depends on the chemical composition of the model environment and the ambient temperature during storage. Bottled alcoholic beverages with ≥ 30% ethyl by volume sealed with polymer stoppers must be stored at temperatures below 20°C.

The three-star cognac sample sealed with a capped polymer stopper (Fig. 15) was rejected for foreign inclusions (Fig. 16): small particles clustered on its surface, which did not correspond with the standard appearance for this type of alcoholic drink.

A detailed examination of the unopened bottle (Fig. 17) revealed droplets on the surface of the stopper. When the

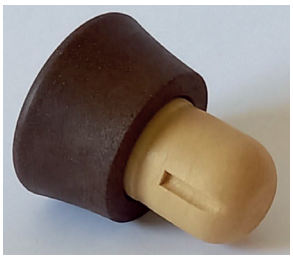

Figure 15 Capped polymer stopper

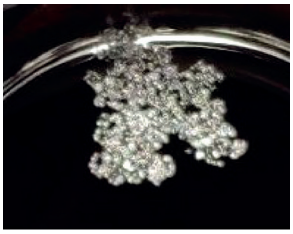

Figure 16 Foreign inclusions on cognac surface, 100× magnification

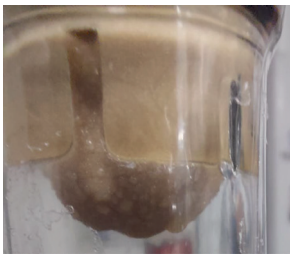

Figure 17 Stopper surface

bottle was tilted, the droplets flowed down the neck into the cognac. Presumably, it happened because the plasticizer protruded onto the stopper surface as a result of poor manufacturing protocol.

Microscopy was performed to study the droplets collected from the stopper surface and the inclusions sampled from the cognac surface. Figure 18 shows the microscopic images of the polymer stopper (a–c) and foreign inclusions on the cognac surface (d).

The foreign inclusions were of different shapes, i.e., plates, scales, and clusters. The inclusions on the surface of the stopper looked similar to those on the surface of the cognac. Logically, the commercial appearance of the cognac had been spoiled by the faulty stopper.

Phthalates have a high sorption capacity in relation to various classes of compounds in alcoholic beverages, especially those with a benzene ring [34]. Polymers have a well-developed spatial structure and a large specific surface area that serves as a platform for chemical interactions. For instance, Fig. 18d shows the accumulation of cognac tannins on the peripheral surface of the inclusions.

A model experiment test made it possible to confirm the role of the polymer stopper in wine quality degradation. The stopper samples were exposed to model solutions that simulated grape vodkas and cognacs. The stoppers were extracted from cognac bottles, rinsed with the abovementioned model solutions, microscoped for cleanliness, and applied to bottles with a water-alcohol solution similar to the model environment. To accelerate the extraction process, the bottles were stored upside down for 72 h to provide continuous contact between the solution and the stopper under normal environmental conditions (t = 20 ± 2°C). Then, the bottles were returned to the vertical position to test the drop on the stopper surface (Fig. 19). The model solutions demonstrated inclusions similar to those in Fig. 18, which were caused by synthetic components that had migrated there from the stopper.

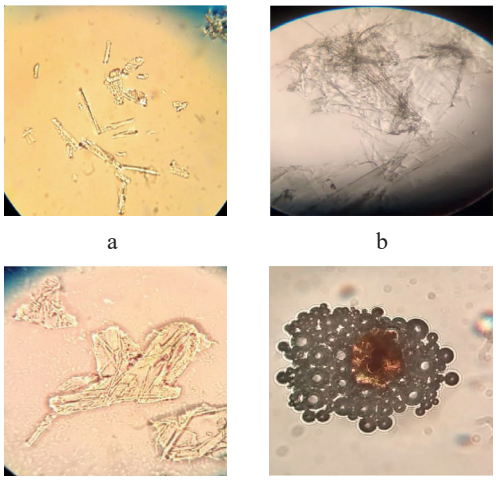

Figure 18 Foreign inclusions from the polymer stopper, 400× magnification: (a–c) polymer stopper surface, (d) cognac surface

Polymer compounds are known to smoke when burning. Depending on the composition, the flame is red-blue or black. A burning test was conducted to define the nature of the sediment. The inclusion components were washed from cognac and burned on a spatula: they indeed emitted smoke, and the flame was red-blue, with occasional black shades. The test proved the presence of polymer stopper components in the foreign inclusions that made the cognac non-saleable.

To validate the result, the cognac samples were tested for phthalates using the standard method described in State Standard 33451-2015. Sample 1 that featured 17-month-old cognac contained 0.18 mg/L of dibutyl phthalate and 0.01 mg/L of dioctyl phthalate. Sample 2 of 12-month-old cognac contained 0.17 mg/L of dibutyl phthalate and 0.03 mg/L of dioctyl phthalate.

Another sample featured a glass bottle of grape vodka sealed with a T-shape polymer stopper. It was obtained from a finished product warehouse and contained tiny scale-like inclusions.

The substances isolated from this product were compared with the components that migrated into the model environment from new stoppers of the same type. The microscope images showed similar inclusions of various sizes in amorphous clusters. Apparently, they resulted from the surface treatment of stoppers and/or polymer inclusions, possibly phthalates (Fig. 20).

To confirm that the identified inclusions belonged to the polymer stoppers, a similar test was conducted for some new polymer stoppers available on the domestic market (Fig. 4).

Microscope images of the sediments showed that the inclusions developed from the substances that migrated

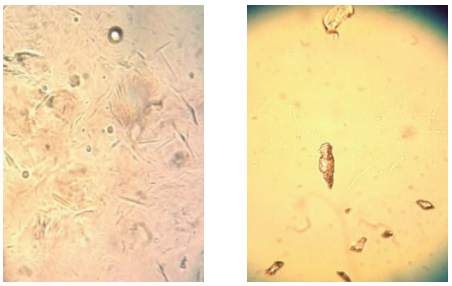

Figure 19 Microscope images of inclusions, 400× magnification

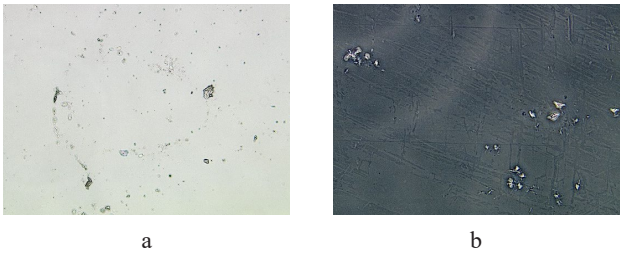

Figure 20 Microscope images of the stopper sample extract, 400× magnification: (a) model environment, (b) finished product

from the stopper surface into the model environments. Fig. 21 demonstrated inclusions similar in appearance and shape to those found in grape vodka. The particles were identical in structure, with minor differences in shape and size. Like in the cognac experiment, a sample of grape vodka was tested for phthalates to validate the assumptions about the nature of the inclusions.

The five samples of grape vodka came from the same batch and had the same bottling date. Their shelf-life was two months at the time of testing. Dibutyl phthalate was identified in all the samples at a concentration of 0.01–0.10 mg/L. Dioctyl phthalate was detected only in two samples at a concentration of 0.01 mg/L (Table 2).

The model environments contacted with T-shape polymer stoppers with different types of flanges: model environment 1 + wooden flange stopper (Fig. 21a); model environment 2 + T-shape stopper with wood-covered flange (Fig. 21b); model environment 3 + T-shape stopper with goldish metal-covered flange (Fig. 21c); and model environment 4 + T-shape stopper with blue metal-covered flange (Fig. 21d). The contact period was 10 days at 5–30°C, as stipulated in Technical Regulation of Customs Union 005/2011, Appendix 1 (Table 2).

Since beverages often become contaminated with microplastics during processing and packaging [35], the phthalates could be attributed to the production process. However, the second test, which took place six months later, showed an increase in the phthalate concentration (Table 2). The cognac sealed with sample 1 had 0.26 mg/L of dibutyl phthalate and 0.08 mg/L of dioctyl phthalate. Sample 2 demonstrated a lower migration rate: 0.20 mg/L of dibutyl phthalate and 0.05 mg/L of dioctyl phthalate.

The continuous migration of phthalates from the stopper would eventually render the cognac unsafe for human health. In addition, the EAEU standards for stoppers prohibit dibutyl phthalate migration. Appendix 2 of Technical Regulation of Customs Union 005/2011 limits the permissible amount of dioctyl phthalate migration as ≤ 2.0 mg/L per ten days of contact.

The grape vodka experiments also revealed a tendency for dibutyl phthalate and dioctyl phthalate to migrate during storage. However, their concentration was much lower than in the cognac: 0.01–0.11 and 0.09–0.18 mg/L after six months of storage (Table 2).

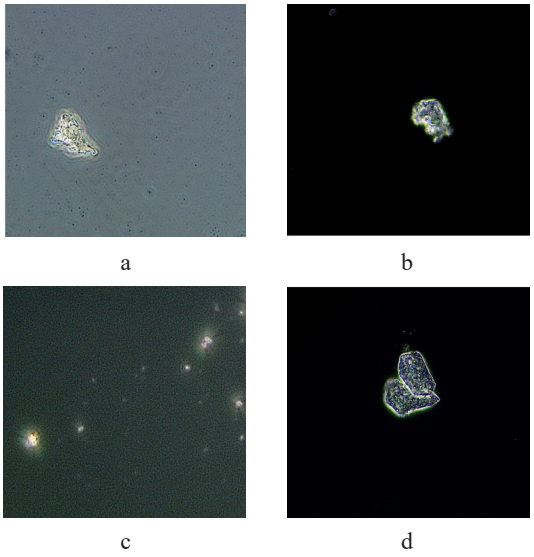

Figure 21 Microscope images of sediment separated from the model environment after contact with various capped polymer stoppers, 400× magnification: (a) wooden flange, (b) T-shape with wood-covered flange, (c) and (d) T-shape with metal-covered flange

Table 2 Stopper-to-beverage phthalate migration during storage at 5–30°C

Sample	Content, mean value, mg/L			
	Dibutyl phthalate		Dioctyl phthalate	
	Initial	After 6 months	Initial	After 6 months
Cognac, sample 1	0.180 ± 0.034	0.260 ± 0.049	0.010 ± 0.002	0.080 ± 0.013
Cognac, sample 2	0.170 ± 0.032	0.200 ± 0.038	0.003 ± 0.005	0.050 ± 0.002
Grape vodka, sample 1	0.010 ± 0.002	0.080 ± 0.015	0.050 ± 0.008	0.110 ± 0.018
Grape vodka, sample 2	0.010 ± 0.002	0.110 ± 0.021	0.010 ± 0.002	0.090 ± 0.014
Grape vodka, sample 3	≤ 0.001*	≤ 0.001*	0.100 ± 0.016	0.180 ± 0.029
Grape vodka, sample 4	≤ 0.001*	0.030 ± 0.006	0.030 ± 0.005	0.130 ± 0.021
Grape vodka, sample 5	≤ 0.001*	0.010 ± 0.002	0.010 ± 0.002	0.100 ± 0.016
Model environment 1 (40% water-alcohol solution + wooden flange stopper, Fig. 4a)	≤ 0.001*	≤ 0.001*	≤ 0.001*	≤ 0.001*
Model environment 2 (40% water-alcohol solution + T-shape stopper with wood-covered flange, Fig. 4b)	≤ 0.001*	0.010 ± 0.002	0.010 ± 0.002	0.010 ± 0.002
Model environment 3 (40% water-alcohol solution + T-shape stopper with goldish metal-covered flange, Fig. 4c)	≤ 0.001*	0.010 ± 0.002	0.010 ± 0.002	0.010 ± 0.002
Model environment 4 (40% water-alcohol solution + T-shape stopper with blue metal-covered flange, Fig. 4d)	≤ 0.001*	≤ 0.001*	≤ 0.001*	≤ 0.001*

* – the result is below the detection range



Figure 22 Contamination on the surface of T-shape polymer stoppers

No dibutyl phthalate was originally detected in grape vodka samples 4 and 5; after six months of storage, it remained as low as 0.01 mg/L. The model environments demonstrated similar results. Model environments 1 and 3 developed dibutyl phthalate overtime, but model environments 2 and 4 remained free of toxic compounds the entire storage time.

To sum it up, the domestic wine market has polymer stoppers that meet safety requirements in terms of phthalate migration alongside with similar stoppers that fail to comply with this control criterion. Obviously, the incoming control should be stricter for wineries that use this type of stoppers.

The appearance of stoppers is another urgent issue. The visual inspection of capped stoppers detected foreign particles, e.g., lint, dust, black stripes, etc. (Fig. 22). According to State Standards 32626-2014 and 34257-2017, polymer stoppers are stored in boxes or bags that protect their quality from contamination, precipitation, and mechanical damage. However, these regulatory documents establish no requirements for the sanitary conditions of the stopper surface. Moreover, they provide no instructions, even of a recommendatory nature, for the pre-bottling treatment. The drinks, on the contrary, are subject to serious quality and safety standards.

Naturally, the absence of sanitary standard and/or recommendations for preliminary processing renders stopper manufacturers unaccountable, while beverage producers have no legal grounds for appropriate demands and claims.

Stoppers with contaminated surface obviously affect the quality of the drink during storage and may lead to microbial spoilage.

CONCLUSION

This research assessed the safety and quality of polymer stoppers on the Russian market, as well as their impact on the finished products. Such aspects as appearance, shape, polymer dust, and sensory properties (changes in flavor, color, and transparency) met the standards introduced by State Standard 32626-2014. However, the low-cost cast stoppers and the medium-cost coextruded stoppers demonstrated permeability, which increased after hot-process bottling. All types of stoppers, except the medium-price coextruded samples, gave the aqueous extract a foreign smell.

The surface contamination detected in some samples is a strong reason for a stricter quality control. The expenditures on preliminary sanitation could be compensated by eliminating potential financial losses from the finished products rejected by inspectors.

In this research, the polymer stoppers proved to contaminate alcoholic beverages with toxic and potentially hazardous substances, such as ethyl acetate, heptane, hexane, acetone, dibutyl and dioctyl phthalates, as well as propyl, butyl, isobutyl, and methyl alcohols. All these substances accumulated during storage as a result of continuous migration from the faulty stoppers.

Based on the research results, beverages with ≥ 30% of alcohol sealed with polymer stoppers should be stored at ≤ 20°C.

Wine-making enterprises should be more careful in planning their production of it involves polymer stoppers because the stopper-beverage migration rate of toxic substances, such as phthalates, is the fastest during the first 7–10 h.

Although this research focused on the polymer stoppers available on the Russian market of alcoholic beverages, the results obtained could be relevant for wine-makers from other countries, especially in the Eurasian Economic Union.

CONTRIBUTION

L.E. Chemisova and N.M. Ageyeva developed the research concept and design and wrote the manuscript. L.E. Chemisova, N.M. Ageyeva, O.N. Sheludko, and Yu.F. Yakuba provided data collection, analyzed the material, and proofread the manuscript. M.V. Antonenko systematized the experimental data. All the authors approved of the final version of the manuscript and are equally responsible for the integrity of the article.

CONFLICT OF INTEREST

The authors declared no conflict of interests regarding the publication of this article.

REFERENCES

1. Silva MA, Julien M, Jourdes M, Teissedre P-L. Impact of closures on wine post-bottling development: A review. European Food Research and Technology. 2011;233:905–914. https://doi.org/10.1007/s00217-011-1603-9
2. Chemisova LE, Ageeva NM, Markovskiy MG, Guguchkina TI. Influence of volatile components contained in cork on the quality and safety of wines. Izvestiya vuzov. Food Technology. 2019;(2–3):24–25. (In Russ.). https://doi.org/10.26297/0579-3009.2019.2-3.6
3. Poças F, Couto JA, Hogg TA. Wine packaging and related sustainability issues. In: Costa MJ, Catarino S, Escalona JM, Comuzzo P, editors. Improving sustainable viticulture and winemaking practices. Academic Press; 2022. pp. 371–390. https://doi.org/10.1016/B978-0-323-85150-3.00001-3

4. Liu N, Song Y-Y, Dang G-F, Ye D-Q, Gong X, Liu Y-L. Effect of wine closures on the aroma properties of Chardonnay wines after four years of storage. South African Journal of Enology and Viticulture. 2015;36(3):296–303. https://doi.org/10.21548/36-3-963
5. Sánchez-González M, Pérez-Terrazas D. Dataset of mechanical properties from different types of wine stopper: Micro-agglomerated, natural cork and synthetic. Data in Brief. 2018;21:2103–2109. https://doi.org/10.1016/j.dib.2018.11.051
6. Takahashi M, Aoyagi H. Analysis of porous breathable stopper and development of PID control for gas phase during shake-flask culture with microorganisms. Applied Microbiology and Biotechnology. 2020;104:8925–8936. https://doi.org/10.1007/s00253-020-10847-x
7. Lopes P, Roseira I, Cabral M, Saucier C, Darriet P, Teissedre P-L, *et al.* Impact of different closures on intrinsic sensory wine quality and consumer preferences. Wine and Viticulture Journal. 2012;27(2):34–41.
8. Marin AB, Durham CA. Effects of wine bottle closure type on consumer purchase intent and price expectation. American Journal of Enology and Viticulture. 2007;58(2):192–201. https://doi.org/10.5344/ajev.2007.58.2.192
9. Risch SJ. Food packaging history and innovations. Journal of Agricultural and Food Chemistry. 2009;57(18):8089–8092. https://doi.org/10.1021/jf900040r
10. Furtado I, Lopes P, Oliveira AS, Amaro F, Bastos ML, Cabral M, *et al.* The impact of different closures on the flavor composition of wines during bottle aging. Foods. 2021;10(9):2070. https://doi.org/10.3390/foods10092070
11. Cantu A, Guernsey J, Anderson M, Blozis S, Bleibaum R, Cyrot D, *et al.* Wine closure performance of three common closure types: Chemical and sensory impact on a Sauvignon Blanc wine. Molecules. 2022;27(18):5881. https://doi.org/10.3390/molecules27185881
12. Lopes P, Silva MA, Pons A, Tominaga T, Lavigne V, Saucier C, *et al.* Impact of oxygen dissolved at bottling and transmitted through closures on the composition and sensory properties of a Sauvignon Blanc wine during bottle storage. Journal of Agricultural and Food Chemistry. 2009;57(21):10261–10270. https://doi.org/10.1021/jf9023257
13. Brotto L, Battistutta F, Tat L, Comuzzo P, Zironi R. Modified nondestructive colorimetric method to evaluate the variability of oxygen diffusion rate through wine bottle closures. Journal of Agricultural and Food Chemistry. 2010;58(6):3567–3572. https://doi.org/10.1021/jf903846h
14. Mucaca CAL, Filho JHT, do Nascimento E, Arruda LLAL. Phenolic composition, chromatic parameters and antioxidant activity "in vitro" in tropical Brazilian red wines. Journal of Food and Nutrition Research. 2017;5(10):754–762. https://doi.org/10.12691/jfnr-5-10-6
15. Pasteur L. Studies on wine: Its diseases, causes that provoke them, new processes for preserving and aging it, 2nd ed. Paris: F. Savy; 1873. 344 p. (In French).
16. Silva MA, Julien M, Jourdes M, Teissedre P-L. Impact of closures on wine post-bottling development: A review. European Food Research and Technology. 2011;233:905–914. https://doi.org/10.1007/s00217-011-1603-9
17. Chemisova LE, Ageyeva NM, Yakimenko EN. Quality and safety of wine during storage: Packaging and stopper. Food Processing: Techniques and Technology. 2023;53(2):281–293. (In Russ.). https://doi.org/10.21603/2074-9414-2023-2-2432
18. Liu D, Xing R-R, Li Z, Yang D-M, Pan Q-H. Evolution of volatile compounds, aroma attributes, and sensory perception in bottle-aged red wines and their correlation. European Food Research and Technology. 2016;242:1937–1948. https://doi.org/10.1007/s00217-016-2693-1
19. Chemisova L, Ageeva N, Mitrofanova E, Sheludko O. Ensuring the preservation of the quality of wine during storage. BIO Web of Conferences. 2022;46:01015. https://doi.org/10.1051/bioconf/20224601015
20. Chemisova LE. Mechanisms of cortical cork influence the biotechnological processes taking place during storage and wine maturation. Fruit Growing and Viticulture of South Russia. 2021;68(2):332–354. (In Russ.). https://doi.org/10.30679/2219-5335-2021-2-68-332-354
21. Furtado I, Lopes P, Oliveira AS, Amaro F, Bastos ML, Cabral M, *et al.* The impact of different closures on the flavor composition of wines during bottle aging. Foods. 2021;10(9):2070. https://doi.org/10.3390/foods10092070
22. Ravikumar A, Malik S, Chitnis A, Paul D, Mishra DK. Wine purchasing decisions in India from a consumer's perspective: An analysis of influencing factors on the buying behavior. Innovative Marketing. 2022;18(2):120–134. https://doi.org/10.21511/im.18(2).2022.11
23. Halloran MW, Nicell JA, Leask RL, Marić M. Small molecule plasticizers for improved migration resistance: Investigation of branching and leaching behaviour in PVC blends. Materials Today Communications. 2021;29:102874. https://doi.org/10.1016/j.mtcomm.2021.102874
24. Kozlov PV, Papkov SP. Physicochemical principles of polymer plasticization. Moscow: Khimiya; 1982. 224 p. (In Russ.).
25. Barshtein RS, Kirillovich VI, Nosovskii YuE. Plasticizers for polymers. Moscow: Khimiya; 1982. 200 p. (In Russ.).

26. Sheftel' VO. Harmful substances in plastics. Moscow: Khimiya; 1991. 544 p. (In Russ.).
27. Le Magueresse-Battistoni B, Labaronne E, Vidal H, Naville D. Endocrine disrupting chemicals in mixture and obesity, diabetes and related metabolic disorders. World Journal of Biological Chemistry. 2017;8(2):108–119. https://doi.org/10.4331/wjbc.v8.i2.108
28. Ventrice P, Ventrice D, Russo E, de Sarro G. Phthalates: European regulation, chemistry, pharmacokinetic and related toxicity. Environmental Toxicology and Pharmacology. 2013;36(1):88–96. https://doi.org/10.1016/j.etap.2013.03.014
29. Zaitseva NV, Ulanova TS, Karnazhitskaya TD, Zavernenkova EO. Study of correlation between growth rate of children and monophtalate concentrations in urine. Izvestiya of Saratov University. New Series. Series: Chemistry. Biology. Ecology. 2017;17(1):62–66. (In Russ.). https://doi.org/10.18500/1816-9775-2017-17-1-62-66
30. Rustemeyer L, Elsner P, John S-M, Maibach HI. Kanerva's occupational dermatology, 2nd ed. Berlin: Springer; 2012. 2058 p. https://doi.org/10.1007/978-3-642-02035-3
31. Lazacovici D. The study of phthalates migration from different materials contacting with food. Journal of Food and Packaging Science, Technique and Technologies. 2012;(1):27–32.
32. Adlard ER. Jokie Bakker and Ronald J. Clarke: Wine flavour chemistry (2nd Edn). Chromatographia. 2018;81:1241. https://doi.org/10.1007/s10337-018-3566-5
33. Kalapos MP, Ruzsányi V. Acetone. In: Wexler P, editor. Encyclopedia of Toxicology (Fourth Edition). Academic Press; 2024. pp. 67–78. https://doi.org/10.1016/B978-0-12-824315-2.00393-6
34. Magerramov AM, Azizov AA, Alosmanov RM, Kerimova ES, Buniyatzade IA. Use of polymers as sorbents. Young Learners. 2015;4(84):38–41. (In Russ.). https://elibrary.ru/TIXEKF
35. Prata JC, Paço A, Reis V, da Costa JP, Fernandes AJS, da Costa FM, *et al.* Identification of microplastics in white wines capped with polyethylene stoppers using micro-Raman spectroscopy. Food Chemistry. 2020;331:127323. https://doi.org/10.1016/j.foodchem.2020.127323

ORCID IDs
Larisa E. Chemisova https://orcid.org/0000-0001-9377-5515
Natalia M. Ageyeva https://orcid.org/0000-0002-9165-6763
Olga N. Sheludko https://orcid.org/0000-0001-8655-3375
Yurii F. Yakuba https://orcid.org/0000-0003-2711-2419

Foods and Raw Materials. 2026;14(1)

ISSN 2308-4057 (Print)
ISSN 2310-9599 (Online)

Review Article
Open Access

Available online at http://jfrm.ru/en
https://doi.org/10.21603/2308-4057-2026-1-668
https://elibrary.ru/QLFZDL

Gut microbiota and its role in development of chronic disease and aging

Anna D. Vesnina[1,*], Anna S. Frolova[1], Darya Yu. Chekushkina[1], Irina S. Milentyeva[1], Sergey L. Luzyanin[1], Larisa M. Aksenova[2]

[1] Kemerovo State University, Kemerovo, Russia
[2] All-Russian Scientific Research Institute of Confectionery Industry, Moscow, Russia

* e-mail: koledockop1@mail.ru

Received 12.12.2024; Revised 03.02.2025; Accepted 05.03.2025; Published online 30.04.2025

Abstract:
The gut microbiota is called the "main organ" of the host organism due to its important role in maintaining the normal functioning of the body. Dysbacteriosis is one of the risk factors for chronic diseases. It can cause metabolic and neural disorders, inflammatory and other reactions that reduce a healthy lifespan. This calls for developing bioactive supplements with a geroprotective effect to promote health. In this review, we aimed to study the relationship between the gut microbiota and the host organism.

This systematic review covered scientific papers published from 2013–2024 and indexed by eLIBRARY.RU, the National Center for Biotechnology Information, and Scopus.

Dysbacteriosis can lead to a number of diseases that have a cumulative negative effect on the gut microbiota. Regardless of the state of health, the following factors affect the gut microbiota in the decreasing order: diet > sleep > circadian rhythm > physical activity. There is a need for developing bioactive supplements with geroprotective potential to normalize the functioning of the microbiota. In particular, these supplements can contain probiotics, prebiotics, and plant metabolites. *Lactococcus*, *Lactobacillus*, and *Bifidobacterium* can be used as probiotics. Prebiotics include arabinogalactan, galactooligosaccharides, inulin, lactulose, oligofructose, xylo-oligosaccharide, fructooligosaccharide, or their mixtures. Among plant metabolites, especially important are polyphenols, including the ones from green tea, fruits and berries, as well as resveratrol, allicin, quercetin, curcumin, and others. However, not all of them are easily bioavailable and soluble. Encapsulation is often used to address the problem of bioavailability. The ketogenic diet and fasting-mimicking diets have the potential to increase a healthy life expectancy. The potential of dietary supplements to normalize the gut microbiota can be studied by *in vitro* experiments that use artificial gastrointestinal tracts.

Our results can provide a foundation for further research into the role of the gut microbiota in maintaining the health of the host organism.

Keywords: Microbiota, gut, nutrition, aging, body functioning gut-host associations, metabolits, life expectancy

Funding: This review was part of the state assignment entitled "The development of bioactive supplements consisting of plant metabolites *in vitro* to protect the population from premature aging" (project FZSR-2024-0008).

Please cite this article in press as: Vesnina AD, Frolova AS, Chekushkina DYu, Milentyeva IS, Luzyanin SL, Aksenova LM. Gut microbiota and its role in development of chronic disease and aging. Foods and Raw Materials. 2026;14(1):174–197. https://doi.org/10.21603/2308-4057-2026-1-668

INTRODUCTION

Despite modern advances in science and technology, longer life expectancy is accompanied with chronic diseases. These include diseases of the musculoskeletal system, immune and cardiovascular systems, metabolic and neurodegenerative disorders, as well as cancer. We know today that the human body health largely depends on the gastrointestinal tract microbiota [1, 2].

The gut microbiota is a community of microorganisms (their common genetic material) that inhabit the gastrointestinal tract of the host organism [3–5]. The microbiota plays an important role in the functioning of the host organism, regulating its immune, endocrine, and other systems (Fig. 1) [6].

Throughout its long evolution, the intestinal microbiota constantly adapts to the unique characteristics of a body, maintaining intestinal homeostasis. Microorganisms

Copyright © 2025, Vesnina *et al.* This is an open access article distributed under the terms of the Creative Commons Attribution 4.0 International License (https://creativecommons.org/licenses/by/4.0/), allowing third parties to copy and redistribute the material in any medium or format and to remix, transform, and build upon the material for any purpose, even commercially, provided the original work is properly cited and states its license.

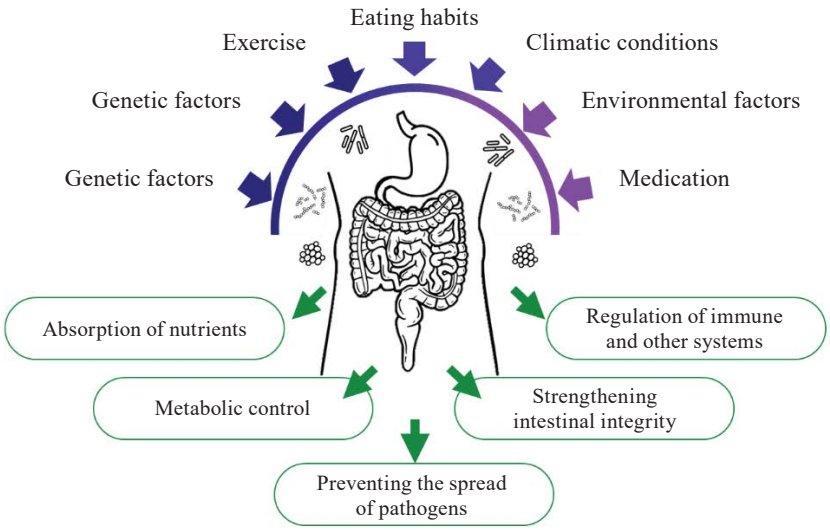

Figure 1 Factors affecting the gut microbiota and its role in regulating the ost organism

that inhabit the intestine extract nutrients from the body, break down hard-to-digest food residues, and participate in the metabolism of nutrients in the intestinal environment [7]. The disruption of their normal functioning creates a risk of developing chronic diseases. Therefore, we need to study the relationship between the microbiota and the health of the host organism in order to be able to regulate it [7, 8].

Old age (60–75 years) is associated with certain changes in the composition of the gut microbiota. They include lower biodiversity of normal microbiota, larger numbers of opportunistic strains, as well as their consequences. Such changes are caused, among other things, by the negative impact of environmental factors, particularly nutrition [1, 9]. Therefore, measures need to be taken to improve the biodiversity and normal functioning of the gut microbiota [1]. One of them is dietary intervention [10–13]. This calls for developing functional foods and food ingredients, as well as dietary supplements that normalize the functioning of the gut microbiota. However, we first need to know what functional food ingredients and nutrients have a positive impact on the gut microbiota and, therefore, exhibit a geroprotective effect. We also need to understand the mechanism of their action.

This review aimed to investigate the role of the gut microbiota in the functioning of the host organism and ensuring its healthy aging. We also explored ways of impacting the microbiota and methods for assessing its changes under the influence of various dietary factors.

To achieve this aim, our objectives were to study:
– the definition of the gut microbiota and its relationship with chronic diseases and aging;
– the main metabolites of the microbiota that regulate the state of the host organism;
– functional food ingredients that can help maintain the normal functioning of the gut microbiota; and
– methods for *in vitro* studies to determine the effect of functional food ingredients on the gut microbiota.

This review can be used as a foundation for designing further research to create bioactive supplements containing functional ingredients with geroprotective activity. It covers the most important representatives of the microbiota, as well as the conditions and methods of conducting microbiota experiments.

STUDY OBJECTS AND METHODS

We reviewed scientific articles published in English and Russian and indexed in the databases of the Russian Scientific Electronic Library (eLIBRARY.RU); National Center for Biotechnology Information (NCBI), including PubMed; and Scopus (Elsevier). Intellectual property information was accessed via the Federal Institute of Industrial Property (https://www.fips.ru/) and the PATENTSCOPE database.

The search keywords included gut microbiota, the influence of gut microbiota on aging, gastrointestinal biotransformation *in vitro*, artificial gastrointestinal tract, microbiota modeling, artificial gastrointestinal tract, probiotics, prebiotics, lactic acid bacteria, nutrition, and aging.

The review covered publications from 2013 to 2024, a well as some highly relevant articles published before 2013.

A total of 187 publications were selected for this review. During the selection process, we prioritized the papers describing the results of clinical or preclinical studies (regardless of the model objects), as well as review papers. Excluded from the review were *in silico* studies, conference proceedings, and studies of the microbiome of the skin, lungs, and other organs.

RESULTS AND DISCUSSION

The gut microbiota is a complex, dynamic, and spatially heterogeneous ecosystem. It is a community of microorganisms that interact both with each other and with the host organism. They include bacteria, fungi,

archaea, and viruses [7]. The gut microbiota is considea symbiotic relationship with the host organism, helping maintain its normal physiological processes and dynamic equilibrium [4, 14].

The normal functioning of the gut microbiota depends on its qualitative and quantitative diversity. The microbiota of an adult human includes four key categories of microorganisms: Firmicutes (Gram-positive), Bacteroides (Gram-negative), Actinomycetes (Gram-positive), and Proteus (Gram-negative) (Table 1). The ratio of Firmicutes and Bacteroidetes is an important indicator of disturbances in the functioning of the microbiota [2, 7, 15].

Five main groups of bacteria inhabit the human gastrointestinal mucosa: *Bacteroides*, *Proteobacteria* (gram-negative), *Actinobacteria*, *Verrucomicrobia* (gram-negative), and *Firmicutes*. The most common anaerobic microorganisms are *Bacteroides*, *Eubacteria*, *Bifidobacteria*, *Peptostreptococci*, *Clostridia*, and *Ruminococci* [17, 18].

Various diseases can be caused by any changes in the composition and diversity of the gut microbiota that lead to a decrease in beneficial bacteria and an increase in opportunistic bacteria (dysbacteriosis). Conversely, the progression of diseases can change the number and diversity of microbiota strains [19].

Gut microbiota and its relation to chronic disease and premature aging. The microbiota inhabiting different parts of the gastrointestinal tract differs in its qualitative and quantitative composition. The stomach, the duodenum, the jejunum, the ileum, and the colon contain about 10^1, 10^3, 10^3, 10^7, and 10^{12} cells/g contents, respectively. Every person has unique microbiota that has adapted to the conditions of his or her life [16].

The composition of the microbiota can be assessed by using various omics technologies. These include polymerase chain reaction (PCR) [20], sequencing fragments of the ribosomal 16S RNA gene of the new generation, and shotgun sequencing of the whole genome [4]. Zhong *et al.* [21] proposed a CRISPR-Cas amplicon sequencing (CCSAS) method to study eukaryotes as representatives of the microbiota.

Microbiotic imbalance can contribute to the development of chronic diseases (Table 2). They include diseases of the digestive tract such as inflammatory bowel diseases (ulcerative colitis and Crohn's disease) and colorectal cancer [22–24].

Caruso *et al.* [22] reported a decrease in the diversity of microorganisms in the intestines of patients with inflammatory bowel disease (IBD) compared to healthy individuals. In particular, the authors found a significant decrease in Firmicutes and an increase in Enterobacter and Proteobacteria, as well as changes in fungal microbiota.

According to Li *et al.* [34], Crohn's disease elevates the diversity of fungi, such as *Candida albicans*, *Aspergillus albicans*, and *Cryptococcus neoformans*, in the colon and ileum. This fungal composition was typical of the inflamed intestinal mucosa compared to the non-inflamed area with no fungi.

Dysbacteriosis is also associated with an increased risk of metabolic disorders and chronic diseases, such as obesity and type 2 diabetes, cardiovascular diseases, and cancer. Among the top causes of death, these diseases pose a serious threat to people's health and life. This calls for research into the relationship between the gut microbiota and the health of the host organism [7, 42–45].

Wu *et al.* [9] explored the role of the gut microbiota in healthy aging and longevity. They conducted their study in Sardinia, a large island in the Mediterranean Sea whose population is homogeneous in terms of diet and lifestyle and is represented by a large number of centenarians. The researchers found that:

1. The taxonomic composition of the microbiota was statistically similar in the young and old people, but differed from that of the centenarians.

2. The gut microbiota of the long-lived islanders was dominated by *Methanobrevibacter smithii* and *Bifido-*

Table 1 Human gastrointestinal tract microbiota (sourced from Bikbavova [16])

Type	Firmicutes	Bacteroidetes	Actinobacteria	Proteobacteria
Genus	*Bacillus*	*Bacteroides*	*Bifidobacterium*	*Enterobacteraceae*
	Acetobacter	*Prevotella*	*Corynebacterium*	*Escherichia*
	Clostridium	*Parabacteroides*	*Propionibacterium*	*Shigella*
	Ruminococcus	*Alistipes*	*Arthrobacter*	*Salmonella*
	Lachnospiraceae	*Porphyromonas*	*Micrococcus*	*Escherichia*
	Roseburia	*Chlorobium*	*Francia*	*Desulfovibrio*
	Faecalibacterium	*Flavobacterium*	*Mycobacterium*	*Klebsiella*
	Eubacterium	*Chlamidia*		*Moraxella*
	Lactobacillus	*Prosthecobacter*		
	Enterococcus	*Verrucomicrobium*		
	Heliobacterium			
	Heliospirillum			
	Leuconostoc			
	Mycoplasma			
	Spiroplasma			
	Sporomusa			
	Staphylococcus			
	Streptococcu			

bacterium adolescentis, with low numbers of *Faecalibacterium prausnitzii*, *Eubacterium rectale*, and *Ruminococcus* sp.

3. The microbiota of the centenarians exhibited a high capacity for glycolysis (glucose oxidation), which was presumably associated with the predominance of *Lactobacillus* and *Escherichia*.

4. The microbiota of the centenarians showed a high capacity to produce short-chain fatty acids despite a reduced capacity to break down carbohydrates.

Other studies have found low microbial diversity in older people. This low diversity is associated with lifestyle factors, including heavy medication use, changes in hormonal status and diet, and severe somatic diseases [46, 47]. Moreover, the gut microbiota is affected by limitations associated with aging. These include problems with digestion, lack of appetite, refusal to eat, or the inability to absorb a number of nutrients.

The influence of the gut microbiota on the health of the host organism is based on complex regulatory mechanisms. Knowing these mechanisms, we can develop new, and improve the existing, preventative and therapeutic measures.

Omics technologies are instrumental in exploring the influence of microbiota on the health of the organism. Today we know that microbiota can regulate the main biological processes of the host organism by producing bioactive substances [7].

Despite some general patterns in microbiotic composition, its individual variations can be quite significant. There is no single model of healthy microbiota that would be applicable to all people. The Human Microbiome project has studied healthy microbiota, i.e. the microbiota of adults with no signs of disease [48]. Its results are used for reference purposes in a number of studies [49]. However, each person has unique microbiota and microbiotic diversity cannot be the only factor in health prognosis.

The composition of the microbiota varies depending on a person's adaptation to environmental factors, as well as their genetic and physiological characteristics [10, 50]. People with the same eating habits and lifestyle can have completely different microbial communities. This suggests that genetic and climatic factors are also key to the microbiome. Changes in the gut microbiota can be caused by antibiotic use [51], stress, or dietary habits, with both short-term and long-term health consequences. Therefore, it is important to study these changes in the microbiota and its response to external stimuli [52].

The genetic consortium of all microorganisms living in the intestine significantly exceeds the human genome [7]. The human genome consists of about 23 000 genes, while the microbiome encodes more than 3 million genes, producing a large number of metabolites that regulate the functions of the host organism [4]. To a certain extent, gene mutations can influence the composition of the gut microbiota. For example, people with mutations in nucleotide oligomerization domain-containing protein 2 (NOD2) have an increased number of *Enterobacteriaceae*.

Table 2 Quantitative composition of microbiota and its relation to diseases

Microorganism	Disease	Model	Source
↑ *Bifidobacterium*, ↑ *Pasteurella*, ↑ *Enterococcus*, ↓ *Brautella*, ↓ *Prevotella,* ↓ *Faecococcus*	Parkinson's disease	Mice	[7]
↑ *Escherichia*, ↑ *Shigella*	Alzheimer's disease	Mice	[7]
↑ *Firmicutes*, ↑ *Bacteroidetes*	Hypertension	Humans	[25]
↑ *Enterobacteriaceae*, ↑ *Enterobacteraerogenes*	Athero-sclerosis	Humans	[26]
↑ *Phylum Firmicutes*, ↓ *Akkermansia muciniphila*, ↑ *Faecalibacterium prausnitzii*, ↓ *Bacteroides*	Obesity	Mice Humans	[27–29]
↑ *Rumenococcus*, ↑ *Desulfovibrio*, ↑ *Enterobacter*, ↑ *Bacteroides*, ↑ *Prevotella*, ↓ *Bifidobacterium*, ↓ *Fischeri*	Type 2 diabetes	Humans	[29, 30]
↑ *Faecalibacteria*, ↑ *Lachnospira*, ↑ *Ruminococcae*, ↑ *Roseburia*, ↓ *Prevotella copri*, ↓ *Bifidobacterium longum*	Type 1 diabetes	Humans	[31, 32]
↑ *Lactobacillus*, ↑ *Streptococcus*, ↓ *Rumenococcus*, ↓ *Prevotella*, ↓ *Flavobacterium*	Non-alcoholic fatty liver disease (NAFLD)	Mice	[33]
↓ *Enterobacter*, ↑ *Proteobacteria*, ↑ *Candida albicans*, ↑ *Aspergillus albicans*, ↑ *Cryptococcus neoformans*	Inflammatory bowel disease (IBD)	Mice Humans	[24, 34, 35]
↑ *Escherichia coli*, ↑ *Bacteroides fragilis*, ↑ *Fusobacterium nucleatum*, ↓ *Bifidobacterium*, ↓ *Lactobacillus*, ↓ *Bacteroides*	Colorectal cancer	Animals	[36]
↑ *Prevotella denticola*, ↑ *Klebsiella*, ↑ *Escherichia*, ↑ *Eisenbergiella*, ↑ *Flavobacterium*, ↑ *Fusicatenibacter*, ↑ *Megamonas*, ↑ *Enterococcus*, ↑ *Verrucomicrobia*, ↑ *Proteobacteria*, ↓ *Bacteroidetes*, ↓ *Pholiota*, ↓ *Scedosporium*, ↓ *Trichosporon*	Rheumatoid arthritis	Humans	[37–41]

↓ – reduced amount of strain; ↑ – increased amount of strain

To further explore the relationship between host genetics and intestinal microbiota, Rothschild *et al.* [53] analyzed the data from the Twins UK study of more than 14 000 twins. Their results showed a significantly greater influence of environmental factors on shaping gut microbiota compared to host genetics.

Zhang *et al.* [54] reported that only 2% of microbiota taxa are inherited, while over 20% of microbiotic differences in people are associated with drug use and anthropometric data. The scientists also found that nutrition accounts for 57% of changes in microbiota, while genetic factors account for at least 12% of these changes. This raises the importance of nutrition in normalizing the functioning of the gut microbiota.

Microbial metabolites related to chronic diseases. Metabolomic analysis of fecal samples and biofluids is an important tool for studying the impact of food components on the intestine and its microbiota [55]. In particular, it can provide insights into which food components are available to the microbiota, as well as how food components are digested, absorbed, and fermented in the gastrointestinal tract [55–57]. Gut microbiota metabolites can be analyzed by proton nuclear magnetic resonance spectroscopy (^{1}H NMR), chromatographic assays (gas chromatography combined with mass spectrometry (GC-MS), liquid chromatography combined with single-stage mass spectrometry (LC-MS)), and other methods [58–60].

Cai *et al.* [61] studied the effect of the substance "Tempol" (4-hydroxy-2,2,6,6-tetramethylpiperidine-N-oxyl) on the intestinal microbiota of mice by using NMR and GC-MS. They found that this substance reduced the amount of short-chain fatty acids. A decrease in acetate, propionate, and butyrate in the cecum was estimated by ^{1}H NMR at 41, 25, and 39%, respectively, and by GC-MS at 28, 63, and 37%, respectively. As can be seen, both methods showed similar results for butyrate, but not for acetate or propionate. The choice of a method for studying microbiota metabolites depends on the study object and aim, as well as the resources available. Yet, it is important to understand their advantages and limitations.

Lanng *et al.* [56] employed NMR analysis to study the gut microbiota and metabolic processes during a diet where meat protein was partially replaced with insect protein. The NMR method is also used to determine the contents of amino acids and their derivatives, organic acids, carbohydrates, short-chain fatty acids, trimethylamine-N-oxide (TMAO), and other food components [55].

He *et al.* [55] and Emwas *et al.* [58] highlighted the advantages and limitations of the NMR method for metabolomic analysis (Table 3).

The NMR method can be applied when there are no limitations for the sample size or when the substances cannot be analyzed chromatographically. The protocols for NMR-based metabolomic research of the gut health have been developed by Bervoets *et al.* [62] for infants and by Cui *et al.* [63] for adults.

Liquid chromatography-tandem mass spectrometry (LC-MS/MS) has become a major tool for analyzing complex metabolite compositions. However, none of the LC-MS/MS methods is suitable for a direct analysis of all metabolites due to insufficient chromatographic retention, low ionization efficiency, and high susceptibility to matrix interference. These limitations are partially addressed by chemical derivatization [64]. Some derivatizing agents include Dansyl-Cl, o-phthalaldehyde (OPA), Fmoc-Cl, Dabsyl-Cl, and Marfey reagent. The choice of an agent depends on the aim of the experiment [65].

The gut microbiota influences the metabolism of the host organism by producing enzymes that are not encoded by the human genome. These enzymes break down polysaccharides and polyphenols, as well as synthesize vitamins [66]. The nutrient medium for the microbiota consists of endogenous mucins and glycoproteins, proteins, oligopeptides, and dietary polysaccharides that are not digested by the host organism. Short-chain fatty acids (SCFAs) are the main product of carbohydrate fermentation.

SCFAs affect the immune responses of the mucosa. They promote the growth of B-cells and maintain the integrity of the mucosa by activating the inflammasome and producing IL-18. Primary acid salts (BAs) play an immunomodulatory role by stimulating the FXR

Table 3 Advantages and limitations of NMR vs. chromatography for metabolomic analysis

Advantages	Limitations
Ensures high reproducibility	Has lower sensitivity compared to chromatographic methods
Allows for relatively simple sample preparation	Is used for non-selective analysis (overlapping peaks from several metabolites create serious problems)
Can be used for quantification without internal standard substances	Requires more sample for testing
Can be automated	
Allows for studying the metabolome in biomaterial without extraction and derivatization	
Can be used for compounds that are difficult to analyze chromatographically (sugars, organic acids, alcohols, polyols, and other highly-polar compounds)	
Allows for several analyses of the same sample due to its non-destructive nature	

receptor. This has an anti-inflammatory effect and protects the body from chemically induced colitis [67].

Among essential SCFAs are acetate, propionate, and butyrate. They are produced during anaerobic fermentation from organic acids and amino acids. SCFAs play an important role in the human body [68], namely:
– provide energy for colon epithelial cells (colonocytes); serve as a substrate for endogenous metabolites [68];
– enhance the secretion of intestinal mucus and protect the mucous layer [69];
– participate in the secretion of insulin [70];
– affect the metabolism of bile acids, cholesterol, and trimethylamine oxide (TMAO);
– serve as signaling molecules that activate host G-protein-coupled receptors [71–75] regulating antitumor and anti-inflammatory functions; as well as
– affect the expression of host genes by inhibiting histone deacetylases (HDAC) [75].

Butyrate and propionate have been found to exhibit anti-inflammatory and antitumorous effects. Propionate also lowers cholesterol levels. Microbiota can obtain propionate from arabinogalactan via three pathways: succinate, acrylate, and propanediol [20, 68].

Louis *et al.* [76] reviewed normal microbiota strains that produce butyrate and propionate. They include the following strains:

1. *Faecalibacterium prausnitzii* is an obligate anaerobe, which can also grow at low oxygen concentrations in the presence of riboflavin, cysteine, and glutathione. The strain grows poorly on starch and hemicellulose but it grows well on inulin, pectin, and uronic acids [77].

2. *Eubacterium rectale* and strains of *Roseburia* spp. produce butyrate (at slightly acidic pH), formate, and lactate. They grow on starch, inulin, and arabinoxylans [78, 79].

3. *Bacteroidetes*, *Negativicutes*, and *Firmicutes* produce propionate from dietary carbohydrates via the succinate pathway [68].

4. Lachnospiraceae (*Roseburia inulinivorans* and *Blautia*) can produce 1,2-propanediol via the propanediol pathway from rhamnose and fucose. *Bacteroides*, *Escherichia coli* and *Anaerostipes rhamnosivorans*, *Clostridium sphenoides* and *Saccharomyces cerevisiae*, *Lactobacillus buchneri* produce 1,2-propanediol via lactaldehyde. *Eubacterium hallii* and *Lactobacillus reuteri*, *Flavonifractor plautii*, *Intestinimonas butyriproducens* and *Veillonella* spp. convert 1,2-propanediol into propionate and propanol [79, 80].

Kytikova *et al.* [2] listed the strains that produce SCFAs (Table 4).

SCFAs affect cell surface receptors, namely GPR43 (Free Fatty Acid Receptor 2), GPR41 (Free Fatty Acid Receptor 3), and Olfr78 (olfactory receptor 78). SCFAs regulate intestinal motility and inflammatory reactions, normalize glucose levels, and exhibit cardioprotective and anticarcinogenic effects [16, 81].

Bacteria also produce intermediate fermentation products such as fumarate, succinate, and lactate. Lactate and pyruvate are known to enhance immunity and resistance to the action of *Salmonella* [82].

In addition to SCFAs, microorganisms also produce branched-chain fatty acids (BCFAs) by degrading valine, leucine, and isoleucine. BCFAs mainly include isobutyrate, methylbutyrate, isovalerate, and isocaproate. The mechanism of their influence on the host organism is not yet fully understood. However, isovaleric acid has been found to activate neurons [83], modulate mitochondrial *β*-oxidation of pyruvate, and alter lipogenesis in adipocytes. It is also important for cholesterol synthesis.

Some microbial metabolites interact with the metabolic and physiological processes in the host organism. They include trimethylamine and trimethylamine-N-oxide, indolepropionic acid, vitamins, and hormones.

Trimethylamine (TMA) can enter the body via the conversion of choline and L-carnitine by microbiota. TMA is synthesized from choline with specific enzymes such as *CutC* (glycylradical enzyme GRE choline TMA-lyase) and *CutD* (activator GRE activase). These enzymes are encoded by the *CutC* and *CutD* genes of the bacteria *Firmicutes* (*Anaerococcus hydrogenalis*, *Clostridium asparagiforme*, *Clostridium hathewayi*, *Clostridium sporogenes*), *Proteobacteria* (*Desulfovibrio desulfuricans*, *Escherichia fergusonii*, *Proteus penneri*, *Providencia rettgeri*, *Edwardsiella tarda*) and *Actinobacteria*.

TMA can be synthesized from L-carnitine by carnitine oxidase and reductase encoded by the genes *YeaW* (Carnitine monooxygenase oxygenase subunit)/*YeaX* (Carnitine monooxygenase reductase subunit). These genes belong to *Proteobacteria* of the *Gammaproteobacteria* class (*Klebsiella pneumoniae*, *E. coli*, *Citrobacter*, *Providencia*, and *Shigella*), *Betaproteobacteria* class (*Achromobacter*), *Firmicutes* type (*Sporosarcina*), and *Actinobacteria* [20]. TMA is subsequently absorbed and converted to trimethylamine-N-oxide (TMAO) [84].

There is a known relationship between TMAO levels and cardiovascular diseases. TMAO is involved in the

Table 4 Gut microbiota bacteria producing SCFAs (sourced from Kytikova *et al.* [2])

SCFA	Strains
Acetate	*Bifidobacterium* spp., *Blautia hydrogentrophica*, *Prevotella* spp., *Streptococcus* spp., *Akkermansia muciniphilia*, *Bacteroides* spp., *Clostridium* spp., *Ruminococcus* spp.
Butyrate	*Coprococcus* spp., *Roseburia inulinivorans*, *Anaerostipes* spp., *Coprococcus comes*, *Coprococcus eutactus*, *Clostridium symbiosum*, *Eubacterium rectale*, *Eubacterium hallii*, *Faecalibacterium* spp., *Roseburia* spp., *Clostridium* spp., *Ruminococcus* spp.
Propionate	*Akkermansia muciniphilia*, *Bacteroides* spp., *Dalister succinatiphilus*, *Eubacterium* spp., *Megasphaera elsdenii*, *Phascolarctobacterium succinatutens*, *Roseburia* spp., *Salmonella* spp., *Veillonella* spp., *Coprococcus* spp., *Roseburia inulinivorans*, *Clostridium* spp., *Ruminococcus* spp.

development of atherosclerosis by converting macrophages into foam cells. Therefore, the higher the TMAO level, the higher the risk of developing cardiovascular diseases [72, 85]. Tang *et al.* [86] showed that elevated TMAO levels in blood plasma can lead to the development of chronic kidney disease and cardiovascular diseases. Regular intake of probiotics and prebiotics can lower TMAO levels by regulating the gut microbiota.

Indolepropionic acid (IPA) is a tryptophan derivative whose synthesis depends on the gut microbiota. Yano *et al.* [87] showed tryptophan as an important source for the synthesis of indoles in the gut microbiota. Indoles regulate immune responses of the intestinal mucosa by activating polycyclic aromatic hydrocarbon receptors [84].

The gut microbiota is capable of synthesizing vitamin K and B vitamins – biotin (B_7), cobalamin (B_{12}), folates (B_9), nicotinic acid (B_3), pantothenic acid (B_5), pyridoxine (B_6), riboflavin (B_2), and thiamine (B_1) [66, 88]. Folates produced by the intestinal microbiota are more accessible than synthetic ones since they do not require enzymatic transformation. Folates can be synthesized *de novo* by *Proteobacteria*, *Firmicutes*, *Actinobacteria*, and *Verrucomicrobia* [89].

The gut microbiota can synthesize hormones and neurotransmitters (Table 5).

Studies have shown that lactic acid bacteria, rather than the central nervous system (CNS), are the main source of serotonin. This neurotransmitter is produced in the presence of glutamate and glucose, which serve as a substrate for the strains. This calls for the development of probiotics that affect the CNS (psychobiotics). However, the mechanisms underlying such action of the microbiota on the CNS are not yet fully understood [90].

To improve the health of the body, microbiota-based preventative strategies are being actively developed [84], namely:

– changing the substrate for microbial fermentation;
– modulating the species composition through nutrition;
– developing probiotic, prebiotic, and synbiotic supplements; and
– transplanting fecal microbiota.

Nutrition plays a special role among these strategies. Therefore, there is a need to adjust dietary recommendations, as well as create functional foods and bioactive supplements that can normalize the gut microbiota.

Functional food ingredients for the gut microbiota. Diet, lifestyle, stress, and antibiotic use significantly affect the microbiotic balance. For example, a diet rich in fat and sugar leads to a decrease in beneficial bacteria and an increase in pathogenic organisms. This, in turn, contributes to the development of inflammatory diseases [7]. Aya *et al.* [19] listed the following factors (in descending order) that cause changes in the microbiota: diet > sleep > circadian rhythm > physical activity. However, the authors ignored the presence of chronic diseases, which is quite an important factor as well.

The consumption of prebiotics and probiotics can help restore the balance of microflora and improve intestinal and overall health [91]. Clinical trials on the use of probiotics in the treatment of inflammatory bowel disease (IBD) have shown positive results. This suggests that probiotic therapy can complement the traditional drug approaches [7]. Probiotics help modify inflammatory responses, improve intestinal permeability, and maintain the immune response. This is extremely important for patients suffering from chronic diseases.

Probiotic microorganisms act in a variety of ways. They modulate the immune function, produce organic acids and antimicrobial compounds, interact with resident microbiota and the host, improve the intestinal barrier integrity, and produce enzymes [92]. The intake of probiotics and prebiotics has beneficial effects on human health and well-being [93].

Prebiotics can be used instead of probiotics or as an additional supplement to stimulate the growth and activity of beneficial bacteria in the gastrointestinal tract (Table 6).

As can be seen from Table 6, *Bifidobacterium* species are most susceptible to prebiotic influence.

Natural products such as inulin and lactulose are important sources of prebiotics. They can be added to food to increase its nutritional content, as well as to benefit health by facilitating the absorption of minerals such as calcium and magnesium. In addition, the oral administration of prebiotics can increase the populations of beneficial microbiota in the gastrointestinal tract, preventing immune-mediated destruction [100].

Table 5 Major bioactive amines synthesized by microbiota (sourced from Gurevich *et al.* [90])

Microorganism	Metabolites	Physiological effect
Lactobacillus spp., Enterococcus	Histamine	Hypotension, allergy
Enterococcus faecalis	Tyramine	Hypertension, headache
	β-phenylethylamine	Control of hunger and satiety
Bacillus	Dopamine	Multiple effects
Bacillus, Escherichia coli	Norepinephrine	Multiple effects
Bifidobacteria	Melatonin	Relaxation of smooth muscles, regulation of sleep and wakefulness
Lactobacillus bulgaricus, Streptococcus, Escherichia coli	Serotonin	Multiple effects
Corynebacterium glutamycum, Lactobacillus plantarum, Lactobacillus paracasei, Lactococcus lactis	Glutamine	Multiple effects
Escherichia coli, Pseudomonas	*γ*-Aminobutyric acid	Muscle relaxation, anxiolytic effect

Table 6 Dietary fibers (prebiotics) modulating the activity of beneficial bacteria in the microbiota [94]

Prebiotic	Model	Effect	Source
Arabinogalactan (15 g/day for 6 weeks)	30 people	↓ isovaleric, valeric, and hexanoic acids No changes in SCFAs ↓ *Firmicutes*, ↑ *Bacteroidetes*, and ↑ *Bifidobacterium*	[95]
Galactooligosaccharides (21.6 g/day for 4 weeks)	24 healthy adults and 20 older people	No changes in SCFAs ↑ *Bifidobacterium* in both groups, but initially less *Bifidobacterium* in older people	[47]
Inulin (7 or 3 g/day for 4 weeks)	50 healthy adults	No changes in SCFAs ↑ *Bifidobacterium*	[96]
(5 or 7.5 g/day for 3 weeks)	29 healthy adults	↑ *Bifidobacterium* and ↑ *Actinobacteria*	[97]
Oligofructose (14 g/day for 1 week)	19 healthy adults	No changes in SCFAs ↑ *Bifidobacterium* ↓ *Lachnospiraceae*	[98]
Xylo-oligosaccharide (5 g/day) or inulin (3 g/day) + xylo-oligosaccharide (1 g/day) for 4 weeks	60 healthy adults	↑ butyrate, propionate, and propionate/acetate ratio ↓ acetate	[99]

↓ – decrease; ↑ – increase

The probiotic strains *Lactococcus*, *Lactobacillus*, and *Bifidobacterium* and the prebiotics inulin, oligofructose, and mannan can normalize the functioning of the gut microbiota and exhibit a cardioprotective effect [43].

Bifidobacteria play an important role in maintaining a healthy human gut microbiome [101, 102]. One of their major functions is to produce acetate and lactate during carbohydrate fermentation. Acetate and lactate can be converted to butyrate by other colonic bacteria through cross-feeding [102–104].

Active probiotic microbiota exerts several biological effects through different mechanisms. Firstly, they compete for nutrients to survive in the gastrointestinal tract and thereby prevent pathogenic microorganisms from adhering to epithelial cells. Secondly, lactic acid bacteria produce antagonistic compounds such as short-chain fatty acids, bacteriocins, and organic acids. They inhibit the growth of pathogens and prevent the colonization of opportunistic microorganisms. In addition, lactic acid bacteria regulate the immune system by stimulating immunoglobulin production, increase the cytotoxicity of natural killer cells, and modulate cytokine secretion [105].

Wilson *et al.* [106] studied the effect of the prebiotic galactooligosaccharide (GOS) on colonic inflammation. Seventeen (17) patients with active ulcerative colitis were administered GOS (2.8 g/day) for 6 weeks. Although the prebiotic did not lower the clinical scores or inflammation, it normalized the patients' stools. The proportions of *Bifidobacterium* and *Christensenellaceae* increased only in the patients with less active diseases, indicating that the prebiotic effect might depend on disease activity.

Du *et al.* [107] investigated the effect of fructooligosaccharides (FOS) on the composition and metabolism of intestinal microbiota in 39 children with functional diarrhea. The 16S rRNA sequencing showed that the FOS significantly improved α- and β-diversity in the volunteers. Particularly, the FOS significantly increased probiotic bacteria (e.g., *Bifidobacterium*) and significantly inhibited pathogenic bacteria (e.g., *Escherichia – Shigella*). The analysis of bacterial metabolites after the FOS treatment showed that the decrease in isobutyric acid, isovaleric acid, NH_3, and H_2S levels positively correlated with the relative abundance of *Lachnoclostridium* and negatively correlated with the abundance of *Streptococcus*.

Zou *et al.* [108] conducted a meta-analysis of gut microbiota in ulcerative colitis (UC) patients to identify UC-associated bacterial strains. They aimed to identify drugs that could specifically target the gut microbiota to mitigate the disease. The scientists screened 164 dietary herbal medicines *in vitro* to identify potential prebiotics for the UC-associated bacteria. The UC patients had a marked decrease in *Bacteroides* compared to the healthy controls. *Bacteroides thetaiotaomicron* showed an inverse association with the UC symptoms, indicating its potential as an anti-colitis agent.

Wang *et al.* [109] studied the prebiotic potential of polysaccharides obtained from *Stellariae Radix* and examined their effects on the composition of the intestinal microbiota in mice. The results demonstrated the high ability of crude polysaccharides to stimulate *Lactobacillus acidophilus* and *Bifidobacterium longum*. In addition, the oral administration of crude polysaccharides to mice significantly increased the populations of beneficial bacteria and, at the same time, decreased the populations of harmful bacteria in their intestinal flora.

The prebiotic potential of epilactose was described by Cardoso *et al.* [110]. The scientists used fecal inocula from individuals following the Mediterranean diet or vegan diet. The prebiotic properties of epilactose were confirmed by the formation of several metabolites (lactate, short-chain fatty acids, and gases). Epilactose significantly stimulated the butyrate-producing bacteria. This suggested that the donor diet did not affect the prebiotic action of epilactose. Butyrate is one of the current golden metabolites due to its benefits for the gut and systemic health. For the Mediterranean diet donor, butyrate production in the presence of epilactose was 70 and 63 times higher compared to lactulose and raffinose,

Table 7 Effects of polyphenols on the gut microbiota [18]

Polyphenols	Effect on microbiota	Effect on health	Model	Source
Grapes	↓ ratio *Firmicutes*/*Bacteroidetes*, ↑ *Akkermansia muciniphila*, ↑ *Bifidobacteria*, ↑ *Lactobacillus*, ↑ *Bacteroides* spp.	Lowering blood pressure; normalizing lipid profile and carbohydrates	Animals and humans *in vivo*	[112–114]
Green tea	Effect on the ratio *Firmicutes*/*Bacteroidetes*	Lowering weight, glucose, total cholesterol, and triglycerides in the blood	Animals and humans *in vivo*	[115, 116]
Cranberries	↑ *Akkermansia*, ↑ *Parvibacter*, ↑ *Barnesiella*	Preventing inflammatory bowel disease, obesity, and insulin resistance, normalizing glucose and lipid homeostasis; contributing to weight loss	Animals and humans *in vivo*	[117–120]
Blueberries	Effect on *Proteobacteria*, *Bifidobacterium*, *Actinobacteria*, *Adlercreutzia*, *Flexispira*, *Prevotella*, *Helicobacter*, *Deferribacteres*, and *Desulfovibrio*	Anti-inflammatory and anti-cancerous effect	Animals and humans *in vivo*	[121–123]
Orange	↑ *Lactobacillus* spp., ↑ *Bifidobacterium* spp., ↑ P*arabacteroides* spp., ↑ *Bacteroides ovatus*, ↑ *Faecalibacterium prausnitzii*, ↑ *Ruminococcus* spp., ↑ *Akkermansia* spp.	Normalizing low-density lipoprotein cholesterol, glucose, and insulin sensitivity	Humans *in vivo*	[124–126]
Resveratrol	↓ *Enterococcus faecalis*, ↑ *Bifidobacterium*, ↑ *Lactobacillus*	Effect on the intestinal enzymes nitroreductase, *α*-glucosidase, *α*-glucuronidase, *β*-galactosidase, and mucinase	Animals *in vivo*	[127]
Seabuckthorn (*Hippophaë rhamnoides*)	↑ ratio *Firmicutes*/*Bacteroidetes*, ↓ *Desulfovibrio*	Effect on expression of genes involved in lipid metabolism and fatty acid oxidation; effect on secretion of short-chain fatty acids	Animals *in vivo*	[128]
Allicin	↑ *Bacteroidales*, ↑ *Clostridiales*, ↑ *Akkermansia*, ↓ *Firmicutes*, ↓ *Corynebacteriales*, ↓ *Lactobacillales*	Reducing weight gain, fat deposition, and low-density lipoprotein cholesterol; increasing high-density lipoprotein levels; effect on expression of lipid metabolism genes	Animals *in vivo*	[129]
Quercetin	↓ *Firmicutes*, ↓ *Erysipelotrichia*, ↓ *Bacillus*	Anti-inflammatory effect; lowering insulin resistance	Animals and humans *in vivo*	[130]
Curcumin	Effect on *Anaerotruncus*, *Exiguobacterium*, *Helicobacter*, *Papillibacter*, *Pseudomonas*, *Serratia*, and *Shewanella*	Antidiabetic effect, anti-obesity effect	Animals *in vivo*	[131, 132]

↓ – strain reduction/growth inhibition; ↑ – increase in strains

respectively. For the vegan diet donor, butyrate production increased 29 and 89 times compared to lactulose and raffinose, respectively.

Shabbir *et al.* [18] reviewed the effects of polyphenols on the gut microbiota (Table 7). We know that a number of strains (*Bifidobacterium* ssp., *Lactobacillus* ssp., *E. coli*, *Bacteroides* ssp., *Eubacterium* ssp., *Enterococcus caccae*, *Ruminococcus gauvreauii*, etc.) can influence the bioavailability and bioactivity of polyphenols. In turn, polyphenols exhibit antimicrobial activity [111] and prebiotic functions suppressing opportunistic strains in the intestine.

The use of polyphenols in functional food products and dietary supplements is limited due to their low solubility in water, as well as low bioavailability and stability (Table 8).

The fact that some substances belong to several classes poses a problem of dosing in research.

According to literature, the bioavailability of polyphenols decreases in the following order: phenolic acids > isoflavones > flavonols > catechins > flavanones, proanthocyanidins > anthocyanins [141, 142]. After oral administration, they begin to degrade and transit to various organs of the gastrointestinal tract. However, their low

Table 8 Classification of some polyphenols according to the biopharmaceutical classification system (BCS) (sourced from Truzzi *et al.* [133])

Polyphenols	Compounds	BCS
Hydroxycinnamic acid	Ferulic acid	III [133, 134]
Flavonoids	Chlorogenic acid	
Flavonoids	Rutin	III [133, 134]
Isoflavones	Quercetin	I [133, 134], II [135], IV [136]
Stilbenes	Apigenin	I [133], II [137]
Tannins	Daizein	II [133], IV [138]
Curcuminoids	Resveratrol	II [133, 138]
Hydroxycinnamic acid	Ellagic acid	IV [133, 139]
Flavonoids	Curcumin	II [133], IV [140]

I – high solubility, high permeability; II – low solubility, high permeability; III – high solubility, low permeability; IV – low solubility, low permeability

metabolism in the small intestine and low permeability through the intestinal barrier limit their further transit into the bloodstream [143].

Nanoencapsulation is an effective means of solving the problem described above. Substances such as lipids and micelles can be used as nanosystems. Encapsulation can improve the stability and solubility of substances, protect them from the gastrointestinal tract, and prolong their time in the intestine [143–147].

Highly relevant are *in vitro* studies that explore the effect of polyphenols or other functional food ingredients on the gut microbiota and the mechanism of their action.

Probiotics and prebiotics improve human health and prevent nutrition-related diseases in addition to providing the body with certain nutrients [148].

Since food products have a complex composition and long shelf life, there is a need to determine effects of food additives (sweeteners, colorants, preservatives, antioxidants, etc.) on the gut microbiota. However, such studies have been mainly *in vitro* or on rodents [149–152].

Limiting the caloric intake is believed to be an effective way to prevent disease and increase life expectancy in model organisms [153, 154]. There are a number of diets that can potentially increase people's life expectancy, such as the ketogenic diet, intermittent fasting, or fasting-mimicking diets.

The ketogenic diet is low in carbohydrates, moderate in protein, and high in fat [43]. This diet leads to the development of ketosis, an increased content of ketone bodies in the blood.

The demand for the ketogenic diet to support healthy aging was fueled by the 2017 publications of Newman *et al.* [155] and Roberts *et al.* [156]. In particular, Newman *et al.* [155] found that the ketogenic diet improved survival, memory, and increases lifespan in aging C57BL/6 mice. Roberts *et al.* [156] reported that this diet increased lifespan in adult male C57BL/6 mice, as well as preserved motor function, memory, and muscle mass in old C57BL/6 mice.

β-hydroxybutyrate (ketone body) carries energy from the liver to peripheral tissues during prolonged fasting and exercise. It is suggested that it can cause epigenetic changes associated with improved health and increased lifespan [153].

Intermittent fasting and fasting-mimicking diets are low-calorie, nutrient-rich diets restricting food intake for 12 or 24 h [157, 158]. Brandhorst *et al.* [159] reported that intermittent fasting alternated with a nutrient-rich diet (every 48 h) in *S. cerevisiae* extended their lifespan and increased their survival under oxidative stress. The scientists found that a low-protein and low-calorie diet reduced visceral fat, normalized glucose and insulin levels, as well as increased the number of ketone bodies in C57BL/6 mice. They also observed a decrease in tumor diseases of the hematopoietic system, a reduced number of lesions, and improved cognitive abilities in the mice.

Clinical studies have shown that a low-calorie and low-protein diet lowered glucose and insulin levels, increased ketone bodies, and reduced body weight due to a lower content of fat alongside increasing muscle mass. The diet also reduced the levels of C-reactive protein, which is a marker of inflammation and cardiovascular disease.

Intermittent fasting is believed to have a positive effect on the gut microbiota, which, in turn, improves the expression of a number of genes and the metabolism of the host organism. It might be that by providing intestinal rest, the fasting diet improved the diversity of microbiota (Table 9), the intestinal barrier function, immune and inflammatory responses, stimulating the production of short-chain fatty acids [160].

However, there has been no evidence to date of the effect of various diets on increasing healthy life expectancy in humans. Clinical studies require a lot of time and large numbers of volunteers. They also need to take into account environmental, climatic, genetic, and other individual factors, as well as circadian rhythms [157].

Today, there is a great need to study the effects of functional nutrients, such as plant-based products, on the gut microbiota to promote their use in preventing chronic diseases and increasing healthy life expectancy.

***In vitro* experimental models for gut microbiota studies.** The composition of, and changes in, the microbiota have been studied in clinical trials, as well as on animal models. Nematodes (*Caenorhabditis elegans*), turquoise killifish (*Nothobranchius furzeri*), naked mole-rat (*Heterocephalus glaber*), *Drosophila*, and rodents have been used to modulate the microbiota through dietary interventions to enhance healthy aging [170–173]. However, highly relevant are studies that use artificial gastrointestinal tract models.

An artificial gastrointestinal tract is a system that models different sections of the gastrointestinal tract *in vitro*. The advantages of *in vitro* models over *in vivo* experiments include their simplicity, low cost, the absence of ethical restrictions, as well as biological variation [174, 175].

In Russia, the first developments of the artificial gastrointestinal tract were patented by the scientists from the Don State Technical University [176]. However, they largely focused on the microbiota of animals [177]. The

Table 9 Preclinical and clinical studies on the effect of fasting diet on the gut microbiota (sourced from Mohr *et al.* [161])

Model organism	Dietary intervention	Results	Source
		Preclinical studies	
db/db male mice, 16-week-old	Fasting for 24 h every other day for 7 months, starting at night	Improved survival with no effect on glycated hemoglobin. ↑ *Firmicutes*, ↓ *Bacteroidetes*, ↓ *Verrucomicrobia*, ↑ *Lactobacillus*, ↑ *Oscillospira*, ↑ *Ruminococcus*, ↓ *Akkermansia*, ↓ *Bacteroides*, ↓ *Bifidobacterium*	[162]
Healthy C57BL/6J female mice, 7-week-old	24 h fasting for 4 weeks	↑ *Lactobacillaceae*, ↑ *Bacteroidaceae*, ↑ *Prevotellaceae*, ↑ Ketone formation, glutathione metabolism, enhanced antioxidant pathways	[163]
Lean and obese C57BL/6J male mice, 4-week-old	Normal chow and HFD treatments for 6 weeks; then 4 days of 50% kcal of baseline needs, 4 days of complete food withdrawal, 4 days of 50% kcal of baseline needs	↑ *Akkermansia muciniphila*, ↑ *Lactobacillus*	[164]
Healthy C57BL/6J male mice, 6-week-old	Three groups of mice fasted for 12, 16 a nd 20 h for 30 days; after fasting, the mice fed *ad libitum* for 1 month	↑ *Akkermansia*, ↓ *Alistipes* in the 16-h fasting group	[165]
db/db male mice, 12-week-old	Fasting for 24 h, then feeding *ad libitum* for 28 days	↑ *Lactobacillus*, ↑ *Odoribacter*	[166]
		Clinical studies	
Healthy adults, 45.0±9.7 yr	Ramadan (17 h of fasting per day from sunset to sunrise over a 29-day period)	↑ *Akkermansia muciniphila*, ↑ *Bacteroides fragilis* ↓ Fasting serum glucose and total cholesterol levels	[167]
Healthy adults, 45.0±9.7 yr	Ramadan (17 h of daily fasting)	↑ *Butyricicoccus*, ↑ *Bacteroides*, ↑ *Faecalibacterium*, ↑ *Roseburia*, ↑ *Allobaculum*, ↑ *Eubacterium*, ↑ *Dialister*, ↑ *Erysipelotrichi*	[168]
Healthy male adults, age not reported	Fasting for 16 h for 25 days	↑ Enrichment of *Prevotellaceae* and *Bacteroideaceae* + Association between microbial richness and Sirt1 and circadian gene expression	[169]

↓ – decrease; ↑ – increase

artificial gastrointestinal tract model developed in Russia was based on the former models, namely the dynamic gastric model (DGM), the TNO gastro-intestinal model (TIM), and the human gastric simulator (HGS).

The first developments of an artificial gastrointestinal tract date back to 1993. Figure 2 shows a cell for pancreatic digestion presented by Savoie in 1993 [178].

In 1995, Minekus *et al.* [173] described a multichamber *in vitro* model that simulated dynamic events occurring in the lumen of the gastrointestinal tract of humans and animals with a single-chamber stomach (Fig. 3).

In 1999, Minekus *et al.* [180] improved their 1995 model. Their new system combined peristaltic mixing to obtain and process physiological concentrations of microorganisms, dry matter, and microbial metabolites, with the removal of metabolites and water (Fig. 4).

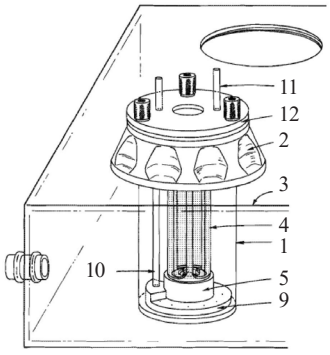

Figure 2 The digestion cell consisting of: outer cylinder (1), cover (2), water bath (3), tubular dialysis membrane (4), inner cylinder (5), annular hollow ring (9), buffer outlet tube (10), buffer idet tube (11), and locking disc (12)

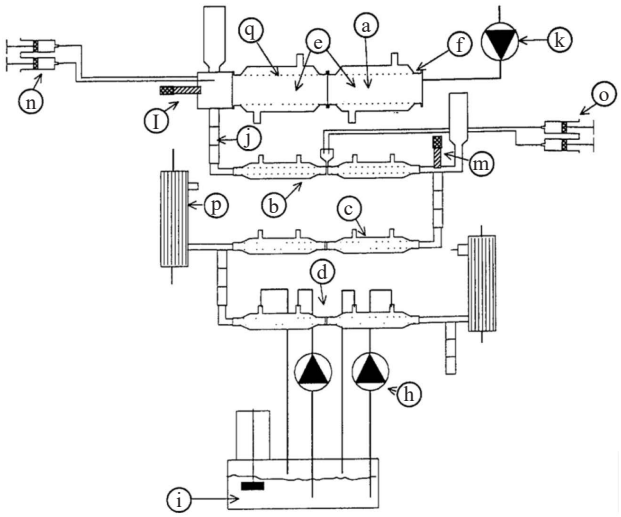

Aspects proposed by A.C. Langland

a) sequential use of enzymes in physiological amounts,
b) Appropriate pH for the enzymes and addition of relevant co-factors such as bile salts and coenzymes,
c) removal of the products of digestion,
d) appropriate mixing at each stage of digestion,
e) physiological transit times for each step of digestion.

Figure 3 The model simulating dynamic physiological processes occurring in the lumen of the stomach and small intestine of humans and monogastric animals (as well as its requirements [179]): (a) gastric compartment, (b) duodenal compartment, (c) jejunal compartment, (d) ileal compartment, (e) basic unit, (f) glass jacket, (g) flexible wall, (h) rotary pump, (i) water bath, (j) peristaltic valve-pump, (k) peristaltic pump, (l, m) pH electrodes, (n, o) syringe pumps, (p) hollow-fiber device

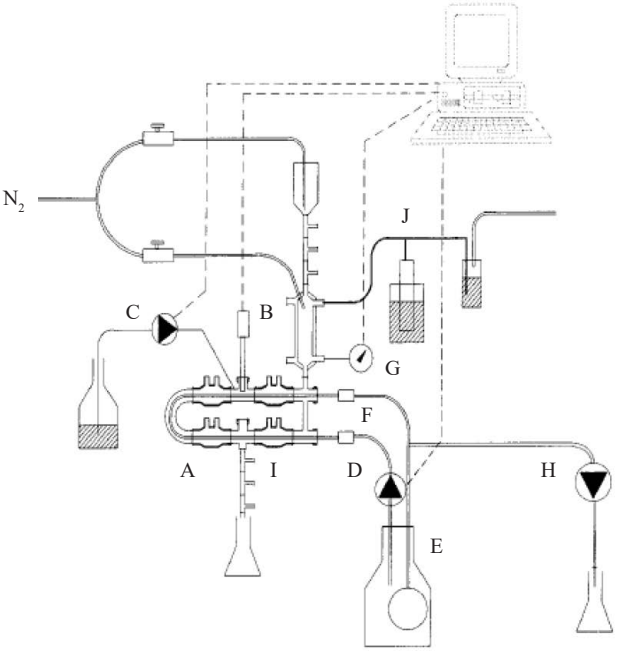

Figure 4 Schematic presentation of the system to simulate conditions in the large intestine: (A) mixing units, (B) pH electrode, (C) alkali pump, (D) dialysis pump, (E) dialysis light, (F) dialysis circuit with hollow fibers, (G) level sensor, (H) water absorption pump, (I) peristaltic valve pump, (J) gas outlet with water lock

The model developed by Minekus was later referred to as the TNO Gastro-Intestinal Model (TIM) after the Dutch Organization for Applied Scientific Research (TNO).

Figure 3 shows the TIM-1 model consisting of four compartments representing the stomach, duodenum, jejunum, and ileum.

Figure 4 shows the TinyTIM or TIM-2 model, a simplified version of TIM-1. It was developed to increase the throughput compared to TIM-1 and was more suitable for studies that do not require separate intestinal stages. In 2015, Minekus *et al.* developed the TIM-agc model simulating the shape and motility of the stomach in a more realistic way [181, 182].

In 2012, the Dynamic Gastric Model (DGM) was developed at the Institute of Food Research (Norwich, UK) [183]. The DGM combined the physical and biochemical characteristics of the human stomach over time (Fig. 5).

The DGM has a wide range of applications. So far, it has been used to study the bioavailability of nutrients, structural changes of food matrices during digestion, and the degradation and dissolution of various drugs [184].

In 2010, Kong and Singh [185] developed a human gastric simulator (HGS) (Figs. 6–8).

The HGS is used to study the biotransformation of food components and gastric contents during digestion. It has also been used to determine the influence of physiological conditions (acid secretion, enzymes, and gastric contractile force) on the kinetics of food breakdown and nutrient release [186].

In 2014, Ménard *et al.* [187] contributed to the development of the dynamic digestive intestinal gastrointestinal system (DIDGI) (Fig. 9).

The DIDGI consists of two or three consecutive compartments simulating the stomach, small intestine, and the ileum. Today, this system is used to study the digestion of milk, milk gels and emulsions, and cheese. It is also used to study the survival of microorganisms in the gastrointestinal tract [188].

There are other systems in addition to the three artificial gastrointestinal tract systems described above. For example, Peeters *et al.* [189] carried out *in vitro* biotransformation using gastrointestinal enzymes and fecal microbiota. Breynaert *et al.* [190] used an *in vitro* continuous flow dialysis model with a colon phase to study the availability and metabolism of polyphenolic compounds (Fig. 10).

Gumienna *et al.* [191] studied changes in wine polyphenols during *in vitro* digestion. For this, they devised an *in vitro* digestion model in a glass bioreactor (Fig. 11).

The only common limitation of all the artificial gastrointestinal tracts is that they do not interact with the host organism, which is beyond *in vitro* experiments. These artificial models have high potential for assessing the safety of food products, antibiotics, and functional food ingredients, as well as their impact on microbiota and its metabolism. They can also be used to study the biotransformation of products.

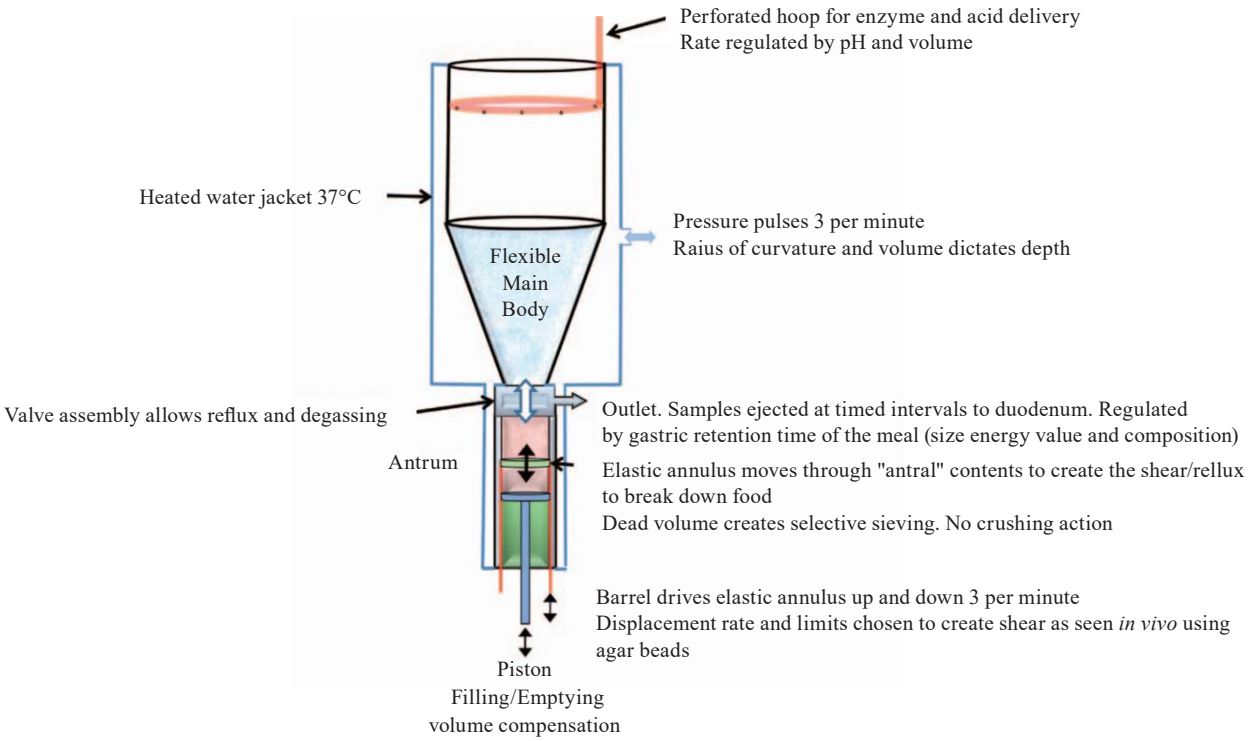

Figure 5 Schematic presentation of the dynamic gastric model designed by Wickham *et al.* [183]

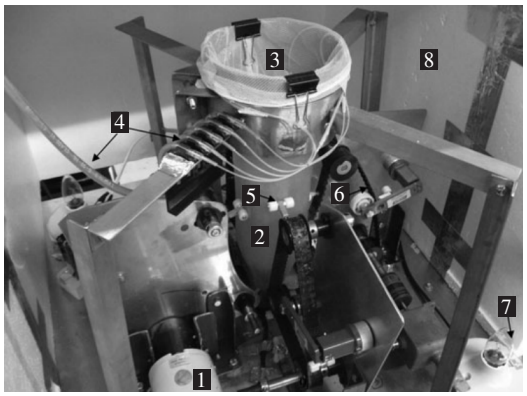

Figure 6 The human gastric simulator: (1) motor, (2) gastric compartment, (3) mesh bag, (4) simulating secretion tubes, (5) Teflon roller set, (6) conveying belt, (7) insulated chamber [185]

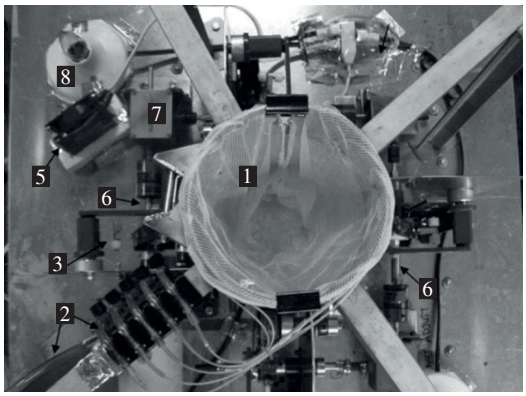

Figure 7 Top view of the human gastric simulator: (1) latex chamber with mesh net, (2) plastic tubing for secretion, (3) roller, (4) motor, (5) fan, (6) drive shaft, (7) right angle gear, (8) light bulb [185]

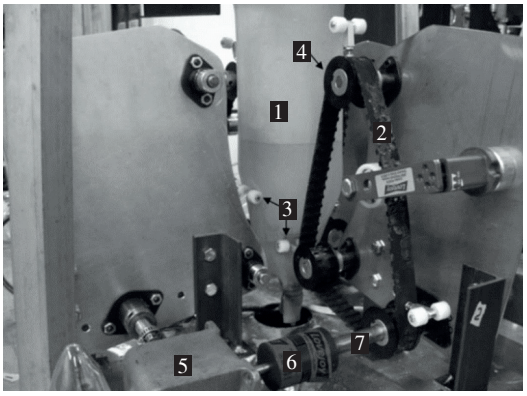

Figure 8 The pulley system and rollers: (1) latex chamber, (2) belt, (3) roller, (4) pulley, (5) right angle gear, (6) Love-Joy joint, (7) shaft [185]

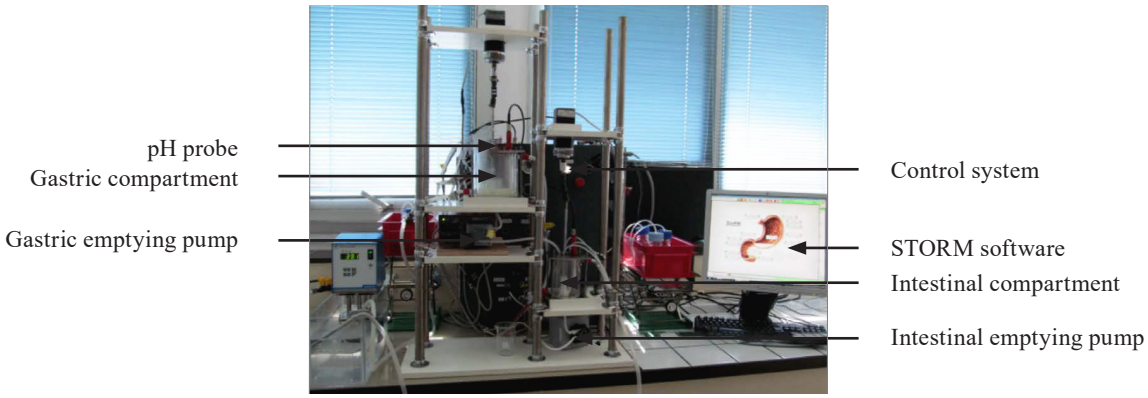

Figure 9 The DIDGI system developed by Ménard *et al.* [187]

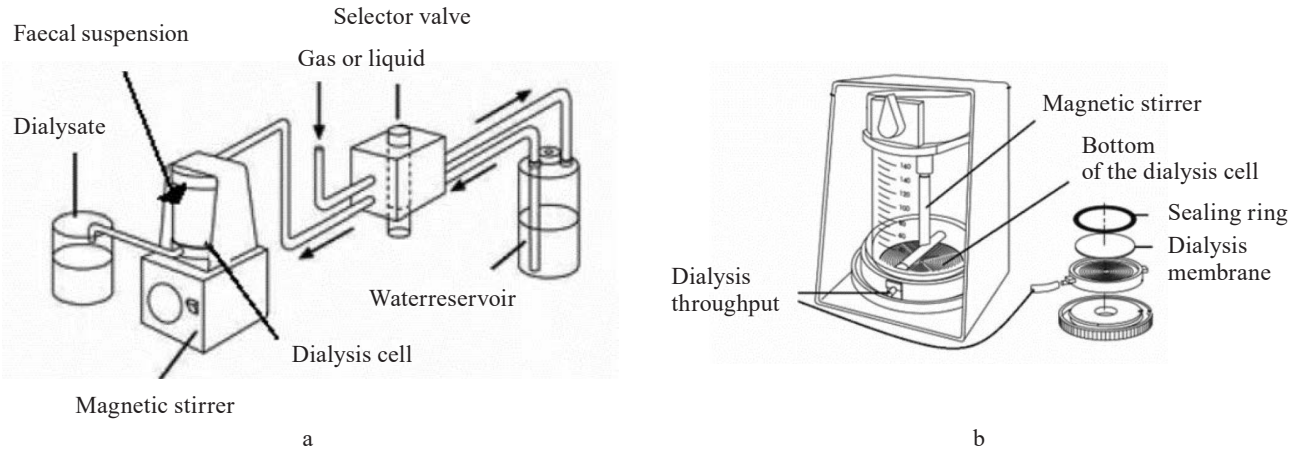

Figure 10 Experimental system designed by Breynaert *et al.* [190]: (a) *in vitro* continuous flow dialysis model with a colon phase, (b) enlarged dialysis cell

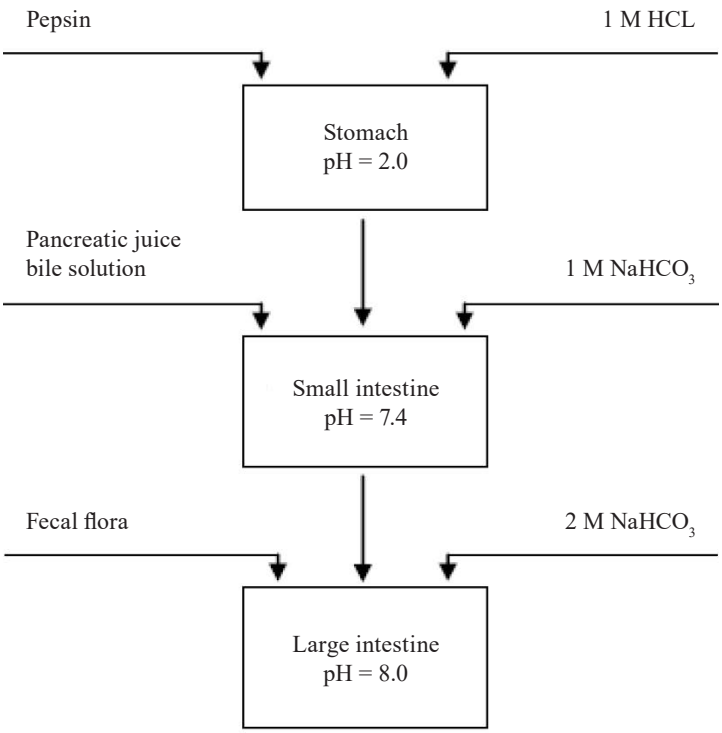

Figure 11 The gastrointestinal tract model consisting of the stomach, small intestine, and colon stages (sourced from Gumienna *et al.* [191])

CONCLUSION

In this review, we explored the basic concepts of the gut microbiota, its relationship with the development of chronic diseases, and its role in the aging process.

We studied the main metabolites of the gut microbiota that regulate the state of the host organism (short-chain fatty acids, branched-chain fatty acids, trimethylamine, trimethylamine-N-oxide, indolepropionic acid, vitamins, and hormones).

The qualitative and quantitative composition of the gut microbiota is studied by the PCR method and sequencing methods. Microbial metabolites are studied by proton nuclear magnetic resonance spectroscopy and chromatographic methods with derivatization.

We presented the main models of artificial gastrointestinal tracts used to study the effects of bioactive substances on the gut microbiota.

Microbiota studies are important for devising diets and functional foods containing polyphenols, probiotics, and prebiotics to prevent chronic diseases and maintain a healthy lifespan.

CONTRIBUTION

A.D. Vesnina – data curation, project administration, validation, visualization, writing – original draft, review & editing. A.S. Frolova – data curation, visualization, writing – original draft. D.Yu. Chekushkina – data curation, writing – original draft I.S. Milentyeva – conceptualization, project administration, writing – review & editing. S.L. Luzyanin and L.M. Aksenova – methodology, writing – review & editing.

CONFLICT OF INTEREST

The authors declare no conflict of interest.

REFERENCES

1. Strasser B, Wolters M, Weyh C, Krüger K, Ticinesi A. The effects of lifestyle and diet on gut microbiota composition, inflammation and muscle performance in our aging society. Nutrients. 2021;13(6):2045. https://doi.org/10.3390/nu13062045
2. Kytikova OYu, Denisenko YuK, Novgorodtseva TP, Antonyuk MV, Gvozdenko TA. The short chain free fatty acids and their receptors in the microbiotic concept for asthma development. Annals of the Russian Academy of Medical Sciences. 2022;77(2):131–142. (In Russ.). https://doi.org/10.15690/vramn1608
3. Hoefer CC, Hollon LK, Campbell JA. The role of the human gutome on chronic disease: A review of the microbiome and nutrigenomics. Advances in Molecular Pathology. 2021;4:103–116. https://doi.org/10.1016/j.yamp.2021.06.003
4. Valdes AM, Walter J, Segal E, Spector TD. Role of the gut microbiota in nutrition and health. BMJ. 2018;361:k2179. https://doi.org/10.1136/bmj.k2179
5. Shishin MV, Prosekov AYu. Investigation of morphological and antimicrobial properties of intestinal tract microorganisms. Food Processing: Techniques and Technology. 2015;39(4):131–137. (In Russ.). https://www.elibrary.ru/VBIUTF
6. Meslier V, Laiola M, Roager HM, de Filippis F, Roume H, Quinquis B, *et al.* Mediterranean diet intervention in overweight and obese subjects lowers plasma cholesterol and causes changes in the gut microbiome and metabolome independently of energy intake. Gut. 2020;69(7):1258–1268. https://doi.org/10.1136/gutjnl-2019-320438
7. Chen Y, Zhou J, Wang L. Role and mechanism of gut microbiota in human disease. Frontiers in Cellular and Infection Microbiology. 2021;11:625913. https://doi.org/10.3389/fcimb.2021.625913
8. Kolokolova AYu, Kishilova SA, Rozhkova IV, Mitrova VA. The role of postbiotic composition in the growth stimulating of bifidobacteria. Food Metaengineering. 2024;2(2):12–21. (In Russ.). https://doi.org/10.37442/fme.2024.2.56
9. Wu L, Zeng T, Zinellu A, Rubino S, Kelvin DJ, Carru C. A cross-sectional study of compositional and functional profiles of gut microbiota in Sardinian centenarians. mSystems. 2019;4(4):e00325-19. https://doi.org/10.1128/mSystems.00325-19
10. Fedorova AM, Dyshlyuk LS, Milentyeva IS, Loseva AI, Neverova OA, Khelef MEA. Geroprotective activity of trans-cinnamic acid isolated from the Baikal skullcap (*Scutellaria baicalensis*). Food Processing: Techniques and Technology. 2022;52(3):582–591. https://doi.org/10.21603/2074-9414-2022-3-2388
11. Milentyeva IS, Vesnina AD, Fedorova AM, Ostapova EV, Larichev TA. Chlorogenic acid and biohanin A from *Trifolium pratense* L. Callus culture extract: functional activity *in vivo*. Food Processing: Techniques and Technology. 2023;53(4):754–765. (In Russ.). https://doi.org/10.21603/2074-9414-2023-4-2475
12. Litvyak VV, Shylau VV, Kuzina LB, Roslyakov YuF. The method of personalized nutrition considering genetically determined factors. Food Metaengineering. 2023;1(1):26–62. (In Russ.). https://doi.org/10.37442/fme.2023.1.5
13. Agarkova EYu. Belyakova ZYu, Kondratenko VV. Principles of formation of modular technologies of enteral nutrition products. Food Metaengineering. 2023;1(3):33–46. (In Russ.). https://doi.org/10.37442/fme.2023.3.26
14. Clemente JC, Ursell LK, Parfrey LW, Knight R. The impact of the gut microbiota on human health: An integrative view. Cell. 2012;148(6):1258–1270. https://doi.org/10.1016/j.cell.2012.01.035

15. Thaiss CA, Itav S, Rothschild D, Meijer MT, Levy M, Moresi C, *et al.* Persistent microbiome alterations modulate the rate of post-dieting weight regain. Nature. 2016;540:544–551. https://doi.org/10.1038/nature20796
16. Bikbavova GR, Livzan MA. Modulation of intestinal microbiome in the formationand progression of ulcerative colitis. Annals of the Russian Academy of Medical Sciences. 2020;75(6):577–584. (In Russ.). https://doi.org/10.15690/vramn1238
17. Sha S, Ni L, Stefil M, Dixon M, Mouraviev V. The human gastrointestinal microbiota and prostate cancer development and treatment. Investigative and Clinical Urology. 2020;61:S43–S50. https://doi.org/10.4111/icu.2020.61.S1.S43
18. Shabbir U, Rubab M, Daliri EB-M, Chelliah R, Javed A, Oh D-H. Curcumin, quercetin, catechins and metabolic diseases: The role of gut microbiota. Nutrients. 2021;13(1):206. https://doi.org/10.3390/nu13010206
19. Aya V, Flórez A, Perez L, Ramírez JD. Association between physical activity and changes in intestinal microbiota composition: A systematic review. PLoS ONE. 2021;16(2):e0247039. https://doi.org/10.1371/journal.pone.0247039
20. Ivashkin VT, Medvedev OS, Poluektova EA, Kudryavtseva AV, Bakhtogarimov IR, Karchevskaya AE. Direct and indirect methods for studying human gut microbiota. Russian Journal of Gastroenterology, Hepatology, Coloproctology. 2022;32(2):19–34. (In Russ.). https://doi.org/10.22416/1382-4376-2022-32-2-19-34
21. Zhong KX, Cho A, Deeg CM, Chan AM, Suttle CA. Revealing the composition of the eukaryotic microbiome of oyster spat by CRISPR-Cas Selective Amplicon Sequencing (CCSAS). Microbiome. 2021;9:230. https://doi.org/10.1186/s40168-021-01180-0
22. Caruso R, Lo BC, Núñez G. Host-microbiota interactions in inflammatory bowel disease. Nature Reviews Immunology. 2020;20:411–426. https://doi.org/10.1038/s41577-019-0268-7
23. Schaubeck M, Clavel T, Calasan J, Lagkouvardos I, Haange SB, Jehmlich N, *et al.* Dysbiotic gut microbiota causes transmissible Crohn's disease-like ileitis independent of failure in antimicrobial defence. Gut. 2016;65(2):225–237. https://doi.org/10.1136/gutjnl-2015-309333
24. Eftychi C, Schwarzer R, Vlantis K, Wachsmuth L, Basic M, Wagle P, *et al.* Temporally distinct functions of the cytokines IL-12 and IL-23 drive chronic colon inflammation in response to intestinal barrier impairment. Immunity. 2019;51(2):367–380.e4. https://doi.org/10.1016/j.immuni.2019.06.008
25. Farhangi MA, Vajdi M. Gut microbiota-associated trimethylamine N-oxide and increased cardiometabolic risk in adults: A systematic review and dose-response meta-analysis. Nutrition Reviews. 2021;79(9):1022–1042. https://doi.org/10.1093/nutrit/nuaa111
26. Li J, Lin S, Vanhoutte PM, Woo CW, Xu A. *Akkermansia muciniphila* protects against atherosclerosis by preventing metabolic endotoxemia-induced inflammation in *Apoe*$^{-/-}$Mice. Circulation. 2016;133(24):2434–2446. https://doi.org/10.1161/CIRCULATIONAHA.115.019645
27. Vallianou N, Stratigou T, Christodoulatos GS, Dalamaga M. Understanding the role of the gut microbiome and microbial metabolites in obesity and obesity-associated metabolic disorders: current evidence and perspectives. Current Obesity Reports. 2019;8:317–332. https://doi.org/10.1007/s13679-019-00352-2
28. Turnbaugh PJ, Ley RE, Mahowald MA, Magrini V, Mardis ER, Gordon JI. An obesity-associated gut microbiome with increased capacity for energy harvest. Nature. 2006;444:1027–1031. https://doi.org/10.1038/nature05414
29. Moreno-Indias I, Cardona F, Tinahones FJ, Queipo-Ortuño MI. Impact of the gut microbiota on the development of obesity and type 2 diabetes mellitus. Frontiers in Microbiology. 2014;5:190. https://doi.org/10.3389/fmicb.2014.00190
30. Crusell MKW, Hansen TH, Nielsen T, Allin KH, Rühlemann MC, Damm P, *et al.* Gestational diabetes is associated with change in the gut microbiota composition in third trimester of pregnancy and postpartum. Microbiome. 2018;6:89. https://doi.org/10.1186/s40168-018-0472-x
31. Chukhlovin AB, Dudurich VV, Kusakin AV, Polev DE, Ermachenko ED, Aseev MV, *et al.* Evaluation of gut microbiota in healthy persons and type 1 diabetes mellitus patients in North-Western Russia. Microorganisms. 2023;11(7):1813. https://doi.org/10.3390/microorganisms11071813
32. van Heck JIP, Gacesa R, Stienstra R, Fu J, Zhernakova A, Harmsen HJM, *et al.* The gut microbiome composition is altered in long-standing type 1 diabetes and associates with glycemic control and disease-related complications. Diabetes Care. 2022;45(9):2084–2094. https://doi.org/10.2337/dc21-2225
33. Jiang C, Xie C, Li F, Zhang L, Nichols RG, Krausz KW, *et al.* Intestinal farnesoid X receptor signaling promotes nonalcoholic fatty liver disease. The Journal of Clinical Investigation. 2015;125(1):386–402. https://doi.org/10.1172/JCI76738
34. Li Q, Wang C, Tang C, He Q, Li N, Li J. Dysbiosis of gut fungal microbiota is associated with mucosal inflammation in Crohn's disease. Journal of Clinical Gastroenterology. 2014;48(6):513–523. https://doi.org/10.1097/MCG.0000000000000035

35. Sukhina MA, Yudin SM, Zagainova AV, Makarov VV, Veselov AV, Anosov IS, *et al.* Peculiarities of microbiota in patients with inflammatory intestinal diseases. Annals of the Russian Academy of Medical Sciences. 2022;77(3): 165–171. (In Russ.). https://doi.org/10.15690/vramn1480

36. Si H, Yang Q, Hu H, Ding C, Wang H, Lin X. Colorectal cancer occurrence and treatment based on changes in intestinal flora. Seminars in Cancer Biology. 2021;70:3–10. https://doi.org/10.1016/j.semcancer.2020.05.004

37. Kishikawa T, Maeda Y, Nii T, Motooka D, Matsumoto Y, Matsushita M, *et al.* Metagenome-wide association study of gut microbiome revealed novel aetiology of rheumatoid arthritis in the Japanese population. Annals of the Rheumatic Diseases. 2020;79(1):103–111. https://doi.org/10.1136/annrheumdis-2019-215743

38. Yu D, Du J, Pu X, Zheng L, Chen S, Wang N, *et al.* The gut microbiome and metabolites are altered and interrelated in patients with rheumatoid arthritis. Frontiers in Cellular and Infection Microbiology. 2022;11:763507. https://doi.org/10.3389/fcimb.2021.763507

39. Chen Y, Ma C, Liu L, He J, Zhu C, Zheng F, *et al.* Analysis of gut microbiota and metabolites in patients with rheumatoid arthritis and identification of potential biomarkers. Aging. 2021;13(20):23689–23701. https://doi.org/10.18632/aging.203641

40. Sun X, Wang Y, Li X, Wang M, Dong J, Tang W, *et al.* Alterations of gut fungal microbiota in patients with rheumatoid arthritis. PeerJ. 2022;10:e13037. https://doi.org/10.7717/peerj.13037

41. Huang Z, Chen C, Tan L, Ling Y, Ma W, Zhang J. 16S rRNA gene sequencing of gut microbiota in rheumatoid arthritis treated with 99Tc-MDP. Pharmacogenomics and Personalized Medicine. 2024;17:237–249. https://doi.org/10.2147/PGPM.S451065

42. Miao Z, Lin J, Mao Y, Chen G, Zeng F, Dong H, *et al.* Erythrocyte n-6 polyunsaturated fatty acids, gut microbiota, and incident type 2 diabetes: A prospective cohort study. Diabetes Care. 2020;43(10):2435–2443. https://doi.org/10.2337/dc20-0631

43. Vesnina A, Prosekov A, Atuchin V, Minina V, Ponasenko A. Tackling atherosclerosis via selected nutrition. International Journal of Molecular Sciences. 2022;23(15):8233. https://doi.org/10.3390/ijms23158233

44. Duque-Molina C. Comprehensive Care Protocols, a strategy for chronic diseases. Revista Médica del Instituto Mexicano del Seguro Social. 2022;60:S1–S3. (In Spanish).

45. Wang T, Wang H, Zeng Y, Cai X, Xie L. Health beliefs associated with preventive behaviors against noncommunicable diseases. Patient Education and Counseling. 2022;105(1):173–181. https://doi.org/10.1016/j.pec.2021.05.024

46. Kaybysheva VO, Zharova ME, Filimendikova KYu, Nikonov EL. Human microbiome: age-related changes and functions. Russian Journal of Evidence-Based Gastroenterology. 2020;9(2):42–55. (In Russ.). https://doi.org/10.17116/dokgastro2020902142

47. Wilms E, An R, Smolinska A, Stevens Y, Weseler AR, Elizalde M, *et al.* Galacto-oligosaccharides supplementation in prefrail older and healthy adults increased faecal bifidobacteria, but did not impact immune function and oxidative stress. Clinical Nutrition. 2021;40(5):3019–3031. https://doi.org/10.1016/j.clnu.2020.12.034

48. Structure, function and diversity of the healthy human microbiome. Nature. 2012;486:207–214. https://doi.org/10.1038/nature11234

49. King CH, Desai H, Sylvetsky AC, LoTempio J, Ayanyan S, Carrie J, *et al.* Baseline human gut microbiota profile in healthy people and standard reporting template. PLoS ONE. 2019;14(9):e0206484. https://doi.org/10.1371/journal.pone.0206484

50. Vesnina A, Prosekov A, Kozlova O, Atuchin V. Genes and eating preferences, their roles in personalized nutrition. Genes. 2020;11(4):357. https://doi.org/10.3390/genes11040357

51. Chaplygina OS, Prosekov AYu, Vesnina AD. Determining the residual amount of amphenicol antibiotics in milk and dairy products. Food Processing: Techniques and Technology. 2022;52(1):79–88. (In Russ.). https://doi.org/10.21603/2074-9414-2022-1-79-88

52. Thriene K, Michels KB. Human gut microbiota plasticity throughout the life course. International Journal of Environmental Research and Public Health. 2023;20(2):1463. https://doi.org/10.3390/ijerph20021463

53. Rothschild D, Weissbrod O, Barkan E, Kurilshikov A, Korem T, Zeevi D, *et al.* Environment dominates over host genetics in shaping human gut microbiota. Nature. 2018;555:210–215. https://doi.org/10.1038/nature25973

54. Zhang C, Zhang M, Wang S, Han R, Cao Y, Hua W, *et al.* Interactions between gut microbiota, host genetics and diet relevant to development of metabolic syndromes in mice. The ISME Journal. 2010;4(2):232–241. https://doi.org/10.1038/ismej.2009.112

55. He W, Bertram HC. NMR-based metabolomics to decipher the molecular mechanisms in the action of gut-modulating foods. Foods. 2022;11(17):2707. https://doi.org/10.3390/foods11172707

56. Lanng SK, Zhang Y, Christensen KR, Hansen AK, Nielsen DS, Kot W, *et al.* Partial substitution of meat with insect (*Alphitobius diaperinus*) in a carnivore diet changes the gut microbiome and metabolome of healthy rats. Foods. 2021;10(8):1814. https://doi.org/10.3390/foods10081814

57. Thøgersen R, Castro-Mejía JL, Sundekilde UK, Hansen LH, Gray N, Kuhnle G, *et al.* Inulin and milk mineral fortification of a pork sausage exhibits distinct effects on the microbiome and biochemical activity in the gut of healthy rats. Food Chemistry. 2020;331:127291. https://doi.org/10.1016/j.foodchem.2020.127291

58. Emwas A-H, Roy R, McKay RT, Tenori L, Saccenti E, Nagana Gowda GA, *et al.* NMR spectroscopy for metabolomics research. Metabolites. 2019;9(7):123. https://doi.org/10.3390/metabo9070123

59. Cameron SJS, Takáts Z. Mass spectrometry approaches to metabolic profiling of microbial communities within the human gastrointestinal tract. Methods. 2018;149:13–24. https://doi.org/10.1016/j.ymeth.2018.04.027

60. Chen MX, Wang S-Y, Kuo C-H, Tsai I-L. Metabolome analysis for investigating host-gut microbiota interactions. Journal of the Formosan Medical Association. 2019;118:S10–S22. https://doi.org/10.1016/j.jfma.2018.09.007

61. Cai J, Zhang L, Jones RA, Correll JB, Hatzakis E, Smith PB, *et al.* Antioxidant drug tempol promotes functional metabolic changes in the gut microbiota. Journal of Proteome Research. 2016;15(2):563–571. https://doi.org/10.1021/acs.jproteome.5b00957

62. Bervoets L, Ippel JH, Smolinska A, van Best N, Savelkoul PHM, Mommers MAH, *et al.* Practical and robust NMR-based metabolic phenotyping of gut health in early life. Journal of Proteome Research. 2021;20(11):5079–5087. https://doi.org/10.1021/acs.jproteome.1c00617

63. Cui M, Trimigno A, Aru V, Khakimov B, Engelsen SB. Human faecal ^{1}H NMR metabolomics: evaluation of solvent and sample processing on coverage and reproducibility of signature metabolites. Analytical Chemistry. 2020;92(14):9546–9555. https://doi.org/10.1021/acs.analchem.0c00606

64. Zhu Y, Deng P, Zhong D. Derivatization methods for LC-MS analysis of endogenous compounds. Bioanalysis. 2015;7(19):2557–2581. https://doi.org/10.4155/bio.15.183

65. Lkhagva A, Shen C-C, Leung Y-S, Tai H-C. Comparative study of five different amine-derivatization methods for metabolite analyses by liquid chromatography-tandem mass spectrometry. Journal of Chromatography A. 2020;1610:460536. https://doi.org/10.1016/j.chroma.2019.460536

66. Rowland I, Gibson G, Heinken A, Scott K, Swann J, Thiele I, *et al.* Gut microbiota functions: metabolism of nutrients and other food components. European Journal of Nutrition. 2018;57:1–24. https://doi.org/10.1007/s00394-017-1445-8

67. Macia L, Tan J, Vieira AT, Leach K, Stanley D, Luong S, *et al.* Metabolite-sensing receptors GPR43 and GPR109A facilitate dietary fibre-induced gut homeostasis through regulation of the inflammasome. Nature Communications. 2015;6:6734. https://doi.org/10.1038/ncomms7734

68. Reichardt N, Duncan SH, Young P, Belenguer A, McWilliam Leitch C, Scott KP, *et al.* Phylogenetic distribution of three pathways for propionate production within the human gut microbiota. The ISME Journal. 2014;8(6):1323–1335. https://doi.org/10.1038/ismej.2014.14

69. Schroeder BO, Birchenough GMH, Ståhlman M, Arike L, Johansson MEV, Hansson GC, *et al.* Bifidobacteria or fiber protects against diet-induced microbiota-mediated colonic mucus deterioration. Cell Host and Microbe. 2018;23(1):27–40.e7. https://doi.org/10.1016/j.chom.2017.11.004

70. Maslowski KM, Vieira AT, Ng A, Kranich J, Sierro F, Yu D, *et al.* Regulation of inflammatory responses by gut microbiota and chemoattractant receptor GPR43. Nature. 2009;461:1282–1286. https://doi.org/10.1038/nature08530

71. Olas B. Probiotics, prebiotics and synbiotics – A promising strategy in prevention and treatment of cardiovascular diseases? International Journal of Molecular Sciences. 2020;21(24):9737. https://doi.org/10.3390/ijms21249737

72. Torres N, Guevara-Cruz M, Velázquez-Villegas LA, Tovar AR. Nutrition and atherosclerosis. Archives of Medical Research. 2015;46(5):408–426. https://doi.org/10.1016/j.arcmed.2015.05.010

73. Barrington WT, Lusis AJ. Association between the gut microbiome and atherosclerosis. Nature Reviews Cardiology. 2017;14:699–700. https://doi.org/10.1038/nrcardio.2017.169

74. Kazemian N, Mahmoudi M, Halperin F, Wu JC, Pakpour S. Gut microbiota and cardiovascular disease: opportunities and challenges. Microbiome. 2020;8:36. https://doi.org/10.1186/s40168-020-00821-0

75. Nicolas GR, Chang PV. Deciphering the chemical lexicon of host-gut microbiota interactions. Trends in Pharmacological Sciences. 2019;40(6):430–445. https://doi.org/10.1016/j.tips.2019.04.006

76. Louis P, Flint HJ. Formation of propionate and butyrate by the human colonic microbiota. Environmental Microbiology. 2017;19(1):29–41. https://doi.org/10.1111/1462-2920.13589

77. Khan MT, Duncan SH, Stams AJM, van Dijl JM, Flint HJ, Harmsen HJM. The gut anaerobe *Faecalibacterium prausnitzii* uses an extracellular electron shuttle to grow at oxic-anoxic interphases. The ISME Journal. 2012;6(8):1578–1585. https://doi.org/10.1038/ismej.2012.5

78. Louis P, Flint HJ. Diversity, metabolism and microbial ecology of butyrate-producing bacteria from the human large intestine. FEMS Microbiology Letters. 2009;294(1):1–8. https://doi.org/10.1111/j.1574-6968.2009.01514.x

79. Vacca M, Celano G, Calabrese FM, Portincasa P, Gobbetti M, de Angelis M. The controversial role of human gut Lachnospiraceae. Microorganisms. 2020;8(4):573. https://doi.org/10.3390/microorganisms8040573

80. Engels C, Ruscheweyh H-J, Beerenwinkel N, Lacroix C, Schwab C. The common gut microbe *Eubacterium hallii* also contributes to intestinal propionate formation. Frontiers in Microbiology. 2016;7:713. https://doi.org/10.3389/fmicb.2016.00713

81. Jose PA, Raj D. Gut microbiota in hypertension. Current Opinion in Nephrology and Hypertension. 2015;24(5):403–409. https://doi.org/10.1097/MNH.0000000000000149

82. Morita N, Umemoto E, Fujita S, Hayashi A, Kikuta J, Kimura I, *et al.* GPR31-dependent dendrite protrusion of intestinal CX3CR1^{+}cells by bacterial metabolites. Nature. 2019;566:110–114. https://doi.org/10.1038/s41586-019-0884-1

83. Bellono NW, Bayrer JR, Leitch DB, Castro J, Zhang C, O'Donnell TA, *et al.* Enterochromaffin cells are gut chemosensors that couple to sensory neural pathways. Cell. 2017;170(1):185–198.e16. https://doi.org/10.1016/j.cell.2017.05.034

84. van Treuren W, Dodd D. Microbial contribution to the human metabolome: implications for health and disease. Annual Review of Pathology: Mechanisms of Disease. 2020;15:345–369. https://doi.org/10.1146/annurev-pathol-020117-043559

85. Zhu Y, Li Q, Jiang H. Gut microbiota in atherosclerosis: focus on trimethylamine N-oxide. APMIS. 2020;128(5):353–366. https://doi.org/10.1111/apm.13038

86. Tang WHW, Wang Z, Kennedy DJ, Wu Y, Buffa JA, Agatisa-Boyle B, *et al.* Gut microbiota-dependent trimethylamine *N*-oxide (TMAO) pathway contributes to both development of renal insufficiency and mortality risk in chronic kidney disease. Circulation Research. 2015;116(3):448–455. https://doi.org/10.1161/CIRCRESAHA.116.305360

87. Yano JM, Yu K, Donaldson GP, Shastri GG, Ann P, Ma L, *et al.* Indigenous bacteria from the gut microbiota regulate host serotonin biosynthesis. Cell. 2015;161(2):264–276. https://doi.org/10.1016/j.cell.2015.02.047

88. Kodentsova VM, Risnik DV. Micronutrients and the gut microbiome: A bidirectional interaction. Medical Alphabet. 2024;(16):40–46. (In Russ.). https://doi.org/10.33667/2078-5631-2024-16-40-46

89. Blagonravova AS, Zhilyaeva TV, Kvashnina DV. Dysbiosis of intestinal microbiota in autism spectrum disorders: New horizons in search for pathogenetic approaches to therapy. Part 2. Gut-brain axis in pathogenesis of autism spectrum disorders. Journal of Microbiology, Epidemiology and Immunobiology. 2021;98(2):221–230. (In Russ.). https://doi.org/10.36233/0372-9311-83

90. Gurevich KG, Nikityuk DB, Nikonov EL, Zaborova VA, Veselova LV, Zolnikova OYu. The role of probiotics and microbiota in digestion, nutrient and hormone metabolism, and hormonal background maintenance. Russian Journal of Preventive Medicine and Public Health. 2018;21(3):45–50. (In Russ.). https://doi.org/10.17116/profmed201821345

91. Dmitrieva A, Kozlova O, Atuchin V, Milentieva I, Vesnina A, Ivanova S, *et al.* Study of the effect of baicalin from *Scutellaria baicalensis* on the gastrointestinal tract normoflora and *Helicobacter pylori*. International Journal of Molecular Sciences. 2023;24(15):11906. https://doi.org/10.3390/ijms241511906

92. Piccioni A, Covino M, Candelli M, Ojetti V, Capacci A, Gasbarrini A, *et al.* How do diet patterns, single foods, prebiotics and probiotics impact gut microbiota? Microbiology Research. 2023;14(1):390–408. https://doi.org/10.3390/microbiolres14010030

93. Mahasneh SA, Mahasneh AM. Probiotics: A promising role in dental health. Dentistry Journal. 2017;5(4):26. https://doi.org/10.3390/dj5040026

94. Vinelli V, Biscotti P, Martini D, Del Bo' C, Marino M, Meroño T, *et al.* Effects of dietary fibers on short-chain fatty acids and gut microbiota composition in healthy adults: A systematic review. Nutrients. 2022;14(13):2559. https://doi.org/10.3390/nu14132559

95. Chen O, Sudakaran S, Blonquist T, Mah E, Durkee S, Bellamine A. Effect of arabinogalactan on the gut microbiome: A randomized, double-blind, placebo-controlled, crossover trial in healthy adults. Nutrition. 2021;90:111273. https://doi.org/10.1016/j.nut.2021.111273

96. Reimer RA, Soto-Vaca A, Nicolucci AC, Mayengbam S, Park H, Madsen KL, *et al.* Effect of chicory inulin-type fructan-containing snack bars on the human gut microbiota in low dietary fiber consumers in a randomized crossover trial. The American Journal of Clinical Nutrition. 2020;111(6):1286–1296. https://doi.org/10.1093/ajcn/nqaa074

97. Holscher HD, Bauer LL, Gourineni V, Pelkman CL, Fahey GC, Swanson KS. Agave inulin supplementation affects the fecal microbiota of healthy adults participating in a randomized, double-blind, placebo-controlled, crossover trial. The Journal of Nutrition. 2015;145(9):2025–2032. https://doi.org/10.3945/jn.115.217331

98. Sloan TJ, Jalanka J, Major GAD, Krishnasamy S, Pritchard S, Abdelrazig S, *et al.* A low FODMAP diet is associated with changes in the microbiota and reduction in breath hydrogen but not colonic volume in healthy subjects. PLoS ONE. 2018;13(7):e0201410. https://doi.org/10.1371/journal.pone.0201410

99. Lecerf J-M, Dépeint F, Clerc E, Dugenet Y, Niamba CN, Rhazi L, *et al.* Xylo-oligosaccharide (XOS) in combination with inulin modulates both the intestinal environment and immune status in healthy subjects, while XOS alone only shows prebiotic properties. British Journal of Nutrition. 2012;108(10):1847–1858. https://doi.org/10.1017/S0007114511007252

100. Sohail MU, Shabbir MZ, Steiner JM, Ahmad S, Kamran Z, Anwa H, *et al.* Molecular analysis of the gut microbiome of diabetic rats supplemented with prebiotic, probiotic, and synbiotic foods. International Journal of Diabetes in Developing Countries. 2017;37:419–425. https://doi.org/10.1007/s13410-016-0502-9

101. Arboleya S, Watkins C, Stanton C, Ross RP. Gut bifidobacteria populations in human health and aging. Frontiers in Microbiology. 2016;7:1204. https://doi.org/10.3389/fmicb.2016.01204

102. Wong CB, Odamaki T, Xiao J. Insights into the reason of Human-Residential Bifidobacteria (HRB) being the natural inhabitants of the human gut and their potential health-promoting benefits. FEMS Microbiology Reviews. 2020;44(3):369–385. https://doi.org/10.1093/femsre/fuaa010

103. Rivière A, Selak M, Lantin D, Leroy F, de Vuyst L. Bifidobacteria and butyrate-producing colon bacteria: importance and strategies for their stimulation in the human gut. Frontiers in Microbiology. 2016;7:979. https://doi.org/10.3389/fmicb.2016.00979

104. Kawasaki S, Watanabe M, Fukiya S, Yokota A. Stress responses of bifidobacteria: oxygen and bile acid as the stressors. In: Mattarelli P, Biavati B, Holzapfel WH, Wood BJB, editors. The bifidobacteria and related organisms. Biology, taxonomy, applications. Academic Press; 2018. pp. 131–143. https://doi.org/10.1016/B978-0-12-805060-6.00007-7

105. Dahiya D, Nigam PS. The gut microbiota influenced by the intake of probiotics and functional foods with prebiotics can sustain wellness and alleviate certain ailments like gut-inflammation and colon-cancer. Microorganisms. 2022;10(3):665. https://doi.org/10.3390/microorganisms10030665

106. Wilson B, Eyice Ö, Koumoutsos I, Lomer MC, Irving PM, Lindsay JO, *et al.* Prebiotic galactooligosaccharide supplementation in adults with ulcerative colitis: exploring the impact on peripheral blood gene expression, gut microbiota, and clinical symptoms. Nutrients. 2021;13(10):3598. https://doi.org/10.3390/nu13103598

107. Du Z, Li J, Li W, Fu H, Ding J, Ren G, *et al.* Effects of prebiotics on the gut microbiota *in vitro* associated with functional diarrhea in children. Frontiers in Microbiology. 2023;14:1233840. https://doi.org/10.3389/fmicb.2023.1233840

108. Zou L, Yang Y, Zhan J, Cheng J, Fu Y, Cao Y, *et al.* Gut microbiota-based discovery of *Houttuyniae Herba* as a novel prebiotic of *Bacteroides thetaiotaomicron* with anti-colitis activity. Biomedicine and Pharmacotherapy. 2024;172:116302. https://doi.org/10.1016/j.biopha.2024.116302

109. Wang H, Li H, Li Z, Feng L, Peng L. Evaluation of prebiotic activity of Stellariae Radix polysaccharides and its effects on gut microbiota. Nutrients. 2023;15(22):4843. https://doi.org/10.3390/nu15224843

110. Cardoso BB, Amorim C, Franco-Duarte R, Alves JI, Barbosa SG, Silvério SC, *et al.* Epilactose as a promising butyrate-promoter prebiotic via microbiota modulation. Life. 2024;14(5):643. https://doi.org/10.3390/life14050643

111. Milentyeva IS, Le VM, Kozlova OV, Velichkovich NS, Fedorova AM, Loseva AI, *et al.* Secondary metabolites in *in vitro* cultures of Siberian medicinal plants: Content, antioxidant properties, and antimicrobial characteristics. Foods and Raw Materials. 2021;9(1):153–163. https://doi.org/10.21603/2308-4057-2021-1-153-163

112. Zorraquín I, Sánchez-Hernández E, Ayuda-Durán B, Silva M, González-Paramás AM, Santos-Buelga C, *et al.* Current and future experimental approaches in the study of grape and wine polyphenols interacting gut microbiota. Journal of the Science of Food and Agriculture. 2020;100(10):3789–3802. https://doi.org/10.1002/jsfa.10378

113. Zheng S, Huang K, Zhao C, Xu W, Sheng Y, Luo Y, *et al.* Procyanidin attenuates weight gain and modifies the gut microbiota in high fat diet induced obese mice. Journal of Functional Foods. 2018;49:362–368. https://doi.org/10.1016/j.jff.2018.09.007

114. Kemperman RA, Gross G, Mondot S, Possemiers S, Marzorati M, van de Wiele T, *et al.* Impact of polyphenols from black tea and red wine/grape juice on a gut model microbiome. Food Research International. 2013;53(2):659–669. https://doi.org/10.1016/j.foodres.2013.01.034

115. Chen T, Liu AB, Sun S, Ajami NJ, Ross MC, Wang H, *et al.* Green tea polyphenols modify the gut microbiome in *db/db* mice as co-abundance groups correlating with the blood glucose lowering effect. Molecular Nutrition and Food Research. 2019;63(8):1801064. https://doi.org/10.1002/mnfr.201801064

116. Zhou J, Tang L, Shen C-L, Wang J-S. Green tea polyphenols boost gut-microbiota-dependent mitochondrial TCA and urea cycles in Sprague-Dawley rats. The Journal of Nutritional Biochemistry. 2020;81:108395. https://doi.org/10.1016/j.jnutbio.2020.108395

117. Anhê FF, Roy D, Pilon G, Dudonné S, Matamoros S, Varin TV, *et al.* A polyphenol-rich cranberry extract protects from diet-induced obesity, insulin resistance and intestinal inflammation in association with increased *Akkermansia* spp. population in the gut microbiota of mice. Gut. 2015;64(6):872–883. https://doi.org/10.1136/gutjnl-2014-307142

118. Anhê FF, Nachbar RT, Varin TV, Vilela V, Dudonné S, Pilon G, *et al.* A polyphenol-rich cranberry extract reverses insulin resistance and hepatic steatosis independently of body weight loss. Molecular Metabolism. 2017;6(12): 1563–1573. https://doi.org/10.1016/j.molmet.2017.10.003

119. Li H, Christman LM, Li R, Gu L. Synergic interactions between polyphenols and gut microbiota in mitigating inflammatory bowel diseases. Food and Function. 2020;11(6):4878–4891. https://doi.org/10.1039/d0fo00713g

120. Choi BS-Y, Varin TV, St-Pierre P, Pilon G, Tremblay A, Marette A. A polyphenol-rich cranberry extract protects against endogenous exposure to persistent organic pollutants during weight loss in mice. Food and Chemical Toxicology. 2020;146:111832. https://doi.org/10.1016/j.fct.2020.111832

121. Jiao X, Wang Y, Lin Y, Lang Y, Li E, Zhang X, *et al.* Blueberry polyphenols extract as a potential prebiotic with anti-obesity effects on C57BL/6 J mice by modulating the gut microbiota. The Journal of Nutritional Biochemistry. 2019;64:88–100. https://doi.org/10.1016/j.jnutbio.2018.07.008

122. Rodríguez-Daza M-C, Roquim M, Dudonné S, Pilon G, Levy E, Marette A, *et al.* Berry polyphenols and fibers modulate distinct microbial metabolic functions and gut microbiota enterotype-like clustering in obese mice. Frontiers in Microbiology. 2020;11:2032. https://doi.org/10.3389/fmicb.2020.02032

123. Lee S, Keirsey KI, Kirkland R, Grunewald ZI, Fischer JG, de La Serre CB. Blueberry supplementation influences the gut microbiota, inflammation, and insulin resistance in high-fat-diet-fed rats. The Journal of Nutrition. 2018;148(2):209–219. https://doi.org/10.1093/jn/nxx027

124. Lima ACD, Cecatti C, Fidélix MP, Adorno MAT, Sakamoto IK, Cesar TB, *et al.* Effect of daily consumption of orange juice on the levels of blood glucose, lipids, and gut microbiota metabolites: controlled clinical trials. Journal of Medicinal Food. 2019;22(2):202–210. https://doi.org/10.1089/jmf.2018.0080

125. Brasili E, Hassimotto NMA, del Chierico F, Marini F, Quagliariello A, Sciubba F, *et al.* Daily consumption of orange juice from *Citrus sinensis* L. Osbeck cv. Cara Cara and cv. Bahia differently affects gut microbiota profiling as unveiled by an integrated Meta-Omics approach. Journal of Agricultural and Food Chemistry. 2019;67(5):1381–1391. https://doi.org/10.1021/acs.jafc.8b05408

126. Fidélix M, Milenkovic D, Sivieri K, Cesar T. Microbiota modulation and effects on metabolic biomarkers by orange juice: A controlled clinical trial. Food and Function. 2020;11(2):1599–1610. https://doi.org/10.1039/c9fo02623a

127. Wang P, Gao J, Ke W, Wang J, Li D, Liu R, *et al.* Resveratrol reduces obesity in high-fat diet-fed mice via modulating the composition and metabolic function of the gut microbiota. Free Radical Biology and Medicine. 2020;156:83–98. https://doi.org/10.1016/j.freeradbiomed.2020.04.013

128. Guo C, Han L, Li M, Yu L. Seabuckthorn (*Hippophaë rhamnoides*) freeze-dried powder protects against high-fat diet-induced obesity, lipid metabolism disorders by modulating the gut microbiota of mice. Nutrients. 2020;12(1):265. https://doi.org/10.3390/nu12010265

129. Shi X, Zhou X, Chu X, Wang J, Xie B, Ge J, *et al.* Allicin improves metabolism in high-fat diet-induced obese mice by modulating the gut microbiota. Nutrients. 2019;11(12):2909. https://doi.org/10.3390/nu11122909

130. Tamura M, Hoshi C, Kobori M, Takahashi S, Tomita J, Nishimura M, *et al.* Quercetin metabolism by fecal microbiota from healthy elderly human subjects. PLoS ONE. 2017;12(11):e0188271. https://doi.org/10.1371/journal.pone.0188271

131. Zhang Z, Chen Y, Xiang L, Wang Z, Xiao GG, Hu J. Effect of curcumin on the diversity of gut microbiota in ovariectomized rats. Nutrients. 2017;9(10):1146. https://doi.org/10.3390/nu9101146

132. Al-Saud NBS. Impact of curcumin treatment on diabetic albino rats. Saudi Journal of Biological Sciences. 2020;27(2):689–694. https://doi.org/10.1016/j.sjbs.2019.11.037

133. Truzzi F, Tibaldi C, Zhang Y, Dinelli G, D'Amen E. An overview on dietary polyphenols and their biopharmaceutical classification system (BCS). International Journal of Molecular Sciences. 2021;22(11):5514. https://doi.org/10.3390/ijms22115514

134. Fong SYK, Liu M, Wei H, Löbenberg R, Kanfer I, Lee VHL, *et al.* Establishing the pharmaceutical quality of Chinese herbal medicine: A provisional BCS classification. Molecular Pharmaceutics. 2013;10(5):1623–1643. https://doi.org/10.1021/mp300502m

135. Madaan K, Lather V, Pandita D. Evaluation of polyamidoamine dendrimers as potential carriers for quercetin, a versatile flavonoid. Drug Delivery. 2016;23(1):254–262. https://doi.org/10.3109/10717544.2014.910564

136. Waldmann S, Almukainzi M, Bou-Chacra NA, Amidon GL, Lee B-J, Feng J, *et al.* Provisional biopharmaceutical classification of some common herbs used in Western medicine. Molecular Pharmaceutics. 2012;9(4):815–822. https://doi.org/10.1021/mp200162b

137. Zhang J, Liu D, Huang Y, Gao Y, Qian S. Biopharmaceutics classification and intestinal absorption study of apigenin. International Journal of Pharmaceutics. 2012;436(1–2):311–317. https://doi.org/10.1016/j.ijpharm.2012.07.002

138. Zhou Z, Li W, Sun W-J, Lu T, Tong HHY, Sun CC, *et al.* Resveratrol cocrystals with enhanced solubility and tabletability. International Journal of Pharmaceutics. 2016;509(1–2):391–399. https://doi.org/10.1016/j.ijpharm.2016.06.006

139. John MK, Xie H, Bell EC, Liang D. Development and pharmacokinetic evaluation of a curcumin co-solvent formulation. Anticancer Research. 2013;33(10):4285–4291.

140. Francioso A, Mastromarino P, Masci A, d'Erme M, Mosca L. Chemistry, stability and bioavailability of resveratrol. Medicinal Chemistry. 2014;10(3):237–245. https://doi.org/10.2174/1573406411309660053

141. Manach C, Williamson G, Morand C, Scalbert A, Rémésy C. Bioavailability and bioefficacy of polyphenols in humans. I. Review of 97 bioavailability studies. The American Journal of Clinical Nutrition. 2005;81(1):230S–242S. https://doi.org/10.1093/ajcn/81.1.230S

142. di Lorenzo C, Colombo F, Biella S, Stockley C, Restani P. Polyphenols and human health: The role of bioavailability. Nutrients. 2021;13(1):273. https://doi.org/10.3390/nu13010273

143. Annunziata G, Jiménez-García M, Capó X, Moranta D, Arnone A, Tenore GC, *et al.* Microencapsulation as a tool to counteract the typical low bioavailability of polyphenols in the management of diabetes. Food and Chemical Toxicology. 2020;139:111248. https://doi.org/10.1016/j.fct.2020.111248

144. Hu B, Liu X, Zhang C, Zeng X. Food macromolecule based nanodelivery systems for enhancing the bioavailability of polyphenols. Journal of Food and Drug Analysis. 2017;25(1):3–15. https://doi.org/10.1016/j.jfda.2016.11.004

145. Ozkan G, Franco P, de Marco I, Xiao J, Capanoglu E. A review of microencapsulation methods for food antioxidants: Principles, advantages, drawbacks and applications. Food Chemistry. 2019;272:494–506. https://doi.org/10.1016/j.foodchem.2018.07.205

146. Zhang Z, Miao W, Ji H, Lin Q, Li X, Sang S, *et al.* Interaction of zein/HP-β-CD nanoparticles with digestive enzymes: Enhancing curcumin bioavailability. Food Chemistry. 2024;460:140792. https://doi.org/10.1016/j.foodchem.2024.140792

147. Rashidinejad A, Boostani S, Babazadeh A, Rehman A, Rezaei A, Akbari-Alavijeh S, *et al.* Opportunities and challenges for the nanodelivery of green tea catechins in functional foods. Food Research International. 2021;142:110186. https://doi.org/10.1016/j.foodres.2021.110186

148. Florowska A, Krygier K, Florowski T, Dłużewska E. Prebiotics as functional food ingredients preventing diet-related diseases. Food and Function. 2016;7(5):2147–2155. https://doi.org/10.1039/c5fo01459j

149. Irwin SV, Fisher P, Graham E, Malek A, Robidoux A. Sulfites inhibit the growth of four species of beneficial gut bacteria at concentrations regarded as safe for food. PLoS ONE. 2017;12(10):e0186629. https://doi.org/10.1371/journal.pone.0186629

150. Zahran SA, Ali-Tammam M, Hashem AM, Aziz RK, Ali AE. Azoreductase activity of dye-decolorizing bacteria isolated from the human gut microbiota. Scientific Reports. 2019;9:5508. https://doi.org/10.1038/s41598-019-41894-8

151. Zhou X, Qiao K, Wu H, Zhang Y. The impact of food additives on the abundance and composition of gut microbiota. Molecules. 2023;28(2):631. https://doi.org/10.3390/molecules28020631

152. Gerasimidis K, Bryden K, Chen X, Papachristou E, Verney A, Roig M, *et al.* The impact of food additives, artificial sweeteners and domestic hygiene products on the human gut microbiome and its fibre fermentation capacity. European Journal of Nutrition. 2020;59:3213–3230. https://doi.org/10.1007/s00394-019-02161-8

153. Newman JC, Verdin E. Ketone bodies as signaling metabolites. Trends in Endocrinology and Metabolism. 2014;25(1):42–52. https://doi.org/10.1016/j.tem.2013.09.002

154. Piper MDW, Bartke A. Diet and aging. Cell Metabolism. 2008;8(2):99–104. https://doi.org/10.1016/j.cmet.2008.06.012

155. Newman JC, Covarrubias AJ, Zhao M, Yu X, Gut P, Ng C-P, *et al.* Ketogenic diet reduces midlife mortality and improves memory in aging mice. Cell Metabolism. 2017;26(3):547–557.e8. https://doi.org/10.1016/j.cmet.2017.08.004

156. Roberts MN, Wallace MA, Tomilov AA, Zhou Z, Marcotte GR, Tran D, *et al.* A ketogenic diet extends longevity and healthspan in adult mice. Cell Metabolism. 2017;26(3):539–546.e5. https://doi.org/10.1016/j.cmet.2017.08.005

157. Lee MB, Hill CM, Bitto A, Kaeberlein M. Antiaging diets: Separating fact from fiction. Science. 2021;374(6570):eabe7365. https://doi.org/10.1126/science.abe7365

158. Longo VD, di Tano M, Mattson MP, Guidi N. Intermittent and periodic fasting, longevity and disease. Nature Aging. 2021;1:47–59. https://doi.org/10.1038/s43587-020-00013-3

159. Brandhorst S, Choi IY, Wei M, Cheng CW, Sedrakyan S, Navarrete G, *et al.* A periodic diet that mimics fasting promotes multi-system regeneration, enhanced cognitive performance, and healthspan. Cell Metabolism. 2015;22(1):86–99. https://doi.org/10.1016/j.cmet.2015.05.012

160. Zhang D, Li H, Li Y, Qu L. Gut rest strategy and trophic feeding in the acute phase of critical illness with acute gastrointestinal injury. Nutrition Research Reviews. 2019;32(2):176–182. https://doi.org/10.1017/S0954422419000027

161. Mohr AE, Gumpricht E, Sears DD, Sweazea KL. Recent advances and health implications of dietary fasting regimens on the gut microbiome. American Journal of Physiology – Gastrointestinal and Liver Physiology. 2021;320(5):G847–G863. https://doi.org/10.1152/ajpgi.00475.2020

162. Beli E, Yan Y, Moldovan L, Vieira CP, Gao R, Duan Y, *et al.* Restructuring of the gut microbiome by intermittent fasting prevents retinopathy and prolongs survival in *db/db* mice. Diabetes. 2018;67(9):1867–1879. https://doi.org/10.2337/db18-0158

163. Cignarella F, Cantoni C, Ghezzi L, Salter A, Dorsett Y, Chen L, *et al.* Intermittent fasting confers protection in CNS autoimmunity by altering the gut microbiota. Cell Metabolism. 2018;27(6):1222–1235.e6. https://doi.org/10.1016/j.cmet.2018.05.006

164. Zheng X, Zhou K, Zhang Y, Han X, Zhao A, Liu J, *et al.* Food withdrawal alters the gut microbiota and metabolome in mice. The FASEB Journal. 2018;32(9):4878–4888. https://doi.org/10.1096/fj.201700614R

165. Li L, Su Y, Li F, Wang Y, Ma Z, Li Z, *et al.* The effects of daily fasting hours on shaping gut microbiota in mice. BMC Microbiology. 2020;20:65. https://doi.org/10.1186/s12866-020-01754-2

166. Liu Z, Dai X, Zhang H, Shi R, Hui Y, Jin X, *et al.* Gut microbiota mediates intermittent-fasting alleviation of diabetes-induced cognitive impairment. Nature Communications. 2020;11:855. https://doi.org/10.1038/s41467-020-14676-4

167. Özkul C, Yalınay M, Karakan T. Islamic fasting leads to an increased abundance of *Akkermansia muciniphila* and *Bacteroides fragilis* group: A preliminary study on intermittent fasting. Turkish Journal of Gastroenterology. 2019;30(12):1030–1035. https://doi.org/10.5152/tjg.2019.19185

168. Ozkul C, Yalinay M, Karakan T. Structural changes in gut microbiome after Ramadan fasting: A pilot study. Beneficial Microbes. 2020;11(3):227–233. https://doi.org/10.3920/BM2019.0039

169. Zeb F, Wu X, Chen L, Fatima S, Haq I, Chen A, *et al.* Effect of time-restricted feeding on metabolic risk and circadian rhythm associated with gut microbiome in healthy males. British Journal of Nutrition. 2020;123(11):1216–1226. https://doi.org/10.1017/S0007114519003428

170. Smith P, Willemsen D, Popkes M, Metge F, Gandiwa E, Reichard M, *et al.* Regulation of life span by the gut microbiota in the short-lived African turquoise killifish. eLife. 2017;6:e27014. https://doi.org/10.7554/eLife.27014

171. Han B, Sivaramakrishnan P, Lin C-CJ, Neve IAA, He J, Tay LWR, *et al.* Microbial genetic composition tunes host longevity. Cell. 2017;169(7):1249–1262.e13. https://doi.org/10.1016/j.cell.2017.05.036

172. Fontana L, Partridge L. Promoting health and longevity through diet: from model organisms to humans. Cell. 2015;161(1):106–118. https://doi.org/10.1016/j.cell.2015.02.020

173. Debebe T, Biagi E, Soverini M, Holtze S, Hildebrandt TB, Birkemeyer C, *et al.* Unraveling the gut microbiome of the long-lived naked mole-rat. Scientific Reports. 2017;7:9590. https://doi.org/10.1038/s41598-017-10287-0

174. Minekus M, Marteau P, Havenaar R, Huis in't Veld JHJ. A multicompartmental dynamic computer-controlled model simulating the stomach and small intestine. Alternatives to Laboratory Animals. 1995;23(2):197–209. https://doi.org/10.1177/026119299502300205

175. Babich O, Larina V, Krol O, Ulrikh E, Sukhikh S, Gureev MA, *et al.* In vitro study of biological activity of *Tanacetum vulgare* extracts. Pharmaceutics. 2023;15(2):616. https://doi.org/10.3390/pharmaceutics15020616

176. Chikindas ML, Mazanko MS, Lukyanov AD, Prazdnova EV, Chistyakov VA. Method for modeling chicken microbiota in an artificial caecum. Patent RU 2773094C1. 2022.

177. Donskoy DYu, Lukyanov AD, Filipović V, Asten TB. Mathematical model of the pH control system in an in vitro model of the gastrointestinal tract of poultry. Advanced Engineering Research (Rostov-on-Don). 2023;23(1):95–106. https://doi.org/10.23947/2687-1653-2023-23-1-95-106

178. Savoie L. Digestion and absorption of food: usefulness and limitations of in vitro models. Canadian Journal of Physiology and Pharmacology. 1994;72(4):407–414. https://doi.org/10.1139/y94-060

179. Langland AC. Digestive enzyme activities in pigs and poultry. In: Fuller MF, editor. In vitro digestion for pigs and poultry. Wallingford: CAB International; 1991. pp. 3–18.

180. Minekus M, Smeets-Peeters M, Bernalier A, Marol-Bonnin S, Havenaar R, Marteau P, *et al.* A computer-controlled system to simulate conditions of the large intestine with peristaltic mixing, water absorption and absorption of fermentation products. Applied Microbiology and Biotechnology. 1999;53:108–114. https://doi.org/10.1007/s002530051622

181. Verhoeckx K, Cotter P, López-Expósito I, Kleiveland C, Lea T, Mackie A, *et al.* The impact of food bioactives on health. In vitro and ex vivo models. Cham: Springer; 2015. 338 p. https://doi.org/10.1007/978-3-319-16104-4

182. Minekus M. The TNO Gastro-Intestinal Model (TIM). In: Verhoeckx K, Cotter P, López-Expósito I, Kleiveland C, Lea T, Mackie A, *et al.*, editors. The impact of food bioactives on health. In vitro and ex vivo models. Cham: Springer; 2015. pp. 37–46. https://doi.org/10.1007/978-3-319-16104-4_5

183. Wickham MJS, Faulks RM, Mann J, Mandalari G. The design, operation, and application of a dynamic gastric model. Dissolution Technologies. 2012;19:15–22. https://doi.org/10.14227/DT190312P15

184. Thuenemann EC, Mandalari G, Rich GT, Faulks MR. Dynamic Gastric Model (DGM) In: Verhoeckx K, Cotter P, López-Expósito I, Kleiveland C, Lea T, Mackie A, *et al.*, editors. The impact of food bioactives on health. In vitro and ex vivo models. Cham: Springer; 2015. pp. 47–59. https://doi.org/10.1007/978-3-319-16104-4_6

185. Kong F, Singh RP. A human gastric simulator (HGS) to study food digestion in human stomach. Journal of Food Science. 2010;75(9):E627–E635. https://doi.org/10.1111/j.1750-3841.2010.01856.x

186. Ferrua MJ, Singh RP. Human Gastric Simulator (riddet model). In: Verhoeckx K, Cotter P, López-Expósito I, Kleiveland C, Lea T, Mackie A, *et al.*, editors. The impact of food bioactives on health. In vitro and ex vivo models. Cham: Springer; 2015. pp. 61–71. https://doi.org/10.1007/978-3-319-16104-4_7

187. Ménard O, Cattenoz T, Guillemin H, Souchon I, Deglaire A, Dupont D, *et al.* Validation of a new *in vitro* dynamic system to simulate infant digestion. Food Chemistry. 2014;145:1039–1045. https://doi.org/10.1016/j.foodchem.2013.09.036

188. Ménard O, Picque D, Dupont D. The DIDGI® system. In: Verhoeckx K, Cotter P, López-Expósito I, Kleiveland C, Lea T, Mackie A, *et al.*, editors. The impact of food bioactives on health. In vitro and ex vivo models. Cham: Springer; 2015. pp. 73–81. https://doi.org/10.1007/978-3-319-16104-4_8

189. Peeters L, Beirnaert C, van der Auwera A, Bijttebier S, de Bruyne T, Laukens K, *et al.* Revelation of the metabolic pathway of hederacoside C using an innovative data analysis strategy for dynamic multiclass biotransformation experiments. Journal of Chromatography A. 2019;1595:240–247. https://doi.org/10.1016/j.chroma.2019.02.055

190. Breynaert A, Bosscher D, Kahnt A, Claeys M, Cos P, Pieters L, *et al.* Development and validation of an *in vitro* experimental gastrointestinal dialysis model with colon phase to study the availability and colonic metabolisation of polyphenolic compounds. Planta Medica. 2015;81(12/13):1075–1083. https://doi.org/10.1055/s-0035-1546154

191. Gumienna M, Lasik M, Czarnecki Z. Bioconversion of grape and chokeberry wine polyphenols during simulated gastrointestinal *in vitro* digestion. International Journal of Food Sciences and Nutrition. 2011;62(3):226–233. https://doi.org/10.3109/09637486.2010.532115

ORCID IDs
Anna D. Vesnina https://orcid.org/0000-0002-4552-7418
Anna S. Frolova https://orcid.org/0000-0003-3988-8521
Darya Yu. Chekushkina https://orcid.org/0009-0002-3826-8048
Irina S. Milentyeva https://orcid.org/0000-0002-3536-562X
Sergey L. Luzyanin https://orcid.org/0000-0001-9293-4377

Foods and Raw Materials. 2026;14(1)

ISSN 2308-4057 (Print)
ISSN 2310-9599 (Online)

Research Article
Open Access

Available online at http://jfrm.ru/en
https://doi.org/10.21603/2308-4057-2026-1-666
https://elibrary.ru/RXPKKQ

Chickpea protein hydrolysates: Production, bioactivity, functional profile, and technological properties

Mahmud Gharaviri[1], Denis I. Aleksanochkin[1], Mahbubeh Ahangaran[1], Ivan A. Fomenko[1,*], Leonid I. Kovalev[2], Marina A. Kovaleva[2], Irina M. Chernukha[1,3], Natalia G. Mashentseva[1]

[1] Russian Biotechnological University (ROSBIOTECH), Moscow, Russia
[2] Bach Institute of Biochemistry, Moscow, Russia
[3] V.M. Gorbatov Federal Research Center for Food Systems of RAS, Moscow, Russia

* e-mail: iv.fomenko@mail.ru

Received 10.01.2025; Revised 04.02.2025; Accepted 04.03.2025; Published online 30.04.2025

Abstract:
Chickpea plant protein hydrolysates are an innovative product on the Russian food market. However, they meet many urgent needs and may solve some fundamental food safety problems. This article describes some effective enzymatic biodegradation methods that yield hydrolysates and biopeptides with advanced functional and technological properties that possess antioxidant and other bioactive potentials.

The study featured Kabuli chickpea (*Cicer arietinum* L.) protein isolate, as well as a number of enzyme preparations of animal, plant, and microbial origin. Hydrolysis was followed by a set of FRAP, DPPH, and ORAC analyses to determine the functional, technological, and antioxidant properties. A combined approach made it possible to reveal the proteomic profile, e.g., a combination of two-dimensional electrophoresis and subsequent mass spectrometry was used to identify peptides. The bioactivity of peptide fragments was predicted *in silico* using bioinformatic databases.

The efficiency of protein destruction depended on the degree of hydrolysis. At 10%, it improved the functional and technological properties. The best results regarding the time and enzyme concentration belonged to Alcalase 2.4 L FG (2%). The enzymes of animal origin, e.g., pepsin at a 10% hydrolysis degree, also improved the functional and technological profile. The samples treated with pepsin and Protoferm FP showed the highest antioxidant activity (FRAP, ORAC), increasing it by more than 200% relative to the initial chickpea isolate. Computer densitometry revealed that the hydrolysates treated with trypsin and papain could destroy more than 55% of the initial protein. Biologically active peptides of the hydrolysates obtained were determined using bioinformatic forecasting.

In this research, chickpea protein hydrolysates provided new technological processing methods for commercial products. They made it possible to obtain biopeptides with antithrombotic, antitumor, antibacterial, antioxidant, and antiamnetic properties, which indicates excellent prospects in the food industry and pharmacy.

Keywords: Peptides, hydrolysate, biological activity, isolate, plant protein, proteomic methods, proteolysis

Please cite this article in press as: Gharaviri M, Aleksanochkin DI, Ahangaran M, Fomenko IA, Kovalev LI, Kovaleva MA, *et al.* Chickpea protein hydrolysates: Production, bioactivity, functional profile, and technological properties. Foods and Raw Materials. 2026;14(1):198–213. https://doi.org/10.21603/2308-4057-2026-1-666

INTRODUCTION

The relationship between nutrition and health is a cluster of highly relevant research topics, as confirmed by regular publications in authoritative scientific journals [1, 2]. In this respect, food proteins and biologically active components are very popular research subjects [3]. Global food security and sustainable development are the most significant challenges in the XXI century. They are triggered by overpopulation, climate change, and depletion of natural resources. These and other environmental issues require innovative approaches to food production and consumption [4, 5].

Advanced food paradigms classify food not only as a source of nutrition but also as a source of beneficial bioactive compounds that improve human health [6]. More and more food scientists consider the production, properties, and efficacy of biologically active ingredients that people may obtain from food products. These ingredients

Copyright © 2025, Gharaviri *et al.* This is an open access article distributed under the terms of the Creative Commons Attribution 4.0 International License (https://creativecommons.org/licenses/by/4.0/), allowing third parties to copy and redistribute the material in any medium or format and to remix, transform, and build upon the material for any purpose, even commercially, provided the original work is properly cited and states its license.

may have lower physiological effect than pharmaceutical therapeutic agents, yet they cause little or no toxic or side effects.

Bioactive peptides are one of such kind of food ingredients [7]. They are small fragments of food proteins that consist of 2–20 amino acid subunits with a molecular weight of ≤ 3 kDa. Bioactive peptides of animal or plant proteins possess numerous beneficial properties and applications [8]. Many of them are multifunctional: they have several mechanisms of action and therefore exercise several physiological activities at once [9]. Plant raw material in general and legumes in particular are by far the most promising source of food protein and biopeptides.

Legumes (*Leguminosae* family) are the second largest family of seed plants that includes about 13 000 species grouped into 600 genera [10]. The most common legumes are common beans (*Phaseolus vulgaris* L.), peas (*Pisum sativum* L.), chickpeas (*Cicer arietinum* L.), lentils (*Lens culinaris* L.), soybeans (*Glycine max* L.), lupines (*Lupinus mutabilis*), mung beans (*Vigna radiata* L.), and peanuts (*Arachis hypogaea* L.) [11, 12]. Legumes occupy 81 million hectares worldwide, with 92 million tons of production capacity. India accounts for almost 25% of the global legume production. China, Myanmar, Canada, Australia, Brazil, Argentina, the United States, and Russia are the largest legume producers [13].

Chickpeas are the most cultivated legume crop number three in the world, with 15 million ha of fields and an annual production volume of 16 million tons [14, 15]. According to the Russian Federal State Statistics Service Rosstat, Russia boasted 492 100 ha of chickpea fields in 2023, which was 34% more than in 2022. Even though this annual legume crop prefers regions with mild climate, it flourishes in arid regions as well because it is highly resistant to hot air if the soil contains enough moisture. Southeast Asia provides about 80% of chickpea production, which makes it the dominant cultivation region. India remains the leader in terms of cultivation volume (11.97 million ha). Geographically, chickpeas come in two types: Kabuli and Desi. The Kabuli type is cultivated in the Mediterranean region, as well as in North and South America. The seeds are large (100–750 mg), round, smooth, and beige, with an energy value of 365 kcal/100 g. The Desi type grows in semi-arid areas; the seeds are small (80–350 mg), angular, rough, and dark, with a thick outer layer and an energy value of 327 kcal/100 g [11, 14, 16, 17].

Chickpeas are rich in carbohydrates (41.1–47.4%) and protein (21.7–23.4%), which makes them a valuable component in different food systems [18]. Chickpea proteins possess an excellent amino acid profile with *in-vitro* digestibility as high as 76%. Chickpea proteins can be classified by solubility, like other plant proteins. They are represented by four fractions: albumins (10–14% total protein content), globulins (55–60%), prolamins (2–3%), and glutelins (18%). Globulins make up the largest fraction, which consists of two main groups, 11S globulins (legumes) and vinicillins (7S vicilin and convicillin, *Cupinaceae* superfamily). The major component of the albumin fraction is 2S albumin. It consists of two subunits of 8–10 and 4–5 kDa, which are linked together by two disulfide bonds. This fraction is rich in cysteine but poor in sulfur amino acids [19–21]. Animal proteins are well studied and popular in the food industry, but their adverse prospects stimulate research into other protein sources, e.g., legumes [22].

As chickpeas are rich in protein, food scientists use them to obtain protein isolates that would enhance the nutritional value of various functional products. Chickpea protein isolate powder typically contains ≥ 90% protein [23]. Alkaline extraction with isoelectric precipitation is the most popular method of protein isolate production in the food industry [24, 25]. Protein isolates are rich in bioactive peptides that are released in the gastrointestinal tract by proteolytic enzymes or during technological processing of high-protein raw materials [26].

Protein hydrolysates are derived from enzymatic or chemical hydrolysis with short-chain peptides and amino acids [27]. Enzymatic hydrolysis is a reliable alternative to the chemical method, which makes it especially important for the food industry. Enzymatic hydrolysis requires milder reaction conditions than the chemical one. In addition, it makes it possible to target specific peptide bond cleavage and minimize the formation of undesirable by-products [28, 29]. As a result, the final protein structure may acquire particular functional properties, e.g., solubility, water-holding, fat-holding, emulsifying, and foaming, but their nutritional value remains the same [30]. Protein hydrolysates are grouped depending on the degree of hydrolysis: partially hydrolyzed (< 10%), intensively hydrolyzed (> 10%), and extensively hydrolyzed (> 20%). At 10%, hydrolysis improves the functional and technological properties of food products that involve hydrolysates [31]. However, the impact depends on the choice of enzyme and substrate.

Protein hydrolysates owe their popularity in the food industry to their functional profile, technological properties, bioactivity, and good digestibility. They give functional products extra nutritional value [32, 33]. Their excellent solubility and bioavailability make them a valuable component in functional drinks [34, 35]. They improve the structure and moisture retention of meat products while increasing their shelf life. Hydrolysates are also part of formulations for modern low-fat and high-protein products [36]. As a result, protein hydrolysates remain a promising research area that renders new innovative foods.

In this research, we used enzyme preparations to modify the physicochemical, functional, and technological properties of Kabuli chickpea (*Cicer arietinum* L.) protein isolates, as well as to identify the bioactive potential of peptides derived from these isolates. The method of enzymatic hydrolysis makes it possible to develop new functional foods with advanced technological and biological properties. In addition, the data obtained may be useful for research and development in the field of food ingredients.

STUDY OBJECTS AND METHODS

The research featured a protein isolate derived from Kabuli chickpeas (*Cicer arietinum* L.) in line with the protocol for obtaining protein isolate from Desi or Kabuli chickpeas (Patent no. 2803851). The experiment also involved enzyme preparations of plant origin – bromelain and papain (Sigma-Aldrich, USA); animal enzyme preparations – pepsin and trypsin (HIMEDIA, India); and microbial enzyme preparations – Protoferm FP (Alfaprom, China) and Alcalase 2.4 L FG (Novozymes, Denmark).

The enzymatic hydrolysis presupposed a ratio of 0.5, 1, 1.5, and 2% enzyme to the substrate amount. The optimal enzyme operating ranges and hydrolysis conditions were based on the manufacturer's recommendations (Table 1).

Degree of hydrolysis. The degree of hydrolysis was the ratio of amino nitrogen to total nitrogen (Kjeldahl method as in State Standard 13496.4-2019). Amino nitrogen was determined by formal titration (Sorensen method as in General Pharmacopoeia Article 1.2.3.0022.15). The volume of NaOH for titration made it possible to calculate the number of free amino groups.

Chickpea proteins underwent a one-dimensional gel electrophoresis in a 12.5% polyacrylamide gel and a vertical electrophoresis chamber (Helicon, USA) followed by staining with Coomassie Blue R-250 (PanReac, Spain).

Functional and technological profile. The functional and technological properties of the chickpea protein hydrolysates were determined at the 10% hydrolysis, followed by centrifugation at 4000 min^{-1} for 15 min. The sediment was dried in a lyophilic dryer (ProfLyo T50.4, Russia).

Solubility. To measure the solubility, we placed 0.4 g of protein powder in a 100-cm^3 conical flask and added 40 cm^3 of distilled water. The contents were then transferred to a shaker and stirred at 180 min^{-1} for 30 min. After centrifuging the resulting suspension at 4000 min^{-1} for 15 min, the centrate went into a 100-cm^3 flask. The sediment was transferred to another 100-cm^3 flask and extracted twice more with water (25 cm^3). The resulting centrate went into the same flask. The final content of dissolved protein in 100 cm^3 was determined using the Lowry method [37].

Water-holding and fat-holding capacity. To prepare protein solutions, we dissolved 1 g of protein in 10 cm^3 of water or sunflower oil. After 1 min of stirring at 1000 min^{-1} and 15 min of centrifugation at 6000 min^{-1}, the supernatant was decanted, and the tubes were put upside down to remove excess water or oil. After 10 min, we weighed the tubes with the sediment to calculate the water-holding and fat-holding capacity, %, as in Eq. (1):

$$\text{Water-holding and fat-holding capacity} = \frac{M_1 - M_0}{M_n} \times 100 \quad (1)$$

where M_1 is the mass of the test tube with the protein preparation, g; M_0 is the mass of the empty test tube, g; M_n is the mass of the test sample, g [38].

Emulsifying capacity and stability. A 7% suspension of protein solution and water was homogenized at 4000 min^{-1} for 1 min. After adding sunflower oil (1:1), we emulsified the suspension at 8000 min^{-1} for 5 min. The resulting emulsion was divided into four centrifuge tubes and centrifuged at 2000 min^{-1} for 5 min. The emulsifying capacity was calculated as in Eq. (2):

$$\text{Emulsifying capacity} = \frac{V_e}{V_0} \times 100 \quad (2)$$

where V_e is the emulsion volume, cm^3; V_0 is the total system volume, cm^3.

To determine the emulsifying stability, we prepared protein solutions as described above. After heating the emulsion at 80°C for 30 min and cooling it with tap water for 15 min, we poured it into centrifuge tubes to be centrifuged at 2000 min^{-1} for 5 min and used Eq. (3) to calculate its stability, %:

$$\text{Emulsifying stability} = \frac{V_e}{V_0} \times 100 \quad (3)$$

where V_e is the emulsion volume, cm^3; V_0 is the total system volume, cm^3 [38].

Critical gelation concentration. This experiment involved a series of three suspensions (10 cm^3) in distilled water with a concentration step of 2, 12, and 20%, which were homogenized by stirring. The test tubes spent 15 min in a thermostat at 75°C. After heating, the test tubes cooled down in a refrigerator at 5°C for 18 h. After that, lead balls (0.53 g each) were placed on top of suspension to remain there at the same temperature for 2 h. The critical gelation concentration at which the gel was not destroyed under the lead ball loading.

Foaming capacity and stability. Homogeneous 3, 5, and 10% suspensions of a protein preparation was prepared in a graduated cylinder and shaken horizontally for 1 min. After verticalizing the cylinder, we measured the height of the foam column above the liquid level and used Eq. (4) to calculate the foaming capacity, %:

$$\text{Foaming capacity} = \frac{H_1}{H_0} \times 100 \quad (4)$$

where H_1 is the height of the foam after shaking, mm; H_0 is the height of the solution, mm.

To determine the foam stability, we followed the same protocol to prepare the protein and left it for 30 min. After that, we measured the height of the remaining foam and calculated its stability, %, as in Eq. (5):

Table 1 Conditions of enzymatic hydrolysis

Enzyme preparation	Bromelain	Papain	Pepsin	Trypsin	Protoferm F	Alcalase 2.4 L FG
Temperature, °C	45	45	37	37	45	45
pH	4.5	6.2	2.6	7.5	3.5	7.0

$$\text{Foaming stability} = \frac{H_2}{H_1} \times 100 \quad (5)$$

where H_1 is the foam height after shaking, mm; H_2 is the foam height after 30 min of rest, mm [39, 40].

Antioxidant activity. The total antioxidant capacity of the hydrolysates was determined by the method of fluorescence recovery after photobleaching (FRAP) in an SF-2000 spectrophotometer (OKB Spektr, Russia). To determine the total antioxidant capacity, we added 1.45 mL of FRAP and 0.05 mL of hydrolysates pre-diluted with distilled water and incubated the reaction mix at 37°C in the dark for 30 min. After that, we measured the optical density at 594 nm. The FRAP values were calculated using a calibration graph.

The DPPH method involved DPPH (2,2-diphenyl-1-picrylhydrazyl) and an SF-2000 spectrophotometer. To measure the DPPH, we added 1.52 mL DPPH and 0.08 mL of each sample into the test tubes. The reaction mix was incubated in the dark at 22°C for 30 min. The optical density was measured at 517 nm.

The oxygen radical absorbance capacity (ORAC) was determined using a Fluoroskan Ascent FL fluorimeter-luminometer (TermoLabsystems, Finland) and black 96-well plates (Greiner bio-one, Germany).

Proteomic research methods. To identify proteins and provide isoelectric focusing, we used two-dimensional electrophoresis in line with the method first described by O'Farrell [41] which involved isoelectric focusing in an ampholine gradient (IEF-PAGE, equilibrium variant). Proteins were identified on two-dimensional electropherograms by first staining with Coomassie Blue R-250 (CBB R-250) and then with silver nitrate.

Computer densitometry involved wet two-dimensional electropherograms. Complete and/or fragmented digital images were taken with an Epson Expression 1680 scanner at 300 dpi resolution in 48-bit color, with the results saved as TIFF files. The digital images were improved in a graphics editor to calculate proteins using ImageMaster 2D Platinum 7 (GE Healthcare, Switzerland). The procedure included ≥ 3 electropherograms with equal application. The optical density range did not exceed ± 1.5%.

To identify proteins, individual fractions were cut out of two-dimensional electrophoresis: the fragments were crushed and treated with trypsin. The corresponding peptide sets were studied using the methods of matrix assisted laser desorption/ionization (MALDI-TOF MS) and tandem mass spectrometry (MS/MS) on an Ultraflex MALDI – time-of-flight mass spectrometer (Bruker, Germany) with an ultraviolet laser (336 nm) in the positive ion mode (mass range of 500–8000 Da calibrated using trypsin autolysis values). The resulting mass spectra (peptide mass fingerprints) were deciphered using traditional bioinformatics technologies.

Bioinformatics mass spectrometry. The obtained mass spectra of tryptic peptides were analyzed using the peptide mass fingerprint search in the Mascot program (Matrix Science, USA). The 0.01% accuracy of MH^+ mass allowed for the acrylamide modification of cysteines and the oxidation of methionines. The data search involved the databases of the US National Center for Biotechnology Information (NCBI).

The peptide bioinformatics, i.e., determination and prediction of their biological activity, covered the NCBI, BIOPEP, ToxinPred, AntiCP, AntiBP, AHTpin, and Anti-TbPred databases.

RESULTS AND DISCUSSION

Effect of enzymatic hydrolysis on the native structure of protein isolate. Enzymatic hydrolysis affects the protein isolate by modifying its secondary and tertiary structure, destroying peptide bonds, and improving functional properties [42]. An effective hydrolysis requires a proper concentration of the enzyme preparation and an optimal biodegradation time. The hydrolysis degree is crucial for monitoring the protein hydrolysis [28]. Figure 1 illustrates the effect of enzymatic exposure time on the hydrolysis rate.

For enzymatic hydrolysis, a 10% substrate hydrolysis (relative to the proteolysis time) is the optimal degree. The degree of hydrolysis is the proportion of split peptide bonds in the protein hydrolysate. In this study, the best results relative to time and enzymatic concentration belonged to Alcalase 2.4 L FG. This sample reached the desired 10% as follows: 0.5% – 27 min; 1% – 24 min; 1.5% – 21 min; 2% – 20 min. Alcalase 2.4 L FG possesses a wide catalytic range and is an effective breaker of higher molecular proteins into peptides [43].

The enzymatic hydrolysis induced by plant and animal enzyme preparations (pepsin, trypsin, and papain) proved to be less effective. The average time it took them to reach the 10% protein destruction was as follows: 0.5% – 36 min; 1% – 30 min; 1.5% – 27 min; 2% – 24 min. Bromelain also failed as a hydrolysis intensifier (0.5% – 51 min; 1% – 42 min; 1.5% – 39 min; 2% – 33 min).

Protoferm FP in its initial doses did not reach 10% hydrolysis due to the specificity of the substrate and the activity of the enzyme preparation. We had to bring the dose up to 4% and increase the hydrolysis time up to 120 min.

The degree of hydrolysis increased with time to the stationary phase in 2 h on average. The overall results fell within the predicted range, given the hydrolysis parameters. Further studies involved the following doses: 1.5% for plant and animal enzyme preparations and 2% for microbial preparations.

Subsequent gel electrophoresis (SDS-PAGE) relied on the results obtained for the hydrolysis. The control sample contained a native chickpea protein isolate; the chickpea protein hydrolysates with a 10% hydrolysis degree served as standards. Figure 2 shows the effect of enzyme preparations on the protein and peptide profile of the chickpea protein hydrolysates.

At 0% hydrolysis, the untreated control isolate developed numerous bands in the molecular weight range from ~ 4 to ~ 110 kDa. The bands of ~ 22–24 kDa are known to correspond to legumes (basic subunit); those of ~ 37–41 kDa belong to legumes (acidic subunit); the bands of ~ 50–55 kDa denote vicilin (α, β, γ); the bands

of ~ 70 kDa refer to the convicillin subunit; and the bands of 7 kDa belong to 2S albumin subunit [31]. The molecular weights obtained by SDS-PAGE were below 50 kDa for all the hydrolysates and below 37 kDa for samples 2, 5, and 6, which were treated with trypsin, Protoferm FP, and Alcalase 2.4 L FG. The most effective protein degradation was demonstrated by trypsin, Protoferm FP, and Alcalase 2.4 L FG. At < 15 kDa, each sample had bands with varying staining degrees, which indicated short peptides that developed as a result of protein degradation. The sample treated with trypsin demonstrated a shift in molecular weight and a partial destruction of protein bands represented by vicilin and legumin. The samples treated with papain and bromelain showed

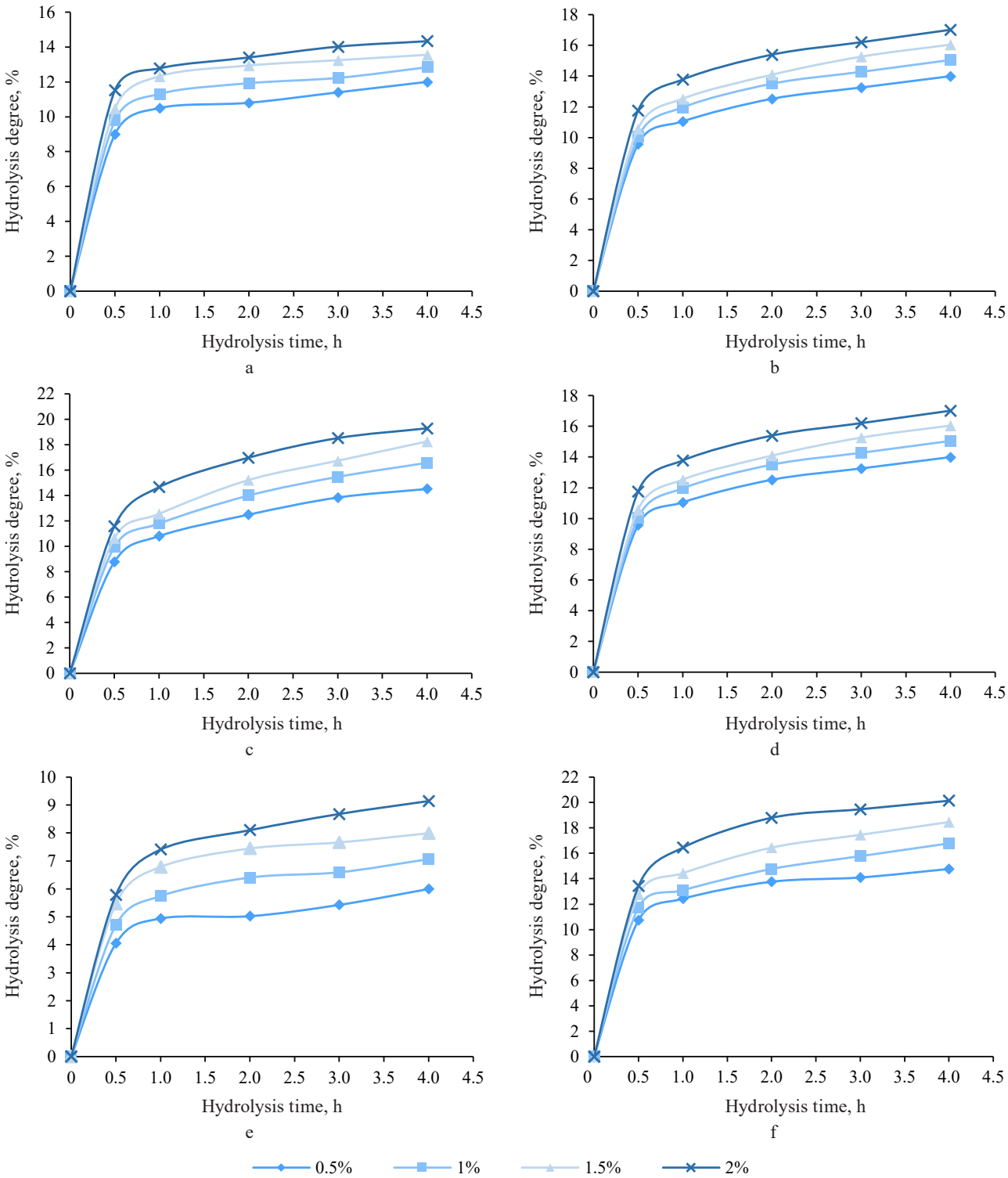

Figure 1 Effect of exposure time to proteolytic enzymes on hydrolysis degree: pepsin (a), trypsin (b), papain(c), bromelain (d), Protoferm FP (e), and Alcalase 2.4 L FG (f)

diffuse tracks of peptides with molecular weights below 25 kDa. These results indicated a stepwise cleavage of amino acid residues from the detected protein fractions. The differences in band profiles between the hydrolysates mean that the associated enzymes were specific for the available catalytic hydrolysis sites.

In addition to nutritional qualities, protein products used in the food industry must possess certain functional and technological properties associated with the operational profile of the final product [44]. The technological characteristics of hydrolysates are known to improve when the protein splits into fragments with a lower molecular weight [45]. Table 2 summarizes the functional and technological properties of the hydrolysates. The control sample contained native chickpea protein isolate, while the experimental samples contained chickpea protein hydrolysates with the 10% hydrolysis.

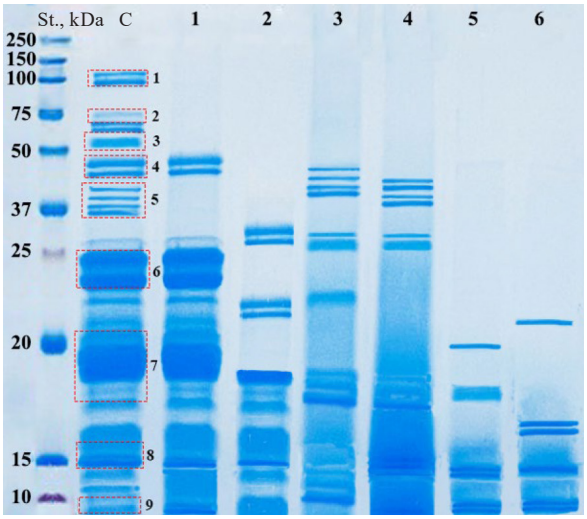

Figure 2 Electrophoresis of hydrolysates: St. – standard, PageRuler™; C – control; 1 – pepsin; 2 – trypsin; 3 – papain; 4 – bromelain; 5 – Protoferm FP; and 6 – Alcalase 2.4 L FG

The samples treated with pepsin and Protoferm FP increased the control solubility by 86.4 and 189.8%, respectively. The hydrolysates treated with pepsin and trypsin also increased their water-holding capacity. All the experimental samples demonstrated an advanced fat-holding capacity. In general, hydrolysate biostructures retain water and fat molecules by accumulating free amino acids and peptides during protein hydrolysis, which, in turn, stabilize food systems. None of the hydrolysates demonstrated significant increases in emulsion properties and stability. The critical gelation concentration in the samples treated with pepsin, papain, and Alcalase 2.4 L FG was approximately the same as in the isolate; other samples demonstrated even lower values. The foaming capacity increased in all samples except the one treated with trypsin. The hydrolysate treated with papain demonstrated one of the highest values (160–168%). Due to the high emulsifying capacity, the foaming stability remained low only in the hydrolysate treated with pepsin, where it was as low as in the original isolate. The hydrolysate treated with pepsin increased all its functional and technological indicators except for critical gelation and foaming stability, which was the same as in the native chickpea protein isolate.

The recent years have seen major scientific interest in natural antioxidants, in particular, the antioxidant potential of bioactive peptides derived from protein products [45, 46]. In this research, we identified the total antioxidant capacity of the experimental hydrolysates using the methods of FRAP, DPPH, and ORAC (Fig. 3).

The highest iron-reducing antioxidant capacity (FRAP) belonged to the hydrolysates treated with pepsin, papain, and Protoferm FP. The highest DPPH radical scavenging activity belonged to the sample treated with pepsin. Peptides with smaller molecular size of protein hydrolysate are known to possess stronger DPPH radical scavenging properties than those with higher molecular weight peptides [47–49]. In addition, a high DPPH

Table 2 Functional and technological properties of hydrolysates and chickpea protein isolate

Properties			Control (native chickpea protein isolate)		Pepsin		Trypsin		Papain		Bromelain		Protoferm FP		Alcalase 2.4 L FG	
Solubility, %			17.23		32.11		13.44		20.72		17.48		49.93		21.79	
Water-holding capacity, %			388		442		563		299		299		275		298	
Fat-holding capacity, %			195		435		488		370		280		299		373	
Emulsion	Emulsifying capacity, %		72		75		80		78		77		79		74	
	Emulsifying stability, %y		95		94		96		95		98		92		96	
Critical gelation concentration, %	Concentration, %	2	1		1		1		2		1		1		2	
		12	4		5		5		5		2		1		6	
		20	15		13		9		13		3		1		14	
Foaming capacity, %	Concentration, %	3	70	47	90	39	70	22	160	31	40	10	80	7	90	6
		5	73	49	92	43	73	30	163	34	42	15	89	10	98	8
		10	76	58	95	52	78	35	168	39	50	17	100	12	103	15
Foaming stability, min			0	30	0	30	0	30	0	30	0	30	0	30	0	30

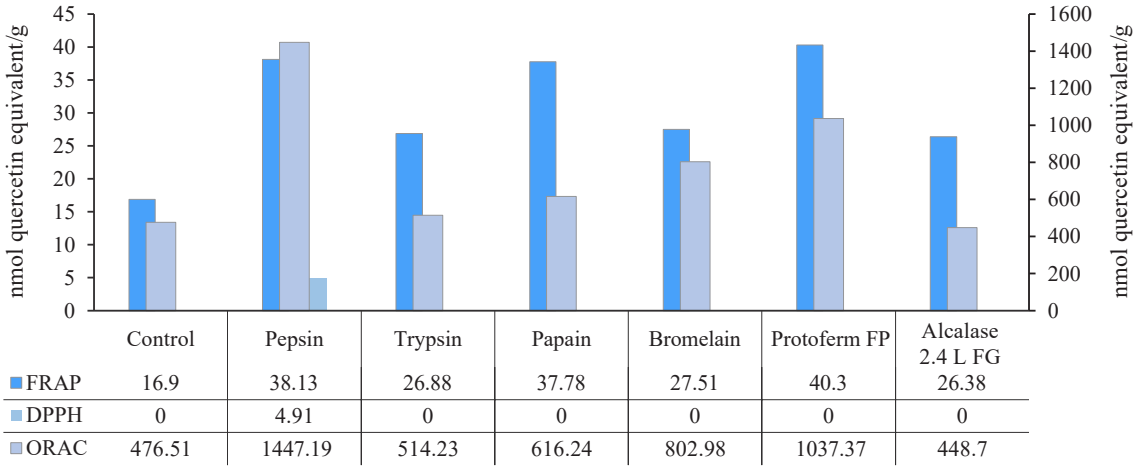

	Control	Pepsin	Trypsin	Papain	Bromelain	Protoferm FP	Alcalase 2.4 L FG
FRAP	16.9	38.13	26.88	37.78	27.51	40.3	26.38
DPPH	0	4.91	0	0	0	0	0
ORAC	476.51	1447.19	514.23	616.24	802.98	1037.37	448.7

Figure 3 Total antioxidant capacity: control vs. experimental samples

activity of protein hydrolysates or peptide fractions was reported to depend on the high content of hydrophobic and positively charged amino acids or biopeptides [50]. In terms of oxygen radical absorption (ORAC), the best results belonged to the hydrolysates treated with pepsin (1447.19 ± 50.60) and Protoferm FP (1037.37 ± 16.80); they increased the initial activity by 303.7 and 217.7%, respectively. The high antioxidant capacity of the hydrolysate treated with Protoferm FP could be explained by the fact that this sample yielded a peptide with the sequence SSSSPDIYIPQAGR, which possesses an antioxidant activity.

Protein composition of chickpea isolates. Proteomic methods proved efficient when applied to proteins of plant origin [51]. They make it possible to assess enzymatic hydrolysis of proteins and determine the biological potential of peptides obtained. Figure 4 shows a two-dimensional electropherogram of proteins in the chickpea isolate: it registers about 100 protein fractions in the mass range of 10–80 kDa and an isoelectric point (pI) of 4.8–10.0.

Only eleven (11) fractions in the chickpea protein isolate corresponded to full-length protein molecules (no. 1–3, 6, 19, 20–22, 24, 26, 27, 29). However, we revealed a certain pattern: some of these proteins changed their physical and chemical properties due to thermochemical effects, and the resulting fractions had different isoelectric points, e.g., no. 21 and 22, 18 and 20, 28 and 30.

Ten (10) fractions proved to be mixes of two or more proteins or their fragments. Some of these proteins retained the native post-translational modifications, e.g., acetylation of the N-terminal part of the molecule (no. 5, 22, 24), lysine methylation (no. 12), and hexoses (no. 10, 11). Twenty fractions demonstrated various protein fragments (no. 4, 5, 7–18, 23, 25, 26, 28, 30).

The two-dimensional electrophoresis revealed the following key proteins: vicilin and its analogues, legumin and its analogues, sucrose-binding proteins, storage proteins, globulins, and some enzymes. Since the chickpea genome remains poorly annotated, it was only the gene locus that was indicated in most cases. As a result, some proteins were identified as resembling (-like), although they might be isoforms of proteins of one and the same gene.

In some cases, we detected tryptic peptides: they were in small quantities, but clearly associated with other proteins (no. 3–5, 9, 21, 22, 24, 29, 30). Table 4 shows their amino acid sequences and positions in the protein chain. Most of these peptides occurred more than once, but in the fractions with different molecular weights.

The mechanism behind this phenomenon is as follows. The thermochemical action yields short peptides, mainly of the legumin and vicilin series. These interact with proteins of other origin, and together they fractionate by charge and molecular weight. When proteins are treated with trypsin for identification, it destroys the corresponding conservative peptides, they are detected in the mass spectra, and tandem mass spectrometry (MS/MS) reveals their amino acid sequence. Figure 5 is an example of tandem mass spectrometry for a peptide with 1623.8 m/z that corresponds to positions 181–193 in

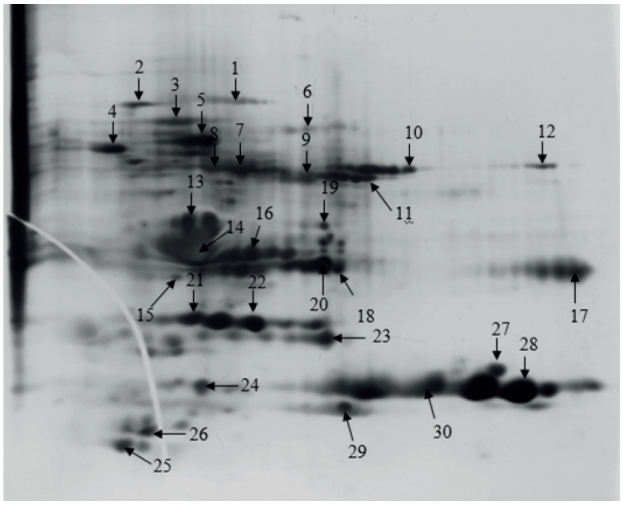

Figure 4 Two-dimensional electropherogram of chickpea isolate proteins (control) stained with silver nitrate. The arrows and numbers mark the fractions identified (see Table 3)

Table 3 Mass spectrometry of protein fractions of chickpea isolate

No. (Fig.3)	Protein (gene symbol)	Protein NCBI	S/M/C*	Mm/pI (experimental)**	Mm/pI (calculated)**
1	Mix of seed biotin-containing protein SBP65 (LOC101504303), legumin (leg3)***(1), and vicilin-like (LOC101515515)	XP_004487170.1 Q9SMJ4.1 XP_004493035.1	180/20/44 135/8/22 80/10/30	71.0/5.40	71.3/5.97 56.2/6.20 51.8/5.73
2	Mix of luminal-binding protein (LOC101513614) ***(1), heat shock 70 kDa protein (LOC101492688), and a fragment of sequence 28-320 of vicilin-like (LOC101510695)***(1)	XP_004503582.1 XP_004507753.1 XP_004496704.1	215/27/53 137/20/45 103/18/30	70.0/4.90	73.5/5.02 71.2/5.21 69.4/5.59
3	Vicilin-like (LOC101510695)	XP_004496704.1	199/41/41	68.0/5.20	69.4/5.59
4	Mix of fragments of protein disulfide-isomerase (LOC101512854) and ruBisCO large subunit-binding protein subunit alpha, chloroplastic (LOC101503231) + Acetyl (Protein N-term)	XP_004502489.2 XP_004506047.1	299/33/64 78/13/32	52.0/4.80	59.7/5.13 62.0/5.12
5	Fragment without N-terminal region of vicilin-like seed storage protein At2g18540 (LOC101506263) + Acetyl (Protein N-term)	XP_004512222.3	155/37/41	54.0/5.30	82.5/5.78
6	Mix of legumin A-like (LOC101489278), vicilin-like (LOC101515515), and provicilin-like (LOC101510367)	XP_004493780.1 XP_004493035.1 XP_004496703.1	67/8/21 65/8/19 49/7/15	56.0/6.50	59.3/5.87 51.8/5.73 64.6/6.61
7	Mix of fragment without N-terminal region of sucrose-binding protein-like (LOC101499776), fragment without N-terminal region of provicilin-like (LOC101510367), and legumin A-like (LOC101489278)***(1)	XP_004495184.1 XP_004496703.1 XP_004493780.1	136/16/38 120/13/29 136/9/18	45.0/5.80	53.8/5.85 64.6/6.61 59.3/5.87
8	Fragment of homologue 8S globulin alpha isoform (ABG02260) [*Vigna radiata* L.]	ABG02260.1	220/27/57	45.0/5.30	52.0/5.81
9	Fragment without N-terminal region of provicilin-like (LOC101510367) + hexose and fragment without N region of sucrose-binding protein-like (LOC101499776)	XP_004496703.1 XP_004495184.1	162/23/51 117/18/45	42.0/6.90	64.6/6.61 53.8/5.85
10	Fragment without N-terminal region of provicilin-like (LOC101510367) + hexose	XP_004496703.1	192/34/61	43.0/9.30	64.6/6.61
11	Fragment without N-terminal region of provicilin-like (LOC101510367) + hexose	XP_004496703.1	226/37/63	41.0/9.00	64.6/6.61
12	Fragment without C region of elongation factor 1-alpha (EF1A) with methylation of K (lysine) at 55K and 87K	NP_001352092.1	87/19/58	42.0/9.60	49.3/9.15
13	Fragment of N-terminal region of legumin A-like (LOC101489278)***(2)	XP_004493780.1	142/24/48	36.0/5.20	59.8/5.87
14	Fragment of N-terminal region of Legumin (LEG3)***(2)	Q9SMJ4.1	168/25/39	32.0/5.20	56.2/5.97
15	Mix of fragments of legumin A-like (LOC101489278)***(1) and vicilin-like (LOC101515515)	XP_004493780.1 XP_004493035.1	168/28/23 60/8/23	32.0/5.00	56.8/5.87 51.9/5.73
16	Fragment without C region of vicilin-like (LOC101515515)***(2)	XP_004493035.1	312/30/50	28.0/5.90	51.8/5.73
17	Central fragment of basic 7S globulin-like (LOC101504144)***(1)	XP_004494958.1	126/16/45	28.0/9.80	48.2/8.37
18	Mix of fragments of vicilin-like (LOC101515515) and NADPH-dependent aldehyde reductase 1, chloroplastic-like (LOC101506833)	XP_004493035.1 XP_004494625.2	107/12/35 80/9/32	28.0/7.80	51.8/5.73 35.5/8.11
19	Mix of fructose-bisphosphate aldolase cytoplasmic isozyme (ALDC) and fragments of legumin A-like (LOC101489278) and vicilin-like (LOC101505411)	NP_001265896.2 XP_004493780.1 XP_004492829.1	195/15/64 74/9/25 71/9/25	36.0/7.60	38.6/6.17 59.8/5.87 51.3/6.10
20	NADPH-dependent aldehyde reductase 1, chloroplastic-like (LOC101505375)	XP_004507706.1	270/16/71	28.0/7.60	32.2/6.40
21	Albumin-2-like (LOC101512722)	NP_001351664.1	184/13/53	25.0/5.10	26.1/5.67
22	Albumin-2-like (LOC101512722) + Acetyl (Protein N-term)	NP_001351664.1	254/24/87	25.0/5.90	26.1/5.67
23	Fragment of N-terminal region of vicilin-like (LOC101505411)	XP_004492829.1	178/32/33	24.0/7.70	51.1/6.10
24	18.5 kDa class I heat shock protein (LOC101514603)***(1) + Acetyl (Protein N-term)	XP_004505083.1	174/25/76	18.5/7.60	18.4/5.57
25	Central fragment of vicilin-like (LOC101505411)	XP_004492829.1	109/13/20	14.0/4.90	51.1/6.10
26	Mix of fragment of C region of vicilin-like (LOC101505411) and fragment of C region of basic 7S globulin-like (LOC101504144)***(1) with admixture of desiccation protectant protein Lea14 homologue (LOC101489566)***(1)	XP_004492829.1 XP_004494958.1 XP_004510736.1	110/19/39 97/13 /20 104/7/46	14.5/5.30	51.1/6.10 48.2/8.37 16.3/5.34
27	P24 oleosin-like (LOC101492171)	XP_004493360.1	64/16/40	21.0/9.30	21.4/9.56
28	Fragment of C region of legumin-like (LEG)***(1)	XP_027188788.1	99/23/30	20.0/9.40	56.2/5.97
29	Mix of 17.5 kDa class I heat shock protein-like (LOC101513658), outer envelope pore protein 16–2, chloroplastic-like (LOC101490648)***(1), and oleosin 16 kDa-like (LOC101488878)***(1)	XP_004490930.1 XP_004487776.1 XP_004501216.1	100/9/59 95/6/46 76/4/26	16.5/7.80	17.4/6.85 18.5/6.90 16.1/8.71
30	Fragment of C region of legumin-A-like (LOC101489278)*** (1)	XP_004493780.1	62/25/28	20.0/9.30	59.3/5.87

* S/M/C – Score, indicator of compliance (significant protein scores are ≥ 68, $p < 0.05$); the number of Matching peptides; Coverage (%) of the complete amino acid sequence of the protein by the peptide; ** Mm/pI (experimental) – estimates based on the electrophoretic mobility on two-dimensional electrophoresis; Mm/pI (calculated) – estimates made from amino acid sequence data based on the removal of the signal peptide but without other postsynthetic modifications (ExPASy Compute pI/Mw tool); *** msms – identification confirmed by tandem mass spectrometry with the number of sequenced tryptic peptides in brackets

Table 4 Peptides in complexes with other proteins

No. (see Table 1)	Source protein	Positions in amino acid sequence	Sequence confirmed by MS/MS	Mass to charge ratio, m/z
3	Legumin	181–193	FYLAGNHEQEFLR	1623.8
4	Legumin Vicilin-like	181–193 176–190	FYLAGNHEQEFLR ILEASFNSDYEEIER	1623.8 1814.9
5	Legumin Vicilin-like	181–193 176–190	FYLAGNHEQEFLR ILEASFNSDYEEIER	1623.8 1814.9
9	Legumin A-like Vicilin-like и seed storage protein At2g18540	181–200 380–388	FYLAGNQEQEFLQYQQQEGR QGDVFLVPR	2476.2 1030.6
21	Vicilin-like	59–69	SQLFENLQNYR	1411.7
22	Vicilin-like	59–69	SQLFENLQNYR	1411.7
24	Legumin-like Vicilin-like	449–472 59–69	LLGASSLINGMPEEVVAAAFNMER SQLFENLQNYR	2519.2 1411.7
29	Outer envelope pore protein 16-2, chloroplastic-like isoform X2 leosin 16 kDa-like	56–75 136–144	QAYFTAIQGGLPPSDVSATR EYGNYAQGR	2079.0 1057.5
30	Vicilin-like	141–157	VLDLAIPVNRPGQFQSF	1901.0

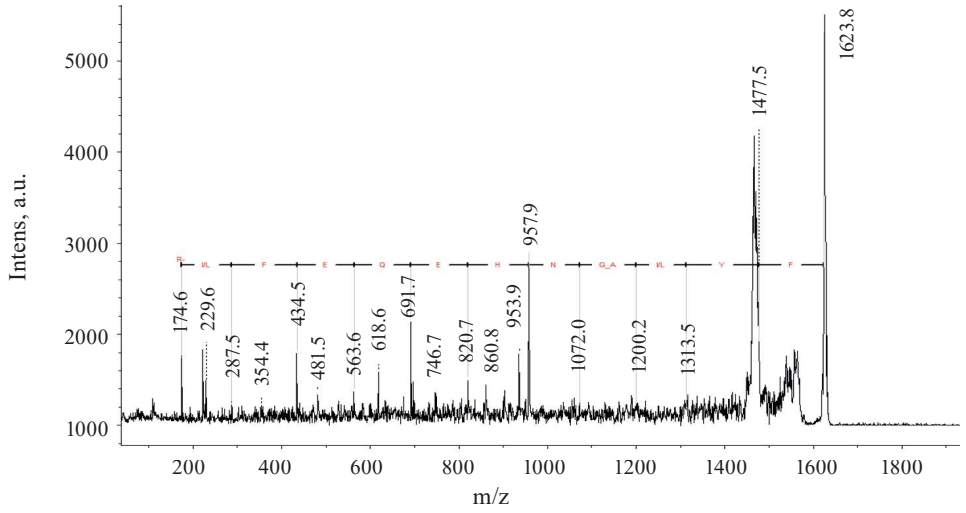

Figure 5 Fragmentation spectrum of ion with 1623.8 m/z as an illustration of amino acid sequence identified: the image is inverted in line with the processing algorithm

the amino acid sequence of chickpea legumin protein. The resulting sequence was FY I/L GA NHEF I/LR, which corresponded to FYLAGNHEQEFLR in Table 2. Isoleucine and leucine are not differentiated by mass during ionization because they are identical in mass (that is why they are often given as a variant, i.e., I/L). Sometimes, it is not one amino acid residue that is cleaved, but two or three. In this case, the program sees them not as single amino acid residues, but as a combination of residues with corresponding masses.

The abovementioned key peptides were generated by thermochemical action during the production of chickpea isolate and could bind to proteins of a different genesis.

Effect of proteases on peptide formation from chickpea protein isolate. Different types of proteases had different effects on the chickpea isolate proteins. Figure 6 shows the two-dimensional electrophoresis of chickpea isolate proteins before and after exposure to proteases.

The protease-induced fractionation of chickpea proteins was visible on the two-dimensional electrophoresis. The proteases demonstrated different efficiency in forming a pool of short peptides. They also differed in the utilization of proteins, especially the genes of legumin and albumin-2-like protein. Computer densitometry made it possible to compare the effect of proteases (Fig. 7) on the amount of total protein in the control.

The computer densitometry results were calculated based on the two-dimensional electrophoresis with Coomassie Blue R-250 staining. This stain binds to proteins more effectively than silver nitrate.

Trypsin and papain proved to be the most effective proteases in terms of functional peptides: they processed ≥ 55% of total protein into short peptides and intermediate forms. Bromelain and Protoferm FP proved to be the least effective proteases (25–35%).

In addition to peptides, the two-dimensional electrophoresis also identified some intermediate, relatively large fragments of chickpea isolate proteins formed by different types of proteases (Fig. 8, Table 5).

The proteomic study revealed that intermediate fragments mostly came from the legumin, vicilin, and albumin-like protein families.

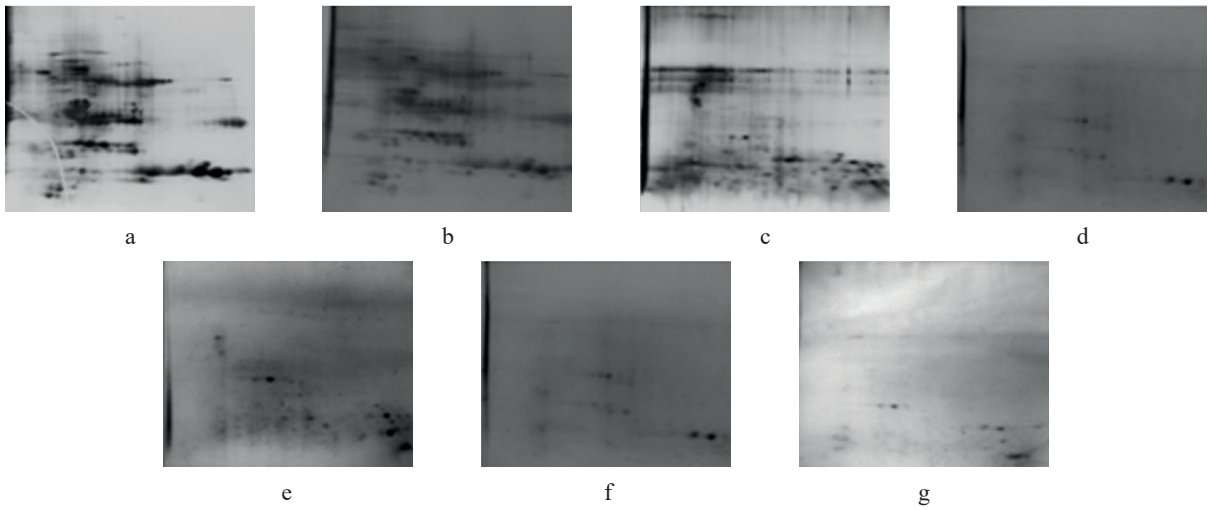

Figure 6 Dimensional electrophoresis of chickpea isolate proteins before and after exposure to proteases: (a) control, (b) trypsin, (c) pepsin, (d) papain, (e) bromelain, (f) Alcalase 2.4 L FG, and (g) Protoferm FP

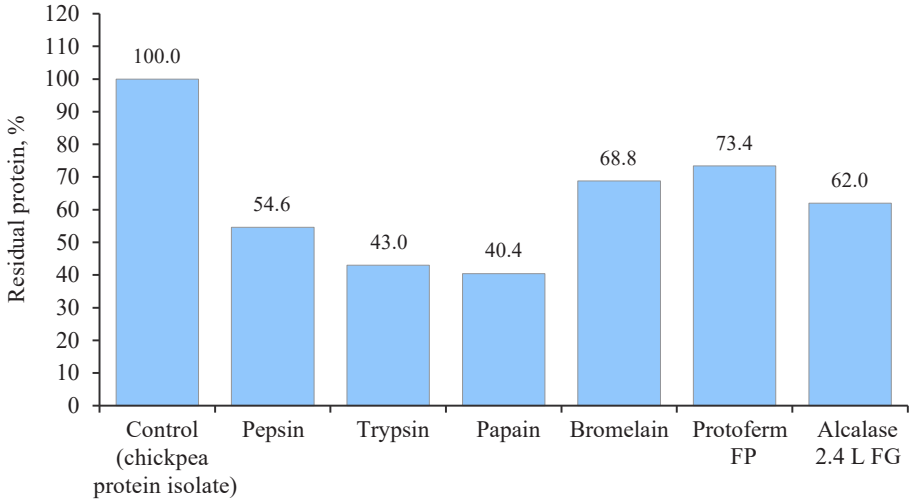

Figure 7 Effect of different proteases on total proteins in chickpea isolate

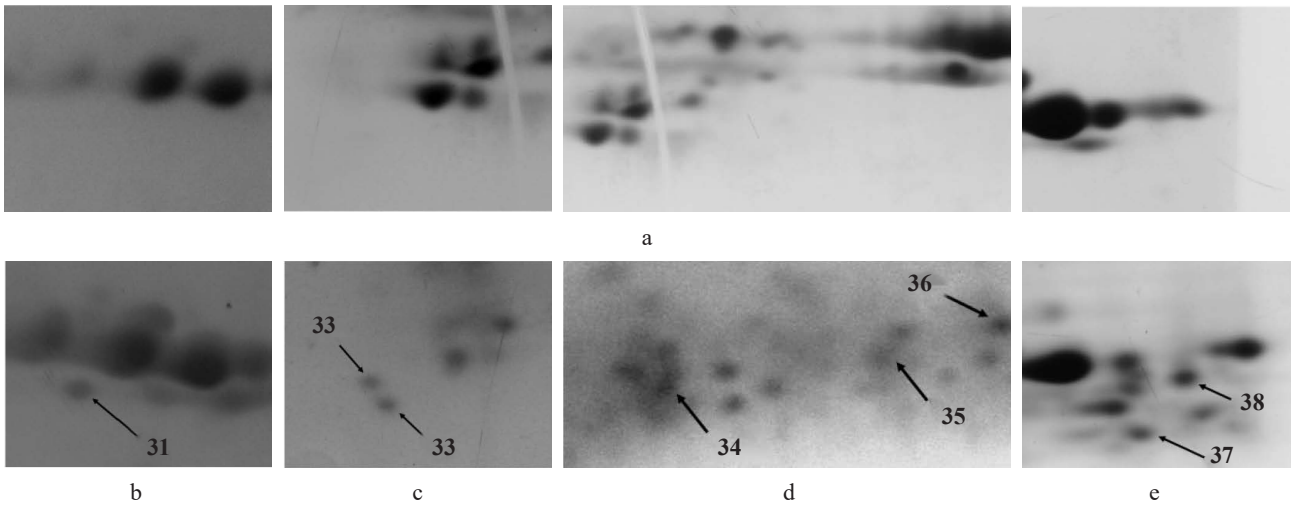

Figure 8 Intermediate peptides on fragments of two-dimensional electrophoresis created by different proteases (Table 5): (a) control, (b) trypsin, (c) bromelain, (d) Alcalase 2.4 L FG, and (e) Protoferm FP

Table 5 Intermediate fragments of protein fractions of chickpea isolate exposed to different proteases: mass spectrometry

No.	Protein (gene symbol)	Protein NCBI	S/M/C*	Mm/pI (experimental)**	Mm/pI (calculated)**
31	Fragment of C-terminal region of positions 344–431, legumin A-like (LOC101489278) + (1)	XP_004493780.1	77/16/25	18.0/9.35	59.3/5.87
32	Fragment of positions 252–448 vicilin-like (LOC101515194) + (2)	NP_001296635.1	114/12/18	14.0/5.00	51.5/6.04
33	Fragment of positions 252–441 vicilin-like (LOC101515194) + (1)	NP_001296635.1	85/12/18	13.5/5.20	51.5/6.04
34	Mix of fragment of positions 24–279 vicilin-like (LOC101515515)***(3), fragment of positions 347–414 legumin-like (LEG)***(1), and positions 154–183 provicilin-like (LOC101510367)***(1)	XP_004493035.1 XP_027188788.1 XP_004496703.1	286/19/33 91/2/4 89/3/4	14.5/5.30	51.9/5.73 56.7/5.97 65.0/6.61
35	Mix of fragment of positions 25–190 vicilin-like (LOC101515515), fragment of positions 105–182 albumin-2-like (LOC101512722)***(1), fragment of positions 252–427 legumin-like (LEG)***(1), and fragment of positions 163–309 provicilin-like (LOC101510367)***(1)	XP_004493035.1 NP_001351664.1 XP_027188788.1 XP_004496703.1	71/7/17 125/3/20 125/5/14 85/2/4	16.0/6.60	51.9/5.73 26.3/5.67 26.3/5.67 65.0/6.61
36	Mix of fragment of positions 219–427 legumin-like (LEG)***(1), fragment of positions 59-251 vicilin-like (LOC101505411), fragment of positions 14–71 17.1 kDa class II heat shock protein-like (LOC101504383)***(1), and fragment of positions 30–154 P24 oleosin (LOC101509783)***(1)	XP_027188788.1 XP_004492829.1 XP_004501442.1 XP_004489219.1	78/6/15 72/6/ 15 118/2/23 80/2/12	8.0/5.90	56.7/6.61 51.2/6.10 21.4/5.46 20.7/7.85
37	Fragment of positions 334–510 legumin A-like (LOC101489278)***(1)	XP_004493780.1	107/10/24	15.0/9.60	59.8/5.87
38	Mix of fragments of positions 325–491 legumin-like (LEG)***(1) and positions of 365–507 legumin J-like (LOC101501269)***(1)	XP_027188788.1 XP_004495100.1	78/18/22 67/18/18	16.0/9.80	56.7/5.97 61.0/5.50

* S/M/C – Score, indicator of compliance (significant protein scores are ≥ 68, $p < 0.05$); the number of Matching peptides; Coverage (%) of the complete amino acid sequence of the protein by the peptides; ** Mm/pI (experimental) – estimates based on the electrophoretic mobility on two-dimensional electrophoresis; Mm/pI (calculated) – estimates made from amino acid sequence data based on the removal of the signal peptide but without other postsynthetic modifications (ExPASy Compute pI/Mw tool); *** msms – identification confirmed by tandem mass spectrometry with the number of sequenced tryptic peptides in brackets.

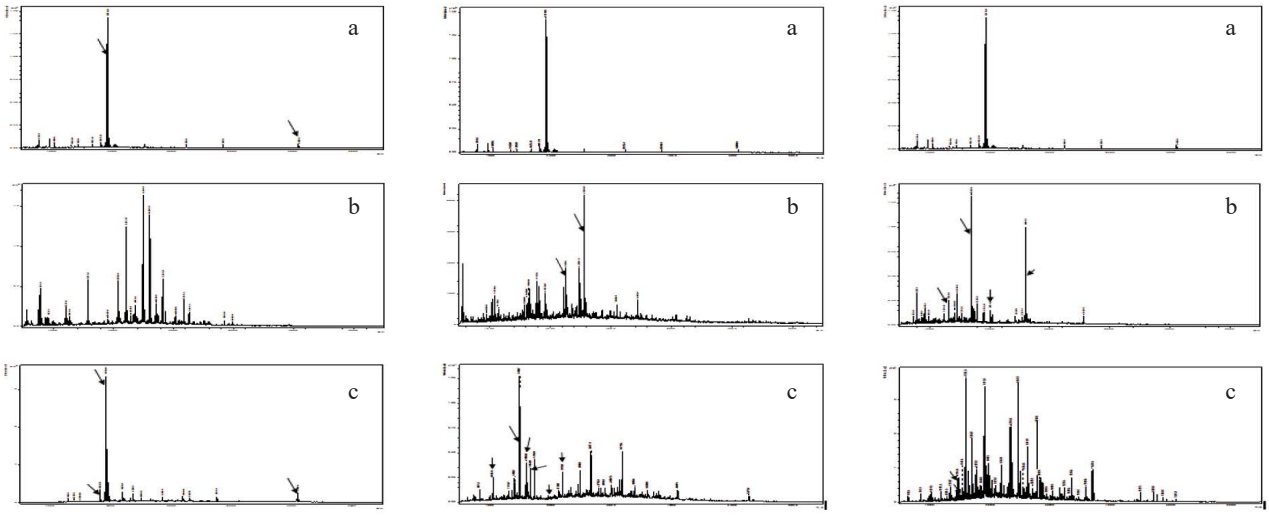

Figure 9 Mass spectra of short peptides after protease treatment. Peptides are marked with arrows

Protease effect on generation of short peptides (m/z ≤ 6000 Da) from chickpea isolate. When dealing with short peptides generated by different types of proteases, we encountered with a technical problem that prevented the identification of mass peaks by tandem mass spectrometry. The isolate samples contained high concentrations of residual chemicals that had been involved in the process of isolate formation, e.g., salts, acids, and alkalis. These substances hindered ionization and identification of the amino acid sequence of particular peptides. Moreover, some of the mass peaks were not of protein nature (high salt concentration). Figure 9 illustrates the mass spectra of short peptides in protease-treated hydrolysates and the control.

The mass spectra of short peptides had clearly different sets. The samples treated with pepsin, papain, bromelain, and Protoferm FP demonstrated a large number of different mass peaks. The hydrolysate treated with

Alcalase 2.4 L FG had fewer peaks and was less effective in biodegrading proteins into biopeptides. Trypsin mainly converted the processed proteins into single amino acid residues.

The mass spectra made it possible to identify eighteen biopeptides; their potential was predicted based on bioinformatic databases (Table 6). The *in-silico* proteolysis was able to connect protein sequence databases and bioactive peptide databases to accelerate the identification of bioactive peptides and their efficiency assessment [52].

The proteolytic enzyme preparations made it possible to determine the amino acid sequence of eighteen (18) peptides generated by different types of proteases. However, pepsin proved useless in this respect. In the trypsin sample, one peptide, which was initially present in the native protein structure, was identical to the control

Table 6 Identified biologically active peptides of chickpea proteins

No.	Source protein	Positions in amino acid sequence	Sequence confirmed by MS/MS	Mass to charge ratio, m/z	Bioactivity
			Control		
1	XP_004487601.1	24–65	SKDEKEEIPESCHKQLKSLNL KHCEKFLMKRMQKDEDEDDDN	5089.1	ACE inhibitor, DPP-IV inhibitor, regulating, AntiCP, non-toxin
			Trypsin		
2	Unknown	–	SSNPFTFLVPPRESEN	1820.9	AntiCP, AHTpin, non-toxin
3	XP_004487601.1	24–65	SKDEKEEIPESCHKQLKSLNL KHCEKFLMKRMQKDEDEDDDN	5089.1	ACE inhibitor, DPP-IV inhibitor, regulating, AntiCP, non-toxin
			Papain		
4	legumin J-like XP_004495100.1	159–178	ITLLDTSNFANQLDSTPRVF	2252.1	ACE inhibitor, DPP-IV inhibitor, AntiCP, non-toxin
5	provicilin-like XP_004496703.1	485–507	FGINAQNNQRNFLAGEDDNVISQ	2564.2	ACE inhibitor, DPP-IV inhibitor, AntiCP, non-toxin
			Bromelain		
6	vicilin-like XP_004492829.1	485–497	FGINAQNNQRNFL	1535.7	ACE inhibitor, DPP-IV inhibitor, AntiCP, AntiBP, non-toxin
7		485–498	FGINAQNNQRNFLA	1606.8	ACE inhibitor, DPP-IV inhibitor, AntiCP, non-toxin
8		485–499	FGINAQNNQRNFLAG	1663.8	ACE inhibitor, DPP-IV inhibitor, AntiCP, non-toxin
9	legumin-like XP_027188788.1	484–492	FSFLVPPRS	1049.6	ACE inhibitor, DPP-IV inhibitor, Renin inhibitor, AntiCP, AHTpin, non-toxin
10	vicilin-like XP_004496704.1	547–563	FPGSAQEVNRLIKNQRQ	1985.0	Regulating, Antithrombotic, Antiamnestic, ACE inhibitor, DPP-IV inhibitor, PAM inhibitor, AntiCP, non-toxin
11		545–563	LTFPGSAQEVNRLIKNQRQ	2199.2	Regulating, Antithrombotic, Antiamnestic, ACE inhibitor, DPP-IV inhibitor, PAM inhibitor, AntiCP, non-toxin
			Alcalase 2.4 L FG		
12	vicilin-like XP_004492829.1	143–154	DLAIPVNRPGQF	1326.7	Regulating, antithrombotic, antiamnestic, ACE inhibitor, DPP-IV inhibitor, PAM inhibitor, AntiCP, AntiBP, AHTpin, non-toxin
13		143–157	DLAIPVNRPGQFQSF	1688.8	Regulating, antithrombotic, antiamnestic, ACE inhibitor, DPP-IV inhibitor, PAM inhibitor, renin inhibitor, AntiCP, non-toxin
14	legumin-like XP_027188788.1	169–184	SFQNQLDQMPRRFYLA	2013.9	ACE inhibitor, DPP-IV inhibitor, renin inhibitor, AntiCP, non-toxin
15		214–235	SGFKRDFLEDALNVNRRIVNKL	2604.3	ACE inhibitor, DPP-IV inhibitor, AntiCP, non-toxin
16	legumin A-like XP_004493780.1	350–364	SSSSPDIYIPQAGR	1477.7	ACE inhibitor, antioxidative, DPP-IV inhibitor, AntiCP, AHTpin, non-toxin
17	vicilin-like XP_004492829.1	143–155	DLAIPVNRPGQFQ	1454.7	Regulating, antithrombotic, antiamnestic, ACE inhibitor, DPP-IV inhibitor, PAM inhibitor, AntiCP, AntiBP, non-toxin
18		143–157	DLAIPVNRPGQFQSF	1688.8	Regulating, antithrombotic, antiamnestic, ACE inhibitor, DPP-IV inhibitor, PAM inhibitor, renin inhibitor, AntiCP, non-toxin
19	legumin-like XP_027188788.1	250–269	VKGGLSIITPPEKEPRQKRG	2190.2	ACE inhibitor, DPP-IV inhibitor, DPP-III inhibitor, AntiCP, AntiBP, AHTpin, non-toxin, Anti-Tb

AntiCP – anticancer, AntiBP – antibacterial, AHTpin – antihypertensive inhibitor, AntiFP – antifungal, AntiTb – anti-tuberculosis, ACE inhibitor – angiotensin-converting enzyme inhibitor

sample with the amino acid sequence SKDEKEEIPES-CHKQLKSLNLKHCEKFLMKRMQKDEDEDDDN. Another peptide was of unknown origin: although its amino acid sequence was identified, its source remained unknown. The plant proteases generated short peptides from legumin and vicilin-like proteins. The bacterial proteases also formed peptides from the same series of proteins, but with a different amino acid sequence. The bromelain sample demonstrated a specific pattern: it yielded complexes of almost identical peptides that differed only in one amino acid residue, which fortified the solution with specific amino acids. A similar effect was observed in the samples with Alcalase 2.4 L FG and Protoferm FP; however, the cleavage yielded 2–3 amino acid residues, forming di- and tripeptides. The treatment with Alcalase 2.4 L FG and Protoferm FP resulted in an absolutely identical peptide with the amino acid sequence DLAIPVNRPGQFQSF. It demonstrated antithrombotic, antiamnestic, and antitumor activities, as well as inhibited the angiotensin-converting enzyme, DPP-4, proton pump, and renin.

According to the bioinformatics forecasting, all the peptides had antitumor activity, promoting the destruction of cancer cells by a direct or indirect mechanism [53]. All hydrolysates, except for the one treated with trypsin, could inhibit the angiotensin-converting enzyme. Some peptides possessed antithrombotic, antibacterial, antioxidant, and antiamnestic activities or could inhibit DPP-4, DPP-3, adenylate cyclase, and renin, as well as control blood glucose.

The remaining mass peaks rendered it impossible to read the amino acid sequence because of the high concentration of salts. Apparently, a different technological base is required for a more complete identification of the peptides generated by different types of proteases, e.g., HPLC combined with tandem mass spectrometry.

CONCLUSION

In this study, the enzymatic processing of plant protein yielded biologically active peptides of low molecular weight. In addition to bioactivity, these biopeptides exhibited good functional, technological, and antioxidant properties. These results may open up new prospects for the application of plant proteins. Hydrolysates treated with proteolytic enzymes of animal origin improved their functional and technological profile. Commercial enzymes of microbial origin proved to be more effective producers of biologically active peptides. The plant proteases demonstrated the greatest balance between the advanced functional and technological properties and the biopeptide yield.

Chickpea protein hydrolysates and biopeptides are a new potential natural source of bioactive substances to be used in the food industry and pharmacy. Advanced hydrolysis technologies may resolve a lot of current issues in the spheres of nutrition, ecology, and economy, contributing to the development of more sustainable and affordable food systems.

CONTRIBUTION

All authors contributed equally to the study and are equally responsible for the information published in this article.

CONFLICT OF INTEREST

The authors declared no conflict of interests regarding the publication of this article.

REFERENCES

1. Aluko RE. Determination of nutritional and bioactive properties of peptides in enzymatic pea, chickpea, and mung bean protein hydrolysates. Journal of AOAC International. 2008;91(4):947–956. https://doi.org/10.1093/jaoac/91.4.947
2. Kandrokov RKh, Yurchenko TI, Rumyantseva VV. New technology of bakery products of whole-ground spelt flour. Food Processing: Techniques and Technology. 2024;54(3):598–609. (In Russ.). https://doi.org/10.21603/2074-9414-2024-3-2529
3. Montesano D, Gallo M, Blasi F, Cossignani L. Biopeptides from vegetable proteins: New scientific evidences. Current Opinion in Food Science. 2020;31:31–37. https://doi.org/10.1016/j.cofs.2019.10.008
4. Gonzalez C. Climate change, food security, and agrobiodiversity: Toward a just, resilient, and sustainable food system. Fordham Environmental Law Review. 2011;22:493–521.
5. Vesnina A, Prosekov A, Atuchin V, Minina V, Ponasenko A. Tackling atherosclerosis via selected nutrition. International Journal of Molecular Sciences. 2022;23(15):8233. https://doi.org/10.3390/ijms23158233
6. Jakubczyk A, Karaś M, Rybczyńska-Tkaczyk K, Zielińska E, Zieliński D. Current trends of bioactive peptides – New sources and therapeutic effect. Foods. 2020;9(7):846. https://doi.org/10.3390/foods9070846
7. Yust MM, Millán-Linares MC, Alcaide-Hidalgo JM, Millán F, Pedroche J. Hydrolysis of chickpea proteins with Flavourzyme immobilized on glyoxyl-agarose gels improves functional properties. Food Science and Technology International. 2013;19(3):217–223. https://doi.org/10.1177/1082013212442197
8. Görgüç A, Gençdağ E, Yılmaz FM. Bioactive peptides derived from plant origin by-products: Biological activities and techno-functional utilizations in food developments – A review. Food Research International. 2020;136:109504. https://doi.org/10.1016/j.foodres.2020.109504

9. Ulug SK, Jahandideh F, Wu J. Novel technologies for the production of bioactive peptides. Trends in Food Science and Technology. 2020;108:27–39. https://doi.org/10.1016/j.tifs.2020.12.002
10. Semba RD, Ramsing R, Rahman N, Kraemer K, Bloem MW. Legumes as a sustainable source of protein in human diets. Global Food Security. 2021;28:100520. https://doi.org/10.1016/j.gfs.2021.100520
11. Faridy J-CM, Stephanie C-GM, Gabriela M-MO, Cristian J-M. Biological activities of chickpea in human health (*Cicer arietinum* L.). A Review. Plant Foods for Human Nutrition. 2020;75:142–153. https://doi.org/10.1007/s11130-020-00814-2
12. Rehm CD, Goltz SR, Katcher JA, Guarneiri LL, Dicklin MR, Maki KC. Trends and patterns of chickpea consumption among United States adults: Analyses of national health and nutrition examination survey data. The Journal of Nutrition. 2023;153(5):1567–1576. https://doi.org/10.1016/j.tjnut.2023.03.029
13. Dutta A, Trivedi A, Nath CP, Gupta DS, Hazra KK. A comprehensive review on grain legumes as climate-smart crops: Challenges and prospects. Environmental Challenges. 2022;7:100479. https://doi.org/10.1016/j.envc.2022.100479
14. Yegrem L. Nutritional composition, antinutritional factors, and utilization trends of Ethiopian chickpea (*Cicer arietinum* L.). International Journal of Food Science. 2021;2021(1):5570753. https://doi.org/10.1155/2021/5570753
15. Calia C, Pulvento C, Sellami MH, Tedone L, Ruta C, de Mastro G. A bibliometric analysis of chickpea agronomic practices in the world during 45 years of scientific research. Legume Science. 2024;6(1):e219. https://doi.org/10.1002/leg3.219
16. Panday H, Sah AK, Rai RK, Panwar GS, Gautam Y, Kamaluddin, *et al.* Economics of chickpea (*Cicer arietinum L.*) production in India: A descriptive view. International Journal of Statistics and Applied Mathematics. 2023;8(5): 403–411.
17. Maya M, Maphosa M. Current status of chickpea production: Opportunities for promoting, adoption and adapting the crop in Zimbabwe: A review. Journal of Dryland Agriculture. 2020;6(1):1–9. https://doi.org/10.5897/JODA2019.0029
18. Księżak J, Bojarszczuk J. The effect of cropping method and botanical form on seed yielding and chemical composition of chickpeas (*Cicer arietinum* L.) grown under organic system. Agronomy. 2020;10(6):801. https://doi.org/10.3390/agronomy10060801
19. Kaur R, Prasad K. Technological, processing and nutritional aspects of chickpea (*Cicer arietinum*) – A review. Trends in Food Science and Technology. 2021;109:448–463. https://doi.org/10.1016/j.tifs.2021.01.044
20. de Santis MA, Rinaldi M, Menga V, Codianni P, Giuzio L, Fares C, *et al.* Influence of organic and conventional farming on grain yield and protein composition of chickpea genotypes. Agronomy. 2021;11(2):191. https://doi.org/10.3390/agronomy11020191
21. Chang L, Lan Y, Bandillo N, Ohm J-B, Chen B, Rao J. Plant proteins from green pea and chickpea: Extraction, fractionation, structural characterization and functional properties. Food Hydrocolloids. 2022;123:107165. https://doi.org/10.1016/j.foodhyd.2021.107165
22. Goldstein N, Reifen R. The potential of legume-derived proteins in the food industry. Grain and Oil Science and Technology. 2022;5(4):167–178. https://doi.org/10.1016/j.gaost.2022.06.002
23. Grasso N, Lynch NL, Arendt EK, O'Mahony JA. Chickpea protein ingredients: A review of composition, functionality, and applications. Comprehensive Reviews in Food Science and Food Safety. 2022;21:435–452. https://doi.org/10.1111/1541-4337.12878
24. Ghribi AM, Gafsi IM, Sila A, Blecker C, Danthine S, Attia H, *et al.* Effects of enzymatic hydrolysis on conformational and functional properties of chickpea protein isolate. Food Chemistry. 2015;187:322–330. https://doi.org/10.1016/j.foodchem.2015.04.109
25. Kolpakova VV, Byzov VA. Functional characteristics and molecular structural modification of plant proteins. Review. Food Systems. 2024;7(3):324–335. (In Russ.). https://doi.org/10.21323/2618-9771-2024-7-3-324-335
26. Ramani A, Kushwaha R, Malaviya R, Kumar R, Yadav N. Molecular, functional and nutritional properties of chickpea (*Cicer arietinum* L.) protein isolates prepared by modified solubilization methods. Journal of Food Measurement and Characterization. 2021;15:2352–2368. https://doi.org/10.1007/s11694-020-00778-6
27. Colla G, Nardi S, Cardarelli M, Ertani A, Lucini L, Canaguier R, *et al.* Protein hydrolysates as biostimulants in horticulture. Scientia Horticulturae. 2015;196:28–38. https://doi.org/10.1016/j.scienta.2015.08.037
28. Xu Y, Galanopoulos M, Sismour E, Ren S, Mersha Z, Lynch P, *et al.* Effect of enzymatic hydrolysis using endo- and exo-proteases on secondary structure, functional, and antioxidant properties of chickpea protein hydrolysates. Journal of Food Measurement and Characterization. 2020;14:343–352. https://doi.org/10.1007/s11694-019-00296-0
29. Czelej M, Garbacz K, Czernecki T, Wawrzykowski J, Waśko A. Protein hydrolysates derived from animals and plants – A review of production methods and antioxidant activity. Foods. 2022;11(13):1953. https://doi.org/10.3390/foods11131953

30. García Arteaga V, Apéstegui Guardia M, Muranyi I, Eisner P, Schweiggert-Weisz U. Effect of enzymatic hydrolysis on molecular weight distribution, techno-functional properties and sensory perception of pea protein isolates. Innovative Food Science and Emerging Technologies. 2020;65:102449. https://doi.org/10.1016/j.ifset.2020.102449
31. Thirulogasundar A, Shi D, Stone AK, Xu C, Bhagwat A, Lu Y, *et al.* Effect of enzyme hydrolysis on the functionality, protein quality, and flavour profile of lentil and chickpea protein isolates. Journal of Food Measurement and Characterization. 2024;18:1592–1609. https://doi.org/10.1007/s11694-023-02228-5
32. Tang T, Wu N, Tang S, Xiao N, Jiang Y, Tu Y, *et al.* Industrial application of protein hydrolysates in food. Journal of Agricultural and Food Chemistry. 2023;71(4):1788–1801. https://doi.org/10.1021/acs.jafc.2c06957
33. Ali C, Metin Y. Effects of hydrolysis degree on the functional properties of hydrolysates from sour cherry kernel protein concentrate. Foods and Raw Materials. 2023;11(2):197–205. https://doi.org/10.21603/2308-4057-2023-2-566
34. Chalamaiah M, Ulug SK, Hong H, Wu J. Regulatory requirements of bioactive peptides (protein hydrolysates) from food proteins. Journal of Functional Foods. 2019;58:123–129. https://doi.org/10.1016/j.jff.2019.04.050
35. Krikunova LN, Meleshkina EP, Vitol IS, Dubinina EV, Obodeeva ON. Grain Bran hydrolysates in the production of fruit distillates. Foods and Raw Materials. 2023;11(1):35–42. https://doi.org/10.21603/2308-4057-2023-1-550
36. Mohan A, Rajendran SRCK, He QS, Bazinet L, Udenigwe CC. Encapsulation of food protein hydrolysates and peptides: A review. RSC Advances. 2015;5(97):79270–79278. https://doi.org/10.1039/C5RA13419F
37. González López CV, Cerón García MC, Acién Fernández FG, Bustos CS, Chisti Y, Fernández Sevilla JM. Protein measurements of microalgal and cyanobacterial biomass. Bioresource Technology. 2010;101(19):7587–7591. https://doi.org/10.1016/j.biortech.2010.04.077
38. Taragjini E, Ciardi M, Musari E, Villaró S, Morillas-España A, Alarcón FJ, *et al.* Pilot-scale production of *A. platensis*: Protein isolation following an ultrasound-assisted strategy and assessment of techno-functional properties. Food and Bioprocess Technology. 2022;15:1299–1310. https://doi.org/10.1007/s11947-022-02789-1
39. Elsohaimy SA, Refaay TM, Zaytoun MAM. Physicochemical and functional properties of quinoa protein isolate. Annals of Agricultural Sciences. 2015;60(2):297–305. https://doi.org/10.1016/j.aoas.2015.10.007
40. Leni G, Soetemans L, Caligiani A, Sforza S, Bastiaens L. Degree of hydrolysis affects the techno-functional properties of lesser mealworm protein hydrolysates. Foods. 2020;9(4):381. https://doi.org/10.3390/foods9040381
41. O'Farrell PH. High resolution two-dimensional electrophoresis of proteins. The Journal of Biological Chemistry. 1975;250(10):4007–4021. https://doi.org/10.1016/S0021-9258(19)41496-8
42. Kostyleva EV, Sereda AS, Velikoretskaya IA, Kurbatova EI, Tsurikova NV. Proteases for obtaining of food protein hydrolysates from proteinaceous by-products. Problems of Nutrition. 2023;92(1):116–132. (In Russ.). https://doi.org/10.33029/0042-8833-2023-92-1-116-132
43. Real Hernandez LM, Gonzalez de Mejia E. Enzymatic production, bioactivity, and bitterness of chickpea (*Cicer arietinum*) peptides. Comprehensive Reviews in Food Science and Food Safety. 2019;18(6):1913–1946. https://doi.org/10.1111/1541-4337.12504
44. Bernardi S, Lupatini-Menegotto AL, Kalschne DL, Flores ÉLM, Bittencourt PRS, Colla E, *et al.* Ultrasound: A suitable technology to improve the extraction and techno-functional properties of vegetable food proteins. Plant Foods for Human Nutrition. 2021;76:1–11. https://doi.org/10.1007/s11130-021-00884-w
45. Zinina O, Merenkova S, Rebezov M, Galimov D, Khayrullin M, Burkov P. Physicochemical, functional, and technological properties of protein hydrolysates obtained by microbial fermentation of broiler chicken gizzards. Fermentation. 2022;8(7):317. https://doi.org/10.3390/fermentation8070317
46. Li Y, Jiang B, Zhang T, Mu W, Liu J. Antioxidant and free radical-scavenging activities of chickpea protein hydrolysate (CPH). Food Chemistry. 2008;106(2):444–450. https://doi.org/10.1016/j.foodchem.2007.04.067
47. Moure A, Domínguez H, Parajó JC. Antioxidant properties of ultrafiltration-recovered soy protein fractions from industrial effluents and their hydrolysates. Process Biochemistry. 2006;41(2):447–456. https://doi.org/10.1016/j.procbio.2005.07.014
48. Pezeshk S, Ojagh SM, Rezaei M, Shabanpour B. Fractionation of protein hydrolysates of fish waste using membrane ultrafiltration: Investigation of antibacterial and antioxidant activities. Probiotics and Antimicrobial Proteins. 2019;11:1015–1022. https://doi.org/10.1007/s12602-018-9483-y
49. Tkaczewska J, Borawska-Dziadkiewicz J, Kulawik P, Duda I, Morawska M, Mickowska B. The effects of hydrolysis condition on the antioxidant activity of protein hydrolysate from *Cyprinus carpio* skin gelatin. LWT. 2020;117:108616. https://doi.org/10.1016/j.lwt.2019.108616
50. Dong Z, Tian G, Xu Z, Li M, Xu M, Zhou Y, *et al.* Antioxidant activities of peptide fractions derived from freshwater mussel protein using ultrasound-assisted enzymatic hydrolysis. Czech Journal of Food Sciences. 2017;35(4):328–338. https://doi.org/10.17221/421/2016-CJFS

51. Chang Y-W, Alli I, Konishi Y, Ziomek E. Characterization of protein fractions from chickpea (*Cicer arietinum* L.) and oat (*Avena sativa* L.) seeds using proteomic techniques. Food Research International. 2011;44(9):3094–3104. https://doi.org/10.1016/j.foodres.2011.08.001
52. Du Z, Comer J, Li Y. Bioinformatics approaches to discovering food-derived bioactive peptides: Reviews and perspectives. TrAC Trends in Analytical Chemistry. 2023;162:117051. https://doi.org/10.1016/j.trac.2023.117051
53. Hilchie AL, Hoskin DW, Power Coombs MR. Anticancer activities of natural and synthetic peptides. In: Matsuzaki K, editor. Antimicrobial Peptides. Basics for Clinical Application. Singapore: Springer; 2019. pp. 131–147. https://doi.org/10.1007/978-981-13-3588-4_9

ORCID IDs
Mahmud Gharaviri https://orcid.org/0000-0002-4318-7077
Denis I. Aleksanochkin https://orcid.org/0009-0000-7677-6583
Mahbubeh Ahangaran https://orcid.org/0000-0003-4796-2066
Ivan A. Fomenko https://orcid.org/0000-0003-2478-1705
Leonid I. Kovalev https://orcid.org/0000-0001-6519-8247
Marina A. Kovaleva https://orcid.org/0000-0002-3486-2122
Irina M. Chernukha https://orcid.org/0000-0003-4298-0927
Natalia G. Mashentseva https://orcid.org/0000-0002-9287-0585

FRM

Foods and Raw Materials. 2026;14(1)

ISSN 2308-4057 (Print)
ISSN 2310-9599 (Online)

Research Article
Open Access

Available online at http://jfrm.ru/en
https://doi.org/10.21603/2308-4057-2026-1-669
https://elibrary.ru/UUOGOW

Rhizobia as complex biofertilizers for wheat: Biological nitrogen fixation and plant growth promotion

Yuliya R. Serazetdinova[1,*], Ekaterina E. Borodina[1], Natalya V. Fotina[1], Adarsh Naik[1], Gaurav Mudgal[2,3], Lyudmila K. Asyakina[1]

[1] Kemerovo State University, Kemerovo, Russia
[2] Saveetha Institute of Medical and Technical Sciences, Saveetha University, Chennai, India
[3] Chandigarh University, Mohali, India

* e-mail: serazetdinova2000@mail.ru

Received 02.12.2024; Revised 31.01.2025; Accepted 04.02.2025; Published online 30.04.2025

Abstract:
The biological fixation of atmospheric nitrogen by rhizobia plays a key role in the cycle of ecosystems and their productivity. In agriculture, it is often used to increase the yield of legumes. We aimed to assess the stimulatory properties of three bacterial strains (*Ensifer meliloti* 441 B-219, *Ensifer mexicanus* B-4064, and *Rhizobium tropici* B-216) and their potential for promoting wheat growth under laboratory conditions.

The bacterial were obtained from the All-Russian Collection of Industrial Microorganisms (National Bioresource Center, Kurchatov Institute). To explore their potential for agronomic practices, we determined their stimulating properties and assessed antagonistic activity against such phytopathogens as *Fusarium graminearum* F-877, *Bipolaris sorokiniana* F-529, *Botrytis cinerea* F-1006, *Erwinia rhapontici* B-9292, and *Xanthomonas campestris* B-4102. Finally, we studied the effect of the strains on germination and the contents of photosynthetic pigments, nitrogen, and protein in the above-ground parts of wheat plants under laboratory conditions.

All the test rhizobia strains demonstrated various stimulating properties. In particular, they produced phytohormones, fixed nitrogen, solubilized phosphates and zinc, and synthesized ACC deaminase. The strains also exhibited pronounced antagonistic activity against *F. graminearum*, *B. sorokiniana*, and *Xanthomonas campestris.* According to the laboratory tests, the wheat seeds treated with *E. meliloti* 441 B-219 and *R. tropici* B-216 had longer shoots and roots, as well as higher contents of chlorophyll and carotenoids in some wheat varieties. *R. tropici* also had a strong positive effect on the weight of shoots and roots in all wheat varieties. *E. mexicanus* B-4064 exhibited a positive effect only on germination in some varieties. However, none of the strains had a significant effect on the nitrogen content.

The test rhizobia strains have significant potential for stimulating plant growth, but they do not contribute to a significant increase in nitrogen availability for wheat.

Keywords: *Triticum aestivum* L., nitrogen fixation, biofortification, phytohormones, siderophores, solubilization

Funding. This research was part of the state assignment on "Studying the potential of growth-promoting bacteria to improve the agronomic biofortification of wheat" (FZSR-2024-0009).

Please cite this article in press as: Serazetdinova YuR, Borodina EE, Fotina NV, Naik A, Mudgal G, Asyakina LK. Rhizobia as complex biofertilizers for wheat: Biological nitrogen fixation and plant growth promotion. Foods and Raw Materials. 2026; 14(1):214–227. https://doi.org/10.21603/2308-4057-2026-1-669

INTRODUCTION

A phytobiome is a community of microorganisms associated with a host plant. It plays a key role in maintaining the plant's health and productivity in a changing environment. Microorganisms, such as bacteria and fungi, inhabit all plant organs but are particularly abundant in the rhizosphere [1, 2]. Bacteria are the most common and diverse microorganisms in this community [3] and they can be referred to as the second genome of the plant [4].

Root nodules of legumes are specialized organs that form as a result of interaction between the plant root system and bacteria of the *Rhizobium* genus. Root nodules have a unique microbiome dominated by rhizobia. These bacteria are crucial for the main stage of nitrogen metabolism, where atmospheric nitrogen (N_2) is reduced to ammonia (NH_3) in the presence of nitrogenase. This enzyme is a complex of MoFe dinitrogenase (molybdenum-iron protein), which is a catalyst, and dinitrogenase

Copyright © 2025, Serazetdinova *et al.* This is an open access article distributed under the terms of the Creative Commons Attribution 4.0 International License (https://creativecommons.org/licenses/by/4.0/), allowing third parties to copy and redistribute the material in any medium or format and to remix, transform, and build upon the material for any purpose, even commercially, provided the original work is properly cited and states its license.

reductase (Fe protein). These two components are encoded by the genes nif, nif D, and nif K (for MoFe dinitrogenase), and the gene nif H (for Fe dinitrogenase reductase) [5–8].

A product of nitrogen fixation, ammonia is assimilated by the plant and converted into organic nitrogen compounds, which are necessary for growth and development. Thus, the specific relationship between the nodule root and its host plant is mainly controlled by the exchange of nitrogen (N) and carbon (C). The plant supplies the reduced carbon (in the form of carbohydrates) to the bacteria, which use it as energy to stimulate the nitrogen fixation process, and the nodules return the reduced nitrogen to the plant [9].

Biological nitrogen fixation provides legumes with an advantage under the conditions of nitrogen deficiency inthe soil, promoting their growth and development [10, 11]. Furthermore, biological nitrogen fixation by legumes is the main source of nitrogen in natural agroecosystems. The total nitrogen fixation is estimated at about 1.75×10^{11} kg worldwide, with nitrogen fixation by legumes accounting for 8.0×10^{10} kg and the industrial production of nitrogen fertilizers accounting for the remaining 8.8×10^{10} kg [12].

Nitrogen-fixing microorganisms are divided into three groups: free-living, associative, and symbiotic. Associative and symbiotic nitrogen fixers are found in the rhizosphere of both legumes and non-legumes [13, 14]. However, most studies have focused on the symbiosis of plants and nitrogen-fixing microorganisms resulting in the formation of root nodules. Research into root nodule metagenomes opens up new prospects for studying the composition and functional diversity of microbial species. However, we need to assess the effectiveness of isolated strains for the host plants, as well as their survivability in different soil conditions, before they can be used in sustainable agricultural practices. The symbiosis of rhizobia and legumes is a good model system for studying complex interactions. In particular, it can be used to study the mechanisms of interspecies recognition and the factors of nitrogen fixation. A better understanding of these interactions can improve crop management practices aimed at increasing the efficiency of atmospheric nitrogen in agriculture.

Diazotrophic bacteria play a key role in biological nitrogen fixation. They are also known to enhance plant growth and increase crop yield [15–18]. Studies show that numerous strains of *Rhizobia*, *Bradyrhizobia*, *Ensifer*, *Azotobacter*, *Azospirillum*, *Pseudomonas*, *Klebsiella*, and *Bacillus* have a beneficial effect on plant development and increase the yield of wheat, rice, and other crops. This is due to phytohormones (e.g., indoleacetic acid), siderophores, and organic acids, which stimulate the growth of stems and roots [17]. Gopalakrishnan *et al.* [19] found this effect on chickpea (*Cicer arietinum* L.). Some *Bradyrhizobial* strains isolated from the rhizosphere of rice and *Azorhizobium caulinodans* are able to fix nitrogen without entering into a symbiotic relationship with the plant [20], as well as under low oxygen conditions [21].

Baset *et al.* [22] reported the beneficial effects of rhizobia inoculation on rice, maize, and wheat. On the other hand, Gopalakrishnan *et al.* [23] and Das *et al.* [24] found that rhizobia can act as biological control agents against pathogenic fungi (*Rhizoctonia*, *Fusarium*, *Macrophomina*, and *Sclerotium*) by synthesizing hydrocyanic acid, antibiotics, and/or mycolytic enzymes. However, there has been inadequate research into the potential PGP properties of many other α-, β- and γ-proteobacteria associated with legume nodules and involved in nitrogen fixation processes. Studying these properties of diazotrophic bacteria, especially rhizobia, is important for selecting the most effective strains to increase crop yields.

In the last few years, significant efforts have been made to extend nitrogen fixation to cereals [25, 26]. Compared to symbiotic nitrogen-fixing bacteria, non-symbiotic bacterial diazotrophs are of limited agronomic use, although they account for about 30% of total biological nitrogen fixation [27]. They may be a source of fixed N in many terrestrial ecosystems [28]. This potential was supported by Pankiewicz *et al.* [29], who showed that *Setaria viridis* inoculated with an ammonia-producing strain showed robust growth under nitrogen-limiting conditions. Van Deynze *et al.* [30] reported that a Mexican maize cultivar fixed nitrogen at up to 82% when its aerial roots were colonized by symbiotic diazotrophic bacteria.

In this study, we aimed to assess the growth properties of three strains of rhizobia (*Ensifer meliloti* 441 B-219, *Ensifer mexicanus* B-4064, *Rhizobium tropici* B-216), as well as to study their potential for stimulating wheat growth under laboratory conditions. The effectiveness of these rhizobia strains as growth stimulants for wheat may promote their subsequent use in agrobiotechnology.

E. (Sinorhizobium) meliloti is an alphaproteobacterium, a gram-negative aerobic microorganism found in soil and capable of forming symbiotic interactions with nitrogen-fixing legumes of the genera *Medicago*, *Melilotus* and *Trigonella*. This bacterium is easily cultivated on various nutrient media and has great trophic capabilities in relation to sources of carbon, nitrogen, and phosphorus. Some *E. meliloti* strains do not colonize the plant's root system and therefore lack the ability to form symbiotic relationships [31]. Studies have shown that *E. meliloti* can act as an endophyte, colonizing various plant tissues, including leaves. There is a need to study the mechanisms of plant infection and intracellular reproduction of *E. meliloti*, including the regulatory mechanisms of the bacterial cell cycle and specific signaling molecules secreted by alfalfa, or lucern, plants (*Medicago* L.) [32, 33].

E. mexicanus is an aerobic, gram-negative, non-spore-forming rod. The ITTG R7 strain was isolated from the root nodules of narrow-leaved acacia (*Acacia angustissima* (Mill.) Kuntz) collected in Tuxtla Gutiérrez, Chiapas, Mexico [34]. Current scientific literature lacks a comprehensive description of the phenotypic and genotypic characteristics of *E. mexicanus*. Further

studies are needed to fully define its physiological, biochemical, and genetic properties, as well as analyze its nitrogen-fixing capacity and host plant specificity in comparison with other Ensifer species. The lack of detailed information on *E. mexicanus* limits our understanding of its role in ecosystems and its potential for agricultural use.

R. tropici is a poorly studied species of rhizobia isolated from root nodules of common bean and members of the *Leucaena* genus (woody legumes common in the tropics and subtropics). *R. tropici* is found in soil samples from various parts of the world. It can form symbiotic relationships with a wide range of legume host plants. The taxonomic group *R. tropici* includes a large number of strains with metabolic diversity [35]. They can synthesize a wide range of lipochito-oligosaccharides [36–38], which can have up to 60 structural configurations [39] depending on the bacterial species and environmental conditions. A lipo-chitooligosaccharide is a chain of 16 to 18 carbon atoms with a fatty acid residue that promotes the growth of non-legume plants. This is due to its ability to mimic the effects of plant hormones such as cytokinins and auxins [40], resulting in increased seed germination and resistance to pathogens [41].

STUDY OBJECTS AND METHODS

The bacterial strains under study were obtained from the All-Russian Collection of Industrial Microorganisms of the National Bioresource Center at the Kurchatov Institute National Research Center (Russia):

– *Ensifer meliloti* 441 B-219 isolated from the surface of alfalfa roots (Alma-Ata Region, 1961) and capable of producing nitragin;
– *Ensifer mexicanus* B-4064 capable of fixing atmospheric nitrogen; and
– *Rhizobium tropici* B-216 isolated from the surface of horse bean roots (Lithuanian Soviet Socialist Republic, 1967) and capable of producing nitragin.

To determine the cultural characteristics of the strains, a suspension of a bacterial strain with a low cell concentration was overlaid with a Drygalski spatula onto the medium containing 21.0 g/L of fermented meat hydrolysate (KhimMedService, Russia), 10.0 g/L peptone (ChemExpress, Russia), and 15.0 g/L agar-agar (LenReaktiv, Russia).

The morphological characteristics of the strains were determined by a microscopic examination of a fixed smear stained with methylene blue (LenReaktiv, Russia) at a total magnification of ×1000 [42].

To study the ability of the strains to produce indole-3-acetic acid, a cell suspension was prepared in 1% peptone water with a McFarland turbidity coefficient of 0.8–1.0 using a Densichek plus densitometer (BioMerieux, France). The cells were then inoculated on Luria-Bertani broth in the Miller modification (HiMedia Laboratories, India) in an amount of 3% of the nutrient medium. They were cultivated in an LSI-3016A shaker-incubator (Daihan Labtech, South Korea) for 24 h at 28 ± 2°C at 110 rpm. The cells were separated from the culture fluid by centrifugation for 10 min at 7500 rpm. Then, 1 mL of the Salkowski reagent (0.1 g iron (III) chloride (LenReaktiv, Russia) dissolved in 100 mL of 50% sulfuric acid (KhimKomponent, Russia)) was added to 1 mL of the resulting supernatant and kept for 30 min at 22 ± 2°C. At the same time, a control sample (nutrient medium with the Salkowski reagent) was prepared under the same conditions. The optical densities of the experimental and control samples were determined on a UV 1800 spectrophotometer (Shimadzu, Japan) at 535 nm [43]. The optical density of the sample (OD) was calculated according to Eq. (1):

$$OD = OD_{sp} - OD_c \quad (1)$$

where OD_{sp} is the optical density of the sample as read by the spectrophotometer; OD_c is the optical density of the control.

The amount of indole-3-acetic acid was determined using a graduated graph of standard solutions of indole-3-acetic acid (Dia-M, Russia) at concentrations from 0.5 to 5.0 μg/mL.

To study the ability of the strains to produce gibberellic acid, a cell-free culture fluid was prepared using the method described earlier. Then, 280 μL of zinc acetate (LenReaktiv, Russia) and potassium ferricyanide (LenReaktiv, Russia) was added to 2 mL of the culture fluid. The mixture was centrifuged for 15 min at 4500 rpm. Then, 1 mL of 30% hydrochloric acid (ChemExpress, Russia) was added to 1 mL of the resulting supernatant and kept for 75 min at 22 ± 2°C. The optical density was determined spectrophotometrically at 254 nm, with a 5% hydrochloric acid solution used as a control [44]. The amount of gibberellic acid was determined using a calibration graph of standard solutions of gibberellic acid (Dia-M, Russia) at concentrations from 0.5 to 5.0 mg/mL.

To study the ability of the strains to produce siderophores, a cell-free culture fluid was prepared using the method described earlier. Then, 1 mL of the resulting culture fluid was mixed with 1 mL of the CAS reagent (1.5 mL of a 0.016% solution of iron III chloride in a 10 M solution of hydrochloric acid mixed with 7.5 mL of a 1.21% solution of chromazurol S (ChemExpress, Russia) and made up to 100 mL with distilled water). The resulting solution was kept in a dark place for 30 min at 22 ± 2°C. At the same time, a control sample (nutrient medium with the CAS reagent) was prepared under the same conditions. The optical density was determined on a spectrophotometer at 630 nm. The concentration of siderophores (C_{sid}, %) was calculated using Eq. (2) [45]:

$$C_{sid} = \frac{OD_s - OD_c}{OD_c} \times 100 \quad (2)$$

where OD_s is the optical density of the sample; OD_c is the optical density of the control.

To study the ability of the strains to produce ammonia, a cell suspension was prepared using the method described earlier and inoculated on 1% peptone water. The cells were cultivated at 28 ± 2°C at 110 rpm for 48 h

and then separated from the culture fluid as described earlier. Then, 150 μL of Nessler's reagent (LenReaktiv, Russia) was added to 3 mL of the culture fluid and shaken. At the same time, a control sample (nutrient medium with Nessler's reagent) was prepared under the same conditions. The optical densities of the experimental and control samples were determined at 450 nm. The optical density of the sample was calculated according to Eq. (1). The amount of ammonia was determined by using a calibration graph of standard ammonium solutions at concentrations from 50 to 300 μg/mL [46].

To study the ability of the strains to fix nitrogen, a cell suspension was prepared in a physiological solution as described above and the resulting suspension was inoculated on Ashby broth (HiMedia Laboratories, India). The cells were cultivated and separated from the culture fluid under the conditions described for the ammonia production analysis. The amount of nitrogen in the culture fluid was measured with a Rapid N Cube nitrogen analyzer (Elementar, Germany) [44].

To study the ability of the strains to solubilize phosphates, a strain suspension was prepared as described above for the nitrogen fixation analysis. The resulting suspension was inoculated on Pikovskaya's broth (HiMedia Laboratories, India) and cultivated. The culture fluid was separated from the cells under the conditions described for the ammonia production analysis. Next, 1 mL of the culture liquid was mixed with 4.5 mL of a chloromolybdic acid solution (1.5 g ammonium molybdate (ChemExpress, Russia) dissolved in 40 mL of distilled water was mixed with 34.2 mL concentrated hydrochloric acid and made up to 100 mL with distilled water) and 25 μL of a chlorostannic acid solution (2.5 g tin chloride (ProfSnab, Russia) dissolved in 10 mL concentrated hydrochloric acid and made up to 100 mL with distilled water). The resulting solution was allowed to stand at 22–24°C for 15 min. The experimental and control optical densities were determined at 600 nm. The optical density of the sample was calculated by using Eq. (1). The amount of dissolved phosphorus was measured by using a calibration graph of a standard solution of dipotassium phosphate (LenReaktiv, Russia) at concentrations from 50 to 300 μg/mL [47].

To study the ability of the strains to solubilize zinc, a strain was inoculated in Petri dishes on the medium consisting of (g/L): 10.0 of glucose (ChemExpress, Russia), 1.0 ammonium sulfate (Dia-M, Russia), 0.2 potassium chloride (LenReaktiv, Russia), 0.1 potassium phosphate disubstituted, 0.2 magnesium sulfate (ChemExpress, Russia), 1.0 zinc oxide (LenReaktiv, Russia), and 15.0 agar-agar. The strain was cultured in a TSO-1/80 SPU thermostat (Smolensk Software Control Systems Design, Russia) for 4 days at 28 ± 2°C. A clearing zone around the colony indicated the strain's ability to solubilize zinc [48].

To study the ability of the strains to produce ACC deaminase, a strain was streaked in Petri dishes on the medium containing (g/L): 2.0 of ammonium sulfate, 4.0 potassium monobasic phosphate (LenReaktiv, Russia), 6.0 sodium dibasic phosphate (LenReaktiv, Russia), 0.2 magnesium sulfate, 0.001 ferrous sulfate (ChemExpress, Russia), 15.0 agar-agar, as well as solutions (1 mL each) of 0.01 g/L boric acid (KhimBaza, Russia), 0.01 g/L manganese sulfate (KhimBaza, Russia), 0.07 g/L zinc sulfate (ChemExpress, Russia), and 0.05 g/L copper sulfate (ChemExpress, Russia). The strain was cultured as described above. The growth of the culture indicated its ability to produce ACC deaminase [46].

To study the ability of the strains to produce biofilms, a strain was streaked in Petri dishes on the medium containing (g/L): 0.8 of Congo red (Dia-M, Russia), 50.0 sucrose (ChemExpress, Russia), 37.0 Brain Heart Infusion Broth (Micro-Lab, Russia), and 15.0 agar-agar. The strain was cultured as described above. The black color of the culture indicated its ability to produce biofilms [46].

The antagonistic activity of the bacterial strains was analyzed by using the following phytopathogens: *Fusarium graminearum* F-877, *Bipolaris sorokiniana* F-529, *Botrytis cinerea* F-1006, Erwinia rhapontici B-9292, and *Xanthomonas campestris* B-4102. The phytopathogenic fungi and bacteria were cultured in test tubes with potato-glucose agar (LenReaktiv, Russia) and GMF agar (LenReaktiv, Russia), respectively. A 24-h culture of a bacterium grown on a liquid Luria-Bertani medium (Miller's modification) was pour-plated into Petri dishes and incubated for 24 h at 28–30°C. Then, an agar block with the test culture was cut out and inserted into the well of an agar disk in the Petri dish with the phytopathogens. The phytopathogens were spread on agar washings. The bacterial suspension with a McFarland turbidity of 0.8 (1.5×10^8 CFU/cm^3) was law-plated. The Petri dishes were refrigerated for 8 h at 4°C to allow the metabolites of bacterial monocultures to diffuse from the block into the thickness of the agar with the test culture. Then, the phytopathogenic fungi were incubated in a thermostat at 26–28°C [49].

The laboratory tests were conducted according to State Standard 12038-84. For them, we used the varieties "Siberian Alliance", "The Hope of Kuzbass", and "In Memory of Aphrodite" of spring soft wheat (*Triticum aestivum* L.) and the microbiological fertilizer "Azofit" (SibBioPharm, Russia) based on nitrogen-fixing bacteria. The seeds were incubated in a Stellar-Fito LINE rack for plant growth (AWTech, Russia) at 20 ± 2°C.

On day 7 of incubation, we determined their germination (Eq. (3)). The length and weight of the sprout and root; as well as the contents of total chlorophyll, carotenoids, nitrogen, and protein.

$$G = \frac{N_{sd}}{N_{sp}} \times 100 \quad (3)$$

where G is the germination, %; N_{sd} is the number of seedlings; N_{sp} is the number of planted seeds.

To determine the pigment content, crushed leaves were extracted with 70% ethanol, kept for 30 min in a boiling water bath, and filtered. The sediment was filled with 70% ethanol and filtered. The pigment absorption was measured spectrophotometrically at 667 (total chlorophyll) and 480 nm (carotenoids) [50].

The nitrogen content in the above-ground part of the plants was determined on a Rapid N Cube nitrogen analyzer as described in the manual.

RESULTS AND DISCUSSION

The cultural and morphological characteristics of the test strains are presented in Fig. 1.

The bacterial strains *Ensifer meliloti* 441 B-219, *Ensifer mexicanus* B-4064, and *Rhizobium tropici* B-216 form white, round colonies. Their cells are rod-shaped and belong to gram-negative bacteria.

The growth-stimulating activity of the test microorganisms is presented in Figs. 2–6.

As can be seen in Fig. 2, *E. meliloti* 441 B-219 produced ACC deaminase and biofilms, *Ensifer mexicanus* B-4064 produced ACC deaminase and solubilized zinc, while *Rhizobium tropici* B-216 produced ACC deaminase.

As can be seen in Fig. 4, the amount of synthesized indolyl-3-acetic acid varied from 0.35 to 8.76 μg/mL, with *E. mexicanus* B-4064 showing the highest activity (8.76 μg/mL). The amount of gibberellic acid varied from 0.58 to 1.19 mg/mL, with *E. meliloti* 441 B-219 exhibiting the highest activity (1.19 mg/mL). The content of siderophores ranged from 43.2 to 51.5%, with *E. mexicanus* B-4064 displaying the highest activity (51.5%).

The ammonia content varied from 186 to 298 μg/mL, with *E. meliloti* 441 B-219 exhibiting the highest activity (298 μg/mL). The nitrogen content ranged from 175 to 194 μg/mL, with *R. tropici* B-216 showing the highest activity (194 μg/mL). The soluble phosphorus content varied from 100 to 229 μg/mL, with *E. mexicanus* B-4064 revealing the highest activity (229 μg/mL).

Our results were consistent with other studies. For example, Metuge *et al.* reported that *R. tropici* formed biofilms by synthesizing extracellular polymeric substances [51]. Imada *et al.* found that *R. tropici* CIAT 899 synthesized indole-3-acetic acid via the indole-3-pyruvate pathway. They also reported that the synthesis of this phytohormone was significantly inhibited by the presence of NH_4+ in the medium [52]. Sijilmassi *et al.* found that *R. tropici* CIAT 899 synthesized gibberellic acid and solubilized insoluble forms of phosphorus [53]. The ability of *R. tropici* to produce ACC deaminase might explain its ability to form rhizobial nodules. In addition, ACC deaminase plays a significant role in the antagonistic activity of the strains against phytopathogens [54].

Spini *et al.* reported that *E. meliloti* 3001 formed biofilms, as well as produced indole-3-acetic acid and siderophores [55]. Primo *et al.* found that the strains of *E. meliloti* had a varying ability to form agglomerates. For example, *E. meliloti* SR9 demonstrated high autoaggregation phenotypes, while *E. meliloti* CU10 was not capable of forming biofilms [56]. The authors suggested that these differences may be associated with metabolic variations, especially with the production of exopolysaccharides. They observed a correlation between the phenotypic morphology of colonies (mucoid colonies are prone to biofilm formation) and their ability to synthesize exopolysaccharides. Our results confirm this relationship: *E. meliloti* 441 B-219, which exhibits a mucoid colony morphology, demonstrated the ability to form biofilms *in vitro*. In another study, Checcucci *et al.* described the ability of *Sinorhizobium meliloti* 1021 to synthesize ACC desamenase, which is probably involved in rhizosphere colonization or endophytic behavior [57]. According to Alami *et al.*, the strains of *E. meliloti* isolated from the plants growing in the abandoned tailings of the Zayda mine had the ability to solubilize insoluble forms of phosphorus [58]. This finding was confirmed by Borj *et al.* [59].

Current literature lacks data on the growth-promoting properties of *E. mexicanus*. Our study is the first to describe the ability of *E. mexicanus* B-4064 to produce phytohormones, siderophores, and ACC deaminase, as well as to mobilize zinc and phosphorus. These properties open up new possibilities for using this strain in agricultural technologies to increase crop yields. Our findings provide an insight into the biological potential of *E. mexicanus* and expand the range of potentially useful microorganisms for sustainable agriculture.

The antagonistic activity of the bacterial strains against the most common fungal and bacterial phytopathogens

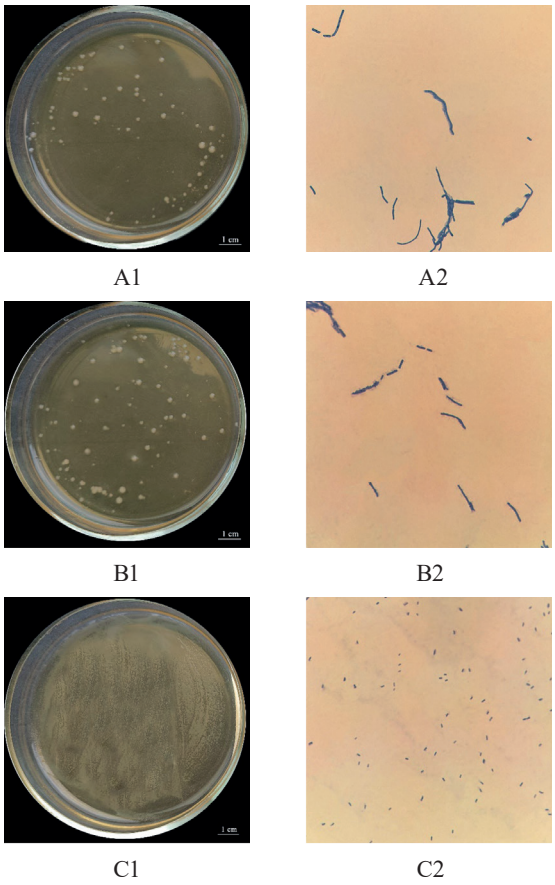

Figure 1 Cultural and morphological characteristics of *Ensifer meliloti* 441 B-219 (A), *Ensifer mexicanus* B-4064 (B), and *Rhizobium tropici* B-216 (C): 1 – cultural characteristics during growth on a solid medium after 24-h cultivation, 2 – morphological characteristics, with methylene blue staining (magnified ×1000)

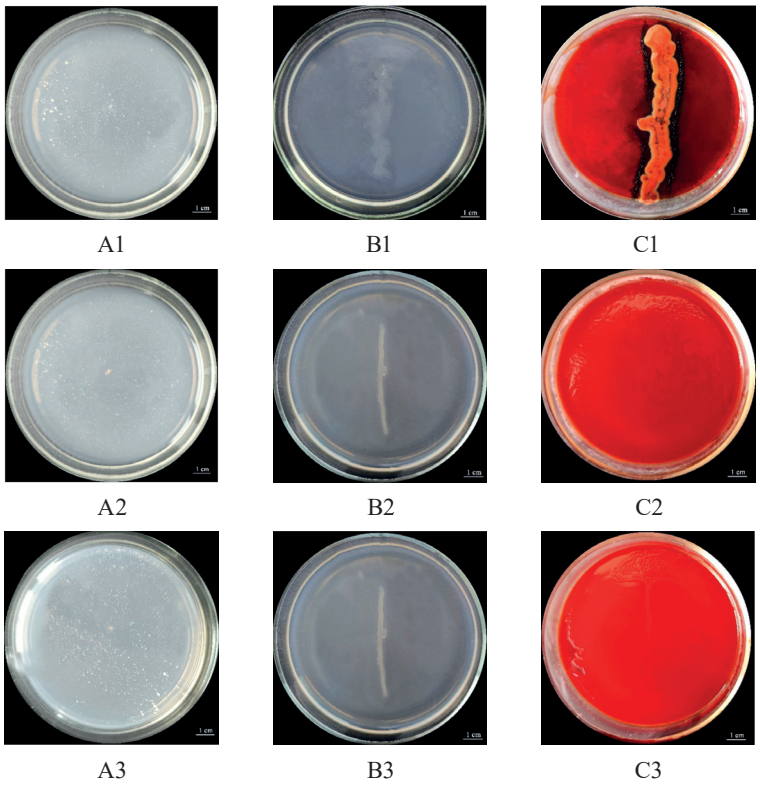

Figure 2 The ability of *Ensifer meliloti* 441 B-219 (1), *Ensifer mexicanus* B-4064 (2), and *Rhizobium tropici* B-216 (3) to solubilize zinc (A), produce ACC deaminase (B), and biofilms (C)

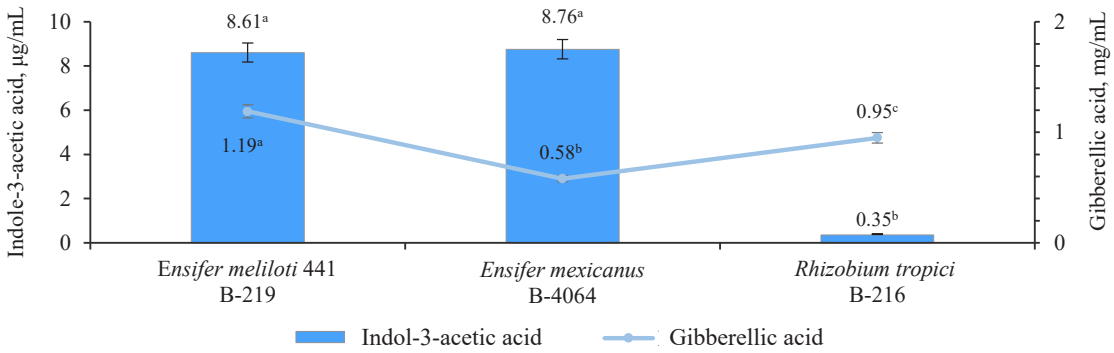

The letters to the right of the values indicate the significance of differences between the strains (within one parameter) according to ANOVA and the Scheffe test. The same letters mean no significance

Figure 3 Phytohormone-producing ability of the strains under study

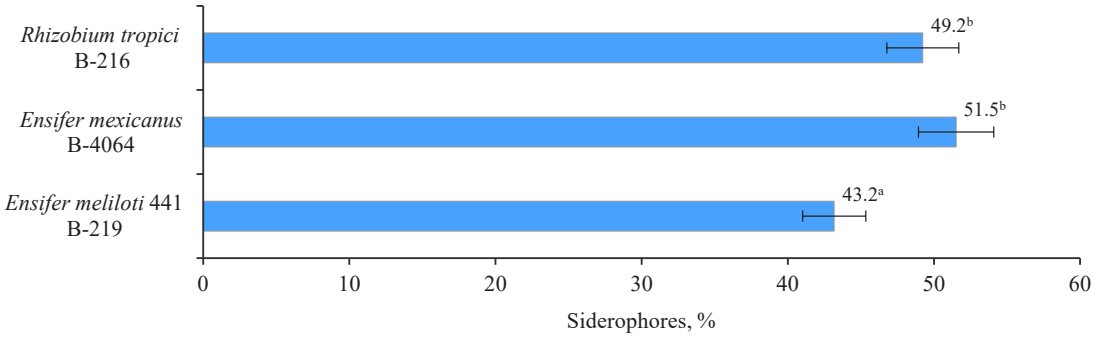

The letters to the right of the values indicate the significance of differences between the strains (within one parameter) according to ANOVA and the Scheffe test. The same letters mean no significance

Figure 4 Siderophore-producing ability

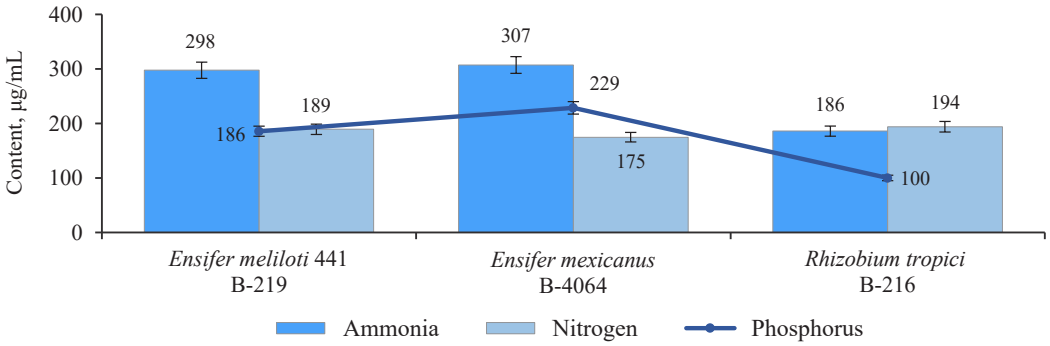

The letters to the right of the values indicate the significance of differences between the strains (within one parameter) according to ANOVA and the Scheffe test. The same letters mean no significance

Figure 5 The ability of the strains to produce ammonia, nitrogen, and phosphorus

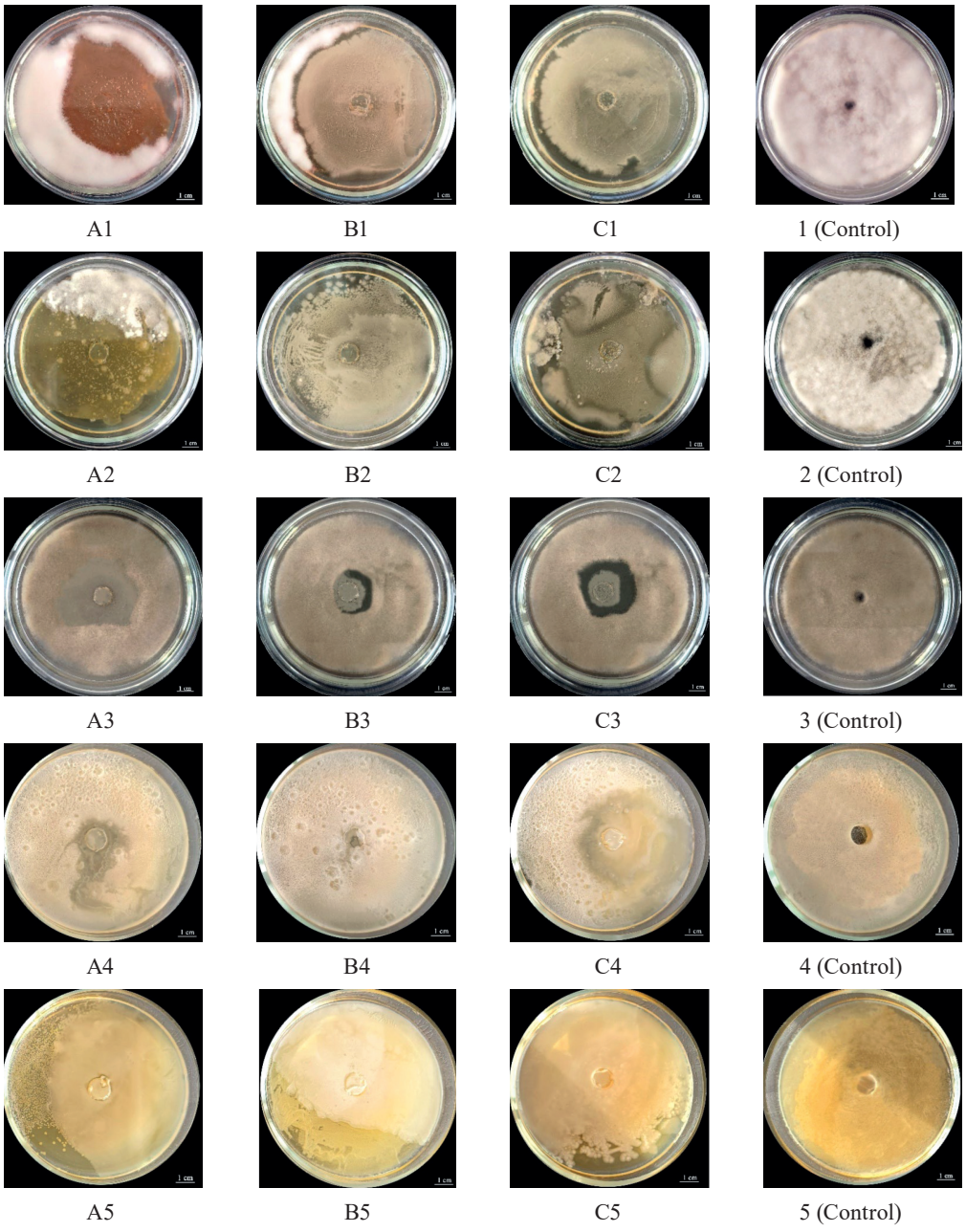

Figure 6 Antagonistic activity of *Ensifer meliloti* 441 B-219 (A), *Ensifer mexicanus* B-4064 (B), and *Rhizobium tropici* B-216 (C) against *Fusarium graminearum* F-877 (1), *Bipolaris sorokiniana* F-529 (2), *Botrytis cinerea* F-1006 (3), Erwinia rhapontici B-9292 (4), and *Xanthomonas campestris* B-4102 (5)

Table 1 Antagonistic activity of the bacterial strains

Strain	Antagonistic activity against, mm				
	Fusarium graminearum F-877	*Bipolaris sorokiniana* F-529	*Botrytis cinerea* F-1006	*Erwinia rhapontici* B-9292	*Xanthomonas campestris* B-4102
Ensifer meliloti 441 B-219	67 ± 3	65 ± 3	55 ± 2	23 ± 1	95 ± 5
Ensifer mexicanus B-4064	90 ± 5	95 ± 5	25 ± 1	–	77 ± 3
Rhizobium tropici B-216	95 ± 5	72 ± 4	40 ± 1	45 ± 2	95 ± 4

Table 2 Laboratory testing of strains on spring soft wheat varieties

Sample treatment	Germination, %	Average sprout length, mm	Average root length, mm	Average weight of one sprout, mg	Average weight of one root, mg
Siberian Alliance					
Water	87 ± 4	124 ± 5	94 ± 3	27.3 ± 1.0	20.9 ± 0.9
Azofit	87 ± 3	125 ± 6	97 ± 3	30.3 ± 1.3	23.4 ± 1.0
Ensifer meliloti 441 B-219	89 ± 4	158 ± 7	138 ± 5	34.5 ± 1.5	24.0 ± 1.0
Ensifer mexicanus B-4064	92 ± 4	133 ± 4	105 ± 4	32.4 ± 1.2	27.6 ± 1.2
Rhizobium tropici B-216	82 ± 4	163 ± 6	102 ± 4	39.0 ± 1.5	29.5 ± 1.0
The Hope of Kuzbass					
Water	88 ± 5	129 ± 5	91 ± 3	27.3 ± 1.2	24.4 ± 1.2
Azofit	89 ± 4	134 ± 6	89 ± 2	28.0 ± 1.3	22.2 ± 1.1
Ensifer meliloti 441 B-219	90 ± 5	172 ± 4	130 ± 4	28.6 ± 1.2	27.0 ± 1.0
Ensifer mexicanus B-4064	95 ± 3	156 ± 7	93 ± 4	32.0 ± 1.0	25.7 ± 1.3
Rhizobium tropici B-216	91 ± 4	191 ± 9	97 ± 5	38.9 ± 1.6	26.9 ± 1.2
In Memory of Aphrodite					
Water	76 ± 3	138 ± 5	91 ± 3	29.5 ± 1.2	22.8 ± 1.1
Azofit	75 ± 3	142 ± 6	91 ± 4	30.7 ± 1.5	21.7 ± 1.0
Ensifer meliloti 441 B-219	78 ± 2	157 ± 4	128 ± 4	31.3 ± 1.3	26.0 ± 1.2
Ensifer mexicanus B-4064	77 ± 4	145 ± 5	95 ± 2	33.1 ± 1.2	24.8 ± 1.0
Rhizobium tropici B-216	81 ± 4	199 ± 6	97 ± 4	41.2 ± 1.8	24.1 ± 1.3

(*Fusarium graminearum* F-877, *Bipolaris sorokiniana* F-529, *Botrytis cinerea* F-1006, *Erwinia rhapontici* B-9292, and *Xanthomonas campestris* B-4102) is shown in Fig. 6 and Table 1.

The bacterial strain *E. meliloti* 441 B-219 showed high antagonistic activity against *F. graminearum* F-877, *B. sorokiniana* F-529, and *X. campestris* B-4102. These results are consistent with those obtained by other scientists. For example, Batnini *et al.* reported that *S. meliloti* inhibited the growth of *Fusarium oxysporum*. In addition, they observed higher contents of proline and sucrose in the above-ground parts of the plants treated with the strain and infected with the phytopathogen. This indicates the ability of *S. meliloti* to mitigate biotic stress caused by *F. oxysporum* [60]. Our study revealed that *E. meliloti* strains have bactericidal properties.

E. mexicanus B-4064 exhibited high antagonistic activity against *F. graminearum* F-877, *B. sorokiniana* F-529, and *X. campestris* B-4102. However, it did not inhibit the growth of *E. rhapontici* B-9292.

The bacterial strain *R. tropici* B-216 showed high antagonistic activity against *F. graminearum* F-877, *B. sorokiniana* F-529, and *X. campestris* B-4102. According to Volpiano *et al.*, this may be due to the production of volatile organic compounds. The authors, who studied the strain *R. tropici* SEMIA 4077, reported that it inhibited 45% of *Sclerotium (Athelia) rolfsii* mycelium *in vitro* [61]. However, our study was the first to observe the inhibitory effect of the strain *R. tropici* B-216 on *F. graminearum*, *B. sorokiniana* and *X. campestris*. Thus, our results expand the understanding of its potential as a biological control agent.

Table 2 and Figs. 7–9 demonstrate the ability of the strains to stimulate the growth and development of the spring soft wheat varieties "Siberian Alliance", "The Hope of Kuzbass", and "In Memory of Aphrodite" under laboratory conditions.

The treatment of spring soft wheat with *E. meliloti* 441 B-219 did not have a significant positive effect on the germination or the weight of the sprout and root. However, it demonstrated a positive effect on the length of the sprout and root compared to the control group (treated with water and the microbial preparation Azofit). In the Siberian Alliance variety, the sprout length increased by 34 and 33 mm and the root length increased by 44 and 41 mm compared to the water-treated and Azofit-treated samples, respectively. In the Hope of Kuzbass variety, the sprout length, root length, and root weight increased by 40.5 mm, 40 mm, and 3.7 mg, respectively. In the variety In Memory of Aphrodite, the root length and root weight increased by 37 mm and 3.8 mg, respectively.

The strain *E. mexicanus* B-4064 had a significant positive effect on the germination of the Siberian Alliance and the Hope of Kuzbass varieties, increasing it

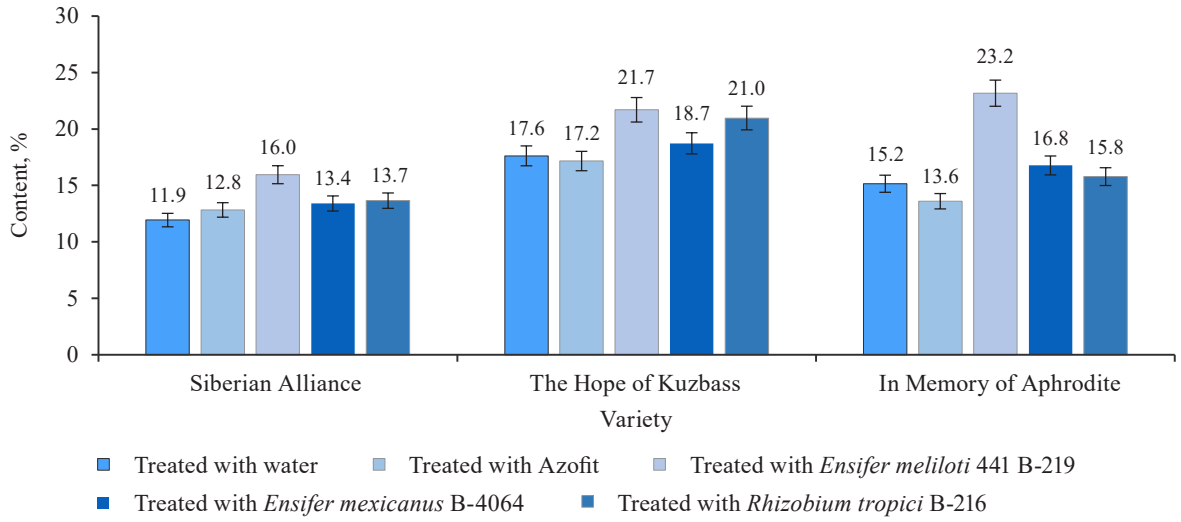

Figure 7 Total chlorophyll content in spring soft wheat sprouts

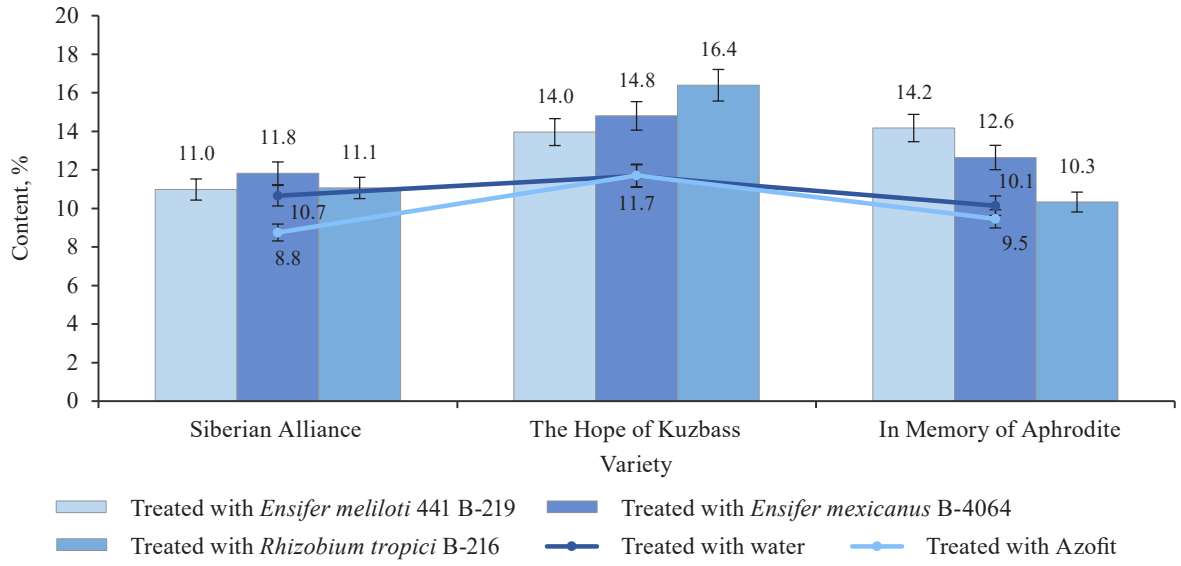

Figure 8 Carotenoid content in spring soft wheat sprouts

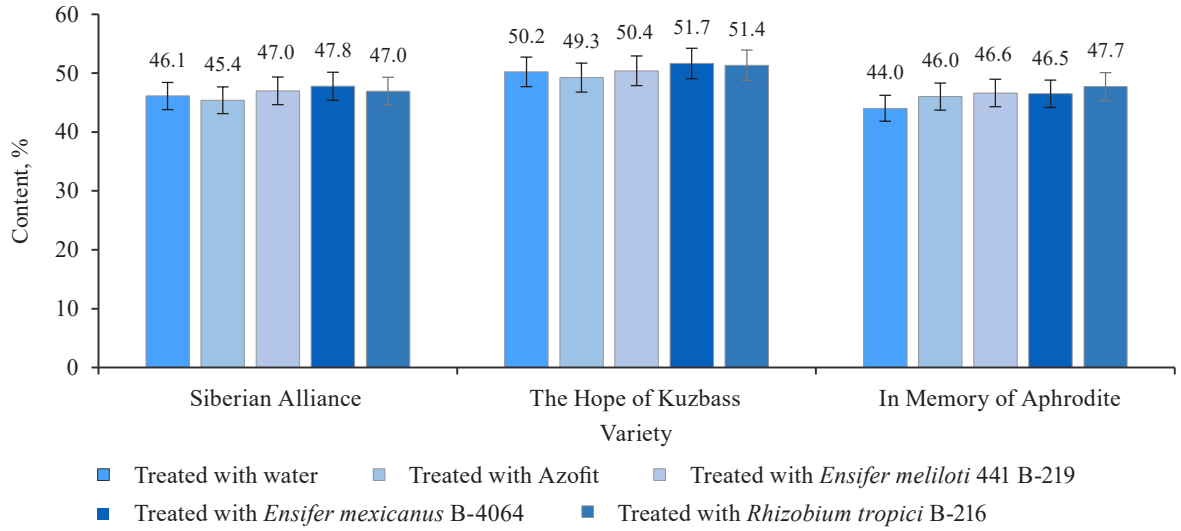

Figure 9 Nitrogen content in spring soft wheat sprouts

by 5 and 6.5%, respectively. However, no such effect was observed on the In Memory of Aphrodite variety.

The strain *R. tropici* B-216 had a positive effect on the three wheat varieties. In the Siberian Alliance variety, it increased the sprout length, sprout weight, and root weight by an average of 39.5 mm, 10.2 mg, and 7.4 mg, respectively, compared to the control group. In the Hope of Kuzbass variety, the strain increased the sprout length, sprout weight, and root weight by an average of 59.5 mm, 11.3 mg, and 3.4 mg, respectively. In the variety In Memory of Aphrodite, the strain increased the sprout length and weight by an average of 59 mm and 11.1 mg, respectively.

As can be seen in Fig. , *E. meliloti* 441 B-219 had a positive effect on the chlorophyll content in the wheat samples. In particular, the chlorophyll content amounted to 16.0, 21.7, and 23.2% of the mass in the Siberian Alliance, the Hope of Kuzbass, and In Memory of Aphrodite varieties, respectively. In the control group, the chlorophyll content reached 11.9, 17.6, and 15.2% in the water-treated samples of the three varieties, respectively; as well as 12.8, 17.2, and 13.6% in the Azofit-treated samples of the three varieties, respectively.

The *E. mexicanus* B-4064 strain did not have a significant positive effect on the total chlorophyll content in any of the spring soft wheat varieties. The *R. tropici* B-216 strain increased the chlorophyll content only in the Hope of Kuzbass variety (to 21.0%).

The *E. meliloti* 441 B-219 strain had a significant positive effect on the carotenoid content in the variety In Memory of Aphrodite (14.2%). In the control group, the carotenoid content reached 10.7, 11.7, and 10.1% in the water-treated samples of the Siberian Alliance, the Hope of Kuzbass, and In Memory of Aphrodite varieties, respectively; as well as 8.8, 11.7, and 9.5% in the Azofit-treated samples of the three varieties, respectively.

E. mexicanus B-4064 strain did not have a significant positive effect on the carotenoid content in any of the spring soft wheat varieties. *R. tropici* B-216 increased the carotenoid content only in the Hope of Kuzbass variety (to 16.4%).

The test rhizobia strains did not exert a significant positive effect on the nitrogen content in any of the three varieties of spring soft wheat. This might be due to the lack of nodules, specialized structures that ensure effective nitrogen fixation in legumes. The absence of nitrogen accumulation in the above-ground part of wheat may also be associated with its accumulation in the root system. However, even if rhizobia assumingly enhance nitrogen accumulation in the root system, their contribution to the total nitrogen content in wheat grain is quite insignificant. Nitrogen accumulation from vegetative organs during the pre-flowering period accounts for 50–95% [62] of the total nitrogen content in grain at harvest. Leaves and stems are the most important sources of nitrogen for grain [63], while the roots contribute only 10–15% [64]. Thus, nitrogen accumulation in the root system that could potentially result from rhizobia treatment is not a determining factor in agricultural practice.

Nevertheless, the rhizobia under study exerted a stimulating effect on the growth parameters and photosynthetic processes, contributing to longer shoots and roots, as well as higher chlorophyll and carotenoid contents. This might indicate that the rhizobia promote the formation of phytohormones, better absorption of other macro- and microelements, and changes in the morphogenesis of the root system. Further studies are needed to fully understand these mechanisms. In particular, there is a need to quantify phytohormones in plant tissues, study the microbial community of the rhizosphere, analyze the morphology of the root system, and determine the content of other nutrients. Controlled field experiments, which take into account the influence of abiotic factors, will allow us to assess the practical potential of the test rhizobia strains as biostimulants to increase wheat productivity. Our results can open up new directions for studying the interaction between rhizobia and cereal crops.

CONCLUSION

Symbiotic nitrogen fixation by rhizobia in association with legumes is a fundamental process of the nitrogen cycle that plays a key role in the productivity of agroecosystems. Although we fully understand the mechanisms of this interaction, the potential of rhizobia as growth promoters for non-legume plants needs to be studied further. In this study, we assessed the phytopromoting properties of three rhizobia strains: *Ensifer meliloti* 441 B-219, *Ensifer mexicanus* B-4064, and *Rhizobium tropici* B-216.

According to our results, *E. meliloti* 441 B-219 produced ACC deaminase and formed biofilms. The strain also produced phytohormones (8.61 μg/mL indolyl-3-acetic acid and 1.19 mg/mL gibberellic acid), siderophores (43.2%), ammonia (297.53 μg/mL), and nitrogen (189.22 μg/mL), as well as solubilized phosphates (185.71 μg/mL). In addition, *E. meliloti* exhibited pronounced antagonistic activity against *Fusarium graminearum* F-877, *Bipolaris sorokiniana* F-529, and *Xanthomonas campestris* B-4102.

E. mexicanus B-4064 synthesized ACC deaminase and solubilized zinc. The strain also produced phytohormones (8.76 μg/mL indolyl-3-acetic acid and 0.58 mg/mL gibberellic acid), siderophores (51.5%), ammonia (307.2 μg/mL), and nitrogen (174.78 μg/mL), as well as solubilized phosphates (228.57 μg/mL). *E. mexicanus* inhibited the growth of *F. graminearum* F-877, *B. sorokiniana* F-529, and *X. campestris* B-4102, but did not exhibit antagonistic activity against *Erwinia rhapontici* B-9292.

R. tropici B-216 synthesized ACC deaminase, phytohormones (0.35 μg/mL indolyl-3-acetic acid and 0.95 mg/mL gibberellic acid), and siderophores (49.2%). It also produced ammonia (185.87 μg/mL) and nitrogen (193.95 μg/mL), as well as solubilized phosphates (100.00 μg/mL). The strain had high antagonistic activity against the phytopathogens *F. graminearum* F-877, *B. sorokiniana* F-529, and *X. campestris* B-4102.

The spring wheat seeds treated with *E. meliloti* 441 B-219 and *R. tropici* B-216 had longer shoots and roots, as well as higher contents of chlorophyll and carotenoids (in some wheat varieties). *R. tropici* B-216 demonstrated the most pronounced positive effect on the length of shoots, as well as on the mass of the above-ground and underground parts in all wheat varieties. *E. mexicanus* B-4064 produced a significant positive effect only on seed germination. However, none of the bacterial strains had a statistically significant effect on the nitrogen content in the above-ground parts of the plants.

Although the rhizobia under study had no effect on the nitrogen content in the above-ground parts of the wheat plants, these strains have potential in agricultural practices due to their complex effect on the plants. In particular, they stimulate growth, increase stress resistance, and improve the absorption of nutrients such as phosphorus and zinc. Therefore, the use of the rhizobia can be more effective than the use of individual chemicals. In addition, the biological methods for increasing plant productivity are more environmentally friendly compared to the use of chemical fertilizers and pesticides.

However, further large-scale field trials under different agro-climatic conditions are needed to confirm the practical potential, long-term effects, and economic feasibility of using the rhizobia.

CONTRIBUTION

The authors were equally involved in writing the manuscript and are equally responsible for plagiarism.

CONFLICT OF INTEREST

The authors declare that there is no conflict of interest regarding this publication.

REFERENCES

1. Kaplan D, Maymon M, Agapakis CM, Lee A, Wang A, Prigge BA, *et al.* A survey of the microbial community in the rhizosphere of two dominant shrubs of the Negev Desert highlands, *Zygophyllum dumosum* (Zygophyllaceae) and *Atriplex halimus* (Amaranthaceae), using cultivation-dependent and cultivation-independent methods. American Journal of Botany. 2013;100(9):1713–1725. https://doi.org/10.3732/ajb.1200615
2. Quiza L, St-Arnaud M, Yergeau E. Harnessing phytomicrobiome signaling for rhizosphere microbiome engineering. Frontiers in Plant Science. 2015;6:507. https://doi.org/10.3389/fpls.2015.00507
3. Leach JE, Triplett LR, Argueso CT, Trivedi P. Communication in the Phytobiome. Cell. 2017;169(4):587–596. https://doi.org/10.1016/j.cell.2017.04.025
4. Berendsen RL, Pieterse CMJ, Bakker PAHM. The rhizosphere microbiome and plant health. Trends in Plant Science. 2012;17(8):478–486. https://doi.org/10.1016/j.tplants.2012.04.001
5. Burén S, Rubio LM. State of the art in eukaryotic nitrogenase engineering. FEMS Microbiology Letters. 2018;365(2):fnx274. https://doi.org/10.1093/femsle/fnx274
6. Dai Z, Guo X, Yin H, Liang Y, Cong J, Liu X. Identification of nitrogen-fixing genes and gene clusters from metagenomic library of acid mine drainage. PLoS ONE. 2014;9(2):e87976. https://doi.org/10.1371/journal.pone.0087976
7. Seefeldt LC, Hoffman BM, Peters JW, Raugei S, Beratan DN, Antony E, *et al.* Energy transduction in nitrogenase. Accounts of Chemical Research. 2018;51(9):2179–2186. https://doi.org/10.1021/acs.accounts.8b00112
8. Nonaka A, Yamamoto H, Kamiya N, Kotani H, Yamakawa H, Tsujimoto R, *et al.* Accessory proteins of the nitrogenase assembly, NifW, NifX/NafY, and NifZ, Are essential for diazotrophic growth in the nonheterocystous canobacterium *Leptolyngbya boryana*. Frontiers in Microbiology. 2019;10:495. https://doi.org/10.3389/fmicb.2019.00495
9. White J, Prell J, James EK, Poole P. Nutrient sharing between symbionts. Plant Physiology. 2007;144(2):604–614. https://doi.org/10.1104/pp.107.097741
10. Andrews M, Raven JA, Lea PJ. Do plants need nitrate? The mechanisms by which nitrogen form affects plants. Annals of Applied Biology. 2013;163(2):174–199. https://doi.org/10.1111/aab.12045
11. Raven JA. Why are mycorrhizal fungi and symbiotic nitrogen-fixing bacteria not genetically integrated into plants? Annals of Applied Biology. 2010;157(3):381–391. https://doi.org/10.1111/j.1744-7348.2010.00435.x
12. Shah A, Nazari M, Antar M, Msimbira LA, Naamala J, Lyu D, *et al.* PGPR in agriculture: A sustainable approach to increasing climate change resilience. Frontiers in Sustainable Food Systems. 2021;5:667546. https://doi.org/10.3389/fsufs.2021.667546
13. Santi C, Bogusz D, Franche C. Biological nitrogen fixation in non-legume plants. Annals of Botany. 2013;111(5):743–767. https://doi.org/10.1093/aob/mct048
14. Mus F, Crook MB, Garcia K, Costas AG, Geddes BA, Kouri ED, *et al.* Symbiotic nitrogen fixation and the challenges to its extension to nonlegumes. Applied and Environmental Microbiology. 2016;82(13):3698–3710. https://doi.org/10.1128/AEM.01055-16
15. Trabelsi D, Mhamdi R. Microbial inoculants and their impact on soil microbial communities: A review. BioMed Research International. 2013;2013(11):863240. https://doi.org/10.1155/2013/863240

16. Gopalakrishnan S, Srinivas V, Prakash B, Sathya A, Vijayabharathi R. Plant growth-promoting traits of *Pseudomonas geniculata* isolated from chickpea nodules. 3 Biotech. 2015;5:653–661. https://doi.org/10.1007/s13205-014-0263-4
17. Gopalakrishnan S, Srinivas V, Samineni S. Nitrogen fixation, plant growth and yield enhancements by diazotrophic growth-promoting bacteria in two cultivars of chickpea (*Cicer arietinum* L.). Biocatalysis and Agricultural Biotechnology. 2017;11:116–123. https://doi.org/10.1016/j.bcab.2017.06.012
18. Ivanova S, Vesnina A, Fotina N, Prosekov A. An overview of carbon footprint of coal mining to curtail greenhouse gas emissions. Sustainability. 2022;14(22):15135. https://doi.org/10.3390/su142215135
19. Gopalakrishnan S, Srinivas V, Vemula A, Samineni S, Rathore A. Influence of diazotrophic bacteria on nodulation, nitrogen fixation, growth promotion and yield traits in five cultivars of chickpea. Biocatalysis and Agricultural Biotechnology. 2018;15:35–42. https://doi.org/10.1016/j.bcab.2018.05.006
20. Yanni YG, Rizk RY, Corich V, Squartini A, Ninke K, Philip-Hollingsworth S, *et al.* Natural endophytic association between Rhizobium leguminosarum bv. trifolii and rice roots and assessment of its potential to promote rice growth. Plant and Soil. 2004;194:99–114. https://doi.org/10.1023/A:1004269902246
21. Gebhardt C, Turner GL, Gibson AH, Dreyfus BL, Bergersen FJ. Nitrogen-fixing growth in continuous culture of a strain of *Rhizobium* sp. isolated from stem nodules on *Sesbania rostrata*. Microbiology. 1984;130(4):843–848. https://doi.org/10.1099/00221287-130-4-843
22. Baset Mia MA, Shamsuddin ZH. Rhizobium as a crop enhancer and biofertilizer for increased cereal production. African Journal of Biotechnology. 2010:9(37):6001–6009.
23. Gopalakrishnan S, Sathya A, Vijayabharathi R, Varshney RK, Gowda CLL, Krishnamurthy L. Plant growth promoting rhizobia: Challenges and opportunities. 3 Biotech. 2015;5:355–377. https://doi.org/10.1007/s13205-014-0241-x
24. Das K, Prasanna R, Saxena AK. Rhizobia: A potential biocontrol agent for soilborne fungal pathogens. Folia Microbiologica. 2017;62:425–435. https://doi.org/10.1007/s12223-017-0513-z
25. Dent D, Cocking E. Establishing symbiotic nitrogen fixation in cereals and other non-legume crops: The Greener Nitrogen Revolution. Agriculture and Food Security. 2017;6:7. https://doi.org/10.1186/s40066-016-0084-2
26. Smercina DN, Evans SE, Friesen ML, Tiemann LK. To fix or not to fix: Controls on free-living nitrogen fixation in the rhizosphere. Applied and Environmental Microbiology. 2019:85:e02546-18. https://doi.org/10.1128/AEM.02546-18
27. Kennedy IR, Islam N. The current and potential contribution of asymbiotic nitrogen fixation to nitrogen requirements on farms: A review. Australian Journal of Experimental Agriculture. 2001;41(3):447–457. https://doi.org/10.1071/EA00081
28. de Oliveira ALM, de Lima Canuto E, Massena Reis V, Ivo Baldani J. Response of micropropagated sugarcane varieties to inoculation with endophytic diazotrophic bacteria. Brazilian Journal of Microbiology. 2003;34:59–61. https://doi.org/10.1590/S1517-83822003000500020
29. Pankievicz VCS, do Amaral FP, Santos KFDN, Agtuca B, Xu Y, Schueller MJ, *et al.* Robust biological nitrogen fixation in a model grass–bacterial association. The Plant Journal. 2015;81(6):907–919. https://doi.org/10.1111/tpj.12777
30. van Deynze A, Zamora P, Delaux P-M, Heitmann C, Jayaraman D, Rajasekar S, *et al.* Nitrogen fixation in a landrace of maize is supported by a mucilage-associated diazotrophic microbiota. PLoS Biology. 2018;16(8):e2006352. https://doi.org/10.1371/journal.pbio.2006352
31. Carelli M, Gnocchi S, Fancelli S, Mengoni A, Paffetti D, Scotti C, *et al.* Genetic diversity and dynamics of *Sinorhizobium meliloti* populations nodulating different alfalfa cultivars in Italian soils. Applied and Environmental Microbiology. 2000;66(11):4785–4789. https://doi.org/10.1128/AEM.66.11.4785-4789.2000
32. Pini F, Frascella A, Santopolo L, Bazzicalupo M, Biondi EG, Scotti C, *et al.* Exploring the plant-associated bacterial communities in *Medicago sativa* L. BMC Microbiology. 2012;12:78. https://doi.org/10.1186/1471-2180-12-78
33. Pan H, Wang D. Nodule cysteine-rich peptides maintain a working balance during nitrogen-fixing symbiosis. Nature Plants. 2017;3:17048. https://doi.org/10.1038/nplants.2017.48
34. Lloret L, Ormeño-Orrillo E, Rincón R, Martínez-Romero J, Rogel-Hernández MA, Martínez-Romero E. *Ensifer mexicanus* sp. nov. a new species nodulating *Acacia angustissima* (Mill.) Kuntze in Mexico. Systematic and Applied Microbiology. 2007;30(4):280–290. https://doi.org/10.1016/j.syapm.2006.12.002
35. Gomes DF, Ormeño-Orrillo E, Hungria M. Biodiversity, symbiotic efficiency, and genomics of *Rhizobium tropici* and related species. In: de Bruijn FJ, editor. Biological nitrogen fixation. John Wiley & Sons; 2015. pp. 747–765. https://doi.org/10.1002/9781119053095.ch74
36. Estévez J, Soria-Díaz ME, de Córdoba FF, Morón B, Manyani H, Gil A, *et al.* Different and new Nod factors produced by *Rhizobium tropici* CIAT899 following Na^+ stress. FEMS Microbiology Letters. 2009;293(2):220–231. https://doi.org/10.1111/j.1574-6968.2009.01540.x

37. del Cerro P, Rolla-Santos AAP, Gomes DF, Marks BB, del Rosario Espuny M, Rodríguez-Carvajal MÁ, *et al.* Opening the "black box" of *nodD3*, *nodD4* and *nodD5* genes of *Rhizobium tropici* strain CIAT 899. BMC Genomics. 2015;16:864. https://doi.org/10.1186/s12864-015-2033-z

38. del Cerro P, Rolla-Santos AAP, Gomes DF, Marks BB, Pérez-Montaño F, Rodríguez-Carvajal MÁ, *et al.* Regulatory *nodD1* and *nodD2* genes of *Rhizobium tropici* strain CIAT 899 and their roles in the early stages of molecular signaling and host-legume nodulation. BMC Genomics. 2015;16:251. https://doi.org/10.1186/s12864-015-1458-8

39. D'Haeze W, Holsters M. Nod factor structures, responses, and perception during initiation of nodule development. Glycobiology. 2002;12(6);79R–105R. https://doi.org/10.1093/glycob/12.6.79R

40. Relić B, Talmont F, Kopcinska J, Golinowski W, Promé JC, Broughton WJ. Biological activity of *Rhizobium* sp. NGR234 Nod-factors on *Macroptilium atropurpureum*. Molecular Plant-Microbe Interactions. 1993;6(6):764–774. https://doi.org/10.1094/mpmi-6-764

41. Miransari M, Smith D. Rhizobial lipo-chitooligosaccharides and gibberellins enhance barley (*Hordeum vulgare* L.) seed germination. Biotechnology. 2009;8(2):270–275. https://doi.org/10.3923/biotech.2009.270.275

42. Atuchin VV, Asyakina LK, Serazetdinova YuR, Frolova AS, Velichkovich NS, Prosekov AYu. Microorganisms for bioremediation of soils contaminated with heavy metals. Microorganisms. 2023;11(4):864. https://doi.org/10.3390/microorganisms11040864

43. Asyakina LK, Vorob'eva EE, Proskuryakova LA, Zharko MYu. Evaluating extremophilic microorganisms in industrial regions. Foods and Raw Materials. 2023;11(1):162–171. https://doi.org/10.21603/2308-4057-2023-1-556

44. Asyakina LK, Isachkova OA, Kolpakova DE, Borodina EE, Boger VYu, Prosekov AYu. The effect of a microbial consortium on spring barley growth and development in the Kemerovo region, Kuzbass. Grain Economy of Russia. 2024;16(1):104–112. (In Russ.). https://doi.org/10.31367/2079-8725-2024-90-1-104-112

45. Serazetdinova YuR, Bogacheva NN, Faskhutdinova ER, Asyakina LK, Proskuryakova LA. Aspects of the joint cultivation of *Bacillus amyloliquefaciens* and *Bacillus aryabhattai* for the intensification of growth-stimulating substances synthesis. Siberian Herald of Agricultural Science. 2024;54(6):41–48. (In Russ.). https://doi.org/10.26898/0370-8799-2024-6-4

46. Parashar M, Dhar SK, Kaur J, Chauhan A, Tamang J, Singh GB, *et al.* Two novel plant-growth-promoting *Lelliottia amnigena* isolates from *Euphorbia prostrata* aiton enhance the overall productivity of wheat and tomato. Plants. 2023;12(17):3081. https://doi.org/10.3390/plants12173081

47. Belkebla N, Bessai SA, Melo J, Caeiro MF, Cruz C, Nabti E. Restoration of *Triticum aestivum* growth under salt stress by phosphate-solubilizing bacterium isolated from southern Algeria. Agronomy. 2022;12(9):2050. https://doi.org/10.3390/agronomy12092050

48. Faskhutdinova ER, Fotina NV, Neverova OA, Golubtsova YuV, Mudgal G, Asyakina LK, *et al.* Extremophilic bacteria as biofertilizer for agricultural wheat. Foods and Raw Materials. 2024;12(2):348–360. https://doi.org/10.21603/2308-4057-2024-2-613

49. Asyakina LK, Mudgal G, Tikhonov SL, Larichev TA, Fotina NV, Prosekov AYu. Study of the potential of natural microbiota of spring soft wheat to increase yield. Achievements of Science and Technology in Agro-Industrial Complex. 2023;37(11):12–17. (In Russ.). https://elibrary.ru/HXXGEC

50. Kazerooni EA, Maharachchikumbura SSN, Adhikari A, Al-Sadi AM, Kang S-M, Kim L-R, *et al.* Rhizospheric *Bacillus amyloliquefaciens* protects *Capsicum annuum* cv. Geumsugangsan from multiple abiotic stresses *via* multifarious plant growth-promoting attributes. Frontiers in Plant Science. 2021;12:669693. https://doi.org/10.3389/fpls.2021.669693

51. Metuge JA, Havugimana E, Rugandirababisha J, Senwo ZM, Mutimawurugo MC. Evaluation of *Rhizobium tropici* – derived extracellular polymeric substances on selected soil properties, seed germination, and growth of black-eyed peas (*Vigna unguiculata*). Agricultural Sciences. 2024;15(5):548–564. https://doi.org/10.4236/as.2024.155031

52. Imada EL, Rolla dos Santos AAP, de Oliveira ALM, Hungria M, Rodrigues EP. Indole-3-acetic acid production via the indole-3-pyruvate pathway by plant growth promoter *Rhizobium tropici* CIAT 899 is strongly inhibited by ammonium. Research in Microbiology. 2017;168(3):283–292. https://doi.org/10.1016/j.resmic.2016.10.010

53. Sijilmassi B, Filali-Maltouf A, Fahde S, Ennahli Y, Boughribil S, Kumar S, *et al.* In-vitro plant growth promotion of rhizobium strains isolated from lentil root nodules under abiotic stresses. Agronomy. 2020;10(7):1006. https://doi.org/10.3390/agronomy10071006

54. Tavares MJ, Nascimento FX, Glick BR, Rossi MJ. The expression of an exogenous ACC deaminase by the endophyte *Serratia grimesii* BXF1 promotes the early nodulation and growth of common bean. Letters in Applied Microbiology. 2018;66(3):252–259. https://doi.org/10.1111/lam.12847

55. Spini G, Decorosi F, Cerboneschi M, Tegli S, Mengoni A, Viti, C, *et al.* Effect of the plant flavonoid luteolin on *Ensifer meliloti* 3001 phenotypic responses. Plant and Soil. 2016;399:159–178. https://doi.org/10.1007/s11104-015-2659-2

56. Primo ED, Cossovich S, Nievas F, Bogino P, Humm EA, Hirsch AM, *et al.* Exopolysaccharide production in *Ensifer meliloti* laboratory and native strains and their effects on alfalfa inoculation. Archives of Microbiology. 2020;202:391–398. https://doi.org/10.1007/s00203-019-01756-3

57. Checcucci A, Azzarello E, Bazzicalupo M, de Carlo A, Emiliani G, Mancuso S, *et al.* Role and regulation of ACC deaminase gene in *Sinorhizobium meliloti*: Is it a symbiotic, rhizospheric or endophytic gene? Frontiers in Genetics. 2017;8:6. https://doi.org/10.3389/fgene.2017.00006

58. Alami S, Bennis M, Lamin H, Kaddouri K, Bouhnik O, Lamrabet M, *et al.* The inoculation with *Ensifer meliloti* sv. rigiduloides improves considerably the growth of *Robinia pseudoacacia* under lead-stress. Plant and Soil. 2023; 497:119–137. https://doi.org/10.1007/s11104-023-05974-z

59. Aslani borj M, Etesami H, Alikhani HA. Silicon improves the effect of phosphate-solubilizing bacterium and arbuscular mycorrhizal fungus on the phosphorus concentration of salinity stressed alfalfa (*Medicago sativa* L.). Rhizosphere. 2022;24:100619. https://doi.org/10.1016/j.rhisph.2022.100619

60. Batnini M, Lopez-Gomez M, Palma F, Haddoudi I, Kallala N, Zribi K, *et al. Sinorhizobium* spp inoculation alleviates the effect of *Fusarium oxysporum* on *Medicago truncatula* plants by increasing antioxidant capacity and sucrose accumulation. Applied Soil Ecology. 2019;150:103458. https://doi.org/10.1016/j.apsoil.2019.103458

61. Gazolla Volpiano C, Lisboa BB, de São José JFB, de Oliveira AMR, Beneduzi A, Pereira Passaglia LM, *et al. Rhizobium* strains in the biological control of the phytopathogenic fungi *Sclerotium* (*Athelia*) *rolfsii* on the common bean. Plant and Soil. 2018;432:229–243. https://doi.org/10.1007/s11104-018-3799-y

62. Palta JA, Fillery IRP. N application enhances remobilization and reduces losses of pre-anthesis N in wheat grown on a duplex soil. Australian Journal of Agricultural Research. 1995;46(3):519–531. https://doi.org/10.1071/AR9950519

63. Critchley CS. A physiological explanation for the canopy nitrogen requirement of winter wheat. PhD thesis. University of Nottingham. 2001. 274 p.

64. Gaju O, Allard V, Martre P, Le Gouis J, Moreau D, Bogard M, *et al.* Nitrogen partitioning and remobilization in relation to leaf senescence, grain yield and grain nitrogen concentration in wheat cultivars. Field Crops Research. 2014;155:213–223. https://doi.org/10.1016/j.fcr.2013.09.003

ORCID IDs
Yuliya R. Serazetdinova https://orcid.org/0000-0002-3044-3529
Ekaterina E. Borodina https://orcid.org/0000-0001-6362-7589
Natalya V. Fotina https://orcid.org/0000-0002-7655-0258
Gaurav Mudgal https://orcid.org/0000-0003-4303-4983
Lyudmila K. Asyakina https://orcid.org/0000-0003-4988-8197

Foods and Raw Materials. 2026;14(1)

ISSN 2308-4057 (Print)
ISSN 2310-9599 (Online)

Review Article
Open Access

Available online at http://jfrm.ru/en
https://doi.org/10.21603/2308-4057-2026-1-670
https://elibrary.ru/VBWIDF

Inhibited and non-inhibited lipid oxidation in colloidal solutions: A review

Ivan V. Moskalenko*, Ilya S. Korolev, Evgeny A. Smirnov, Ekaterina V. Skorb

ITMO University, St. Petersburg, Russia

* e-mail: ivmoskalenko@itmo.ru

Received 04.10.2024; Revised 29.11.2024; Accepted 03.12.2024; Published online 30.04.2025

Abstract:
Fatty acids possess special structural features that allow them to form surfactants. Their weak C–H bonds trigger oxidation by the radical-chain mechanism. As a result, various colloidal solutions develop in aqueous media, and the new conditions affect the mechanism of fatty acid oxidation.

This review summarizes scientific publications on fatty acid oxidation in colloidal systems registered in Scopus and WoS in 2014–2024. It involved articles on the kinetics of fatty acid oxidation in water-lipid colloidal solutions, e.g., emulsions and micellar solutions.

The main stages of lipid oxidation – initiation, continuation, and chain termination – depend on various factors. The oxidation rate can be affected by the composition of the system, oxygen concentration, distribution of the initiator between the lipid or aqueous phases, type of surfactant, and pH. Each of these factors can change the mechanism of radical chain oxidation, thus affecting the shelf-life and quality of food products. The behavior of antioxidants in colloidal solutions differs from that in true solutions. The oxidation rate, the concentrations of various components, and the antioxidant activity in water-lipid solutions can be measured by different methods. These days, machine learning and artificial intelligence predict oxidation rates and assess the properties of antioxidants in various food systems. If combined together, they improve their predictive ability of the oxidation rate of fatty acids in colloidal solutions.

By establishing the mechanism of fatty acid oxidation in colloidal systems, food scientists design the optimal conditions to preserve antioxidants in various foods and increase their shelf-life.

Keywords: Fatty acids, lipid peroxidation, radical chain oxidation, micelles, emulsion, antioxidants

Funding: The research was supported by the Ministry of Science and Higher Education of the Russian Federation (Minobrnauka), Agreement no. 075-15-2021-1349.

Please cite this article in press as: Moskalenko IV, Korolev IS, Smirnov EA, Skorb EV. Inhibited and non-inhibited lipid oxidation in colloidal solutions: A review. Foods and Raw Materials. 2026;14(1):228–246. https://doi.org/10.21603/2308-4057-2026-1-670

INTRODUCTION

Fatty acids are among the most crucial food components. They are essential for human and animal nutrition and health. Fatty acids are prevalent in various food products, e.g., nuts, fish, oils, meat, and dairy products [1–5]. The fatty acids found in these foods typically contain 14–22 carbon atoms [6]. Their hydrocarbon chains may be fully saturated, or they may contain 1–6 double bonds (usually in the *cis*-configuration), with a bis-allylic group between them. Figure 1 illustrates this kind of bond-dissociation energy.

These two structural features lead to two key observations:

1. The structural residues of fatty acids are soluble in organic media, and the presence of easily removable acidic groups provides numerous opportunities for the development of fatty acids-based surfactants, e.g., phospholipids.

2. Weak C–H bonds in unsaturated and polyunsaturated fatty acids facilitate oxidation, thereby reducing the shelf-life of food products.

Considering that many foods that contain water and fatty acids are surfactants, fatty acid oxidation occurs not in their pure form, but rather in colloidal solutions, i.e., emulsions and micellar solutions. Recent reviews [7–10] address the process of fatty acid oxidation in colloidal solutions. However, several unresolved issues remain despite the recent progress in colloidal studies [11]. For example, most reviews fail to consider the instrumental methods for determining oxidation

Copyright © 2025, Moskalenko *et al.* This is an open access article distributed under the terms of the Creative Commons Attribution 4.0 International License (https://creativecommons.org/licenses/by/4.0/), allowing third parties to copy and redistribute the material in any medium or format and to remix, transform, and build upon the material for any purpose, even commercially, provided the original work is properly cited and states its license.

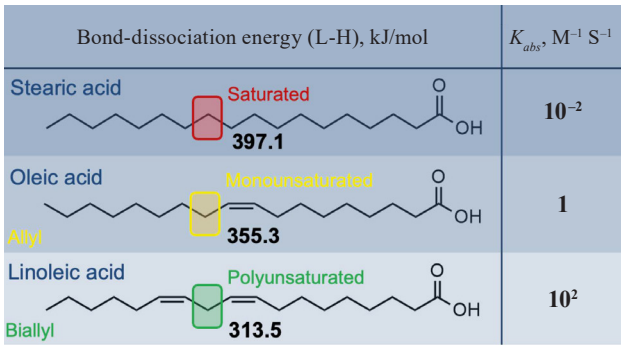

Figure 1 Structures of fatty acids, C–H bond energies, and rate constants for hydrogen abstraction from various functional groups

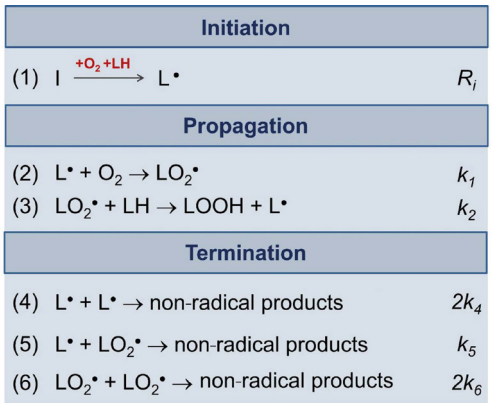

Figure 2 Mechanism of free radical chain oxidation

rates. Such issues as machine learning and artificial intelligence in predicting oxidation rates and inhibitor strengths also remain beyond their scope. Finally, most of them adhere to a strictly phenomenological perspective. This review focuses on examining the kinetics of fatty acid oxidation in colloidal solutions.

STUDY OBJECTS AND METHODS

This review covered publications registered in Google Scholar, ResearchGate, and Scopus in 2002–2023, with the focus on original studies published within the last 10 years in peer-reviewed sources. The search involved such keywords as *lipids oxidation*, *lipid oxidation in emulsion*, *lipid oxidation in micelles*, *antioxidants in emulsion*, and *machine learning lipid peroxidation*. Priority was given to articles published in specialized journals on the kinetics of radical chain reactions and food chemistry.

RESULTS AND DISCUSSION

General issues of fatty acid oxidation. Oxidation mechanisms in colloidal solutions may differ significantly from those in true solutions: their mechanisms are more complex (Fig. 2).

The mechanism of fatty acid oxidation in true solutions is a variety of the free radical chain oxidation mechanism. It closely resembles the oxidation of hydrocarbons (Fig. 2) [12] and is identical for saturated fatty acids. At high oxygen concentrations (~ 10^{-3} M), the likelihood of Reactions 4 and 5 is virtually zero, as the rate of Reaction 1 is close to the diffusion rate [13]. The system contains almost no free alkyl radicals (L•). Consequently, the oxidation rate R_{O_2}, mol/(L·s)) (can be described by Eq. (1) [14]:

$$R_{O_2} = \frac{k_2}{\sqrt{2k_6}}[\mathrm{LH}]\sqrt{R_i} \quad (1)$$

where k_n is the rate constant for the n-th reaction (Fig. 2), L/(mol·s); [LH] is the substrate concentration, mol/L; R_i is the initiation rate, mol/(L·s). The chain propagation is the rate-limiting step in free radical chain processes. Notably, the rate constant k_2 for fatty acids is an additive function of the bis-allylic and allylic groups [15, 16], as illustrated by Eq. (2):

$$k_2 = 4k_a + 2nk_{ba} \quad (2)$$

where is the rate constant for the abstraction of a hydrogen atom from the allylic group, L/(mol·s); is the rate constant for the abstraction of a hydrogen atom from the bis-allylic group, L/(mol·s). Considering that k_a is much lower than k_{ba}, the greatest contribution comes from the bis-allylic groups. Thus, oxidation proceeds in a co-oxidation mode. The oxidation rate can be reduced by increasing the concentration of allylic groups. In [17], diluting fish oil with oleic acid-rich sunflower oils decreased the oxidation rate. Another method to reduce the oxidation rate involves protecting bis-allylic groups by replacing hydrogen with deuterium [18–21]. These substances proved effective antioxidants in model systems, as well as inhibitors of oxidative stress and related pathologies in biological systems [22, 23]. However, these substances are relatively expensive dietary supplements [24], and their effects on the body remain understudied and questionable [25].

Oxygen is another important component that affects oxidation. At high oxygen concentrations, the oxidation rate follows Eq. (1). At low oxygen concentrations, Reactions 4 and 5 are also possible, and the oxidation rate exhibits a more complex dependence [26–28], as illustrated by Eq. (3):

$$\frac{[\mathrm{O_2}]}{[\mathrm{LH}]}\left(\frac{R_\infty^2}{R_{O_2}^2}-1\right)=\frac{k_2k_5}{k_1k_6}+\frac{k_2^2k_4}{k_1^2k_6}\frac{[\mathrm{LH}]}{[\mathrm{O_2}]} \quad (3)$$

where R_∞ is the oxidation rate calculated using Eq. (1); R_{O_2} is the oxidation rate at a specific oxygen concentration, mol/(L·s); $[O_2]$ is the oxygen concentration, mol/L. Since the oxygen concentration in water is approximately an order of magnitude lower than in organic solvents [29], a high-water content in a water/oil system significantly reduces the overall oxygen concentration. Unfortunately, scientific literature rarely provides data on the effect of oxygen concentration on the oxidation rate of fatty acid derivatives [30]. The oxygen concentra-

tion within a micelle depends on the surfactant concentration [31], and the surface area does not affect the rate of oxygen diffusion into the micelle [32].

Additionally, oxygen participates in autoxidation. The rates of auto-initiation are as low as ~ 10^{-8} mol/(L·s) at 70°C and can often be neglected. These processes combine two reactions [33], as illustrated below:

$$LH + O_2 \rightarrow L^{\bullet} + HO_2^{\bullet}$$
$$2LH + O_2 \rightarrow 2L^{\bullet} + H_2O_2$$

The mechanism of this third-order reaction apparently consists of two stages: first, a substrate-oxygen complex develops; second, it is attacked by a substrate molecule. From a chemical kinetics perspective, it is a relatively rare termolecular reaction.

Thus, autoxidation produces not only fatty acid radicals but also the hydroperoxyl radical ($HO_2^{\bullet}$) and hydrogen peroxide. Interestingly, polar solvents increase the rate of auto-initiation [33, 34] and reduce the proportion of termolecular reactions. This effect can be attributed to the disruption of the pre-reaction complex, which decreases the likelihood of the slow termolecular reaction. In this respect, the kinetics of fatty acid oxidation in polar organic solvents requires further research. The formation of $HO_2^{\bullet}$ was also reported in [35], which examined the inhibition of autoxidation in various foods containing fatty acid residues by superoxide dismutase. Additionally, superoxide dismutase inhibited the oxidation of fish oil emulsions [36], indicating the formation of $HO_2^{\bullet}$. The same authors determined that catalase also reduces the oxidation rate [37], which indirectly supports the formation of $HO_2^{\bullet}$ during oxidation because catalase decomposes hydrogen peroxide.

As indicated in the previous paragraph, oxidation may trigger the formation of $HO_2^{\bullet}$ radicals. Only one research featured the rate constant for the reaction of hydrogen atom abstraction from fatty acids by the hydroperoxyl radical [38]: it was approximately 10^3 L/(mol·s) for the bis-allylic group, while allylic groups did not react with $HO_2^{\bullet}$. Additionally, trans-isomers of linoleic acid also did not react with $HO_2^{\bullet}$ [39]. For liquid-phase reactions, all other publications primarily include rate constants for the addition to the double bonds of certain vinyl compounds [40–42], the dependency of rate constants on solvent polarity [43–45], and the reactivity of some inhibitors with $HO_2^{\bullet}$ [46, 47].

Initiation in multiphase systems. The rate of auto-initiation is negligible for the kinetics of fatty acid oxidation. As a result, special initiators are needed to enhance the oxidation process. They can be water-soluble, e.g., AAPH, AMEP, SOTS-1; lipid-soluble, e.g., AIBN, AMVN, and Fenton-like or enzymatic catalysis, e.g., xanthine oxidase-xanthine [48–56]. In all the cases, the position of the initiator influences both the oxidation rate and its mechanism (Fig. 3).

From a kinetic perspective, the decomposition of hydroperoxides is a chain-branching event. This decomposition occurs relatively slowly and is accelerated by temperature or light [57]. Metal ions with variable valency may initiate the oxidation of lipoproteins in emulsions. Iron and copper ions are the most popular ones [58–61]. Yet, the initiation rate depends on multiple factors, such as pH or chelating agents. When studying oxidation kinetics with other types of initiation, this reaction is usually eliminated as an additional source of chain branching. For instance, solutions are prepared using deionized water, and further purification is achieved with ion-exchange resins.

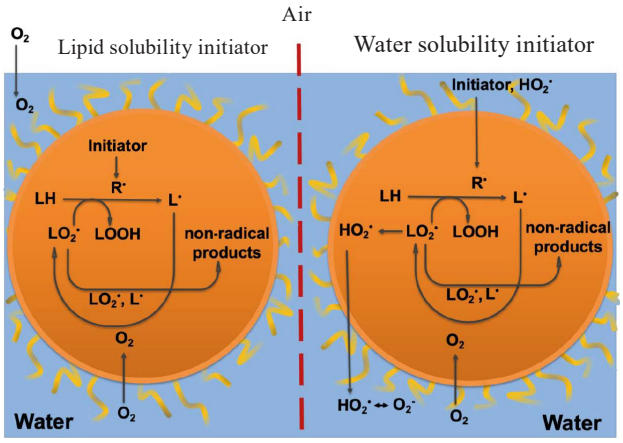

Figure 3 Reaction mechanisms in the presence of water-soluble and lipid-soluble initiators

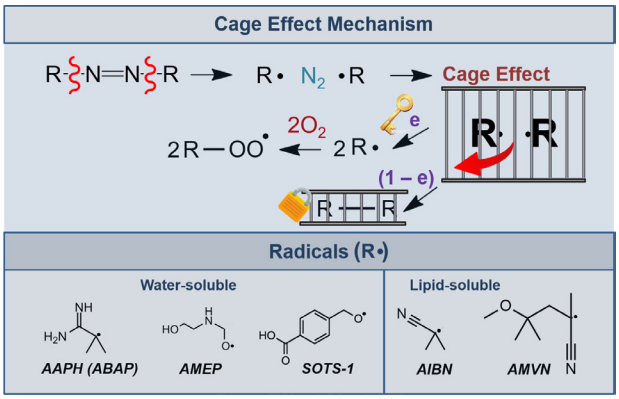

Figure 4 Radical formation during azo-initiator decomposition

Surfactants are often used to form micelles and emulsions, except when the oxidation substrate itself acts as a surfactant, e.g., phospholipids [62]. As a rule, it is either non-ionic or anionic surfactants. Cationic surfactants, however, can degrade the formed hydroperoxides, leading to chain branching [63–66].

Hydroperoxides decompose under the effect of a magnetic field generated by cationic surfactants [67].

Water-soluble initiators are the most popular variant for initiation in micelles, e.g., AAPH (Fig. 4). In this case, the initiation rate depends on pH. At low pH, the initiation rate is higher than at neutral pH, and it is similarly elevated at high pH. The increased initiation rate at low pH is attributed to the additional protonation in the diamine fragment, which enhances the

Coulomb interactions and increases the likelihood of the initiator cage exit [49].

SOTS-1 is a special case [51]. Upon decomposition in water, it generates a superoxide radical. To generate $O_2^{\bullet-}$ (superoxide), it needs an enzymatic system of xanthine oxidase and hypoxanthine [68].

Lipid-soluble initiators are primarily used in emulsions and occasionally in micelles. However, the rate constants for initiation in micelles differ significantly from those in true solutions. For instance, k_i(AMVN) is 2.5×10^{-7} s^{-1} [54], while the rate constant for decomposition is 5.4×10^{-6} s^{-1} [14]. Thus, the likelihood of the radical escaping from the micelle is only about 0.05. In our previous work [69], we observed that it happens because:
– the micelle forms a secondary cell, within which the probability of the radical escaping is significantly lower;
– the lower concentration of oxygen promotes chain termination via Reaction 5 (Fig. 2), which is thermodynamically more favorable than Reaction 6 (Fig. 2).

Interestingly, the rate constant k_i for the lipid-soluble AIBN depends on pH, even though it is within the micelle. The publication in question provided no explanation for this observation, which means that inhibition methods for micellar solutions require further clarification.

Chain propagation. Measuring the rate constants for chain propagation under colloidal conditions is quite challenging. One of the few experimentally determined rate constants for the chain propagation of linoleates in bilayers was found to be several times lower than in true solutions: 16.6 and 70 L/(mol·s), respectively [70]. This result was attributed to the peroxyl radical being "somewhat expelled outward" [48]. In molecular dynamics simulations, the peroxyl radical is more favorably positioned within the lipid region while the hydroperoxide aligns with the aqueous phase [71].

For water-soluble initiators, the "loading" of the micelle is a factor that affects the rate of chain propagation [72, 73]. At 2–20 nm, the oxidation rate exhibits a linear dependence on the number of fatty acid molecules within the micelle. Such sizes allow for the containment of a relatively small number of molecules (up to several hundred), which limits the oxidation rate. Conversely, oxidation in water/oil systems with a droplet size of hundreds of nanometers is much closer to ideal solutions [74]. Similar conclusions were reported in [75] concerning the oxidation of olive oil and fish oil emulsions in water with sizes ranging from 80 to 1300 nm. The lipid oxidation rate in emulsions actually decreased as the droplet size went up [76].

Figure 5 illustrates the mechanism of decomposition hydroperoxyls in micelles. When using water-soluble initiators, some chains in micelles may be propagated by the hydroperoxyl radical ($HO_2^{\bullet}$) [77]. Its presence in the oxidation process of methyl linoleate and methyl linolenate was detected using superoxide dismutase, which converts $HO_2^{\bullet}$ into hydrogen peroxide [78]. For the monounsaturated ester (methyl oleate), the authors observed no superoxide dismutase inhibition, which means that oleate oxidation did not produce $HO_2^{\bullet}$. However, superoxide dismutase inhibition confirms only the cases where $HO_2^{\bullet}$ is both generated and propagates the chain. Remarkably, $HO_2^{\bullet}$ was unable to propagate chains in saturated and monounsaturated fatty acids [38, 39]. Additionally, $HO_2^{\bullet}$ did not participate in chain propagation for linoleates where hydrogen was replaced with deuterium at the bis-allylic position [39].

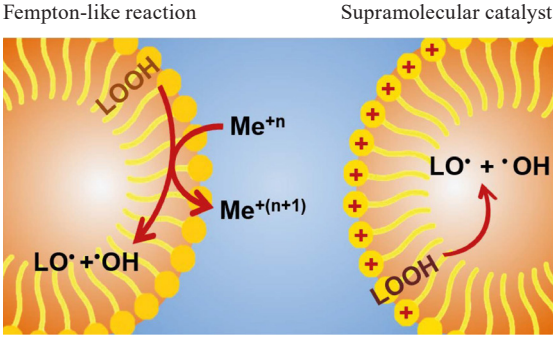

Figure 5 Mechanism of decomposition hydroperoxyls in micelles

A more accurate method for detecting $HO_2^{\bullet}$ described in [79] involved a combination of superoxide dismutase and nitroxide radicals. Nitroxide radicals appeared in the presence of $HO_2^{\bullet}$, but the presence of superoxide dismutase reduced the concentration of $HO_2^{\bullet}$ and shortened the induction period. This method was found lacking because nitroxide radicals were weak antioxidants, which resulted in a poorly defined induction period. Another confirmation of $HO_2^{\bullet}$ formation was the decreased induction period of nitroxide radicals during the oxidation of methyl linoleate in Triton X100 micelles in heavy water [80]. Heavy water led to the replacement of $HO_2^{\bullet}$ with $DO_2^{\bullet}$, which cannot regenerate nitroxide radicals [47, 81].

As for lipid-soluble initiators, the formation of $HO_2^{\bullet}$ did not occur in Triton X100 micelles [69]. It happened because peroxyl radicals are more likely to be destroyed inside the micelle. However, the number of fatty acid molecules inside the micelle interior is limited. When initiated with water-soluble initiators, the chain length exceeded the number of molecules inside the micelle [79]. This phenomenon can partly be explained by the formation of $HO_2^{\bullet}$, but even with the introduction of superoxide dismutase, the chain length remained greater than the number of molecules inside the micelle [79]. Thus, some chains can be transferred through collisions between two micelles, one of which contains a radical [9, 73, 82].

Such chain propagation mechanisms as radical diffusion into the solution and co-oxidation with surfactants [83] are virtually impossible. In the first case, the solubility of fatty acid radicals in aqueous media is minimal. In the second case, it primarily affects hydrophilic regions that do not interact with the micelle interior. However, some non-ionic surfactants, e.g., Triton X100, Tween 65, and Pluronic F68, could undergo oxidation [83, 84]. Thus, we can only discuss parallel oxidation of surfactants and fatty acids.

Chain termination in true solutions occurs via Reactions 4–6 (Fig. 2). At high oxygen concentrations, Reactions 4 and 5 can be neglected since the concentration of alkyl radicals is extremely low. Since the oxygen concentration in an aqueous medium is almost an order of magnitude lower than in organic solvents, Reactions 4 and 5 predominate during chain termination in the micelle. Chain termination is most likely to occur inside the micelle because the concentration of radicals in the organic phase is much higher than in the aqueous phase.

No consensus has been reached so far on the type of chain termination in micellar solutions. AAPH demonstrates both mixed and linear chain terminations. Linear termination might be related to the fact that only one initiator radical enters the micelle whereas quadratic termination requires two chains. In [85], linear termination was explained by the formation of the hydroperoxyl radical: upon exiting the micelle, it converts into a less reactive superoxide anion radical:

$$O_2^{\bullet-} + H^+ \leftrightarrow HO_2^{\bullet} \ (pK_a = 4.8)$$

However, these processes do not terminate the chain but rather slow it down and eventually lead to chain transfer, as evidenced by the higher oxidation rates observed under nanoheterogenous conditions.

The decay of $HO_2^{\bullet}$ in aqueous environments can occur through two reactions [86, 87]:

$$HO_2^{\bullet} + HO_2^{\bullet} \rightarrow H_2O_2 + {}^1O_2$$
$$k = 8.3\times10^5 \text{ L/(mol·s)}$$

$$HO_2^{\bullet} + O_2^{\bullet-} + H_2O \rightarrow H_2O_2 + O_2 + OH^-$$
$$k = 9.7\times10^7 \text{ L/(mol·s)}$$

These reactions have high-rate constants, but under neutral pH conditions, the concentration of $HO_2^{\bullet}$ is low, and the chain termination is minimal. In organic solvents, the rate of chain termination depends on the formation of the $HO_2^{\bullet}$-solvent complex [45]. This conclusion for $HO_2^{\bullet} + HO_2^{\bullet}$ was reported in studies that featured rate constants in various solvents.

Loshadkin *et al.* [84, 88–90] explained the gradual increase in the oxidation rate by "radical accumulation". This effect is likely caused by the presence of antioxidant impurities, as evidenced by the increased reaction order with respect to the initiator during the reaction and the longer induction period with decreased initiation rates. Therefore, thoroughly purified reagents are crucial for more accurate kinetic models of lipid oxidation.

Studying chain termination with lipid-soluble initiators is challenging because their concentration is difficult to vary: a lower initiator concentration decreases the already low oxidation rate while a higher concentration may complicate its solubility in micelles.

Inhibited oxidation. Oxidation is often an undesirable process. Equation (1) clearly demonstrates that the oxidation rate can be reduced by decreasing the chain propagation rate (Reaction 2, Fig. 2), by slowing down the initiation rates, or by hydroperoxide decomposition. The types of inhibitors for optimal lipid oxidation are listed below [91]:

– chain-breaking inhibitors that react with peroxyl radicals, e.g., aromatic amines and phenols;
– chain-breaking inhibitors that react with alkyl radicals, e.g., nitroxyl radicals; and
– metal deactivators for variable valency metals.

For metal deactivators, the rate of oxidation initiated by variable valency metal ions depends on pH and the presence of chelating agents, such as EDTA [92]. Acidic pH is known to reduce the rate of oxidation initiated by iron ions. Such surfactants as Tween can also form chelate complexes. Such amino acids as L-lysine and L-asparagine develop complexes with iron ions [93], thereby reducing the oxidation rate in meat products. Sodium citrate additives also reduce oxidation rates [94]. Conversely, monovalent salts tend to increase the oxidation rate, probably due to their impact on the surface of emulsion droplets. Phosphate groups [95], e.g., in sodium caseinate [96], reduce oxidation rates by forming complexes. Buffer solutions based on citrates and phosphates lower oxidation rates by stabilizing iron ions in the solution [97]. An innovative approach to creating new inhibitory materials involves the complexation of variable valency metal ions with poly(hydroxyethyl acrylate) [98]. This method provides coatings for poly(ethylene terephthalate) containers, which extends the shelf-life of food products.

Chain-breaking inhibitors that react with alkyl radicals are generally less effective due to the relatively low concentration of alkyl radicals. The most common inhibitors are various nitroxyl radicals, such as TEMPO and its derivatives. However, they are primarily utilized as radical traps and spin labels in oxidation kinetics (Fig. 6) [39, 79, 99–103]. In practice, the antioxidant action of nitroxyl radicals is not limited to reactions with alkyl radicals [104] because nitroxyl radicals exist as alkoxyamines and hydroxylamines in aqueous environments [105, 106]. Hydroxylamines are particularly strong inhibitors. Nitroxyl radicals also react with $HO_2^{\bullet}$, and this reaction regenerates nitroxyl radicals, facilitating the formation of antioxidant systems. For instance, Amorati *et al.* [47, 107, 108] proposed an antioxidant system based on nitroxyl radicals and 1,4-cyclohexadiene

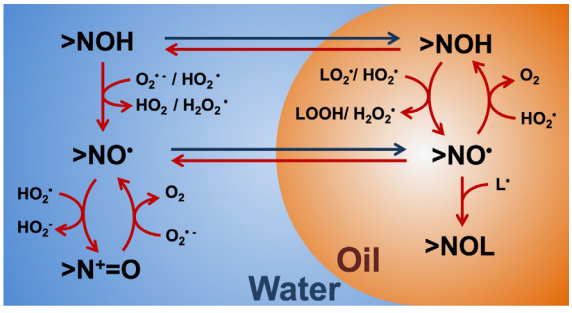

Figure 6 Mechanism of nitroxyl radical-inhibited oxidation of methyl linoleate in micelles (Adapted from [99])

and its derivatives, where $HO_2^•$ is produced upon oxidation. Other potential substrates for similar systems include 1,2-disubstituted ethylenes and 1,4-disubstituted butadienes, which also produce $HO_2^•$ upon oxidation [42]. Additionally, $HO_2^•$ can be generated in systems with oxygen peroxide [109]; however, its concentration in the lipid phase is usually minimal.

The most extensive group of oxidation inhibitors consists of those that react with peroxyl radicals. Various polyphenols and phenols (PhOH) are the most popular inhibitors in this category [46, 110]: vitamin E, epicatechins, Trolox, 2,6-di-tert-butyl-4-methylphenol (BHT), etc. [111–114]. Their mechanism of action in nonpolar organic solutions is typically represented as a hydrogen atom transfer:

$$PhOH + LO_2^• \rightarrow PhO^• + LOOH$$
$$PhO^• + LO_2^• \rightarrow NRP$$

Thus, phenols can terminate two oxidation chains. However, numerous side reactions may reduce their effectiveness e.g., autoxidation reactions, reactions between phenolic radicals, etc. In the case of hydrogen atom transfer, the key parameter is the bond dissociation energy of the O–H bond [115]. The lower the bond energy, the more active the inhibitor. At lower bond energies, autoxidation reactions become more favorable, which can lead to a pro-oxidant effect [116, 117].

$$PhOH + O_2 \rightarrow PhO^• + HO_2^•$$

In this case, autooxidation is accelerated due to the catalytic oxidation of phenols in the presence of iron ions [118, 119].

Assessing antioxidant activity by the bond dissociation energy can yield intriguing results: in [120] the authors demonstrated that the C–H bond energy in flavonoids was lower than the O–H bond energy in phenolic groups.

In multiphase systems, the dependence of antioxidant activity on the structure and polarity of inhibitors differs somewhat from that in true solutions (Fig. 7). Among inhibitors of the same class, the most polar phenolic inhibitors exhibit the highest antioxidant activity in true solutions. In water/oil systems, less polar inhibitors are more effective [121]. This phenomenon is known as the polar paradox [122]: nonpolar antioxidants dissolve better on the lipid surface where the primary oxidation processes occur [123]. Clearly, hydrophobicity can be enhanced by increasing the number of hydrophobic groups in the inhibitor molecule. However, the antioxidant activity of inhibitors gradually reaches a limit with the increasing length of the alkyl tail, a phenomenon termed the cut-off effect [124–126].

Some researchers believe that concentration is also important [127, 128]. For instance, they compared the antioxidant activity of epigallocatechin gallate (EGCG) with its lipophilic ester derivative (tetrastearate) in oil. The ester was more effective at lower concentrations whereas epigallocatechin gallate proved more active at higher concentrations. At low concentrations, the effect of solubility in oil predominates over the interfacial phenomena on antioxidant effectiveness. Thus, non-polar antioxidants with better fat solubility are more effective than their polar counterparts while the reverse is true at higher concentrations. As a result, the polar paradox theory is applicable only when the antioxidant concentration exceeds a critical value to let the interfacial phenomena dominate over solubility parameters.

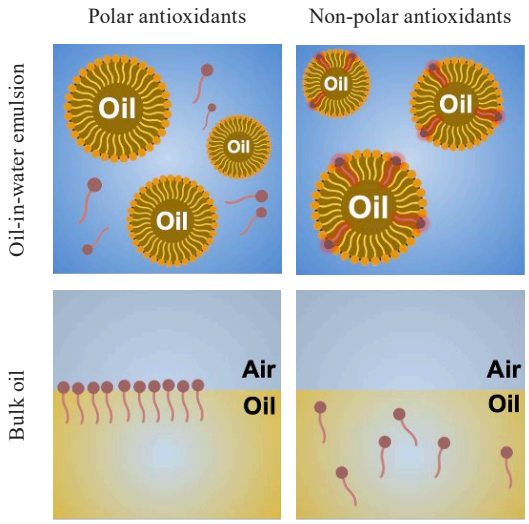

Figure 7 Interfacial phenomena as a possible action mechanism of polar paradox in oil-in-water emulsion and bulk oil

A more complex approach to the effect of the inhibitor at the phase boundary is introduced in [129–131]. For instance, Bravo-Díaz *et al.* [132] developed a pseudophase model: they divided the entire solution into oil, interfacial, and aqueous regions, with surfactants located at the boundary between the lipid and aqueous phases. Each region demonstrated distinct solvent properties and was considered a separate phase, or pseudo-phase. Reagents and other components distributed thermodynamically in line with the Gibbs free energy of transfer. This effect means that the distribution of reagents is always described by partition constants, which remain constant throughout the reaction. Phenolic radicals and their concentration are detected with 4-hexadecylbenzenediazonium, which reacts with phenolates to form colored compounds.

Such polar environments as water or alcohols have a different inhibition mechanism. Previously, polar solvents were believed to reduce the rate of inhibition by forming associates with polar functional groups of inhibitors [133], which required the disruption of hydrogen bonds before the group could react with radicals. Nowadays, there are more complex mechanisms of inhibition in polar media. For example, in medium-polarity environments, e.g., methanol, the preferred mechanism is a single electron transfer-proton transfer (SET-PT) [134]:

$$PhOH + LO_2^• \rightarrow PhOH^{+•} + LO_2^-$$
$$PhOH^{+•} + LO_2^- \rightarrow PhO^• + LOOH$$

Aqueous environments have a tendency to the mechanism of sequential proton loss electron transfer (SPLET) [135–137]:

$$PhOH \rightarrow PhO^- + H^+$$
$$PhO^- + LO_2^{\bullet} \rightarrow PhO^{\bullet} + LO_2^-$$
$$LO_2^- + H^+ \rightarrow LOOH$$

Inhibitors can terminate chain reactions through all three mechanisms, with the sequential proton loss electron transfer predominantly occurring in the aqueous phase, single electron transfer-proton transfer at the interface, and hydrogen atom transfer in the lipid phase. Thus, the effectiveness of antioxidants may vary depending on their location within a multiphase system, with different mechanisms being more favorable in specific regions due to the local environment and solvent properties.

Evaluation of antioxidant activity. Antioxidant activity can be characterized by such parameters as the stoichiometric inhibition coefficient (f) and the chain termination rate constant (k_7). The stoichiometric inhibition coefficient essentially represents the number of broken chains on one inhibitor molecule. For phenols, the most common stoichiometric inhibition coefficient is around 2, but this value may decrease with an increase in the probability of side reactions. Experimentally, the stoichiometric inhibition coefficient f depends on the induction period (τ_{ind}). These quantities correlate as in Eq. (4) [138, 139]:

$$\tau_{ind} = \frac{f[InH]}{R_i} \quad (4)$$

where [*In*H] is the concentration of the antioxidant, mol/L.

The induction period is usually determined by two methods. In line with the geometric method, a tangent is drawn from the section of the exit from the induction period. In this case, the induction period is the intersection of the time axis and the tangent (Fig. 8) [49, 140]. The integral method means that the induction period is calculated as in Eq. (5) (Fig. 9):

$$\tau_{ind} = \int_0^{\infty} \left(1 - \frac{R}{R_0}\right) dt \quad (5)$$

where R is the rate at time t, mol/(L·s); R_0 is the rate of uninhibited oxidation, mol/(L·s).

The chain breakage rate constant k_7 is calculated using Eqs. (6) and (7):

$$F_1 = \ln\left(\frac{1 + R/R_0}{1 - R/R_0}\right) - \frac{R}{R_0} = \frac{k_7 R_0}{fk_2[LH]} t + const \quad (6)$$

$$F_2 = \frac{R_0}{R} - \frac{R}{R_0} = \frac{2k_7 R_0}{fk_2[LH]R_{in}}[InH] \quad (7)$$

In the first case, the dependence of F_1 on time is plotted for the section leaving the induction period. In Eq. (6), the derivative equals,

$$\frac{k_7 R_0}{fk_2[LH]}$$

from which it is easy to calculate k_7. In the second case, the oxidation rate is measured at different inhibitor concentrations, and then a graph of F_2 is plotted against the antioxidant concentration: the resulting derivative reveals the value of k_7. Initially developed for true solutions [141], these approaches are also applicable to colloidal solutions but with some reservations, e.g., the true chain transfer rate constant is unknown.

Measuring the oxidation rate. The oxidation kinetics can be monitored either by the reaction reagents, e.g., oxygen consumption, or by the product accumulation, e.g., hydroperoxides. The antioxidant concentration can be monitored even if oxidation is inhibited. The simplest analysis option is to control the oxygen concentration. One option is to measure the volume of absorbed oxygen [142, 143]. Another one is to determine the concentration of dissolved oxygen in the solution, e.g., with the help of the Clark electrode in aqueous solutions [144]. Photosensors offer a more universal option: they detect singlet oxygen fluorescence [145–148].

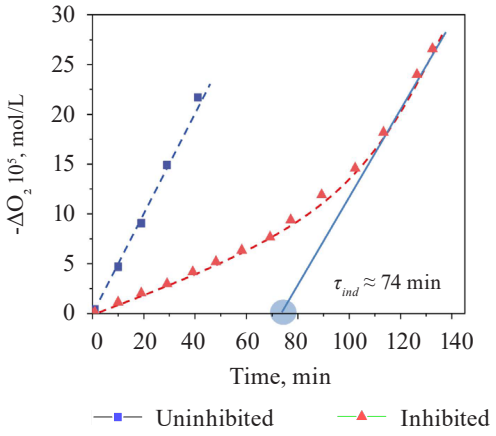

Figure 8 Kinetics of inhibited vs. uninhibited lipid oxidation in micelles

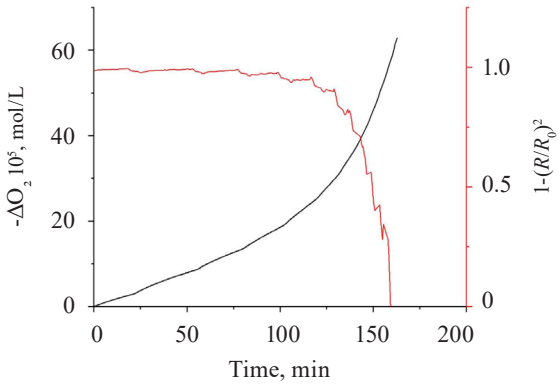

Figure 9 Integral method of determining the induction period

In this case, however, the generation of singlet oxygen may lead to a slight increase in the oxidation rate.

Electrochemical approaches detect oxidation of various species and their oxidation rates. For examples, an amperometric test based on pseudo-titration approach could measure the antioxidant power of wine, orange juice [149], and complex samples [150], such as blood. Voltametric measurements can be applied in a similar way [151]. Other publications report calculating the electrochemical reaction rates based on the Butler-Volmer equation [152, 153].

Recent studies that focus on hydrogen peroxide and hydroperoxide-ion monitor the intra- and extracellular concentration in biological processes by using intermetallic catalytic particles deposited in hydrogel [154] or by applying oxide particles [155] to screen-printed carbon electrode or glassy carbon electrode. The latter option involves electrocatalysis driven by equilibration of Fermi-levels with the surrounding solutions [156, 157]. Highly conductive materials and additives with high specific surface area improve the kinetics of hydroperoxide oxidation and lower the limit of detection in electrochemical methods. The list includes carbon nanotubes, graphene [158], or gold nanoparticles [159, 160].

Since hydroperoxides are subject to decomposition, their accumulation is difficult to monitor directly. Russian researchers prefer this method for determining hydroperoxides that consists of back titration of iodine reduced by hydroperoxide. More complex methods include spectral determination of iodine or iron ions, as well as chromatographic, infrared, and titrimetric determination of triphenylphosphine oxide (TPPO), formed from triphenylphosphine (TPP) [161–171]. However, these methods are not convenient for studying kinetics because they require additional sample processing and a large sample volume for analysis.

Online methods based on high-power laser-irradiation can detect peroxide concentration in the sample. For example, the rapidly developing technique of Raman spectroscopy was applied to oxidation of fat acids and oils, as well as to monitoring reactions in liposomes [172–176]. The fingerprint region (300–1900 cm^{-1}) in Raman spectroscopy [177] is a powerful tool to detect structural changes in compounds, especially

Table 1 Machine learning algorithms in lipid oxidation and stability studies

Prediction	Algorithm	Reference
Evaluate the usefulness of orange by-product flour in the stabilization of oil-in-water emulsions and compare it with purified citrus pectins. Optimize the formulation of emulsion stabilized with orange by-product flour and vegetable proteins, using artificial neural networks	Feed-Forward Backpropagation Network **Input**: orange by-product flour content (0–3.40%) and protein content (0–0.60%) **Output**: emulsion profile (apparent viscosity; d10, d50, and d90 percentiles; ξ-potential; flocculation; creaming index)	[182]
Paired with ATR-FTIR spectroscopy, identify and classify pure njangsa seed oil, palm kernel oil, coconut oil, njangsa seed oil-palm kernel oil, and njangsa seed oil-coconut oil margarine	Support Vector Machines, Decision Tree, Light Gradient-Boosting Machine, K-Nearest Neighbors, Logistic Regression, Random Forest **Input:** FTIR spectra. **Output**: classification of oil.	[183]
Identify off-flavors and compounds of lipid oxidation in dairy powders	Random Forest, Leave-One-Out Cross-Validation, Root Mean Square Error classification of regression **Input:** GC/MS data; sensory data **Output**: Top peak identification, list of compounds	[184]
Define lipid peroxidation activity	Quantitative Structure-Activity Relationship Models **Input:** Top relevant descriptors previously selected by forward stepwise method based on *p*-value criteria **Output:** LP = lipid peroxidation activity/No LP = no lipid peroxidation activity	[185]
Define water and lipid content in emulsion	Self-learning Monte Carlo with Deep Neural Networks **Input:** SWIR spectra **Output:** Water and lipid content	[186]
Measure biorelevance gap in antioxidant assays	Quantitative Structure–Activity Relationship, K-Nearest Neighbors, Support Vector Machine, Bayesian Probabilistic Learning, Random Forest **Input:** Factors governing antioxidant activity *in vivo* **Output**: antioxidation activity of polyphenol	[187]
Detect lipid and protein oxidative damage in thawed pork	Convolutional Neural Network, Multi-Task Convolutional Neural Network **Input:** Raw 1D vis-NIR spectral data at 480–1002 nm **Output**: Malondialdehyde and carbonyl content of samples	[188]
Predicts the antioxidant activity of polyphenols	Neural differential equations **Input:** Concentration headspace hexanal (GC), polyphenols (HPLC) **Output**: Induction period	[189, 190]

in complex composition of many chemical compounds. In this regard, methods of artificial intelligence and chemo-informatics may be useful, too [178]. The technique of Surface Enhance Raman Spectroscopy (SERS) detects lower contents of chemicals with relatively high scattering intensity due to plasmonic resonance and hot-spots between those particles. It proved effective in detecting low concentrations of polyphenols, e.g., chlorogenic acid, caffeic, and gallic acids [179–181]. In addition, SERS-substrates are reusable [176].

Perspectives of machine learning. Predicting lipid oxidation and stability in various systems is a complex process, particularly due to the diverse physicochemical conditions, input data, and algorithms required. Lipid oxidation depends on a number of factors, making it difficult to develop a single, universal algorithm capable of providing accurate predictions across all conditions. Currently, machine learning techniques can predict certain aspects of these systems. For example, such machine learning algorithms as Feed-Forward Backpropagation Networks optimize emulsions stabilized with orange by-product flour (OBPF) and proteins. Support Vector Machines and other models analyze spectroscopy data to classify oils. Deep learning algorithms, such as Neural Differential Equations, perform well in predicting the induction period of polyphenols in bulk lipid oxidation (Table 1).

These models operate on different input data and use various algorithms, such as Random Forest and Convolutional Neural Networks, to address specific challenges, such as predicting lipid content or oxidative damage in meat. Due to the wide range of approaches, a single model may not be sufficient to accurately predict lipid oxidation and antioxidant activity in different systems. As a result, future advancements will likely require new algorithms or combinations of existing ones to improve predictive capabilities across diverse colloidal conditions. An integrated approach is essential for advancing our understanding of lipid oxidation and stability in complex systems.

The prediction of oxidation rate and antioxidant activity often depends on such factors as droplet size, distribution of components between phases, and concentration of components. Components can be split into phases to predict their concentrations using Random Forest and Feed-Forward Backpropagation Network [191]. Since chemical kinetics of oxidation and inhibited oxidation are described by equations, Deep Neural Networks and Neural Differential Equations methods are the most successful methods [192, 193]. The effect of antioxidants on oxidation kinetics can be predicted using Quantitative Structure-Activity Relationship models. Thus, a combination of these three methods (Random Forest/ Feed-Forward Backpropagation Network + Deep Neural Networks/Neural Differential Equations + Quantitative Structure-Activity Relationship) can give an excellent result in terms of predicting the oxidation rate and antioxidant properties.

CONCLUSION

Even though the oxidation of fatty acids in colloid solutions occurs by a radical-chain mechanism, it still depends on the redistribution of components between phases, droplet sizes, oxygen concentration, type of surfactant, and pH. Each of these factors affects the oxidation mechanism.

Unlike oxidation in true solutions, the hydroperoxyl radical is an important oxidation factor in colloidal systems. It participates in the stages of chain propagation and inhibitor regeneration, as well as slows down the chain termination. Apparently, the hydroperoxyl radical is formed from the peroxyl radical in the process of chain initiation.

The role of oxygen concentration remains understudied. Oxidation in water/lipid colloidal solutions occurs with a lack of oxygen, which increases the likelihood of chain termination by the reaction of alkyl and peroxyl radicals.

The study of oxidation kinetics in colloidal solutions requires some caution because unpurified commercial reagents may lead to incorrect conclusions about the oxidation mechanism.

Machine learning will soon be able to predict lipid oxidation rates and antioxidant activity of inhibitors in colloidal systems. Given that various physicochemical processes complicate the development of the model, a combination of algorithms may be an effective solution.

This review examined the kinetics and the main stages of oxidation and inhibition of fatty acids, as well as the main research methods in oxidation kinetics. A more detailed study of the kinetics of fatty acid oxidation in colloidal solutions may predict and increase the shelf-life of various food products.

CONTRIBUTION

I.V. Moskalenko developed the research concept, conducted the research, wrote and proofread the manuscript, supervised the project, and obtained funding. I.S. Korolev contributed to the writing of the manuscript and prepared the illustrations. E.A. Smirnov contributed to the writing and proofreading. E.V. Skorb developed the research concept, provided text editing, and obtained funding.

CONFLICT OF INTEREST

The authors declared no conflict of interests regarding the publication of this article.

REFERENCES

1. Polmann G, Badia V, Danielski R, Ferreira SRS, Block JM. Nuts and nut-based products: A meta-analysis from intake health benefits and functional characteristics from recovered constituents. Food Reviews International. 2023;39(8):5021–5047. https://doi.org/10.1080/87559129.2022.2045495

2. Xu H, Turchini GM, Francis DS, Liang M, Mock TS, Rombenso A, *et al.* Are fish what they eat? A fatty acid's perspective. Progress in Lipid Research. 2020;80:101064. https://doi.org/10.1016/j.plipres.2020.101064
3. Cherif A, Slama A. Stability and change in fatty acids composition of soybean, corn, and sunflower oils during the heating process. Journal of Food Quality. 2022;2022(1):6761029. https://doi.org/10.1155/2022/6761029
4. Heck RT, Lorenzo JM, dos Santos BA, Cichoski AJ, de Menezes CR, Campagnol PCB. Microencapsulation of healthier oils: An efficient strategy to improve the lipid profile of meat products. Current Opinion in Food Science. 2020;40:6–12. https://doi.org/10.1016/j.cofs.2020.04.010
5. Cerdó T, Ruíz A, Acuña I, Nieto-Ruiz A, Diéguez E, Sepúlveda-Valbuena N, *et al.* A synbiotics, long chain polyunsaturated fatty acids, and milk fat globule membranes supplemented formula modulates microbiota maturation and neurodevelopment. Clinical Nutrition. 2022;41(8):1697–1711. https://doi.org/10.1016/j.clnu.2022.05.013
6. Niki E. Lipid peroxidation. In: Chatgilialoglu C, Studer A, editors. Encyclopedia of radicals in chemistry, biology and materials. John Wiley & Sons; 2012. pp. 1577–1598. https://doi.org/10.1002/9781119953678.rad052
7. Musakhanian J, Rodier J-D, Dave M. Oxidative stability in lipid formulations: A review of the mechanisms, drivers, and inhibitors of oxidation. AAPS PharmSciTech. 2022;23:151. https://doi.org/10.1208/s12249-022-02282-0
8. Villeneuve P, Bourlieu-Lacanal C, Durand E, Lecomte J, McClements DJ, Decker EA. Lipid oxidation in emulsions and bulk oils: A review of the importance of micelles. Critical Reviews in Food Science and Nutrition. 2023;63(20):4687–4727. https://doi.org/10.1080/10408398.2021.2006138
9. Laguerre M, Tenon M, Bily A, Birtić S. Toward a spatiotemporal model of oxidation in lipid dispersions: A hypothesis-driven review. European Journal of Lipid Science and Technology. 2020;122(3):1900209. https://doi.org/10.1002/ejlt.201900209
10. Miyashita K. Paradox of omega-3 PUFA oxidation. European Journal of Lipid Science and Technology. 2014; 116(10):1268–1279. https://doi.org/10.1002/ejlt.201400114
11. Villeneuve P, Durand E, Decker EA. The need for a new step in the study of lipid oxidation in heterophasic systems. Journal of Agricultural and Food Chemistry. 2018;66(32):8433–8434. https://doi.org/10.1021/acs.jafc.8b03603
12. Denisov ET, Afanas'ev IB. Oxidation and antioxidants in organic chemistry and biology. Boca Raton: CRC Press; 2005. 1024 p. https://doi.org/10.1201/9781420030853
13. Nikolayev AI, Safiullin RL, Komissarov ND. Reaction kinetics of alkyl and alkylperoxide radicals. Reaction Kinetics and Catalysis Letters. 1986;31:355–359. https://doi.org/10.1007/BF02072970
14. Yin H, Xu L, Porter NA. Free radical lipid peroxidation: Mechanisms and analysis. Chemical Reviews. 2011; 111(10):5944–5972. https://doi.org/10.1021/cr200084z
15. Kitaguchi H, Ohkubo K, Ogo S, Fukuzumi S. Additivity rule holds in the hydrogen transfer reactivity of unsaturated fatty acids with a peroxyl radical: Mechanistic insight into lipoxygenase. Chemical Communications. 2006;(9):979–981. https://doi.org/10.1039/b515004c
16. Tikhonov IV, Moskalenko IV, Pliss EM, Fomich MA, Bekish AV, Shmanai VV. Kinetic isotope H/D effect in the oxidation of ethers of linoleic acid in solutions. Russian Journal of Physical Chemistry B. 2017;11:395–399. https://doi.org/10.1134/S1990793117030113
17. Qi YY, Gong T, Zhao PT, Niu YJ, Hu YY, Hu CY, *et al.* Hydroxytyrosyl oleate is a promising safe additive to inhibit the oxidation of olive oil. Food Control. 2023;153:109895. https://doi.org/10.1016/j.foodcont.2023.109895
18. Lamberson CR, Xu L, Muchalski H, Montenegro-Burke JR, Shmanai VV, Bekish AV, *et al.* Unusual kinetic isotope effects of deuterium reinforced polyunsaturated fatty acids in tocopherol-mediated free radical chain oxidations. Journal of the American Chemical Society. 2014;136(3):838–841. https://doi.org/10.1021/ja410569g
19. Andreyev AYu, Tsui HS, Milne GL, Shmanai VV, Bekish AV, Fomich MA, *et al.* Isotope-reinforced polyunsaturated fatty acids protect mitochondria from oxidative stress. Free Radical Biology and Medicine. 2015;82:63–72. https://doi.org/10.1016/j.freeradbiomed.2014.12.023
20. Shah R, Shchepinov MS, Pratt DA. Resolving the role of lipoxygenases in the initiation and execution of ferroptosis. ACS Central Science. 2018;4(3):387–396. https://doi.org/10.1021/acscentsci.7b00589
21. Liu Y, Bell BA, Song Y, Zhang K, Anderson B, Axelsen PH, et al. Deuterated docosahexaenoic acid protects against oxidative stress and geographic atrophy-like retinal degeneration in a mouse model with iron overload. Aging Cell. 2022;21(4):e13579. https://doi.org/10.1111/acel.13579
22. Shchepinov MS, Chou VP, Pollock E, Langston JW, Cantor CR, Molinari RJ, *et al.* Isotopic reinforcement of essential polyunsaturated fatty acids diminishes nigrostriatal degeneration in a mouse model of Parkinson's disease. Toxicology Letters. 2011;207(2):97–103. https://doi.org/10.1016/j.toxlet.2011.07.020
23. Hill S, Lamberson CR, Xu L, To R, Tsui HS, Shmanai VV, *et al.* Small amounts of isotope-reinforced polyunsaturated fatty acids suppress lipid autoxidation. Free Radical Biology and Medicine. 2012;53(4):893–906. https://doi.org/10.1016/j.freeradbiomed.2012.06.004

24. Fomich MA, Bekish AV, Vidovic D, Lamberson CR, Lysenko IL, Lawrence P, *et al.* Full library of (*Bis*-allyl)-deuterated arachidonic acids: Synthesis and analytical verification. ChemistrySelect. 2016;1(15):4758–4764. https://doi.org/10.1002/slct.201600955

25. Tsikas D. Combating atherosclerosis with heavy PUFAs: Deuteron not proton is the first. Atherosclerosis. 2017;264: 79–82. https://doi.org/10.1016/j.atherosclerosis.2017.07.018

26. Johnson DR, Decker EA. The role of oxygen in lipid oxidation reactions: A review. Annual Review of Food Science and Technology. 2015;6:171–190. https://doi.org/10.1146/annurev-food-022814-015532

27. Koelsch CM, Downes TW, Labuza TP. Hexanal formation via lipid oxidation as a function of oxygen concentration: Measurement and kinetics. Journal of Food Science. 1991;56(3):816–820. https://doi.org/10.1111/j.1365-2621.1991.tb05389.x

28. Moskalenko IV, Grobov AM, Pliss EM. The rate constants of cross recombination reaction of alkyl and peroxyl radicals during the oxidation of styrene, acrylonitrile and methyl methacrylate. Bashkir Chemical Journal. 2015;22(4):60–62. (In Russ.). https://www.elibrary.ru/VIURYT

29. Bozorg-Haddad O, Delpasand M, Loáiciga HA. Water quality, hygiene, and health. In: Bozorg-Haddad O, editor. Economical, political, and social issues in water resources. Elsevier; 2021. pp. 217–257. https://doi.org/10.1016/B978-0-323-90567-1.00008-5

30. Zhang J, Freund MA, Culler MD, Yang R, Chen PB, Park Y, *et al.* How to stabilize ω-3 polyunsaturated fatty acids (PUFAs) in an animal feeding study? – Effects of the temperature, oxygen level, and antioxidant on oxidative stability of ω-3 PUFAs in a mouse diet. Journal of Agricultural and Food Chemistry. 2020;68(46):13146–13153. https://doi.org/10.1021/acs.jafc.9b08298

31. Nissim R, Batchelor-Mcauley C, Compton RG. Measuring oxygen solubility in micelles. ChemElectroChem. 2015;3(1):105–109. https://doi.org/10.1002/celc.201500380

32. Roppongi T, Miyagawa Y, Fujita H, Adachi S. Effect of oil-droplet diameter on lipid oxidation in O/W emulsions. Journal of Oleo Science. 2021;70(9):1225–1230. https://doi.org/10.5650/jos.ess21145

33. Sirick A, Lednev S, Moskalenko I, Machtin V, Pliss E. Kinetic features of chain initiation reactions during the oxidation of unsaturated compounds in media of different polarity. Reaction Kinetics, Mechanisms and Catalysis. 2016;117:405–415. https://doi.org/10.1007/s11144-015-0957-6

34. Petrova SN, Sultanova IK. Oxidative stability of sunflower oil in the presence of organic solvents. ChemChemTech. 2010;53(4):105–107. (In Russ.).

35. Wawrzykowski J, Kankofer M. Superoxide dismutase from hen's egg yolk can protect fatty acids from peroxidative damage. European Food Research and Technology. 2014;239:1041–1049. https://doi.org/10.1007/s00217-014-2300-2

36. Ke L, Tan Y, Xu Y, Gao G, Wang H, Luo S, *et al.* Effects of peroxidase and superoxide dismutase on physicochemical stability of fish oil-in-water emulsion. npj Science of Food. 2022;6:31. https://doi.org/10.1038/s41538-022-00146-2

37. Ke L, Xu Y, Gao G, Wang H, Yu Z, Zhou J, *et al.* Catalase to demulsify oil-in-water fish oil-polysorbate emulsion and affect lipid oxidation. Food Research International. 2020;133:109169. https://doi.org/10.1016/j.foodres.2020.109169

38. Bielski BH, Arudi RL, Sutherland MW. A study of the reactivity of HO_2/O_2^- with unsaturated fatty acids. The Journal of Biological Chemistry. 1983;258(8):4759–4761.

39. Moskalenko IV, Tikhonov IV, Pliss EM, Fomich MA, Shmanai VV, Rusakov AI. Kinetic isotope effect in the oxidation reaction of linoleic acid esters in micelles. Russian Journal of Physical Chemistry B. 2018;12:987–991. https://doi.org/10.1134/S1990793118050196

40. Pliss EM, Machtin VA, Grobov AM, Pliss RE, Sirick AV. Kinetics and mechanism of radical-chain oxidation of 1,2-substituted ethylene and 1,4-substituted butadiene-1,3. International Journal of Chemical Kinetics. 2017; 49(3):173–181. https://doi.org/10.1002/kin.21065

41. Pliss RE, Machtin VA, Loshadkin DV, Rusakov AI, Pliss EM. The mechanism of inhibited oxidation of norbornene series bicycloolefins. Petroleum Chemistry. 2014;54:382–386. https://doi.org/10.1134/S0965544114050089

42. Zaikov GE, Howard JA, Ingold KU. Absolute rate constants for hydrocarbon autoxidation. XIII. Aldehydes: photo-oxidation, co-oxidation, and inhibition. Canadian Journal of Chemistry. 1969;47:3017–3029. https://doi.org/10.1139/v69-500

43. Pliss E, Machtin V, Soloviev M, Grobov A, Pliss R, Sirik A, *et al.* The role of solvation in the kinetics and the mechanism of hydroperoxide radicals addition to π-bonds of 1,2-diphenylethylene and 1,4-diphenylbutadiene-1,3. International Journal of Chemical Kinetics. 2018;50(6):397–409. https://doi.org/10.1002/kin.21169

44. Pliss E, Machtin V, Pliss R, Sirik A, Loshadkin D, Rusakov A. The effect of solvation on the reactivity of 1,1-substituted ethylenes in hydroperoxyl radical addition reactions. Reaction Kinetics, Mechanisms and Catalysis. 2018;123: 559–571. https://doi.org/10.1007/s11144-017-1336-2

45. Foti MC, Sortino S, Ingold KU. New insight into solvent effects on the *formal* HOO· + HOO· reaction. Chemistry – A European Journal. 2005;11(6):1942–1948. https://doi.org/10.1002/chem.200400661
46. Cedrowski J, Litwinienko G, Baschieri A, Amorati R. Hydroperoxyl radicals (HOO·): Vitamin E regeneration and H-bond effects on the hydrogen atom transfer. Chemistry – A European Journal. 2016;22(46):16441–16445. https://doi.org/10.1002/chem.201603722
47. Baschieri A, Valgimigli L, Gabbanini S, DiLabio GA, Romero-Montalvo E, Amorati R. Extremely fast hydrogen atom transfer between nitroxides and HOO· radicals and implication for catalytic coantioxidant systems. Journal of the American Chemical Society. 2018;140(32):10354–10362. https://doi.org/10.1021/jacs.8b06336
48. Barclay LRC. 1992 Syntex Award Lecture. Model biomembranes: Quantitative studies of peroxidation, antioxidant action, partitioning, and oxidative stress. Canadian Journal of Chemistry. 2011;71(1):1–16. https://doi.org/10.1139/v93-001
49. Musialik M, Kita M, Litwinienko G. Initiation of lipid autoxidation by ABAP at pH 4–10 in SDS micelles. Organic and Biomolecular Chemistry. 2008;6(4):677–681. https://doi.org/10.1039/b715089j
50. Konya KG, Paul T, Lin S, Lusztyk J, Ingold KU. Laser flash photolysis studies on the first superoxide thermal source. First direct measurements of the rates of solvent-assisted 1,2-hydrogen atom shifts and a proposed new mechanism for this unusual rearrangement. Journal of the American Chemical Society. 2000;122(31):7518–7527. https://doi.org/10.1021/ja993570b
51. Ingold KU, Paul T, Young MJ, Doiron L. Invention of the first azo compound to serve as a superoxide thermal source under physiological conditions: Concept, synthesis, and chemical properties. Journal of the American Chemical Society. 1997;119(50):12364–12365. https://doi.org/10.1021/ja972886l
52. Yakupova LR, Safiullin RL. Kinetics of the initiated and inhibited oxidation of methyl oleate in homogeneous and aqueous emulsion media. Kinetics and Catalysis. 2011;52:785–792. https://doi.org/10.1134/S002315841106022X
53. Niki E, Saito M, Yoshikawa Y, Yamamoto Y, Kamiya Y. Oxidation of lipids. XII. Inhibition of oxidation of soybean phosphatidylcholine and methyl linoleate in aqueous dispersions by uric acid. Bulletin of the Chemical Society of Japan. 1986;59(2):471–477. https://doi.org/10.1246/bcsj.59.471
54. Yazu K, Yamamoto Y, Ukegawa K, Niki E. Mechanism of lower oxidizability of eicosapentaenoate than linoleate in aqueous micelles. Lipids. 1996;31(3):337–340. https://doi.org/10.1007/BF02529881
55. Pyrzynska K, Pękal A. Application of free radical diphenylpicrylhydrazyl (DPPH) to estimate the antioxidant capacity of food samples. Analytical Methods. 2013;5(17):4288–4295. https://doi.org/10.1039/c3ay40367j
56. Olshyk VN, Melsitova IV, Yurkova IL. Influence of lipids with hydroxyl-containing head groups on Fe^{2+} (Cu^{2+})/H_2O_2-mediated transformation of phospholipids in model membranes. Chemistry and Physics of Lipids. 2014;177:1–7. https://doi.org/10.1016/j.chemphyslip.2013.10.010
57. Li X, Wu G, Huang J, Zhang H, Jin Q, Wang X. Kinetic models to understand the coexistence of formation and decomposition of hydroperoxide during lipid oxidation. Food Research International. 2020;136:109314. https://doi.org/10.1016/j.foodres.2020.109314
58. Wang G, Wang T. Oxidative stability of egg and soy lecithin as affected by transition metal ions and pH in emulsion. Journal of Agricultural and Food Chemistry. 2008;56(23):11424–11431. https://doi.org/10.1021/jf8022832
59. Wang S. A comparative study of fenton and fenton-like reaction kinetics in decolourisation of wastewater. Dyes and Pigments. 2008;76(3):714–720. https://doi.org/10.1016/j.dyepig.2007.01.012
60. Pinchuk I, Lichtenberg D. Deuterium kinetic isotope effect (DKIE) in copper-induced LDL peroxidation: Interrelated effects of on inhibition and propagation. Chemistry and Physics of Lipids. 2017;205:42–47. https://doi.org/10.1016/j.chemphyslip.2017.04.009
61. Pinchuk I, Lichtenberg D. The effect of compartmentalization on the kinetics of transition metal ions-induced lipoprotein peroxidation. Chemistry and Physics of Lipids. 2016;195:39–46. https://doi.org/10.1016/j.chemphyslip.2015.11.004
62. Yurkova IL. Free-radical reactions of glycerolipids and sphingolipids. Russian Chemical Reviews. 2012;81(2):175–190. https://doi.org/10.1070/RC2012v81n02ABEH004205
63. Trunova NA, Krugovov DA, Bogdanova YuG, Kasaikina OT. Micellar free radical initiators. Moscow University Chemistry Bulletin. 2008;63(4):214–218. https://doi.org/10.3103/S0027131408040093
64. Kasaikina OT, Krugovov DA, Mengele EA, Berezin MP, Fokin DA. Heterogeneous radical-generating catalysts based on cationic surfactants. Petroleum Chemistry. 2015;55:679–682. https://doi.org/10.1134/S0965544115080101
65. Potapova NV, Kasaikina OT, Berezin MP, Plashchina IG. Catalytic generation of radicals in supramolecular systems with acetylcholine. Kinetics and Catalysis. 2020;61:786–793. https://doi.org/10.1134/S0023158420050079

66. Potapova NV, Kasaikina OT, Berezin MP, Plashchina IG, Gulin AA. Supramolecular catalysts for the radical destruction of hydroperoxides based on choline derivatives. Kinetics and Catalysis. 2023;64:67–73. https://doi.org/10.1134/S0023158423010056

67. Krugovov DA, Gatin AK, Potapova NV, Kondratovich VG, Mengele EA, Kasaikina OT. The effect of a magnetic field on the generation of free radicals in the interaction of quaternary ammonium compounds with hydroperoxides. Russian Journal of Physical Chemistry B. 2024;18:656–662. https://doi.org/10.1134/S199079312470012X

68. Tikhonov IV, Pliss EM, Borodin LI, Sen VD. Superoxide radicals in the kinetics of nitroxide-inhibited oxidation of methyl linoleate in micelles. Russian Journal of Physical Chemistry B. 2017;11:400–402. https://doi.org/10.1134/S1990793117030253

69. Moskalenko IV, Borodin LI, Novikov AS. Oxidation of methyl linoleate in Triton X-100 micelles initiated by lipid-soluble initiator 2,2′-azobis (2,4-dimethylvaleronitrile). ChemistrySelect. 2023;8(25):e202301357. https://doi.org/10.1002/slct.202301357

70. Antunes F, Pinto RE, Barclay LRC, Vinqvist MR. Determination of propagation and termination rate constants by using an extension to the rotating-sector method: Application to PLPC and DLPC bilayers. International Journal of Chemical Kinetics. 1998;30(10):753–767. https://doi.org/10.1002/(SICI)1097-4601(1998)30:10<753::AID-KIN8>3.0.CO;2-U

71. Garrec J, Monari A, Assfeld X, Mir LM, Tarek M. Lipid peroxidation in membranes: The peroxyl radical does not "float." The Journal of Physical Chemistry Letters. 2014;5(10):1653–1658. https://doi.org/10.1021/jz500502q

72. Roginskii VA. Kinetics of the chain oxidation of methyl linoleate in aqueous micellar solutions of sodium dodecyl sulfate. Kinetics and Catalysis. 1996;37(4):488–494. https://elibrary.ru/LDTWWR

73. Moskalenko IV, Petrova SYu, Pliss EM, Rusakov AI, Buchachenko AL. Effect of microheterogeneity on the kinetics of oxidation of methyl linoleate in micelles. Russian Journal of Physical Chemistry B. 2016;35(4):36–39. (In Russ.). https://doi.org/10.7868/S0207401X16040087

74. Jiang T, Charcosset C. Encapsulation of curcumin within oil-in-water emulsions prepared by premix membrane emulsification: Impact of droplet size and carrier oil on the chemical stability of curcumin. Food Research International. 2022;157:111475. https://doi.org/10.1016/j.foodres.2022.111475

75. Costa M, Freiría-Gándara J, Losada-Barreiro S, Paiva-Martins F, Bravo-Díaz C. Effects of droplet size on the interfacial concentrations of antioxidants in fish and olive oil-in-water emulsions and nanoemulsions and on their oxidative stability. Journal of Colloid and Interface Science. 2020;562:352–362. https://doi.org/10.1016/j.jcis.2019.12.011

76. ten Klooster S, Boerkamp VJP, Hennebelle M, van Duynhoven JPM, Schroën K, Berton-Carabin CC. Unravelling the effect of droplet size on lipid oxidation in O/W emulsions by using microfluidics. Scientific Reports. 2024;14:8895. https://doi.org/10.1038/s41598-024-59170-9

77. Soloviev M, Moskalenko I, Pliss E. Quantum chemical evaluation of the role of $HO_2^{\bullet}$ radicals in the kinetics of the methyl linoleate oxidation in micelles. Reaction Kinetics, Mechanisms and Catalysis. 2019;127:561–581. https://doi.org/10.1007/s11144-019-01613-w

78. Roginsky V, Barsukova T. Superoxide dismutase inhibits lipid peroxidation in micelles. Chemistry and Physics of Lipids. 2001;111(1):87–91. https://doi.org/10.1016/S0009-3084(01)00148-7

79. Tikhonov IV, Pliss EM, Borodin LI, Sen' VD. Effect of superoxide dismutase on the oxidation of methyl linoleate in micelles inhibited by nitroxyl radicals. Russian Chemical Bulletin. 2016;65:2985–2987. https://doi.org/10.1007/s11172-016-1690-7

80. Moskalenko IV, Tikhonov IV. H/D Kinetic solvent isotope effect in the oxidation of methyl linoleate in Triton X-100 micelles. Russian Journal of Physical Chemistry B. 2022;16:602–605. https://doi.org/10.1134/S1990793122040121

81. Harrison KA, Haidasz EA, Griesser M, Pratt DA. Inhibition of hydrocarbon autoxidation by nitroxide-catalyzed cross-dismutation of hydroperoxyl and alkylperoxyl radicals. Chemical Science. 2018;9(28):6068–6079. https://doi.org/10.1039/C8SC01575A

82. Laguerre M, Bily A, Roller M, Birtić S. Mass transport phenomena in lipid oxidation and antioxidation. Annual Review of Food Science and Technology. 2017;8:391–411. https://doi.org/10.1146/annurev-food-030216-025812

83. Kasaikina OT, Mengele EA, Plashchina IG. Oxidation of nonionic surfactants with molecular oxygen. Colloid Journal. 2016;78:767–771. https://doi.org/10.1134/S1061933X16060065

84. Loshadkin DV, Pliss EM, Kasaikina OT. Features of methyl linoleate oxidation in Triton X-100 micellar buffer solutions. Russian Journal of Applied Chemistry. 2020;93:1090–1095. https://doi.org/10.1134/S1070427220070216

85. Pliss EM, Loshadkin DV, Grobov AM, Kuznetsova TS, Rusakov AI. Kinetic study and simulation of methyl linoleate oxidation in micelles. Russian Journal of Physical Chemistry B. 2015;9:127–131. https://doi.org/10.1134/S1990793115010091

86. Bielski BHJ, Cabelli DE, Arudi RL, Ross AB. Reactivity of HO_2/O^-_2 radicals in aqueous solution. Journal of Physical and Chemical Reference Data. 1985;14:1041–1100. https://doi.org/10.1063/1.555739

87. Belovolova LV. Reactive oxygen species in aqueous media (a review). Optics and Spectroscopy. 2020;128:932–951. https://doi.org/10.1134/S0030400X20070036

88. Pliss EM, Soloviev ME, Loshadkin DV, Molodochkina SV, Kasaikina OT. Kinetic model of polyunsaturated fatty acids oxidation in micelles. Chemistry and Physics of Lipids. 2021;237:105089. https://doi.org/10.1016/j.chemphyslip.2021.105089

89. Molodochkina SV, Loshadkin DV, Pliss EM. Kinetics and mechanism of methyl linoleate oxidation in cetyltrimethylammonium bromide micelles. Russian Chemical Bulletin. 2024;73:728–732. https://doi.org/10.1007/s11172-024-4183-0

90. Molodochkina SV, Loshadkin DV, Pliss EM. Kinetic features of methylinoleate oxidation in micelles of sodium dodecyl sulfate. Russian Journal of Physical Chemistry B. 2024;18:136–142. https://doi.org/10.1134/S1990793124010160

91. Denisov ET, Denisova TG. Handbook of antioxidants: bond dissociation energies, rate constants, activation energies, and enthalpies of reactions. CRC Press; 2000. 289 p.

92. Haahr A-M, Jacobsen C. Emulsifier type, metal chelation and pH affect oxidative stability of *n*-3-enriched emulsions. European Journal of Lipid Science and Technology. 2008;110(10):949–961. https://doi.org/10.1002/ejlt.200800035

93. Xu P, Zheng Y, Zhu X, Li S, Zhou C. L-lysine and L-arginine inhibit the oxidation of lipids and proteins of emulsion sausage by chelating iron ion and scavenging radical. Asian-Australasian Journal of Animal Sciences. 2018;31(6):905–913. https://doi.org/10.5713/ajas.17.0617

94. Liu J, Guo Y, Li X, Si T, Mcclements DJ, Ma C. Effects of chelating agents and salts on interfacial properties and lipid oxidation in oil-in-water emulsions. Journal of Agricultural and Food Chemistry. 2019;67(49):13718–13727.

95. Cui L, Decker EA. Phospholipids in foods: Prooxidants or antioxidants? Journal of the Science of Food and Agriculture. 2015;96(1):18–31. https://doi.org/10.1002/jsfa.7320

96. Guzun-Cojocaru T, Koev C, Yordanov M, Karbowiak T, Cases E, Cayot P. Oxidative stability of oil-in-water emulsions containing iron chelates: Transfer of iron from chelates to milk proteins at interface. Food Chemistry. 2011;125(2):326–333. https://doi.org/10.1016/j.foodchem.2010.08.004

97. Daoud S, Bou-Maroun E, Waschatko G, Cayot P. Lipid oxidation in oil-in-water emulsions: Iron complexation by buffer ions and transfer on the interface as a possible mechanism. Food Chemistry. 2021;342:128273. https://doi.org/10.1016/j.foodchem.2020.128273

98. Johnson DR, Tian F, Roman MJ, Decker EA, Goddard JM. Development of iron-chelating poly(ethylene terephthalate) packaging for inhibiting lipid oxidation in oil-in-water emulsions. Journal of Agricultural and Food Chemistry. 2015;63(20):5055–5060.

99. Tikhonov IV, Pliss EM, Borodin LI, Sen' VD, Kuznetsova TS. Stable nitroxyl radicals and hydroxylamines as inhibitors of methyl linoleate oxidation in micelles. Russian Chemical Bulletin. 2015;64:2438–2443. https://doi.org/10.1007/s11172-015-1175-0

100. Tikhonov IV, Pliss EM, Borodin LI, Sen′ VD. Five-membered cyclic nitroxyl radicals as inhibitors of the oxidation of methyl linoleate in micelles. Russian Chemical Bulletin. 2015;64:2869–2871. https://doi.org/10.1007/s11172-015-1240-8

101. Merkx DWH, Plankensteiner L, Yu Y, Wierenga PA, Hennebelle M, van Duynhoven JPM. Evaluation of PBN spin-trapped radicals as early markers of lipid oxidation in mayonnaise. Food Chemistry. 2021;334:127578. https://doi.org/10.1016/j.foodchem.2020.127578

102. Zhao Q, Wang M, Zhang W, Zhao W, Yang R. Impact of phosphatidylcholine and phosphatidylethanolamine on the oxidative stability of stripped peanut oil and bulk peanut oil. Food Chemistry. 2020;311:125962. https://doi.org/10.1016/j.foodchem.2019.125962

103. Krudopp H, Sönnichsen FD, Steffen-Heins A. Partitioning of nitroxides in dispersed systems investigated by ultrafiltration, EPR and NMR spectroscopy. Journal of Colloid and Interface Science. 2015;452:15–23. https://doi.org/10.1016/j.jcis.2015.03.001

104. Amorati R, Pedulli GF, Pratt DA, Valgimigli L. TEMPO reacts with oxygen-centered radicals under acidic conditions. Chemical Communications. 2010;46(28):5139–5141. https://doi.org/10.1039/C0CC00547A

105. Tikhonov IV, Sen' VD, Borodin LI, Pliss EM, Golubev VA, Rusakov AI. Effect of the structure of nitroxyl radicals on the kinetics of their acid-catalyzed disproportionation. Journal of Physical Organic Chemistry. 2014;27(2):114–120. https://doi.org/10.1002/poc.3247

106. Sen' VD, Tikhonov IV, Borodin LI, Pliss EM, Golubev VA, Syroeshkin MA, *et al.* Kinetics and thermodynamics of reversible disproportionation-comproportionation in redox triad oxoammonium cations – nitroxyl radicals – hydroxylamines. Journal of Physical Organic Chemistry. 2015;28(1):17–24. https://doi.org/10.1002/poc.3392

107. Amorati R, Guo Y, Budhlall BM, Barry CF, Cao D, Challa SSRK. Tandem hydroperoxyl-alkylperoxyl radical quenching by an engineered nanoporous cerium oxide nanoparticle macrostructure (NCeONP): toward efficient solid-state autoxidation inhibitors. ACS Omega. 2023;8(43):40174–40183. https://doi.org/10.1021/acsomega.3c03654

108. Mollica F, Gelabert I, Amorati R. Synergic antioxidant effects of the essential oil component γ-terpinene on high-temperature oil oxidation. ACS Food Science and Technology. 2022;2(1):180–186. https://doi.org/10.1021/acsfoodscitech.1c00399

109. Opeida IA, Sheparovych RB. Inhibition by hydrogen peroxide in the radical chain oxidation of hydrocarbons by molecular oxygen. Theoretical and Experimental Chemistry. 2019;55:36–42. https://doi.org/10.1007/s11237-019-09593-7

110. Mukai K, Oka W, Watanabe K, Egawa Y, Nagaoka S, Terao J. Kinetic study of free-radical-scavenging action of flavonoids in homogeneous and aqueous Triton X-100 micellar solutions. The Journal of Physical Chemistry A. 1997;101(20):3746–3653. https://doi.org/10.1021/jp9706745

111. Aizpurua-Olaizola O, Navarro P, Vallejo A, Olivares M, Etxebarria N, Usobiaga A. Microencapsulation and storage stability of polyphenols from *Vitis vinifera* grape wastes. Food Chemistry. 2016;190:614–621. https://doi.org/10.1016/j.foodchem.2015.05.117

112. Liang H, Liang Y, Dong J, Lu J. Tea extraction methods in relation to control of epimerization of tea catechins. Journal of the Science of Food and Agriculture. 2007;87(9):1748–1752. https://doi.org/10.1002/jsfa.2913

113. Huang S-W, Hopia A, Schwarz K, Frankel EN, German JB. Antioxidant activity of α-tocopherol and trolox in different lipid substrates: Bulk oils *vs* oil-in-water emulsions. Journal of Agricultural and Food Chemistry. 1996;44(2):444–452. https://doi.org/10.1021/jf9505685

114. Cuomo F, Cinelli G, Chirascu C, Marconi E, Lopez F. Antioxidant effect of vitamins in olive oil emulsion. Colloids and Interfaces. 2020;4(2):23. https://doi.org/10.3390/colloids4020023

115. Zhu Y, Yang J, Qin L, He C, Zhou S. Selecting phenolics by means of thermodynamics for scavenging free radicals in camellia oil induced by heating. LWT. 2024;201:116222. https://doi.org/10.1016/j.lwt.2024.116222

116. Kazin VN, Guzov EA, Moshareva VA, Pliss EM. Influence of a constant magnetic field on the mechanism of adrenaline oxidation. Magnetochemistry. 2022;8(7):70. https://doi.org/10.3390/magnetochemistry8070070

117. Umek N. Cyclization step of noradrenaline and adrenaline autoxidation: A quantum chemical study. RSC Advances. 2020;10(28):16650–16658. https://doi.org/10.1039/D0RA02713H

118. Ebrahimi P, Bayram I, Lante A, Decker EA. Antioxidant and prooxidant activity of acid-hydrolyzed phenolic extracts of sugar beet leaves in oil-in-water emulsions. Journal of the American Oil Chemists' Society. 2024;102(2):339–349. https://doi.org/10.1002/aocs.12891

119. Pan Y, Qin R, Hou M, Xue J, Zhou M, Xu L, *et al.* The interactions of polyphenols with Fe and their application in Fenton/Fenton-like reactions. Separation and Purification Technology. 2022;300:121831. https://doi.org/10.1016/j.seppur.2022.121831

120. Vo QV, Nam PC, Thong NM, Trung NT, Phan C-TD, Mechler A. Antioxidant motifs in flavonoids: O–H versus C–H bond dissociation. ACS Omega. 2019;4(5):8935–8942. https://doi.org/10.1021/acsomega.9b00677

121. Budilarto ES, Kamal-Eldin A. The supramolecular chemistry of lipid oxidation and antioxidation in bulk oils. European Journal of Lipid Science and Technology. 2015;117(8):1095–1137. https://doi.org/10.1002/ejlt.201400200

122. Frankel EN, Huang S-W, Kanner J, German JB. Interfacial phenomena in the evaluation of antioxidants: Bulk oils vs emulsions. Journal of Agricultural and Food Chemistry. 1994;42(5):1054–1059. https://doi.org/10.1021/jf00041a001

123. Nahas R, Berdahl D. The polar paradox: How an imperfect conceptual framework accelerated our knowledge of antioxidant behavior. In: Logan A, Nienaber U, Pan X, editors. Lipid oxidation: Challenges in food systems. Academic Press, AOCS Press; 2013. pp. 243–260. https://doi.org/10.1016/B978-0-9830791-6-3.50010-2

124. Aliaga C, López de Arbina A, Rezende MC. "Cut-off" effect of antioxidants and/or probes of variable lipophilicity in microheterogeneous media. Food Chemistry. 2016;206:119–123. https://doi.org/10.1016/j.foodchem.2016.03.024

125. Costa M, Losada-Barreiro S, Paiva-Martins F, Bravo-Diaz C, Romsted LS. A direct correlation between the antioxidant efficiencies of caffeic acid and its alkyl esters and their concentrations in the interfacial region of olive oil emulsions. The pseudophase model interpretation of the "cut-off" effect. Food Chemistry. 2015;175:233–242. https://doi.org/10.1016/j.foodchem.2014.10.016

126. Laguerre M, López Giraldo LJ, Lecomte J, Figueroa-Espinoza M-C, Baréa B, Weiss J, *et al.* Chain length affects antioxidant properties of chlorogenate esters in emulsion: The cutoff theory behind the polar paradox. Journal of Agricultural and Food Chemistry. 2009;57(23):11335–11342. https://doi.org/10.1021/jf9026266

127. Zhong Y, Shahidi F. Antioxidant behavior in bulk oil: Limitations of polar paradox theory. Journal of Agricultural and Food Chemistry. 2012;60(1):4–6. https://doi.org/10.1021/jf204165g

128. Shahidi F, Zhong Y. Revisiting the polar paradox theory: A critical overview. Journal of Agricultural and Food Chemistry. 2011;59(8):3499–3504. https://doi.org/10.1021/jf104750m

129. Romsted LS, Bravo-Díaz C. Modeling chemical reactivity in emulsions. Current Opinion in Colloid and Interface Science. 2013;18(1):3–14. https://doi.org/10.1016/j.cocis.2012.11.001

130. Losada Barreiro S, Bravo-Díaz C, Paiva-Martins F, Romsted LS. Maxima in antioxidant distributions and efficiencies with increasing hydrophobicity of gallic acid and its alkyl esters. The pseudophase model interpretation of the "cutoff effect". Journal of Agricultural and Food Chemistry. 2013;61(26):6533–6543. https://doi.org/10.1021/jf400981x

131. Laguerre M, Bayrasy C, Panya A, Weiss J, McClements DJ, Lecomte J, *et al.* What makes good antioxidants in lipid-based systems? The next theories beyond the polar paradox. Critical Reviews in Food Science and Nutrition. 2015;55(2):183–201. https://doi.org/10.1080/10408398.2011.650335

132. Bravo-Díaz C, Romsted LS, Liu C, Losada-Barreiro S, Pastoriza-Gallego MJ, Gao X, *et al.* To model chemical reactivity in heterogeneous emulsions, think homogeneous microemulsions. Langmuir. 2015;31(33):8961–8979. https://doi.org/10.1021/acs.langmuir.5b00112

133. Tamer TM, ElTantawy MM, Brussevich A, Nebalueva A, Novikov A, Moskalenko IV, *et al.* Functionalization of chitosan with poly aromatic hydroxyl molecules for improving its antibacterial and antioxidant properties: Practical and theoretical studies. International Journal of Biological Macromolecules. 2023;234:123687. https://doi.org/10.1016/j.ijbiomac.2023.123687

134. Stepanić V, Gall Trošelj K, Lučić B, Marković Z, Amić D. Bond dissociation free energy as a general parameter for flavonoid radical scavenging activity. Food Chemistry. 2013;141(2):1562–1570. https://doi.org/10.1016/j.foodchem.2013.03.072

135. Antonijević M, Avdović E, Simijonović D, Milanović Z, Žižić M, Marković Z. Investigation of novel radical scavenging mechanisms in the alkaline environment: Green, sustainable and environmentally friendly antioxidative agent(s). Science of The Total Environment. 2024;912:169307. https://doi.org/10.1016/j.scitotenv.2023.169307

136. Amorati R, Baschieri A, Cowden A, Valgimigli L. The antioxidant activity of quercetin in water solution. Biomimetics. 2017;2(3):9. https://doi.org/10.3390/biomimetics2030009

137. Amorati R, Baschieri A, Morroni G, Gambino R, Valgimigli L. Peroxyl radical reactions in water solution: A gym for proton-coupled electron-transfer theories. Chemistry – A European Journal. 2016;22(23):7924–7934. https://doi.org/10.1002/chem.201504492

138. Tichonov I, Roginsky V, Pliss E. Natural polyphenols as chain-breaking antioxidants during methyl linoleate peroxidation. European Journal of Lipid Science and Technology. 2010;112(8):887–893. https://doi.org/10.1002/ejlt.200900282

139. Tikhonov I, Roginsky V, Pliss E. The chain-breaking antioxidant activity of phenolic compounds with different numbers of O-H groups as determined during the oxidation of styrene. International Journal of Chemical Kinetics. 2009;41(2):92–100. https://doi.org/10.1002/kin.20377

140. Jodko-Piórecka K, Litwinienko G. Antioxidant activity of dopamine and L-DOPA in lipid micelles and their cooperation with an analogue of α-tocopherol. Free Radical Biology and Medicine. 2015;83:1–11. https://doi.org/10.1016/j.freeradbiomed.2015.02.006

141. Loshadkin D, Roginsky V, Pliss E. Substituted *p*-hydroquinones as a chain-breaking antioxidant during the oxidation of styrene. International Journal of Chemical Kinetics. 2002;34(3):162–171. https://doi.org/10.1002/kin.10041

142. Amorati R, Baschieri A, Valgimigli L. Measuring antioxidant activity in bioorganic samples by the differential oxygen uptake apparatus: Recent advances. Journal of Chemistry. 2017;2017(1):6369358. https://doi.org/10.1155/2017/6369358

143. Yakupova LR, Proskurjakov SG, Zaripov RN, Rameev ShR, Safiullin RL. Measurement of the reaction rate proceeding with gas absorption or gas evolution. Butlerov Communications. 2011;28(19):71–78. (In Russ.). https://www.elibrary.ru/OWFPXP

144. Roginsky VA, Tashlitsky VN, Skulachev VP. Chain-breaking antioxidant activity of reduced forms of mitochondria-targeted quinones, a novel type of geroprotectors. Aging. 2009;1(5):481–489. https://doi.org/10.18632/aging.100049

145. Jansen J, Knoll J, Beyreuther E, Pawelke J, Skuza R, Hanley R, *et al.* Does FLASH deplete oxygen? Experimental evaluation for photons, protons, and carbon ions. Medical Physics. 2021;48(7):3982–3990. https://doi.org/10.1002/mp.14917

146. Quaranta M, Murkovic M, Klimant I. A new method to measure oxygen solubility in organic solvents through optical oxygen sensing. Analyst. 2013;138(21):6243–6245. https://doi.org/10.1039/C3AN36782G

147. Guo Y, Cariola A, Matera R, Gabbanini S, Valgimigli L. Real-time oxygen sensing as a powerful tool to investigate tyrosinase kinetics allows revising mechanism and activity of inhibition by glabridin. Food Chemistry. 2022;393:133423. https://doi.org/10.1016/j.foodchem.2022.133423

148. Genovese D, Baschieri A, Vona D, Baboi RE, Mollica F, Prodi L, *et al.* Nitroxides as building blocks for nanoantioxidants. ACS Applied Materials and Interfaces. 2021;13(27):31996–32004. https://doi.org/10.1021/acsami.1c06674

149. Tacchini P, Lesch A, Neequaye A, Lagger G, Liu J, Cortés-Salazar F, *et al.* Electrochemical pseudo-titration of water-soluble antioxidants. Electroanalysis. 2013;25(4):922–930. https://doi.org/10.1002/elan.201200590

150. Lesch A, Cortés-Salazar F, Prudent M, Delobel J, Rastgar S, Lion N, *et al.* Large scale inkjet-printing of carbon nanotubes electrodes for antioxidant assays in blood bags. Journal of Electroanalytical Chemistry. 2014;717–718:61–68. https://doi.org/10.1016/j.jelechem.2013.12.027

151. Souza LP, Calegari F, Zarbin AJG, Marcolino-Júnior LH, Bergamini MF. Voltammetric determination of the antioxidant capacity in wine samples using a carbon nanotube modified electrode. Journal of Agricultural and Food Chemistry. 2011;59(14):7620–7625. https://doi.org/10.1021/jf2005589

152. Smirnov E, Peljo P, Scanlon MD, Girault HH. Interfacial redox catalysis on gold nanofilms at soft interfaces. ACS Nano. 2015;9(6):6565–6575. https://doi.org/10.1021/acsnano.5b02547

153. Peljo P, Smirnov E, Girault HH. Heterogeneous versus homogeneous electron transfer reactions at liquid–liquid interfaces: The wrong question? Journal of Electroanalytical Chemistry. 2016;779:187–198. https://doi.org/10.1016/j.jelechem.2016.02.023

154. Li G, Chen Y, Liu F, Bi W, Wang C, Lu D, *et al.* Portable visual and electrochemical detection of hydrogen peroxide release from living cells based on dual-functional Pt-Ni hydrogels. Microsystems and Nanoengineering. 2023;9:152. https://doi.org/10.1038/s41378-023-00623-y

155. Rajendran S, Manoj D, Suresh R, Vasseghian Y, Ghfar AA, Sharma G, *et al.* Electrochemical detection of hydrogen peroxide using micro and nanoporous CeO_2 catalysts. Environmental Research. 2022;214:113961. https://doi.org/10.1016/j.envres.2022.113961

156. Peljo P, Scanlon MD, Olaya AJ, Rivier L, Smirnov E, Girault HH. Redox electrocatalysis of floating nanoparticles: determining electrocatalytic properties without the influence of solid supports. The Journal of Physical Chemistry Letters. 2017;8(15):3564–3575. https://doi.org/10.1021/acs.jpclett.7b00685

157. Scanlon MD, Peljo P, Méndez MA, Smirnov E, Girault HH. Charging and discharging at the nanoscale: Fermi level equilibration of metallic nanoparticles. Chemical Science. 2015;6(5):2705–2720. https://doi.org/10.1039/C5SC00461F

158. Nagaraju DH, Pandey RK, Lakshminarayanan V. Electrocatalytic studies of Cytochrome c functionalized single walled carbon nanotubes on self-assembled monolayer of 4-ATP on gold. Journal of Electroanalytical Chemistry. 2009;627(1–2):63–68. https://doi.org/10.1016/j.jelechem.2008.12.020

159. Smirnov E, Peljo P, Scanlon MD, Girault HH. Gold nanofilm redox catalysis for oxygen reduction at soft interfaces. Electrochimica Acta. 2016;197:362–373. https://doi.org/10.1016/j.electacta.2015.10.104

160. Gotti G, Evrard D, Gros P. Simultaneous electrochemical detection of oxygen (O_2) and hydrogen peroxide (H_2O_2) in neutral media. International Journal of Electrochemical Science. 2023;18(9):100262. https://doi.org/10.1016/j.ijoes.2023.100262

161. Saad B, Wai WT, Lim BP, Saleh MI. Flow injection determination of peroxide value in edible oils using triiodide detector. Analytica Chimica Acta. 2006;565(2):261–270. https://doi.org/10.1016/j.aca.2006.02.039

162. Kwon CW, Park K-M, Park JW, Lee J, Choi SJ, Chang P-S. Rapid and sensitive determination of lipid oxidation using the reagent kit based on spectrophotometry (FOODLAB*fat* system). Journal of Chemistry. 2016;2016(1):1468743. https://doi.org/10.1155/2016/1468743

163. Feng X, Yan J, Chen Y, Tan C, Lin H, Ge X. Effects of Fe(III) and Fe(II) on the peroxidation value of soybean oil under different conditions and product characterization. Journal of Food Processing and Preservation. 2020;44(7):e14515. https://doi.org/10.1111/jfpp.14515

164. Zhang N, Li Y, Wen S, Sun Y, Chen J, Gao Y, *et al.* Analytical methods for determining the peroxide value of edible oils: A mini-review. Food Chemistry. 2021;358:129834. https://doi.org/10.1016/j.foodchem.2021.129834

165. Ivanova AS, Merkuleva AD, Andreev SV, Sakharov KA. Method for determination of hydrogen peroxide in adulterated milk using high performance liquid chromatography. Food Chemistry. 2019;283:431–436. https://doi.org/10.1016/j.foodchem.2019.01.051

166. Yu X, van de Voort FR, Sedman J. Determination of peroxide value of edible oils by FTIR spectroscopy with the use of the spectral reconstitution technique. Talanta. 2007;74(2):241–246. https://doi.org/10.1016/j.talanta.2007.06.004

167. Deyrieux C, Villeneuve P, Baréa B, Decker EA, Guiller I, Michel Salaun F, *et al.* Measurement of peroxide values in oils by triphenylphosphine/triphenylphosphine oxide (TPP/TPPO) assay coupled with FTIR-ATR spectroscopy: Comparison with iodometric titration. European Journal of Lipid Science and Technology. 2018;120(8):1800109. https://doi.org/10.1002/ejlt.201800109

168. Lopez C, Genot C. Multidimensional characterization of dietary lipids [Internet]. New York: Humana; 2024. 379 p. https://doi.org/10.1007/978-1-0716-3758-6

169. Wind J, Villeneuve P, Taty MPE, Figueroa-Espinoza MC, Baréa B, Pradelles R, *et al.* Improving the triphenylphosphine/triphenylphosphine oxide (TPP/TPPO)-based method for the absolute and accurate quantification by FTIR-ATR of hydroperoxides in oils or lipid extracts. European Journal of Lipid Science and Technology. 2024;126(9):2400030. https://doi.org/10.1002/ejlt.202400030

170. Roohi H, Rajabi M. Iodometric determination of hydroperoxides in hydrocarbon autoxidation reactions using triphenylphosphine solution as a titrant: A new protocol. Industrial and Engineering Chemistry Research. 2018;57(20):6805–6814. https://doi.org/10.1021/acs.iecr.7b05403

171. Benrabah R, El Sayah Z, Glaude PA, Arnoux P, Fournet R, Sirjean B. Quantification of hydroperoxides in liquid fuels: A systematic comparison of titration and absorption methods and their coupling to HPLC. Fuel. 2024;365:131218. https://doi.org/10.1016/j.fuel.2024.131218

172. Faroux JM, Ureta MM, Tymczyszyn EE, Gómez-Zavaglia A. An overview of peroxidation reactions using liposomes as model systems and analytical methods as monitoring tools. Colloids and Surfaces B: Biointerfaces. 2020;195:111254. https://doi.org/10.1016/j.colsurfb.2020.111254

173. Jiang Y, Su M, Yu T, Du S, Liao L, Wang H, *et al.* Quantitative determination of peroxide value of edible oil by algorithm-assisted liquid interfacial surface enhanced Raman spectroscopy. Food Chemistry. 2021;344:128709. https://doi.org/10.1016/j.foodchem.2020.128709

174. Killeen DP, Marshall SN, Burgess EJ, Gordon KC, Perry NB. Raman spectroscopy of fish oil capsules: Polyunsaturated fatty acid quantitation plus detection of ethyl esters and oxidation. Journal of Agricultural and Food Chemistry. 2017;65(17):3551–3558. https://doi.org/10.1021/acs.jafc.7b00099

175. Du S, Su M, Jiang Y, Yu F, Xu Y, Lou X, *et al.* Direct discrimination of edible oil type, oxidation, and adulteration by liquid interfacial surface-enhanced Raman spectroscopy. ACS Sensors. 2019;4(7):1798–1805. https://doi.org/10.1021/acssensors.9b00354

176. Qi Z, Akhmetzhanov T, Pavlova A, Smirnov E. Reusable SERS substrates based on gold nanoparticles for peptide detection. Sensors. 2023;23(14):6352. https://doi.org/10.3390/s23146352

177. Langer J, de Aberasturi DJ, Aizpurua J, Alvarez-Puebla RA, Auguié B, Baumberg JJ, *et al.* Present and future of surface-enhanced Raman scattering. ACS Nano. 2020;14(1):28–117. https://doi.org/10.1021/acsnano.9b04224

178. Li W, You Z, Cao D, Liu N. A machine learning-driven SERS platform for precise detection and analysis of vascular calcification. Analytical Methods. 2024;16(40):6829–6838. https://doi.org/10.1039/D4AY01061B

179. Liu E, Han L, Fan X, Yang Z, Jia Z, Shi S, *et al.* New rapid detection method of total chlorogenic acids in plants using SERS based on reusable Cu_2O–Ag substrate. Talanta. 2022;247:123552. https://doi.org/10.1016/j.talanta.2022.123552

180. Aguilar-Hernández I, Afseth NK, López-Luke T, Contreras-Torres FF, Wold JP, Ornelas-Soto N. Surface enhanced Raman spectroscopy of phenolic antioxidants: A systematic evaluation of ferulic acid, *p*-coumaric acid, caffeic acid and sinapic acid. Vibrational Spectroscopy. 2017;89:113–122. https://doi.org/10.1016/j.vibspec.2017.02.002

181. Huguenin J, Ould Saad Hamady S, Bourson P. Monitoring deprotonation of gallic acid by Raman spectroscopy. Journal of Raman Spectroscopy. 2015;46(11):1062–1066. https://doi.org/10.1002/jrs.4752

182. Umaña M, Llull L, Bon J, Eim VS, Simal S. Artificial neural networks to optimize oil-in-water emulsion stability with orange by-products. Foods. 2022;11(23):3750. https://doi.org/10.3390/foods11233750

183. Tachie CYE, Obiri-Ananey D, Alfaro-Cordoba M, Tawiah NA, Aryee ANA. Classification of oils and margarines by FTIR spectroscopy in tandem with machine learning. Food Chemistry. 2024;431:137077. https://doi.org/10.1016/j.foodchem.2023.137077

184. Chen C, Husny J, Rabe S. Predicting fishiness off-flavour and identifying compounds of lipid oxidation in dairy powders by SPME-GC/MS and machine learning. International Dairy Journal. 2018;77:19–28. https://doi.org/10.1016/j.idairyj.2017.09.009

185. Galvez-Llompart M, Zanni R, Manyes L, Meca G. Elucidating the mechanism of action of mycotoxins through machine learning-driven QSAR models: Focus on lipid peroxidation. Food and Chemical Toxicology. 2023;182:114120. https://doi.org/10.1016/j.fct.2023.114120

186. Spink SS, Pilvar A, Wei LL, Frias J, Anders K, Franco ST, *et al.* Shortwave infrared diffuse optical wearable probe for quantification of water and lipid content in emulsion phantoms using deep learning. Journal of Biomedical Optics. 2023;28(9):094808. https://doi.org/10.1117/1.JBO.28.9.094808

187. Idowu SO, Fatokun AA. Artificial intelligence (AI) to the rescue: Deploying machine learning to bridge the biorelevance gap in antioxidant assays. SLAS Technology. 2021;26(1):16–25. https://doi.org/10.1177/2472630320962716

188. Cheng J, Sun J, Yao K, Xu M, Dai C. Multi-task convolutional neural network for simultaneous monitoring of lipid and protein oxidative damage in frozen-thawed pork using hyperspectral imaging. Meat Science. 2023;201:109196. https://doi.org/10.1016/j.meatsci.2023.109196

189. Parra-Escudero C, Bayram I, Decker EA, Singh S, Corvalan CM, Lu J. A machine learning-guided modeling approach to the kinetics of α-tocopherol and myricetin synergism in bulk oil oxidation. Food Chemistry. 2024(463);141451. https://doi.org/10.1016/j.foodchem.2024.141451

190. Fulkerson A, Bayram I, Decker EA, Lu J, Corvalan CM. Machine learning reveals parsimonious differential model for myricetin degradation from scarce data. 2023. https://doi.org/10.21203/rs.3.rs-3122091/v1

191. Mallikarjunaiah SM. A deep learning feed-forward neural network framework for the solutions to singularly perturbed delay differential equations. Applied Soft Computing. 2023;148:110863. https://doi.org/10.1016/j.asoc.2023.110863

192. Michoski C, Milosavljević M, Oliver T, Hatch DR. Solving differential equations using deep neural networks. Neurocomputing. 2020;399:193–212. https://doi.org/10.1016/j.neucom.2020.02.015

193. Ruthotto L, Haber E. Deep neural networks motivated by partial differential equations. Journal of Mathematical Imaging and Vision. 2020;62:352–364. https://doi.org/10.1007/s10851-019-00903-1

ORCID IDs
Ivan V. Moskalenko https://orcid.org/0000-0003-2272-2103
Ilya S. Korolev https://orcid.org/0000-0003-3252-0329
Evgeny A. Smirnov https://orcid.org/0000-0001-7930-7758
Ekaterina V. Skorb https://orcid.org/0000-0003-0888-1693

FRM
Foods and Raw Materials. 2026;14(1)
ISSN 2310-9599 (Print)
ISSN 2308-4057 (Online)
Available online at https://jfrm.ru/en/
DOI: https://doi.org/10.21603/2308-4057-2026-1

CONTENTS

Editor's column i

Elena V. Guseva, Natalya Yu. Khromova, Boris A. Karetkin, Artem I. Artemiev, Kirill M. Demkin, Julia M. Puzankova, Irina V. Shakir, Victor I. Panfilov Biological value of berry polyphenols and prospects for supercritical extraction application for their isolation: A review 1

Ishrat Perveen, Nazia Koser, Rozina Shahadat Khan, Maryam Maqsood, Nida Saleem, Farhat Naseem Alvi, Syed Muhammad Aun, Maria Fareed Siddiqui, Tallat Anwar Faridi, Hafiz Muhammad Abrar Awan, Yasar Saleem, Naaz Abbas, Sania Mazhar, Shaista Nawaz, Quratulain Syed, Syed Hussain Imam Abidi Dietary consumption of pre-carcinogenic amines and mutagenicity in humans: An evidence-based study 14

Khalid El Moutaouakil, Noureddine Falih, Karim Doumi Predictive analytics of cattle behavior using machine learning techniques: A case study 26

Olumayowa Joseph Iyanda, Akeem Abdulai Oyekanmi, Mufutau Olaoye Atayese, Christopher Adejuyigbe, Ayomide Afolabi Enhancing lowland rice physiology with integrated nitrogen nutrient sources in Nigeria's derived savannah 37

Sergey N. Golovin, Evgeniya Yu. Kirichenko, Maxim M. Khanukaev, Alexander K. Logvinov 3D bioprinting of hybrid cultured meat from rabbit cells and sunflower protein 52

Maria R. Ramirez, Debora Manuale, Juan C. Yori Fiber supplements from agro-industrial waste: Effect on valproic acid hepatotoxicity in rats 61

Yee Mun Chin, Lejaniya Abdul Kalam Saleena, Lee Ying Lim, Liew Phing Pui, Mahmud Iwan Solihin Kelulut stingless bee honey stored under different thermal conditions: Non-destructive assessment 71

Himanshu, Nishant Kumar, Ishu Khangwal Functional attributes and bio-prospects of fruit peel waste 81

Manoj Kumar Sharma, Anupama Diwan, Satish Sardana, Kapil Kumar Derivation of hazardous wastes: Pharmaceutical and food applications 104

Francesca Girotto Sunflower press-cake and its protein extract for food applications: Effects of sonication on functional properties 117

Durga R. Priyadarshin, Annette D. Beatrice, Tinhoithem Haokip Antioxidant and anti-inflammatory activities of the Black Bean (*Phaseolus vulgaris* L.): A systematic review 123

Safia Ali Haimoud, Fatiha Arioui, Meriem Medjekane, Leila Ali Haimoud, Khelifa Bahri, Asma Cheikh, Saadia Ghiboub, Hanane Benabed, Ikram Boudali, Besma Ayache, Chaima Beskri Antilithiasic and antioxidant activities of propolis and bee pollen extracts: *In vitro* and *in silico* studies 138

Fidelis C.K. Ocloo, Joyce Agyei-Amponsah, Bernard T. Odai, Tahiru Mahami, Jonathan O. Armah, Ernestina A. Ayeh, Isaac Adjei, Jacob Basugilo, Sarah Asomaniwaa, Martin N.Y.H. Egblewogbe, Bernard Darfour Irradiated sorghum grain: Phytochemical, physicochemical, and functional properties 148

Larisa E. Chemisova, Natalia M. Ageyeva, Olga N. Sheludko, Mikhail V. Antonenko, Yurii F. Yakuba Polymer stoppers: Quality of alcohol beverages during storage 159

Anna D. Vesnina, Anna S. Frolova, Darya Yu. Chekushkina, Irina S. Milentyeva, Sergey L. Luzyanin, Larisa M. Aksenova Gut microbiota and its role in development of chronic disease and aging 174

Mahmud Gharaviri, Denis I. Aleksanochkin, Mahbubeh Ahangaran, Ivan A. Fomenko, Leonid I. Kovalev, Marina A. Kovaleva, Irina M. Chernukha, Natalia G. Mashentseva Chickpea protein hydrolysates: Production, bioactivity, functional profile, and technological properties 198

Yuliya R. Serazetdinova, Ekaterina E. Borodina, Natalya V. Fotina, Adarsh Naik, Gaurav Mudgal, Lyudmila K. Asyakina Rhizobia as complex biofertilizers for wheat: Biological nitrogen fixation and plant growth promotion 214

Ivan V. Moskalenko, Ilya S. Korolev, Evgeny A. Smirnov, Ekaterina V. Skorb Inhibited and non-inhibited lipid oxidation in colloidal solutions: A review 228